UNIVERSITY OF MILANO-BICOCCA

Department of Biotechnology and Biosciences

PhD program in *Chemical, Geological and Environmental Sciences*
XXXI Cycle

PhD in Chemical Sciences

Design, synthesis and bioconjugation of TLR4 ligands to understand and modulate innate immunity processes

Florent Cochet
811128

Tutor: Prof. Francesco Peri
Co-tutor: Dr. Christina Airoldi
Co-tutor: Prof. Luca Bertini

Academic year 2017/2018

Although nature commences with reason and ends in experience it is necessary for us to do the opposite, that is to commence with experience and from this to proceed to investigate the reason.

- Leonardo Da Vinci

TABLE OF CONTENTS

TABLE OF ILLUSTRATIONS

ABBREVIATIONS

- AIM2, Interferon-inducible protein (Absent In Melanoma 2)
- ALRs, AIM2-Like Receptors
- ALS, amyotrophic lateral sclerosis
- AP-1, Activator protein 1
- ATP, adenosine-5'-triphosphate;
- BPI, bactericidal/permeability-increasing protein
- CAC, critical aggregate concentration
- CD, Crohn's disease
- CD14, cluster of differentiation 14
- CETP, cholesteryl ester transfer protein
- CLRs, C-type lectin receptors
- CMC, critical micellar concentration
- CpG DNA, Cytosine triphosphate deoxynucleotide phosphodiester Guanine triphosphate deoxynucleotide DNA
- CRDs, carbohydrate-recognition domains
- DAMPs, Damage-Associated Molecular Patterns
- DCs, Dendritic cells
- DC-SIGN, dendritic cell-specific ICAM3-grabbing nonintegrin
- DMARDs, disease-modifying antirheumatic drugs
- DNGR-1, DC NK lectin group receptor-1
- FA, Fatty acid
- Gal, Galactose
- Glc, Glucose
- GlcN, Glucosamine
- GlcN3N, 2,3-diamino-2,3-dideoxy-D-glucose
- GlcNAc, *N*-Acetyl-Glucosamine
- GLs, Glycolipids
- GPI, glycosylphosphatidylinositol
- HEK, Human Embryonic Kidney Cell 293
- Hep, heptosyl-2-keto-3-deoxy-octulosonate
- HLADR, Human Leukocyte Antigen D Related
- HMGB1, high mobility group box 1
- HSPs, heat shock proteins
- IBD, inflammatory bowel diseases
- IFN, Interferon
- IL, Interleukin

- IRAK, interleukin-1 receptor-associated kinase
- IRF, Interferon regulatory factor
- ISGs, IFN-stimulated genes
- Kdo, 3-deoxy-D-manno-oct-2 ulosonic acid
- Ko, 2-keto-D-glycero-D-talo-octonic acid
- LBP, Lipid Binding Protein
- LCs, liquid crystals
- LOS, Lipooligosaccharide (Hep3-Kdo2-lipid A)
- LPS, lipopolysaccharide;
- LRR, Leucine-Rich Repeat
- LRRCT, Leucin-Rich Repeat C-terminal
- LRRNT, Leucin-Rich Repeat N-terminal
- MAL, MyD88 adaptor-like protein;
- MAPK, mitogen-activated protein kinase
- MC, Mast Cells
- MD, molecular dynamics
- MD-2, Myeloid Differentiation factor 2
- MDDC, Human Monocyte Derived Dendritic Cell
- Mincle, macrophage-inducible C-type lectin
- MMR, macrophage mannose receptor
- MurNAc, *N*-Acetyl-Muramic acid
- MyD88, Myeloid differentiation primary response gene 88
- NBD Nucleotide-Binding Domain
- NF-κB, nuclear factor-kappa B
- NLRP, NOD-like receptor family, pyrin domain-containing protein
- NLRs, (NOD)-like receptors
- NODs, Nucleotide-binding Oligomerization Domain receptors
- PAMPs, Pathogen-Associated Molecular Patterns
- PDB, Protein Data Bank
- PGN, Peptidoglycan
- PIP2, phosphatidylinositol-4,5-bisphosphate
- PLTP, phospholipid transfer protein
- PRRs, pattern recognition receptors
- RA, rheumatoid arthritis
- RAGE, receptor for advanced glycation end products
- Ra-LPS, Lipid A + core
- Re-LPS, $(Kdo)_2$-Lipid A

- RIG-I, retinoid acid-inducible gene I
- R-LPS, Rough LPS
- RLRs, RIG-I-like receptors
- RNS, Reactive oxygen species
- ROS, Reactive oxygen species
- RSV, respiratory syncytial virus
- SAR, Structure Activity Relationship
- SEAP, secreted embryonic alkaline phosphatase
- S-LPS, Smooth LPS
- SNP, single nucleotide polymorphism
- SPR, Surface plasmon resonance
- TAK, transforming growth factor-beta–activated kinase-1
- TANK, TRAF family member-associated NF-κ-B activator
- TBK1, TANK-binding kinase 1
- TEM, Transmission Electron Microscopy
- THP-1, Human Leukemic Monocyte Cell Line
- TICAM-1, TIR domain-containing adaptor molecule-1 (TRIF)
- TICAM-2, TIR domain-containing adaptor molecule-2 (TRAM)
- TIR, toll-interleukin-1 receptor
- TIRAP, TIR adapter protein
- TLRs, Toll-like receptors;
- TNF, Tumor Necrosis Factor
- TRAF, TNF receptor-associated factor
- TRAM, TRIF-related adapter molecule (TICAM-2)
- TRIF, TIR-domain containing adapter-inducing interferon-β (TICAM-1)
- UC, ulcerative colitis

ABSTRACT

Toll-like receptors (TLRs) are among the first receptors activated during host-pathogen interactions. They act as key mediators in the pathogen-associated molecular patterns (PAMPs) detection and are responsible for the innate and adaptive immune responses in mammal.

Belonging to this family, Toll-like receptor 4 (TLR4) is the mammalian sensor of bacterial endotoxin, lipopolysaccharide (LPS). Its activation results in the rapid triggering of pro-inflammatory processes essential for optimal host immune responses. TLR4 activation is a complex event which involves several proteins (LBP, CD14, and MD-2) and ends with the dimerization as an activated $(TLR4/MD\text{-}2/LPS)_2$ complex.

Dysregulated TLR4 activation is related to an impressively broad spectrum of disorders still lacking specific pharmacological treatment, including autoimmune disorders, chronic inflammations, allergies, asthma, infectious and central nervous system diseases, cancer, and sepsis. TLR4 modulation by small molecules of synthetic and natural origin provides access to new TLR-based therapeutics. Indeed, compounds able to block TLR4 activation (antagonists) are promising drug candidates against thee pathologies while TLR4 activating compounds (agonists) may be use as vaccines adjuvants and antitumoral agents.

The work of this PhD thesis is described in four papers. The aim of the thesis is to study the processes and requirements leading to TLR4 activation/inhibition. The first study, Chap. IX, focuses on the contribution of carbohydrates to bacterial endotoxin (lipopolysaccharide, LPS, lipooligosaccharide, LOS, and lipid A) activity and in the switch from TLR4 agonism to antagonism. In particular, the structure-activity relationship and contribution of core saccharides 3-deoxy-D-manno-octulosonic acid (Kdo) and heptosyl-2-keto-3-deoxy-octulosonate (Hep) to TLR4/MD-2 binding and activation by LPS and LOS have been investigated in detail.

This study allows the rational design of new structures of potential TLR4 modulators. These compounds were projected by computer-assisted design and their binding to MD-2 was evaluated through docking studies. A set of the most promising compounds was defined. They are composed of a glucosamine-bis-succinyl core (two carboxylate groups as phosphates bioisosteres) linked to different unsaturated and saturated fatty acid chains. The binding of the synthetic compounds to MD-2 was studied by four independent methods using functional recombinant human MD-2 protein purified. It was demonstrated that all compounds bound to MD-2 with similar affinities and inhibited, in a concentration-dependent manner, the LPS-stimulated TLR4 signaling and cytokine production in human and murine cells. Therefore, the compounds were patented (Chap. X) and the study of these compounds was pushed forward.

One compound of the panel was tested *in vivo* and resulted unable to inhibit the production of pro-inflammatory cytokines. The lack of activity was investigated and hypothesized to be due to their sequestration by serum proteins (albumin). Since the macromolecular structure of the compounds in biological media may lead to such effects, computational and cryo-TEM microscopy study of a representative of this series of amphiphilic molecules was performed. Interestingly, it displayed self-assembly property in solution with the formation of large and regular vesicles (Chap. XI). This discovery explains the sequestration by serum proteins but, more importantly, permits to think about a pharmacological use, as carrier for example.

The chapter XII details the synthesis of a new cyanine-label (Cy7N) and its bioconjugation to *E. coli* K-12 endotoxin (LOS-Cy7N) for the intracellular imaging and *in vivo* microscopy. Fluorescent LPS/LOS are fundamental molecular tools for the investigation of their distribution into the body and the understanding of receptor-dependent cellular trafficking of gram-negative bacteria endotoxins. Conjugation of fluorescent agents labelling LOS is still undocumented and should provide useful complementary information. Cy7 derivatives are known for their fluorescence in the near-infrared region providing an excellent contrast on biological samples. We explored the possibility to exploit the far-red fluorescence emission of amino-heptamethine fluorophore (Cy7N), featuring a large Stokes-shift. Dye was functionalized with a carboxyl-diethylenglycolamine to permits its bioconjugation to a phospho-ethanolamine group of LOS. The fluorophore Cy7N, featuring sulfonate side-chains, provides a good solubility in aqueous medium and the central amino substitution, while allowing a convenient bio-conjugation to LOS, confers optimal optical properties such as an important stokes shift and a strong emission in the biological transparency window, increasing the imaging contrast. It was showed that Cy7N can be excited by default filter-set of Cy5 and fluoresces into deep red spectrum for low-background imaging. The large Stoke-shift feature of Cy7N, which trespasses beyond the Cy5 emission, also permits to obtain two-colors images by using one excitation for double-labeling of two cyanine dyes. Moreover, contrarily to commercially available fluorescent LPS, the fluorescently labelled endotoxin LOS-Cy7N was purified by chromatography with a high level of chemical purity. LOS-Cy7N experiments demonstrated that LOS internalization is CD14-dependent but, by co-treatment with two types of fluorescent endotoxins, it was showed for the first time that LOS and LPS undergo different internalization speed in cells: endocytosis of LOS is much faster than LPS upon cell surface binding. LOS-Cy7N showed interesting physicochemical properties for biological media microscopy and its wider use as a tagged tool to study the role of endotoxin molecules is currently evaluated.

INTRODUCTION

I. Immunity

The immune system is a complex machinery dedicated to the body's defense against infectious organisms as well as endogenous toxins. Through a cascade of reaction, called immune response, the immune system attacks the organisms and substances that invade the body system and causes diseases. Different kind of immune systems exist for the plant,[1] the invertebrates[2] and the vertebrates.[3]

The human immune system is made up of special cells, proteins, tissues and organs (Fig. 1 and 2), that work together to protect the body, defending people against germs and microorganisms every day. In most cases, the immune system does a great job, keeping people healthy and preventing infections. But, sometimes, problems with the immune system can lead to illness and infection.

One of the important cells involved are white blood cells, also called leukocytes, which come in two basic types combining the abilities to seek out and to destroy disease-causing organisms or substances.

Leukocytes are produced or stored in many locations in the body, including the bone marrow, the spleen and the thymus. For this reason, they are called the lymphoid organs. There are also lymphoid tissue concentrations throughout the body, mainly in the form of lymph nodes, that house the leukocytes. The leukocytes circulate through the body between the organs and nodes via lymphatic vessels and blood vessels. In this way, the immune system works in a coordinated manner to monitor the body for invaders or substances that might cause problems.

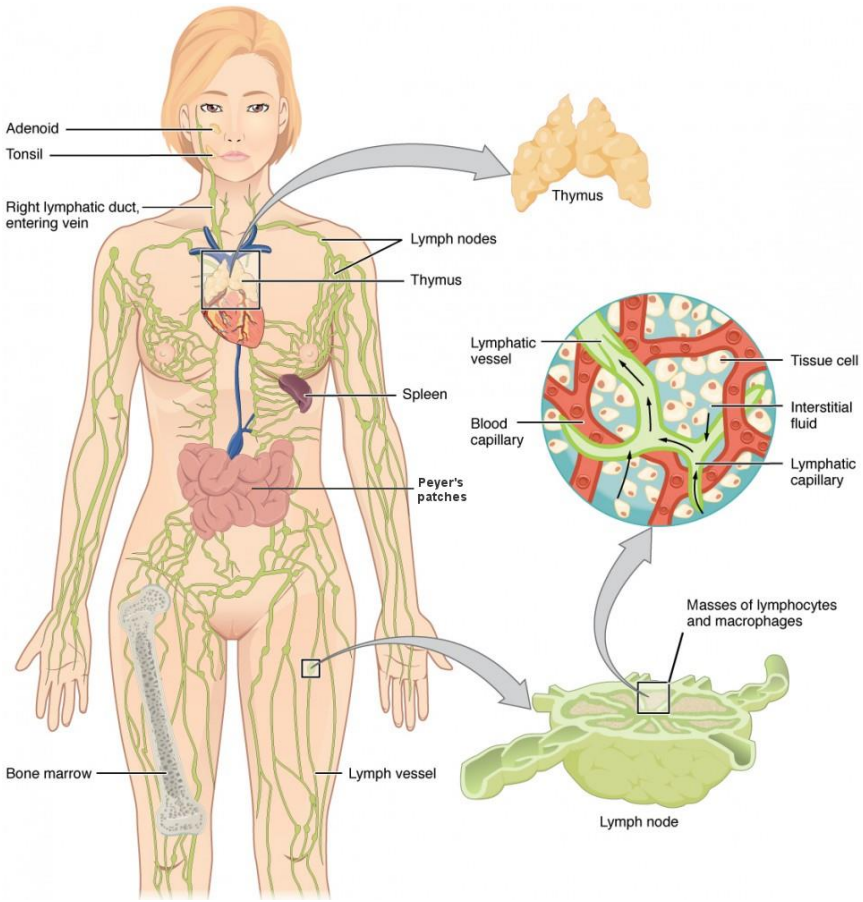

Figure 1. Lymphoid organs

The two basic types of leukocytes are phagocytes and lymphocytes. Phagocytes (neutrophil, macrophages, monocytes and dendritic cells) chew up invading organisms to destroy them. On the other hand, lymphocytes are divided in two sub-classes: B lymphocytes (seek out their targets and send defences to lock onto them) and T lymphocytes (destroy the invaders identified by B lymphocytes).

1. Adaptive and Innate immunity

The adaptive (or active) immunity is developed throughout our lives. Adaptive immunity involves the lymphocytes, mediated by B and T cells, and is developed as people are exposed to diseases or immunized against diseases through vaccination. It is characterized by immunological memory through the production of specific antibody. Therefore, adaptive immunity is slow, highly adaptable and highly specific to a given antigen.

On the other hand, innate (or natural) immunity is a type of fast general protection present and active since birth. Innate immunity includes the external barriers of the body, like the skin and mucous membranes (nose, throat, and gastrointestinal tract) which are the first line of defence

in preventing diseases from entering the body. It is not only a physical barrier, for example, the gastrointestinal tract possesses gastric acid, bile acids, digestive enzyme that are able to kill the microorganism or cleave bacterial cell walls. Specialised innate immune cells, mainly granulocytes and monocytes, work at the elimination of the pathogens by phagocytose or thanks to cytotoxic substances such as nitric oxide, cytokines and histamines.

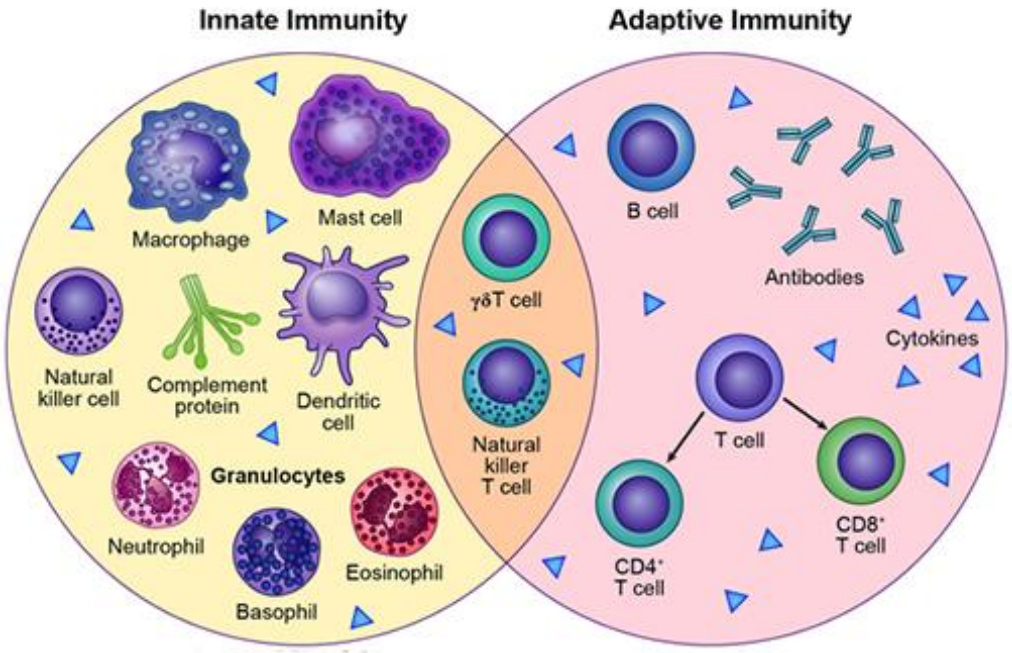

Figure 2. Innate vs adaptive players [4]

2. PAMPs, DAMPs, PRRs and Toll-like receptors

The immune strategy is based on the recognition of molecular patterns, called PAMPs (Pathogen-Associated Molecular Patterns) and DAMPs (Damage-Associated Molecular Patterns. The PAMPs come from exogenous microorganisms and can be constituted by proteins, nucleic acids, lipid-bearing molecules and carbohydrates (peptidoglycans, lipoteichoic acid or lipoproteins). On the other hand, DAMPs are cell-derived endogenous molecules that initiate and perpetuate immunity in response to trauma, ischemia and tissue damage, regardless of the presence or absence of pathogenic infection. Most PAMPs and DAMPs serve as so-called 'Signal 0s' which is the first sensing process occurring for an immunological response.[5] Detection of such molecular pattern triggers a general activation of the immune system, mainly autophagy, a conserved lysosomal degradation pathway essential for the cell survival

mechanism. It permits to eliminate most of the dangerous microorganisms before the activation of the adaptive immune system.

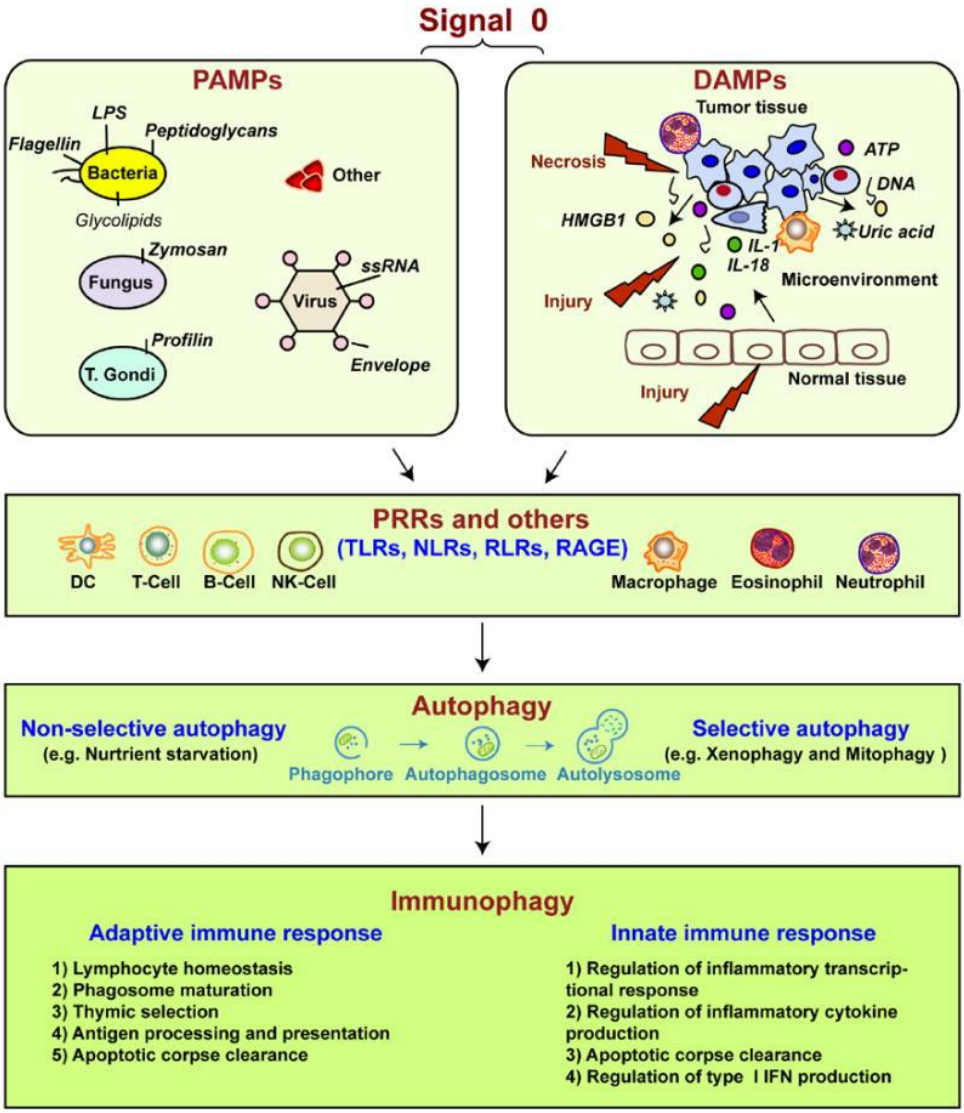

Figure 3. Signal 0s play critical roles in autophagy and immunity. Pathogen-associated molecular patterns (PAMPs) and damage-associated molecular patterns (DAMPs) serve as signal 0s, inducing autophagy and immunophagy in the emergent immune response before the later Signal 1 (antigenic peptide and major histocompatability molecules), Signal 2 (costimulatory molecules such as CD80 and CD86), both present on the surface of DCs recruited by the signal 0s. Signal 3 represents the DC provided IL-6 family cytokine expression such as IL-12 and IL-23 which promote polarization of emergent T-cell response. Signal 4 represents the integrin expression on DCs, defining the origin of the DCs and driving specialized molecules on T-cells promoting T-cell traffic to tissues.[5]

The recognition of PAMPs and DAMPs occur with specific receptors called Pattern-Recognition Receptors (PRRs). They can be divided in two major classes regarding their cytoplasmic or transmembrane localization.

Cytoplasmic PRRs are NOD-like receptors (NLR, family of ≈ 20 proteins), which mainly recognizes bacterial peptidoglycans, and retinoid acid-inducible gene I (RIG-I)-like receptors (RLR, three known proteins: RIG-I, MDA5, LGP2), which participate in the intracellular

recognition of viral double-stranded (ds) and single stranded RNA. They are succinctly described in Fig. 4 but will not be further treated since this thesis is focused on TLR4.

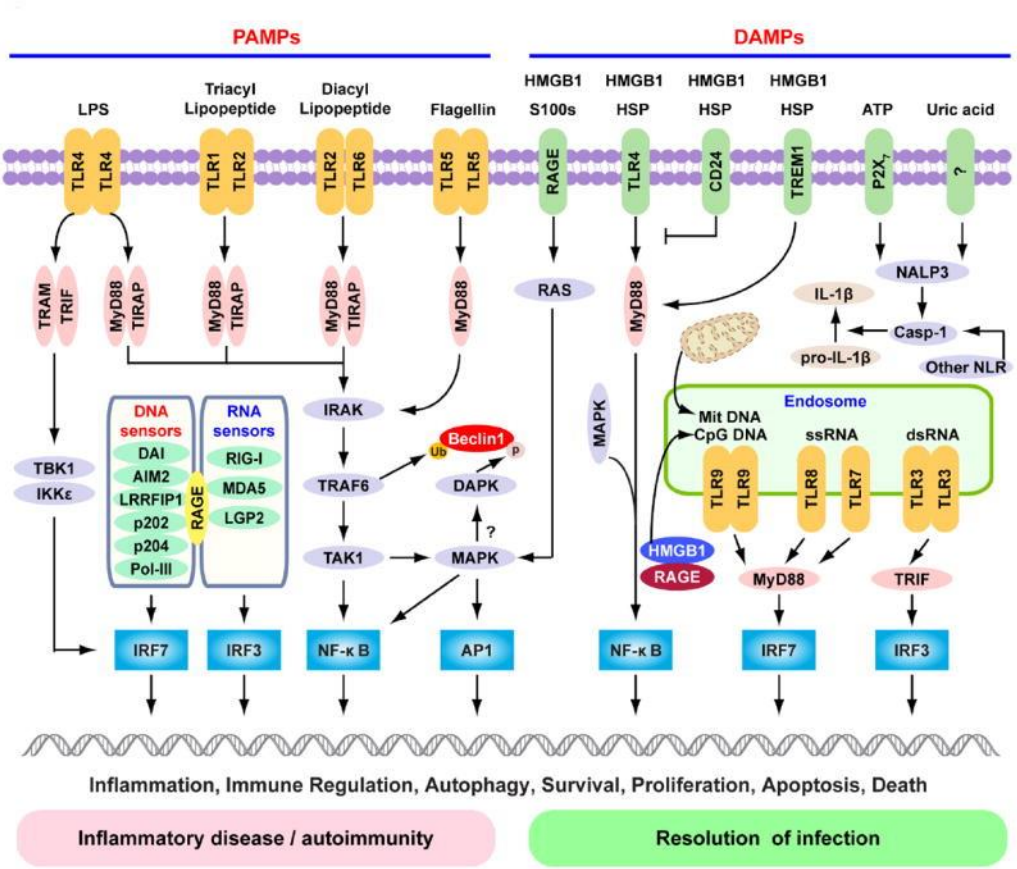

Figure 4. The role of TLRs, RLRs, and NLRs in PAMP and DAMP Signaling pathways triggered by pathogen-associated molecular pattern (PAMPs) and damage-associated molecular pattern molecules (DAMPs). Lipopolysaccharide (LPS) activates both the myeloid differentiation factor 88 (MyD88)-dependent and TIR-domain containing adapter-inducing interferon-β (TRIF)-dependent Toll-like receptor 4 (TLR4) pathways. The MyD88-dependent pathway is responsible for NF-κB and mitogen-activated protein kinase (MAPK) activation, which controls induction of proinflammatory cytokines. The TRIF-dependent pathway activates IRF3 by TANK-binding kinase 1 (TBK1)/IKKε, which is required for the induction of IFN-inducible genes. TLR1-TLR2 and TLR2-TLR6 recognize bacterial triacylated lipopeptide or diacyl lipopeptide, respectively, and recruit TIR adapter protein (TIRAP) and MyD88 at the plasma membrane to activate the MyD88- dependent pathway. TLR5 recognizes flagellin and activates the MyD88-dependent pathway. TLR3, TLR7, TLR8, and TLR9 reside in the endosome and recognize dsRNA, ssRNA, CpG DNA, or mitochondrial DNA (Mit DNA), respectively. They recruit TRIF or MyD88 to activate the IRF3 or IRF7 pathway. All immunogenic nucleic acids bind indicated cytosolic DNA sensors or RNA sensors, including retinoid acid-inducible gene I (RIG-I)-like receptors (RLRs), which are required for subsequent recognition by specific pattern recognition receptors to activate innate immune responses. DAMPs such as HMGB1, S100 proteins (S100s), and heat shock proteins (HSPs) recognize the receptor for advanced glycation end products (RAGE), TLR4, or trigger the receptor expressed on myeloid cells-1 (TREM-1) and activate the MyD88-MAPK-NF-κB pathway. HMGB1 and RAGE activate the TLR9-MyD88 dependent pathway, which contributes to autoimmune pathogenesis. CD24 is a negative receptor to inhibit the DAMP-induced TLR4 pathway. ATP binding of the P2X7 receptor and uric acid, as well as asbestos and alum, increase activation of caspase-1 by the NALP3 inflammasome and other nucleotide-binding oligomerization domain (NOD)-like receptors (NLRs) to promote secretion of IL-1β and IL-18. PAMP and DAMP-mediated signaling and induction of an innate immune response usually results in resolution of infection, but may also cause chronic inflammation or autoimmunity by altering various cell death and survival mechanisms.[5]

The membrane-bound PRRs are divided in two types: the C-type lectin receptors (CLRs) and the Toll-like receptors (TLRs).

The CLRs comprise a large family of receptors that bind to carbohydrates in a calcium-dependent manner. The lectin activity of these receptors is mediated by conserved carbohydrate-recognition domains (CRDs). Based on their molecular structure, two groups of membrane-bound CLRs and a group of soluble CLRs can be distinguished. For example, DEC-205 and the macrophage mannose receptor (MMR), important in antigen uptake, are type I transmembrane proteins containing several CRDs or CRD-like domains. Type II transmembrane CLRs typically carry a single CRD domain and include Dectin-1, Dectin-2, macrophage-inducible C-type lectin (Mincle), the dendritic cell-specific ICAM3-grabbing nonintegrin (DC-SIGN), and DC NK lectin group receptor-1 (DNGR-1). These receptors are mainly involved in fungal recognition and are presented in Fig. 5.

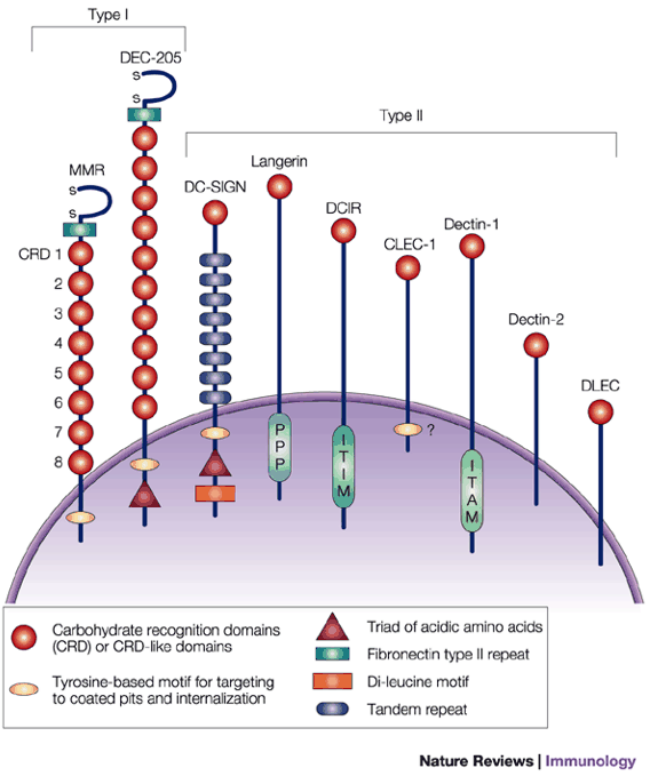

Figure 5. C-type lectins and lectin-like proteins are produced by dendritic and Langerhans cells

The Toll-like receptors were the first PRRs identified in mammals and to date are the best characterized. They initiate key innate inflammatory responses and shape adaptive immunity. All TLRs (10 in humans and 12 in mice) are type I transmembrane proteins characterized by an extracellular leucine-rich domain and a cytoplasmic tail. They recognize diverse PAMPs from bacteria, fungi, parasites and viruses, including lipid-based bacterial cell wall components such as lipopolysaccharide (LPS) and lipopeptides, microbial protein components such as flagellin,

nucleic acids such as single-stranded or double-stranded RNA and CpG DNA. They also react to certain damage-associated molecular patterns (DAMPs) from endogenous cells and the environment (Fig. 4).

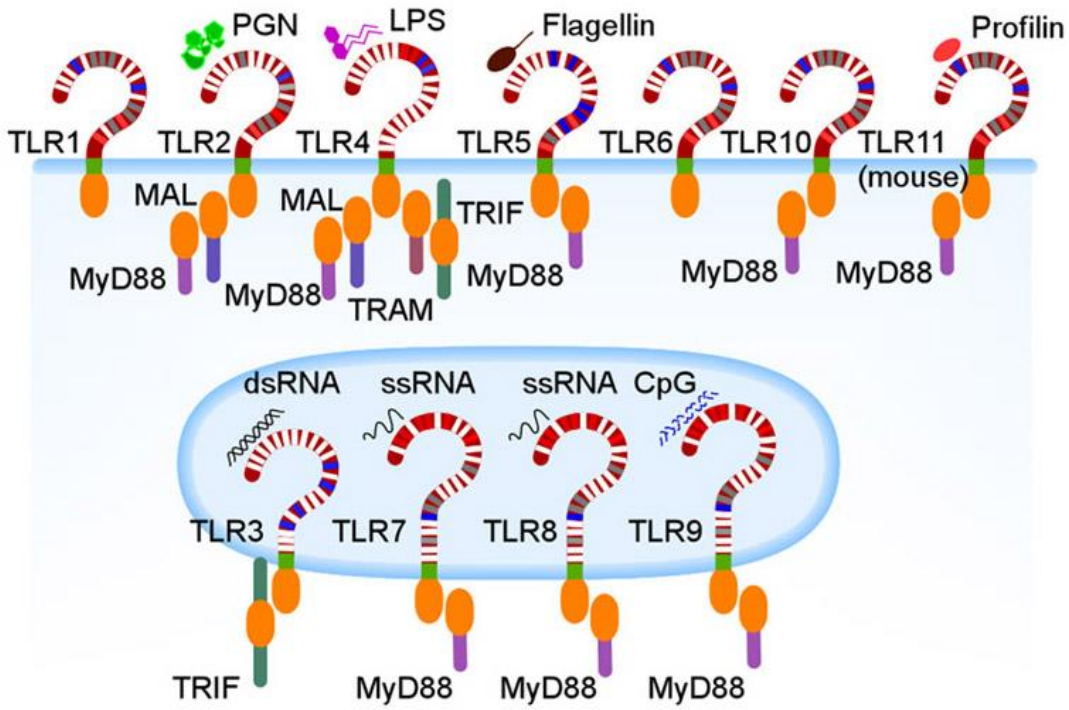

Figure 6. Toll-like receptors (TLRs) family, their ligands and adaptor proteins

.

TLRs are expressed on the cell surface and in endosomes (Fig. 6, 7 and Table 1), their activation by ligands lead to the recruitment of downstream adaptor and signalling molecules such as Myeloid Differentiation primary response 88 protein (MyD88) and/or TIR domain-containing adaptor protein inducing IFNβ (TRIF). TLRs activation results in the up-regulation of pro-inflammatory mediators that favours host immune responses (described in Chap. III).

TLRs are type I transmembrane glycosylated receptor proteins, all of them are composed of a highly variable extracellular leucine-rich repeat (LRR) ectodomain (purple and white portions in Fig. 6), a transmembrane portion (green portions in Fig. 6) and a highly conserved region in the short intracellular tail, called toll-interleukin-1 receptor (TIR) domain (orange portion in Fig. 6). The LRRs motifs of the TLRs ectodomain commonly fold together to form a solenoid domain, resulting in a characteristic horseshoe shape. Ten TLRs have been described in humans and each of them detect a specific PAMP: TLR2 associated with TLR1 or TLR6 sense lipopeptides, TLR3 is specific of viral dsRNA, TLR4 recognise lipopolysaccharide, TLR5 sense bacterial flagellin, TLRs 7 and 8 are specific of viral ssRNA and TLR9 recognise CpG-rich non-methylated DNA (Table 1).[6,7]

Receptor	Cellular localization	Microbial component(s)	Origin(s)
TLRs			
TLR1/TLR2	Cell surface	Triacyl lipopeptides	Bacteria
TLR2/TLR6	Cell surface	Diacyl lipopeptides	*Mycoplasma*
		Lipoteichoic acid	Gram-positive bacteria
TLR2	Cell surface	Lipoproteins	Various pathogens
		Peptidoglycan	Gram-positive and -negative bacteria
		Lipoarabinomannan	Mycobacteria
		Porins	*Neisseria*
		Envelope glycoproteins	Viruses (e.g., measles virus, HSV, cytomegalovirus)
		GPI-mucin	Protozoa
		Phospholipomannan	*Candida*
		Zymosan	Fungi
		β-Glycan	Fungi
TLR3	Cell surface/endosomes	dsRNA	Viruses
TLR4	Cell surface	LPS	Gram-negative bacteria
		Envelope glycoproteins	Viruses (e.g., RSV)
		Glycoinositolphospholipids	Protozoa
		Mannan	*Candida*
		HSP70	Host
TLR5	Cell surface	Flagellin	Flagellated bacteria
TLR7/8	Endosome	ssRNA	RNA viruses
TLR9	Endosome	CpG DNA	Viruses, bacteria, protozoa
RLRs			
RIG-I	Cytoplasm	dsRNA (short), 5′-triphosphate RNA	Viruses (e.g., influenza A virus, HCV, RSV)
MDA5	Cytoplasm	dsRNA (long)	Viruses (picorna- and noroviruses)
NLRs			
NOD1	Cytoplasm	Diaminopimelic acid	Gram-negative bacteria
NOD2	Cytoplasm	MDP	Gram-positive and -negative bacteria
NALP1	Cytoplasm	MDP	Gram-positive and -negative bacteria
NALP3	Cytoplasm	ATP, uric acid crystals, RNA, DNA, MDP	Viruses, bacteria, and host
Miscellaneous			
DAI	Cytoplasm	DNA	DNA viruses, intracellular bacteria
AIM2	Cytoplasm	DNA	DNA viruses
PKR	Cytoplasm	dsRNA, 5′-triphosphate RNA	Viruses

Table 1. Recognition of microbial components by PRRs

TLR10, not expressed in mice, is the only human TLR with unknown ligands and biological function. However, recent studies revealed that TLR10 is a modulatory PRR with mainly inhibitory and anti-inflammatory properties.[8] TLR11, 12 and 13 are present only in mouse, both TLR11 and 12 recognise profilin, a PAMP involved in many process of *toxoplasma* infections, while TLR13 is known to sense bacterial RNA (bRNA).[9,10] TLRs can be classified into two subgroups based on their cell localization: TLR1, 2, 4, 5, 6, and 10 are mainly present on the cell surface while TLR3, 7, 8, 9, 11, 12, and 13 are intracellular, localized within the membrane of endosomes (Table 1 and Figure 7).[11]

TLRs ligands generally derive from pathogens, however, during “sterile” inflammation, autoimmune syndromes and hypertension, TLRs are activated by endogenous signal molecules named DAMPs derived from damaged or necrotic tissues.[12,13] These molecules are extracellular matrix components (e.g., fragments of hyaluronan), plasma membrane, nuclear, and cytosolic

proteins (e.g., high-mobility group box protein 1), and elements of damaged/fragmented organelles (e.g., mitochondrial DNA).[14]

Multiple signalling pathways are activated by TLRs upon stimuli and some of these pathways are unique. TLR triggering lead to the up-regulation of pro-inflammatory mediators like cytokines, chemokines, and adhesion molecules, either through a MyD88-dependent pathway (TLR1, 2, 4, 5, 6, 7, 8, and 9) or a MyD88-independent (TRIF-dependent) pathway (TLR3 and TLR4).[15,16] The pathway activated depends on the ligand and on the adaptor molecules who get recruited to associate with the respective TLR cytosolic TIR domain. The TIR domain is the actor of the interactions between homo- and heterodimeric TLR subunits and recruit the cytosolic adapter proteins necessary to initiate the downstream signalling cascades. The TIR domain is not only shared between TLRs but is also used by other receptors such as the IL-1R family.[17] The major consequence resulting from the activation of one pathway or the other, upon TLR signalling, is the induction of pro-inflammatory cytokines (TNF-α and IL) with the MyD88-dependent pathway while, in the case of the endosomal TLRs, the induction of type I IFN (Fig. 7).[18]

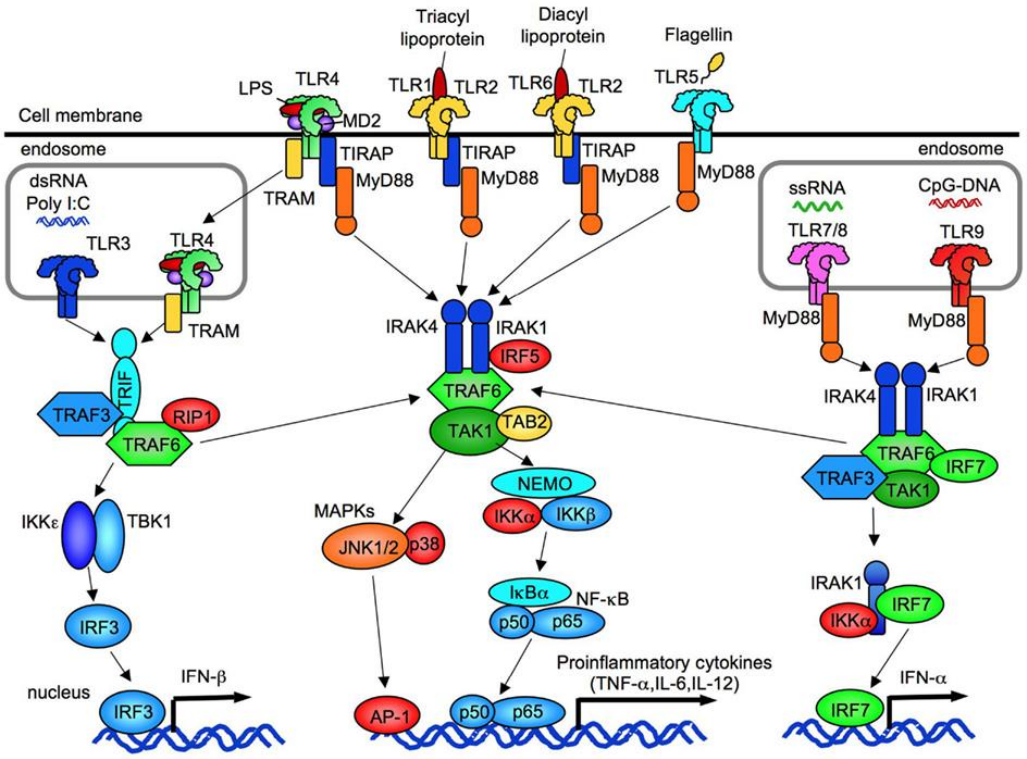

Figure 7. The overview of TLRs signalling. TLR1, 2, 4, 5, and 6 are expressed on cell membrane while TLR3, 7/8, and 9 are expressed in endosomes. All TLRs, expect for TLR3, activate MyD88-dependent pathway to induce NF-κB and p38/JNK activation. TLR2 and TLR4 signalling require TIRAP and MyD88. TLR3 requires TRIF to activate TBK1/IKKε. After TLR4 internalization, TLR4 signalling activates the TRAM/TRIF-dependent pathway. The TLR3/4-dependent TRIF-dependent signalling induces IRF3 activation and IFN-β production. TLR7/8 and TLR9 induce IFN-α production through IRF7.[18]

The adaptors recruited are TIR domain-containing proteins: MyD88, TIR domain-containing adaptor protein (TIRAP), MYD88-adaptor-like protein (MAL), Toll/IL-1 receptor (TIR)-domain containing adapter-inducing IFN-β (TRIF), and TRIF-related adaptor molecule (TRAM). After the ligand-induced TLRs dimerization, the cytosolic TIR domain of TLRs may either engage MyD88 and MAL (MyD88-dependent pathway), or TRIF and TRAM adaptors (TRIF-dependent pathway) (Fig. 6 and 7).[18]

TLR4 possesses a dual activation mechanism as it can be internalised from the plasma membrane to endosomes which lead to switch the signalling pathway from MyD88 to TRIF (Figure 8).[19,20] TLR4 is the only TLR that is able to produce a signal through two distinct pathways. It will be extensively described in the next chapters.

3. TLR4

TLR4 is fundamental for the host immunity as it is involved in many key functions. As mentioned above, its main role is to sense and respond to minute amounts (picomolar) of LPS which is generally considered as the most potent immunostimulating PAMP. Furthermore, TLR4 strongly promotes the recruitment of other immune cells to the infection site to efficiently neutralize the threat.[21] In this respect, TLR4 is a link between innate and adaptive immunity.

TLR4 is the cell sensor dedicated to endotoxin (LPS and LOS), the major components of the outer leaflet of Gram-negative bacteria's outer membrane. TLR4 plays a crucial role in initiating the innate immune response, it trigger the production and secretion of pro-inflammatory cytokines.[22] TLR4 can also be activated by some endogenous DAMPs such as heat-shock protein 70, fibronectin, oxidized phospholipids, and other molecules released by the host in certain situation of danger.[14] Located on the plasma membrane of the main cells of innate immunity, it is highly expressed by monocytes, macrophages and dendritic cells, but is also present in lymphocytes and epithelial cells.[23,24]

TLR4 is part of the Leucine-Rich Repeat (LRR) family proteins, defined by many copies of LRR modules. An individual LRR module is 20~30 amino acids long and contains a highly conserved "LxxLxLxxN" motif.[25,26] This conserved part of the module forms a strand which stack in parallel with the neighboring LRR modules, forming a large sheet. Thus, the overall structures of LRR-family proteins share a characteristic horseshoe shape.[27] The leucine in the conserved motif point inside forming a hydrophobic core while the variable "x" residues are exposed to the solvent area. Some of these variable residues play functional roles by interacting with ligands. The LRR modules are capped by two specialized modules, LRRNT and LRRCT,

at the N- and C-terminal ends respectively. The LRRNT and LRRCT modules do not have LRR motifs in their sequences, instead, they often have multiple di-sulfur bridges that stabilize the structures of these special modules.[25,26,28] LRR-family proteins play diverse physiological roles in the cell by interacting mostly with protein ligands. The most frequent site for protein interaction is the concave side of the protein.

TLR4 is a type I transmembrane protein composed of 839 amino acids: 608 residues belong to the extracellular domain (ectodomain), 44 to the transmembrane helical domain and 187 residues compose the cytosolic tail.[29,30] TLR4 ectodomain is formed of tandem copies of the LRR motif which give the characteristic horseshoe-like structure of TLR4 ectodomain.[31,32] The concave surface is composed by parallel β-strands and the convex surface is formed by loops (Figure 8).[33] TLR4 ectodomain, on his own, does not bind LPS directly, it needs an adaptor protein so-called Myeloid Differentiation factor 2 (MD-2) to bind LPS.[34] MD-2 is a 22 kDa protein, anchored by several hydrogen bonds to the lateral and concave surface of the TLR4 ectodomain, depicted as A and B patch in Fig. 8 and representing the residues from the LRR2 to the LRR10.[29]

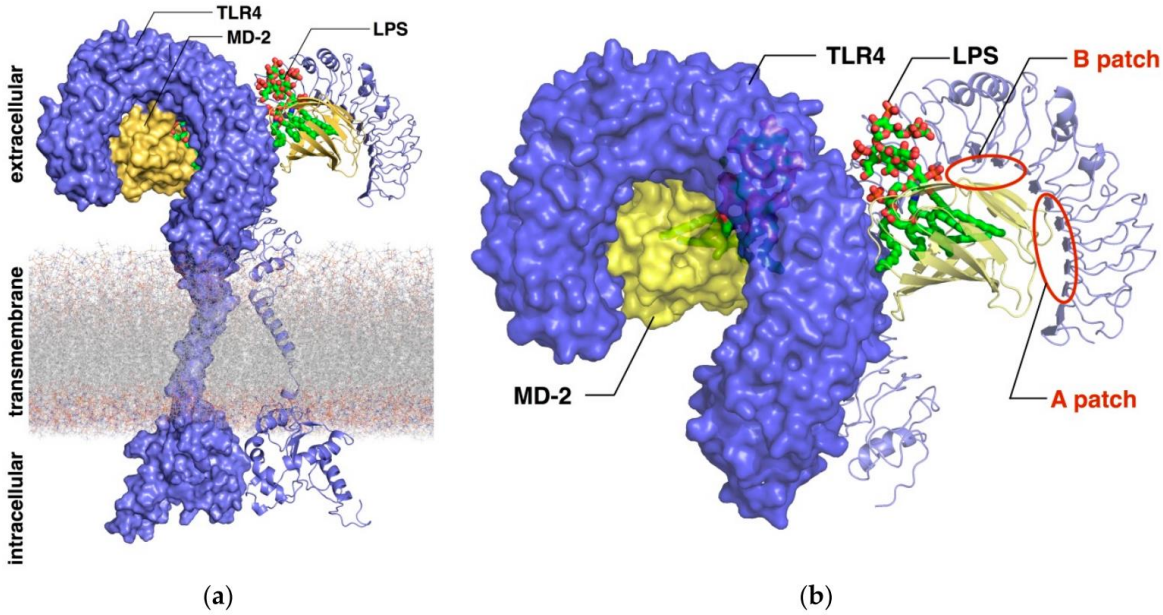

Figure 8. Representation of the 3D structure of TLR4/MD-2/LPS (**a**) Large-scale representation showing the intracellular, transmembrane and extracellular domains of TLR4/MD-2 in complex with *E. coli* LPS. 3D Structures correspond to the X-ray crystallographic structure for the extracellular domain (PDB ID 3FXI) and homology modeling for the transmembrane and intracellular domains. (**b**) Close-up look at the TLR4 extracellular domain (purple) along with MD-2 (yellow) and LPS (CPK colors with carbon atoms in green) from PDB ID 3FXI.[33]

MD-2 is essential for LPS recognition since it is the actual binder of LPS. Furthermore, no physiological TLR4 activation has been observed in the absence of MD-2.[29]

II. Inflammation

Inflammation is, generally speaking, the body's immune system's response to stimulus. This stimulus can either be bacteria colonizing a wound or a splinter piercing a finger, in most cases. inflammation happens when the immune system fights against something that may turn out to be harmful.

Inflammations may have many different causes and the most commons are pathogens (germs, bacteria, viruses or fungi), external injuries (like scrapes or foreign objects) and effects of chemicals or radiation.

An acute inflammation may be indicated by the following five signs: redness, heat, swelling, pain, loss of function (e.g. inflamed limb can no longer be moved properly). Not all five signs occur in every inflammation, some inflammations occur "silently" and do not cause any symptoms. This means that an inflammation does not start when a wound has been infected by bacteria, festers, or heals poorly, but already as the body is trying to fight against the harmful stimulus or a viral infection. If the inflammation is severe, it may cause general reactions in the body. This may include the signs and symptoms like a change in the blood such as an increased number of defence cells and general symptoms of feeling sick, exhausted and feverish. These symptoms are a sign that the immunes defences are very active and need a lot of energy (it may lack for other activities). If the rate of metabolism is higher due to a fever, even more defence substances and cells can be produced. A highly dangerous complication of an inflammation is called sepsis (between six and nine million deaths worldwide every year). It may occur if bacteria multiply quickly in a localised part of the body and then, suddenly, enter into the bloodstream in large quantities. It happens if the body fails in fighting the inflammation locally, if the pathogens are very aggressive or if the immune system is severely weakened.

As described before, many different immune cells can take part in an inflammation. They release different substances: the inflammatory mediators including the tissue hormones bradykinin and histamines. They trigger the expansion of narrow blood vessels in the tissue allowing more blood to reach the injured tissue. For this reason, the inflamed area turns red and becomes hot. More defence cells are also brought along with the blood to the injured tissues to help with the healing process. The inflammatory mediators permit also to increase the permeability of the narrow vessels so that more defence cells can enter into the affected tissue. Furthermore, the defence cells carry more fluid into the inflamed tissue which is why it often swells up.

The mucous membranes also release more fluid during inflammation. And those secretions can help to quickly flush the viruses out of the body.

An inflammation is not always a helpful response of the body. In autoimmune diseases the immune system fights against its own cells by mistake, causing harmful inflammatory responses. These include, for example: rheumatoid arthritis (the joints throughout the body are permanently inflamed), psoriasis (a chronic skin disease), inflammations of the bowel (like Crohn's disease or ulcerative colitis). These diseases are called chronic inflammatory diseases and can last for years or even a lifetime with very different degrees of severity and activity.

1. Gram-positive and Gram-negative bacteria

Bacteria is the most common and widespread human pathogens responsible of inflammation. Of all the different classification systems, the Gram stain is the preferred method used.[35,36] Developed by Hans Christian Joachim Gram in 1884, this protocol permits to classify them either as Gram-positive or Gram-negative bacteria, based on their differential staining properties and morphology. Cell envelope of Gram-positive bacteria possesses a single membrane and a thick layer of peptidoglycans known as cell wall (Fig. 9). On the other hand, Gram-negative bacteria's cell envelope is made up of two distinct membranes, the inner and the outer membrane, that enclose a region known as periplasmic space, a gel-like matrix which has an important function since it acts as a buffer layer between the external environment and the interior, it is essential for the survival and operation of the bacterium. The cell wall of Gram-positive bacteria membrane are two to eight times as thick as the Gram-negative cell wall.

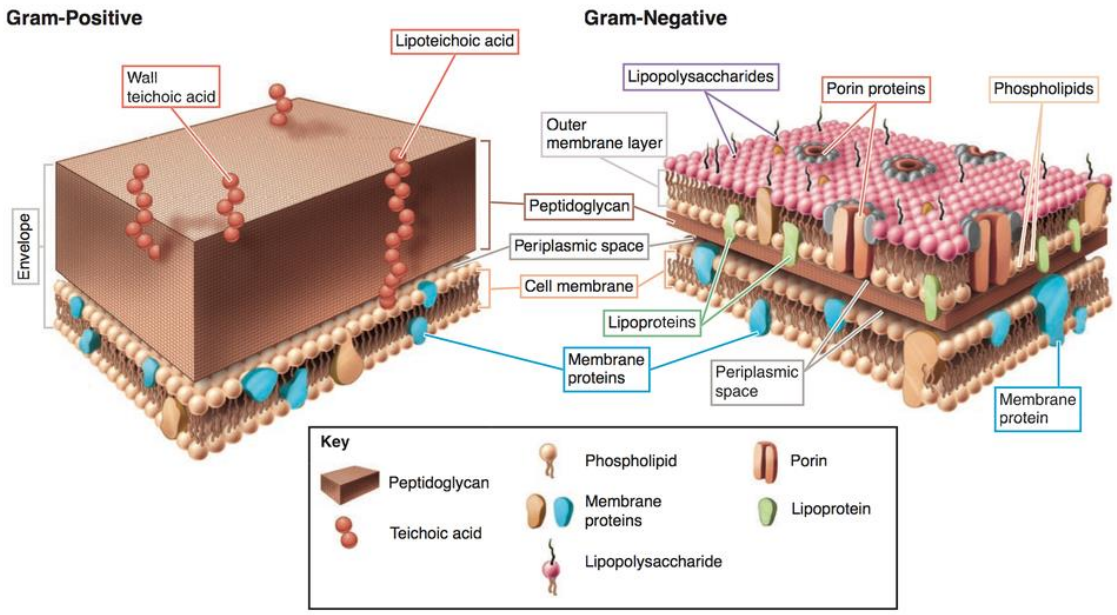

Figure 9. Envelope of Gram-positive vs Gram-negative bacteria

The Gram staining method uses iodine and crystal violet, they precipitate in the thickened cell wall of "Gram-positive" bacteria and are not eluted during alcohol washes. On the contrary, the "Gram-negative" bacteria, which present a thin peptidoglycan layer, do not fix the crystal violet which is readily eluted. It allows Gram-negative bacteria to stain red and Gram-positive bacteria to stain blue-purple Therefore, bacteria can be distinguished based on their morphology and staining properties.[35]

Bacterial membranes are composed by 40% of phospholipids and 60% of proteins. In the membrane of Gram-positive bacteria and in the inner membrane of Gram-negative bacteria, phospholipids are arranged evenly on either leaflet (Fig. 9). Contrariwise, the outer membrane of Gram-negative bacteria is asymmetrically distributed. Most of the phospholipids are located at the inner leaflet of the membrane while the outer leaflet is mainly constituted by a glycolipid termed lipopolysaccharide (LPS), beside some phospholipids and proteins (Fig. 9).[37]

2. Lipopolysaccharide (LPS, LOS and lipid A) in inflammation

As previously described, lipopolysaccharide (LPS) is the main component of the outer-leaflet of the outer-membrane of Gram-negatives bacteria including commensal and human pathogenic bacterial species. It guarantees the viability and survival of bacteria, contributing to the correct assembly of the outer membrane. Moreover, LPS provides an efficient barrier towards a large pool of molecules, including antibiotics, detergents and metals. The low fluidity, due to the highly ordered structure of the LPS monolayer act as an impervious barrier and protect the bacteria from the surrounding dangers.[38]

Therefore, thanks to the evolutionary process, LPS is a potent elicitor of the immune system and a marker for the detection of bacterial pathogen invasion. Its detection initiates the immunological response leading to inflammation and in extreme cases septic shock.

LPS is a heterogeneous population of extremely heat-stable amphiphilic molecules sharing the same general structure (Fig. 10). It is composed by a poly- or oligosaccharide chain named O-Antigen (repeated carbohydrate units, highly variable) covalently linked to the core region (constant oligosaccharide portion composed of usual and unusual carbohydrates) itself bound to lipid A (phospholipidic portion).

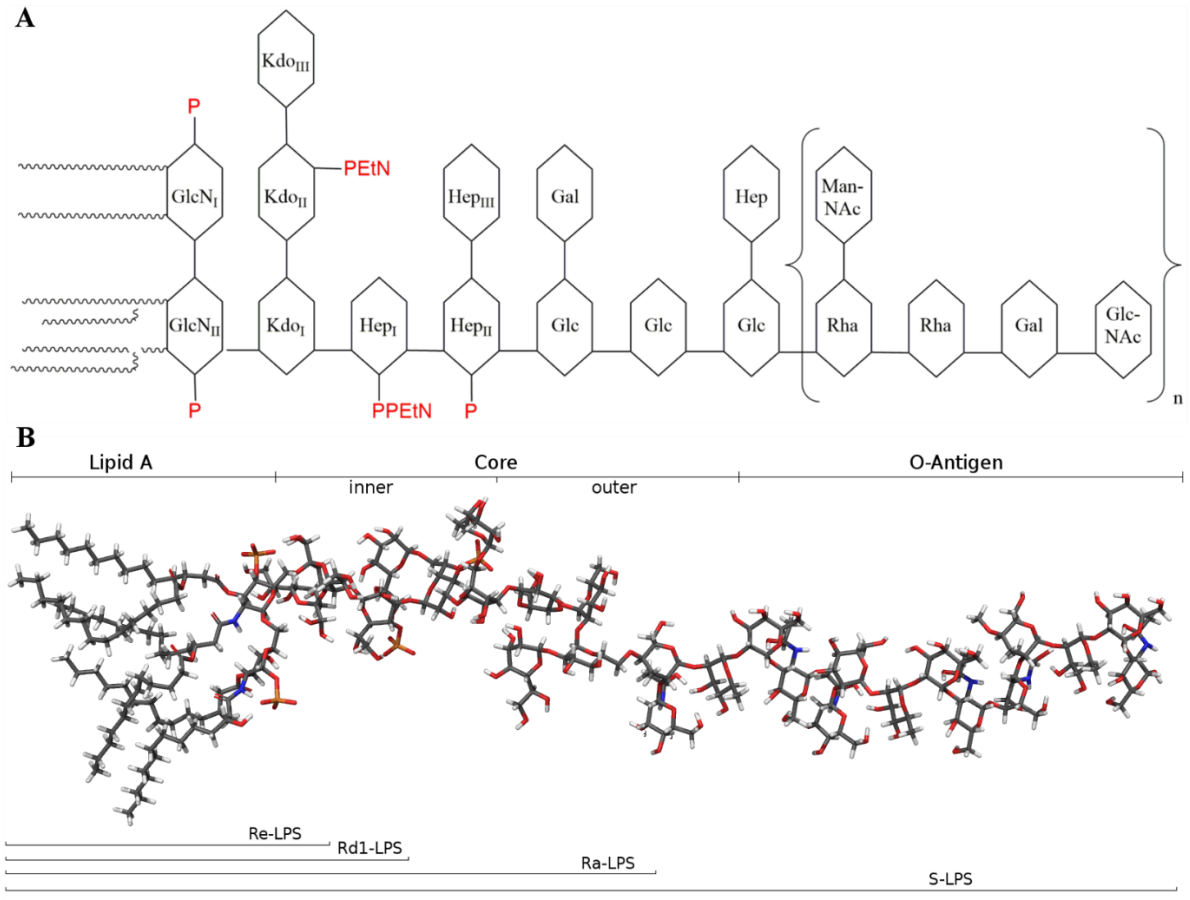

Figure 10. Two diverse representations of *E. coli* (K-12) LPS (**A**) Schematic structure of *E. Coli* LPS; O-Antigen is extremely variable and gives serological specificity to the different LPS variants. The core region is more conserved than O-chain and is divided in outer and inner core. The outer core contains common sugars like hexoses and hexosamines, while the inner core is highly conserved and composed of unusual sugars such as kdo and heptose. The di-glucosamine backbone bounded to fatty acid chains (Lipid A) is the most conserved portion of the LPS and the number and length of acyl chains are crucial determinants for endotoxicity. (**B**) 3D structure of *E. Coli* LPS: They can be classyfied into Smooth-LPS (S-LPS) if the O-Antigen is present and Rough-LPS (R-LPS or LOS) when O-Antigen is lacking. Shorter versions are also founded in nature and called Ra-LPS when LPS is composed of lipid A and the oligosaccharide core, Rd1-LPS when LPS ic composed of lipid A and the inner core, Re-LPS is the shorter version in which lipid A is linked to two or three Kdo carbohydrates.

In most Gram-negative bacteria, the O-antigen consists of up to 50 repeating oligosaccharide units formed by 2 to 8 monosaccharide moieties. In most of the LPS structures, the O-antigen is characterized by an extremely high structural variability even within a given bacterial strain.[39] The core region is more conserved than O-antigen and is divided in outer and inner core. The outer core typically consists of common hexose sugars (glucose, galactose, N-acetyl galactosamine and N-acetyl glucosamine) and is generally more variable than the inner core.

The inner core is characterised by more unusual sugars, one to three heptose bound to one to three 3-deoxy-D-manno-oct-2 ulosonic acid (Kdo) linked via an α-(2-6) linkage to the distal GlcN of lipid A. The later of these is seen in almost every LPS looked at to date, being α-bound to the carbohydrate backbone of lipid A in every case. The only exceptions yet seen are

Acinetobacter and *Burkholderia cepacia* in which LPS employ the alternative 2-keto-D-glycero-D-talo-octonic acid (Ko) in its place. The bond between the lipid A and this first Kdo residue is normally very acid labile (at pH < 4.4) which allows an easy release of the core (and with it the O-antigen) from the lipid A.[21, 38, 39]

Lipid A is considered as the conserved primary immunoreactive part of LPS, because it is the smallest LPS unit effectively detected by TLR4 and able to trigger a potent inflammatory response (pharmacophoric part of LPS).[38,42] Most of lipid A are composed by a central di-glucosamine backbone β-D-GlcN-(1-6)-α-D-GlcN. *Campylobacter jejuni* LPS is the notable exception to this rule, in which the GlcN II is replaced by the related molecule 2,3-diamino-2,3-dideoxy-D-glucose (GlcN3N).[43] The disaccharide backbone carries two phosphoryl groups (at positions 1 and 4') and both phosphates can be further substituted with groups such as phosphate, ethanolamine, ethanolamine phosphate, ethanolamine diphosphate, GlcN, 4-amino-4-deoxy-L-arabino- pyranose.[42] To this structure are attached up to four acyl chains by ester or amide linkage. These chains can then in turn be substituted by further fatty acids to provide LPS molecules with up to seven acyl substituents. The acylation state vary quite considerably between species in nature, number, length, order and saturation.[44] Lipophilic chains can be attached to the lipid A backbone either symmetrically (3 + 3, *Neisseria meningitidis*) or asymmetrically (4 + 2, *E. coli*). Unsaturated fatty acids are rarely seen in lipid A but have been reported for *Rhodobacter sphaeroides* and *R. capsulatus* LPS as well as *enterobacteriaceae* grown at low temperature.[45]

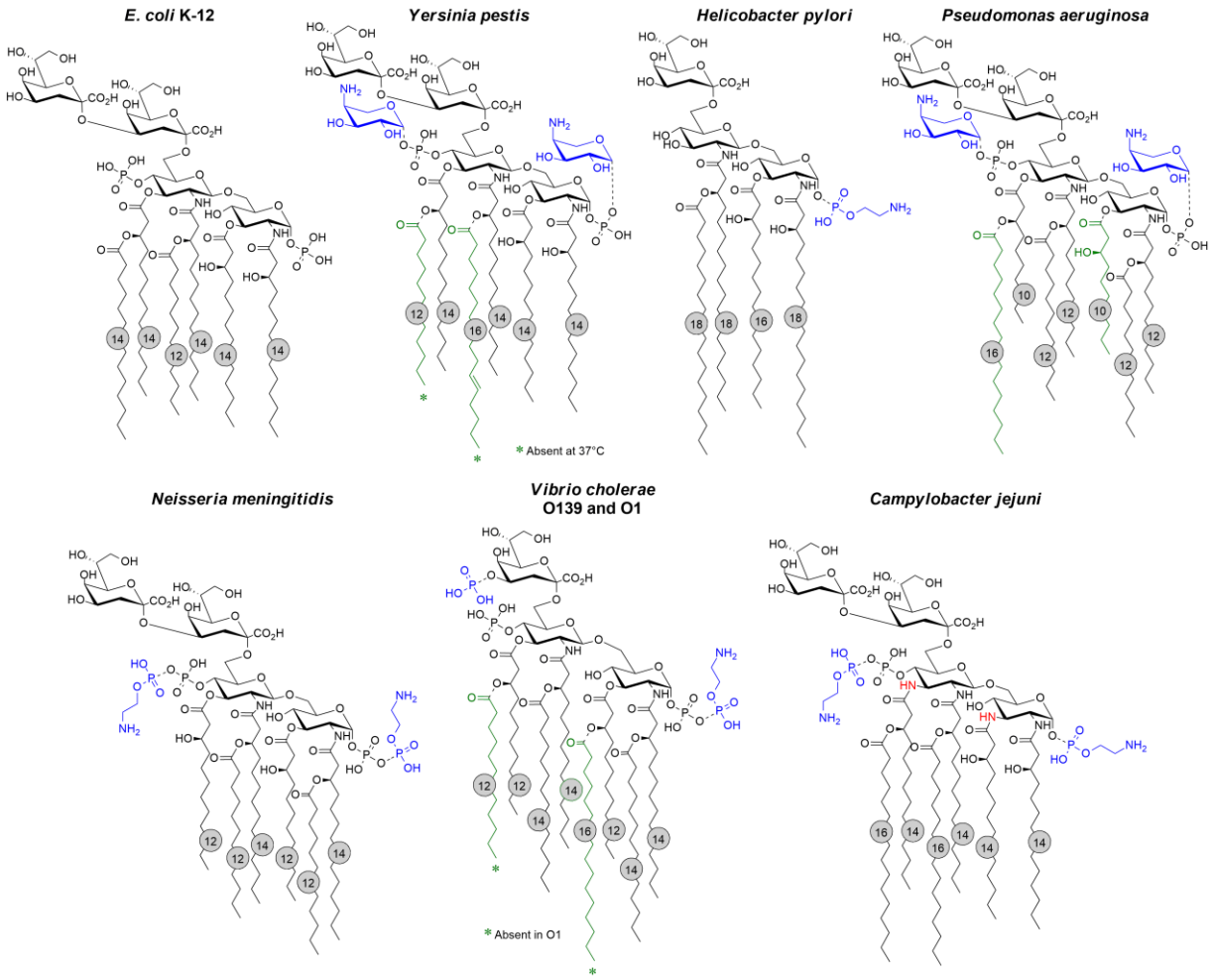

Figure 11. Structural diversity of endotoxin found in pathogenic bacteria The Re-LPS structures of several human pathogens are compared to *E. Coli* K-12. Partial covalent modifications are indicated with blue color for the hydrophylic groups and green for the hydrophobic groups. The length of each fatty acyl chain is indicated by the enclosed circles.

It is possible though not yet proven that this helps the bacteria regulate membrane fluidity. The acylation pattern is highly linked to the biological activity of the compounds and will be discussed further in Chap. VI.

The oligo/polysaccharide chains, covalently linked to the lipid A anchor, protrude in the extracellular compartment mediating many host-bacterium interactions including colonization, adhesion, virulence and symbiosis.[38] LPS is among the most potent pro-inflammatory and immunostimulating molecule. Its presence is a strong indicator of Gram-negative bacteria infections for many eukaryotes.

The amphiphilic properties of LPS allows it to aggregate with a low sub-micromolar/nanomolar values of critical micellar concentration (CMC) in aqueous environment. The critical aggregate concentration (CAC) of some LPS serotypes have been reported in literature: *E. coli* 0111:B4 (22 μM), *S.minnesota* wt (11 μM), *S.minnesota* Re 595

(4 μM).[46] More recent studies highlight that temperature is an important factor for the aggregation: differential scanning calorimetry of *E. coli* Re-LPS suspensions showed a gel-to-liquid crystalline phase transition at 36.4 °C (Tm). Its nominal critical aggregation concentration, determined by dynamic light scattering, was found to be 41.2 ± 1.6 nM below the Tm (25 °C), but only 8.1 ± 0.3 nM above the Tm (37 °C).[47]

Therefore, it aggregates in the concentration range relevant for biological responses. The issue of the biologically active unit of endotoxins, whether as large or small aggregates, or monomers, has been amply debated in the literature and will be discussed further.

III. TLR4 recognition process and structure of the adaptor proteins

The lipid A recognition is a complex procedure and depends on the coordinated action of three adaptor proteins that work together to initiate the TLR4-mediated signalling (Fig. 12).

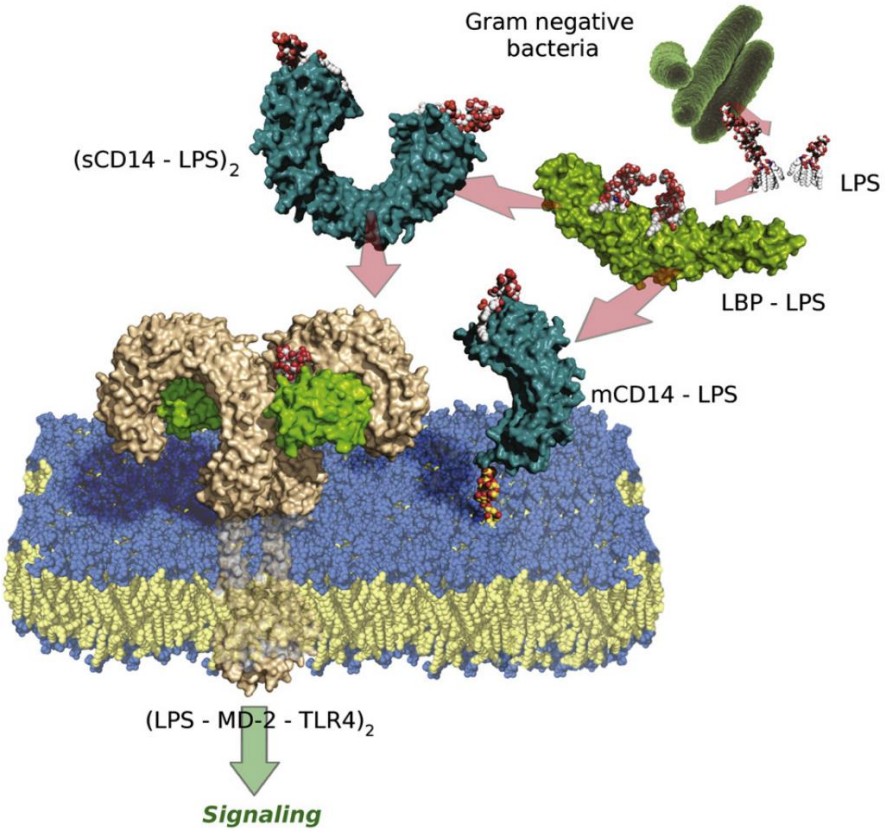

Figure 12. The LPS transport chain and signal amplification: from LPS aggregates to the (TLR4-MD-2-LPS)$_2$ activated complex. In the body, LPS are extracted from bacteria or aggregates named Endotoxin. The LPS Binding Protein (LBP) extract a monomer and transfer it to the cluster of differentiation 14 (CD14) which, in turn, present LPS to the heterodimer (TLR4/MD-2). Two TLR4/MD-2/LPS complexes are then associated and it triggers the TLR4-dependent pro-inflammatory pathway. Picture from PDB ID: 3FXI (for TLR4·MD-2 complex), 1O77 (for the TIR domain of TLR4), 2OBD and 1BPI (for LBP, 1WWL (for CD14) and 1QFG (for LPS).

As seen before, LPS is part of the outer membrane of Gram-negative bacteria, however, it can also be released in the extracellular compartment. *In vivo*, Gram-negative bacteria release minute amounts of endotoxin while growing. It is known that small amounts of endotoxin may be released in a soluble form by young cultures grown in the laboratory. But for the most part, endotoxins remain associated with the cell wall until disintegration of the organisms. An efficient sensing system is therefore needed to detect this low amount of endotoxin. In a physiological environment, LPS spontaneously forms aggregates or micelles due to its amphiphilic nature.

1. Lipid Binding Protein (LBP)

Multimeric clusters of LPS are extracted from bacterial membranes or from the vesicles released from them by a serum glycoprotein known as the lipopolysaccharide binding protein (LBP).[48] LBP is an acute response protein with a transient expression: increasing by hundreds of times shortly after infection. LBP is a boomerang-shaped protein composed of three domains: one N-terminal, one central and one C-terminal domains (Fig. 13). Both the N and C-terminal domains share a similar folding with a long helical spine supporting a barrel-shaped sheet. Experiments of mutagenesis suggest that the primary LPS binding site of LBP is located near the N-terminal tip of the boomerang-like structure.[49,50] The tip is composed of two loops connecting antiparallel hairpins. Their sequences contain multiple Lys and Arg that can interact with negatively charged phosphate groups in the LPS aggregates. In LBP, both the N- and C-terminal barrels have phospholipid-binding pockets but the N-terminal pocket contains a well-fixed phospholipid molecule. The long hydrophobic channel in the pocket surrounds the lipid chain and a number of positively charged amino acid residues, near the entry of the pocket, interact with the negatively charged phosphate group in the bound phospholipid. The C-terminal pocket is more open and loosely bound to a lipid molecule. The biological role of the phospholipid pockets remains unclear, although it has been proposed that they may interact with the lipid chains of the LPS.

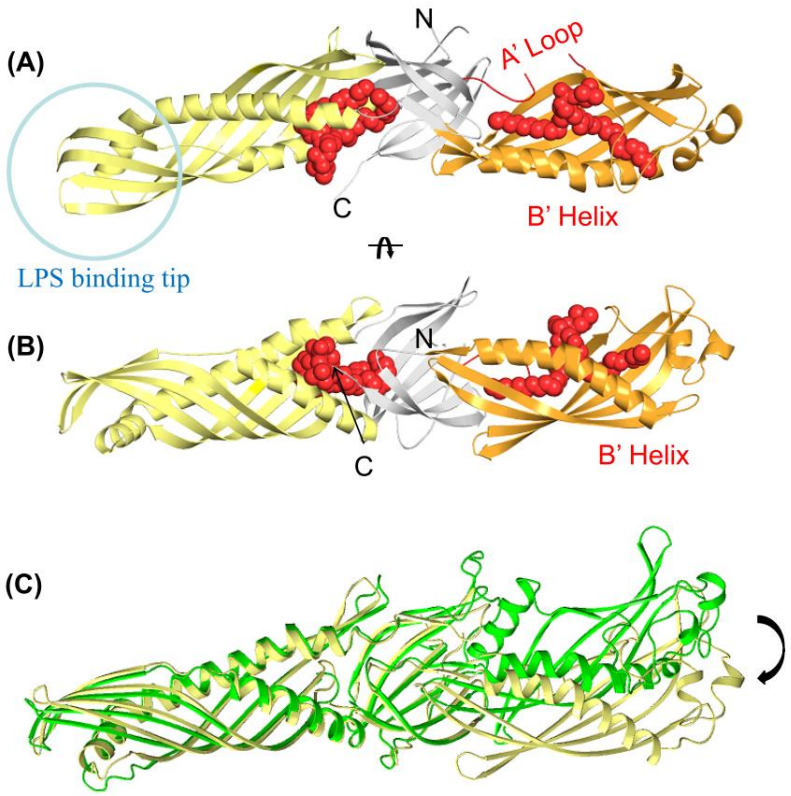

Figure 13. Structure of LBP (**A**) Schematic diagram of the N-terminal (yellow), central (grey) and C-terminal (orange) domains of LBP. Bound phospholipid molecules are shown by red space-filling models. (**B**) The view is rotated by 270˚. (**C**) Structural comparison of LBP and BPI. Ribbon diagrams of LBP and BPI are colored in yellow and green, respectively. The N- and central domains of the two proteins are superimposed. The A' loop and B' helix that connect the N- and C-terminal ends, respectively, of the C-terminal domain to the central domain are labeled.

LBP belongs to a small family of lipid-binding proteins, including cholesteryl ester transfer protein (CETP), phospholipid transfer protein (PLTP), bactericidal/permeability-increasing protein (BPI) and several yet uncharacterized proteins. Among these, BPI is the protein most closely related to LBP with ~50% sequence similarity. The sequences of the two proteins can be aligned with only two single amino acid gaps.[51] Both BPI and LBP can bind to LPS, although only LBP can transfer bound LPS to CD14.[52] Even if individual N- and C-terminal domains show a clear structural homology with that of BPI,[53] the relative orientation of the two domains shows unexpectedly large deviation (Fig. 13C). When the N-terminal domain of LBP is superimposed on BPI, the C-terminal domain of LBP appears bent by ~20 degrees and rotated by ~30 degrees.[54] This large rearrangement of the C-terminal domain appears to be due to small changes in the sequences connecting the N- and C-terminal domains. Therefore, the A' helix connecting the N-terminal domain and the C-terminal domain can be defined as the A' loop (Fig. 13A). The B' helix connecting the C-terminal domain to the central domain is found switched by ~10 degrees in LBP. A single nucleotide polymorphism (SNP) is present near the B' helix and it leads to an altered structure and defects in the LPS response. Populations with

this SNP show increased mortality rates during sepsis and pneumonia. This evidences demonstrates that the structural integrity of the C-terminal domain and the relative orientation of the N- and C-terminal domains are critical for normal LBP activity.[54]

2. Cluster of Differentiation 14 (CD14)

CD14 is expressed either on the surface of myelomonocytic cells, as a glycoprotein attached to the cell membrane with a glycosylphosphatidylinositol (GPI) anchor, either as a soluble protein in the serum.[21,55] The LPS extracted by LBP is transferred to the N-terminal hydrophobic pocket of CD14.[56] (Fig. 14).

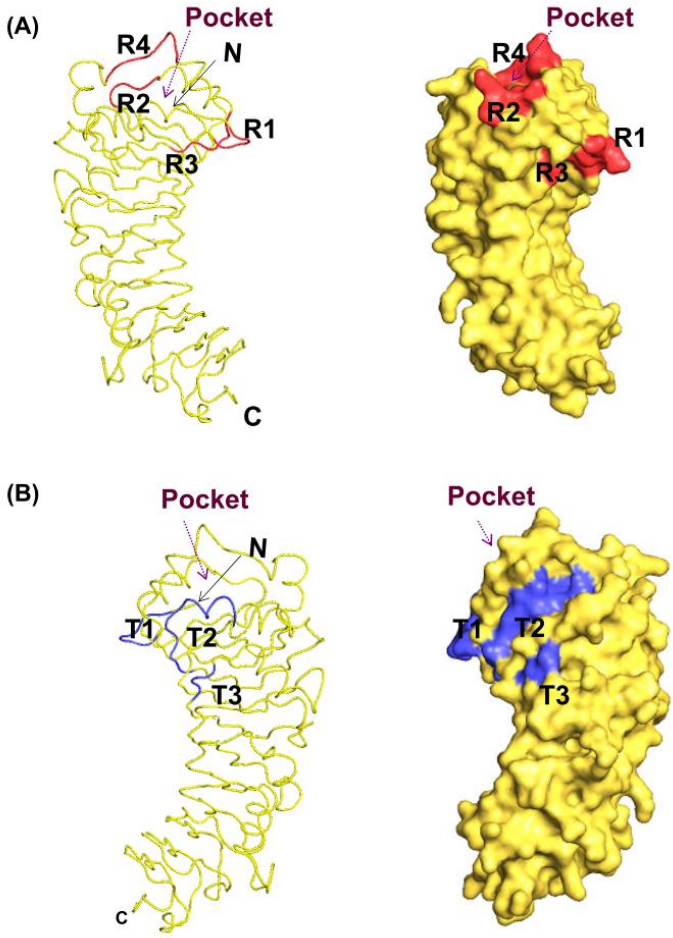

Figure 14. Ribbon and surface representation of CD14 (**A**) Region critical for LPS binding are colored in red and labeled R1-R4. The position of NH2-terminal pocket is marked by N. (**B**) The view is rotated by 180˚. The regions critical in LPS signaling are colored in blue and labeled T1-T3.

CD14 belongs to the leucine-rich repeat (LRR) family and has the characteristic curved solenoid structure. The Asp in the motif make stable hydrogen bonds with the carbonyl backbone of the neighbouring β strands throughout the entire protein, forming an extended hydrogen bonding

network called ‘asparagine ladder’. As a result, the β strands are closely packed, and assemble into a large β sheet making up the entire concave surface of the horseshoe. CD14 is an exception among LRR proteins as its ligand-binding site is located in the convex part of the structure. CD14 has a large hydrophobic pocket between the LRRNT and the first LRR module (Fig. 14A).[56] The convex surface between these two modules is split open, and some of the internal hydrophobic residues are exposed to the solvent area. Mutagenesis and other biochemical experiments strongly suggest that this pocket is the one responsible for LPS binding.[57–62] The size of the pocket is large enough to bind at least part of the lipid chains of LPS. Interestingly, the opening area of the pocket does not have positively charged residues, it suggests that the CD14 pocket may not be fully optimized for the binding of negatively charged LPS. Indeed, it appears that CD14 is a fairly nonspecific lipid binder. This structural observation is consistent with biochemical data showing that CD14 is involved in recognizing not only LPS but also many lipid-containing molecules, such as peptidoglycan, lipoteichoic acid, lipoarabinomannan and lipoproteins. Therefore, it has broad ligand specificity and functions as a pattern recognition receptor by recognizing structural motifs in diverse microbial products. Some of them do not have negatively charged chemical groups. A mutagenesis study also identified three regions that are important for an LPS transfer to TLR4/MD2.[63–65] These sites are clustered in a small area near the LPS binding pocket (Fig. 14B). This surface may be responsible for transient interaction with the TLR4/MD-2 complex for efficient LPS transfer.

3. Complex of Myeloid differentiation protein 2 (MD-2) and the Toll-Like Receptor 4 (TLR4)

MD-2 is a ~14 kDa serum glycoprotein and the LPS binding unit of the TLR4/MD-2 complex. MD-2 belongs to a small family of lipid-binding proteins known as “cup family”. This family of proteins are involved in either the transport or storage of lipid molecules using a large hydrophobic pocket (Fig 15). The cup fold is made of two antiparallel sheets, similar to the immunoglobulin fold. In the immunoglobulin fold, the two sheets are held by a conserved disulfide bridge. In contrast, the cup fold proteins do not have this structurally important disulfide bridge, and the two β sheets can be separated. Hence, the hydrophobic core of the protein is exposed to the solvent area and is used for the binding of the lipid chains of the ligands. Because a large portion of the protein internal core is disturbed for ligand binding, the cup fold proteins contain multiple disulfide bridges that reinforce the stability of the protein. Among the cup proteins, MD-2 has a particularly large pocket that is suitable for the binding of large and

flat hydrophobic ligands such as LPS.[29,66–69] Furthermore, MD-2 possesses a particular flexible loop and some studies indicate that Phe126 (at the middle of the loop) act as a "molecular switch" in endotoxin signalling. The entry of the five lipid A acyl chains into the MD-2 hydrophobic cavity induces a local conformational change that involve the Phe126 side chain and the surrounding residues from 123 to 129 (Fig. 15). Phe126 loop switch may play a key role in supporting the formation of the hydrophobic interface to allow TLR4 dimerization to occur.[69]

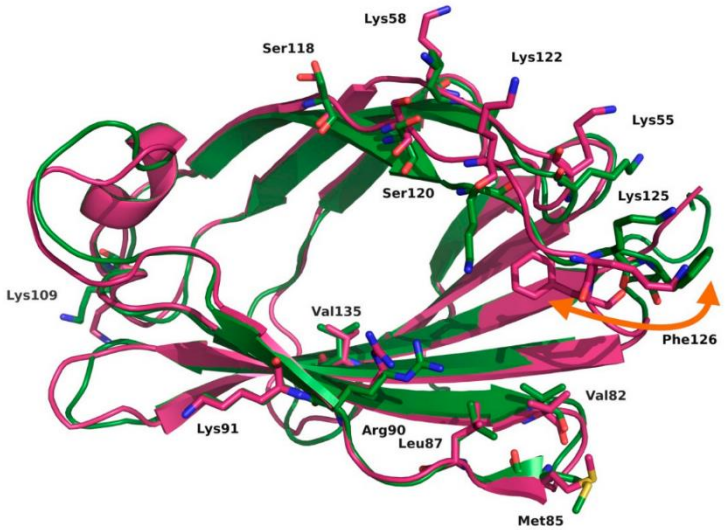

Figure 15. Superimposition of the MD-2 X-ray crystallographic structures The agonist (magenta) and the antagonist (green) conformations of MD-2 from, PDB ID 3FXI and 2E56 respectively. Bound ligands have been hidden for the sake of clarity (*E. coli* LPS in 3FXI; three myristic acids in 2E56). Conformational change of the molecular switch Phe126 is marked.[33]

The extracellular domain of TLR4 responsible for LPS binding belongs to the LRR family, like CD14. The TLR4 LRR domain belongs to the "typical" subfamily, it has 22 LRR modules protected by one LRRNT module in the N-terminal end and one LRRCT module in the C-terminal end.[29] The central sheet of the typical subfamily has uniform twist and tilt angles. Interestingly, the central sheet of TLR4 has two sharp structural transitions and the LRR domain can be divided into three subdomains, the N-terminal, the central and the C-terminal subdomains.

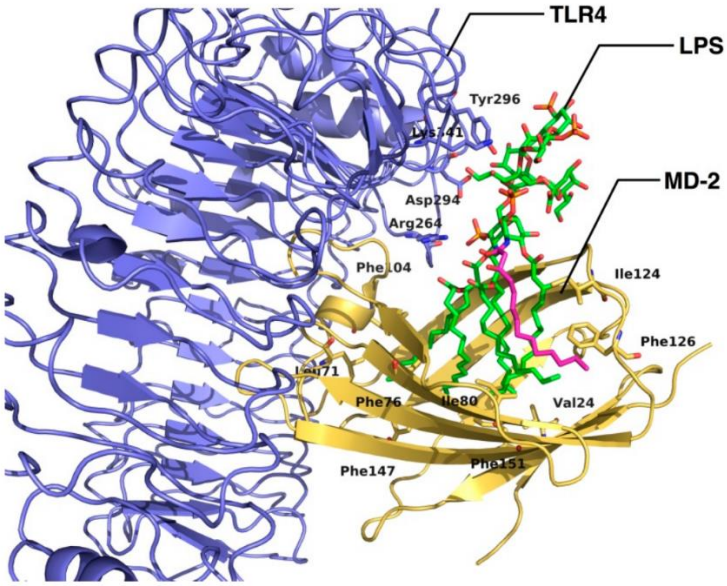

Figure 16. Representation of the LPS in complex with TLR4/MD-2 Detail of the 3D structure of the complex between TLR4/MD-2 and *E. coli* LPS (CPK colors with C atoms in green and R2 C atoms in magenta) from the X-ray crystallographic structure (PDB ID 3FXI); The R2 FA chain (magenta) placed at the channel of MD-2 completes the dimerization interface.[33]

TLR4 is tightly associated with MD-2, forming a stable heterodimeric complex. When LPS, monomerized by LBP and CD14, is transferred to the TLR4/MD-2 complex for signal initiation, the lipid A part of LPS binds into the hydrophobic pocket of MD-2. The LPS used, in the crystallographic study presented, was isolated from *E. coli* as Re-LPS. It contains six lipid chains and two phosphate groups.[29,70–73] All of the lipid chains of lipid A can accommodate into the hydrophobic pocket of MD-2 as the volume of the MD-2 pocket is large enough to contain all its lipid chains. The phosphate groups of the LPS are anchored to the polar rim of MD-2 (Arg90, Lys91, Ser118 and Lys122; Fig. 16), and the polysaccharide moiety establishes a network of polar interactions with TLR4.[22,29,70] MD-2 with bound LPS has two TLR4 binding interfaces, the primary and the dimerization interfaces (Fig. 17). Because the MD-2/LPS complex has these two interfaces, it can bridge two TLR4 molecules, creating a symmetric TLR4/MD-2 hetero-tetramer.

The primary interface of the TLR4/MD-2 heterodimer does not require bound LPS and is located on the concave surface of the horseshoe-like structure. It can be divided into two chemically distinctive areas termed the A and B patches.[29] The A patch (LRR 1 to 7) is predominantly composed of negatively charged amino acids provided by the N-terminal domain of TLR4. It interacts with the positively charged amino acids at the surface of MD-2. The B patch (LRR 7 to 10) is predominantly positively charged and composed of residues from the N- and central domains of the TLR4 extracellular domain (Fig.17). The majority of the TLR4 and MD-2 interactions are due to charges and hydrogen bonds caused by hydrophilic residues. Only

few hydrophobic residues are found on the TLR4/MD-2 interaction surface, and they do not seem to contribute significantly to the protein interaction.[54]

In contrast, the dimerization interface is generated only after the binding of LPS. A lipid chain of LPS (pink chain, Fig. 16) directly participates for the dimerization interface. When bound to the MD-2 pocket, five of the six lipid chains of the *E. coli* LPS are fully inserted inside the hydrophobic pocket. However, the remaining sixth lipid chain (pink chain, Fig. 16) is partially exposed to the MD-2 surface and interacts with a small hydrophobic surface, composed of phenylalanine and leucine from the partner, TLR4*. Extensive research have been performed to determine structure-activity relationships associated with LPS.[44,74,75] These studies demonstrated that the optimal inflammatory activity requires six lipid chains and two phosphate groups attached to the di-glucosamine backbone of lipid A. The core and O-specific chain of LPS supposed to have minimal impact on the immunological activity of LPS.[74,76,77]

The structure of TLR4/MD-2/LPS complex explains these biochemical and immunological data (Fig. 16 and 17). The volume of the MD-2 pocket appears to be optimized for six lipid chains. LPS with four lipid chains has minimal inflammatory activity, although binding to the TLR4/MD-2 complex remains possible. In fact, some of them are strong antagonists to TLR4/MD-2. This structure suggests that LPS with less than six lipid chains has reduced activity because all the lipid chains are submerged inside the pocket and cannot provide an adequate hydrophobic interaction surface necessary for the stable binding between two TLR4. On the contrary, LPS with more than six lipid chains has additional lipid chains that may disturb the optimal interaction distance between MD-2 and TLR4. The two phosphate groups attached to the glucosamine backbone also play an indispensable role in the LPS activity. Deletion of any of these phosphates can reduce the inflammatory activity of LPS by more than one hundred folds.[78]

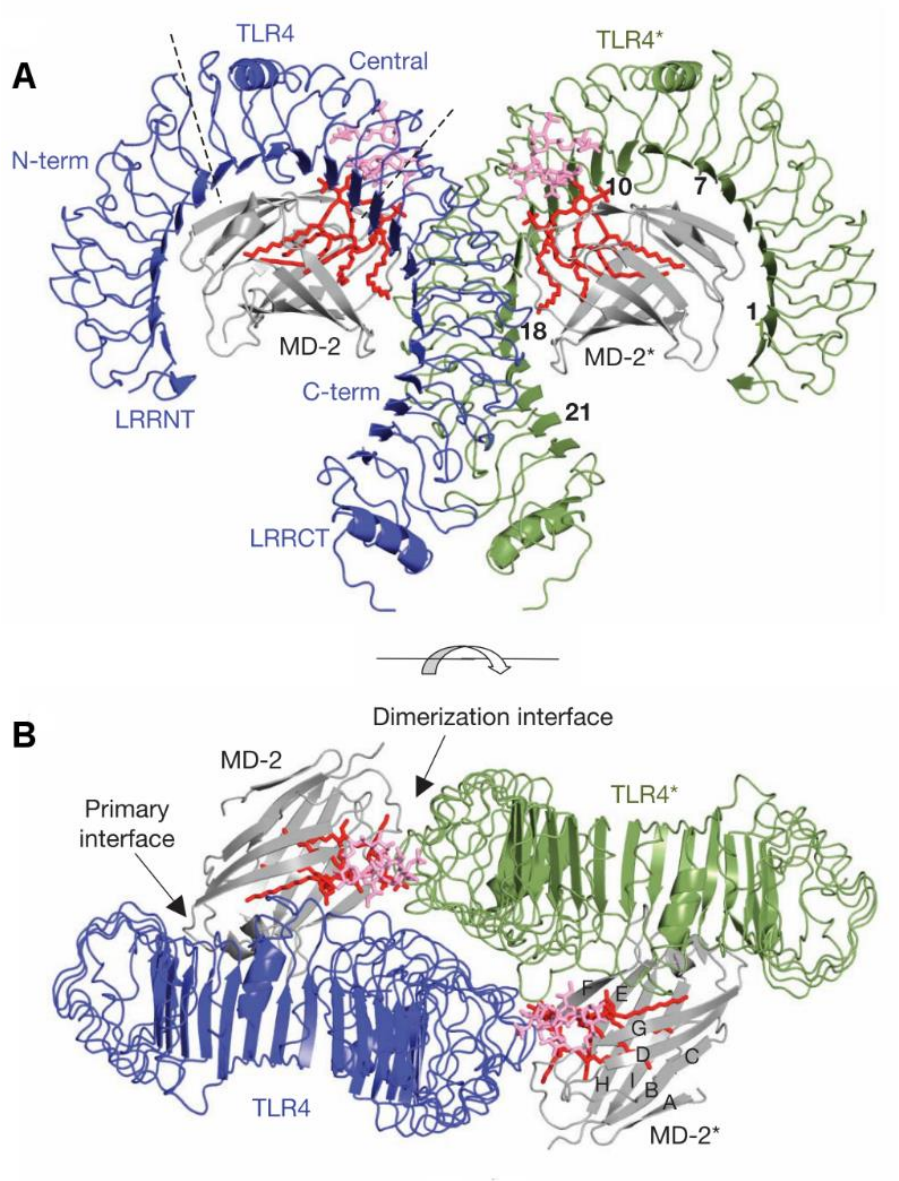

Figure 17. Overall structure of the dimerized [TLR4/MD-2/LPS]2 complex (PDBID 3FXI) A, Side view of the complex. The lipid A component of LPS is coloured red, and the inner core carbohydrates of LPS are coloured pink. The module numbers of the LRRs in TLR4 and the names of the β strands in MD-2 are written in black. TLR4 is divided into N-, central and C-terminal domains. The LRRNT and LRRCT modules cover the N- and C-termini of the LRR modules. **B**, Top view of the symmetrical dimer of the $[TLR4/MD\text{-}2/LPS]_2$ complex. The primary interface between TLR4 and MD-2 is formed before binding LPS, and the dimerization interface is induced by the binding of LPS.[70]

LPS binding to MD-2 co-receptor promotes the dimerization of TLR4 by forming the complex $[TLR4/MD\text{-}2/LPS]_2$ (Fig. 17).[70,79] TLR4 and MD-2 are essentials for LPS detection; the absence of one of these two proteins completely abolishes the activation of the LPS-triggered intracellular signaling.[80]

4. TLR4/MD-2 complex and antagonist interaction

The crystal structures of two antagonists of TLR4, Eritoran (E5564) and lipid IVa, have been solved in complex with murine TLR4/MD-2 for Eritoran (PDB ID 2Z64)[29] and with human MD-2 alone for lipid IVa (PDB ID 2E59).[69] Eritoran is an experimental drug developed as an anti-sepsis drug and is a powerful antagonist of TLR4. It reached phase III clinical study, conducted in patients with severe sepsis, but did not meet its primary endpoint of 28-day all-cause mortality.[81–84] Lipid IVa is an intermediate of LPS biosynthesis and act as an antagonist to human TLR4.[85,86] Both Eritoran and lipid IVa have four lipid chains and two phosphate groups attached to a di-glucosamine backbone. Regardless of the substantial structural discrepancies in their lipid chains, the positions of the phosphate groups and the glucosamines are practically conserved in both structures. Compared to hydrogen bonds and other hydrophilic interactions, the hydrophobic interaction between the lipid chains and the MD-2 pocket seems not to be very sensitive to the distance and orientation of the interacting groups. Therefore, it appears that somehow the total interaction surface area, not the actual chemical structures of the lipid chains, is to consider for MD-2 binding. This observation is consistent with experimental data showing that variation of the chemical structure of the lipid chains can be tolerated,[87] although the total number of lipid chains or the chain length can have a serious effect on the inflammatory activity of LPS and LPS-like.[88] When the structure of LPS bound to MD-2 are compared to the synthetic antagonists, the positions and orientation of antagonists display interesting differences. In the antagonist-bound structure, the glucosamine backbone positions move down inside the pocket by ~ 5 angstroms and the 1 and 4’ phosphate groups swap their positions. The deeper insertion of the glucosamine backbone is supposed to be due to the fewer lipid chains composing the antagonists.

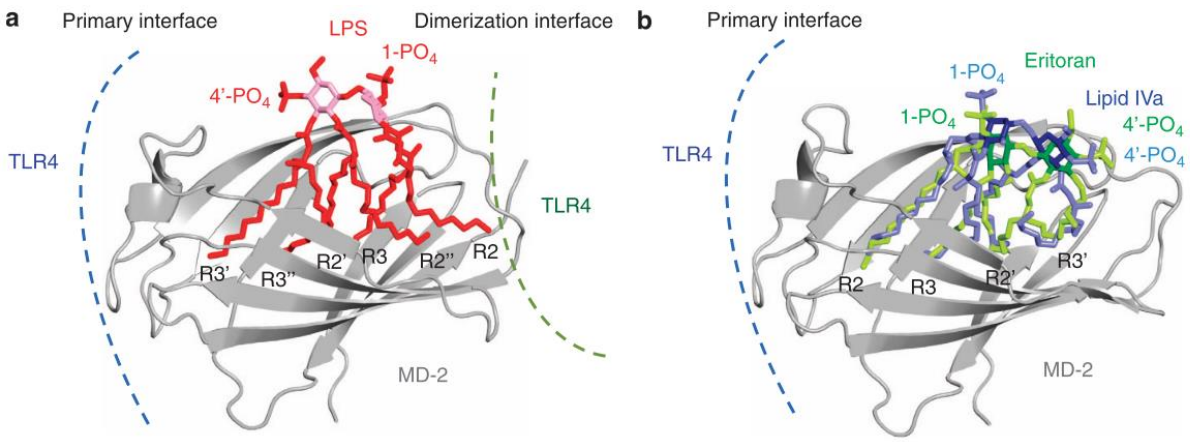

Figure 18. Binding of LPS and antagonistic ligands to the TLR4– MD-2 complex Structure of the primary and dimerization interfaces of the TLR4/MD-2/LPS complex. The lipid chains of LPS are labeled. MD-2 is colored grey. (**a**) The lipid chains and phosphate groups of LPS are shown in red. The glucosamine backbone is pink. (**b**) Structures of Eritoran and lipid IVa bound to MD-2.[89]

As mentioned before, MD-2 possesses a flexible loop, containing Phe126, which is very important for the dimerization interface. It affects also the position and surrounding environment of the bound fatty acyl chains of LPS. These effects of Phe126 are manifest before interactions with TLR4 and are likely driven by hydrophobic interactions between the fatty acyl chains of LPS and the aromatic side chain of Phe126. Therefore, Phe126 acts as a "hydrophobic switch" driving the agonist-dependent recognition of TLR4/MD-2 and promoting, or not, the formation of the binding surface allowing a proper dimerization interface.

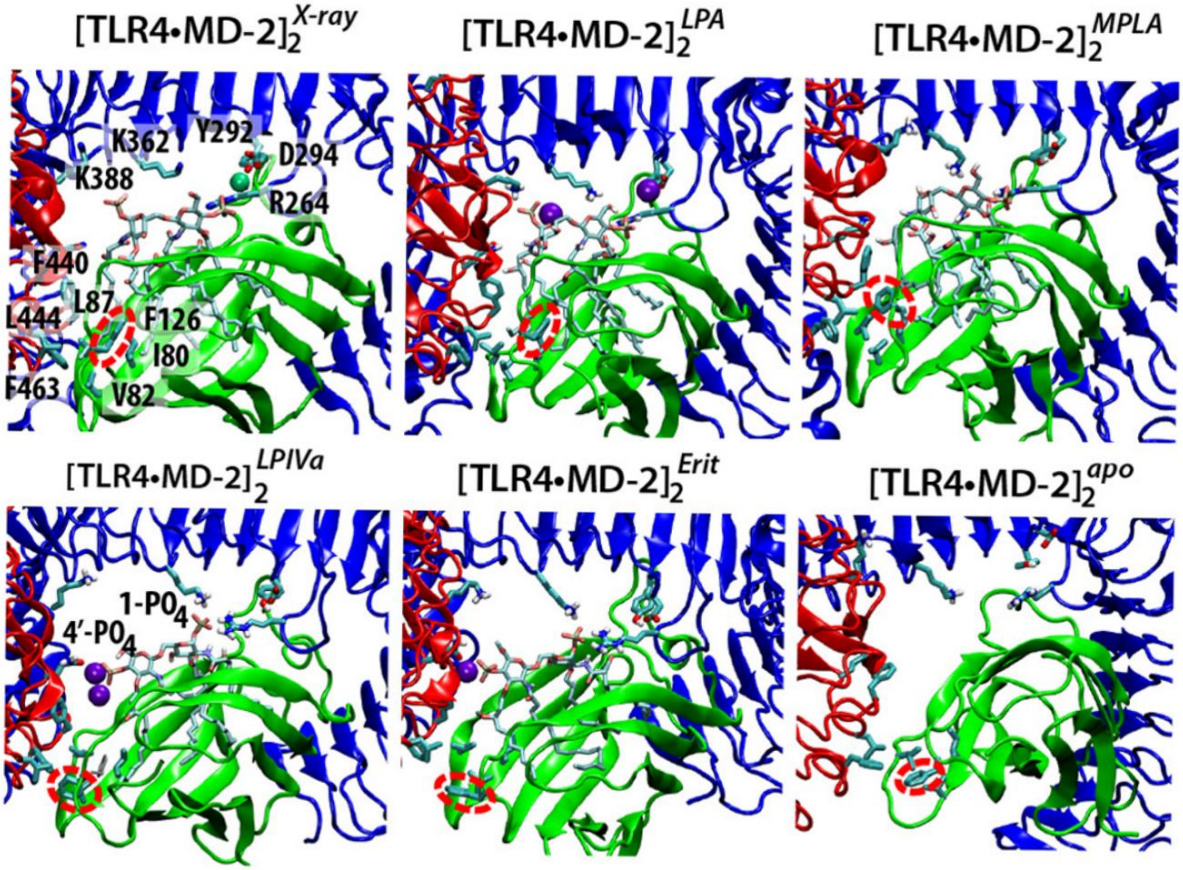

Figure 19. Molecular signaling within the receptor complex the x-ray structure of LPS-bound $[TLR4/MD\text{-}2]_2$ at one of the MD-2 bound sites (*X-ray*, PDB ID 3FXI) is compared with the final simulation structure of the complex when bound to a range of ligands: *LPA* (lipid A), *MPLA* (mono-phosphoryl lipid A), *LPIVa* (lipid IVa), *Erit* (Eritoran) or *apo* (ligand-free state). Protein chains are shown in schematic representation and coloured green for MD-2, red for TLR4 and blue for TLR4* with bound ligand and adsorbed sodium ions in wireframe or space fill format, respectively. Key interacting residues are labelled for the x-ray structure. The orientation of Phe126 is highlighted with a red, dashed ellipse.[90]

The comparison of the X-ray crystal structure of human TLR4 bound to Re-LPS (PDB ID 3FXI) and the simulated structure bound to agonist (lipid A), partial agonist (MPLA) and antagonists (lipid IVa and Eritoran) confirm the importance for the Phe126. In the simulation with lipid A, the conformation of Phe-126 remains close to that of the x-ray structure, forming a hydrophobic cluster of interactions with the FA chain exposed of lipid A and residues including Ile80, Val82, and Leu87 in MD-2, and Phe440, Leu444, and Phe463 in TLR4* (Fig. 19). The association is also supported by a salt bridge formed between Lys125 of MD-2 and Glu422 of TLR4*. This is in total contrast to the agonist-free interfaces in which was observed a spontaneous reorientation of Phe-126 from the closed to open state, in the presence of lipid IVa, Eritoran, and in the ligand-free apo state (Fig. 19). The open state led to complete loss of interactions with lipid and destruction of the TLR4/MD-2 hydrophobic cluster, crucial for maintaining the receptor dimerization interface. In the case of MPLA, the partial agonism induces a reoriented Phe126

state that is intermediate between the agonist and antagonist systems (Fig. 19).[90] Additionally, while the 1-phosphate group of lipid A interacts electrostatically with Lys388 on TLR4*, it is the more "buried" phosphate group which was consistently coordinated, by the Lys362 of TLR4*. Intriguingly, these residues are part of a hypervariable region important for species-dependent specificity.[91]

IV. Two different signaling pathways downstream to TLR4

In several ways, TLR4 is unique among TLRs. First, it is the only known TLR able to activate both MyD88-dependent pathway (inducing the transcription of genes encoding inflammatory molecules) and TRIF-dependent pathway (producing type I interferon).[92] Second, with the exception of TLR4, all other known receptors that induce the production of type I interferon are sensors of nucleic acids and induce activation of IRF3 or IRF7 from intracellular compartments (TLR3, TLR7 and TLR9 signal from endolysosomes).[93,94] Finally, TLR4 is the only known TLR that engages all five TIR domain-containing adaptors.[95]

TLR dimerization brings the two C terminus sequences of the two ectodomains and the TIR signaling domains into close proximity. The association of the receptor TIR domains provides a new scaffold that allows the recruitment of specific adapter proteins to form a post-receptor signaling complex. Depending on their localisation, dimerized TLR4 recruits two distinct adapter protein pairs, Mal/MyD88 (myeloid differentiation primary response gene 88) at the plasma membrane and TRAM (TRIF-related adapter molecule)/TRIF (TIR-domain protein inducing interferon) when endocytosed (Fig. 20). Mal (also known as TIRAP) and TRAM (also known as TICAM2) probably engage directly with the receptor to act as "bridging adapters" for the recruitment of MyD88 and TRIF (also known as TICAM1), respectively.[96]

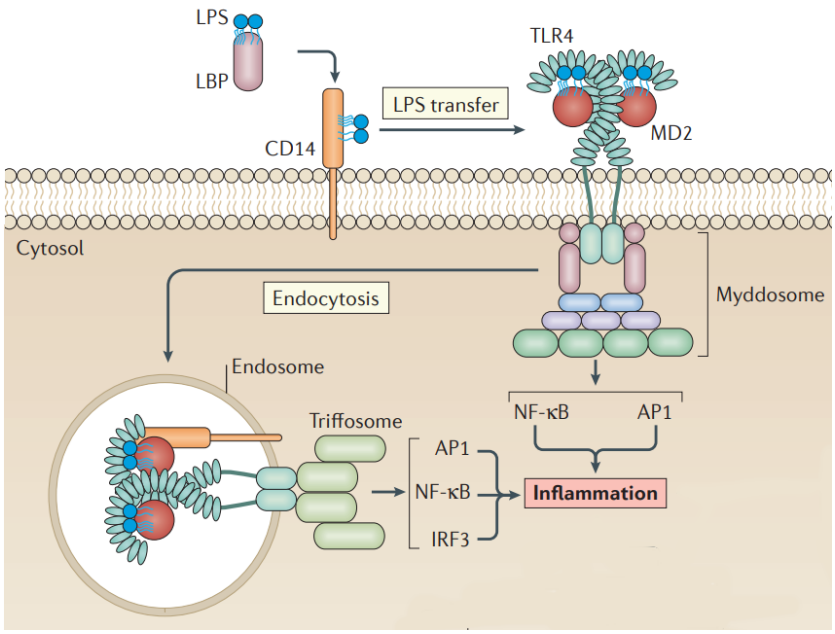

Figure 20. Two different signaling pathways upon TLR4 triggering to promote inflammation Lipopolysaccharide (LPS) is sensed at the plasma membrane initially by LPS-binding protein (LBP), which helps CD14 to extract this pathogen-associated molecular pattern (PAMP) from bacterial cell walls. CD14 delivers LPS to TLR4/MD-2, prompting the dimerization and activation of TLR4, a process that leads to myddosome assembly. CD14 may deliver the dimerized TLR4 to endosomes to promote TIR domain-containing adaptor protein inducing IFN β (TRIF) signalling through the putative triffosome. Both pathways result in inflammation.[97]

The supramolecular organizing centre containing MyD88 is called Myddosome, in opposition to the TRIFF-containing supramolecular organizing centre which is called Triffosome. Therefore, it seems that the adaptor 'choice' determines the transcriptional response induced after microbial detection by TLR4. The use of TIRAP and MyD88 induces the production of proinflammatory cytokines, whereas the use of TRAM and TRIF elicits a type I interferon response.[98–101]

1. Myddosome or TIRAP/MyD88-dependent pathway

The myddosome formation is a process shared between all the TLRs besides TLR3, therefore, it has been highly studied. The LPS-induced TLR4 dimerization usually occurs at phosphatidylinositol 4,5-bisphosphate (PIP2)-rich regions of the plasma membrane. The first cytosolic event is the recruitment of the sorting adaptor Toll/interleukin-1 receptor domain-containing adapter protein (TIRAP) on the TLR4 cytosolic TIR domain, which is necessary for the assembling of a higher-order filamentous structure called myddosome.[102,103] The Myddosome is a supramolecular organizing centre composed of the signalling adaptor MyD88 and several IRAK family kinases, which initiates signalling events leading to the activation of pro-inflammatory transcription factors such as AP-1, NF-κB (p50/p65) and IRF5 (Fig. 21).[95,104,105] Transcription factors activation is the crucial event that leads to the production and secretion of pro-inflammatory cytokines such as TNFα, IL-1β, IL-6 and IL-8.

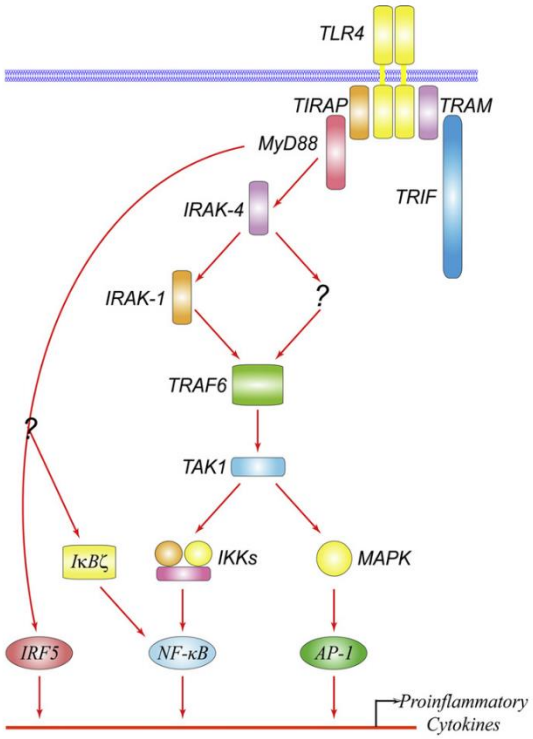

Figure 21. The MyD88-dependent pathway MyD88 activates IRAKs/TRAF6 as well as the transcription factors NF-κB, AP-1 and IRF-5 further downstream. These transcription factors induce expression of proinflammatory cytokine genes.[80]

IRF5 is also produced and acts as a molecular switch that controls whether macrophages will promote or inhibit inflammation. Blocking the production of IRF5 in macrophages may help to treat a wide range of autoimmune diseases and, conversely, boosting IRF5 levels might help to treat people whose immune systems are weak, compromised, or damaged. IRF5 seems to work either by interacting with DNA directly, or by interacting with other proteins that themselves control which genes are switched on.

The structure of the myddosome assembly has been solved (Fig. 22 and 23), it is a complicated supramolecular organizing centre composed of the Toll/Interleukin-1 receptor (TIR) domains associated to myeloid differentiation primary response protein 88 (MyD88) and MyD88 adaptor-like protein (MAL or TIRAP). The adaptor protein TIR domains are linked to amino-terminal domains that contain a phosphatidylinositol-4,5-bisphosphate (PIP2)-binding motif in MAL and a death domain (DD) in MyD88. The TLR TIR domain is composed of a central parallel five-stranded β-sheet with α-helices between them (Fig. 22c and d). The structure of the MAL TIR domain revealed either a symmetric association and an asymmetric association, involving the E helix (orange, Fig. 22e). Moreover, the isolated MyD88 TIR domain forms head-to-tail dimers and allows multiple interactions between TIR domain dimers.

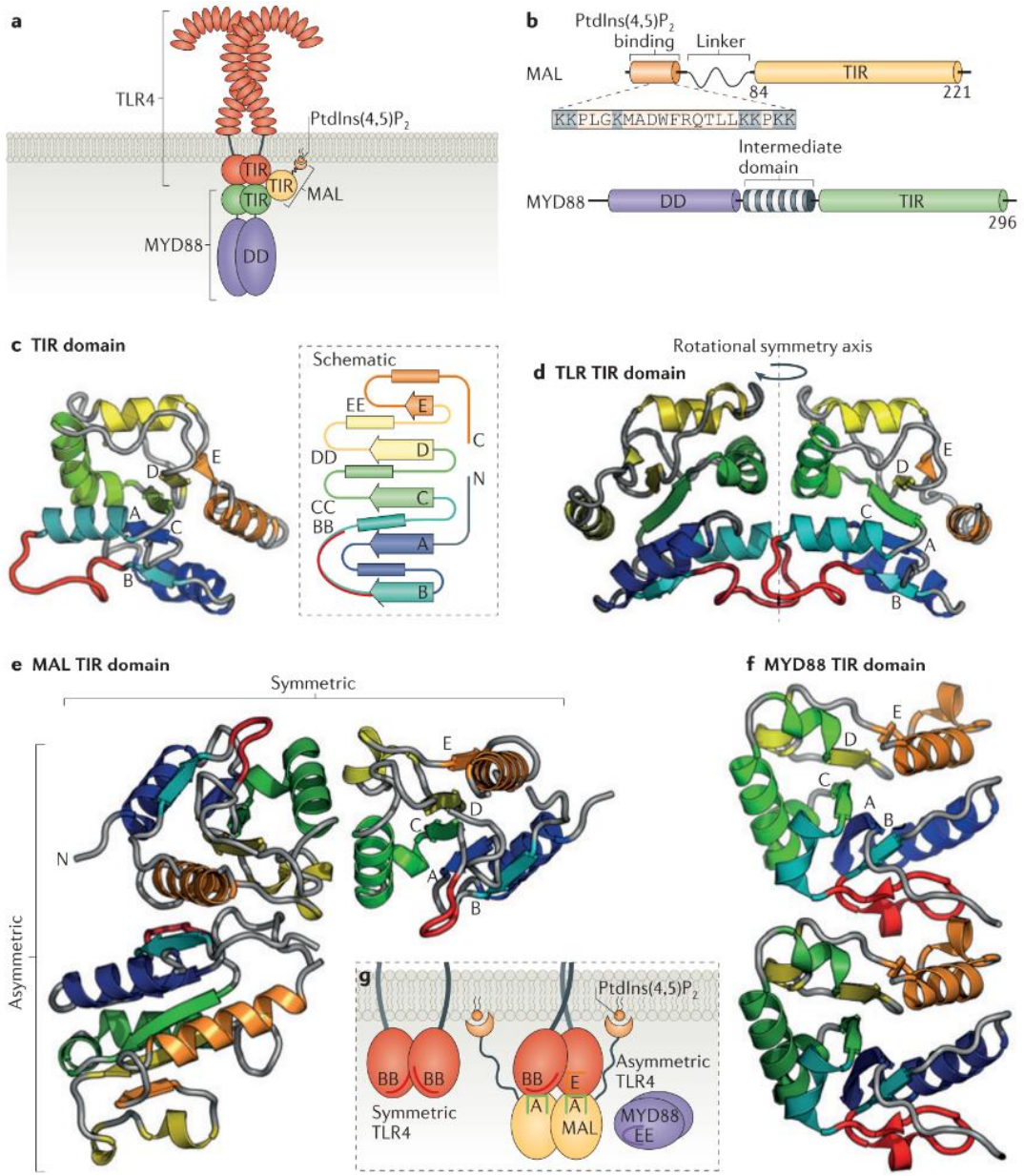

Figure 22. Interactions underlying signalling through TIR domain-containing complexes (**a**) A scheme showing the assembly of the adaptor proteins myeloid differentiation primary response protein 88 (MyD88) and MyD88 adaptor-like protein (MAL) with Toll-like receptor 4 (TLR4) through their Toll/IL-1R (TIR) domains. (**b**) The adaptor protein TIR domains are linked to amino-terminal domains that contain a phosphatidylinositol-4,5-bisphosphate (PIP2)-binding motif in MAL (sequence boxed with positively-charged lysine residues highlighted in blue) and a death domain (DD) in MyD88. (**c**) The TIR domain has a central parallel five-stranded β-sheet and flanking α-helices, shown here as a three-dimensional structure with a two-dimensional schematic for clarity. (**d**) Structures of TLR TIR domains have revealed a dimer with a rotational symmetry axis shown here for TLR10. (**e**) The structure of the MAL TIR domain revealed a similar symmetric association (viewed along the symmetry axis here) and an asymmetric association, involving the E helix (orange). (**f**) The MyD88 TIR domain in isolation has been observed to form head-to-tail dimers. (**g**) The multiple interactions that are made between TIR domain dimers that are involved in TLR4 signalling are shown schematically.[96]

Biophysical and crystallographic work have revealed that 6 to 8 MyD88 molecules form an oligomeric macromolecular platform with four IRAK-4 and four IRAK-2 molecules through death domain (DD) interactions (Fig. 23).[96,103] The process of myddosome assembly is, for now,

believed to be highly allosteric. The engagement of the MyD88 DD by IRAK-4 and IRAK-1 permits their association which results in IRAK-4 mediated phosphorylation of IRAK-1. In turn, it stimulates a cascade of IRAK-1 autophosphorylation.[106] IRAK-1 is ultimately released from the active receptor complex and, in conjunction with TRAF-6, binds to TAK (transforming growth factor-beta–activated kinase-1). This leads to the ubiquitination and degradation of IRAK-1, phosphorylation of IKK (IκB kinase) and activation of NF-κB-mediated proinflammatory genes.

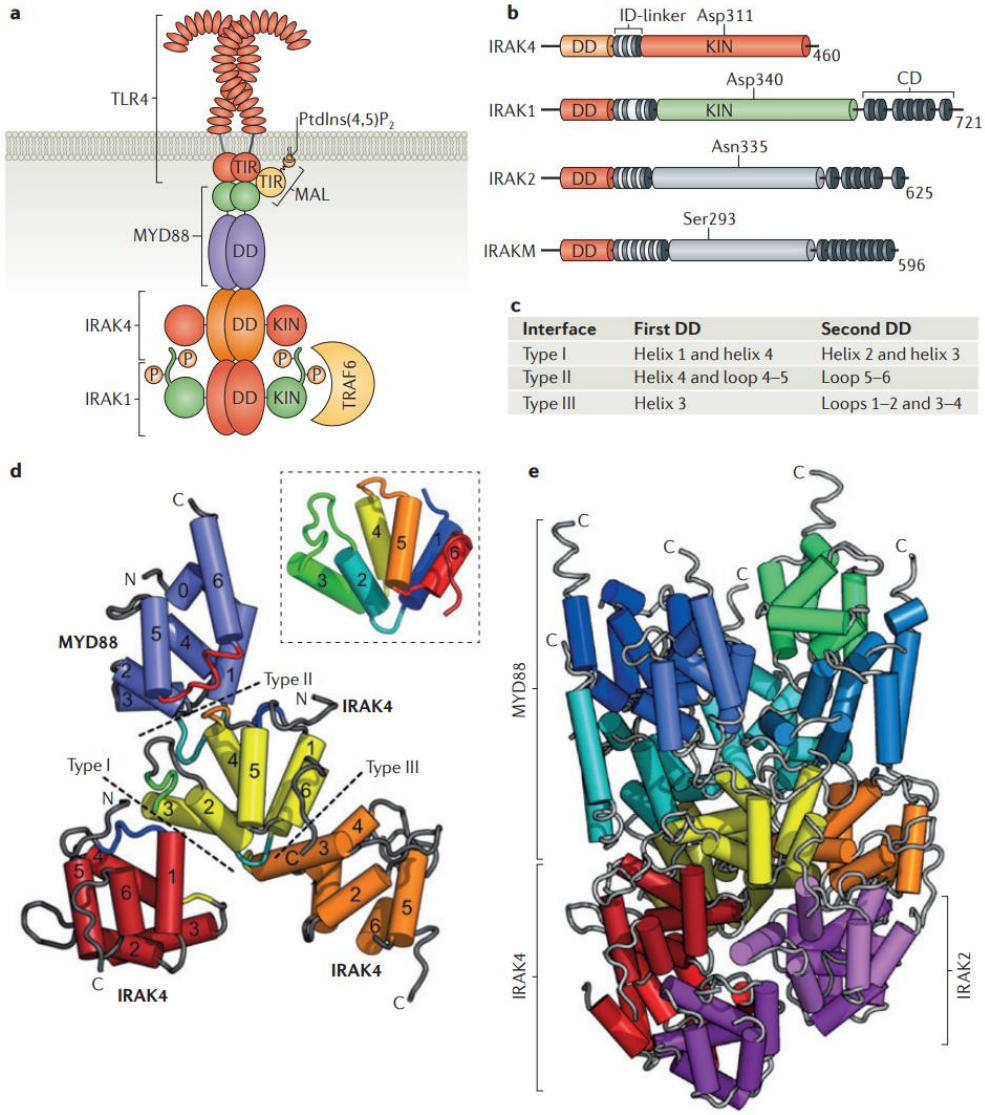

Figure 23. Death domain interactions and position of protein kinases in the Myddosome assembly (**a)** Schematic arrangement of adaptor protein death domains (DDs) and kinase (KIN) domains in association with the Toll/IL-1R (TIR) domains of Toll-like receptor 4 (TLR4). (**b**) Domains of IL-1R-associated kinase (IRAK) family proteins including the DD, the intermediate domain (ID), the KIN domain and the carboxy-terminal domain (CD). The key catalytic aspartate residues that are present in IRAK4 and IRAK1 (Asp311 and Asp340, respectively) are mutated in the inactive kinases IRAK2 and IRAKM (Asn335 and Ser293, respectively). (**c**) The interfaces that are involved in DD assembly are listed. (**d**) DDs involved in myeloid differentiation primary response protein 88 (MyD88) and IRAK4 contacts in the Myddosome. The inset shows an equivalent view of the IRAK4 DD with helices in rainbow colours. (**e**) Complete Myddosome DD assembly shown with MyD88 DDs in blues and green, IRAK4 DDs red, orange and yellow and IRAK2 DDs in violets.[96]

2. Triffosome or TRAM/TRIF-dependent pathway

Concomitant with TLR4 signalling from the plasma membrane, LPS binding to GPI anchored CD14 promotes TLR4 endocytosis.[20] Recent studies have shown that, in contrast to the endocytosis process of other transmembrane receptors, TLR4 internalization is entirely promoted by extracellular interactions. In particular, LPS binding to CD14 is the crucial event that allows TLR4 ectodomain to be selected as a cargo for the endocytosis process and that adaptor protein MD-2 is the cargo-selected agent accomplishing the process.[107] Thus CD14 is not only an accessory protein able to present and increase the sensitivity of the LPS-detection process, but it possesses a dual function in ligand transport and receptor transport.[20,107] Once internalized, TLR4 engages another sorting adaptor, called translocating chain-associated membrane protein (TRAM) or TIR domain-containing adaptor molecule-2 (TICAM-2), and the signalling adaptor TRIF or TICAM-1*, which lead to the subsequent expression of IFNs and IFN-stimulated genes (ISGs) (Fig. 24).[108]

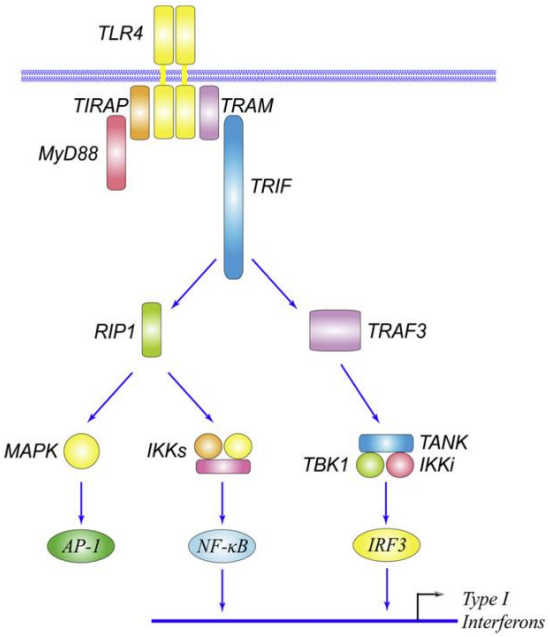

Figure 24. The MyD88-independent pathway TRIF signals the induction of Type I interferons by recruiting TRAF3 and RIP1 to activate transcription factor IRF3, as well as NF-kB and AP-1.[80]

IRF3 is a key transcriptional regulator of type I interferon (IFN)-dependent immune responses which plays a critical role in the innate immune response against DNA and RNA viruses.[109] It regulates the transcription of type I IFN genes (IFN-α and -β) as well as IFN-stimulated genes (ISG) by binding to an interferon-stimulated response element (ISRE) in their promoters. It acts

* TRAM and TICAM-2 are homonyms such as TRIF and TICAM-1. One or the other is used regarding the discipline of study. Immunologists mainly use TRAM/TRIF while Crystallographers use TICAM-2/ TICAM-1.

as a more potent activator of the IFN-β gene than the IFN-α gene and plays a critical role in both the early and late phases of the IFN-α and -β gene induction. IRF3 is phosphorylated by IκB Kinase ε and TANK Binding Kinase 1. This induces a conformational change, leading to its dimerization and nuclear localization and association with C-AMP Response Element-binding protein to form dsRNA-activated factor 1, a complex which activates the transcription of the type I IFN and ISG genes. It can also activate distinct gene expression programs in macrophages and can induce significant apoptosis in primary macrophages.[110,111]

TLR4 interacts with a TIR domain-containing adaptor molecule-2 (TICAM-2)/TRAM [TRIF (TIR domain-containing adaptor-inducing interferon-β)-related adaptor molecule] via its Toll–interleukin-1 receptor homology (TIR) domain. TICAM-2 acts as a scaffold protein and activates TIR domain-containing adaptor molecule-1 (TICAM-1)/TRIF. According to the structural and NMR analysis, TICAM-2 interacts with TICAM-1 by the acidic amino acids' motif, Glu87/Asp88/Asp89. The TIR domain of TICAM-2 couples with the dimer of TIR domain of TLR4 below the membrane, and TICAM-2 itself also forms dimer and constitutes a binding site with TICAM-1. Endosomal localization of TICAM-2 is essential for TLR4-mediated type I interferon-inducing signal from the endosome. The N-terminal myristoylation allows TICAM-2 to anchor to the endosomal membrane. Additionally, two acidic amino acids were identified as a functional motif (Asp91/Glu92) and cooperatively determines endosomal localization of TICAM-2. This structural information of TICAM-2 suggests that this specific structure is indispensable for the endosomal localization and type I interferon production of TICAM-2.[112]

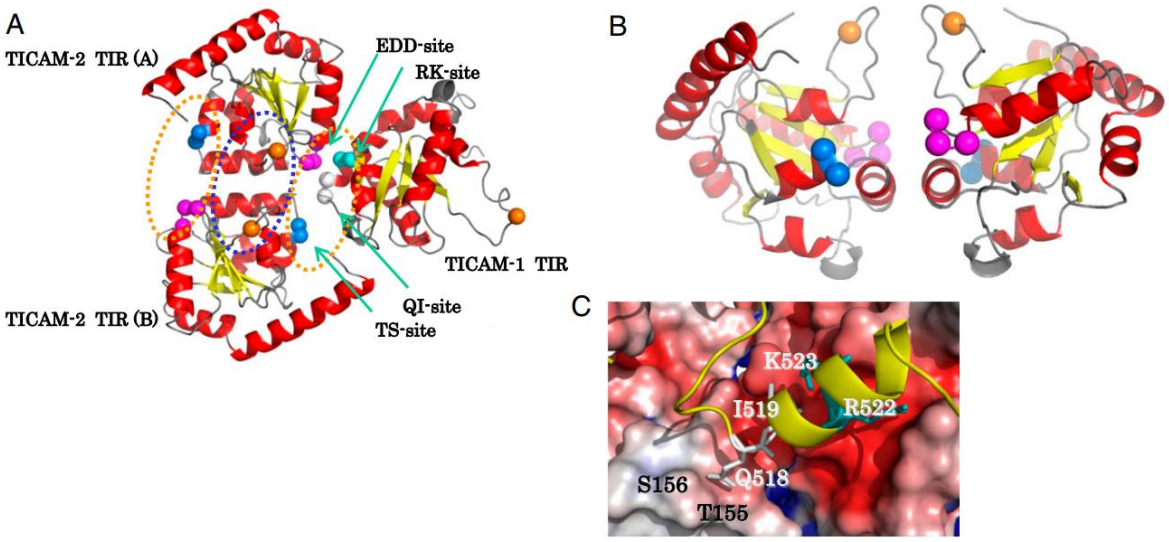

Figure 25. Docking model of the TIR domains of TICAM-2 and TICAM-1 (A) Docking structure of TICAM-2 dimer and TICAM-1 monomer. Homotypic and heterotypic interfaces are enclosed by blue and orange dotted lines respectively. (B) TICAM-2 dimer presenting the binding surface with TICAM-1 TIR. The EDD and TS sites are located at the front surface (also at the back surface) that interact with

the wedge of the TICAM-1 TIR (the RK and QI sites). (C) The front view of the interacting surface of TICAM-2 is shown in electrostatic surface potential presentation whereas the wedge of the TICAM-1 is presented in ribbon model. The residues on the RK and QI sites are shown in wire model and labeled.[112]

Despite substantial recent progress, the understanding of the dynamics and molecular mechanisms of TLR4 signalling remains incomplete. Unresolved issues include the stoichiometry of signalling *in vivo*, the nature of the allosteric processes that are essential for regulation and the importance of lipid microdomains. Progress in these areas will be facilitated by the development of new methodologies, including super-resolution single-molecule imaging, and an interdisciplinary approach involving low and high resolution structural techniques.[113–115] Further studies, should facilitate the development of new therapies directed to the innate signalling network in autoimmune, inflammatory and infectious diseases.

V. TLR4 related pathologies

The TLR4 activation and the associated release of pro-inflammatory mediators are crucial for an optimal host immune response against invading Gram-negative bacteria. Inflammation is generally beneficial for the host as it allows the tissue to repair and heal. However, dysregulated, persistent or excessive immune system activation may be deleterious by generating a broad spectrum of disorders. In particular, the over-activation of the TLR4 pathway is the main cause of acute septic shock and sepsis. Furthermore, aberrant TLR4 signaling is related to many other important pathologies such as inflammatory bowel diseases (IBD) including Crohn's disease (CD) and ulcerative colitis (UC),[116] vascular inflammations,[117] obesity-linked type II diabetes,[118,119] atherosclerosis,[120,121] skin inflammations (dermatitis),[122] psoriasis,[123] rheumatoid arthritis (RA),[124] neuroinflammatory disorders such as neuropathic pain,[125–127] Alzheimer disease,[128] haemorrhagic shock[129] and amyotrophic lateral sclerosis (ALS).[130,131] Moreover, TLR4 has recently been suggested as a promising therapeutic target for drug abuse[132] and major depressive disorders.[133,134] Consequently, TLR inhibitors are an emerging target for drug development.[135]

1. Sepsis

Sepsis is strongly increasing its incidence in the past decades, even exceeding diseases as stroke, cancer and myocardial infarction.[136,137] Its mortality rate is very high, from 20% to 50% in case of organ dysfunction and frequently over 50% in septic shock.[136–138] Sepsis is a time-dependent disease, and prognosis may improve if early diagnosis and appropriate treatment is achieved.[139,140] Severe sepsis and septic shock occur with a high incidence and prevalence in emergency rooms and intensive care units. The evaluation of hospital admissions between 1979 and 2000 in USA, using a representative sample of American hospitals, showed an increase in sepsis incidence from 83 episodes per 100,000 in 1979 to 240 episodes per 100,000 habitants in 2000.[141] Recently, the World Health Organization estimated 30 million cases of sepsis, 19.4 million by severe sepsis and 6 million deaths per year in the world.[142]

The definition of sepsis evolved several times since its first definition in 1991 at a Critical Care Medicine Consensus Conference.[143] The initial and implemented sepsis definitions included: sepsis (systemic inflammatory response syndrome [SIRS] and suspected infection), severe sepsis (sepsis and organ dysfunction) and septic shock (sepsis and hypotension despite adequate fluid resuscitation).[144]

Since the "Third International Consensus Definitions for Sepsis and Septic Shock" (Sepsis-3, 2016), sepsis is defined as: "life-threatening organ dysfunction caused by a dysregulated host response to infection. The clinical criteria for sepsis include suspected or documented infection and an acute increase of two or more Sequential Organ Failure Assessment (SOFA) points as a proxy for organ dysfunction." While septic shock is defined as: "a subset of sepsis in which underlying circulatory and cellular/metabolic abnormalities are profound enough to increase mortality substantially. Septic shock is defined by the clinical criteria of sepsis and vasopressor therapy needed to elevate mean arterial pressure ± 65mmHg and lactate >2 mmol/L (18 mg/dL) despite adequate fluid resuscitation."[145,146]

In principle, many pathogens can trigger sepsis, it includes Gram-negative and positive bacterial cells, virus, fungi and parasites.[145] In order to cause the pathology, infective agents have to overcome the host anatomical barrier, evade host innate immune system and replicate in the targeted organs.[147] The bacterial capacity to trigger sepsis is dependent of the virulence factors of expression, related to the stage of infection and its intrinsic composition.[148] As previously described, LPS is the most potent immunostimulant among microbial products and, although other PAMPs and DAMPs are involved in sepsis onset, LPS is probably the main trigger of the pathology. LPS cause endothelial cell injury and apoptosis by promoting the expression of tissue factors and pro-inflammatory mediators.[149] Therefore, TLR4-mediated signal plays a crucial and central role in sepsis pathogenicity, indeed studies conducted on $TLR4^{-/-}$ murine models (knockout mice that lack TLR4) revealed their hypo-responsivity to LPS and their incapacity to develop septic shock, even upon massive LPS exposure.[150]

Numerous studies have been performed to find compounds able to block the inflammatory cascade: corticosteroids,[151] anti-endotoxin antibodies,[152] TNF-α antagonists,[153,154] IL-1 receptor antagonists,[155] and others.[156,157] The majority of the pharmaceutical products were unsuccessful to treat sepsis, probably because of the highly complex nature of the sepsis. Currently, no drug specific to sepsis is available. A hope was given in 2001 when Eli Lilly and Co. received the Food & Drug Administration approval for Xigris (drotrecogin alfa (activated)), a recombinant human activated protein C that possesses anti-inflammatory and anti-thrombotic properties. It blocks the coagulation cascade, playing crucial role in the organ failure due to severe sepsis. However, the company withdrew its sepsis directed drug Xigris from all markets in 2011 claiming: "While there were no new safety findings, the study failed to demonstrate that Xigris improved patient survival and thus calls into question the benefit-risk profile of Xigris and its continued use," Timothy Garnett, Lilly's chief medical officer.

The identification of TLR4 as a sepsis target and the comprehension of its behavior permit to envisage novel modulators as drug against sepsis. Among the most important antagonists developed so far, are **CRX-526**, **E5531**, **E5564** (Eritoran) and **TAK-242** (Resatorvid). Eritoran and **TAK-242** reach clinical trials.

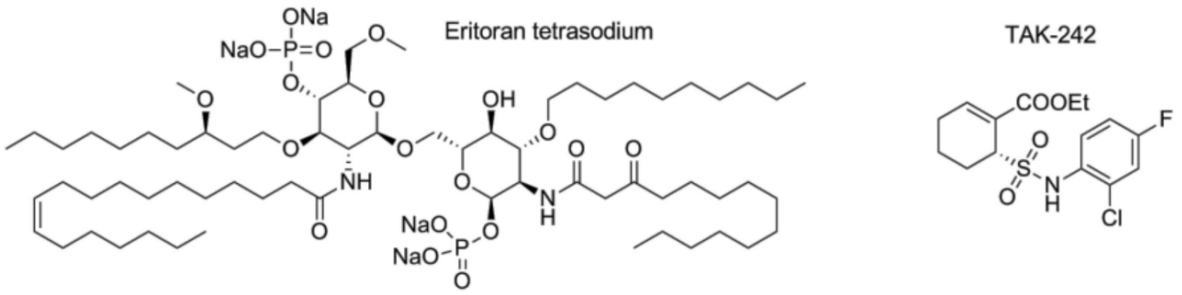

Figure 26. Chemical structure of Eritoran and TAK-242

Ethyl-(6R)-6-[N-(2-chloro-4-fluorophenyl)sulfamoyl]cyclohex-1-ene-1-carboxylate or **TAK-242** (Fig. 26) binds covalently to Cys747 of TLR4-TIR domain and blocks TLR4/TIRAP and TLR4/TRAM interactions.[158] TAK-242 was discarded in 2011 because it failed to suppress cytokine levels in patients with sepsis, sceptic shock or respiratory failure.[159]

The lipid A mimic, Eritoran (Fig. 26), binds to MD-2 as an antagonist. It prevents TLR4 dimerization by competing for LPS binding site.[29] Its clinical development conducted in patients with severe sepsis, was discontinued at Phase III, because it did not meet its primary endpoint of 28-day all-cause mortality.[84]

The research of new TLR4 antagonists for the cure of sepsis is still ongoing.

2. Other pathologies related to TLR4

As previously described, besides LPS-triggered TLR4 activation, TLR4 bind and is activated by endogenous DAMPs, initiating a pro-inflammatory response. Most of them are the endogenous molecules derived from damaged and necrotic tissues (sterile inflammation): fibronectins, small fragments of hyaluronan, high-mobility group box 1 (HMGB1) and even saturated fatty acids in response to cellular damage.[160–162] Therefore, this receptor not only plays a crucial role in LPS-related pathologies like septic shock, but also in many other inflammatory disorders mediated by DAMPs. In addition, a growing amount of data revealed that TLR4 expression is significantly higher in these pathologies, increasing the patient's sensitivity towards DAMPs.

While different LPS shares a conserved lipid A moiety with chemical determinants that ensure the optimal interaction with CD14 and MD-2, DAMPs are chemically diverse molecules and the roles of CD14 and MD-2 in the molecular mechanism of TLR4 activation by these molecules are not entirely understood.

1.1) Inflammatory Bowel Diseases (IBD), including Crohn's Disease and Ulcerative Colitis

An important role for TLR4 signalling in IBD pathogenesis was established through many studies over the last decade.[116] In normal intestine, tolerance towards the gut microbiota is maintained by keeping low levels of expression and activity of TLR4 and others TLRs.[159,163–165] Indeed, circulating monocytes can leave the peripheral blood to become resident macrophages of the intestinal mucosa, it modify their gene expression profile (by reducing the expression of surface CD14 co-receptor for instance) inducing higher tolerance to TLRs antigens.[29] Furthermore, different molecular mechanisms, such as receptors compartmentalization and negative regulation, attenuate or abrogate TLRs activation in gut mucosa.[116,166]

The IBD-associated gut dysbiosis and inflammation may alter TLRs expression and signalling.[116,167] Abrogation of TLRs inhibitory mechanisms (TLRs up-regulation) triggers downstream signal activation and consequently initiates immune responses against commensals.[168] In IBD-susceptible hosts, uncontrolled TLRs signalling generally contribute to destructive host responses and chronic inflammation, leading to many different clinical phenotypes.[169]

For example, the expression of TLR4 and its co-receptors (CD14 an MD-2) is significantly increased in intestinal epithelial cells and in lamina propria mononuclear cells collected from the lower gastrointestinal tract of patients with Crohn's disease (CD) and ulcerative colitis (UC), maximizing their sensitivity to microbial antigens.[170–172] However, even if aberrant TLR4 hyper-responsiveness towards commensals may be the result of microbiota composition variations in genetically susceptible hosts, the up-regulation may also reflect functional loss of receptor immune responses.[116]

Current medical therapies aim to induce and maintain remission as well as to prevent post-surgical recurrences. The type of pharmacological treatment is highly dependent on the stage of the disease, the condition of the patient and the body's ability to respond to a specific drug.[173] Patients with mild-moderate IBD are treated with aminosalicylates, while corticosteroids and antibiotics are preferably prescribed in case of moderate to severe diseases.[174,175] The cost of

these treatments is generally low but these drug can cause multiple side effects and, in many case, do not lead to clinical remission.[176] Table 2 presents and compares the main IBD therapies, their mechanisms of action and their adverse effects.

Treatment type	Related drugs	Mechanism of action	Features	Potentials adverse effects
Aminosalicylates	Mesalamine Olsalazine Balsalazide Sulfasalazine	Inhibition of IL-1, TNF-α, and platelet activating factor (PAF), decreased antibody secretion.	Locally immunosuppressive, nonspecific inhibition of cytokines; medium cost.	Headache, dizziness, dyspepsia, epigastric pain, abdominal pain, nausea, vomiting, and diarrhea.
Immunomodulators	Azathioprin 6-mercaptopurin Methotrexate	Blockage of *de novo* pathway of purine synthesis.	Antiproliferative effects, reduction of inflammation.	Black, tarry stools, bleeding gums, chest pain, fever, chills, swollen glands, pain, cough, and weakness.
Corticosteroids	Prednisone Methylpred-nisolone Hydrocortisone Budesonide	Blockage of phospholipase A2 in the arachidonic acid cascade altering the balance between prostaglandins and leukotrienes; stimulation of apoptosis of lamina propria lymphocytes; suppression of the transcription of cytokines.	High immunosuppression, risk of potential infections, adverse effects with long periods of use, low cost.	Full moon face, difficulty of healing, acne, sleep and mood disturbances, glucose intolerance, osteoporosis, osteonecrosis, subcapsular cataracts, myopathy, infections, acute adrenal insufficiency, myalgia, malaise, arthralgia or intracranial hypertension, and pseudorreumatism syndrome.
Biologicals: anti-cytokine drugs	Infliximab Adalimumab Certolizumab-pegol Golimumab Ustekinumab (phase 3 trial)	Induction of apoptosis in proinflammatory cells; binding specifically to TNF-α, blockage of the interaction the receptor.	Specific inhibition of cytokine, immunosuppression, high cost, advanced technology required.	Abdominal or stomach pain, chest pain, chills, cough, dizziness, fainting, headache, itching, muscle pain, nasal congestion, nausea, sneezing, weakness, vomiting, bloody urine, cracks in the skin, diarrhea, pain, fever, abscess, back or side pain, bone or joint pain, constipation, falls, facial edema, general feeling of illness, hernia, irregular heartbeat, unusual bleeding, weight loss, increased risk of reactivation of latent tuberculosis, and increased risk for developing infections and lymphoma.
Biologicals: anti-cell adhesion molecule	Vedolizumab Natalizumab	Inhibition of migration.	Specific inhibition of cell adhesion molecules high cost, advanced technology required.	Nasopharyngitis, headache and abdominal pain, increased risk of infections, serious infections, and progressive multifocal leukoencephalopathy (natalizumab).

Table 2. IBD treatments: drugs in use, mechanisms of action, and side effects.[173]

Many new therapies are currently in experimentation with the aim to improve patients' life quality.[173] The majority of these therapies are based on monoclonal antibodies (mAb) designed to specifically target pro-inflammatory mediators, particularly upregulated in the gut of IBD patients. Two main strategies are used, on one hand, Infliximab and Adalimumab which specifically target and neutralize TNF-α, a cytokine that plays a key role in maintain a persistent and prolonged state of inflammation in the gut mucosa.[177] On the other hand, Natalizumab (for

CD) and Vedolizumab (for CD and UC) selectively block lymphocyte-endothelial interactions preventing leukocytes migration and recruitment to inflamed districts.[178]

Even if mAb-based therapies represent a valid alternative to classical approaches with a specific and directed mechanism of action, the high cost of mAb prevents this therapy to be widely used. Furthermore, long-term biological molecules-based treatments may cause side effects like renal complications and trigger immunogenicity through the production of anti-drug Ab.[179,180]

The abrogation of TLR4-induced signaling by small-molecules antagonist of the TLR4/MD-2 complex remains a valid strategy not yet developed in the case of IBD.

1.2) Rheumatoid Arthritis (RA)

In the case of patients suffering of RA, it was showed that the peripheral blood monocytes and fibroblast cells express higher levels of TLR4 compared to cells of healthy patients.[181,182] In addition, the increased expression of TLR2 and TLR4 was recently demonstrated *in vitro* on differentiated macrophages from RA synovial fluid.[183]

This over-expression of TLRs allow the cells to strongly respond to the great amount of DAMPs present in the inflamed district and lead to a persistent state of inflammation.[184] Indeed, the presence of potential endogenous TLR ligands in the synovial tissue of patients with RA were identified, it includes fibrinogen, HSP 60 and 70 and EDA fibronectin.[185] HSP 22 was identified as another endogenous TLR4 ligand and expressed in the joints of patients with RA.[186] High Mobility Group Box chromosomal protein 1 (HMGB-1), a highly conserved nuclear protein stabilizing the nucleosome formation, is increased in RA synovial fluid, and is highly expressed in RA tissue macrophages.[187] The NF-κB activation induced by HMGB-1 appears to be mediated through TLR2, TLR4 and RAGE.[187,188] Furthermore, the extracellular matrix component biglycan is expressed in RA synovial tissue fibroblasts[185] and it has been shown to activate through TLR2 and TLR4.[189]

It was demonstrated that RA synovial fluids activated HEK293 cells expressing TLR4, suggesting that RA-synovial fluids contain TLR4 ligands.[190] RA synovial membrane cultures stimulates normal macrophages in a MyD88, Mal/TIRAP-dependent manner, which is consistent with an activation through TLR2 and/or TLR4.[191] Together, these observations suggest the presence of functional extracellular TLR4 and/or TLR2 ligands within the joints of patients with RA.

Type of TLR	Microbial Pathogen Associated Molecular Patterns (PAMPs)(1)	Potential endogenous TLR ligands (DAMPs) in RA	Defined source in RA (synovial tissue, cells or fluid)
TLR2 (dimerization with TLR1or 6)	Lipoglycans (Mycobacterium) Lipoteichoic Acids (Gram-positive bacteria) Peptidoglycan (Gram-positive bacteria) Zymosan (Yeast)	HSP 60	Macrophage(2), synovial tissue*
		HSP70	fibroblast(2), macrophage(2) synovial tissue
		gp96	fibroblast(2), macrophage(2), synovial tissue and synovial fluid(2)
		HMGB-1	synovial tissue macrophages, synovial fluid
		Biglycan	fibroblast(2)
		Serum amyloid A	serum, synovial tissue
TLR4	LPS (Gram-negative bacteria) Mannan (Candida) Envelope protein (Virus)	HSP22	synovial tissue, fibroblast
		HSP 60	Macrophage(2), synovial tissue
		HSP70	fibroblast(2), macrophage(2) synovial tissue
		EDA fibronectin	synovial fibroblast, synovial fluid
		fibrinogen	Synovial tissue, synovial fluid
		low molecular weight hyaluronic acid	synovial fluid
		HMGB-1	synovial tissue macrophages, synovial fluid
		Biglycan	fibroblast
TLR3	ds RNA (virus)	Undetermined	necrotic synovial fluid cells
TLR8	ss RNA(virus)	Undetermined	necrotic synovial fluid cells
TLR9	CpG motif (bacteria, virus)	immunostimulatory CpG motifs	serum

Table 3. Toll-like receptors and their ligands involved in RA

People with inflammatory arthritis are living full active lives thanks to disease-modifying antirheumatic drugs (DMARDs) For now, this condition cannot be cured but a combination of medications exist to protect the joints.

DMARDs are devided into two sub-families.

- The traditional DMARDs (Methotrexate, Hydroxychloroquine, Leflunomide, Mycophenolate mofetil and Sulfasalazine) restrict broadly the immune system and are often used in combination with methotrexate as the base. Methotrexate, or 4-amino-10-methylfolic acid, is a folic acid antagonist known to inhibits the reduction of folic acid and the proliferation of tissue cells. The adenosine signaling is the most widely accepted explanation for the methotrexate mechanism in RA: methotrexate increases adenosine

levels and, on engagement of adenosine with its extracellular receptors, an intracellular cascade is activated promoting an overall anti-inflammatory state [192]

- The targeted DMARDs (Tofacitinib) is a potent and selective inhibitor of the Janus Kinases (JAK) family, it inhibits the heterodimeric receptor signaling of cytokines associated with JAK3 and/or JAK1 and exhibits functional selectivity for cytokine receptors that signal via JAK2 pairs. Inhibition of JAK1 and JAK3 with tofacitinib attenuates interleukin (IL-2, -4, -6, -7, -9, -15, -21) and type I and type II interferon signaling.[193]

The treatment with direct TLR4 modulators are not available for this disease even if promising results comes from chaperonin 10, a small molecular weight heat shock protein, well tolerated and clinically effective in a study of patients with RA, providing proof that the TLR pathway is important in the pathogenesis of RA.[194]

1.3) Atherosclerosis, vascular inflammations and cardiovascular diseases

Atherosclerosis is characterized by a local and chronic inflammation of the vascular wall resulting in the accumulation of lipids and macrophage-derived foam cells in the sub-endothelial compartment.[195] Even if the inflammatory nature of the disease process has been widely accepted, the precise components of the atherogenic pro-inflammatory cascade is still controversial.

The TLR4 involvement in various cardiovascular diseases has been widely described.[196,197] Epidemiologic studies have shown that bacterial infection and atherosclerosis are connected, suggesting a link between atherosclerosis and TLRs activation. Experimental data are in line with the clinical findings since several TLRs (TLR1, 2, 4 and 5) are expressed in atherosclerotic plaques by leukocytes and resident cells that migrate into the arterial wall.[198,199] Notably, TLR4 levels can be upregulated by pro-atherogenic proteins such as oxidized LDL.[200]

TLRs are not only expressed and functional in immune or vascular cells but they are also readily detectable in cardiac myocytes. Among the classes tested so far, TLR2, 3, 4 and 6 are expressed in cardiac myocytes, whereas TLR1 and 5 are not.[201,202] TLR4 activation has been shown to reduce apoptosis of cardiac myocytes through an effect mediated by nitric oxide synthase[203] suggesting that TLR4 signaling could be important for development of myocardial diseases (Fig. 27). The importance of myocardial TLR4 signaling was first established *in vivo* in septic cardiomyopathy,[204] and extended to ischemia–reperfusion injury,[205] heart failure[201,206] and cardiac hypertrophy.[207]

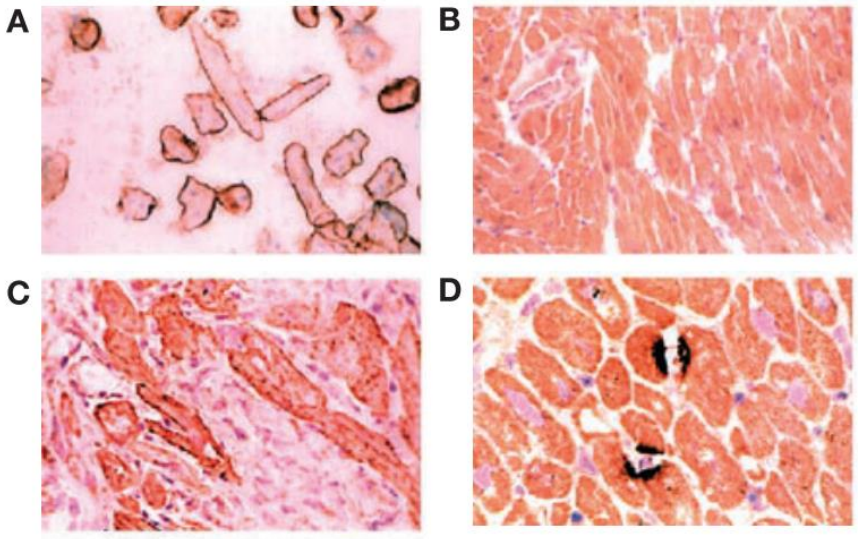

Figure 27. Toll-like receptor 4 expression in rat, murine and human myocardium (**A**) Primary isolates of adult rat ventricular myocytes 24 h after isolation, stained with a pAb targeted to a TLR4-specific epitope adjacent to the cytoplasmic hTLR4 TIR domain. (**B**) Normal murine cardiac muscle (×200 magnification) exhibits diffuse, homogeneous myocyte staining. (**C**) Cardiac myocytes adjacent to an area of ischemic injury induced by coronary artery ligation exhibit intense sarcolemmal TLR4 staining. (**D**) Cardiomyocytes from humans with dilated cardiomyopathy displayed intensely stained focal expression of TLR4.

The effectiveness of immune response inhibition in primarily non-immune-related diseases has not yet been established. Although experimentally well proven, inhibition of immune responses in cardiovascular non-immune diseases has failed in clinical practice. The role of TNF has been extensively studied experimentally in the context of heart failure, giving evidence that excess of TNF increases the progression of heart failure. However, several clinical trials failed to demonstrate a clinical improvement with TNF inhibition in patients with heart failure.[208] The trial of the complement cascade inhibition by an anti-C5 complement Ab, although experimentally protective in ischemia-reperfusion injury, had no effect on patients treated with fibrinolysis for acute myocardial infarction.[209] Recent studies revealed that a specific treatment, based on anti-TLR4 Ab, ameliorated the pathological phenotype.[210] Further studies will however be needed to develop it as a clinical drug.

The failure of immuno-suppressive studies in cardiovascular diseases is related to the fact that activation of the immune system under these circumstances is a double-edged sword: an intact immune system is necessary for many protective pathways, but prolonged immune activation activates unfavorable signal cascades, allowing disease progression. The major challenge faced is to limit the effect of detrimental innate immune responses while simultaneously maintaining the adequate and appropriate innate immune defense mechanisms. Fine tuning of TLR4 signaling with suitable antagonists seems an interesting way to address this issue.

1.4) Obesity-linked type II diabetes

In order to investigate a possible link between TLR4 signaling and obesity, two mouse models of TLR4 expressing cells were generated, they are either deficient in hepatocyte (Tlr4LKO) or in myeloid cell (Tlr4ΔmΦ).[119] This strategy allowed to discover that hepatocytes are important mediators of diet-induced inflammation via TLR4 pathway. Surprisingly, the removal of TLR4 from macrophages did not reduce the levels of circulating inflammatory cytokine. It suggests a compensatory mechanism increasing TLR4 expression in other cell types (dendritic cells, B cells or endothelial cells) which contributes to this elevated inflammatory response.[119]

Many studies were conducted to reveal the ligands responsible of the TLR4 activation in diet-induced obesity. It was found that both type II diabetic patients and obese mice models exhibited high levels of LPS in plasma.[211] Further analysis revealed that both high-fat and high-fructose diets influence the amount of circulating LPS by altering the growth and composition of gut microbiota[212] and gut epithelial permeability.[213,214] Even if the mechanisms increasing the LPS plasma levels in obese subjects are not clarified, it seems that diet-introduced lipids promote the incorporation of LPS into chylomicrons, favouring its absorption by gut enterocytes.[118] This event strongly contribute to postprandial endotoxemia resulting in a persistent and systemic pro-inflammatory stimulation of TLR4 singalling.[215]

As in the case of RA, expression of TLR4 is increased in obesity-linked type II diabetic subjects suggesting a pivotal role of this receptor in the pathogenesis of insulin resistance and diabetes. Moreover, chronic, low-grade inflammation is one of the main characteristics of obesity leading to an increased production of pro-inflammatory mediators thought to contribute to the onset of the disease. Studies conducted on $TLR4^{-/-}$ mice showed that its absence reduced the diet-induced insulin resistance and inflammation.[216] TLR4 is expressed in many cytotypes of insulin target tissues: liver, adipose tissue, skeletal muscle, vasculature, pancreatic β cells, and brain. Thus, the TLR4 activation in these districts can mediates the insulin action both directly, through pro-inflammatory kinases activation and ROS production, and indirectly, via activation and release of pro-inflammatory insulin-desensitizing factors.[215] Furthermore, recent works reported that mutations inhibiting the TLR4 activity allow type II diabetic mice to be protected against endothelial dysfunction and hyperglycemia.[217]

No specific drugs, targeting TLR4, are yet developed for obesity-linked type II diabetes but evidences point toward their possibility to be interesting solutions for the mediation of TLR4-induced inflammation.

1.5) Neuroinflammatory disorders, neuropathic pain, Amyotrophic Lateral Sclerosis (ALS)

In the central nervous system, TLR4 is localized on microglia and protects neurons from invading microorganisms. However, the presence of typical amyloid protein aggregates due to neurodegenerative diseases are able to trigger a potent TLR4-dependent inflammatory and neurotoxic response that exacerbates the disease.[130] This observation was confirmed by the fact that loss-of-function mutation in TLR4 gene strongly ameliorate neurotoxicity.[218] This part will be widely described below, within the description of **FP7** (Chap VIII).

VI. TLR4-directed therapies

The potential of targeting TLRs is illustrated by existing small-molecule agonists of TLR7 (**Imiquimod**) that have shown efficacy in the treatment of viral infections, such as human papillomavirus.[219] In addition, a novel TLR8 agonist (**VTX-2337**) has shown promises in Phase I clinical trials against metastatic head and neck cancers, and it has now entered Phase II clinical trials.[220] By contrast, small-molecule antagonists of TLR8 effectively inhibit TNF production in synovial explants and could replace TNF-targeted biological agents in the treatment of rheumatoid arthritis.[221] Targeting the post-receptor pathway is also feasible, cell-permeable peptides that inhibit the interaction of TRIF and TRAM in the TLR4 pathway are effective in a murine models of sepsis and thus are candidate therapeutics for human endotoxic shock.[222] The importance of phosphorylation in the assembly of the signaling complex raises interesting possibilities for the pharmacological manipulation of myddosome assembly. This may also be affected by the presence of tissue-specific variants of IRAK-1 and IRAK-4, which could also influence TLR signaling.

As described, the majority of the TLR4-related pathologies are still lacking specific pharmacological treatment. Therefore, targeting the TLR4 pathway arises growing interest in the last decades.[223] As TLR4 is a complex target involving many adaptor proteins, several approaches may be envisaged to treat the TLR4-mediated inflammatory disorders.[224] The main methods employed for TLR4 modulation are:

- TLR agonists for the development of adjuvant vaccines
- Neutralization of LPS by LPS sequestrants
- Inhibition of LPS interaction with up-stream receptors (LBP and CD14)
- TLR4 antagonist competing with LPS for MD-2 binding
- Down-stream modulators, targeting the intracellular second-messengers.

1. TLR4 agonist as immunostimulants and vaccines adjuvants

According to their potent immunogenicity, Lipid A or partial lipid A structures, may find applications as vaccine adjuvants. Indeed, the activation of the immune responses without deleterious effects is the purpose of vaccines. After the discovery of the natural role of TLR4 in controlling a large number of infectious diseases and its ability to pass by either MyD88-dependent or TRIF-dependent pathways, significant interest has been given to the development of lipid A-like agonists targeting TLR4 for their use as adjuvants in vaccine formulations.

Moreover, TLR4 has been shown to play a non-redundant role in eliciting the maturation of dendritic cells (DC). It is a vital component to adjuvant-mediated vaccine-antigen immunogenicity since DCs play a significative role in priming naïve T cells and initiating immune responses.[225]

Vaccines can be prophylactic, administered to reduce or prevent the development of a future infection by a wild-type pathogen, or therapeutic, with the aim to cure a particular pathology. The active principle of a vaccine is an antigenic substance, prepared from the causative agent of a disease or a synthetic substitute, used to provide immunity against one or several diseases. The formulation commonly used in the production of vaccines include a suspending fluid (sterile saline water or fluids containing protein); preservatives and stabilizers (excipients: albumin, phenols, glycine…); and adjuvants that help to improve the vaccine's effectiveness.

The word "adjuvant" comes from the Latin word *adiuvare*, meaning to help or aid. An immunologic adjuvant is defined as any substance that acts to accelerate, prolong, or enhance antigen-specific immune responses when used in combination with specific vaccine antigens.

Early studies demonstrated that the LPS of Gram-negative bacteria cell wall was a potent adjuvant when delivered with protein antigens.[226] However, the administration of LPS or its biologically active component "lipid A" caused strong systemic responses and these bacterial extracts were considered too toxic to be used as adjuvants for human vaccines. Then, subsequent efforts have been focused on research to chemically modify the LPS/lipid A in an attempt to generate compounds with no-toxicity while keeping the desired immune stimulatory activity.

In the 1970s, the first success in the chemical modification of LPS permit to obtain a mixture composed of Monophosphoryl hexa-acylated lipid A, called 4'MPL or **MPL**, as the major component. It showed a greatly reduced pyrogenicity while maintaining the immune stimulatory activity.[227]

This mixture was further purified resulting in a clinical-grade version currently manufactured by GlaxoSmithKline (GSK) biologicals. It is used in the widespread vaccines FENDrix® (GSK Biologicals) for hepatitis B and Cervarix® (GSK Biologicals) against HPV (human papillomavirus).

However, despite achieving significant success as vaccine adjuvant, the use of **MPL** still faces several challenges. The product, purified from *S. minnesota*, is highly heterogeneous in its acylation state, it contains a mixture of tetra-, penta- and hexa-acylated MPL which induce major differences in term of potency on human immune cells.

Since the acylation state drastically affects the biological activity, a careful verification of the **MPL** composition is imperative to maintain a consistent end-product. However, even if

nowadays the most active component of **MPL**, hexa-acylated **MPL**, could be obtained as a pure compound from chemical synthesis, the **MPL** mixture obtained from *S. minnesota* is still the one used in vaccines. The choice of the manufacturing company was probably guided by important drawbacks of the synthesis, in particular, the difficulty and cost of the synthesis and purification as well as tremendous trouble encountered during scale-up.

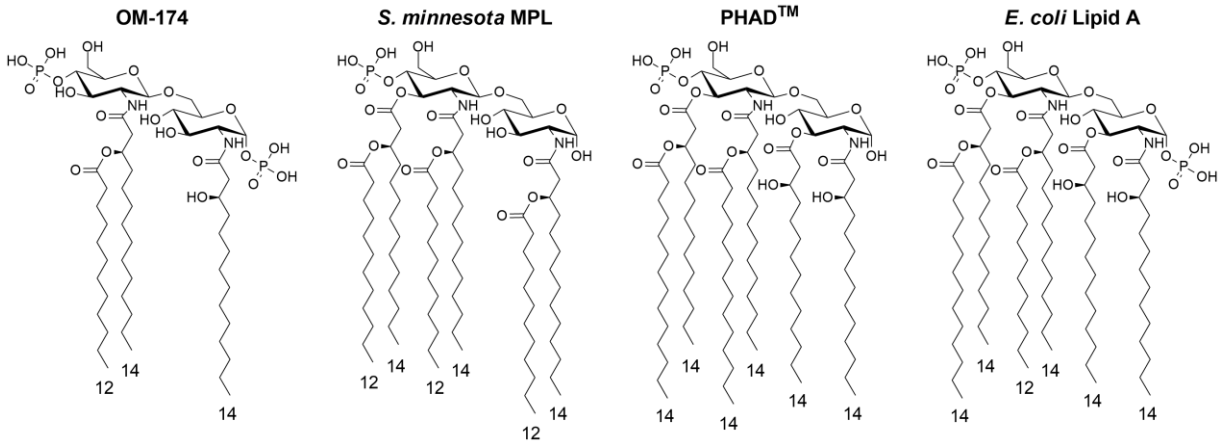

Figure 28. Structure of the lipid A and derivatives used as vaccine adjuvants

Two major compounds were developed through the years, **OM-174** which is a diphosphoryl, triacyl disaccharide lipid A derivative was developed by OM Pharma (Meyrin, Switzerland) and is currently in Phase I clinical trial for the treatment of cancer, this compound is as well extracted from *E. coli*. In addition, the *E. coli* lipid A disaccharide itself is currently evaluated as vaccine adjuvant. Extracted from *E. coli* cell pellets by the company WRAIR, their lyposomic formulation is currently tested in Phase II clinical trial against malaria.

As discussed for **MPL**, despite the huge chemical synthesized panel of lipid A analogues, no synthetic lipid A compound underwent clinical evaluation as vaccine adjuvants until recently. Mostly because of the manufacturing issues of this class of compounds.

The only disaccharide currently in clinical evaluation in **PHAD™**, also referred to as "synthetic MPL", which is completely homogeneous and composed of a Monophosphoryl disaccharide with six C14 fatty acid (FA) chains asymmetrically distributed (4+2) as in *E. coli* lipid A. **PHAD™** has been developed by the USA Infectious Diseases Research Institute (IDRI) in 2011 and then has been manufactured by Avantis Polar Lipids (USA). The synthetic lipid was shown to be 10- to 100-folds more active than *S. minnesota* RE595-derived MPL on human monocyte-derived DCs. The difference in the activity has been attributed to the lack of tetra- and penta-acylated lipid A compounds that contaminate **MPL** derived from natural sources while not present in synthetic MPL. Early results from clinical trials of **PHAD™** indicate excellent safety

profiles that are accompanied the enhancement of antigen-specific responses.[228] **PHAD™** has been tested in a phase I clinical trial against influenza and is in preclinical development as an adjuvant for vaccines against tuberculosis, leishmaniasis, schistosomiasis and hookworm.
Being so little the number of disaccharides that entered clinical evaluation and being so difficult and cost-demanding their synthesis, TLR4 antagonists with a monosaccharide have been also developed as vaccine adjuvants. Of the eight adjuvants currently approved for vaccines or in clinical evaluation, three of them are monosaccharide-based compounds: **RC-529**, an amino alkyl glucosaminide 4-phosphates (AGPs), **ONO-4007**. The activity and chemical structures of **RC-529** and **ONO-4007** and **PET lipid A** will be discussed in the section monosaccharides based TLR4 modulators (Chap. VII section 3.3).[225]
Summarizing the results obtained until now, it can be concluded that TLR4 agonists represent a safe and effective class of molecules that have demonstrated to possess interesting potential as vaccine adjuvants

2. TLR4 and cancer

Finally, TLR4 modulation also found application in the treatment of cancer and represents an important application of immunostimulants. Non-toxic TLR4 agonists are potential candidates as anticancer agents since the activation of macrophages and induction of cytokines secretion, particularly tumor necrosis factor alpha (TNF-α), are implicated in host defense against cancer. Therefore, immunostimulants have been studied and clinically tested as antitumoral agents.[225], [229] Antitumor polysaccharides and bacterial-derived agents such as LPS have been shown to induce intra-tumoral TNF production, corresponding to their individual antitumor activity.[230] Different types of lipid A, total and partial structures, have been tested for this application. One example is **ONO-4007** which entered phase I clinical trials with this purpose. Lipid A monosaccharide mimetic **PET-lipid A**, thanks to the remarkable results shown, has already proceeded till phase III clinical trials in liposomal formulation for the treatment of cancer.

3. LPS sequestrants

Inactivation of LPS may occurs with the use of compounds that binds and sequesters it, thus abrogating its activity. It is a promising approach against sepsis as well as many more

inflammatory diseases related to increased bacterial translocation and in many infectious diseases mediated by LPS.[231]

A variety of cationic synthetic LPS-sequestering agents have been developed and reviewed exhaustively by David and co-workers.[232] The amphiphilic nature of lipid A enables it to interact with a variety of cationic hydrophobic ligands. Various proteins such as LPS-binding protein (LBP), bactericidal/permeability-increasing protein (BPI) and limulus anti-LPS factor (LALF) have a strong affinity for LPS and display antimicrobial activity against Gram-negative bacteria. Synthetic peptides based on the putative LPS-binding domain of LBP, BPI and LALF proteins, were specifically designed and synthesized to target Gram-negative bacteria. Cationic antimicrobial peptides with diverse structures binds LPS and suppress its ability to stimulate TLR4-dependent cytokine production.[233,234] Polymyxin B (PMB) is a membrane-active peptide antibiotic that binds to LPS and inhibits its toxicity *in vitro* and in animal models of endotoxemia. Approved for clinical use in Japan in late 2000, PMB provides a clinically validated proof-of-concept of the therapeutic potential of sequestering circulation LPS.[235]

A major goal over the past decade was to develop small-molecules analogues of PMB that would sequester LPS with similar potency while non-toxic and safe, so to be used parenterally for the prophylaxis or therapy of sepsis. To this end, various class of synthetic cationic amphiphiles were developed including acyl and sulfonamido-homospermines (Chap. VII section 4.4).

4. LBP/LPS and CD14/LPS interaction inhibitors

Inhibition of LPS-LBP and/or LPS-CD14 interactions was envisaged as another promising strategy. Using LBP or CD14 ligands that bind to a vicinal (allosteric) or identical binding site of LPS lipid A or polysaccharide O-chain should preclude TLR4 signaling. Indeed, although LPS is the most studied and characterized ligand, CD14 interacts with many other molecules.[231] For example, both LBP and CD14 are able to bind lipoteichoic acid (LTA) derived from *Bacillus subtilis*. Additionally, the whole bacteria are recognized by CD14 in an LBP-dependent reaction, but only after pre-incubation with serum. As well, CD14 is important to enhance the recognition of soluble peptidoglycans (PGN), recognized by TLR2.[236]

In vitro studies provide evidences that the PGN binding interface on CD14 can overlap with the binding site of LPS polysaccharide O-chain, although the biological relevance of PGN binding to CD14/TLR2 is under debate. It was demonstrated that PGN competes with LPS for binding to CD14, then PGN and LPS binding sites must overlap, at least partially.[237] The glycoconjugate preparation from *Treponema spirochetes* inhibited the interaction of TLR4 ligands (lipid A,

LPS, Taxol) and TLR2 ligands (PGN) with LBP and CD14, acting as an antagonist of the corresponding TLR4 or TLR2-dependent pathways.[238] Our group also developed synthetic cationic amphiphiles who belong to this category, they will be discussed in the next chapter.

VII. General trend and common features for TLR4 modulators

Through the years, numbers of different studies were conducted to rationalize the behavior of TLR4 modulators. The following part will describe the correlation between the biological activity and the supramolecular shape of the compounds (state of aggregation). In addition, the information grasped from SAR and ligand base design of TLR4 modulators will be discussed.

1. Role of aggregates in TLR4 activation

Since natural lipid As and their synthetic analogues are amphiphilic compounds with long hydrophobic chains and polar phosphate heads, they are expected to form micelles in solution, above their critical micellar concentration (CMC). LPS has been reported to form very stable supramolecular micellar aggregates in solution, with very low CMC values, estimated in the pM range.[239]

Micelles or supramolecular aggregates may have different 3D shapes and these shapes may, in turn, influence the availability of the lipid A or its interaction with TLR4 and co-receptors. Several studies have been performed through the years to determine lipid A aggregates shape. It was expected to find a correlation between the molecular structure of the compounds and their shape in solution. However, it was surprising to see that even small variations in the structure of lipid A molecules, that means a change in number, length or type of the FA chains, as well as the number of anionic groups, can modify the shape of the aggregates from lamellar to cubic or hexagonal. It was even more relevant to discover that the already known correlations between molecular structures and activity of lipid As insert themselves into specific correlations between aggregates shape and activity.[240,241]

Using conformational energy calculations, TEM and X-ray investigations, it has been demonstrated that the most powerful immune-stimulator (*E. coli* lipid A), with six FA chains asymmetrically distributed and two phosphate groups, possesses a non-lamellar structure. Contrariwise, the inactive or antagonist lipid As from *Rb. Capsulatus* and *C. violaceum*, respectively tetra- and penta-acylated, adopt lamellar structures.[242] Moreover, monophosphoryl lipid A and lipid A from *Campylobacter jejuni*, which have intermediate activities, assume a mixed lamellar/cubic structure.

Defining their molecular shape in solution and relating it to the different types of aggregates created the first consensus regarding the correlations between aggregation state and activity.[243–245]

Computational calculations studies showed that the minimum energy conformation of the different types of lipid A are related to the "tilt angle": angle formed between the glucosamine backbone and the FA chains (packed almost parallel to each other, Fig. 29).[242]

This angle, determined by ATR spectroscopy using polarized light, showed that *E. coli* lipid A, that forms non-lamellar aggregates, has an tilt angle > 50°, thus defining a conical molecular shape.[246] For the species with lamellar aggregates, the tilt angle was found < 25°, thus generating a cylindrical shape. These species include lipid IVa, the penta-acylated and the symmetrically (3+3) hexa-acylated species of *Rhodobacter sphaeroides* and *Rhodobacter capsulatus.* Specie with an intermediate tilt angle (between 25° and 50°), as Monophosphoryl lipid A, present intermediate conformations.

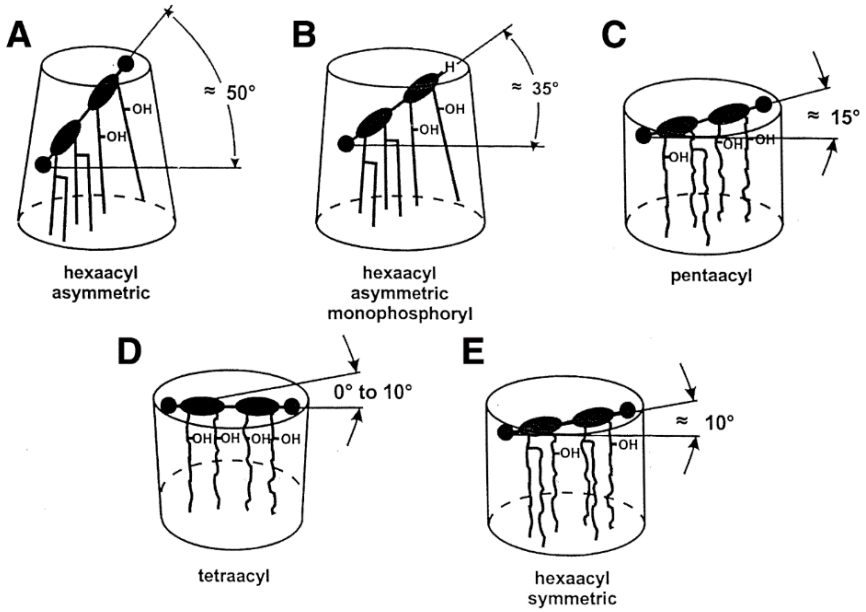

Figure 29. Intrinsic conformations several lipid As: (A) endotoxically highly active *E. coli*-type lipid A, (B) medium active monophosporyl lipid A, and inactive, (C) antagonistic pentaacyl lipid A, (D) tetraacyl lipid A and (E) lipid A from *C. violaceum.*

It strongly suggests that the active agonist molecules assume a conical shape in solution, with the hydrophobic chains distributed on higher area with respect to the polar part of the molecule (sugar core with phosphates). Contrariwise, this area is similar for the cylindrical inactive/antagonist molecules.

Further studies on glycolipids (GLs) permit to understand that the temperature strongly influences the shape of the aggregates as well (Fig 30).[244]

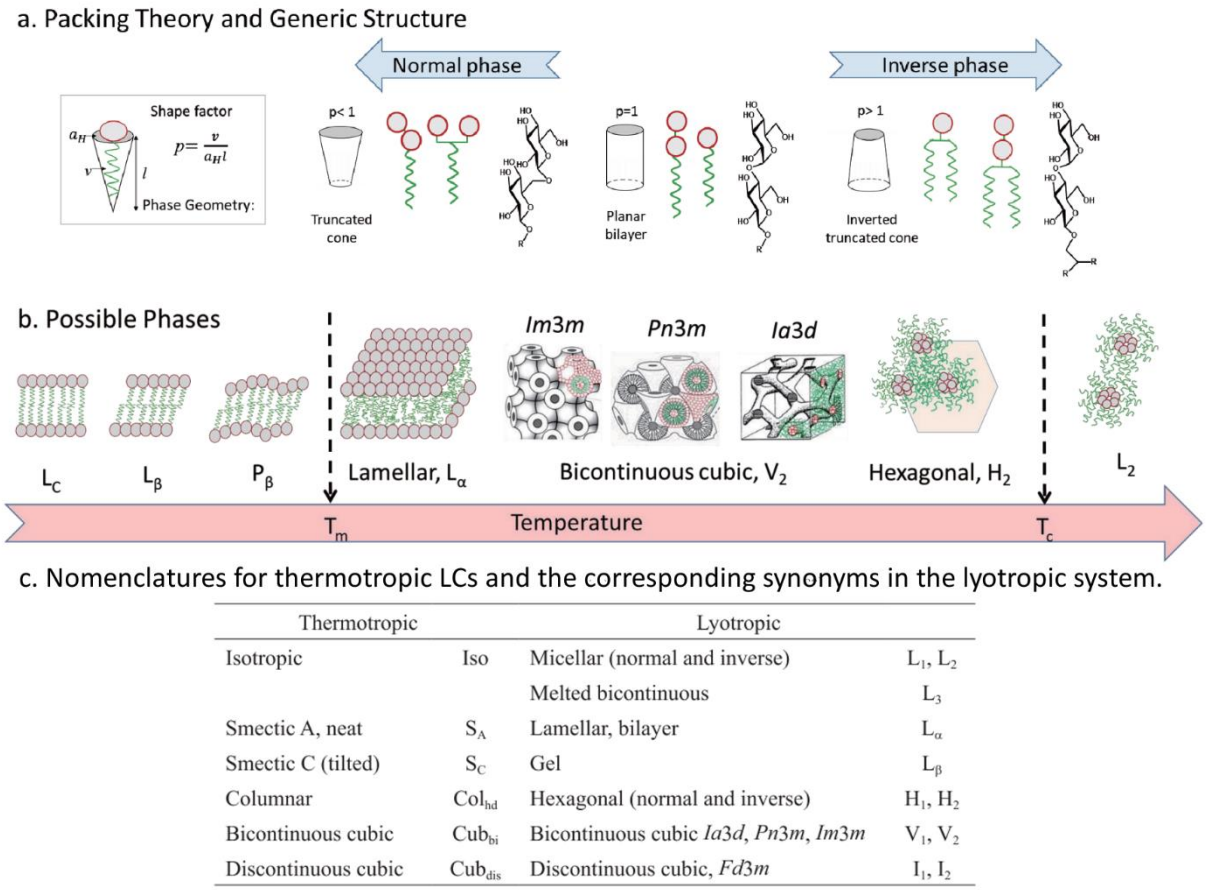

c. Nomenclatures for thermotropic LCs and the corresponding synonyms in the lyotropic system.

Thermotropic		Lyotropic	
Isotropic	Iso	Micellar (normal and inverse)	L_1, L_2
		Melted bicontinuous	L_3
Smectic A, neat	S_A	Lamellar, bilayer	L_α
Smectic C (tilted)	S_C	Gel	L_β
Columnar	Col_{hd}	Hexagonal (normal and inverse)	H_1, H_2
Bicontinuous cubic	Cub_{bi}	Bicontinuous cubic *Ia3d*, *Pn3m*, *Im3m*	V_1, V_2
Discontinuous cubic	Cub_{dis}	Discontinuous cubic, *Fd3m*	I_1, I_2

Figure 30. Generic glycolipids (GLs) structures, possible liquid crystals (LCs) phases and nomenclature (**a**) The packing theory[247] that predicts phase based on the shape factor; and the possible generic structures of GL[248] with a few selected examples and (**b**) Possible LC phases for GL, where only the inverse types are drawn, although normal phases (V1, H1 and L1) are also possible. (**c**) Nomenclatures for thermotropic[249] LCs and the corresponding synonyms in the lyotropic[250] system. Both are used in literature.

GLs are "amphitropic" (IUPAC recommended terminology[251]): able to self-assemble in dry state (thermotropic) as well as solvated (lyotropic)[252]. Due to the amphoteric behavior of sugars, the term "amphotropic" is also widely used for carbohydrate LCs.[253] These thermotropic GLs are able to form a range of self-assemblies (Fig. 30) as a function of molecular structures. Since these are thermally driven LC, a thermotropic nomenclature was adopted: bilayer or lamellar shapes are named "smectic" while hexagonal shape is named "columnar".[249] However, these are amphiphilic materials, and the lyotropic nomenclature is more suitable since it is capable to describe more complex phases (Fig. 30c).[250] The type of phase formed by a lipid can be predicted from the critical packing parameter or shape factor (p).[247] The equation is given as $p = \upsilon / \alpha_H l$ where υ is the volume of the hydrophobic chain, α_H is the interfacial area occupied by the hydrophilic head group, and l is the length of the hydrocarbon chain. Lamellar phases are predicted when $p < 1$ and if it is equal to one. On the other hand, if $p > 1$, it will give micellar structures. In lyotropic systems, the normal phases are also referred to as the water continuous-

phases, assuming water as solvent. On the contrary, the reverse phases are the hydrocarbon chain-continuous phases. For non-lamellar structures, the lyotropic nomenclature distinguishes the normal and the inverse phases with the subscripts 1, and 2 respectively. For example, the dry columnar phase may be labelled as H_1 for normal hexagonal while it would be labelled H_2 for an inverse hexagonal structure. Recent studies of dry GL thermotropic phases (lamellar, hexagonal and bi-continuous cubic) including molecular dynamics using dielectric spectroscopy[254,255] established the tilted organization of bilayer.[256,257] Some fundamental ideas have emerged from thermotropic studies of GLs such as the fact that the cubic phases may be induced by mixing the hexagonal and lamellar phases.[258]

Furthermore, DFT studies demonstrate that electron density distribution of the sugar ring is different when viewed from the top or the bottom.[259] The sugar amphoterism has direct consequences to lipidic heterogeneity in cell membrane. Moreover, saccharide have been reported binding to aromatic groups (Tyr, Phe and Trp) of proteins, it strongly suggests that sugar-lipid interactions occur.[260] The sugar-lipid interaction seems to support the lipid flip mechanism, essential for apoptosis process in cell membrane system.[261] Therefore, studies of dry GL self-assemblies uncovered some basic knowledge, important for the hydrated systems.

Correlations between the aggregate structures and the biological activities can be extended to synthetic lipid A mimetics since it has been observed for some of them to date (tri-acylated monosaccharides, GLA compounds and phospholipids with non-sugar backbone).

Summarizing what was previously stated, molecular structure, molecular shape, aggregate shape and biological activity correlations can be expressed as follow:[242]

- The compounds assembling as non-lamellar (Q and H_2) structures (conical conformation) such as enterobacterial hexa-acyl lipid A have an important tilt angle (> 50°) and are highly active as TLR4 agonists.
- Lipid A adopting lamellar structures (cylindrical conformation) such as *Rb. Capsulatus, C. violaceum*, tetra- and penta-acylated lipid As, are antagonist or inactive and have a very low tilt angle (0 to 15°).
- Those assuming mixed lamellar/cubic structures (partially conical conformation such as MPLA an lipid A from *Campylobacter jejuni*) have intermediate activity and a higher inclination angle (≈ 25°).
- The inactive lipid A samples adopting lamellar structures were found to act as efficient antagonists against biologically active LPS if sufficient negative charges are present on the backbone.

- Uncharged lipid A with lamellar structures such as lipid A from *Rhodomicrobium vannielli* and de-phosphono hexa-acyl lipid A turned out to be neither agonists nor antagonists.
- The temperature impacts the aggregate shape of such amphiphilic compounds, transition may be envisaged between micellar and lamellar shapes as well as hexagonal and micellar inversed. It may find applications for the generation of well-shaped aggregates enhancing the interaction between receptors and macromolecular structures.

The role of the aggregate shape in the interaction with TLR4 has been extensively studied in search of rationalization. However, it is still on debate whether the correlation of aggregates shape with activity is related to the binding with receptors upstream (LBP or CD14), with TLR4/MD-2 heterodimer or to unspecific intercalation into the cell membrane.
In the later stage of such intercalation, which seems to happen to some extent, it was showed that active forms of aggregates induce activation of transmembrane ion channels (like MaxiK), which in turn enhance the influx of potassium ions.[262–266] These ions would, in principle, exert their effects on intracellular caspases which are important proteins of the so-called non-canonical inflammasome. Moreover, the intercalation could exert an effect on the TLR4/MD-2 complex dimerization by inhibiting or accelerating the process.
Another crucial information emerging from these studies is that the addition of substances like peptides, protein or other agents, which strongly reduce the immunoactivity of LPS, also cause a conversion of the non-lamellar cubic structure of lipid A into the lamellar one. This was found to be true for lysozyme, lactoferrin and polymyxin. Moreover, the addition of chlorpromazine (CPZ) to the antagonistic pentaacyl lipid A of *E. coli*, which led to the conversion from lamellar to inverted cubic aggregates also resulted in the switch of its activity to agonism.[87]

Highlighting the importance of the aggregate shapes in solution has however had a great impact in the field of TLR4 since it gave an explanation to the different biological activities (agonism, antagonism or inactivity) observed for lipid As. The correlations outlined have then been confirmed by X-ray studies in which MD-2 was crystalized with natural and synthetic ligands. It permits to define the binding-activity relationship of MD-2 with several lipid As. On the contrary, in the field of monosaccharides molecular simplification of lipid A, where little is known about MD-2 binding-activity relationship, it still constitutes a key explanation.

2. SAR-based drug design

The following sections will be focalized, first, on the disaccharides as agonists and, then, on monosaccharides. Each of the section describes the SAR of the compounds as agonist and, then, as antagonists.

1.1) SAR of the disaccharides

According to the previous sections, studies of TLR4 recognition process as well as determination of the biological activity of endotoxin (lipid A, LPS and LOS) and synthetic TLR4 modulators permit to define two key factors modulating TLR4 signaling:

- The interaction of lipid A/LPS monomer with MD-2, favorizing (or not) $[TLR4/MD\text{-}2]_2$ dimerization process.
- The 3D structure of lipid A/LPS aggregates, that very likely influences the firsts steps of LPS recognition process, involves LBP and CD14 proteins.

First of all, it must be stated that murine immune-stimulants (TLR4 agonists) may be antagonists in human, while usually an agonist in human is also an agonist in murine. While murine and human TLR4 have 62.4% sequence identity and are therefore expected to have highly homologous structures, however, small variations induce important modifications. The species-specific recognition has been elucidated (Fig. 31) and seems dependent of the intrinsic composition of the MD-2 proteins. The slight differences found between human MD-2 (hMD-2) and murine MD-2 (mMD-2) revealed the reason why **lipid IVa** behave as an antagonist in human while being agonist in murine.

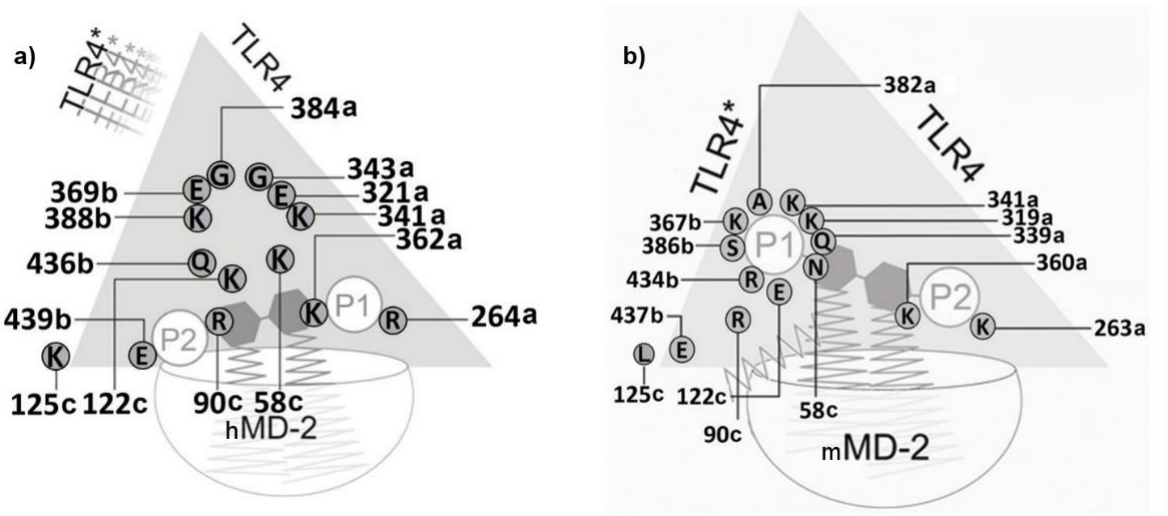

Figure 31. Schematic view of the computed side chain interactions of TLR4/MD-2 complex with Lipid IVa (**a**) human TLR4/MD-2 conplex, (**b**) murine TLR4/MD-2 complex.[267]

Computational studies pointed out the receptor antagonistic action of Lipid IVa in the human system (Fig. 31a) as well as the agonistic action of **Lipid IVa** in the murine system (Fig. 31b) **Lipid IVa** binds with an inverted (flipped) orientation in the two species and it was proposed that the indicated charged/polar side chains of TLR4* form a "repulsive region" preventing the association of two [TLR4/MD-2/**Lipid IVa**] complexes in the human system. Indeed, **lipid IVa** does not provide the dimerization into an active m-shaped receptor complex and acts as a competitive inhibitor of LPS/lipid A. The counter-subunit (TLR4*) is leaving or never was in place, as indicated by the shaded label of TLR4* (upper left side of wedge). On murine systems, **lipid IVa** appeared less buried inside MD-2 hydrophobic pocket, allowing a FA chain to accommodate outside of the pocket, at the dimerization interface. Furthermore, the flipped conformation seems to favor the upward shift of the phosphate residue (1-PO_4) at GlcN-I into a bridging position formed by a cluster of residues of TLR4, MD-2 and TLR4*. It was in complete agreement with the current consensus model of agonist-induced TLR4/MD-2 dimerization (**lipid IVa** itself will be described extensively further).[267,268]

- **TLR4 agonism**

The features defining an agonist, activator of the TLR4/MD-2 complex and subsequent intracellular signaling both in human and murine, have been actively sought. Nowadays, it is commonly accepted that three structural features are fundamentals for the agonist activity of a disaccharide on TLR4/MD-2 complex:

- The presence of six acyl chains, allowing a chain to protrude outside of the MD-2 pocket and providing the hydrophobic surface necessary for the interaction with the TLR4*/MD-2* complex nearby.

- The presence of two phosphate groups (anionic moiety) to interact with the positive residues at the rim of the MD-2 pocket (one phosphate may be sufficient to induce a lower immune-stimulation).
- A conical shape of the molecule in solution, forming cubic (V_2) or hexagonal (H_2) supramolecular micellar aggregates. The six acyl chains should be asymmetrically distributed (3 + 2) since it was observed that a symmetrical distribution rather generates cylindrical compounds.

Structural variations of *E. coli* lipid A were analyzed, for instance, the number, length and position of the acyl chains as well as the number of phosphate groups. Most of the modifications resulted in a reduced or absent activity (Fig. 32).[269]

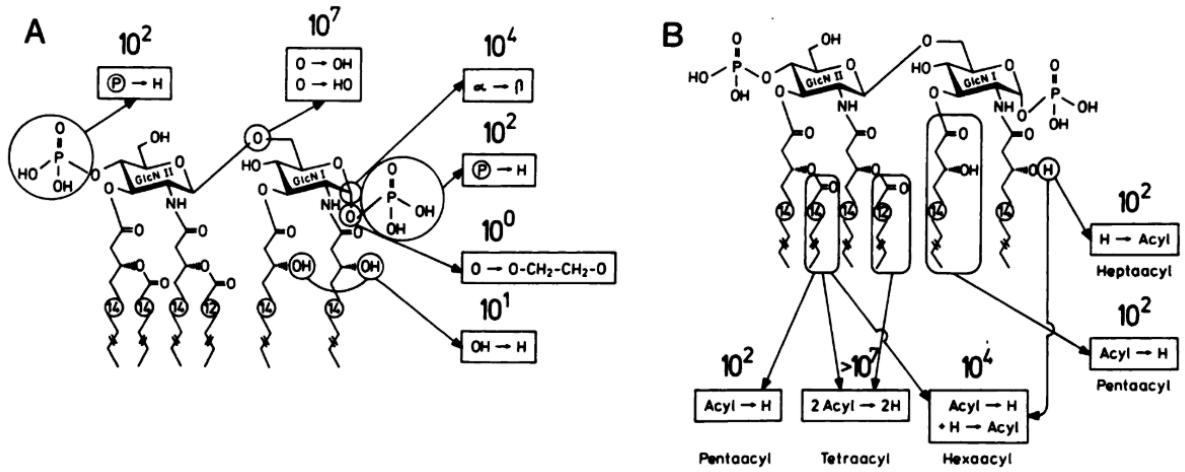

Figure 32. Schematic representation of lipid A structure-activity relationships Chemical modification of the *E. coli* lipid A structure is represented with the factor by which the structure generated is less active than lipid A. (**A**) Modifications of the hydrophilic region of lipid A. (**B**) Modifications of the hydrophobic region of lipid A.[269]

One of the few exceptions to the first and third features is **OM-174** (described below). Interestingly, this tri-acyl lipid A mimetic, with a normal disaccharide backbone, exhibited an hexagonal (H_1) structure, connected with lower but not vanishing activity.[242]

- **TLR4 antagonism**

On the other hand, there is compounds that are able to block the immuno-stimulation, meaning that they are able to prevent TLR4 activation by LPS by competing for MD-2 binding site. These compounds interact with MD-2 in a non-productive way, preventing TLR4/MD-2 dimerization while obstructing the binding of agonist. However, not every compound lacking immuno-stimulation can be an antagonist of TLR4. The structural features necessary for

antagonism cannot be described as specifically as for agonism, nevertheless, they are surely related to two major effects:

- The ability of the disaccharide to fill as much as possible the MD-2 pocket, enhancing the hydrophobic interactions. However, the full capacity of the MD-2 pocket should not be reached in order to avoid the protrusion of one FA chain and the switch to agonism. It may be the reason for which LPS with five or four FA chains are less active (or inactive) compared to lipid A. Indeed, they should stay deeper in the pocket than lipid A, then, energetical penalties would apply when chains move back to the surface of MD-2 for an eventual dimerization with TLR4*.
- A cylindrical or inverted conical shape of the molecule in solution which auto-assemble as fluid lamellar aggregates (vesicles or liposomes).

1.2) SAR of the monosaccharides

As stated earlier, it was surprising to see monosaccharide, as lipid A partial structures, to be able to act as LPS antagonists and even more surprisingly as immune-stimulants (like the much more complex disaccharide structures). Since the majority of these compounds were synthesized in the 80's and 90's, nothing was known at that time about the role nor the structure of the TLR4/MD-2 complex. Therefore, in search of a possible rationalization of such effects and a correspondence with the disaccharides, researchers focused on CD14 and in particular on the aggregate shape of the compounds. After many multidisciplinary studies, a correlation was found: monosaccharides that assemble as non-lamellar aggregates are active as agonists both in human and murine while those generating lamellar aggregates possess antagonistic activity in both or are inactive. Finally, as for disaccharides, monosaccharides possessing agonistic activity in murine and antagonistic activity in human have mixed aggregate shapes.[270]

- **TLR4 agonism**

It was known since 1998 that few monosaccharides, assuming lipid A partial structure, were able to express immune-stimulation both in human and in murine models. Similarly to their much more complex disaccharide counterpart, studies were conducted to rationalize the specific structural features necessary to define compounds as TLR4 agonists and the specific correlation with the active disaccharide structures. It emerged that a typical active compound should possess a glucosamine scaffold, one anionic group (phosphate, sulfate or carboxylic acid) linked at C1 or C4 position and three FA chains. The lipophilic chains are usually myristic (C14) or lauric

(C12) FA chains, distributed as one linear and one branched (acyloxy acyl) chain (like SDZ MRL 953). Furthermore, it was revealed, comparing GLA analogs (monosaccharide 4-monophosphoryl triacyl lipid As), that the position of the branched chain strongly influences the biological activity. If it is linked near the phosphate, the compound generates a non-lamellar aggregate and exhibit agonist activity. On the contrary, if the branched chain is further away, the compound generates a lamellar aggregate and do not show agonism.[270–273]

It was proposed that the structural features corelate with the accepted requisite defined for disaccharides since: one glucosamine scaffold, one phosphate and three FA chains are exactly the half of a typical disaccharide agonist: 2 glucosamines scaffold, 2 phosphates and six FA chains.

It was also suggested that two-monosaccharide may bind into one MD-2 pocket and therefore activate the dimerization. If two tri-acylated molecules enter the MD-2 pocket maybe a sixth acyl chain could protrude outside the pocket to permit dimerization. Despite the great interest of such compounds, the number of lipid A-like monosaccharide available for SAR definition (meaning variation in chain length but also in chain type) is, for now, very limited.

- **TLR4 antagonism**

As for monosaccharides agonists, the number of lipid A monosaccharide antagonists is very limited and the structural features required for antagonism are not clearly defined.

An important part of work has been done by our group during the last years thanks to the synthesis of a lipid X-like compound **FP7**.[274] In particular, this compound and variants showed high specificity on direct MD-2 binding assays as well as promising biological results *in vivo* and *in vitro*, thus confirmed the role of MD-2 and the specificity of the compounds.

The fundamental features accessed to date for antagonism are:

- Two phosphate groups allowing the ligand to anchor strongly to the rim of the MD-2 pocket.
- Two FA chains of C12 or C14 length. It has been demonstrated that C10 chains possesses a lower antagonistic effect while C16 lead to inactivity.

Similarly to the rationalization regarding agonists, little is known about the actual binding mode of the compounds, research is still at the beginning. It has however been established that monosaccharides possess a much lower antagonistic activity than disaccharides.

3. Ligand-based drug design

The most commonly used and well-established approach for the design and synthesis of TLR4 modulators is the design of *E. coli* lipid A chemical modifications (ligand-based drug design). SAR of natural lipid A and analogs provide the basis allowing us to envisage the structural requirements for TLR4 agonist or antagonist. Moreover, the resolution of several "ligand/MD-2" crystal structures permitted to clarify the binding mode of such ligands and made possible the computational studies (docking and molecular dynamics) of newly designed compounds.

On the contrary, the other ligands of TLR4 (DAMPs) are rarely used for the design of TLR4 modulators, mainly because of the high chemical diversity of the DAMPs. Moreover, DAMPs have different modes of interaction with TLR4. Finally, the role of the accessory proteins (CD14 and MD-2) is still controversial in the case of DAMPs stimulation.

As already described in previous sections, *E. coli* lipid A (Fig. 33) consists of a D-GlcN-β(1−6)-D-GlcN disaccharide unit carrying two phosphates groups (one α-oriented at position C1 and one equatorial at position C4') and six acyl chains of 14 carbon atoms besides the branch on the C2' chain which is a C12 FA chain. These chains have an asymmetrical (4+2) distribution: two linear chains at C2 and C3 positions, and two branched chains at C2' and C3' positions.

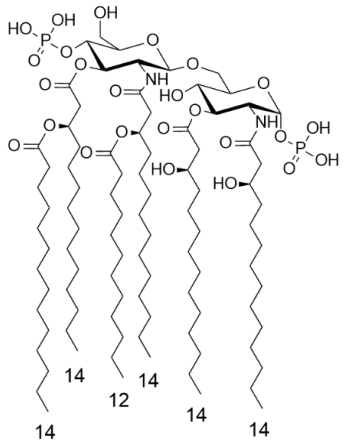

Figure 33. Chemical structure of E. coli lipid A

The first total synthesis of *E. coli* lipid A was accomplished by Imoto *et al.* in 1985, therefore it has been extensively and deeply studied to highlight all the aspects of its activity and binding.[275,276] However, due to the complexity of the system, the knowledge of the exact geometry of the lipid A/MD-2 complex has been realized years later, in 2009 by Park *et al.*[70]

To understand the ligand specificity and receptor activation mechanism of the hTLR4/MD-2/Ra-LPS complex, the crystal structure was realized by incubating the Ra-LPS with a purified and partially unglycosylated TLR4/MD-2 complex. The crystal structure showed the dimerized complex, with a resolution at 3.1Å. It appeared that the overall folding of TLR4 and MD-2 is not disturbed by LPS binding or dimerization. TLR4 adopts the characteristic horseshoe-like shape of the LLR superfamily and MD-2 has a β–cup fold structure composed of two anti-parallel β sheets forming a large hydrophobic pocket for ligand binding. LPS binds to MD-2 cavity and directly mediates dimerization of the two TLR4/MD-2 complexes.[70]

In the crystal structure, the FA chains of lipid A interact with the hydrophobic pocket of MD-2 with five chains buried inside the pocket, the sixth chain (lipid chain linked to the position C2 of the glucosamine) is partially exposed to the MD-2 surface composing the core hydrophobic interface for the interactions with TLR4*.

Ester and amide groups connecting the lipids to the glucosamine backbone or to the other lipid chains are exposed to the surface of MD-2. They interact with hydrophilic amino acid side chains located on one of the β strands of the MD-2 pocket and on the surface of the two TLR4. Finally, the two phosphate groups of lipid A bind to the TLR4/MD-2 complex by interacting with positively charged residues in the two TLR4 and MD-2. Both hydrophobic and hydrophilic interactions contribute to the main dimerization interaction between TLR4, MD-2, LPS and TLR4*, that is fundamental for TLR4 activation.

In particular, the role of the sixth chain (R2) of lipid A appears crucial. The hydrophobic R2 lipid chain of LPS protruding outside the MD-2 pocket indeed interacts directly with a small hydrophobic patch of the C-terminal convex face of the horseshoe structure of TLR4* thus inducing the interaction with the second MD-2. TLR4 complex and the formation of the "M"-shaped 2:2:2 hTLR4/MD-2/LPS complex. The close proximity of the C-terminus of the extracellular domain in the complex induced by binding to LPS may allow for the dimerization and signaling by the intracellular TIR domain.[277]

Moreover, the 3-hydroxyl group of the R2 chain of LPS contributes, by forming a hydrogen bond with TLR4*. The hydrophobic residue of MD-2 supplement this core hydrophobic interface, while hydrophobic residues in the Phe126 loop and the Arg90 residue of MD-2 form hydrogen bond and ionic interactions with TLR4* that surround and support the hydrophobic core of the dimerization interface. The two phosphate groups, 1-phosphate and 4'-phosphate of lipid A, also play an important role in TLR4 dimerization. They both bind to a positively charged cluster of Lys and Arg from TLR4, TLR4* and MD-2. LPS binding induces local changes in the structure of the Phe126 loop of MD-2 and in the radius and bending angle of TLR4.

While lipid A from *E. coli* is considered the typical chemical structure associated with the strongest endotoxic properties, a variety of natural lipid A variants exist with modifications in the number and disposition of FA chains and with other covalent modifications that impact pathogenesis, bacterial physiology and bacterial interactions with the host immune system. As *E. coli*, different LPS chemotypes (and their lipid A portions) have been used as templates for the design and synthesis of TLR4 agonists and antagonists. However, results should be considered as contributive only if lipid As and analogs were synthesized and obtained as single molecular species. Indeed, since it has been possible to demonstrate that the state of acylation strongly impacts the biological activity, biological extracts get a trend but cannot be used for the design *de novo*. Moreover, since TLR4 recognizes a range of diverse structures, it is not always possible to exclude the effects of other components present in the natural extracts tested.

VIII. TLR4 modulators

According to the previous statements, numbers of different TLR4 modulators were developed during the last decades. The following sections will describe the main compounds developed focusing on their design, structures and properties. We will first focus on the agonists and, then, we would be interested on the antagonists.

1. TLR4 agonists

Great synthetic efforts have been done through the years to obtain synthetic lipid A analogues and lipid A mimetics. Several TLR4-active compounds have been synthesized starting from the lipid A structure and modifying:

- The number, length, position or nature of the FA chains.
- The number of phosphate groups or replacement with phosphate bioisosteres.
- The disaccharide scaffold, which was also reduced to monosaccharide (molecular simplification approach).

This works allowed scientists to understand better the chemical groups requested to obtain efficient TLR4 agonists or antagonists and how these parameters alters the relationship between activity and toxicity. In the next section will be described the most important TLR4 agonists.

- **Hepta-acyl lipid As**

Each bacterial strain expresses mostly its unique type of LPS structure, it leads to tremendous variations between lipid As but permits to classify the LPS by bacterial strain. Early structural investigations of Re-LPS from *Salmonella minnesota* revealed that its major lipid A specie was hepta-acylated (Fig. 34). This compound is identical to *E. coli* lipid A, but it has an additional palmitoyl (C16) FA chain esterified at the (R)-3-hydroxymiristoyl chain linked at the C2 position.

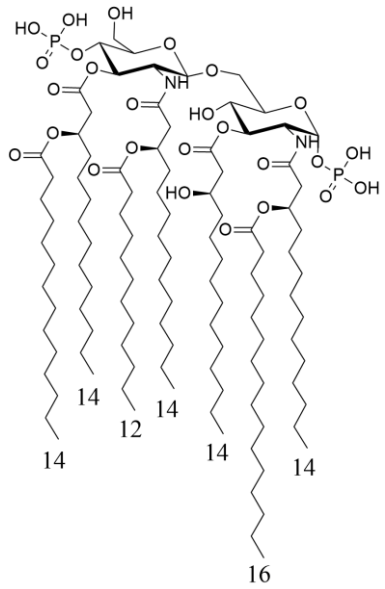

Figure 34. Chemical structure of Salmonella typhimurium lipid A

The corresponding synthetic hepta-acyl lipid A (compound **516** in literature),[243] despite the increased lipophilic area, has been shown to display still profound, but significantly lower, immune-stimulation compared to the highly active hexa-acylated *E. coli* lipid A.[278]

- **Monophosphoryl lipid A (MPL)**

It was early demonstrated (1970s) that the endotoxic effects of *Salmonella minnesota* lipid A (strain R595) could be ameliorated by selective hydrolysis of the 1-phosphate and the (R)-3-hydroxytetradecanoate groups. *S. minnesota* lipid A modified in this way is an effective adjuvant in both prophylactic and therapeutic human vaccines.[225]

Through the use of mild acid hydrolysis, the polysaccharide side chains, a phosphoryl group and one of the seven acyl chains of *S. minnesota* LPS were removed, leaving a mixture of lipid A molecules that were devoid of polysaccharide with a single phosphate and had predominantly six FA chains. This compound, defined as 4'MPL, showed greatly reduced pyrogenicity while maintaining immune stimulatory activity. However, since preparations were still mixtures of

tetra-acyl, penta-acyl and hexa-acyl monophosphoryl lipid As, it was impossible to define the actual structure. It was resolved by the total synthesis of the putative major constituents of *S. minnesota* MPL mixture and the most active component was identified.[279,280] It resulted to be an hexa-acylated monophosphoryl disaccharide thus confirming previous studies showing that a β(1-6) di-glucosamine moiety bearing six FA chains is a prerequisite to the full expression of endotoxic activities. This mixture was further purified and perfected thus resulting in the clinical-grade version currently manufactured by GlaxoSmithKline (GSK) Biologicals and now referred to as **MPL**.

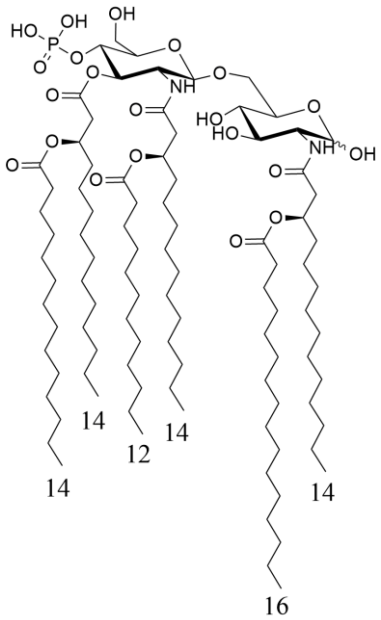

Figure 35. Chemical structure of S. minnesota MPL

Early clinical development of **MPL** focuses on its use as an adjuvant for cancer therapy. However, despite promising results in phase II clinical trials (1993), further development was not continued. In contrast to its limited use in therapeutics clinical trial, **MPL** has been widespread used as an adjuvant in prophylactic vaccines. Several vaccines already received regulatory approval while many more are in development. The first approved vaccines containing **MPL** were produced by GSK Biologicals, it is FENDrix®, directed against hepatitis B and Cervarix®, which targets the Human Papilloma Virus (HPV). Cervarix® has not been approved in every country but it received the US regulatory approval, making MPL the first defined adjuvant to be approved for widespread use in human since aluminum salts.

- **Hexa-acyl lipid A PHAD™**

Since the strategy of modifying natural LPS seemed to be promising, **PHAD™** was developed by the USA Infectious Disease Research Institute (IDRI) in 2011. Instead of using *S.*

minnesota lipid A as starting point, they worked with the potent and well-known *E. coli* lipid A. The modified structure, depicted in Fig. 36, is a monophosphoryl disaccharide with six myristic (C14) FA chains, distributed asymmetrically as in *E. coli* (4+2).[225,281]

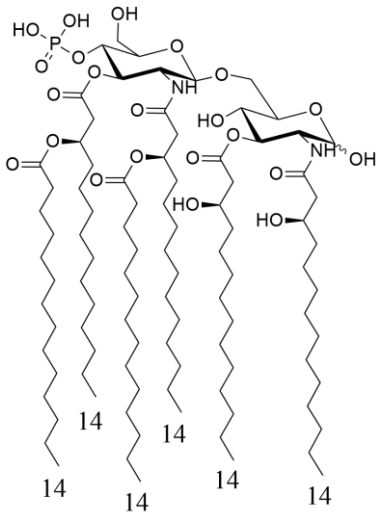

Figure 36. Chemical structure of the synthetic PHAD

This synthetic lipid A was shown to be a powerful immune-stimulator, 10- to 100-fold more active than *S. minnesota* Re-595-derived MPL on human monocyte-derived DCs, its increased activity was attributed to the lack of tetra-acylated and penta-acylated lipid A moieties in the purified hexa-acylated material.[281] Upon *in vivo* administration and properly formulated, this synthetic compound induces strong systemic innate immune responses and prime the antigen-specific Th1 cells.[281] This compound is still not used commercially but it advances into the clinic tests in several component vaccines (HIV, Epstein-Barr, Schistosomiasis, Respiratory syncytial virus).[282–286]

1.1) Disaccharides mimetics

The chemical approach, to find new and well-defined TLR4 modulators, led also to the synthesis of monosaccharides-derived compounds, still mimicking the structure of lipid A with a proper distance between the anionic groups. This idea come from the consideration that one of the glucosamines may be removed from the scaffold without affecting the biological activity. It was speculated that the activity would be retained if the proper distance between acyl chain and phosphate groups was maintained.

Based on this strategy, both derivative of the reducing and non-reducing part of lipid A with a proper linker carrying an anionic group and acyl chains as an analogue of the second sugar have been synthesized.

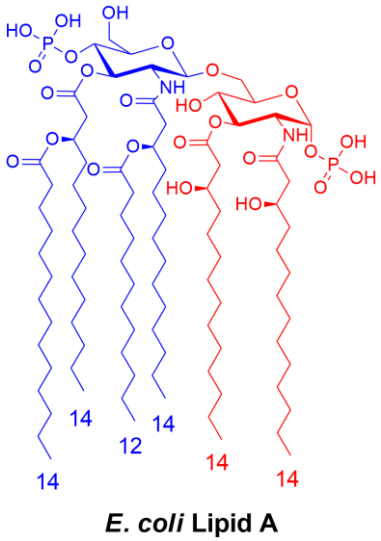

***E. coli* Lipid A**

Figure 37. Chemical structure of E. coli lipid A with the non-reducing part in blue and the reducing part of lipid A in red.

- **Dimeric monosaccharide as lipid A mimetics**

Both molecular modeling and MD-2 docking suggested that the use of a bridge between two monosaccharides would ensure the conformational flexibility required to allow the accommodation of the FA chains into hMD-2 binding cavity. Therefore, the design and synthesis of dimeric monosaccharide structures using a spacer of variable nature to link the monosaccharide units was developed.

The first compounds of this kind were designed as two monophosphorylated di-acyl glucosamines linked through a (1-1') ethylene linker (Fig. 38A and B). Preliminary biological studies indicated that such compounds was not active as agonist nor as antagonist despite the significant synergistic effect on LPS-induced ICAM-1 expression by THP-1 cells. [287]

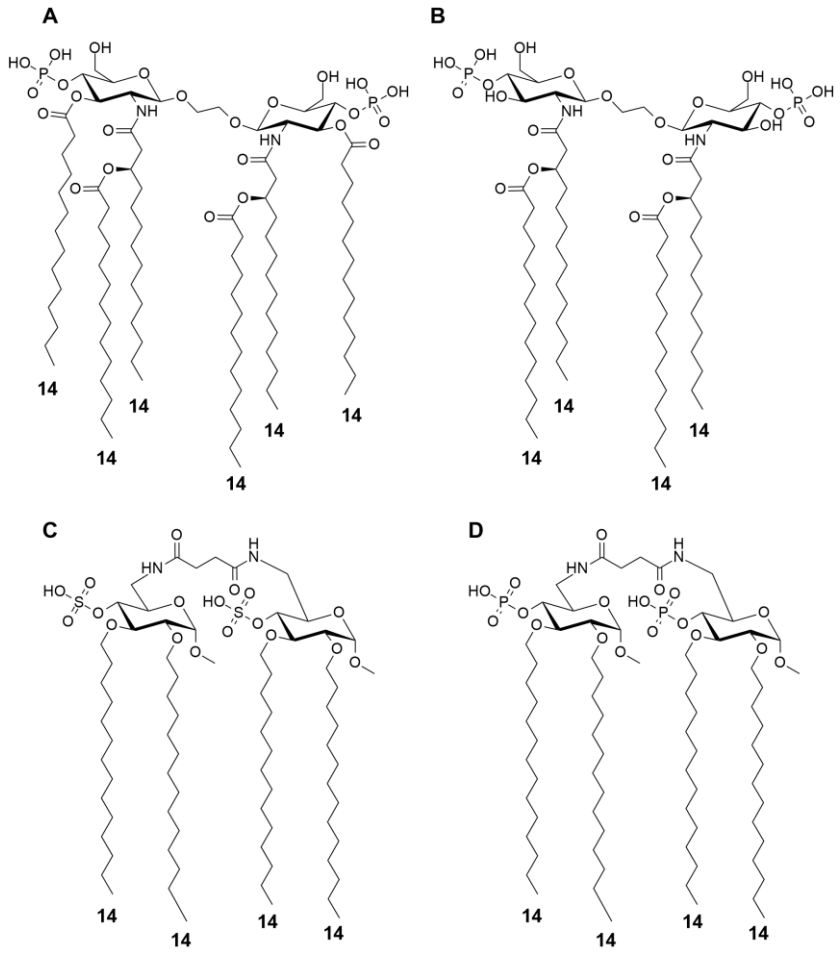

Figure 38. Chemical structures of dimeric monosaccharide as disaccharide mimetics (**A**, **B**) compounds developed by Lewicky et al.[288] (**C**, **D**) Compounds from our lab, Piazza et al.[289]

Two lipid A analogs (Fig. 38C and D), were later designed and synthesized by our group using a convergent strategy. They possess a rotational symmetry and are composed by two glucose monosaccharides symmetrically linked through a (6-6') linker. **C** has two anionic sulphate groups while **D** possesses two phosphates groups. Unfortunately, the diphosphate **D** appeared to be insoluble in water, precluding its biological characterization. On the other hand, **C** was tested on HEK-Blue cells and showed a dual activity: it behaved as TLR4 antagonist if co-administered with *Neisseria meningitidis* LOS, and as TLR4 agonist if administered alone. Further experiments showed that **D** inhibited the interaction of LOS with both CD14 and TLR4/MD-2, presumably occupying the same receptor binding sites.[289]

- **Amino alkyl glucosaminide 4-phosphate (AGP):** Corixa compounds (CRX), ethanolamine mimetics **CRX-527**, **CRX-526**, **RC-529** and **PET-lipid A**

In 1999, a new class of monosaccharide molecules called amino alkyl glucosaminide 4-phosphate (AGPs) was developed by Johnson *et al.* from Ribi ImmunoChem.[290] Later, the

company became Corixa Corp. (MT, USA) and they were eventually called Corixa compounds or CRX.

They were synthesized based on the non-reducing part of lipid A. These family of compounds are lipid A mimetics in which the reducing sugar has been replaced by an acylated amino acid, ethanolamine or pentaerythritol. AGPs generally possess two anionic groups (4-phosphate linked to the glucosamine and a carboxylic group on the aglycon) and six FA chains. The carboxylic group is also tested as stable bioisostere of the labile 1-phosphate present in lipid A. The authors speculated that coupling a flexible N-acylated aglycon to the non-reducing sugar of lipid A may favor the close packing of the FA chains in a hexagonal array crucial to obtain supramolecular aggregates with TLR4 activity.

Serine has been used as the aglycon unit since it presents the three requested functional groups: an amino group to be acylated with a FA chain, a carboxyl group as a bioisostere of reducing 1-phosphate and a hydroxyl group to be linked to the monosaccharide (Fig. 39A and B). Moreover, the serine-derived flavolipin and other naturally occurring N-(3-acyloxyacyl) amino acids were already known for their immuno-stimulant properties.

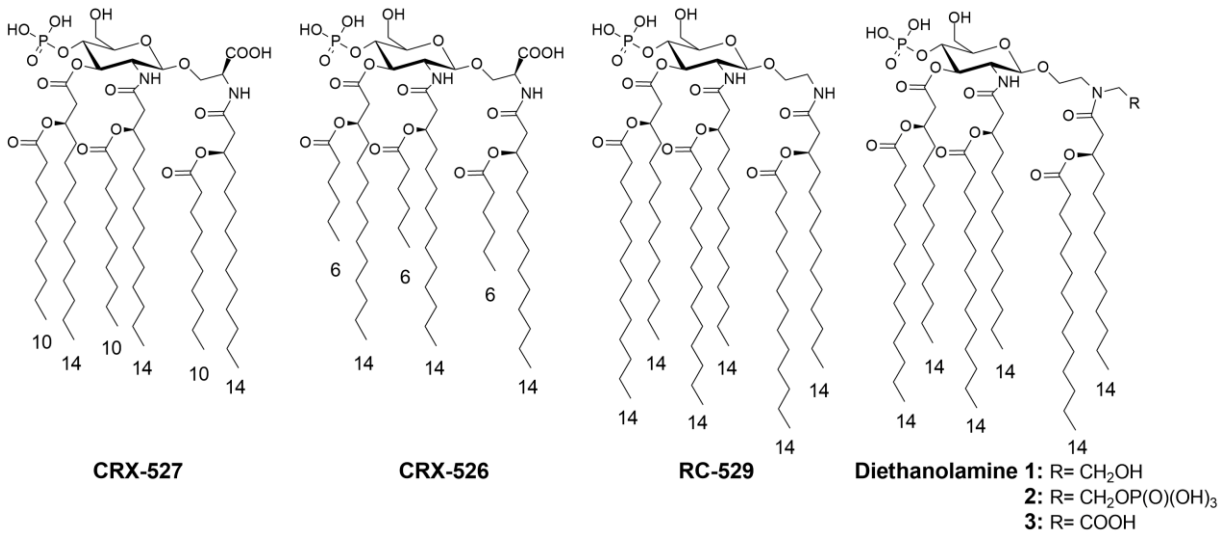

Figure 39. Chemical structures of some AGPs based on the non-reducing part of lipid A (**A**) compound **CRX-527**, (**B**) compound **CRX-526**, (**C**) compound **RC-529**, (**D**) diethanolamine derivatives.

As depicted in Fig.39C and D, ethanolamine and other hydroxyalkyl amines, with or without ramifications, have been synthesized and reported in literature. The synthesis of compounds with different length of acyl chains permit to hamper the SAR knowledge for this type of molecules.

Compounds have been tested for their ability to induce nitric oxide synthase (iNOS) in murine macrophage and cytokine production in human peripheral monocytes. Toxicity was also

evaluated in a standard three-rabbit USP pyrogen test. AGPs and hydroxyalkyl amines proved to induce immune-stimulation and their activity as well as their toxicity showed an important chain-length dependence. Moreover, it was demonstrated that the immuno-stimulation triggered by hydroxyalkyl amines compounds, lacking the carboxylic acid (like **RC-529**), was associated to their toxicity. On the other hand, AGPs like compound **CRX-527** showed an extremely powerful immune-stimulation with low toxicity.

These data show that the carboxyl group of serine-based AGPs can be assumed as a bioisostere of the 1-phosphate moiety of lipid A. The second anionic group which seemed not fundamental for the activity (lipid A/**MPL**), is in turn essential to express a powerful immune-stimulation for AGPs. Analogs presenting ether links instead of the ester links were also synthesized and they showed equivalent results.[291] **CRX-527** and its ether analogue were virtually indistinguishable regarding their ability to induce cytokine production in human cell. This strongly suggests that the AGP motif can be a potent and non-toxic biomimetic of lipid A.

Contrariwise, compound **CRX-526**, which possesses shorter ramified chains, showed a potent antagonist activity being able to block the induction of pro-inflammatory cytokines induced by LPS both *in vitro* and *in vivo*.[291]

Studies of the aggregation state showed that **CRX-527** molecules possess a conical shape and adopt a non-lamellar, inverted hexagonal (H_2) aggregate structure in solution, which is consistent with its high agonist activity. Meanwhile, physicochemical analysis of **CRX-526**, revealed that it forms lamellar aggregates in solution, characteristic of the antagonist or inactive molecules.

Most importantly, while AGPs activation of TLR4 proceeded also in the absence of co-receptor CD14, even if less efficiently, the response to the most potent compound **CRX-527** was strictly dependent of TLR4 and MD-2 but not CD14, suggesting that **CRX-527** may be able to engage both MyD88-independent pathway (TRIF, that requires CD14) and MyD88 pathway in the absence of CD14.[292] Similar results were obtained in murine infectious disease models with these hybrid molecules.[293]

Numerous variants of the acyloxy ethanolamine have been successively synthesized like, for example, the diethanolamines (Fig. 39). Those compounds showed different immuno-stimulatory potency depending on the di-ethanolamine substituent (alcohol, phosphate or carboxylic acid) when tested on human monocyte cell line THP-1. The greatest activity was found for **diethanolamine 3**, bearing a carboxylic group and six FA chains.[245,287]

Several members of this class of lipid A mimetics, including the prototypical AGPs (**CRX-526**, **CRX-527** and **RC-529**) demonstrated their ability to improve humoral and cell-mediated

immune responses to several antigens as well as to enhance non-specific resistance to viral and bacterial infections in mice.[290,291] To further demonstrate the potential anti-infective effect of AGPs, **CRX-527** was evaluated in a pre-clinical model for respiratory syncytial virus (RSV) and it was found to effectively inhibit the RSV replication in BALB/c mice when intranasally administered 24h prior to infection via the same route.[312]

RC-529 was shown to induce antigen specific serum and mucosal IgG and IgA antibodies and reduced nasal colonization in mouse intranasal challenge models for both *Neisseria meningitidis* and non-typable *Haemophilis influenzae* (NTHi).[294,295] Since **RC-529** demonstrated an adjuvant profile similar to MPL, it was further studied as a vaccine adjuvant. Nowadays, the adjuvants used for the formulation of the approved recombinant hepatitis B vaccine Supervax®, produced by Crucell, are a combination of **RC-529** and aluminum hydroxide.[225]

Another compound related to this kind is **PET-lipid A** (Fig. 40). It is composed of the reducing part of lipid A linked at C1 with a propyl chain amine and two additional hydroxy acyl groups in the middle of this propyl chain. This compound showed a powerful immune-stimulatory activity and it has been tested in different systems showing its more promising results in anticancer therapy. It is currently in phase III clinical trials.[225]

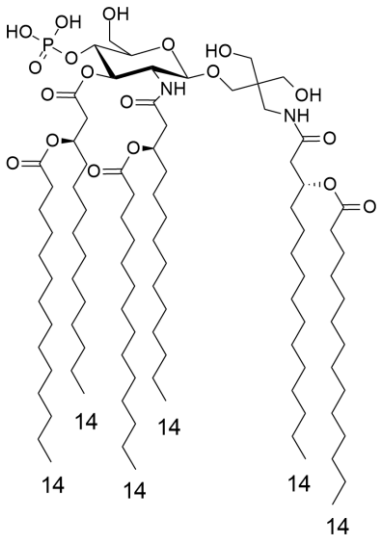

Figure 40. Chemical structure of PET-lipid A

1.2) Monosaccharides as TLR4 agonists

The synthesis of natural lipid As or lipid A mimetics with a disaccharide scaffold is a complex process involving many synthetic steps. Moreover, the two glycosylation steps must

be stereo-controlled with the selective formation of β(1-6) glycosidic and 1-α–phosphate as in natural lipid As for an optimal biological activity.

Therefore, an important trend in lipid A mimicry has been the design of simplified structures, with the aim to partially or totally preserve the lipid A biological activity while reducing the chemical complexity of the molecules and improving, in parallel, the synthetic affordability and solubility properties.[245]

- **Gifu lipid As (GLA)**

GLAs were developed at the Gifu University (Japan) in 1984. They were working on the synthesis of analogs of the non-reducing part of *E. coli* lipid A in order to test their immuno-stimulating activities.[296,297] GLA processes a phosphate group at C4 position while different type of linear or branched chain have been inserted in C2 and C3 positions. These compounds have been tested on murine and human cells and the results have been summarized in 1999 by Matsuura *et al.*[271,272]

It has been demonstrated that compounds with two (**GLA-26**) or four chains (**GLA-47**) possess an agonist activity in murine while being antagonist in human. On the other hand, compounds **GLA-60**, **GLA-63**, **GLA-64** and **GLA-89**, containing a linear chain at C2 and a branched chain at C3 next to the phosphate group with variable chain length, demonstrated an agonistic activity in both murine and human.

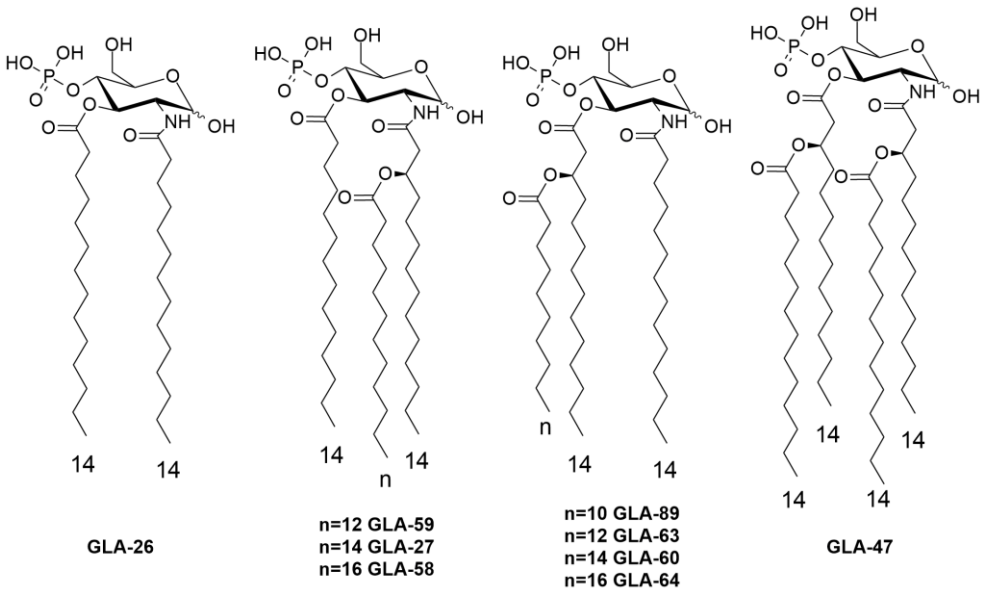

Figure 41. Chemical structure of the biologically active GLA compounds

It was unexpected to see a monosaccharide expressing an agonistic activity as the much more complex disaccharides. The studies also demonstrate that the elongation to 16 carbon atoms or

shortening to 10 on the ramified chain (branch of the chain at C3) caused a switch from agonism to antagonism in human cells (**GlA-64** and **GLA-89**). The same effect was observed with the branched chain linked to C2 position (**GLA-27** and **GLA-59**).[270] However, if the branched chain is linked at C2 and possesses the elongation of the third chain to C16 (**GLA-58**), it results a strong antagonistic activity both in murine and in human.[271] These data gave an important contribution for the rationalization of the monosaccharides SAR toward TLR4.

It was also showed that GLAs possessing non-lamellar aggregate shapes are active as agonist both in human and in murine while those displaying an antagonistic activity (or no activity) on both generate lamellar aggregate shapes.[270]

These observations are consistent with the relationship between aggregate structure and agonism/antagonism found for lipid A variants and previously presented. Moreover, it was found that the position of the branched chain influence activity: if the acyloxy acyl (branched) chain is near the phosphate, compounds generate non-lamellar aggregates and exhibit agonism whereas, if the branched chain is further away, compounds generate a lamellar aggregated form.

After the identification of TLR4 and MD-2 role in immuno-stimulation, scientists searched another rational for their interaction with the receptorial system. Studies aiming to define the actual receptor of these compounds were conducted.[273,282] The induction of pro-inflammatory factors by GLA compounds was investigates in human peripheral blood mononuclear cells (PBMC) with or without addition of monoclonal antibodies directed against human TLR2 or TLR4. It appeared that only monoclonal antibodies directed against TLR4 were able to block the biological response to active GLAs.[282,284] Thus, it established for the first time the correlation between monosaccharide activity and TLR4 modulation.

Early results from clinical trials using vaccines containing GLA formulations indicate excellent safety profiles that are accompanied by the enhancement of antigen-specific responses.[228]

The GLA compounds has been used in phase I clinical studies for influenza and are in preclinical development as vaccines adjuvant against tuberculosis, leishmaniasis, schistomiasis and hookworm.[225,283,284]

- **Lipid X and its derivatives (SDZ-880.431 and SDZ MRL 953)**

Molecular simplification of lipid A structure was historically inspired by the discovery of **lipid X** (compound **401**). This monosaccharide is the biosynthetic precursor of *E. coli* lipid A reducing sugar moiety and induces immune responses.[298]

The first synthetic **lipid X** obtained showed an apparent immuno-stimulatory activity.[299] It was later found to be contaminated by small amounts of the immuno-stimulant N,O-acylated disaccharide-1-phosphate which can from during the last step of its synthesis.[300]

Finally, the purified **lipid X** (Fig. 42) appeared to behave as a competitive inhibitor of LPS, able to block the activation of monocytes and macrophages by endotoxin as well as the priming of human neutrophils.[301] The anti-endotoxic activity of **lipid X** led to consider the simplified monosaccharide scaffolds as suitable for the development of TLR4 antagonists. Nowadays, this principle is called molecular simplification.

Starting from **lipid X** structure, many analogs were synthesized with modifications on the acyl chains (acetyl group or branched chains), the scaffold (glucosamine or glucose) and the anionic groups (phosphates or sulfates).[301,302] These derivatives of **lipid X** were found to have reduced inhibitory activity until **SDZ-880431** and **SDZ-MRL-953** were developed (Fig.42).[302,303] **SDZ-880431** possesses one additional phosphate in C4 compared to **lipid X** and demonstrated the most potent antagonistic activity with respect to all synthetic **lipid X** analogs synthesized, being more potent than **lipid X** itself both on murine macrophages and human monocytes.[245,302,304]

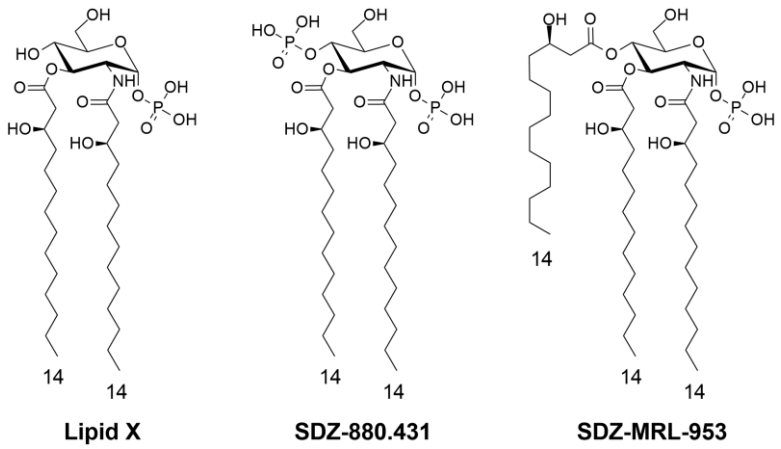

Figure 42. Chemical structure of monosaccharides based on molecular simplification of lipid A

However, the most interesting discovery of these studies was **SDZ-MRL-953**. This lipid A reducing part derivative differs from **lipid X** because of the insertion of a third linear acyl chain at C4 position. Unlike **lipid X**, **SDZ-MRL-953** does not showed anti-toxin effect in the tests *in vitro*. On the contrary, it stimulated mouse macrophages to release high level of granulocytes colony-stimulating factor (G-CSF) and low level of pro-inflammatory cytokines such as Il-6, IL-8, TNF–α (thus a cytokine profile being markedly different from the endotoxin-induced cytokine pattern) at relatively high concentration (10^3 higher than lipid A).[305]

Tests were conducted *in-vitro* and it appears that **SDZ-MRL-953** was able to induce the release a range of cytokines comparable to LPS, in human macrophages. The total amounts of cytokines induced were lower and **SDZ-MRL-953** had to be used in 1 to $5x10^4$ times higher concentration compared to LPS. Even if significant induction of TNF–α and IL-6 was seen with the dose of 5 μg/ml, higher doses of **SDZ-MRL-953** do not increase the number of cytokines produced (5ng/ml). Furthermore, at concentration up to 500 μg/ml, neither release of IL-1 nor of G-CSF was observed.[306] **SDZ-MRL-953** was proved to be less toxic in the galactosamine-sensitized mice than LPS by a factor of $1.7x10^4$ to > $7.4\ 10^5$. Thus, the therapeutic indices of **SDZ-MRL-953** were significantly improved over those of endotoxin and ranged from about 5 to > 500, depending on the infection model and mode of administration.

SDZ-MRL-953 can be considered as the first potential monosaccharide adjuvant discovered and the first compound showing the promising approach of monosaccharide molecular simplification in the clinical perspective. It entered in clinical exploration for cytokine induction in the setting of chemotherapy-induced cytopenia.[306]

Based on the known antitumor activity of endotoxins due to their immuno-stimulatory property, **SDZ-MRL-953** entered in phase I clinical trial to evaluate its biologic response and safety once administration in human.[307] It resulted that **SDZ-MRL-953** was at least 10^4 times less toxic than LPS. Apparently, the improved tolerability of **SDZ-MRL-953** was most likely related to its low activity, particularly for TNF-α and IL-1β induction.

Unfortunately, even after the positive results, this study dated 1997 is the last scientific report available on compound **SDZ-MRL-953** and still little is known about its mechanism of action. *In vitro* studies suggest that **SDZ-MRL-953** may act independently of CD14.[308] Unlike endotoxin, its action on TNF-α released in human peripheral blood by mononuclear cells could not be blocked by monoclonal antibodies directed against CD14. Then, data seem to point toward a direct interaction with MD-2, but since MD-2 was not known at this time, no studies were performed.

- **Monosaccharides with aromatic moiety**

Monosaccharides analogues of the non-reducing part of lipid A were developed with the initial aim of obtaining anti-cancer agents. Compounds are composed of a glucosamine linked to a phosphate group (C4) and FA chains (C2 and C3 positions) displaying an aromatic group. These compounds differ for the length of the chains as well as the position of the phenyl-ring, whether in C2 or C3, in the branched or in the "main" chain (Fig. 43). Naphthalene have also been used, as a highly hydrophobic moiety. In most of the case, a sulphate was used instead of

the phosphate group except in two variants. Different results of biological activities and toxicities were found with respect to type of structural modification.

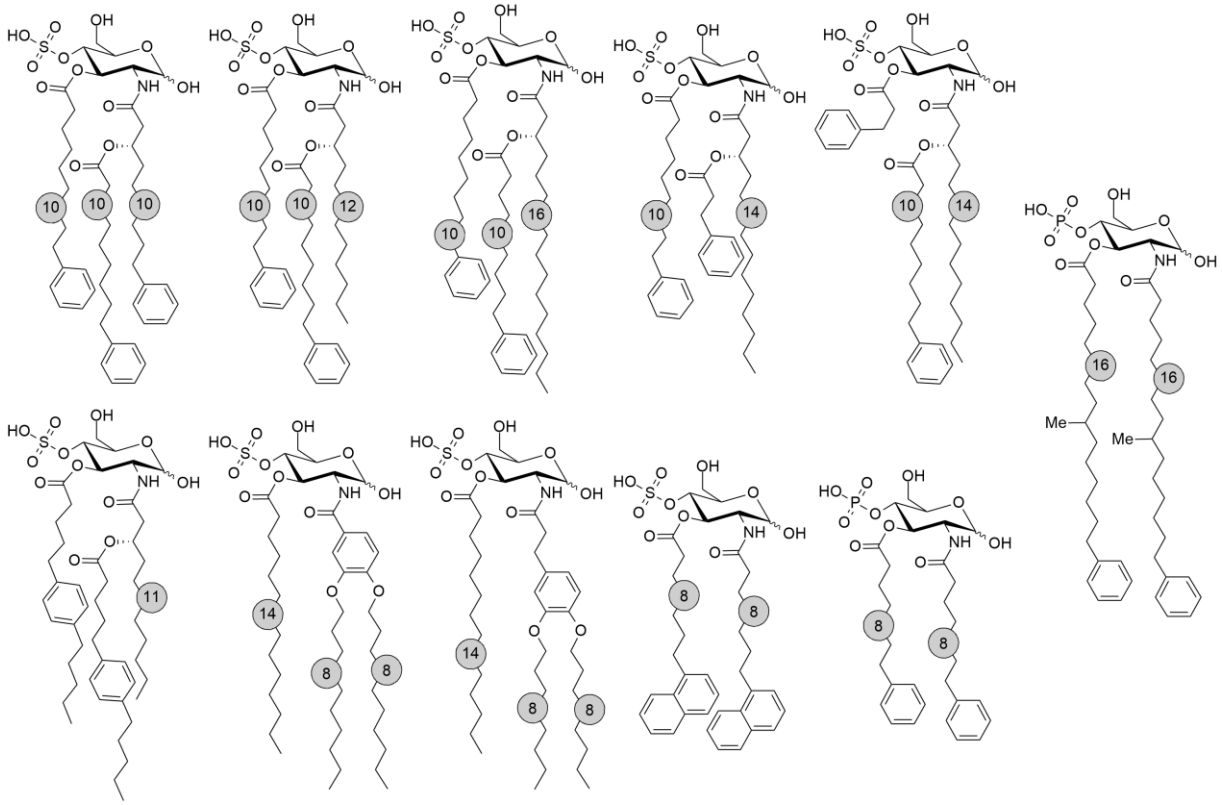

Figure 43. Chemical structure of lipid As partial structure presenting aromatic groups[309,310] Numbers represent the number of carbon atoms of the alkane chain

One of the main contributors was ONO Pharmaceuticals, which developed most of those compounds.[309,310] Some of them showed enhancing activity of cellular immunity (e.g. mitogenic activity) to living tissue in murine, induced the production of TNF−α, IL-1 and IFN and presented a low toxicity.[311]

One of the compounds produced, called **ONO-4007** and possessing a sulfate in position C4, three alkyl chains in which two display an aromatic group at the end (Fig. 44). This compound showed unique properties: it greatly diminished the toxicity against animals (less than 1/1000 compared to natural *E. coli* LPS), it has a potent anti-tumor effect against implanted MethA sarcoma and MH-134 hepatoma in the murine system and is water soluble.[230] All these features suggest advantageous property for the therapeutic use and allowed **ONO-4007** to be a possible candidate for anti-tumor therapy. Therefore, it entered in phase I clinical trial.[225]

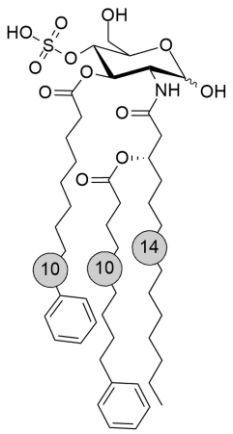

Figure 44. Chemical structure of ONO-4007

As a result, it was showed that **ONO-4007** exhibit its anti-tumor effect by activating TIM *in situ* producing intra-tumoral TNF–α which permit to be cytotoxic against MM46 mammary carcinoma tumor cells.[230]. Due to its immuno-stimulatory activity and its safe profile, **ONO-4007** was also tested as adjuvant in vaccine. Nowadays **ONO-4007** is in phase I clinical studies as adjuvant vaccine against Leischmania.[225]

Despite the relevant results of **ONO-4007**, the effect of aromatic chains has been tested only on the few monosaccharides molecular simplifications of the non-reducing part lipid A presented. It would be interesting to look at di-sulphated or di-phosphorylated analogs or to the analogs of the reducing part of lipid A.

1.3) Dimer of phospholipids

Based on the lipid A structure and the knowledge of pharmacologic groups required, it was hypothesized that a dimer of phospholipid bounded with a diamine linker containing six FA chains symmetrically distributed (three FA chains per monomeric unit), may be able to mimic lipid A structure and therefore be sufficient to obtain biological activity.[312]

Following this rational design, six-lipid chain dimeric molecules with stereochemistry, functionality, and lipid chain lengths similar to that found in the natural lipid As, with a stable linker between the monomeric units, were synthesized (Fig. 45). **ER112022**. It turned out that the designed compounds possessed effectively an agonistic lipid A-like activity *in vitro* in human whole blood. They showed a significant increase of the TLR4-mediated cytokines (TNF-α from human whole blood and Il-6 from adherent human glioma cell line, U373, in the absence of added sCD14).[312] The promising results led to the synthesis of additional dimeric molecules to investigate the structural requirements needed for a maximal stimulation. Further

simplification provided the more active compounds **ER111232** with a shorter dimer linker, **ER112066** with saturated lipids and **ER119327** with non-functionalized lipids.

A

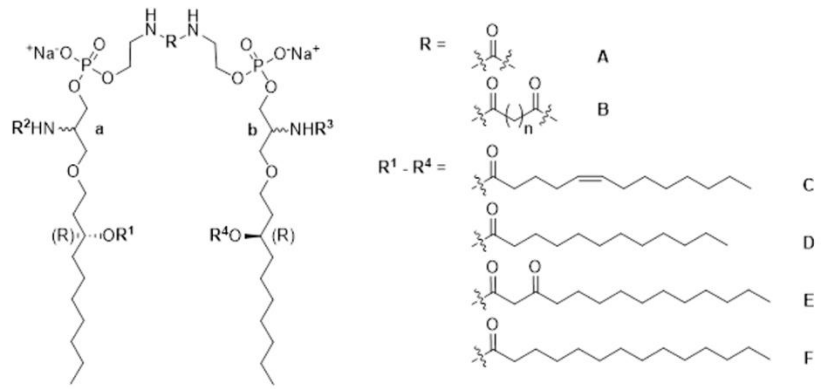

B

ER No.	Configuration		R	n^a	R^1/R^4	R^2/R^3	TNF-α^b
	a	*b*					
112022	*R,S*	*R,S*	B	4	C	E	0.42 ± 0.33
111232	*R,S*	*R,S*	A		C	E	0.03 ± 0.02
113651	*R,S*	*R,S*	B	1	C	E	0.7 ± 0.9
112066	*R,S*	*R,S*	A		D	E	0.04 ± 0.02
119327	*R,S*	*R,S*	A		D	F	0.02 ± 0.003
803022	*R*	*R*	A		D	F	0.01 ± 0.03
803789	*R*	*S*	A		D	F	0.54 ± 0.26
803732	*S*	*S*	A		D	F	8.34 ± 3.7
804057	*R*	*R*	A		D	E	0.01 ± 0.003
804053	*S*	*S*	A		D	E	4.23 ± 5.0
804058	*R*	*R*	B	1	C	E	0.03 ± 0.02
804059	*S*	*S*	B	1	C	E	≥10.0 ± 0

[a] *n* denotes the number of methylenes between the carbonyls as shown in Fig. 1, where **R** = **B**.
[b] The number shown is the half-maximal stimulatory concentration, defined under *Materials and Methods,* in micromoles. TNF-α release was measured in human whole blood stimulated with compounds as described under *Materials and Methods* and is the mean of 2 to 22 separate assessments. In calculating the mean and standard error, we assigned a value of 10 if the half-maximal stimulatory concentration was 10 μM or greater.

Figure 45. Structure, stereochemistry and activity of dimeric phospholipid structures(A) Phospholipid dimer structures, the linker, **R**, between the monomeric units can be either a urea **A** or a diamide **B** having one or four methylene separating the amide carbonyls. The stereochemistry of positions **a** and **b** are either racemic, R-, or S- in configuration. The acyl chains connected as esters, $\mathbf{R^1}$ and $\mathbf{R^4}$, are unsaturated, **C**, or saturated, **D**, while the acyl chains connected as amides, $\mathbf{R^2}$ and $\mathbf{R^3}$, are either **E** or **F**. (**B**)The table provides the appropriate substitutions for all discussed structures.

The distance between the **ER111232** phosphates was designed to approximates the one separating the anionic groups in lipid As, using modelling calculation techniques. To learn whether these synthetic agonists activates cells through similar signaling mechanisms than LPS, they were tested for their ability to trigger NF-κB production in HEK293 cells stably expressing TLR4, MD-2 and an NF-κB reporter gene (HEK293-TLR4/MD-2/ELAM-luc). The results showed that the synthetic agonists up-regulated NF-κB by TLR4-dependent activation. Results were confirmed by antagonist (Eritoran) co-administration assay. Indeed, the release of TNF-α induced by **ER111232** was inhibited in presence of **Eritoran**, confirming that the actual target of these agonists is the TLR4/MD-2 complex.

Furthermore, this study indicates that while arrangement in space, chain length and number of FA chains is essential for the immune-stimulant activity of lipid As, the disaccharide scaffold seems not to be that important, or to a lesser extent. However, it was showed that the compound stereochemistry, and more precisely the chirality of its serine portion, plays a large role in

activity. Starting from the most active diastereomeric mixture, **ER119327**, the R,R,R,R-, R,S,S,R-, and R,R,S,R-isomers (equivalent to R,S,R,R) showed activity differences. As predicted by computational studies, the R,R,R,R-isomer was found to be the most active of the three diastereomers. The all-R stereochemistry version of **ER112066**, is currently the most relevant compound of this class, it demonstrates TLR4 agonist activity both in murine and human. It has been licensed to Sanofi Pasteur and is in preclinical phase development as vaccine adjuvant for several applications: *Trypanosoma cruzi*, Meningococcus, Influenza and Cancer.[225]

2. TLR4 antagonists

As described in the previous sections, lipid-based antagonists have been observed to possess anti-endotoxic properties essentially competing with LPS for the binding to the receptor proteins. Several compounds were synthesized with the aim to find efficient and non-toxic TLR4 antagonists and they are discussed in the following sections.

1.1) Disaccharides compounds as TLR4 antagonists

- **Lipid IVa (compound 406)**

The **Lipid IVa** (also found as precursor Ia or compound **406** in literature) is a tetra-acylated di-phosphoryl version of *E. coli* lipid A and corresponds to a biosynthetic precursor of lipid A. Compared to *E. coli* lipid A, **lipid IVa** lacks the two branched chains linked at C3 and C3' positions (Fig. 46). Its total synthesis was accomplished in 1984, even before the one of lipid A, thus representing an historical milestone.[85,313,314] As explained at the beginning of this chapter, tetra-acylated **lipid IVa** acts as an antagonist in human but as an agonist on mouse TLR4.[245,267]

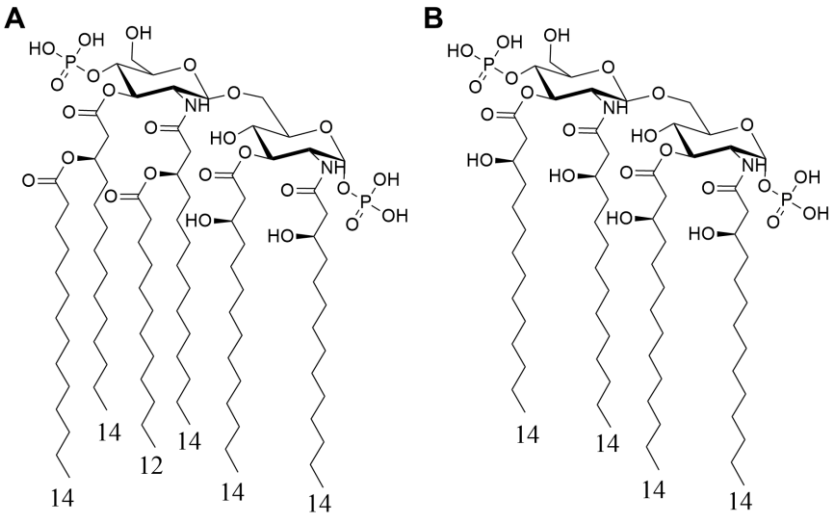

Figure 46. Chemical structure of (A) E. coli lipid A and (B) the synthetic lipid IVa

In order to better understand the interactions of **lipid IVa** with hMD-2, the crystal structure of human MD-2 in complex with **lipid IVa** was achieved in 2007.[69] The crystal structure showed that the two phosphates groups of **lipid IVa** interact with the positively charged lysine and arginine residues of hMD-2 while they do not form direct hydrogen bonding with MD-2 atoms. Its four FA chains are all deeply confined in the cavity and are packed next to each other through Van Der Waals interactions.[69] It also revealed that an additional space is generated by the displacement of the glucosamine backbone of lipid A upwards by 5 Å. Therefore, **lipid IVa** is deeply buried into the MD-2 cavity and it may be the reason why LPS with five or less lipid chains are less active, antagonist or inactive in biological assays. The study was later completed (2012) by the crystal structure of mouse TLR4/MD-2 (mTLR4/MD-2) in complex with tetra-acylated **lipid IVa**. It permits to compare to the crystal structure available: mTLR4/MD-2/**lipid IVa** (PDB ID: 3VQ1),[277] hTLR4/MD-2/**lipid IVa** (PDB ID: 2E59),[69] mTLR4/MD-2/Re-LPS (Re chemotype of *E. coli* LPS, PDB ID: 3VQ2),[277] and hTLR4/MD-2/Ra-LPS (Ra chemotype of *E. coli* LPS, PMB ID: 3FXI).[70]

Interestingly, similar structural changes were observed for the Phe126 loop in all the four crystal structures. Moreover, although **lipid IVa** lacks two acyl chains compared with hexa-acylated LPS, it showed the same overall orientation as LPS. The phosphate atoms are displaced about 1.3 and 2.6 Å in the 1-PO_4 and 4'-PO_4 groups respectively when ligands of mTLR4/MD-2/**lipid IVa** and mTLR4/MD-2/Re-LPS are superimposed.

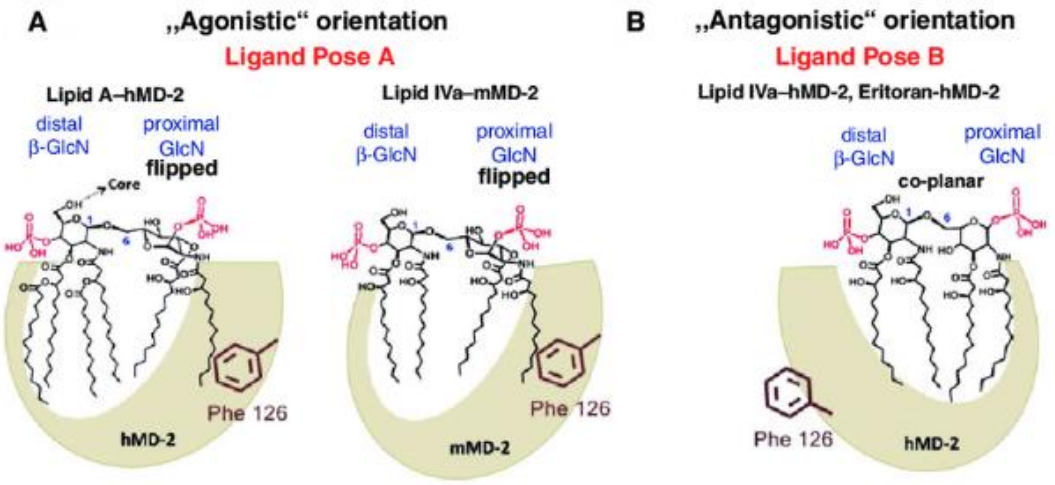

Figure 47. Orientations of the lipid A ligands within the binding pocket of MD-2. (**A**) Schematic representation of the orientation of the agonistic ligands resolved in the co-crystal structures: *E. coli* lipid A hMD-2/TLR4 (PDB ID: 3FXI) and **lipid IVa** mMD-2/TLR4 (PDB ID: 3VQ1) wherein the proximal (reducing) GlcN ring of the GlcN(β1-6)GlcN backbone faces the Phe126 loop. Phe126 is shifted inward to stabilize the exposure of the 2N-acyl chain on the surface of MD-2 and to allow the dimerization with the second MD-2*/TLR4* complex. (**B**) Orientation of the antagonistic ligand lipid IVa hMD-2 (PDB ID: 2E59) wherein the distal (non-reducing) GlcN ring faces the Phe126 loop. Phe126 is oriented outwards and exposed to solvent, which prevents the dimerization of two receptor complexes.

It was speculated that the favorable interaction induced by the interaction of the exposed R2 chain with the hydrophobic patch of TLR4* should compensate the energetically unfavored arrangement of **lipid IVa** related to its acyl chain partially exposed to the protein surface (and solvent) and the hydrophobic cavity left partially unoccupied.[268]

Another big change between mMD-2/**lipid IVa** and the hMD-2/Ra-LPS crystal structures is the flipped orientation of the ligand. It is most likely due to the charged polar residues present at the rim of the MD-2 proteins, being slightly different between human and murine, they should modify the electrostatic potential of the cavity entrance.[267] Indeed, while in mTLR4/MD-2 the two phosphates groups of **lipid IVa** were surrounded by positively charged Arg266, Lys319, Arg337, Lys367 and Arg434, they are substituted by Glu266, Thr319, Leu337, Glu367 and Gln434 in hTLR4.[69,277]

Notably, Lys367 and Arg434 were located near the dimerization interface. It was reported that, when these residues were replaced with their human counterparts, Glu367 and Gln434, the responsiveness of the mTLR4/MD-2 to **lipid IVa** was abolished.[315] Hence, these two residues play an important role in species specificity for **lipid IVa**, possibly by enhancing the interaction with the 1-PO_4* group of **lipid IVa**. These residues most likely modulate the electrostatic surface potentials to favor the suitable positioning of the negatively charged 1-PO_4 group for an efficient dimerization of the [mTLR4/MD-2/**lipid IVa**]$_2$ complexes. It was also reported that mMD-2 mutation at Glu122 to its human counterpart Lys122, substantially reduced the

responsiveness to **lipid IVa**.[315] Once again, modifications of the positively charged Lys residue would change the electrostatic potential of the cavity entrance and therefore, the interactions with the charged phosphate groups of **lipid IVa**.

As a consequence of the overall orientation change, **lipid IVa** is more deeply buried into the hydrophobic pocket of hMD-2 than it is for the mTLR4/MD-2/**lipid IVa** complex and is not available to enhance the dimerization process. [69,277]

These results confirm the central role of the charge distribution for the correct positioning of lipid As and the efficient dimerization of TLR4/MD-2.

- **Penta-acyl lipid As: RsDPLA and RcDPLA**

These two compounds were initially studied because of their inactivity as agonists and their curious structure, leading to a challenge for its characterization. Indeed, *Rhodobacter sphaeroides* (ATCC 17023 strain) and *Rhodobacter capsulatus* (37B4 strain) have two penta-acylated di-phosphoryl lipid As (**RsDPLA** and **RcDPLA** respectively).[316] Both of them have a common and unique structural feature, having 3-keto acids at their N-bound acyl moieties (C2 and C2' positions) in place of ordinary 3-hydroxy acids in other lipid As.[317–320] In addition, both contain an unsaturated FA acid chain, these unique features where hypothesized to be responsible for their strong antagonistic activity, suppressing the endotoxic action of LPS when administered simultaneously, both *in-vitro* and *in-vivo*.[321,322]

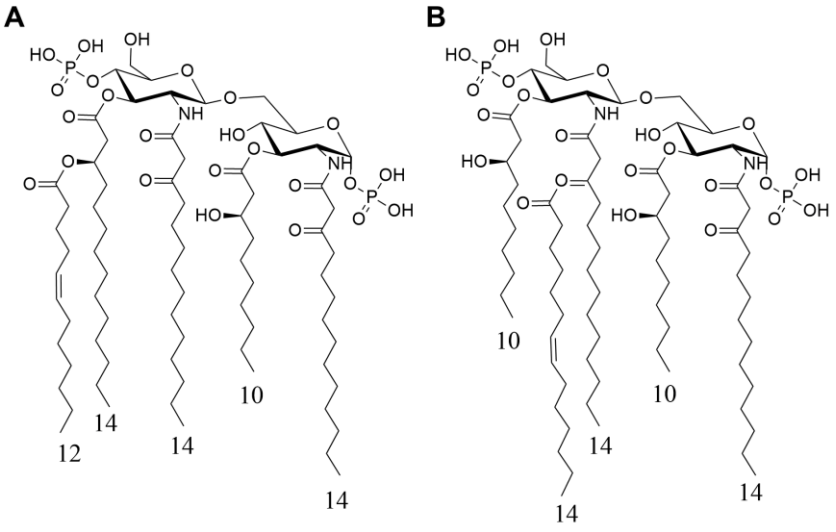

Figure 48. Chemical structures of penta-acyl Rhodobacter: (**A**) Rhodobacter capsulatus (**RcDPLA**) and (**B**) Rhodobacter sphaeroides (**RsDPLA**).

Therefore, these two compounds became extensively characterized. In particular, their total synthesis were realized, allowing the test of pure compounds, which confirmed the previous

data.[323] [324] They appear to be able to block LPS-induced cytokine production (TNF-α and Interleukins) *in vivo* as well as *in vitro* on monocytes/macrophages and RAW264.7 (murine macrophage cell line).[325–327] Moreover, it was also reported that **RsDPLA** blocks LPS-induced pre-B cell activation[328] and CD18 surface expression on human neutrophils.[329]

- **Eritoran (E5564)**

Since the synthetic **RsDPLA** and **RcDPLA** showed promising results with a powerful antagonistic activity combined to a low toxicity, chemists focused on the synthesis of analogs. From these studies, two compounds emerged as interesting: **Eritoran** (or compound **E5564**) and compound **E5531**.[330]

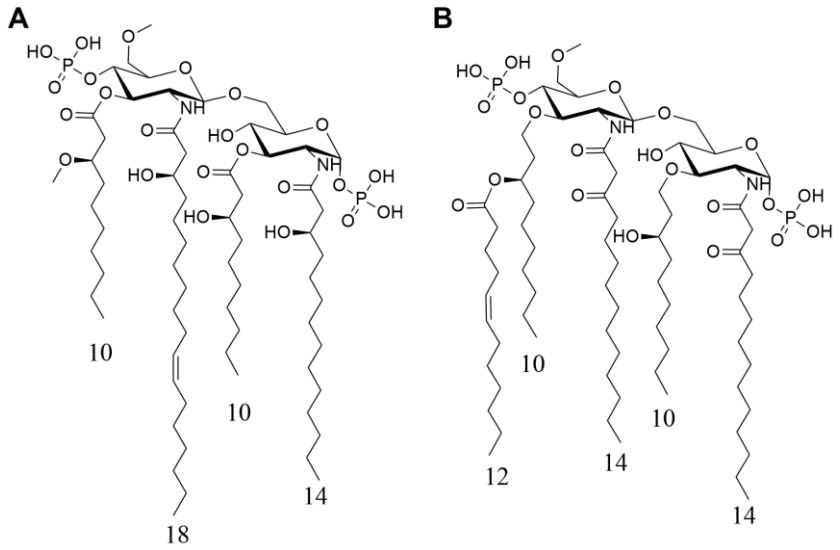

Figure 49. Chemical structure of (A) Eritoran (E5564) and (B) compound E5531

Both were designed as a combination of **lipid IVa** and the DPLAs, they possess a di-glucosamine scaffold with two phosphate groups in (C1 and C4' positions), four FA chains for **Eritoran** and five FA chains for **E5531**. **Eritoran** (Fig. 49A) is linked to the classical (R)-3-hydroxytetradecanoate (C14) chain in position C2, (R)-3-hydroxydecanoate (C10) at C3, (R)-3-methoxydecanoate at C3' and the (R, Z)-3-hydroxy-11-octadecenoate (C18:1) linked to the C2' position. In contrast, compound **E5531** (Fig. 49B) is linked to two 3-oxotetradecanoate chains at position C2 and C2', (R)-3-hydroxydecyloxy ether in position C3 and a branched chain in C3' as (Z)-1-hydroxydecan-3-yl dodec-5-enoate).

Eritoran and **E5531** demonstrated a powerful antagonist activity both in human and in murine cells. These compounds are able to reduce, in a dose dependent manner, the production of LPS-induced cytokines. They block LPS/ sCD14-induced reporter activity in TLR4/MD-2-

expressing HEK293 but not TLR2-mediated signaling by heat-killed *S. aureus*. Thus indicating that they most likely inhibits LPS signaling via TLR4/MD-2.[331]

Similarly to **Eritoran**, **E5531** associates with plasma proteins, reducing the compounds concentration, which prevent the activity in a dose- and time-dependent manner.[332] However, compared with **E5531**, **Eritoran** is a more potent inhibitor of cytokine generation, and higher doses retain the activity for duration sufficient to permit clinical application.[332]

Structure-activity relationship between **Eritoran** and TLR4/MD-2 complexes have emerged from the crystal structures of the compound with human and murine TLR4/MD-2.[29] They revealed that **Eritoran** binds into the hydrophobic pocket of hMD-2 without any direct interaction between **Eritoran** and TLR4. **Lipid IVa** and **Eritoran** bind to the same area of the MD-2 pocket and the presence of long unsaturated chain (C2') seems to have an important role in determining its powerful antagonistic activity. The *cis* double bound appears to enhance the space filled into the pocket because of its bent shape. The chain makes a 180° turn at the *cis* double bond so that it occupies a larger space in the pocket, it fits better with the concave shape of the MD-2 pocket and can display π–π interactions.

These results indicate that **Eritoran** is a potent antagonist and may be a potential therapeutic agent for the treatment of diseases like sepsis. It was also envisaged as a promising treatment for influenza since it is able to abolish the bacterial-induced lethality due to LPS in primed mice.[81,332]

Eritoran entered clinical trials for the treatment of sepsis and appeared to be significantly protective in animal model of sepsis and, in healthy volunteers, blocking the signs and symptoms of endotoxemia in a dose-dependent manner.[231] Despite the first encouraging results, the clinical phase III was discontinued in 2011 because: **Eritoran** showed a lack of statistically significant activity when tested on a panel of 2000 septic patients.[83]

- **Triacyl disaccharide OM-174**

In 2000, OM Pharma (Meyrin, Switzerland) purified a di-phosphoryl, triacyl, disaccharide lipid A derivative from *E. coli* and called it **OM-174** (Fig. 50).

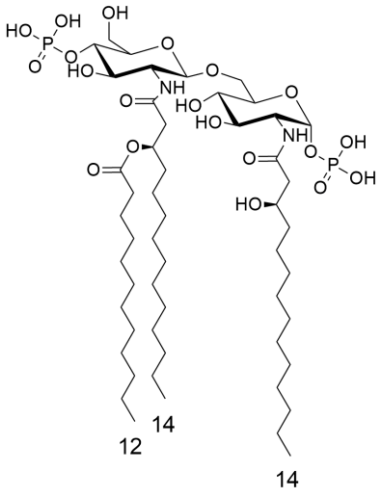

Figure 50. Chemical structure of OM-174

Surprisingly, while the tri-acyl lipid A is known to be more than 10^5-fold less active than the hexa-acyl lipid A, it was only 10-fold less active in inducing IL-6 in human mononuclear cells, and equally active in inducing NO production in murine macrophages. Despite the fact that the 1,4-bisphosphorylated β(1-6) diglucosamine backbone is identical for **OM-174** and lipid A, their overall physicochemical behaviour, as well as biological reactivity, are very different. For example, the reduction of the acyl chains number leads to a decrease in Tc from 43°C for the hexa-acyl lipid A, 30 °C for a penta-acyl structure, 15 °C for a tetra-acyl partial structure and down to 0 °C for the triacyl **OM-174**. Concomitantly, the supramolecular structures at 37 °C changes from inverted cubic (hexa-acyl lipid A), through lamellar (tetra-acyl lipid A) to micellar H_1 (**OM-174**) structure. Interestingly, the decrease of the acyl chains number and the concomitant change in the supramolecular conformation are accompanied by the ability to bind increasing amounts of water in the interface region. [242,333]

OM-174 has been reported to induce regression of tumours in rats bearing established colon tumours and is in Phase I clinical trials as anticancer treatment.[225,334,335]

1.2) Dimer of phospholipids as antagonists

Inspired by phospholipid **ER112022**, were developed the tri-acylated di-phosphorylated pseudopeptides called **OM-174**, **OM-294-DP** (DP=diphosphorylated) and **OM-294-MP** (MP=monophosphorylated). The **OM-294** compounds are similar to **OM-174** but carrying only the essential functionalities of the parent lipid A structure.[336]

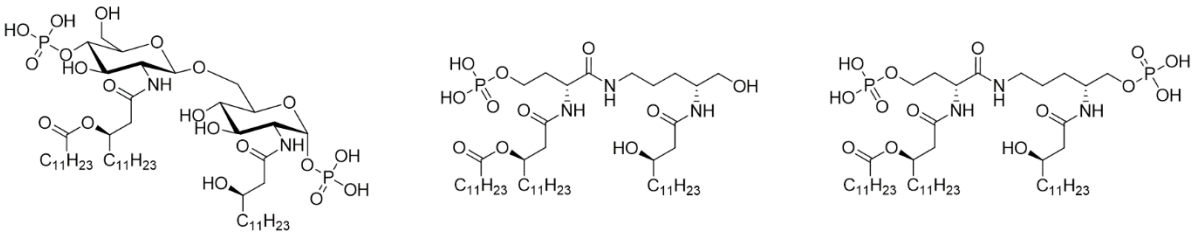

Figure 51. Chemical structure of the OM-174, OM-294-MP and DP compounds

This scaffold is a pseudo-dipeptide of ornithine (C-terminal amino acid (AA)) and homoserine or aspartic acid (N terminal AA). All the stereochemical combinations of the AA have been synthesized and biologically tested. These compounds showed mixed immunological activities (agonistic/antagonistic), comparable to that of the parent lipid A, while being practically devoid of endotoxicity. Indeed, all **OM-294-DP** diastereomers are powerful inducers of NO production, comparable to the effect of the parent biological molecule **OM-174**, but they do not induce IL-6. They act as strong LPS antagonist but only when LPS is added before the compounds. **OM-294-MP** diastereomers showed lower agonistic and antagonistic activities than **OM-294-DP** compounds. It suggests that these compounds, even if they showed an effect towards LPS, seem not to be specific TLR4/MD-2 binders.

1.3) Lipid A reducing part mimetics

The molecular simplification approach was used to synthesize AGPs based on the reducing part of lipid A. For those compounds, the non-reducing part was substituted with acylated phosphoserine or aspartic acid with L- or D-configurations at the α-position of the amino acids.[337]

A series of those mimetics was designed with two anionic groups, three acyl- or four acyl-groups as well as four linear chains or one branched and two linear. These analogs were evaluated for the induction of human cytokines and their inhibitory activities against LPS.

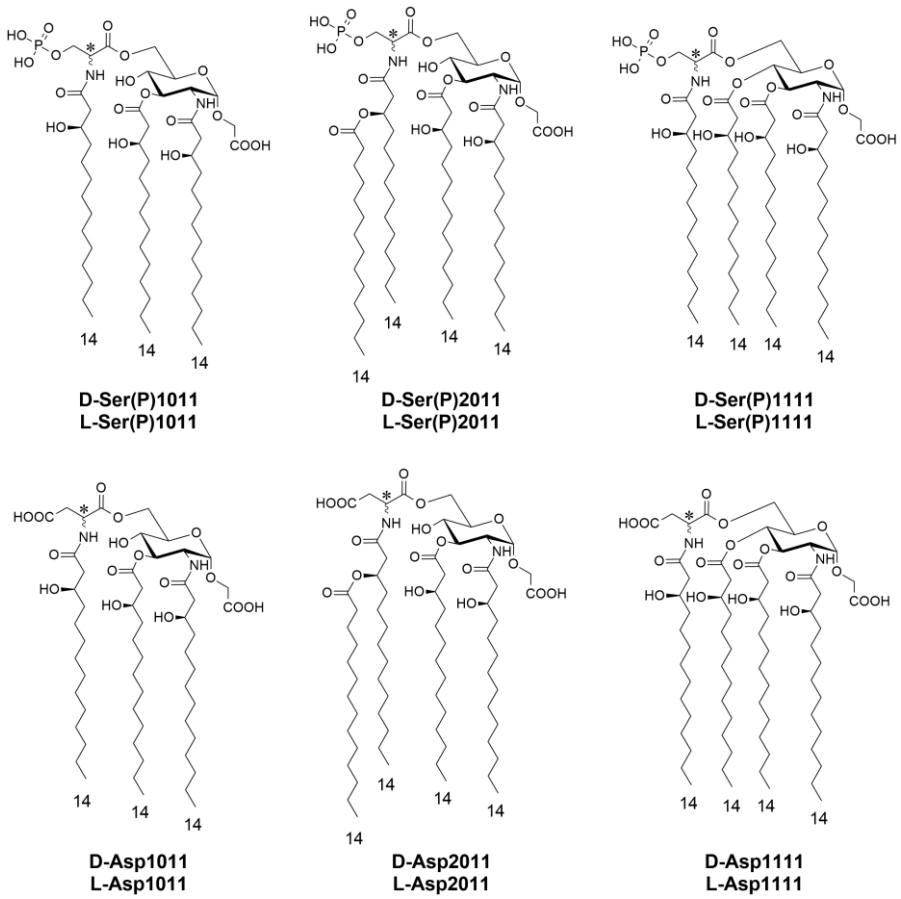

Figure 52. Chemical structure of lipid A reducing part linked to acidic N-acyl-amino acids analogs

The phosphoserine analogues displayed an antagonistic activity regardless of the acylation pattern. On the other hand, aspartic acid analogues showed varying results: the tri-acylated **L-Asp1011** showed a weak antagonist effect as well as a weak agonistic activity; the branched tetra-acylated **D-Asp2011** is agonist and was found 100-fold stronger than **L-Asp2011**; finally, the linear tetra-acylated **D-Asp1111** and **L-Asp1111** are antagonists.[337]

As a result of the study, it appears that the phosphoserine-containing analogues were stronger inhibitors than the corresponding aspartic acid-containing analogues (comparing the same acylation patterns). The agonistic and antagonistic activities were switched with the modification of the functional group (**D-Ser(P)2011** and **D-Asp2011**). The inhibition is stronger for the tetra-acylated analogs than the tri-acylated compounds. The two negatively charged groups are needed, as for lipid As, to interact with the positively charged groups at the MD-2 binding site to obtain the maximal activity. Moreover, the distance between ionizable groups, intrinsically fixed for the disaccharides, seems to be a critical determinant for MD-2 binding.

1.4) Monosaccharides as TLR4 antagonists

- **FP7**

Compounds were designed and synthesized by our group back to 2014.[274] They were originally designed as analogs of **SDZ-880.431** itself being a derivative of **lipid X** (Fig. 53). Compared to **lipid X**, **SDZ-880.431** possess an additional 4-posphate and resulted to be the most potent monosaccharide antagonist on human and on murine models.[245,302–304] This powerful antagonist was, however, synthesized before the discovery of TLR4/MD-2 role in immuno-modulation, and never tested for its ability to bind MD-2.

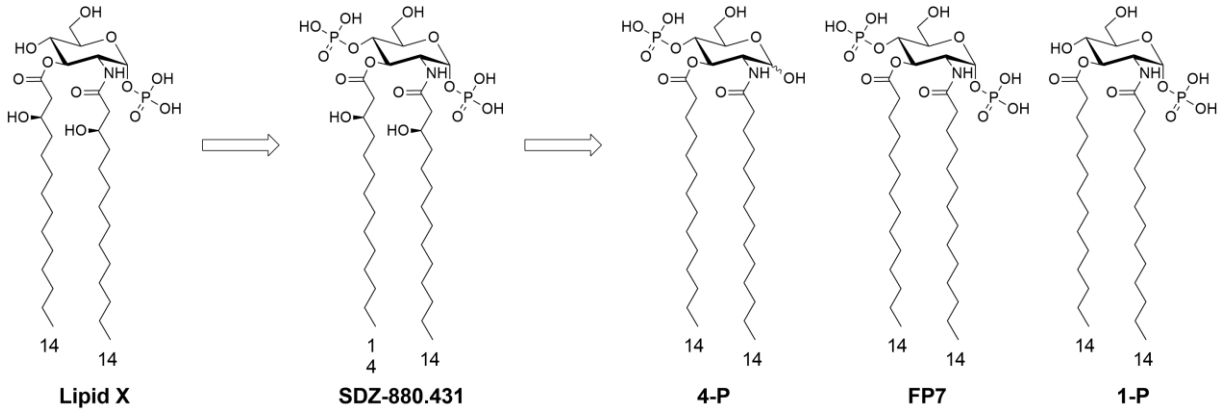

Figure 53. Structures of lipid X, SDZ-880.431 and designed 4-P, FP7 and 1-P

Based on the promising results of **SDZ-880.431**, compounds were designed and synthesized as simplified version of **SDZ-800.431** with myristic chains replacing the β-hydroxyl myristic chains and phosphorylated in position C1 (**1-P**), C4 (**4-P**) or both (**FP7**). The initial divergent synthetic strategy is depicted below in Figure 54. Briefly, through three sequential -synthetic steps, glucosamine was protected with an azido group at position C2, a *para*-methoxybenzylidene (PMB) was inserted, blocking position C4 and C6 as an acetal and the anomeric position was protected as a *tert*-butyldimethylsilyl ether (TBDMS). Then, the azido group was cleaved to an amine by a Staudinger reduction and position C2 and C3 were esterified with myristic acid in the presence of the 1-ethyl-3-(3-dimethylaminopropyl) carbodiimide (EDC) as a condensing agent and a catalytic amount of dimethyl aminopyridine (DMAP). From this point, the batch were splitted to produce the three compounds
Deprotection of the TBDMS, subsequent phosphorylation and hydrogenation on Pd/C gave **1-P**. The regioselective ring opening of PMB with sodium cyanoborohydride ($NaBH_3CN$) permit to obtain two different compounds (**9** and **12**). Indeed, $NaBH_3CN$ open the benzylidene to selectively give the hydroxyl at position C4 and PMB at position C6 (compound **9**) but, adding

a stoichiometric amount of hydrochloric acid, TMDMS was also cleaved from the anomeric position giving compound **12** with free hydroxyls at C1 and C4 positions and PMB at C6. Compound **9** was phosphorylated, TMDMS was cleaved by TBAF, and final hydrogenation gave **4-P** while compound **12** was phosphorylated and hydrogenated to obtain **FP7**.

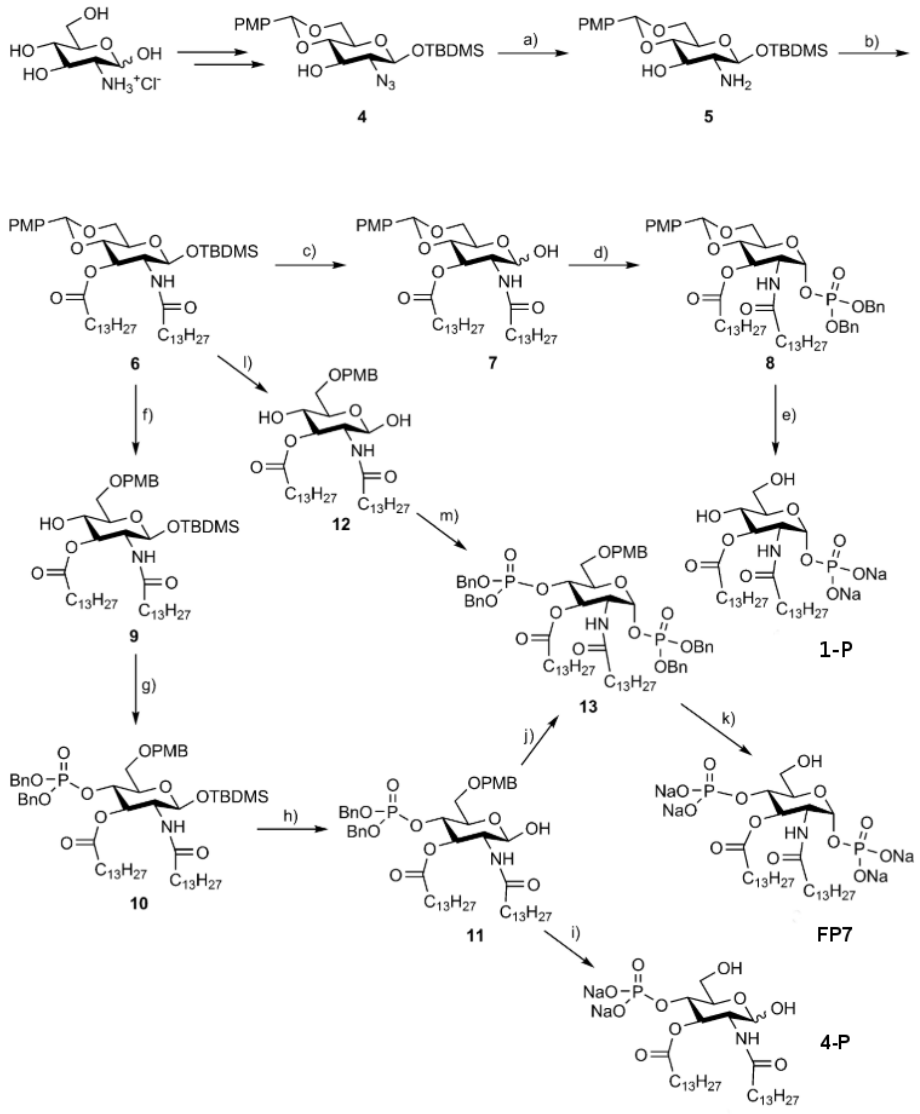

Figure 54. Divergent strategy for the synthesis of 1-P, 4-P and FP7. Reagents and conditions: a) PPh_3, THF/H_2O, 60°C, 87%; b) myristic acid, EDC, DMAP, DCM,97%; c) TBAF, AcOH, THF, - 15 °C to RT, 76%; d) tetrabenzyl diphosphate, $LiN(TMS)_2$, THF_{dry}, - 78 to – 20 °C, 43%; e) H_2, Pd/C, AcOH, dry MeOH/DCM, quant.; f) $NaBH_3CN$, 4Å MS, THF_{dry}, 84%; g) $(BnO)_2PN(iPr)_2$, imidazolium triflate, DCM_{dry}, then m-CPBA, 0 °C, 42%; h) TBAF, AcOH, THF, - 15 °C to RT, 57%; i) H_2, Pd/C, AcOH, dry MeOH/DCM quant.; j) $P_2O_3(BnO)_4$, $LiN(TMS)_2$, THF_{dry}, - 78 to – 20 °C, 71%; k) H_2, Pd/C, AcOH, dry MeOH/DCM quant.; l) $NaBH_3CN$, 4Å MS, THF_{dry}, then HCl in dioxane until pH 1.5, 61%; m) $(BnO)_2PN(iPr)_2$, imidazolium tosylate, DCM_{dry}, then m-CPBA, 0 °C, 38%.[274]

The biological activity of the three derivatives was investigated on HEK293 cells and none of them showed agonist activity. MTT was performed and the compounds reveal limited to no toxicity up to highest concentration tested (50 μM). When cells were pre-treated with increasing concentrations of the synthetic compounds (0 to 50 μM) and then stimulated with *E. coli* LPS,

compound **FP7** turned out to be a powerful antagonist while compounds **1-P** and **4-P** were only weakly active in inhibiting LPS-stimulated TLR4 signaling.[274]

The compound **FP7** appeared to have a low IC_{50} of 0.46 when tested at low LPS concentration (10 ng/ml) and it increase to 3.42 μM for more concentrated LPS solutions (1 μg/ml).[88,274]

The study was extended to animal cell model as bone-marrow-derived murine (BM) macrophages from wild type and $CD14^{-/-}$ mice. It appears that the TNF-α production was reduced in the same way also in murine. **FP7** showed a dose-dependent agonistic activity at low LPS concentration for wild type cells and at higher LPS concentration for $CD14^{-/-}$ BM macrophage cells. The activity in both cell types strongly suggest that **FP7** competes with LPS for both CD14 and the TLR4/MD-2 complex.

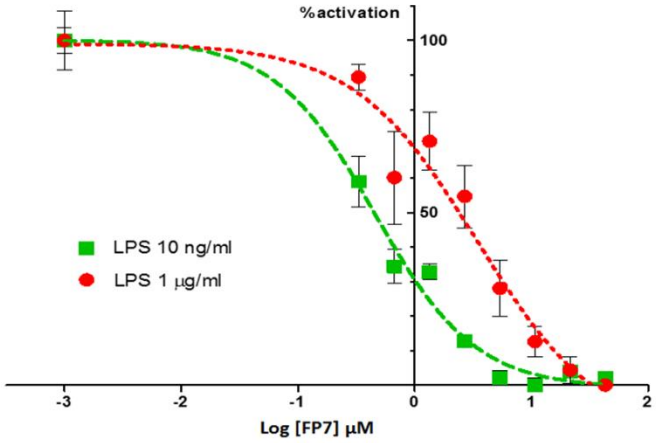

Figure 55. FP7 inhibition of LPS-induced TLR4-dependent activation on HEK-blue cells

These promising results led our group to focus on this compound to understand its mechanism of action, search for possible applications and use it as lead compound for novel TLR4 antagonists.

a. Aggregation state

Even if the issue of whether large or small aggregates, or monomers, are the biologically active units is still unclear, as stated before, the aggregation state in solution is an important information to acquire. The activation of TLR4 could in principle be triggered by diverse effects generated by the aggregates shape of such amphiphilic compounds (intercalation into the membrane and/or activation of potassium channels and caspases).

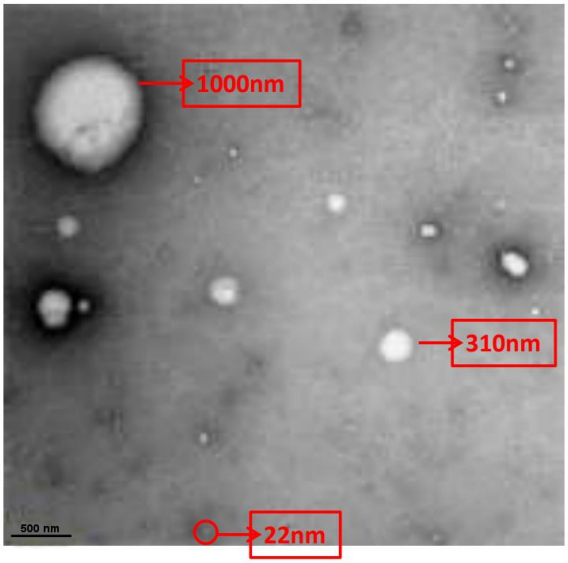

Figure 56. TEM-Negative Staining of FP7 Lipid (2.5 mg/ml).
Nominal magnification x10,000 (1.1nm/pixel).

Thus, Transmission Electron Microscopy (TEM) with negative staining analysis (Fig. 57) was used to obtain the required the morphological information and revealed that **FP7** assemble mainly as small to medium micelles (20 to 300 nm) but may also form large micelles, 1 μm of diameter.

A study of co-administration of antimicrobial peptides was recently conducted.[234] The co-administration of two LPS-neutralizing peptides (a cecropin A–melittin hybrid peptide and a human cathelicidin) proved to enhances by an order of magnitude the potency of **FP7** in blocking the TLR4 signal. NMR experiments, TEM with negative staining and cryo-TEM show that peptide addition changes the aggregation state of **FP7**, promoting the formation of larger micelles. It reinforces the already suggested relationship between the aggregation state of lipid A-like ligands and the type and intensity of the TLR4 response.

b. Docking studies

To study the possible binding of **FP7** to TLR4 complex, docking studies were performed by Jean-marc Billod (ESR1) and collaborators from the group of Professor Sonsoles Martin-Santamaria (CIC CSIC, Madrid, Spain) with AutoDock[338] and AutoDock Vina[339] programs. Computational programs were validated by docking the natural antagonist **lipid IVa**, using the X-ray crystallographic structure of hMD-2 protein in complexation with lipid IVa as the starting geometry (PDB ID: 2E59).[69] Once the docking procedures were validated, the same docking protocol was applied to **FP7**. Reasonable binding poses were predicted showing that this compound may be a suitable binder. The docked theoretical MD-2 binding energies for compounds **1-P** and **4-P** were significantly higher than for compound **FP7** (~8 $kJ.mol^{-1}$),

validating furthermore the model since in accord to *in vitro* data. Analysis of the binding poses showed that **FP7** may bind in two different fashions, with close predicted binding energies. Most of the best docked solutions corresponded to binding poses with the two FA chains deeply buried inside the MD-2 pocket, similarly to what had been seen with lipid IVa. One of the FA chains establishes hydrophobic contacts and CH–π interactions with Leu74, Phe76, Phe104, and Ile117, in a similar way to the FA chain of **lipid IVa** (Fig. 57A). The second FA chain is directed into a region delimited by Ile52, Leu54, Phe121, Ile124, Tyr131, and Ile153, the "sub-pocket" occupied by the FA chain in the MD-2/**lipid IVa** complex.

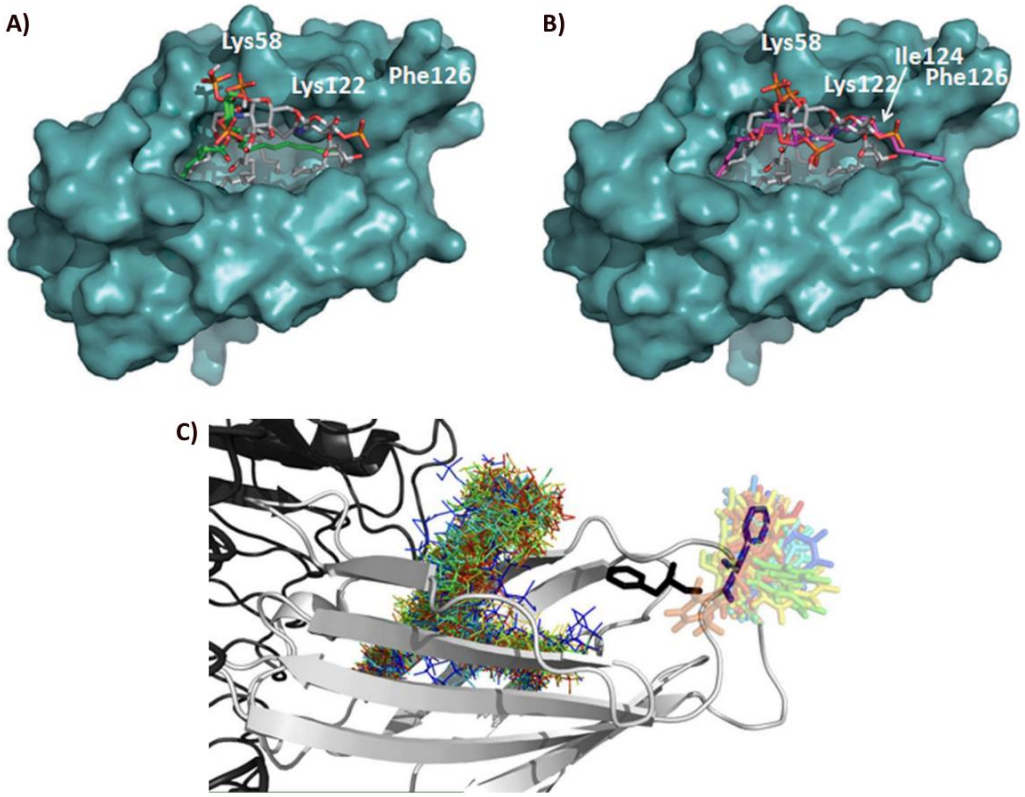

Figure 57. Binding poses of FP7 Autodock binding poses of FP7characterized with either two (green, **A**) or one (magenta, **B**) FA chains oriented inside the lipophilic MD-2 pocket. Lipid IVa is shown as reference in CPK colours. (**C**) Superimposition of snapshots (one for each simulated nanosecond), from the Molecular Dynamic simulations of the TLR4/MD-2/FP7 complex, coloured from blue (t=0 ns) to red (t=50 ns). Only FP7 (as lines) and Phe126 (in sticks) are made visible. Side chains of Phe126 from the X-ray crystallographic structures have been superimposed to the snapshots to illustrate the antagonist (dark blue, PDB-ID 2E59) and agonist (black, PDB-ID 3FXI) conformations of MD- 2.

In few cases, a second binding mode appears, with one FA chain extending towards Val82 and placed over Ile124 (Fig. 57B). Moreover, this Ile124 moves in the agonist conformation letting its position is occupied by Phe126 (as the previously described agonist/antagonist switch, Fig. 57C). One phosphate group participates in hydrogen bonds with Ser118 and is always found in near Lys58 and/or Lys122, similarly to one phosphate of **lipid IVa**. The second phosphate group position is found move variable between the docking poses, near the positively charged side

chains of Arg96 or exposed to the outside. These predicted binding poses provided a 3D model for the hydrophobic interaction of the FA chains and as well as the polar interactions involving the phosphate groups with the MD-2 protein.

c. Specific binding to MD-2

Then, during its doctoral thesis, Lenny Zaffaroni (ESR3) from our group, set-up a protocol to express hMD-2 on *Pichia pastoris* and purify hMD-2 protein. Our collaboration and the availability of the hMD-2 protein in its monomeric form lead us to perform several binding studies: ELISA assay of LPS competition and LPS-biotin displacement, **bis-ANS** displacement assay and Surface plasmon Resonance (SPR).

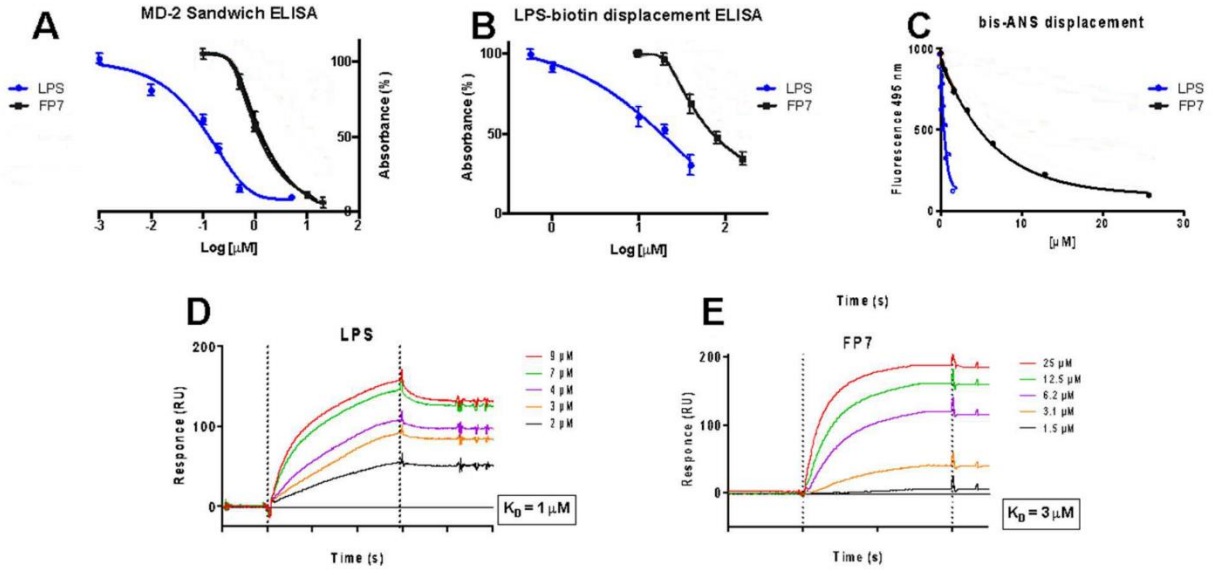

Figure 58. Cell-free binding studies on purified MD-2 receptor (A) LPS and FP7 prevent anti-human MD-2 monoclonal antibody binding in a dose-dependent manner; (B) LPS and FP7 activity in competing with biotin-LPS for hMD-2 binding; (C) Fluorescence measurements show that LPS and FP7 dose-dependently inhibit the binding of bis-ANS to MD-2; (D-E) SPR analysis show direct interaction between LPS or FP7 and MD-2; KD values are reported. Results are mean ± SEM from three parallels representative of at least three independent experiments.

All these experiments were in complete accord and confirm the data extracted from cell assays since **FP7** binds to MD-2 (Fig. 58A), is able to displace LPS and **bis-ANS** from the MD-2 pocket (Fig. 58B and C) and possess a reasonable measured dissociation constant (K_D~3 µM, Fig. 58E). The evidence were numerous to be convinced that this compound actualy binds to MD-2 and was even able to displace LPS.

d. NMR studies

Nuclear Magnetic Resonance (NMR) assay in solution were also performed in collaboration with Helena Coelho (ESR9) from the group of Director Jesus Jimenez-Barbero (CIC bioGUNE, Bilbao, Spain). The recording of ^{1}H NMR spectra of **FP7**, of MD-2, and of a **FP7**/MD-2 mixture (ratio 5:1, at a 150 mM ligand concentration, Figure 59 showed selective attenuation of the signals corresponding to the myristic FA chain protons of **FP7** upon addition of MD-2 to the monosaccharide sample solution. Broadening of the overall resonance signals was detected but the decrease in signal intensities was significantly higher for the hydrogen atoms belonging to the FA aliphatic chains, particularly for the signals of the ω-methyl groups and contiguous CH2 moieties. Contrariwise, the signals corresponding to the hydrogen atoms of the sugar ring proved to be practically unaltered. The reductions in intensity observed experimentally are due to specific line broadening of these signals and arise from the changes in their transverse relaxation times. This drastic modification of the signals points, again, toward the existence of interaction between **FP7** and MD-2 and more precisely at the aliphatic side chain region. These data enriched the already suggested existence of a major interaction of both FA chains of the sugar ligand with the hydrophobic binding cavity of MD-2.

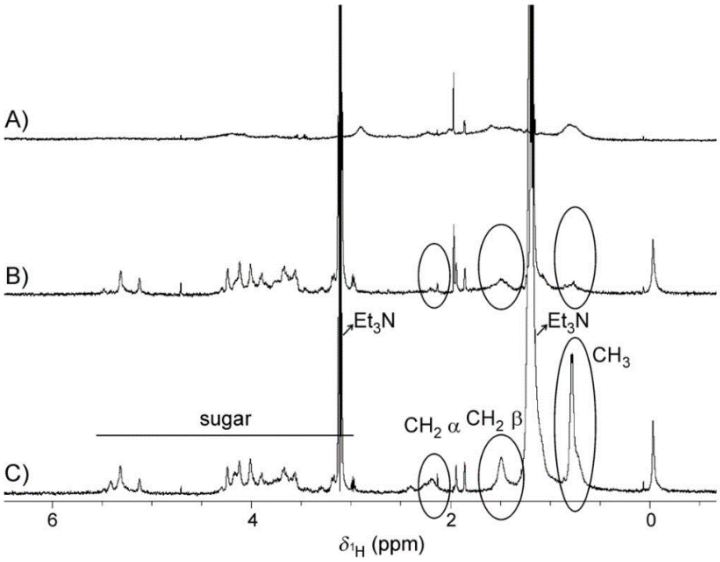

Figure 59. 1H NMR experiment upon addition of MD-2 to FP7 (**A**) ^{1}H NMR of 30 mM MD-2 protein in ^{2}D acetate buffer at pH 5, 298 K, 120 scans. B) ^{1}H NMR of 30 mm MD-2 protein and 150 mM **FP7** in ^{2}D acetate buffer at pH 5, 298 K, 120 scans. C) ^{1}H NMR of 150 mm **FP7** in ^{2}D acetate buffer at pH 5, 298 K, 120 scans.

e. LPS-induced activation of human monocytes and maturation of DCs

As stated previously, monocytes and dendritic cells (DCs) are essential actors of the innate immunity and inflammation regulation. Monocytes circulates in the peripheral blood stream detecting pathogens and danger signal, upon activation they produce cytokines and chemokines, triggering tissue-infiltrating DCs that are potent antigen-presenting cells. Both cell types express TLR4 at their surface and their stimulation by LPS lead them to produce pro-inflammatory

cytokines which varies according to the cell type. Therefore, the TLR4-antagonistic activity of **FP7** was tested *in vitro* on human monocytes and DCs (Fig. 60).[340]

It was observed that **FP7** is able to block almost completely the induction of IL-8, IL-6 and MIP-1β (Fig. 60a), which are the major cytokines secreted by LPS-stimulated monocytes.

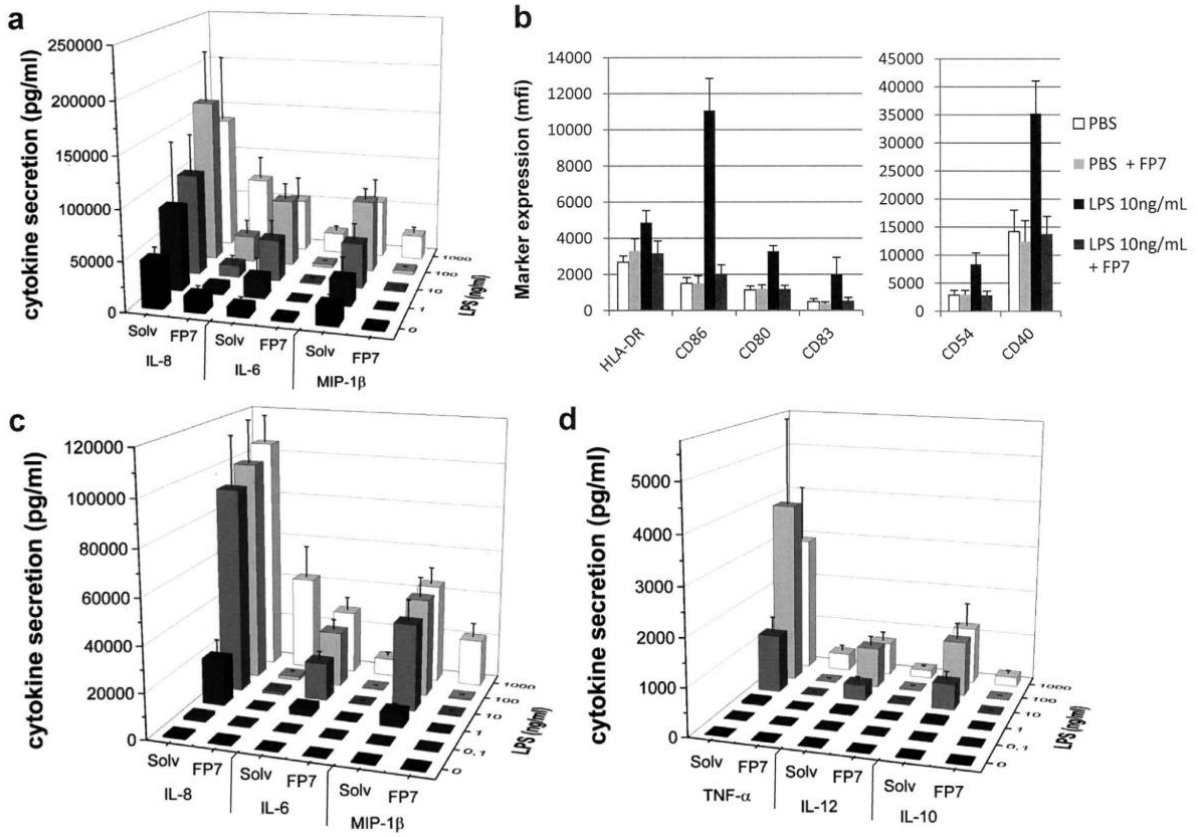

Figure 60. FP7 antagonizes LPS-induced human monocyte stimulation and DC maturation (**a**) Monocytes were isolated from peripheral human blood, stimulated for 24 h with increasing amounts of LPS or the same volume of PBS as control, in the presence of 10 μM **FP7** or solvent (Solv). Data represents mean cytokine secretion in monocyte supernatants from 4 independent experiments. (**b–d**) Dendritic cells (DCs) were differentiated from human peripheral blood monocytes for 6 days. DCs were stimulated for 24 h with increasing amounts of LPS or the same volume of PBS as control, in the presence of 10 μM **FP7** or solvent. Surface expression of DC maturation markers was monitored by flow cytometry and means ± SEM of fluorescence intensity are shown (**b**). Cytokine secretion was assayed in DC supernatants by Cytometric Bead Array (CBA). Data represents mean cytokine secretion from 6 independent experiments.

In is of common knowledge that TLR4 stimulation of DCs induces their phenotypic and functional maturation. To become mature DCs, they should be stimulated by PAMPs (as LPS) or DAMPs (released upon stress, infection or necrosis). During maturation process, DCs develop their capability to present antigens and therefore their capturing activity. They also increase their expression of major histocompatibility complex (MHC) antigens and cytokines genes-encoding. An important task devoted to mature DCs is the presentation of antigens to naive T cells in the lymph nodes.

DCs stimulated with LPS presented the classical response of human mature DCs with a strong induction of CD86 and CD40 (Fig. 60b), as well as increasing level HLA-DR, CD80, CD83 and CD45. The study demonstrates that **FP7** is able to abrogate the expression all these phenotypic markers (Fig. 60b). Moreover, DCs stimulated with LPS produce high levels of IL-8, IL-6, MIP-1β and TNF-α, as well as limited production of IL-10 and IL-12. The treatment with **FP7**, after DC differentiation, demonstrate that it also prevents the LPS-induced secretion of IL-8, IL-6, MIP-1β and TNF-α, IL-10 and IL-10 up to 100 ng/ml of LPS and inhibits the cytokine secretion induced by 1 μg/ml (Fig.60c and d). Therefore, it was demonstrated that **FP7** prevents LPS-induced maturation of DCs.

The IC_{50} may vary between cell lines and primary cells, thus IC_{50} was evaluated on monocytes and DCs looking at every previously cited cytokine. Monocytes and DCs were pre-treated with increasing dose of **FP7** before their stimulation with LPS.[340] It appears that **FP7** inhibits, in a dose-dependent manner, the secretion of pro-inflammatory cytokines on both monocytes and DCs.

	IC_{50} on monocytes (nM)	IC_{50} on DCs (nM)
IL-6	60	220
IL-8	130	440
MIP-1β	70	320

Table 4. IC50 of LPS in monocytes and DCs cells based in cytokine secretion inhibition

These results correlate with the previous experiment obtained in HEK-blue cells[274] and viability measurement, on primary cells, revealed that **FP7** was not toxic until a concentration of 10 μM. The specificity of **FP7** for TLR4 was also studied, indeed, for example, TLR4 and TLR2 share the capacity to be activated by lipid ligands. To test its specificity toward TLR4, **FP7** (10 μM) was incubated with several cell lines prior to 24h exposure to their natural ligand (Fig. 61):

a. HEK293 cells co-expressing human TLR4, MD-2 and CD14 were treated with ultrapure LPS (natural TLR4 ligand).
b. HEK293 cells co-expressing human TLR1 and TLR2 were treated with Pam3CSK4 (Pam3, natural TLR1/TLR2 ligand)
c. HEK293 cells co-expressing human TLR2 and TLR6 were treated with peptidoglycan (PGN, natural TLR2/TLR6 ligand).
d. DCs were stimulated with 10 ng/ml of ultrapure LPS or 10 μg/ml of PGN, PAM3, or pIC (double-stranded RNA poly(I:C), natural TLR3 ligand) in the absence or presence of **FP7** (10 μM).

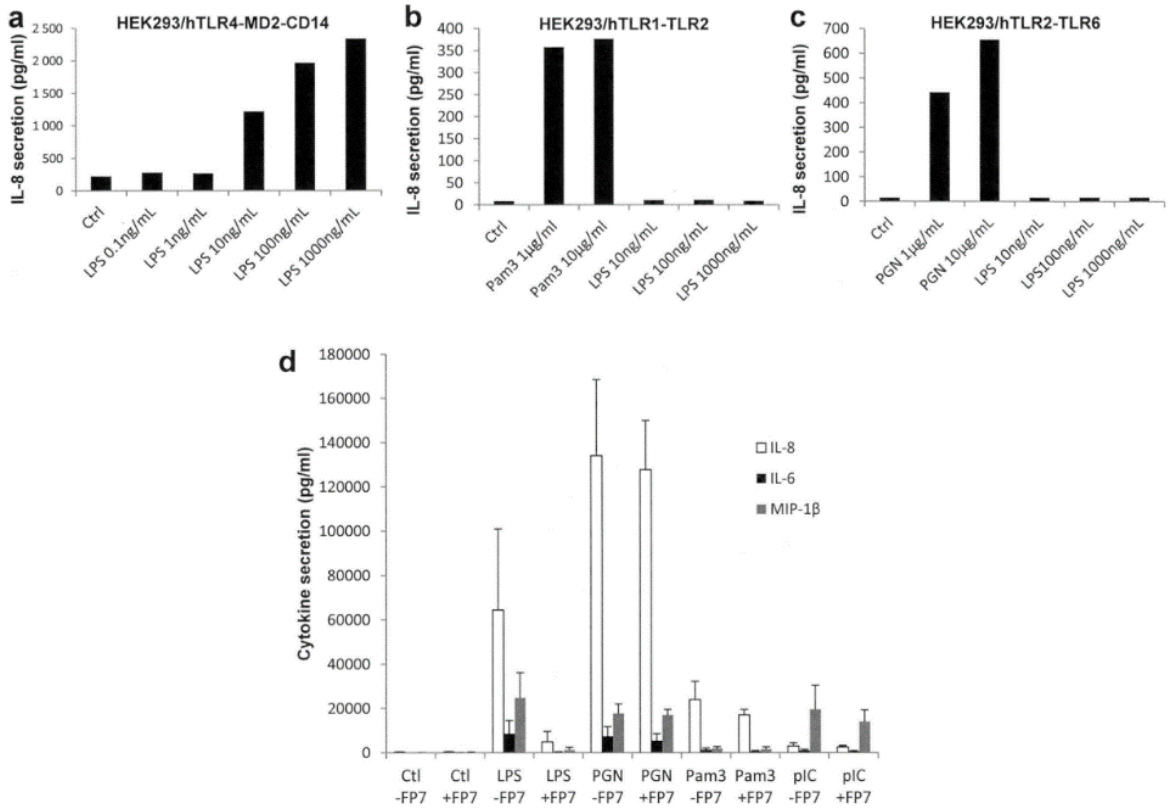

Figure 61. FP7 selectively antagonizes TLR4 (**a–c**) HEK293/hTLR4-MD2-CD14, HEK293/hTLR1-TLR2, HEK293/hTLR2-TLR6 cells were treated 24 h with ultrapure LPS, peptidoglycan (PGN), or Pam3CSK4 (Pam3). Supernatants were collected and IL-8 secreted in response to TLR stimulation was assayed. (**d**) DCs were stimulated for 24 h with 10 ng/ml ultrapure LPS or 10 µg/ml PGN, PAM3, or pIC in the absence or presence of 10 µM **FP7**. Control cells (Ctrl) received PBS instead of TLR ligand. Cytokine secretion was assayed in DC supernatants means ± SEM from 3 independent experiments are shown.

These experiments proved that while **FP7** is a strong antagonist of TLR4, it did not affect the stimulation of TLR1/TLR2, TLR2/TLR6 or TLR3 and can therefore be considered as a TLR4-selective ligand.

f. Activity on influenza-induced lethality

It was reported in literature that influenza-induced lethality due to acute lung injury occurs successively to the cytokine storm triggered by the stimulation of TLR4 by host-derived DAMPs (OxPAPC and HMGB1) which are TLR4 agonists.[341,342] As well, the TLR4 antagonist, **Eritoran**, showed to protect mice from lethal influenza infection and blunted air lung injury.[81,342] Eritoran was suspected to act inhibiting the binding of DAMPs to TLR4 in the late phase of the viral infection. **FP7** was therefore a good candidate and was tested *in vivo* against lethal influenza (Fig. 62).

Mice were treated with a mouse adapted influenza strain (PR8) and treated with vehicle (saline solution, NT) or with **FP7** (10 µM) for 5 consecutive days on 2 days post-influenza challenge

(day 2 to 6). The treatment of PR8-infected mice with 10 μM **FP7** *in vivo* resulted in a strong reduction of influenza infection-induced lethality (Fig. 62a) with significant protection ($P < 0.01$).

The analysis of hematoxylin and eosin-stained lung tissue sections (scored blindly for peribronchiolitis, intestinal pneumonia, perivasculitis and alveolitis) reveal that **FP7** improve significantly the histopathology score of infected lungs and prevent excessive inflammation and lung damage induced by influenza infection (Fig. 62b and c).

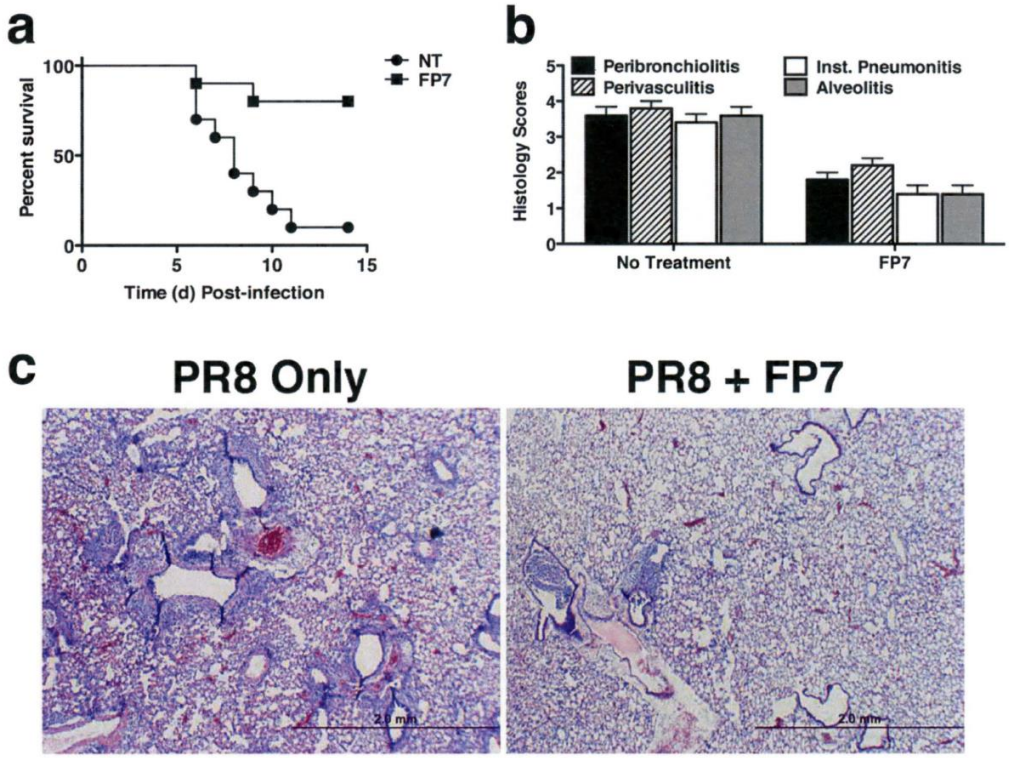

Figure 62. FP7 treatment protects mice from lethal influenza challenge C57BL/6 J mice were infected with mouse-adapted influenza, strain PR8 (~7500 $TCID_{50}$, i.n.; ~LD90). Two days later, mice received vehicle (saline; i.v.), or **FP7** (200 μ g/mouse; i.v.) once daily from days 2 to 6 post-infection. (**a**) Mice were monitored daily for survival for 14 days (5 mice/treatment group) (**a**). (**b**) On day 7 post-infection, another group of 5 mice per treatment were euthanized and lungs were extracted and stained for histopathology and examined for tissue damage, necrosis, apoptosis, and inflammatory cellular infiltration. Mean histopathology scores for each group were determined blindly. (**c**) Representative H&E- stained lung sections are shown.

The non-treated infection by influenza induces the production of cytokines, mainly TNF-α, IL-1β and IFN-β, chemokines (KC, murine IL-8) and the accumulation of oxidized phospholipids in infected lungs or circulating HMGB1. These responses to influenza infection were showed to be effectively inhibited by the Eritoran therapy.[81,342] In a comparative manner, **FP7** lead to significant reduction of influenza-induced genes expression of TNF-α, IL-1β, IFN-β, KC, IL-6 and RANTES. This inhibitory effect of **FP7** on cytokines levels and HMGB1, induced by PR8 infection, and subsequent protection of the tissues, are most likely resulting

from the ability of **FP7** to inhibit the TLR4 signaling by DAMPs like HMGB1 and the subsequent TLR4-dependent cytokine storm.

g. Modulation of CNS-related diseases.

Studies of the central nervous system (CNS) and more precisely the amyotrophic lateral sclerosis (ALS) disease, reveal that inflammatory responses probably play a critical role in the pathogenesis of the motoneuron injury. Since TLRs are much more understood and studied, it appears that they may be involved in both innate and adaptive immune responses in ALS: TLR4 abnormal signaling in pro-inflammatory microglia cells has been related to motoneuron degeneration leading to ALS. Therefore, **FP7** was a good candidate and was tested *in vitro* on ALS cells models (SMI32-positive motoneurons , Fig. 63).[131]

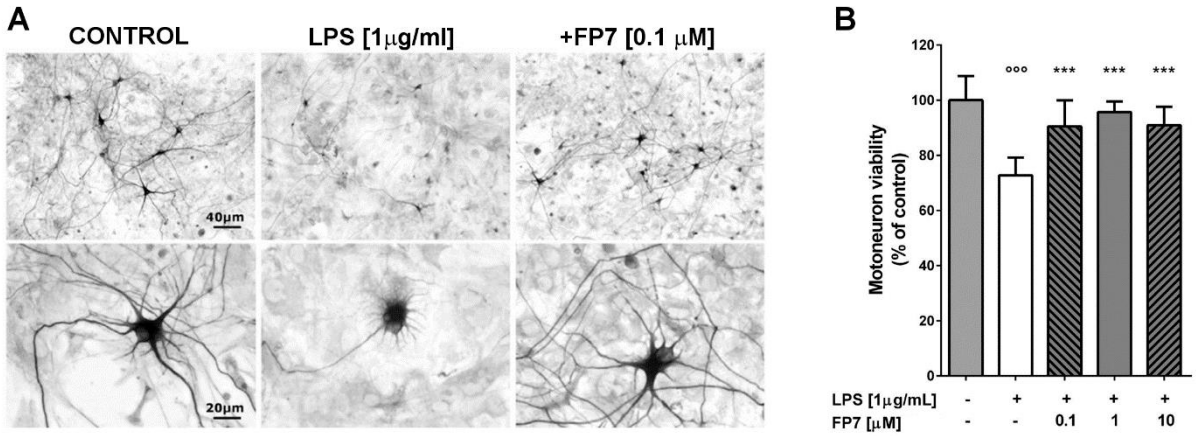

Figure 63. Motoneuron death in cocultures stimulated by LPS: protective effects of FP7 Motoneuron death induced by LPS (alone or in co-treatment with **FP7**) was assessed in motoneuron/glia cocultures after 24 h of exposure. (**A**) Low- (upper line) or high- (lower line) magnified representative pictures of SMI32-positive motoneurons maintained in control conditions, treated with LPS alone or in combination with **FP7** (0.1 μM). (**B**) Bars represent mean percentage ± standard deviation of motoneuron death compared to control. Data from at least three independent experiments were analyzed. °°°$p < 0.001$ vs control; ***$p < 0.001$ vs LPS. One-way ANOVA and Tukey's test.

The results were really encouraging as it appears that 100 nM of **FP7** were highly efficient to reduce the LPS-induced motoneuron death, increasing the viability of motoneurons from 70 to 90%. Higher concentrations of **FP7** (1 and 10 μM) do not enhance significantly the viability of the motoneurons suggesting that 100 nM or lower concentrations may be sufficient to be tested as potential drug toward ALS *in vivo*.

The exposition of the microglia to LPS is known to trigger two main inflammatory events. The release of nitric oxide (NO) and the activation of the microglia itself (increased production of IL-1β and TNF-α). **FP7** was tested on LPS-activated microglial cells to observe the probable modulation of the pro-inflammatory released cytokines.

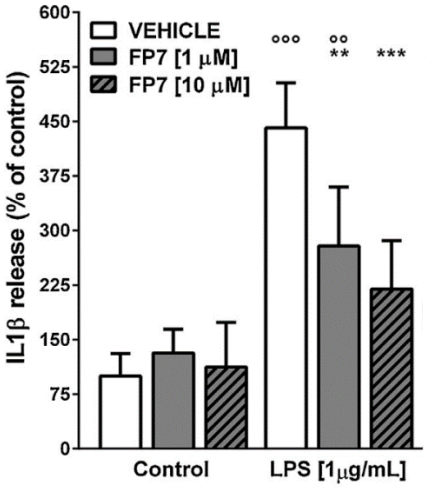

Figure 64. FP7 reduced the IL-1□ release by LPS-activated microglia Purified microglia cultures were co-treated with LPS and 1 or 10 mM FP7. IL-1b concentrations in culture medium was assessed after 24 h by ELISA assay. Bars represent the mean percentage ± standard deviation of cytokine concentrations in medium, normalized to control. Data from at least three independent experiments were analyzed. ◦◦◦$p < 0.001$ vs control; **$p < 0.01$, ***$p < 0.001$ vs LPS. Two-way ANOVA and Bonferroni's test.

The co-treatment with **FP7** resulted to significantly reduce the LPS-mediated IL-1β release (Fig. 64) while no significant effects were observed on either TNF-α nor NO. It suggests a cross signaling between the receptors (NO is not directly under control of TLR4 and TNF-α release can be triggered by multiple receptors).

The different studies based on **FP7** are encouraging. The use of molecular simplification of lipid A structure seems to be a valid approach toward new TLR4 modulators. The *in silico* and *in vitro* results were highly consistent and strongly suggest that **FP7** is a specific ligand of MD-2. The *in vivo* and *in vitro* studies showed good results and proved that **FP7** may be a powerful and interesting compound to be developed either as a drug for TLR4-associated diseases modulation (Influenza, ALS…) and as a lead compound for further drug development.

Indeed, the main work realized during this PhD was the design of novel TLR4 modulators, based on the SAR and ligand-based design previously described, the computational molecular modeling of the designed ligands, the synthesis of the most promising compounds and their suggestion for relevant *in vitro* and *in vivo* assays.

3. Non-sugar and natural compounds as modulators of TLR4

Chemically diverse compounds, that do not possess a sugar scaffold but still possess an effective disposition of hydrophobic and ionic groups, showed interesting LPS-like or LPS antagonistic activities mediated by MD-2. Some of these structures have been designed to mimic lipid A (like phospholipid dimers) while others have been proposed or repurposed after theirs virtual screening and/or structural comparison to lipid As (**bis-ANS**).[312,343] The biological evaluation of this compounds permit also to grasp important SAR information. TLR4 modulators, totally unrelated to lipid A structural features, were discovered: **auranofin**, **JTT705**, **coprohemin** and **thalidomide**.[231] Moreover, unexpected natural compounds were found to be TLR4-active, it is the case of opioids (**naloxone** and **naltrexone**), **taxane paclitaxel**, **cinnamaldehyde**, **isoliquiritigenin**, **6-shogaol**, **caffeic acid ester** and **curcumin** compounds.[344]

1.1) TLR4 antagonist TAK-242

TAK-242 is an interesting compound,[345] it was developed as a derivative of the lead compound discovered by an extensive screening of the Takeda chemical library toward potential therapeutic agent for sepsis. It was a biological screening, done on mouse macrophages stimulated with lipopolysaccharide (LPS).

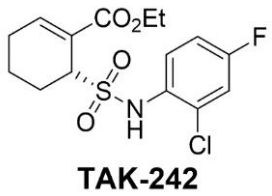

Figure 65. Chemical structure of TAK-242

TAK-242 is a cyclohexane bearing a 2-chloro,4-fluorophenylsulfonamoyl ethyl ester group.

It selectively inhibits TLR4 signal, efficiently protects mice against LPS-induced lethality and showed high potency as antisepsis agent in animal models. Thus, **TAK-242** was tested in clinic, and passed Phase I and II clinical trials.[231]

However, the clinical development of **TAK-242** was discontinued after Phase III since the compound failed to supress cytokine levels in patients with severe sepsis and septic shock or respiratory failure.

The mode of action of **TAK-242** was elucidated recently, it appears that **TAK-242** binds directly to Cys747, in the intracellular domain of TLR4. As **TAK-242** is a Michael acceptor, it has been proposed that this compound may form a covalent adduct with Cys747. However, the actual reason of the TLR4 signaling inhibition remains controversial. Upon binding to TLR4, **TAK-242** could inhibit the myristoylation and phosphorylation of intracellular TRAM protein.

These post-translational modifications are essentials for the correct formation of the supramolecular organizing centres and therefore for the signaling through TLR4.

1.2) bis-ANS

The compound **bis-ANS** (4,4'-Dianilino-1,1'-Binaphthyl-5,5'-Disulfonic Acid) is composed of a hydrophobic binaphthyl core that keep the two anionic sulphates at a distance of 11Å, its structural pattern is therefore similar to lipid As in which phosphates are distant by 13Å. This distance is important to match the one between the basic clusters on the surface of MD-2 structure models.[346]

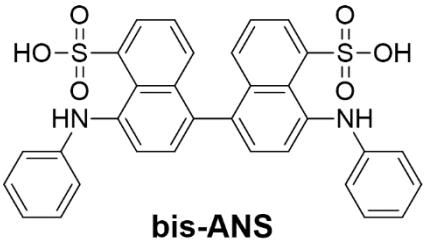

Figure 66. Chemical structure of bis-ANS

This compound is a dye and it was found to bind functional MD-2 *in vitro* with high affinity. Its binding to a hydrophobic surface leads to an increase in its fluorescence intensity due to fluorescence resonance energy transfer (FRET). The decrease in the **bis-ANS** fluorescence, upon LPS addition, shows that the binding site of **bis-ANS** overlaps with the LPS binding site (MD-2 hydrophobic pocket). Consequently, **bis-ANS** acts as a weak LPS antagonist, inhibiting TLR4/MD-2 complex signalling.

Its weaker affinity and antagonistic activity are probably due to the incomplete match of the two anilino-naphthalene rings of **bis-ANS** with the hydrophobic pocket. Those groups occupy a volume significantly smaller than the LPS FA chains, resulting in a weaker hydrophobic interaction with the protein and therefore a lower biological activity.

1.3) Cationic TLR4 modulators

In the literature, the great majority of the cationic TLR4 modulators are based on non-saccharide structures. However, these compounds mostly act as "LPS sequestrants", neutralising its toxicity rather than interacting with the TLR4/MD-2 complex. They may also interact directly with LBP or CD14 upstream preventing the LPS sensing by TLR4/MD-2.[245]

Due to their behaviour, they act mainly as LPS antagonists, surprisingly, some compound interacting with CD14 were founded to act as agonists.

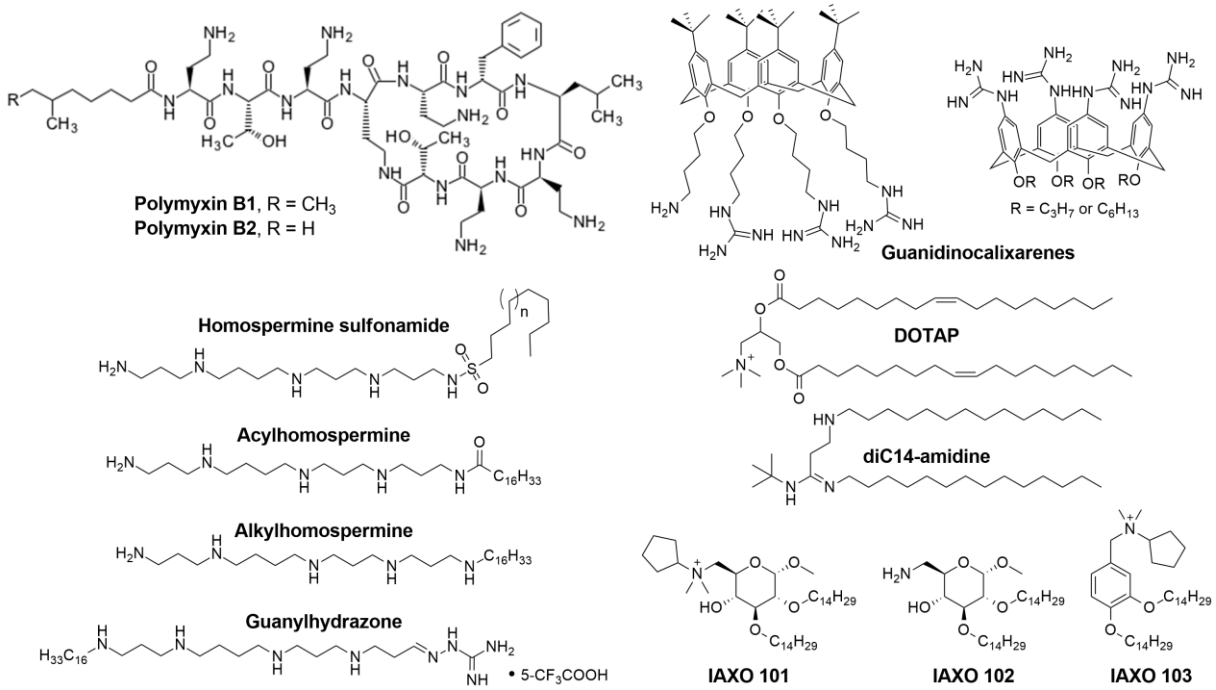

Figure 67. Structure of cationic TLR4 modulators

Examples includes the cationic decapeptide **Polymyxin B** and its non-toxic derivatives,[347,348] homospermines derivatives (alkyl,[349] acyl,[350] guanylhydrazone[351] and sulphonamide[352]), **DOTAP**[353] and **diC14-amidine**,[354] calixarenes[355,356] and the antagonistic IAXO compound developed by our group.[357]

1.4) Natural compounds as TLR4 modulators

Plants were used since ages in medicine without knowing the actual structure of the bioactive effectors nor their mechanism of action. Still nowadays, plants seem to provide an endless source of pharmacologically active compounds.

Recent studies showed plant extracts as potential modulators of TLRs. Interestingly, many herbs used in traditional Chinese medicine and Ayurvedic medicine appeared to be rich in molecules that interfere with TLR4 activation and signaling. It includes: green tea, licorice (*Glycyrrhiza uralentis*), *Magnolia officinalis*, ginger (*Zingiber officinalis*), Red sage (*Salvia miltiorrhiza*) and curcumin.[358] Research have thus been devoted to isolate the bioactive molecules contained in the active extracts and a lot of natural TLR4 modulators have been discovered:

- **Sulforaphane** (**SFN**) identified from cruciferous vegetables such as broccoli or cabbages
- **Curcumin** identified from the rhizomes of the plant *Curcuma longa* (turmeric)
- **Cinnamaldehyde** from the cinnamon bark of cinnamon threes
- **Glycyrrhizin** and **chalcone Isoliquiritigenin**, identified from roots and rhizomes of Glycyrrhiza plants (**licorice**)
- **Ginger**, the rhizome of the herb *Zingiber officinalis*
- **Caffeic acid phenethyl ester** (**CAPE**), isolated as an active constituent of honeybee propolis
- **(-)-epigallocatechin 3-gallate** (**EGCG**), from green tea

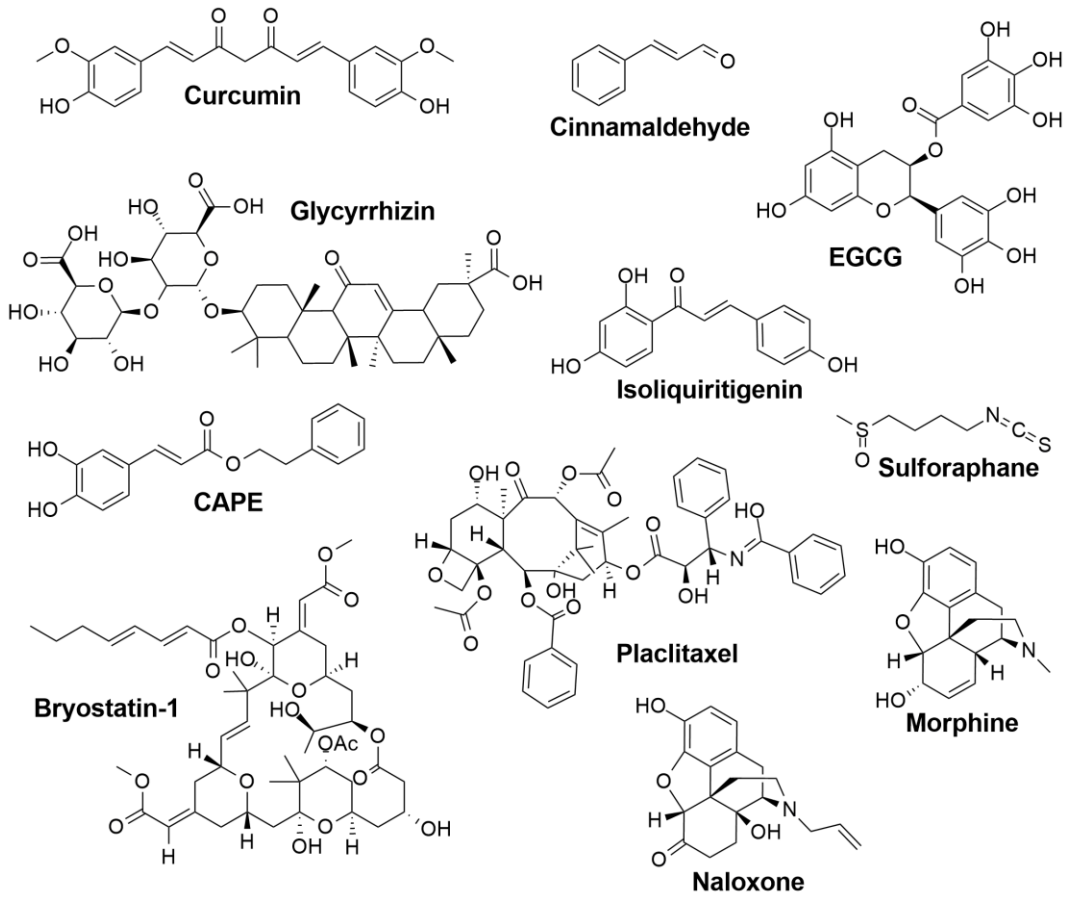

Figure 68. Natural compounds actives as TLR4 modulators

Furthermore, known anticancer drugs such as **Taxane Placlitaxel** and the macrocyclic lactone **Bryostatin-1** as well as opioids (**morphine** and **naloxone**) were tested on TLR4 and found to be active as TLR4 modulators.

Despite the great structural differences of such compounds, the molecules share common features like the presence of phenolic rings.

Moreover, **cinnamaldehyde**, **isoliquiritigenin**, **curcumin** and **caffeic acid ester** contain α,β−unsaturated carbonyl moieties, proposed to be crucial for their activity. Indeed, the main mechanism of action envisaged for these compounds is the disruption of TLR4/MD-2 heterodimer by formation of covalent bonds with solvent-exposed MD-2 and/or TLR4 cysteines through a Michael addition on the compound itself.

Sulforaphane, that contains an isothiocyanate moiety, showed to form a covalent adduct with the exposed Cys133 of MD-2 hydrophobic pocket, thus preventing the binding of LPS.[359] On the contrary **1-dehydro-10-gingerdione** (**1D10G**) and **curcumin**, despite the presence of an unsaturated carbonyl moiety in the later, seems to inhibit the formation of TLR4 activated complex by interacting non-covalently with MD-2 and competing with endotoxin for MD-2 binding.

All the data on these compounds increase the interest in the identification of active natural compounds and the study of their mechanism of action in search of new chemical scaffolds for the development of innovative non-toxic TLR4 modulators. The main advantage of such compounds is, in principle, their better solubility and bioavailability with respect to lipid A analogues (characterized by low solubility in aqueous media due to their amphiphilic nature).

Finally, since olive oil has been associated with the many benefits conferred by the Mediterranean diet, it has been inspected in search of the bioactive molecules responsible for its beneficial effect.[360,361] Phenolic constituents of extra-virgin olive oil were found to possess very interesting biological activities as anti-oxidant, anti-inflammatory and anti-thrombotic agents.[362] In particular, the most active anti-inflammatory phenolic compounds were found to be **oleuropein**,[363] **hydroxytyrosol**[364] and **oleocanthal**.[365,366] Flavonoids and ligands contained in olive oil such as **apigenin**, **luteolin** and **pinoresinol** have also been associated with anti-inflammatory activity (Fig. 69).[367,368]

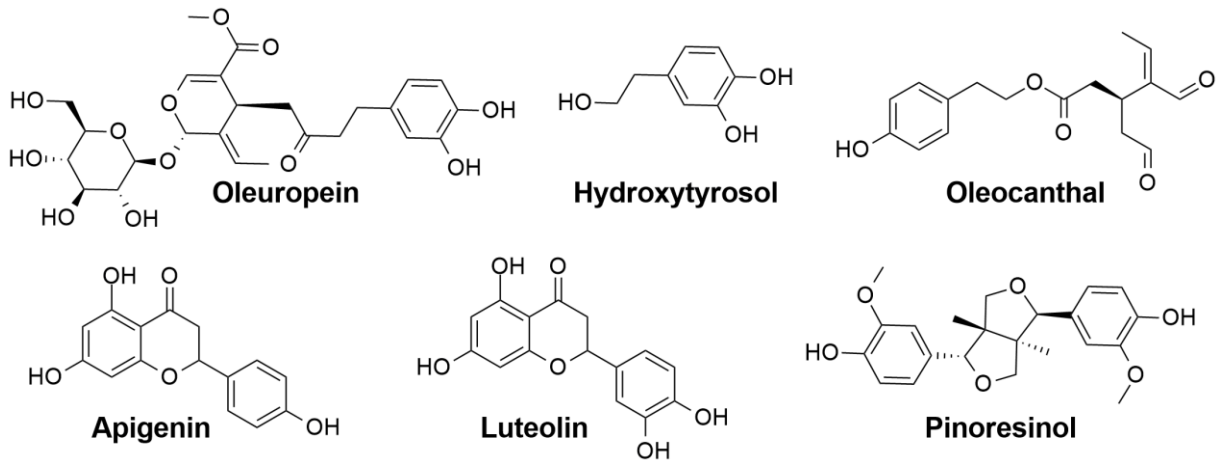

Figure 69. Structure of olive oil compounds

However, despite hydroxytyrosol and oleuropein appears very likely to be related to TLR4 antagonism,[369] the activity of the anti-inflammatory compounds of olive oil has not been directly corelated to the activity of TLR4 system to date.

TOLLERANT PROJECT AND AIM OF THE WORK

This PhD thesis is part of the MSCA-ITN-2014 ETN project "Toll-like receptor 4 activation and function in diseases: an integrated chemical-biology approach" (www.tollerant.eu, acronym TOLLerant) and is based on international group interactions and synergies. TOLLerant is a combination of chemistry, biology, biophysics, biochemistry and pharmacology expertise, and is aiming to gain information on molecular aspects of TLR4 activation and signaling. The short-term scientific objective was to develop novel, non-toxic, synthetic and natural TLR4 modulators and to assess their therapeutic potential. The long-term scientific objective was to develop a generation of innovative, TLR4-based therapeutics, to be used as vaccine adjuvants, anti-sepsis and anti-inflammatory agents to treat chronic inflammations (allergy, asthma).

The training programme aims to provide broad competences to Early Stage Researchers (ESR). During the training, ESR were supported by senior scientists to cultivate their scientific, entrepreneurial and inter-cultural mindset. The non-academic sector was committed to provide ESRs with entrepreneurship and company management skills, in order to enhance their employability by the private sector or even to motivate them to create own start-up companies.

The project was divided in work packages (WP) and the one regarding this thesis was WP1: "Design synthesis of new TLR4-active compounds, structural studies on potential TLR4 modulators from bacteria and plants". Starting from the structure-activity data obtained from previous generations of TLR4-active cationic and anionic amphiphiles developed by our group, new synthetic compounds were rationally designed (collaboration and secondment at CSIC) and synthesized. The rational design was based on chemical structures of existing ligands. Ligand-based design was integrated with structure-based design and virtual screening approaches to create novel, high affinity ligands for MD-2 and CD14 co-receptors. These compounds were designed to act as TLR4 antagonists (blockers) or agonists (activators) and could also be considered for the exploitation as TLR4 probes with the appropriate chemical modifications (insertion of fluorescent moieties or other chemical labels).

These ligands cannot be tracked in vivo and therefore it is not possible to apply molecular imaging techniques in the drug development process. The possibility of combining precise in vitro and/or in vivo delivery with accurate imaging is considered important for clinical development, as it can maximize the effectiveness of drugs, minimise the invasiveness and toxic side effects and speed up the clinical development program. To address these problems, TLR4

ligands developed will be assembled on nanoparticles (NP), taking advantage of the unique physicochemical properties of the NP. This study has the scope to enlarge the repertoire of chemical structures (scaffolds) available for TLR4 modulation and to undertake the elucidation of the mechanistic aspects of the TLR4 activation/inactivation.

doi:10.3390/ijms18112318

RESULTS AND DISCUSSION

IX. The Role of Carbohydrates in the Lipopolysaccharide (LPS)/Toll-Like Receptor 4 (TLR4) Signalling

International Journal of
Molecular Sciences

MDPI

Review

The Role of Carbohydrates in the Lipopolysaccharide (LPS)/Toll-Like Receptor 4 (TLR4) Signalling

Florent Cochet and Francesco Peri *

Department of Biotechnology and Biosciences, University of Milano Bicocca, Piazza della Scienza, 2, 20126 Milano, Italy; f.cochet@campus.unimib.it

***** Correspondence: francesco.peri@unimib.it; Tel.: +39-02-6448-3453

Received: 24 July 2017; Accepted: 30 October 2017; Published: 3 November 2017

1. Abstract:

The interactions between sugar-containing molecules from the bacteria cell wall and pattern recognition receptors (PRR) on the plasma membrane or cytosol of specialized host cells are the first molecular events required for the activation of higher animal's immune response and inflammation. This review focuses on the role of carbohydrates of bacterial endotoxin (lipopolysaccharide, LPS, lipooligosaccharide, LOS, and lipid A), in the interaction with the host Toll-like receptor 4/myeloid differentiation factor 2 (TLR4/MD-2) complex. The lipid chains and the phosphorylated disaccharide core of lipid A moiety are responsible for the TLR4 agonist action of LPS, and the specific interaction between MD-2, TLR4, and lipid A are key to the formation of the activated complex $(TLR4/MD\text{-}2/LPS)_2$, which starts intracellular signalling leading to nuclear factors activation and to production of inflammatory cytokines. Subtle chemical variations in the lipid and sugar parts of lipid A cause dramatic changes in endotoxin activity and are also responsible for the switch from TLR4 agonism to antagonism. While the lipid A pharmacophore has been studied in detail and its structure-activity relationship is known, the contribution of core saccharides 3-deoxy-D-manno-octulosonic acid (Kdo) and heptosyl-2-keto-3-deoxy-octulosonate (Hep) to TLR4/MD-2

binding and activation by LPS and LOS has been investigated less extensively. This review focuses on the role of lipid A, but also of Kdo and Hep sugars in LPS/TLR4 signalling.

Keywords: lipopolysaccharide; TLR4 (Toll-like receptor 4); MD-2 (myeloid differentiation factor 2); Kdo (3-deoxy-D-manno-octulosonic acid)

2. Innate Immunity Response in Higher Organisms to Pathogen-Associated Molecular Patterns

Mammalian innate immunity relies on a family of pattern recognition receptors (PRRs) to detect conserved microbial molecules, termed pathogen-associated molecular patterns (PAMPs) [1,2]. PRRs engagement by microbial PAMPs activates inflammatory pathways, such as the nuclear factor kappa B (NF-κB) and interferon regulatory factor (IRF) signalling for cytokine transcription and the clearance of the infections. The PRR family includes Toll-like receptor (TLR), C-type lectin receptor (CLR), RIG-I-like receptor (RLR), AIM2-like receptor (ALR), and NOD-like receptors (NLR) containing a Nucleotide-binding domain (NBD) and a Leucine-rich Repeat (LRR) domain. TLR and CLR are localized on the plasma or endosomal membranes, while RLR, ALR, and NLR are cytoplasmic [3,4]. The host receptorial system is redundant in the sense that a collection of structurally diverse PRRs recognizes the same bacterial cell wall component. PRRs then induce various signalling pathways that depend on structurally diverse signalling components [5].

Some of the most inflammatory PAMPs, such as lipopolysaccharide (LPS), lipoproteins, peptidoglycan (PGN), and flagellin, are molecules derived from the bacterial cell wall and are recognized, respectively, by specific PRRs.

Organic chemistry synthesis of chemically homogeneous molecules greatly contributed to the unequivocal determination of the minimal and chemically defined structure that is essential for the immunostimulating actions of LPS [6–8]. LPS is composed of three distinct domains (Figure 70) that are covalently linked to each other, which are genetically, biosynthetically, biologically, and chemically distinct: a glycolipid portion termed lipid A, a glycan, and between them a core oligosaccharide.

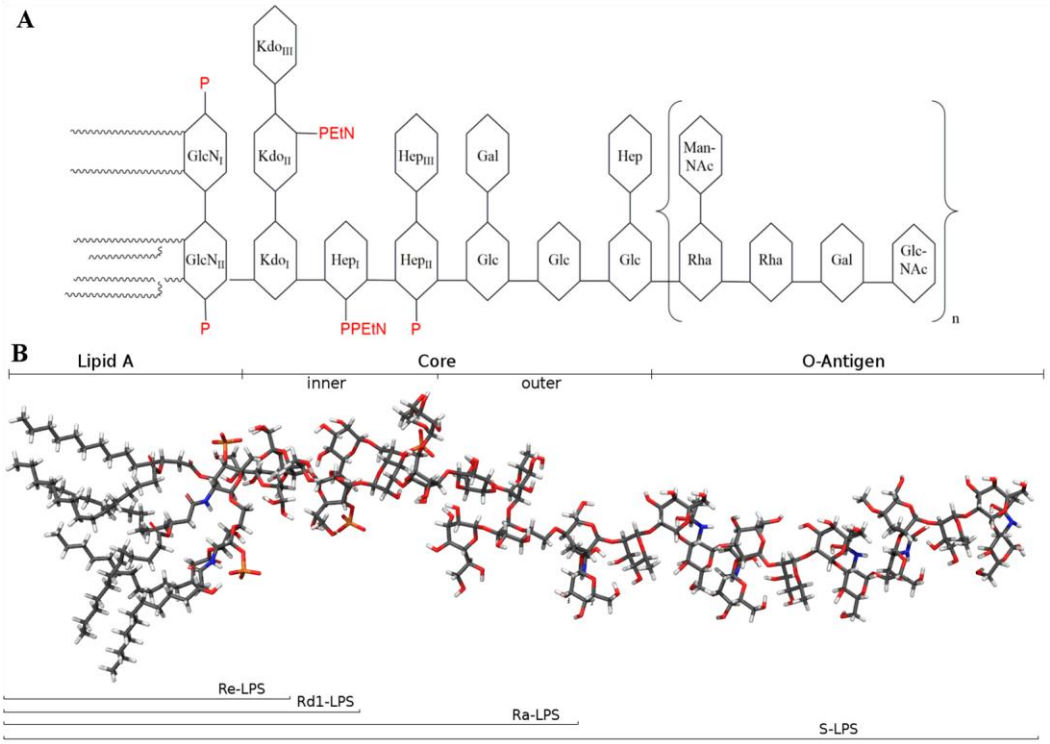

Figure 70. ***E. coli*** **lipopolysaccharide (LPS)** smooth-lipopolysaccharide (S-LPS) is composed by lipid A, core and O-antigens; truncated rough-LPS (R-LPS) are named Ra, Rd1, and Re depending on the number of sugar units of the core. (**A**) Schematic representation (**B**) Chemical structure

The glycan usually is the O-specific polysaccharide (or O-antigen). The membrane-anchoring portion called lipid A is also the biologically active unit (endotoxic principle). The first chemically synthesised lipid A [9], according to the newly elucidated structure, exhibited full activity described for LPS endotoxin.

In the classical nomenclature [10] (Figure 70) LPS is identified by the appearance of the corresponding bacterial colony surface: smooth colonies express complete LPS that has been accordingly termed smooth-lipopolysaccharide (S-LPS). Mutants that express LPS lacking O-antigens form colonies with rough appearance, so that the corresponding truncated LPS variants have been named rough-LPS (R-LPS). However, not all of the mutants lose all O-antigen, so that there are three types of R-LPS (Figure 70). Ra-LPS mutant is composed of the Lipid A and the complete oligosaccharide core, Rd1-LPS mutant is formed by Lipid A and the inner core and the smaller variant, Re-LPS, also called deep rough mutant, only contains two or three Kdo units linked to Lipid A [11,12].

Complete LPS (S-LPS), and its truncated rough variants (R-LPS) including lipid A (Figure 70) are generally defined as endotoxin and have potent pro-inflammatory and immunostimulating action.

Free LPS released from gram-negative cell wall, in form of single molecules or aggregates, is detected by the Toll-like Receptor 4 (TLR4), which is mainly expressed on the surface of haematopoietic cells including monocytes, dendritic cells, and macrophages [11].

A recent review by Kieser and Kagan [5] presents an updated, more complex picture of the LPS recognition by innate immunity cells, suggesting that several membrane and cytosolic receptors are activated by LPS variants. Membrane receptor Brain-specific angiogenesis inhibitor 1 (BAI1) also detects LPS at the bacteria surface and, after promoting phagocytosis, triggers reactive oxygen species (ROS) production and the induction of inflammation. Moreover, LPS that has reached the cytosol is recognized by caspases, initiating formation of the non-canonical inflammasome [12].

From a molecular point of view, glycoconjugate/protein interactions are the key events of activation of innate immunity PRRs, including cytosolic caspases, triggering cytokine production and inflammation. In this review, we will focus on molecular details of sugar-protein interactions in the case of TLR4/MD-2/LPS signalling, the most important and studied pathway in innate immunity and inflammation.

3. Physicochemical Properties of LPS and Molecular Mechanism of LPS/TLR4 Signalling

The amphiphilic character of endotoxin chemical variants (S-LPS, R-LPS or lipid A), results in the formation of micelles in aqueous environment above their critical micellar concentration (CMC) [13]. CMC values between 10^{-8} M and 10^{-7} M for deep rough mutant (Re-LPS) [14,15], and between 1.3 and 1.6 μM for *E. coli* S-LPS [16], were reported. In balanced salts solutions containing physiologic extracellular concentrations of Mg^{2+} and Ca^{2+}, CMC values of 1 nM or lower are likely [17,18].

From these data and from the fact that LPS aggregates are usually highly stable, aggregated forms of LPS should predominate in the concentration range that is relevant for biological responses. In physiological fluids, LPS aggregates were also found as membrane “blebs”, which are constitutively released from growing Gram-negative bacteria. Transmission electron microscopy (TEM) revealed that blebs exist predominantly as vesicles with an average size of 40–80 nm [19].

The current view of mammalian endotoxin sensing and signalling (Figure 71) is that it is initiated by the lipid-binding protein (LBP), which is able to extract LPS monomer from the aggregates and to transfer it to the cluster of differentiation 14 (CD14) [20,21]. CD14, then, transfer the LPS monomer to Myeloid Differentiation factor 2 (MD-2) adaptor in the final

hexamer complex $(TLR4/MD\text{-}2/LPS)_2$ (Figure 71) [22–25]. This unidirectional flow of LPS from LBP to TLR4/MD-2 is explained by the increasing affinity of each LPS receptor for its ligand [26]. TLR4 crosslinking through the formation of the $(TLR4/MD\text{-}2/LPS)_2$ complex is the first step in the inflammatory process. The CD14 receptor, in the membrane-bound form, promotes the formation of hexamer complex $(TLR4/MD\text{-}2/LPS)_2$ by binding monomeric LPS and transferring it to MD-2, thus initiating the Myeloid differentiation primary response 88 (MyD88)-dependent intracellular signalling [26,27]. CD14 also plays a fundamental role in the endocytosis of $(TLR4/MD\text{-}2/LPS)_2$ and in subsequent intracellular signalling based on triffosome formation [28–32].

In general, the activation of TLRs by their ligands is the first molecular event of innate immunity, preceding and triggering cytokine production, inflammation and adaptive immune response [33]. From a pharmacological point of view, TLR4 stimulation by non-toxic LPS/lipid A variants is considered as an innovative approach towards potent and selective immunostimulants to be used as vaccine adjuvants and in tumor immunotherapy [34,35]. On the other hand, natural LPS variants or synthetic molecules that inhibit the formation of $(TLR4/MD\text{-}2/LPS)_2$ hexamer complex by competing with LPS or other agonists for TLR4/MD-2 and/or CD14 binding are interesting drug candidates targeting diseases that are caused by excessive TLR4 activation by bacterial LPS (sepsis and septic shock) and by endogenous molecules (inflammatory and autoimmune diseases) [36].

The knowledge of the molecular aspects of LPS recognition by CD14 and TLR4/ MD-2 is essential to understand the different TLR4-mediated responses to different LPS/lipid A variants or chemotypes, whose activity varies from toxic (TLR4 agonists), to non-toxic and even LPS with endotoxin-neutralizing activity, corresponding to TLR4 antagonism. The same molecular mechanisms play a fundamental role in innate memory and tolerance to LPS [37]. Finally, the rational design of TLR4 agonists and antagonists as drug candidates relies on the precise knowledge of the molecular aspects of the interaction between lipid A and CD14 and/or MD-2 receptors.

doi:10.3390/ijms18112318

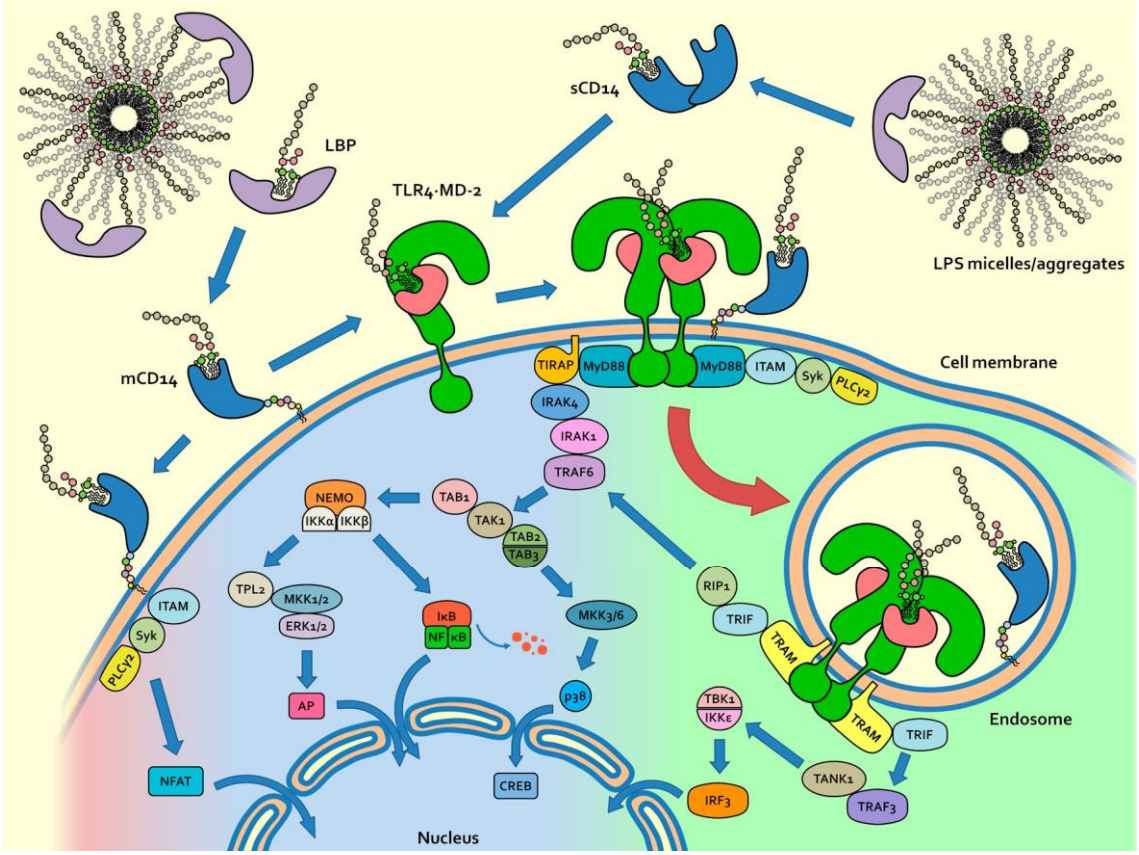

Figure 71. TLR4 activation and signalling from cell membrane and from endosomes MyD88 and TRIF-dependent pathways are distinct signal pathways leading to cytokine production.

4. Structure-Activity Relationship in Natural and Synthetic Lipid A Variants

The chemical pattern consisting in the disaccharide β(1–6) glucosamine core with two phosphates at C1 and $C4^0$ positions and branched or linear fatty acid chains linked to C2, C3, $C2^0$, and $C3^0$ positions is highly conserved in lipid As of different bacterial species. It is the pharmacophore associated to endotoxic activity. This motif can be found in the natural and synthetic lipid A variants that bind and activate TLR4, thus behaving as agonists. The structural variations of lipid A found in different bacterial species (different acylation patterns, variation in the chemical structure and length of fatty acid chains, covalent modification of phosphate groups), are associated to different biological activity.

Natural Lipid A variants produced by *E. coli*, *Neisseria meningitidis*, *Campylobacter jejuni*, *Salmonella minnesota* or *tiphimurium*, *Rhodobacter capsulatus* or *sphaeroides* species, as well as biosynthetic precursor lipid IVa and synthetic analogue Eritoran [38] (Figure 72), provided complete information on structure-activity relationship (SAR) of this class of compounds.

Lipid A variants differ in the acylation pattern, that is the location of fatty acid chains on the disaccharide: 4 + 3 (corresponding to four chains attached to the non-reducing and three chains in the reducing glucosamine) in *S. tiphimurium*, 4 + 2 in *E. coli*, *C. jejuni* and *S. minnesota*, 3 + 3 in *N. meningitidis*, 3 + 2 in *R. capsulatus* and *sphaeroides*, 2 + 2 in Lipid IVa. Synthetic Eritoran presents a 2 + 2 arrangement as well. Lipid As also presents different composition and length of chains (*E. coli* contains mainly C_{14} chains while *N. meningitides* contains mainly C_{12} chains).

Crucial information on SAR of lipid A variants has been collected by Boons and co-workers by means of fully synthetic derivatives [39]. This study highlighted that synthetic lipid A from *N. meningitidis* was significantly more potent than *E. coli* lipid A. According to these results, the 3 + 3 arrangement of fatty acid chains in *N. meningitidis* is associated with a stronger endotoxic activity than the 4 + 2 disposition found in *E. coli*. Moreover, shorter fatty acids chains with 12 instead of 4 carbon atoms are associated to a higher potency in TLR4 stimulation (1–2 orders of magnitude) [39].

It is quite unusual to observe unsaturated fatty acids in lipid A, but it has been reported in *Rhodobacter sphaeroides* and *R. capsulatus* LPS and in the *Enterobacteriaceae* family when they grow at low temperature. *Campylobacter jejuni* LPS is an exception, in which GlcN are replaced by 2,3-diamino-2,3-dideoxy-D-glucose (GlcN3N) [40] (Figure 72).

In some natural lipid A variants, phosphates in positions C1 and $C4^0$ are covalently functionalized with phosphate, ethanolamine, ethanolamine phosphate, ethanolamine di-phosphate (*C. jejuni*), and sugars as glycosylamine, 4-amino-4-deoxy-L-arabinopyranose and D-arabinofuranose [41].

doi:10.3390/ijms18112318

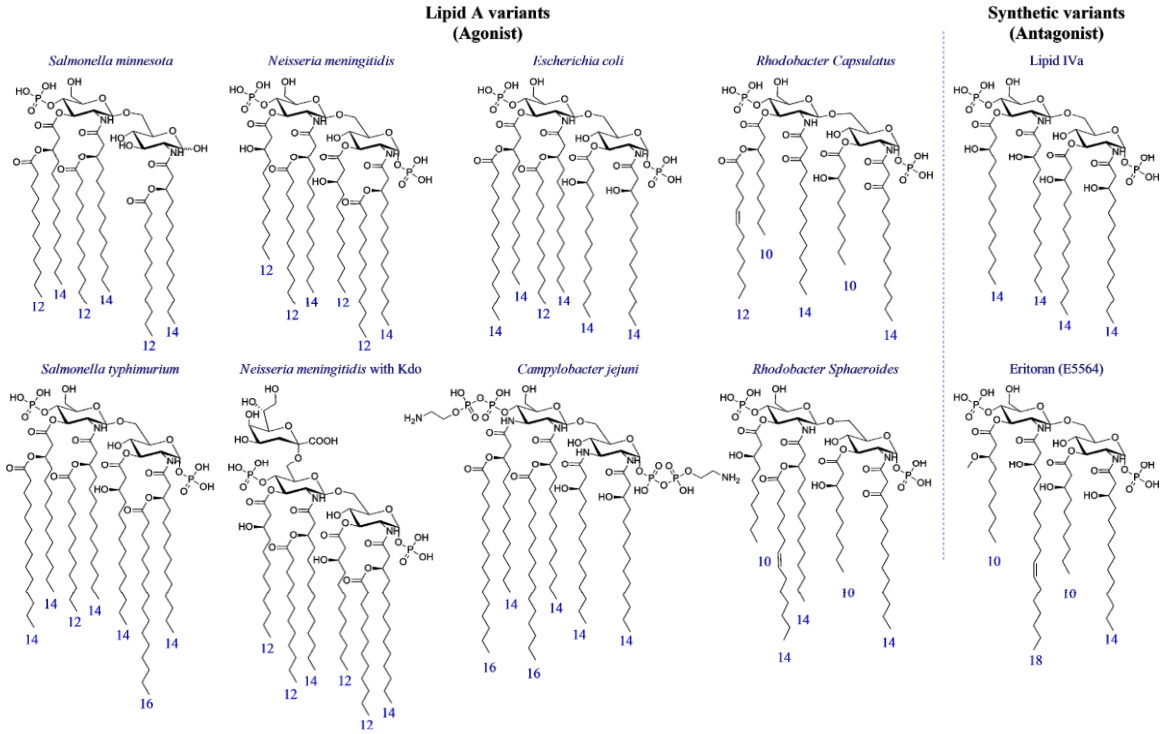

Figure 72. Natural and synthetic lipid As Natural agonists from Salmonella minnesota, Salmonella typhimurium, Neisseria meningitides (with and without Kdo), Escherichia coli, Campylobacter jejuni, Rhodobacter capsulatus and Rhodobacter sphaeroides; the biosynthetic antagonists: Lipid IVa and Eritoran. The numbers of carbon atoms of each fatty acid chain are displayed in blue.

In general, while the presence of six fatty acid (FA) chains is associated with endotoxic action (TLR4 agonism), variants with 7 FA, as *Salmonella typhimurium*, or with less than 6 FA, as in lipid IVa or in the synthetic derivative Eritoran, are on the contrary associated to non-toxic or even anti-endotoxic activity. The anti-endotoxic activity is defined as the competitive antagonist action of lipid A or LPS variants that, when co-administered with endotoxin, neutralize its TLR4 activating effect. A general pharmacophore can be associated to antagonism, consisting of four or five FA that are linked to a disaccharide core bearing in C1 and $C4^0$ positions in one or two negatively charged groups (phosphates or their bioisosteres) [42].

Monosaccharide-based TLR4 modulators allowed for extending the agonism/antagonism rules to the monosaccharide scaffold. The 3:1 ratio between lipid chains and phosphate groups present in lipid A seem an important prerequisite to have agonistic activity both in lipid A variants and in monosaccharides derivatives [43]. Synthetic monosaccharides derivatives with one or two phosphates and two to four fatty acid chains showed in some cases potent TLR4 antagonism in cells and in vivo [44–47]. In mono- and di-saccharides scaffolds, the phosphate groups have been substituted

with bioisosteric, negatively charged carboxylates, and showed similar activities [48–51].

The elucidation of new lipid A chemical structures deriving from bacteria species is a field in continuous evolution, and SAR in new lipid A types will provide important information for designing new synthetic TLR4 modulators [41,52].

In addition, some natural or synthetic molecules having a chemical structure that is unrelated to lipid A can bind to MD-2 and activate TLR4. The natural compounds Taxol and some opioids activate TLR4 [53,54]. Synthetic pyrimido[5,4-b]indoles [55] and 4-substituted aminoquinazolines [56] were shown to specifically activate TLR4 in a MD-2 dependent and CD14 independent manner, in both mouse and human cells. Synthetic compounds with a linear scaffold instead of glucosamine disaccharide such as ER-112022 [57] are active as TLR4 agonist, thus showing that the disaccharide connecting the two anionic phosphates can be substituted by chemical spacers of different chemical structure and with increased conformational mobility. More recently, new classes of non-LPS-like small molecules, the neoseptins [58,59], Euodenine A and analogues [60], have been reported to be MD-2-dependent TLR4 agonists [5,59,61–63].

5. Role of Sugar/Protein and Lipid/Protein Interactions in the Formation and Stability of TLR4/MD-2/Endotoxin Complex

The crystal structures of the hexamer complex $(TLR4/MD\text{-}2/LPS)_2$, in which two TLR4 are crosslinked [22] (Figure 73A), has revealed that binding of LPS (Ra-LPS from *E. coli*) to MD-2 induces agonist-dependent contacts with the C-terminal domain of the second TLR4 molecule of the hexamer (TLR4*). This binding mode is typical of agonists since it is responsible for TLR4 dimerization and activation. Five of the six aliphatic chains of lipid A moiety are deeply inserted into the hydrophobic pocket of MD-2. The FA chain linked to C2 of GlcN I protrudes from MD-2 binding cavity forming, with MD-2 residues (V82, M85, L87, I124, and F126), a binding interface that interacts with hydrophobic residues on the surface of TLR4* (mainly F440*, L444*, and F463*), thus promoting the assembly of the activated hexamer. Additional hydrophilic interactions are also present and involve lipid A's hydroxyls and phosphates groups. These groups interact with MD-2 and TLR4* residues and stabilize the hexameric complex (Figure 73B: C1 phosphate interacts with K388*, K341 and K362 for the two TLR4 as well as K122 for MD-2; $C4^0$ phosphate is in contact with R264, K362 for TLR4, and K58, S118 for MD-2. Moreover, C4-hydroxyl group of the GlcN I interact with K122 residue).

Upon lipid A binding, MD-2 experiences a local conformational change, which involves the side chain of F126 and its immediate neighbours [64]. The interaction between lipid A and

TLR4/MD-2 has been investigated by NMR in solution and suggests a dynamic role of F126. This phenylalanine residue is located at the rim of the LPS binding cavity of MD-2, and acts as a conformational switch allowing, or not, the formation of activated hexamer [65].

In contrast to hexa-acylated lipid A forms, tetra-acylated lipid IVa is a weak agonist in murine TLR4/MD-2 but is an antagonist in human TLR4/MD-2. The crystal structures of human and mouse TLR4/MD-2 in the complex with tetra-acylated lipid IVa provided the structural basis of this species-specific agonistic or antagonistic activities [66,67]. In human MD-2 complex with lipid IVa, the GlcN-P backbone of lipid IVa was shifted upward and rotated by about 180° in comparison to hexa-acylated LPS [64,68] (Figure 74).

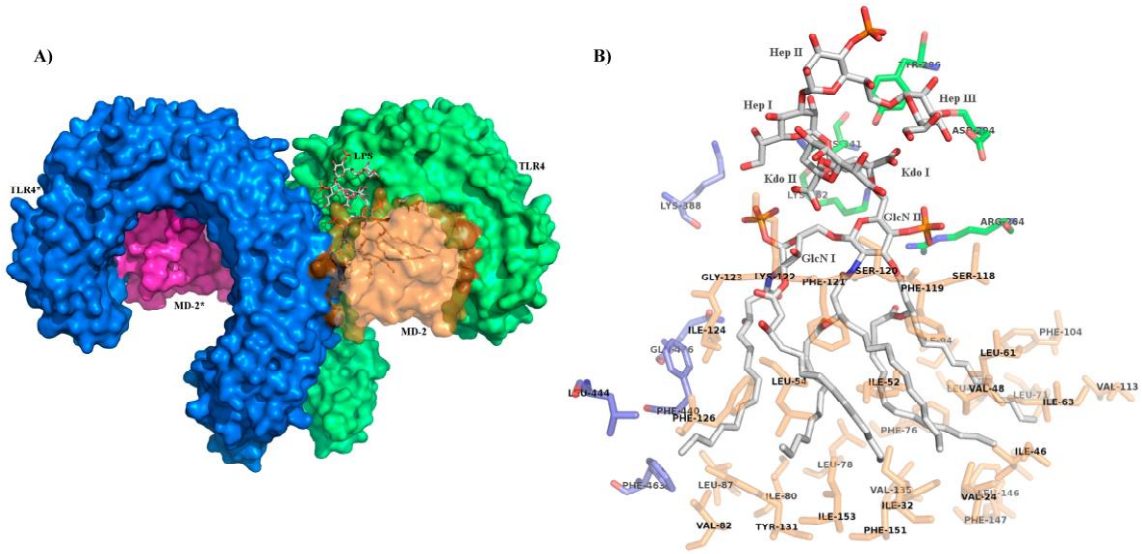

Figure 73. Figure 1. Picture of the interactions between LPS, (TLR4/MD-2) complexes. (**A**) $(TLR4/MD\text{-}2/LPS)_2$ signalling complex; (**B**) *E. coli* Lipid A with inner-core and its interactions with MD-2 (residues in orange) and TLR4 (residues in green) of the same complex and with the second TLR4 molecule, TLR4* (blue), as observed by crystallography (PDBID: 3FXI). LPS is displayed in gray for carbon atoms, red for oxygen, blue for nitrogen and dark orange for phosphate.

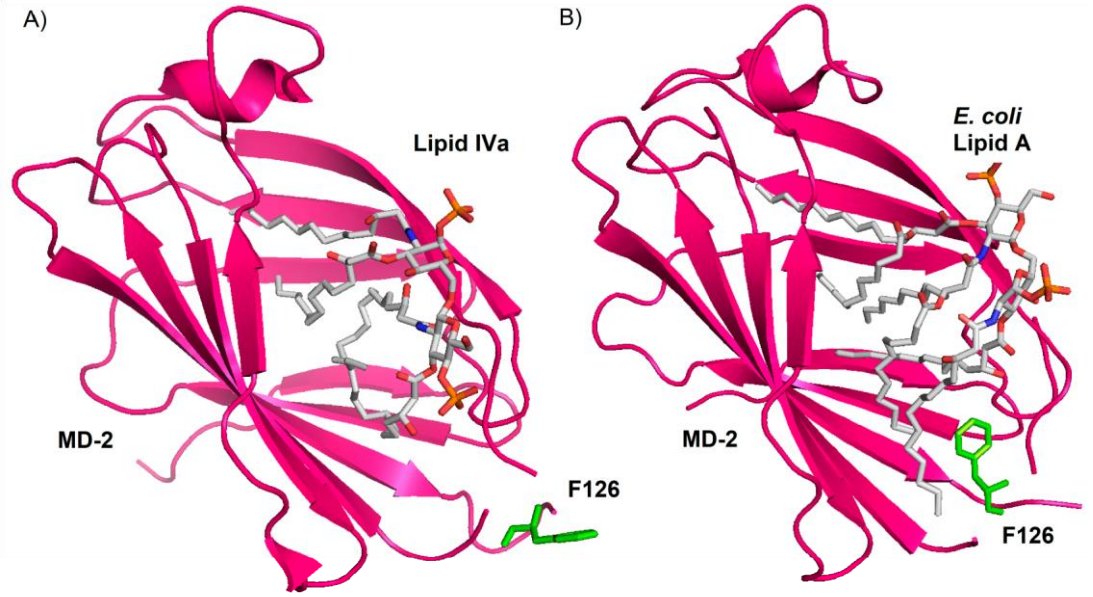

Figure 74. hMD-2 crystal structure present two conformations (**A**) Cristal structure of human MD-2 with Lipid IVa (PDBID: 2E59) (**B**) Cristal structure of human MD-2 with *E. coli* Lipid A (PDBID: 3FXI). Human MD-2 is displayed in purple as ribbon, F126 are displayed in green as sticks and Lipid IVa and Lipid A are displayed according to the color of the atoms as sticks.

This binding mode is not productive and it does not promote the formation of the signalling complex, it is typical of antagonists. Eritoran binds both human and mouse MD-2 with the disaccharide core rotated of 180° respect to agonist lipid A [69]. The interactions of hydrophilic and hydrophobic groups of lipid A with MD-2 and TLR4* have been studied in order to understand the affinity of lipid A variants with the receptor complex, and to explain the switch from agonism to antagonism [61,70,71]. The ligand-based design of new synthetic TLR4 agonist and antagonists has been guided so far by the necessity to reproduce the most important supramolecular interactions among lipid A, MD-2, TLR4, and TLR4* [46,72–74].

6. Role of the Sugar Kdo in the TLR4 Interaction of Natural and Synthetic LPS Variants

The LPS inner core (Figure 70) is typically composed by two or three Kdo units, linked via an α-(2 → 6) linkage to the distal GlcN of the lipid A backbone and three units of Hep. The outer core is composed by more common monosaccharides, such as Glucose (Glc) and galactose (Gal) [75]. The inner core structure is reasonably well conserved (Figure 70) [76], and it is therefore an epitope that is capable of inducing a specific antibody to cross-react with the LPS of many different strains of Gram-negative LPS. Immuno-response directed against the inner core has been exploited in vaccines to elicit widely cross-reactive antibodies in human sera [77]

and in the production of a monoclonal antibody that is able to bind to a wide range of *E. coli* and *Salmonella* LPSs [78,79].

It has long been thought that the inflammatory properties of S-LPS and R-LPS reside only in the lipid A moiety [6,80], and that the nature and number of core saccharides do not have major impact on modulating endotoxicity [81].

From a structural point of view, the inner core sugars, three units of 3-deoxy-D-manno-2octulosonic acid (Kdo I, II, III) and three units of heptosyl-2-keto-3-deoxy-octulosonate (Hep I, II, III) seem to contribute only marginally to the interactions with receptors. However, Kdo I, Hep I, and Hep III are interacting with the TLR4 residues Y296, K341, and D294, respectively (Figure 73). The fact that the inner core sugar interacts only with TLR4, and not with MD-2 and TLR4* as lipid A, confirms that the presence of the inner core sugars is not essential for the endotoxic activity of LPS [9,80], but also suggests that such additional interaction with TLR4 could be important for increasing LPS binding affinity and specificity to the MD-2/TLR4 heterodimer.

Additionally, recent studies have indicated that Kdo moieties of the inner core are likely to contribute to inflammatory responses [7,82–87]. It has also been proved that the *N. meningitidis* Ra-LPS is a potent agonist of MyD88-dependent and independent cytokines [88].

Several other studies have indicated that Kdo moieties of LPS and/or Ra-LPS importantly contribute to inflammatory responses and to TLR4 activation and signalling [85,89].

Boons and co-workers used chemically pure synthetic lipid A variants, with or without Kdo glycosylation [39], and showed that the activity of *N. meningitidis* Re-LPS in eliciting TNF-α and IFN-β production in murine macrophages was significantly higher compared to the synthetic *N. meningitidis* lipid A. As well, the induction of TNF-α was dramatically decreased, to levels like those of the lipid A,
when penta-acylated Ra-LPS was subjected to mild acid hydrolysis (pH 4.3), thus separating lipid A from Kdo.

The loss of the two Kdo from penta-acylated meningococcal Re-LPS resulted in a dramatic attenuation in biologic activity [90]. It is worth noting that *N. meningitidis* Re-LPS is recognized by the CD14, TLR4/MD-2 receptors of both human and murine cells. It suggests that the two Kdo of Re-LPS are not determinant for species-specific differentiation, noted for other LPS structures.

Zughaier et al. compared the responses of human monocyte derived dendritic cell (MDDC) to *Neisseria meningitidis* LPS, Re-LPS, and lipid A [85]. These three endotoxin variants were

obtained from genetically modified bacteria to afford highly controlled serotypes [91–93]. It was found that similar to LPS, Re-LPS induced MDDC maturation and significantly up-regulated the expression of CD80 and
CD86 co-stimulatory molecules, the MDDC maturation marker, CD83 and HLADR (Human Leukocyte
Antigen D Related). On the contrary, lipid A was much less active in inducing the production of the same co-stimulatory molecules. Again, these data suggest that the presence of the two Kdo in Re-LPS greatly increases the activity of lipid A and the authors concluded that Re-LPS is the minimal structure required to induce optimal MDDC maturation and activation.

The same authors produced different endotoxin variants in *N. meningitidis* and compared their activities in terms of cytokine release (TNF-α) and inflammatory mediators (nitric oxide) in macrophages. By a combination of genetic modification and mild acidic hydrolysis of S-LPS they obtained Rd1-LPS, Re-LPS, and lipid A [94–96]. They observed that Rd1-LPS and Re-LPS have similar activities while lipid A is ~10-fold less active. These data suggest that, while Kdo presence is necessary to optimal TLR4 agonism, the Hep units are dispensable [84]. Boons et al. examined the activity of a range of chemically defined, synthetic Lipid As [39,97,98] that were derived from *E. coli*, *S. typhimurium*, *S. minnesota*, and *N. meningitidis* bacterial strains on mouse macrophages and dendritic cells. It was found that the *N. meningitidis* Re-LPS was more potent than the Re-LPS from *E. coli*, which, in turn, were significantly more potent that the synthetic *E. coli* and *N. meningitidis* Lipid A [99].

In this case too, the two Kdo units linked to *N. meningitidis* lipid A were essential to TLR4 activity, even more important than having the two phosphate groups. Monophosphorylated *N. meningitidis* Lipid A was only slightly less active than the diphosphorylated *N. meningitidis* Lipid A, and *N. meningitidis* Re-LPS structures with variable 1 or 4’ phosphorylation were equal agonists. [100].

Muroi and Tanamoto observed similar trend in the case of *Salmonella* endotoxins activity on human THP-1 cells and TLR4-transfected HEK cells. In this case, the order of endotoxic activity was also S-LPS ≈ Re-LPS >> Lipid A. [82].

Schromm et al. [101] found that the number, nature, and location of negatively charged Kdo monosaccharide units modulate the molecular conformation of *E. coli* LPS and Lipid A, and that conformation is tightly linked to endotoxicity. Recently, synthetic Re-LPS (containing two or three Kdo) was found to have an enhanced agonist activity compared to Lipid A linked to one Kdo and Lipid A alone [7,42]. A decreased number or lack of Kdo and hydroxymyristic

acid is proposed as main contributors to low endotoxic activity of *Leptospira interrogans* [102], *Francisella tularensis* [103], *Legionella pneumophila* [104], and different *Rhizobium* species LPSs [105].

From a structural point of view, the negatively charged Kdo sugars of LPS may facilitate the binding to leucine-rich repeats (LRR) of TLR4 (most likely to residues 190 to 194 that contain positively charged amino acids [106]) The presence of Kdo moiety plays also a fundamental role in the conformational change of the glucosamine backbone [101]. When linked to Kdo, an upward shift of GlcN I was observed (~4 Å) [22]. This shifted conformation permits to have an additional space for R2 and R3 acyl chains and bring phosphate group closer to TLR4 protein [107].

7. Conclusions and Future Perspectives

While the polysaccharide O-chain seems dispensable to TLR4 activation and signalling, sugars of the core oligosaccharide play a significant role in TLR4 activation. Kdo is important for agonist activity: fully synthetic lipid A containing Kdo units (also called Re-LPS) are always more active than their counterparts lacking Kdo [39]. This increase in the agonist activity is somehow not paralleled by the number of interactions between the Kdo units and MD-2/TLR4/TLR4*, as observed by crystallography: just one interaction per Kdo unit. It should however be considered that the number of interactions actually observed with X-ray may not be exhaustive, since Kdo and Hep carbohydrates protrude from MD-2 binding site, the high rotational freedom of core oligosaccharide can hamper the observation of the interactions with the TLR4/MD-2 complex. The Kdo role in TLR4 antagonism has not or has only partially been investigated. In analogy with agonists, also antagonists should benefit from additive interaction of Kdo units with TLR4/MD-2 complex. Thanks to the production of lipid A variants with different number of Kdo units linked by chemical [7] or enzymatic [108] processes, it can be assessed that Re-LPS is the minimal chemical motif required for the maximal activation of $(TLR4/MD\text{-}2/LPS)_2$ complex.

The synthesis of lipid A mimetics, bearing one to three Kdo units linked with non-natural bonds resistant to enzymatic hydrolysis, would provide a new generation of TLR4 antagonists that should improve potency and specificity.

Another important parameter that determines the efficiency of agonist and antagonist presentation to the TLR4/MD-2 receptor complex is the tendency of the ligands to form supramolecular aggregates in solution. The amphiphilic character of natural lipid As and synthetic lipid A analogues favours the formation of aggregates in solution. The stability of

aggregates determines, in turn, the affinity of the ligands for LBP, the first receptor of the extracellular LPS/TLR4 signal pathway. In this context, the addition of hydrophilic sugar moieties to lipid A analogues could improve water solubility, increase the CMC values of molecules, and favour interaction with LBP.

In addition, the role of Kdo and Hep sugars in the binding with LBP and CD14 receptors has still to be investigated. Due to the important function of these two LPS-binding proteins in determining the efficiency of agonist or antagonist presentation to the final TLR4/MD-2 complex, an increase in affinity due to the presence of additive sugars could greatly influence the type and intensity of TLR4 response. CD14 has a leading role in the process of endocytosis of TLR4/MD-2 complex ending by intracellular signalling through the TRAM/TRIF complex formation. The differential affinity of different LPS forms for CD14 (complete S-LPS versus R-LPS lacking the O-chain) was clearly evidenced.

This review presents some examples in which the presence of Kdo in natural or synthetic lipid A variants (mono- or di-saccharides) improves the TLR4 activity if compared to simple lipid A or complete LPS with O-chain. The synthesis and the biological characterization of lipid A analogues glycosylated with Kdo and/or Hep (or mimetics of these sugars) is still largely unexplored.

We suggest that glycosylated lipid A analogues can provide in the next future a new generation of synthetic molecules to be developed as drugs targeting TLR4 signal.

Acknowledgments: This study was financially supported by the H2020-MSC-ETN-642157 project “TOLLerant”.

We acknowledge the Italian Ministry for Foreign Affairs and International Cooperation (MAECI) and Roberto Cighetti for Figure 71.

Conflicts of Interest: The authors declare no conflict of interest.

ABBREVIATIONS

AIM2 Interferon-inducible protein (Absent In Melanoma 2)

ALR AIM2-Like Receptor

CD14 Cluster of Differentiation 14

CD80 Cluster of Differentiation 80

CD83 Cluster of Differentiation 83

CD86 Cluster of Differentiation 86

CLR C-type Lectin Receptor

CMC Critical Micellar Concentration

FA Fatty acid

Gal Galactose

Glc Glucose

GlcN Glucosamine

GlcN3N 2,3-diamino-2,3-dideoxy-D-glucose

GlcNAc *N*-Acetyl-Glucosamine

GPI Glycosylphosphatidylinositol

HEK Human Embryonic Kidney Cell 293

Hep heptosyl-2-keto-3-deoxy-octulosonate

HLADR Human Leukocyte Antigen D Related

IL Interleukin

INF Interferon

IRF Interferon Regulatory Factor

IRF3 Interferon Regulatory Factor 3

Kdo 3-Deoxy-D-manno-oct-2-ulosonic acid

LBP Lipid Binding Protein

LOS Lipooligosaccharide (Hep3-Kdo2-lipid A)

LPS Lipopolysaccharide

LRR Leucine-Rich Repeat

MC Mast Cells

MD-2 Myeloid Differentiation factor 2

MDDC Human Monocyte Derived Dendritic Cell

MurNAc *N*-Acetyl-Muramic acid

MyD88 Myeloid differentiation primary response gene 88

NBD Nucleotide-Binding Domain

NF-κB Nuclear Factor-kappa B

NLR NOD-Like Receptors

NMR Nuclear Magnetic Resonance

NOD 1 & 2 Nucleotide-binding Oligomerization Domain receptor 1 & 2

PAMP Pathogen Associated Molecular Pattern

PGN Peptidoglycan

PRR Pattern Recognition Receptor

Ra-LPS Lipid A + core

Re-LPS (Kdo)2-Lipid A
RIG-1 Retinoic Acid Inducible Gene 1
R-LPS Rough LPS
RLR RIG-I-Like Receptor
SAR Structure Activity Relationship
S-LPS Smooth LPS
TANK TRAF family member-associated NF-κ-B activator
TBK1 TANK-Binding Kinase 1 (Serine/Threonine-protein Kinase TBK1)
TEM Transmission Electron Microscopy
THP-1 Human Leukemic Monocyte Cell Line
TIR Toll/interleukin-1 receptor
TLR4 Toll Like Receptor 4
TNF Tumor Necrosis Factor
TRAM TNF Receptor Associated Modulator
TRIF TIR-domain-containing adapter-inducing interferon-β

References

1. Janeway, C.A.; Medzhitov, R. Innate immune recognition. *Annu. Rev. Immunol.* **2002**, *20*, 197–216. [CrossRef] [PubMed]
2. Takeuchi, O.; Akira, S. Pattern Recognition Receptors and Inflammation. *Cell* **2010**, *140*, 805–820. [CrossRef] [PubMed]
3. Chen, G.; Shaw, M.H.; Kim, Y.-G.; Nuñez, G. NOD-Like Receptors: Role in Innate Immunity and Inflammatory Disease. *Annu. Rev. Pathol.* **2009**, *4*, 365–398. [CrossRef] [PubMed]
4. Song, D.H.; Lee, J.-O. Sensing of microbial molecular patterns by Toll-like receptors. *Immunol. Rev.* **2012**, *250*, 216–229. [CrossRef] [PubMed]
5. Kieser, K.J.; Kagan, J.C. Multi-receptor detection of individual bacterial products by the innate immune system. *Nat. Rev. Immunol.* **2017**, *17*, 376–390. [CrossRef] [PubMed]
6. Imoto, M.; Yoshimura, H.; Sakaguchi, N.; Kusumoto, S.; Shiba, T. Total synthesis of lipid A. *Tetrahedron Lett.* **1985**, *26*, 1545–1548. [CrossRef]
7. Yoshizaki, H.; Fukuda, N.; Sato, K.; Oikawa, M.; Fukase, K.; Suda, Y.; Kusumoto, S. First Total Synthesis of the Re-Type Lipopolysaccharide. *Angew. Chem. Int. Ed.* **2001**, *40*, 1475–1480. [CrossRef]

8. Uehara, A.; Fujimoto, Y.; Kawasaki, A.; Kusumoto, S.; Fukase, K.; Takada, H. Meso-Diaminopimelic Acid and Meso-Lanthionine, Amino Acids Specific to Bacterial Peptidoglycans, Activate Human Epithelial Cells through NOD1. *J. Immunol.* **2006**, *177*, 1796–1804. [CrossRef] [PubMed]
9. Homma, J.Y.; Matsuura, M.; Kanegasaki, S.; Kawakubo, Y.; Kojima, Y.; Shibukawa, N.; Kumazawa, Y.; Yamamoto, A.; Tanamoto, K.; Yasuda, T.; et al. Structural Requirements of Lipid A Responsible for the Functions: A Study with Chemically Synthesized Lipid A and Its Analogues. *J. Biochem.* **1985**, *98*, 395–406. [CrossRef] [PubMed]
10. Huber, M.; Kalis, C.; Keck, S.; Jiang, Z.; Georgel, P.; Du, X.; Shamel, L.; Sovath, S.; Mudd, S.; Beutler, B.; et al. R-form LPS, the master key to the activation of TLR4/MD-2-positive cells. *Eur. J. Immunol.* **2006**, *36*, 701–711. [CrossRef] [PubMed]
11. Akira, S.; Takeda, K. Toll-like receptor signalling. *Nat. Rev. Immunol.* **2004**, *4*, 499–511. [CrossRef] [PubMed]
12. Yang, J.; Zhao, Y.; Shao, F. Non-canonical activation of inflammatory caspases by cytosolic LPS in innate immunity. *Curr. Opin. Immunol.* **2015**, *32*, 78–83. [CrossRef] [PubMed]
13. Gutsmann, T.; Schromm, A.B.; Brandenburg, K. The physicochemistry of endotoxins in relation to bioactivity. *Int. J. Med. Microbiol.* **2007**, *297*, 341–352. [CrossRef] [PubMed]
14. Takayama, K.; Din, Z.Z.; Mukerjee, P.; Cooke, P.H.; Kirkland, T.N. Physicochemical properties of the lipopolysaccharide unit that activisit. *J. Biol. Chem.* **1990**, *265*, 14023–14029. [PubMed]
15. Takayama, K.; Mitchell, D.H.; Din, Z.Z.; Mukerjee, P.; Li, C.; Coleman, D.L. Monomeric Re lipopolysaccharide from Escherichia coli is more active than the aggregated form in the Limulus amebocyte lysate assay and in inducing Egr-1 mRNA in murine peritoneal macrophages. *J. Biol. Chem.* **1994**, *269*, 2241–2244. [PubMed]
16. Yu, L.; Tan, M.; Ho, B.; Ding, J.L.; Wohland, T. Determination of critical micelle concentrations and aggregation numbers by fluorescence correlation spectroscopy: Aggregation of a lipopolysaccharide. *Anal. Chim. Acta* **2006**, *556*, 216–225. [CrossRef] [PubMed]
17. Giardina, P.C.; Gioannini, T.; Buscher, B.A.; Zaleski, A.; Zheng, D.S.; Stoll, L.; Teghanemt, A.; Apicella, M.A.;

Weiss, J. Construction of Acetate Auxotrophs of *Neisseria meningitidis* to Study Host-Meningococcal Endotoxin Interactions. *J. Biol. Chem.* **2001**, *276*, 5883–5891. [CrossRef] [PubMed]

18. Iovine, N.; Eastvold, J.; Elsbach, P.; Weiss, J.P.; Gioannini, T.L. The carboxyl-terminal domain of closely related endotoxin-binding proteins determines the target of protein-lipopolysaccharide complexes. *J. Biol. Chem.* **2002**, *277*, 7970–7978. [CrossRef] [PubMed]
19. Post, D.M.B.; Zhang, D.; Eastvold, J.S.; Teghanemt, A.; Gibson, B.W.; Weiss, J.P. Biochemical and functional characterization of membrane blebs purified from *Neisseria meningitidis* serogroup B. *J. Biol. Chem.* **2005**, *280*, 38383–38394. [CrossRef] [PubMed]
20. Schromm, A.B.; Brandenburg, K.; Rietschel, E.T.; Flad, H.D.; Carroll, S.F.; Seydel, U. Lipopolysaccharidebinding protein mediates CD14-independent intercalation of lipopolysaccharide into phospholipid membranes. *FEBS Lett.* **1996**, *399*, 267–271. [CrossRef]
21. Schumann, R.R. Function of lipopolysaccharide (LPS)-binding protein (LBP) and CD14, the receptor for LPS/LBP complexes: A short review. *Res. Immunol.* **1992**, *143*, 11–15. [CrossRef]
22. Park, B.S.; Song, D.H.; Kim, H.M.; Choi, B.-S.; Lee, H.; Lee, J.-O. The structural basis of lipopolysaccharide recognition by the TLR4-MD-2 complex. *Nature* **2009**, *458*, 1191–1195. [CrossRef] [PubMed]
23. Wright, S.D.; Ramos, R.A.; Tobias, P.S.; Ulevitch, R.J.; Mathison, J.C. CD14, a receptor for complexes of lipopolysaccharide (LPS) and LPS binding protein. *Science* **1990**, *249*, 1431–1433. [CrossRef] [PubMed]
24. Ulevitch, R.J.; Tobias, P.S. Recognition of Gram-negative bacteria and endotoxin by the innate immune system. *Curr. Opin. Immunol.* **1999**, *11*, 19–22. [CrossRef]
25. Jiang, Q.; Akashi, S.; Miyake, K.; Petty, H.R. Cutting Edge: Lipopolysaccharide Induces Physical Proximity Between CD14 and Toll-Like Receptor 4 (TLR4) Prior to Nuclear Translocation of NF-κB. *J. Immunol.* **2000**, *165*, 3541–3544. [CrossRef] [PubMed]
26. Gioannini, T.L.; Teghanemt, A.; Zhang, D.; Coussens, N.P.; Dockstader, W.; Ramaswamy, S.; Weiss, J.P. Isolation of an endotoxin-MD-2 complex that produces Toll-like receptor 4-dependent cell activation at picomolar concentrations. *Proc. Natl. Acad. Sci. USA* **2004**, *101*, 4186–4191. [CrossRef] [PubMed]

27. Teghanemt, A.; Prohinar, P.; Gioannini, T.L.; Weiss, J.P. Transfer of monomeric endotoxin from MD-2 to CD14: Characterization and functional consequences. *J. Biol. Chem.* **2007**, *282*, 36250–36256. [CrossRef] [PubMed]
28. Deguine, J.; Barton, G.M. MyD88: A central player in innate immune signaling. *F1000Prime Rep.* **2014**, *6*, 97. [CrossRef] [PubMed]
29. Kagan, J.C.; Su, T.; Horng, T.; Chow, A.; Akira, S.; Medzhitov, R. TRAM couples endocytosis of TLR4 to the induction of interferon beta. *Nat. Immunol.* **2008**, *9*, 361–368. [CrossRef] [PubMed]
30. Fitzgerald, K.A.; Rowe, D.C.; Barnes, B.J.; Caffrey, D.R.; Visintin, A.; Latz, E.; Monks, B.; Pitha, P.M.; Golenbock, D.T. LPS-TLR4 Signaling to IRF-3/7 and NF-κB Involves the Toll Adapters TRAM and TRIF. *J. Exp. Med.* **2003**, *198*, 1043–1055. [CrossRef] [PubMed]
31. Brieger, A.; Rink, L.; Haase, H. Differential Regulation of TLR-Dependent MyD88 and TRIF Signaling Pathways by Free Zinc Ions. *J. Immunol.* **2013**, *191*, 1808–1817. [CrossRef] [PubMed]
32. Zanoni, I.; Granucci, F. Role of CD14 in host protection against infections and in metabolism regulation. *Front. Cell. Infect. Microbiol.* **2013**, *3*, 32. [CrossRef] [PubMed]
33. Mogensen, T.H. Pathogen recognition and inflammatory signalling in innate immune defenses. *Clin. Microbiol. Rev.* **2009**, *22*, 240–273. [CrossRef] [PubMed]
34. Mata-Haro, V.; Cekic, C.; Martin, M.; Chilton, P.M.; Casella, C.R.; Mitchell, T.C. The Vaccine Adjuvant
    Monophosphoryl Lipid A as a TRIF-Biased Agonist of TLR4. *Science* **2007**, *316*, 1628–1632. [CrossRef] [PubMed]
35. Johnson, D. A Synthetic TLR4-active glycolipids as vaccine adjuvants and stand-alone immunotherapeutics. *Curr. Top. Med. Chem.* **2008**, *8*, 64–79. [CrossRef] [PubMed]
36. Scior, T.; Alexander, C.; Zaehringer, U. Reviewing and identifying amino acids of human, murine, canine and equine TLR4/MD-2 receptor complexes conferring endotoxic innate immunity activation by LPS/lipid A, or antagonistic effects by Eritoran, in contrast to species-dependent modulation. *Comput. Struct. Biotechnol. J.* **2013**, *5*. [CrossRef] [PubMed]
37. Seeley, J.J.; Ghosh, S. Molecular mechanisms of innate memory and tolerance to LPS. *J. Leukoc. Biol.* **2017**, *101*, 107–119. [CrossRef] [PubMed]

38. Shiozaki, M.; Doi, H.; Tanaka, D.; Shimozato, T.; Kurakata, S.I. Syntheses of glucose analogues of E5564 as a highly potent anti-sepsis drug candidate. *Bioorg. Med. Chem.* **2006**, *14*, 3011–3016. [CrossRef] [PubMed]
39. Gaekwad, J.; Zhang, Y.; Zhang, W.; Reeves, J.; Wolfert, M.A.; Boons, G.J. Differential induction of innate immune responses by synthetic lipid A derivatives. *J. Biol. Chem.* **2010**, *285*, 29375–29386. [CrossRef] [PubMed]
40. Moran, A.P. Biological and serological characterization of Campylobacter jejuni lipopolysaccharides with deviating core and lipid A structures. *FEMS Immunol. Med. Microbiol.* **1995**, *11*, 121–130. [CrossRef] [PubMed]
41. Di Lorenzo, F.; Billod, J.-M.; Martín-Santamaría, S.; Silipo, A.; Molinaro, A. Gram-Negative Extremophile
Lipopolysaccharides: Promising Source of Inspiration for a New Generation of Endotoxin Antagonists. *Eur. J. Org. Chem.* **2017**, *2017*, 4055–4073. [CrossRef]
42. Kusumoto, S.; Fukase, K.; Fukase, Y.; Kataoka, M.; Yoshizaki, H.; Sato, K.; Oikawa, M.; Suda, Y. Structural basis for endotoxic and antagonistic activities: Investigation with novel synthetic lipid A analogs. *J. Endotoxin Res.* **2003**, *9*, 361–366. [CrossRef] [PubMed]
43. Tamai, R.; Asai, Y.; Hashimoto, M.; Fukase, K.; Kusumoto, S.; Ishida, H.; Kiso, M.; Ogawa, T. Cell activation by monosaccharide lipid A analogues utilizing Toll-like receptor 4. *Immunology* **2003**, *110*, 66–72. [CrossRef] [PubMed]
44. Cighetti, R.; Ciaramelli, C.; Sestito, S.E.; Zanoni, I.; Kubik, Ł; Ardá-Freire, A.; Calabrese, V.; Granucci, F.; Jerala, R.; Martín-Santamaría, S.; et al. Modulation of CD14 and TLR4/MD-2 activities by a synthetic lipid A mimetic. *ChemBioChem* **2014**, *15*, 250–258. [CrossRef] [PubMed]
45. Perrin-Cocon, L.; Aublin-Gex, A.; Sestito, S.E.; Shirey, K.A.; Patel, M.C.; André, P.; Blanco, J.C.; Vogel, S.N.; Peri, F.; Lotteau, V. TLR4 antagonist **FP7** inhibits LPS-induced cytokine production and glycolytic reprogramming in dendritic cells, and protects mice from lethal influenza infection. *Sci. Rep.* **2017**, *7*, 40791. [CrossRef] [PubMed]
46. Ciaramelli, C.; Calabrese, V.; Sestito, S.E.; Pérez-Regidor, L.; Klett, J.; Oblak, A.; Jerala, R.; Piazza, M.; Martín-Santamaría, S.; Peri, F. Glycolipid-based TLR4 modulators and fluorescent probes: Rational design, synthesis and biological properties. *Chem. Biol. Drug Des.* **2016**, *88*, 1–13. [CrossRef] [PubMed]

47. Rodriguez Lavado, J.; Sestito, S.E.; Cighetti, R.; Aguilar Moncayo, E.M.; Oblak, A.; Lainšcˇek, D.; Jiménez Blanco, J.L.; García Fernández, J.M.; Ortiz Mellet, C.; Jerala, R.; et al. Trehalose- and Glucose-Derived Glycoamphiphiles: Small-Molecule and Nanoparticle Toll-Like Receptor 4 (TLR4) Modulators. *J. Med. Chem.* **2014**, *57*, 9105–9123. [CrossRef] [PubMed]

48. Fukase, Y.; Fujimoto, Y.; Adachi, Y.; Suda, Y.; Kusumoto, S.; Fukase, K. Synthesis of Rubrivivax gelatinosus lipid A and analogues for investigation of the structural basis for immunostimulating and inhibitory activities. *Bull. Chem. Soc. Jpn.* **2008**, *81*, 796–819. [CrossRef]

49. Artner, D.; Oblak, A.; Ittig, S.; Garate, J.A.; Horvat, S.; Arrieumerlou, C.; Hofinger, A.; Oostenbrink, C.; Jerala, R.; Kosma, P.; et al. Conformationally constrained lipid a mimetics for exploration of structural basis of TLR4/MD-2 activation by lipopolysaccharide. *ACS Chem. Biol.* **2013**, *8*, 2423–2432. [CrossRef] [PubMed]

50. Seydel, U.; Oikawa, M.; Fukase, K.; Kusumoto, S.; Brandenburg, K. Intrinsic conformation of lipid A is responsible for agonistic and antagonistic activity. *Eur. J. Biochem.* **2000**, *267*, 3032–3039. [CrossRef] [PubMed]

51. Fort, M.M.; Mozaffarian, A.; Stover, A.G.; Correia, J.D.S.; Johnson, D.A.; Crane, R.T.; Ulevitch, R.J.; Persing, D.H.; Bielefeldt-Ohmann, H.; Probst, P.; et al. A Synthetic TLR4 Antagonist Has Anti-Inflammatory Effects in Two Murine Models of Inflammatory Bowel Disease. *J. Immunol.* **2005**, *174*, 6416–6423. [CrossRef] [PubMed]

52. Billod, J.-M.; Lacetera, A.; Guzmán-Caldentey, J.; Martín-Santamaría, S. Computational Approaches to Toll-Like Receptor 4 Modulation. *Molecules* **2016**, *21*, 994. [CrossRef] [PubMed]

53. Kawasaki, K.; Akashi, S.; Shimazu, R.; Yoshida, T.; Miyake, K.; Nishijima, M. Mouse Toll-like Receptor 4 MD-2 complex Mediates Lipopolysaccharide-mimetic Soìignal Transduction by Taxol. *J. Biol. Chem.* **2000**, *275*, 2251–2255. [CrossRef] [PubMed]

54. Kawasaki, K.; Gomi, K.; Kawai, Y.; Shiozaki, M.; Nishijima, M. Molecular basis for lipopolysaccharide mimetic action of Taxol™ and flavolipin. *J. Endotoxin Res.* **2003**, *9*, 301–307. [CrossRef] [PubMed]

55. Chan, M.; Hayashi, T.; Mathewson, R.D.; Nour, A.; Hayashi, Y.; Yao, S.; Tawatao, R.I.; Crain, B.; Tsigelny, I.F.; Kouznetsova, V.L.; et al. Identification of Substituted Pyrimido[5,4-b]indoles as Selective Toll-Like Receptor 4 Ligands. *J. Med. Chem.* **2013**, *56*, 4206–4223. [CrossRef] [PubMed]

56. Nour, A.; Hayashi, T.; Chan, M.; Yao, S.; Tawatao, R.I.; Crain, B.; Tsigelny, I.F.; Kouznetsova, V.L.; Ahmadiiveli, A.; Messer, K.; et al. Bioorganic & Medicinal Chemistry Letters Discovery of substituted 4-aminoquinazolines as selective Toll-like receptor 4 ligands. *Bioorg. Med. Chem. Lett.* **2014**, *24*, 4931–4938. [CrossRef] [PubMed]
57. Lien, E.; Chow, J.C.; Hawkins, L.D.; McGuinness, P.D.; Miyake, K.; Espevik, T.; Gusovsky, F.; Golenbock, D.T. A novel synthetic acyclic lipid A-like agonist activates cells via the lipopolysaccharide/toll-like receptor 4 signaling pathway. *J. Biol. Chem.* **2001**, *276*, 1873–1880. [CrossRef] [PubMed]
58. Morin, M.D.; Wang, Y.; Jones, B.T.; Su, L.; Surakattula, M.M.; Berger, M.; Huang, H.; Beutler, E.K.; Zhang, H.; Beutler, B.; et al. Discovery and Structure—Activity Relationships of the Neoseptins: A New Class of Toll-like Receptor-4(TLR4) Agonists. *J. Med. Chem.* **2016**, *59*, 4812–4830. [CrossRef] [PubMed]
59. Wang, Y.; Su, L.; Morin, M.D.; Jones, B.T.; Whitby, L.R.; Surakattula, M.M.R.P.; Huang, H.; Shi, H.; Choi, J.H.; Wang, K.-W.; et al. TLR4/MD-2 activation by a synthetic agonist with no similarity to LPS. *Proc. Natl. Acad. Sci. USA* **2016**, *113*, 1695–1705. [CrossRef] [PubMed]
60. Neve, J.E.; Wijesekera, H.P.; Du, S.; Jenkins, I.D.; Ripper, J.A.; Teague, S.J.; Campitelli, M.; Garavelas, A.; Nikolapoulos, G.; Le, P.V.; et al. Euodenine A: A Small-Molecule Agonist of Human TLR4. *J. Med. Chem.* **2014**, *57*, 1252–1275. [CrossRef] [PubMed]
61. Peri, F.; Calabrese, V. Toll-like receptor 4 (TLR4) modulation by synthetic and natural compounds: An update. *J. Med. Chem.* **2014**, *57*, 3612–3622. [CrossRef] [PubMed]
62. Xie, N.; Gomes, F.P.; Deora, V.; Gregory, K.; Vithanage, T.; Nassar, Z.D.; Cabot, P.J.; Sturgess, D.; Shaw, P.N.; Parat, M.-O. Activation of mu-opioid receptor and Toll-like receptor 4 by plasma from morphine-treated mice. *Brain Behav. Immun.* **2017**, *61*, 244–258. [CrossRef] [PubMed]
63. Shanmugam, A.; Rajoria, S.; George, A.L.; Mittelman, A.; Suriano, R.; Tiwari, R.K. Synthetic Toll Like Receptor-4 (TLR-4) Agonist Peptides as a Novel Class of Adjuvants. *PLoS ONE* **2012**, *7*, e30839. [CrossRef] [PubMed]
64. Ohto, U.; Fukase, K.; Miyake, K.; Shimizu, T. Structural basis of species-specific endotoxin sensing by innate immune receptor TLR4/MD-2. *Proc. Natl. Acad. Sci. USA* **2012**, *109*, 7421–7426. [CrossRef] [PubMed]

65. Yu, L.; Phillips, R.L.; Zhang, D.; Teghanemt, A.; Weiss, J.P.; Gioannini, T.L. NMR studies of hexaacylated endotoxin bound to wild-type and F126A mutant MD-2 and MD-2·TLR4 ectodomain complexes. *J. Biol. Chem.* **2012**, *287*, 16346–16355. [CrossRef] [PubMed]
66. Oblak, A.; Jerala, R. The molecular mechanism of species-specific recognition of lipopolysaccharides by the MD-2/TLR4 receptor complex. *Mol. Immunol.* **2015**, *63*, 134–142. [CrossRef] [PubMed]
67. Yoon, S.; Hong, M.; Han, G.W.; Wilson, I. A Crystal structure of soluble MD-1 and its interaction with lipid IVa. *Proc. Natl. Acad. Sci. USA* **2010**, *107*, 10990–10995. [CrossRef] [PubMed]
68. Scior, T.; Lozano-Aponte, J.; Figueroa-Vazquez, V.; Yunes-Rojas, J.A.; Zähringer, U.; Alexander, C. Three-Dimensional Mapping of Differential Amino Acids of Human, Murine, Canine and Equine Tlr4/Md-2 Receptor Complexes Conferring Endotoxic Activation By Lipid a, Antagonism By Eritoran and Species-Dependent Activities of Lipid IVa in the Mammalian Lps Se. *Comput. Struct. Biotechnol. J.* **2013**, *7*, 1–11. [CrossRef] [PubMed]
69. Kim, H.M.; Park, B.S.; Kim, J.I.; Kim, S.E.; Lee, J.; Oh, S.C.; Enkhbayar, P.; Matsushima, N.; Lee, H.; Yoo, O.J.; et al. Crystal Structure of the TLR4-MD-2 Complex with Bound Endotoxin Antagonist Eritoran. *Cell* **2007**, *130*, 906–917. [CrossRef] [PubMed]
70. Molinaro, A.; Holst, O.; Di, L.F.; Callaghan, M.; Nurisso, A.; D'Errico, G.; Zamyatina, A.; Peri, F.; Berisio, R.; Jerala, R.; et al. Chemistry of Lipid A: At the Heart of Innate Immunity. *Chemistry* **2015**, *21*, 500–519. [CrossRef] [PubMed]
71. Peri, F.; Piazza, M. Therapeutic targeting of innate immunity with Toll-like receptor 4 (TLR4) antagonists. *Biotechnol. Adv.* **2012**, *30*, 251–260. [CrossRef] [PubMed]
72. Hennessy, E.J.; Parker, A.E.; O'Neill, L.A.J. Targeting Toll-like receptors: Emerging therapeutics? *Nat. Rev. Drug Discov.* **2010**, *9*, 293–307. [CrossRef] [PubMed]
73. Gay, N.J.; Gangloff, M. Structure and Function of Toll Receptors and Their Ligands. *Annu. Rev. Biochem.* **2007**, *76*, 141–165. [CrossRef] [PubMed]
74. Tom, J.K.; Dotsey, E.Y.; Wong, H.Y.; Stutts, L.; Moore, T.; Davies, D.H.; Felgner, P.L.; Esser-Kahn, A.P. Modulation of Innate Immune Responses *via* Covalently Linked TLR Agonists. *ACS Cent. Sci.* **2015**, *1*, 439–448. [CrossRef] [PubMed]
75. Huang, J.X.; Azad, M.A.K.; Yuriev, E.; Baker, M.A.; Nation, R.L.; Li, J.; Cooper, M.A.; Velkov, T. Molecular Characterization of Lipopolysaccharide Binding to Human α-1-Acid Glycoprotein. *J. Lipids* **2012**, *2012*, 1–15. [CrossRef] [PubMed]

76. Knirel, Y.A.; Valvano, M.A. *Bacterial Lipopolysaccharides*; Springer: Berlin, Germany, 2011.
77. Bennett-guerrero, E.; Mcintosh, T.J.; Robin, G.; Snyder, D.S.; Gibbs, R.J.; Michael, G.; Poxton, I.R.; McIntosh, T.J.; Barclay, G.R.; Mythen, M.G.; et al. Preparation and Preclinical Evaluation of a Novel Liposomal Complete-Core Lipopolysaccharide Vaccine. *Infect. Immun.* **2000**, *68*, 6202–6208. [CrossRef] [PubMed]
78. Di Padova, F.E.; Brade, H.; Barclay, G.R.; Poxton, L.R.; Liehl, E.; Schuetze, E.; Kocher, H.P.; Ramsay, G.; Schreier, M.H.; Mcclelland, D.B.L.; et al. A Broadly Cross-Protective Monoclonal Antibody Binding to Escherichia coli and Salmonella Lipopolysaccharides. *Infect. Immun.* **1993**, *61*, 3863–3872. [PubMed]
79. Luk, J.M.; Lind, S.M.; Tsang, R.S.; Lindberg, A.A. Epitope mapping of four monoclonal antibodies recognizing the hexose core domain of Salmonella lipopolysaccharide. *J. Biol. Chem.* **1991**, *266*, 23215–23225. [PubMed]
80. Galanos, C.; Luderitz, O.; Rietschel, E.T.; Westphal, O.; Brade, H.; Brade, L.; Freudenberg, M.; Schade, U.; Imoto, M.; Yoshimura, H.; et al. Synthetic and natural Escherichia coli free lipid A express identical endotoxic activities. *Eur. J. Biochem.* **1985**, *148*, 1–5. [CrossRef] [PubMed]
81. Erridge, C.; Bennett-guerrero, E.; Poxton, I.R. Structure and function of lipopolysaccharides. *Microbes Infect.* **2002**, *4*, 837–851. [CrossRef]
82. Muroi, M.; Tanamoto, K. The polysaccharide portion plays an indispensable role in Salmonella LPS-induced activation of NF-kB through human TLR-4. *Infect. Immun.* **2002**, *70*, 6043–6047. [CrossRef] [PubMed]
83. Demchenko, A.V.; Wolfert, M.A.; Santhanam, B.; Moore, J.N.; Boons, G.J. Synthesis and biological evaluation of Rhizobium sin-1 lipid A derivatives. *J. Am. Chem. Soc.* **2003**, *125*, 6103–6112. [CrossRef] [PubMed]
84. Zughaier, S.M.; Tzeng, Y.; Zimmer, S.M.; Carlson, R.W.; Stephens, D.S.; Datta, A. Neisseria meningitidis Lipooligosaccharide Structure-Dependent Activation of the Pathway Neisseria meningitidis
Lipooligosaccharide Structure-Dependent Activation of the Macrophage CD14/Toll-Like Receptor 4 Pathway. *Infect. Immun.* **2004**, *72*, 371–380. [CrossRef] [PubMed]
85. Zughaier, S.; Agrawal, S.; Stephens, D.S.; Pulendran, B. Hexa-acylation and KDO2-glycosylation determine the specific immunostimulatory activity of Neisseria meningitidis

lipid a for human monocyte derived dendritic cells. *Vaccine* **2006**, *24*, 1291–1297. [CrossRef] [PubMed]

86. Vasan, M.; Wolfert, M.A.; Boons, G.-J. Agonistic and antagonistic properties of a Rhizobium sin-1 lipid A modified by an ether-linked lipid. *Org. Biomol. Chem.* **2007**, *5*, 2087–2097. [CrossRef] [PubMed]
87. Zhang, Y.; Wolfert, M.A.; Boons, G.J. The influence of the long chain fatty acid on the antagonistic activities of Rhizobium sin-1 lipid A. *Bioorg. Med. Chem.* **2007**, *15*, 4800–4812. [CrossRef] [PubMed]
88. Zughaier, S.M.; Zimmer, S.M.; Datta, A.; Carlson, R.W.; Stephens, D.S. Differential Induction of the Toll-Like Receptor 4-MyD88-Dependent and -Independent Signaling Pathways by Endotoxins. *Infect. Immun.* **2005**, *73*, 2940–2950. [CrossRef] [PubMed]
89. Raetz, C.R.; Garrett, T.A.; Reynolds, C.M.; Shaw, W.A.; Moore, J.D.; Smith, D.C.; Ribeiro, A.; Murphy, R.C.; Ulevitch, R.J.; Fearns, C.; et al. Kdo2-Lipid A of Escherichia coli, a defined endotoxin that activates macrophages via TLR-4. *J. Lipid Res.* **2006**, *47*, 1097–1111. [CrossRef] [PubMed]
90. Lien, E.; Means, T.K.; Heine, H.; Yoshimura, A.; Kusumoto, S.; Fukase, K.; Fenton, M.J.; Oikawa, M.; Qureshi, N.; Monks, B.; et al. Toll-like receptor 4 imparts ligand-specific recognition of bacterial lipopolysaccharide. *J. Clin. Investig.* **2000**, *105*, 497–504. [CrossRef] [PubMed]
91. Raetz, C.R.; Whitfield, C. Lipopolysaccharide Endotoxins. *Annu. Rev. Biochem.* **2002**, *71*, 635–700. [CrossRef] [PubMed]
92. Brabetz, W.; Müller-Loennies, S.; Holst, O.; Brade, H. Deletion of the heptosyltransferase genes rfaC and rfaF in Escherichia coli K-12 results in an Re-type lipopolysaccharide with a high degree of 2-aminoethanol phosphate substitution. *Eur. J. Biochem.* **1997**, *247*, 716–724. [CrossRef] [PubMed]
93. Murphy, R.C.; Raetz, C.R.H.; Reynolds, C.M.; Barkley, R.M. Mass Spectrometry Advances in Lipidomica: Collision Induced Decomposition of Kdo2-Lipid A. *Prostaglandins Other Lipid Mediat.* **2005**, *77*, 131–140. [CrossRef] [PubMed]
94. Rosner, M.R.; Tang, J.; Barzilay, I.; Khorana, H.G. Structure of the Lipopolysaccharide Mutant from an Escherichia coli Heptose-less Mutant. *J. Biol. Chem.* **1979**, *254*, 5906–5917. [PubMed]

95. Zhou, Z.; Lin, S.; Cotter, R.J.; Raetz, C.R.H. Lipid A Modifications Characteristic of Salmonella Typhimurium Are Induced by NH 4VO3 in Escherichia Coli K1. *Biochemistry* **1999**, *274*, 18503–18514.
96. Zhou, Z.; Ribeiro, A.A.; Lin, S.; Cotter, R.J.; Miller, S.I.; Raetz, C.R.H. Lipid A modifications in polymyxin-resistant Salmonella typhimurium. *J. Biol. Chem.* **2001**, *276*, 43111–43121. [CrossRef]
97. Zhang, Y.; Gaekwad, J.; Wolfert, M.A.; Boons, G.J. Modulation of Innate Immune Responses with Synthetic Lipid A Derivatives. *J. Am. Chem. Soc.* **2007**, *129*, 5200–5216. [CrossRef] [PubMed]
98. Zhang, Y.; Gaekwad, J.; Wolfert, M.A.; Boons, G.J. Innate immune responses of synthetic lipid a derivatives of Neisseria meningitidis. *Chemistry* **2008**, *14*, 558–569. [CrossRef] [PubMed]
99. Mariathasan, S.; Weiss, D.S.; Newton, K.; McBride, J.; O'Rourke, K.; Roose-Girma, M.; Lee, W.P.; Weinrauch, Y.; Monack, D.M.; Dixit, V.M. Cryopyrin activates the inflammasome in response to toxins and ATP. *Nature* **2006**, *440*, 228–232. [CrossRef] [PubMed]
100. Roth, R.I.; Yamasaki, R.; Mandrell, R.E.; Griffiss, J.M. Ability of gonococcal and meningococcal lipooligosaccharides to clot Limulus amebocyte lysate. *Infect. Immun.* **1992**, *60*, 762–767. [PubMed]
101. Schromm, A.B.; Brandenburg, K.; Loppnow, H.; Zähringer, U.; Rietschel, E.T.; Carroll, S.F.; Koch, M.H.; Kusumoto, S.; Seydel, U. The charge of endotoxin molecules influences their conformation and IL-6-inducing capacity. *J. Immunol.* **1998**, *161*, 5464–5471. [PubMed]
102. Vinh, T.; Adler, B.; Faine, S. Ultrastructure and chemical composition of lipopolysaccharide extracted from *Leptospira interrogans* serovar copenhageni. *J. Gen. Microbiol.* **1986**, *132*, 103–109. [CrossRef] [PubMed]
103. Vinogradov, E.; Perry, M.B.; Conlan, J.W. Structural analysis of *Francisella tularensis* lipopolysaccharide. *Eur. J. Biochem.* **2002**, *269*, 6112–6118. [CrossRef] [PubMed]
104. Petzold, M.; Thürmer, A.; Menzel, S.; Mouton, J.W.; Heuner, K.; Lück, C. A structural comparison of lipopolysaccharide biosynthesis loci of *Legionella pneumophila* serogroup 1 strains. *BMC Microbiol.* **2013**, *13*, 198. [CrossRef] [PubMed]

105. Russa, R.; Urbanik-Sypniewska, T.; Choma, A.; Mayer, H. Identification of 3-deoxy-lyxo-2-heptulosaric acid in the core region of lipopolysaccharides from Rhizobiaceae. *FEMS Microbiol. Lett.* **1991**, *68*, 337–343. [CrossRef] [PubMed]
106. Frecer, V.; Ho, B.; Ding, J.L. Interpretation of biological activity data of bacterial endotoxins by simple molecular models of mechanism of action. *Eur. J. Biochem.* **2000**, *267*, 837–852. [CrossRef] [PubMed]
107. Liu, J. Use of Receptor-Based Drug Design and Applications in the Study of Finding Antagonists for MD-2/TLR4, GLP and CXCR4. Ph.D. Thesis, Faculty of the James T. Laney School of Graduate Studies of Emory University, Atlanta, GA, USA, 2012.
108. Henderson, J.C.; O'Brien, J.P.; Brodbelt, J.S.; Trent, M.S. Isolation and chemical characterization of lipid A from gram-negative bacteria. *J. Vis. Exp.* **2013**, *966*, e50623. [CrossRef] [PubMed]

X. Italian Patent: "NUOVI ANTAGONISTI DEL TLR4 UMANO"

"NUOVI ANTAGONISTI DEL TLR4 UMANO"

1. DESCRIZIONE

L'invenzione riguarda nuovi antagonisti del TLR4, composizioni che li comprendono e loro uso come medicamenti.

2. STATO DELLA TECNICA ANTERIORE

Il Toll-like Receptor 4 (TLR4) è il "sensore" delle endotossine batteriche (lipopolisaccaride, LPS), presente nelle cellule dell'immunità innata (macrofagi e cellule dendritiche) nell'uomo e negli animali superiori. Il TLR4 è capace di riconoscere quantità molto piccole di LPS rilasciato da batteri Gram-negativi in circolazione nell'organismo ed attivare di conseguenza una cascata di segnali all'interno delle cellule che porta alla produzione di molecole pro-infiammatorie come le citochine.

L'attivazione del TLR4, la produzione di citochine infiammatorie e l'attivazione dell'immunità innata e successivamente adattive, sono meccanismi di difesa dell'organismo dalle infezioni batteriche. Tuttavia, un'attivazione troppo potente del TLR4 porta ad una sindrome molto grave e spesso mortale, la sepsi acuta (detta anche shock settico). Inoltre l'attivazione del TLR4 da parte di fattori endogeni derivanti da tessuti danneggiati, è alla radice di malattie auto infiammatorie ed autoimmuni.

È noto in letteratura (Gaikwad et al. Neural Regen Res. 2016 Apr; 11(4): 552–553. doi: 10.4103/1673-5374.180732 Toll-like receptor-4 antagonism mediates benefits during neuroinflammation e Lin et al Cardiovasc Ther. 2009 Summer; 27(2): 117–123 Innate Immunity and Toll-like Receptor Antagonists: A Potential Role in the Treatment of Cardiovascular Diseases) che antagonisti TLR4 sono utili nel trattamento di patologie associate con l'attivazione dell'immunità innata come infezioni, sepsi, aterosclerosi, trombocitopenia, trombosi, disturbi coronarici, cardiomiopatia, danno da riperfusione post ischemia miocardica (MI/R), disturbi alle valvole cardiache, malattie neurodegenerative, cancro, diabete.

C'è dunque un interesse farmacologico crescente nello sviluppare sostanze capaci di bloccare lo stimolo del TLR4. Queste molecole, di origine sintetica o naturale, hanno un'azione da antagonisti del TLR4. Gli antagonisti del TLR4 competono con il ligando naturale (LPS o ligandi endogeni) per il sito di legame del co-recettore (o adattatore) MD-2. Una volta spiazzato

il ligando naturale, queste molecole bloccano l'MD-2 in uno stato non produttivo per l'interazione con il TLR4 bloccando così a monte la trasmissione del segnale infiammatorio e la produzione di citochine.

Uno degli antagonisti del TLR4 più attivi su modelli animali è il composto sintetico E5564 (Eritoran), un mimetico del lipide A, formato da un disaccaride della glucosammina con due gruppi fosfato in posizione C1 e C4' e quattro catene lipofile. Altri antagonisti derivanti dalla semplificazione della struttura dell'Eritoran e del lipide A, sono composti da monosaccaridi variamente acilati con catene lipofile, che mimano la parte riducente e quella non riducente del disaccaride (Figura 1).

In alcuni mimetici del lipide A, il gruppo fosfato anionico è stato sostituito dal gruppo bio-isosterico carbossilato che ne riproduce la carica negativa (Figura 1).

Sono stati sintetizzati disaccaridi con un gruppo carbossilico che sostituisce il fosfato sulla posizione C1 le cui formule sono riportate sotto (T. Mochizuki, Tetrahedron 56, 2000, 7691-7703). In altri analoghi del lipide A lo zucchero riducente ed il fosfato sono stati sostituiti con una dietanolammina acilata legata ad un fosfato o ad un acido carbossilico (Lewicky, J. D.; Ulanova, M.; Jiang, Z. H. Improving the immunostimulatory potency of dietanoloamine-containing lipid A mimics. Bioorg Med Chem 2013, 21, 2199-209). Questi composti, chiamati glucosaminide-4-fosfati (AGPs, Figura 1) sono stati dapprima progettati e sintetizzati da D. Johnson nel 1999 (Johnson, D., Sowell, C., Johnson, C., Livesay, M., Keegan, D., Rhodes, M., Ulrich, J., Ward, J., Cantrell, J., and Brookshire, V. (1999). Synthesis and biological evaluation of a new class of vaccine adjuvants: amminoalkil glucosaminide 4-phosphates (AGPs). Bioorg Med Chem Lett 9, 2273-2278.). Sono stati in seguito sviluppati come adiuvanti vaccinali in quanto conservano un'attività immunostimolante dovuta ad un'azione agonista sul TLR4. L'attività immunostimolante degli AGP è la prova concreta di come la sostituzione bioisosterica del gruppo fosfato in C-1 con un carbossilato che conserva la carica negativa (anionico) non alteri le proprietà di agonismo sul TLR4.

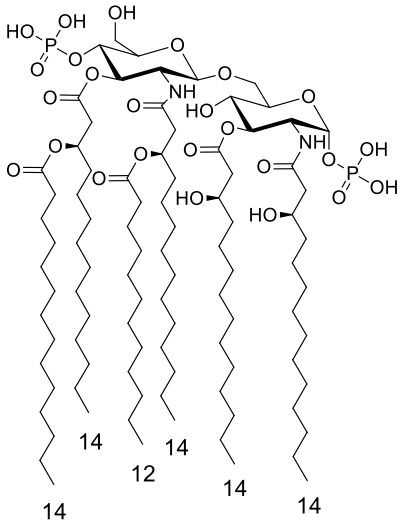

E. coli Lipid A

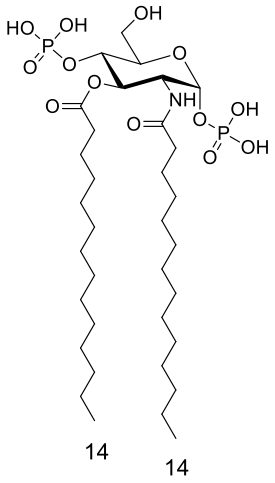

FP7

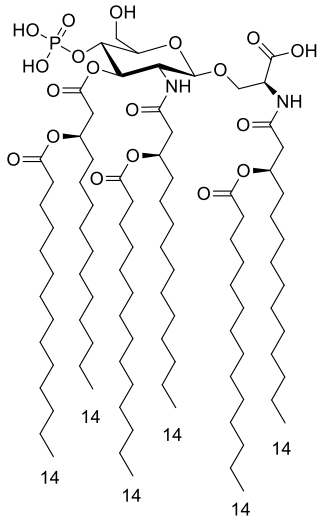

glucosaminide-4-fosfati (AGPs)

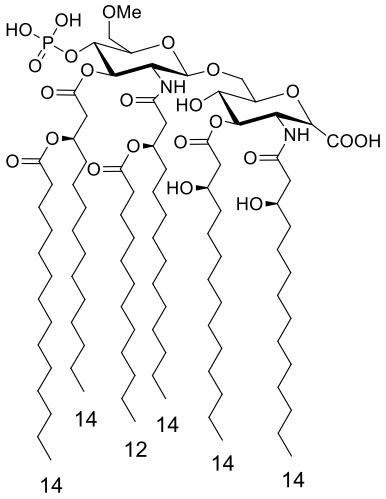

6'-*O*-Methyl-lipid A
tipo acido pirancarbossilico

È sopra riportata la struttura chimica del lipide A di *E. coli*, del monosaccaride sintetico FP7, del disaccaride carbossilato e del glucosaminide-4-fosfato (AGP). Tutti questi composti mimano il lipide A (o una sua parte) e sono attivi come modulatori del TLR4.

3. SOMMARIO DELL'INVENZIONE

La presente invenzione è relativa a nuove molecole sintetiche con attività antagonista del recettore Toll-like Receptor 4 (TLR4) umano. La novità principale consiste nella formula chimica di queste molecole, radicalmente diversa da quella di altri antagonisti sintetici sinora noti. La base strutturale delle molecole è quella del monosaccaride glucosammina, cui sono

legate due catene lipofile sature o insature e due gruppi carbossilici. Le molecole mimano la struttura tridimensionale del lipide A, l'agonista (attivatore) naturale del recettore TLR4.
Sono quindi oggetto dell'invenzione un composto avente formula (I)

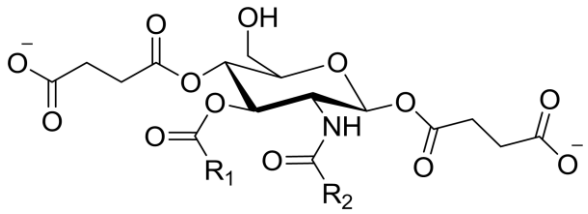

in cui R1 ed R2 possono essere, indipendentemente l'uno dall'altro catene di acido oleico, linoleico, miristico o laurico; una composizione farmaceutica comprendente un composto come definito sopra e il loro uso in terapia.

4. DESCRIZIONE DETTAGLIATA DELLE FIGURE

La figura 1 mostra l'inibizione dose-dipendente dell'attivazione NF-κB in cellule HEK-Blue™ innescata da LPS, dipendente da TLR4 esercitata dai composti FP13-16. (A) Cellule HEK-Blue™ Htlr4 sono state pre-incubate con concentrazioni crescenti (da 0,1 a 10 μM) dei composti FP13-16 e stimolate con LPS (100ng/ml) dopo 30 minuti. I dati sono stati normalizzati rispetto a stimolazioni con solo LPS e adattate ad una equazione logistica sigmoidale a 4 parametri per determinare i valori IC_{50}. I punti rappresentano la media percentuale ±SEM di almeno 3 esperimenti indipendenti. (B) Paragone tra le curve dose-effetto per i composti FP13-16 nell'inibire l'attivazione NF-□B innescata da LPS, dipendente da TLR4.

5. GLOSSARIO

Il termine antagonista del TLR4 nella presente descrizione ha il significato comunemente utilizzato in letteratura e indica un composto che compete con il ligando naturale del TLR4 (LPS o altri ligandi endogeni) per il sito di legame del co-recettore (o adattatore) MD-2.
L'antagonista del TLR4 secondo la presente descrizione, una volta spiazzato il ligando naturale, o una volta legatosi al recettore al posto del ligando naturale, blocca l'MD-2 in uno stato non produttivo per l'interazione con il TLR4 bloccando a monte la trasmissione del segnale infiammatorio e la produzione delle citochine.

Il termine FP13 è utilizzato nella presente descrizione e nei disegni per indicare il composto avente formula

(I^a)

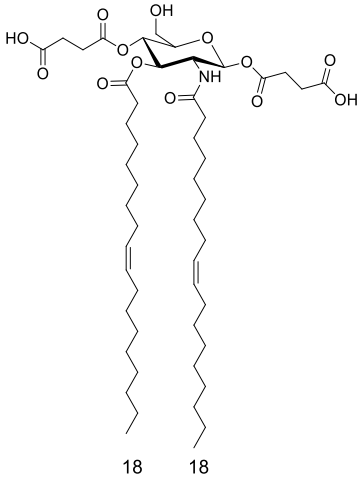

FP13

Il termine FP14 è utilizzato nella presente descrizione e nei disegni per indicare il composto avente formula

(I^b)

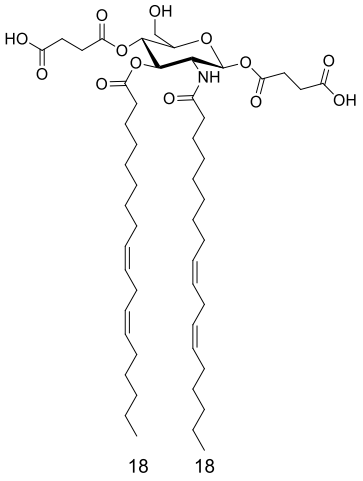

FP14

Il termine FP15 è utilizzato nella presente descrizione e nei disegni per indicare il composto avente formula

(I^c)

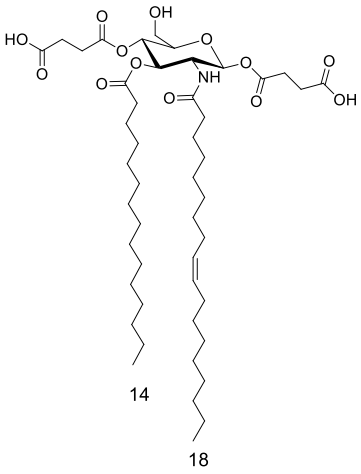

FP15

Il termine FP16 è utilizzato nella presente descrizione e nei disegni per indicare il composto avente formula

(I^d)

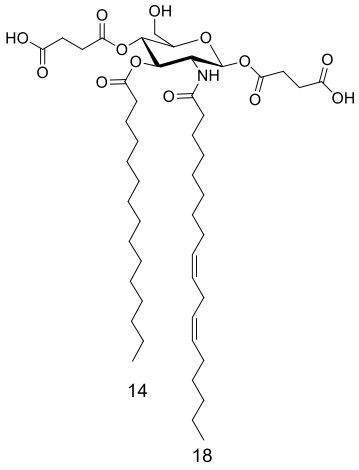

FP16

Il termine FP17 è utilizzato nella presente descrizione e nei disegni per indicare il composto avente formula

(I^e)

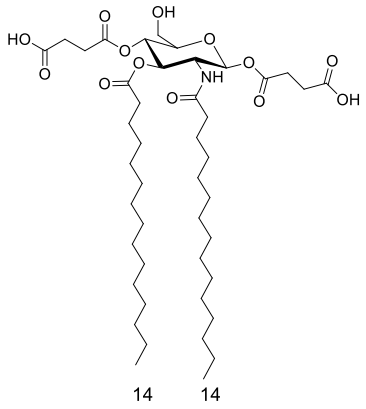

FP17

Il termine FP18 è utilizzato nella presente descrizione e nei disegni per indicare il composto avente formula

(I^f)

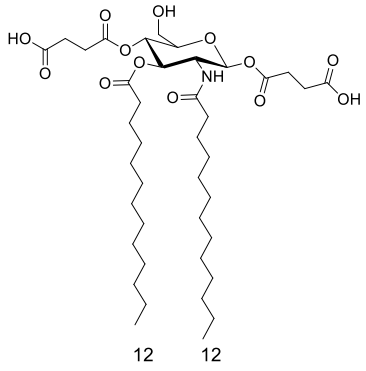

FP18

6. DESCRIZIONE DETTAGLIATA DELL'INVENZIONE

La presente invenzione riguarda antagonisti del recettore umano TLR4, in grado di inibire la risposta infiammatoria scatenata dal legame di tale recettore quando legato dal suo ligando naturale LPS, inibendo quindi il segnale infiammatorio e la secrezione di citochine alla base dell'immunità innata.

E' oggetto dell'invenzione un composto avente formula (I)

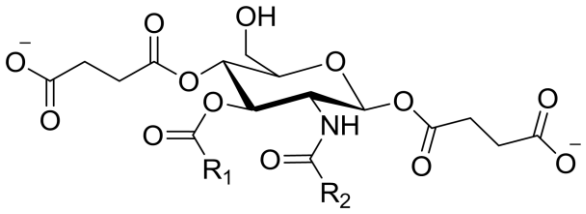

in cui R1 ed R2 possono essere, indipendentemente l'uno dall'altro catene di acido oleico, linoleico, miristico o laurico.

In una forma di realizzazione, quando R1 è una catena di acido oleico R2 è una catena di acido oleico o una catena di acido linoleico.

Secondo una ulteriore forma di realizzazione, quando R1 è una catena di acido linoleico R2 è una catena di acido linoleico.

Secondo una ancora ulteriore forma di realizzazione, quando R1 è una catena di acido miristico R2 è una catena di acido oleico, linoleico o miristico.

Come mostrato in figura 1, il composto dell'invenzione, in una qualsiasi delle sue forme di realizzazione, è un efficace antagonista del recettore TLR4 e può quindi essere utilizzato in campo terapeutico per i fini terapeutici in cui sono utilizzati antagonisti del recettore TLR4 noti in letteratura come quelli descritti nel background dell'invenzione, sopra.

E' quindi oggetto dell'invenzione il composto avente formula (I)

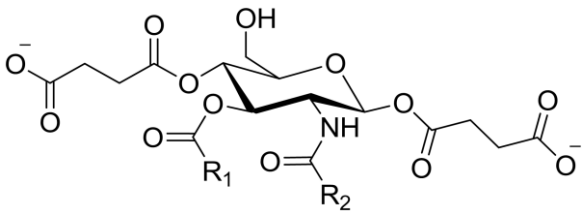

in cui R1 ed R2 possono essere, indipendentemente l'uno dall'altro catene di acido oleico, linoleico, miristico o laurico, o come definito in una qualsiasi delle forme di realizzazione sopra, per uso come principio attivo farmacologico.

In particolare, il composto come sopra definito, in una qualsiasi delle sue forme di realizzazione, è idoneo, in quantità terapeuticamente efficace, per l'uso come principio attivo farmacologico nel trattamento di patologie in cui è necessaria una inattivazione del recettore TLR4.

Un esempio non limitante di tali patologie è rappresentato da infezioni, sepsi, aterosclerosi, trombocitopenia, trombosi, disturbi coronarici, cardiomiopatia, danno da riperfusione post ischemia miocardica (MI/R), disturbi alle valvole cardiache, malattie neurodegenerative, cancro, diabete.

E’ quindi oggetto dell’invenzione anche una composizione farmaceutica comprendente un composto avente formula (I)

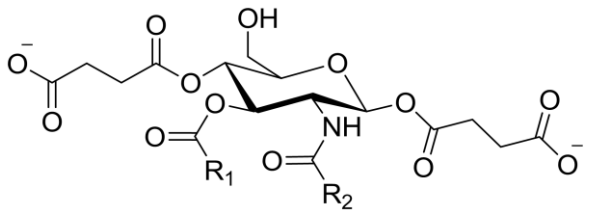

in cui R1 ed R2 possono essere, indipendentemente l’uno dall’altro catene di acido oleico, linoleico, miristico o laurico, o come definito in una qualsiasi delle forme di realizzazione sopra, e almeno un veicolante o un eccipiente farmacologicamente accettabile.

L’esperto del settore potrà scegliere uno o più veicolanti e/o eccipienti farmacologicamente accettabili in base al metodo di somministrazione desiderato, sulla base della comune pratica farmacologica.

La composizione secondo l’invenzione potrà essere formulata, ad esempio, in forma liquida, iniettabile, solida, granulato, polvere, emulsione, spray, aerosol, crema.

L’esperto del settore potrà quindi formulare la composizione scegliendo eccipienti e/o veicolanti opportuni, ad esempio, per somministrazione orale, sistemica, endovenosa, topica, rettale, nebulizzata.

La composizione farmaceutica dell’invenzione può quindi essere utilizzata come farmaco. Il dosaggio e le modalità di somministrazione possono essere scelte dal medico curante sulla base dell’anamnesi clinica del paziente, del suo stato di salute, del sesso, del peso e dell’età.

La composizione comprenderà quantità farmacologicamente efficaci del composto come sopra definito in una qualsiasi delle sue forme di realizzazione.

Per quantità farmacologicamente efficace s’intende una quantità di principio attivo che producono una risposta terapeutica o l’effetto desiderato in almento una parte dei soggetti che la assume.

La composizione farmaceutica dell’invenzione, in una qualsiasi delle sue forme di realizzazione, può essere utilizzata nel trattamento di patologie in cui è necessaria o che beneficiano da una inattivazione del recettore TLR4.

Un esempio non limitativo di tali patologie comprende infezioni, sepsi, aterosclerosi, trombocitopenia, trombosi, disturbi coronarici, cardiomiopatia, danno da riperfusione post ischemia miocardica (MI/R), disturbi alle valvole cardiache, malattie neurodegenerative, cancro, diabete.

E’ ulteriormente oggetto dell’invenzione un metodo terapeutico per il trattamento di patologie in cui è necessaria o che beneficiano da una inattivazione del recettore TLR4 che comprende la somministrazione di dosi terapeuticamente efficaci del composto avente formula (I)

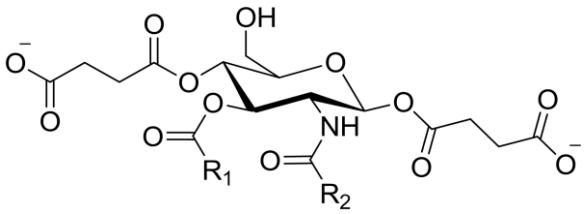

in cui R1 ed R2 possono essere, indipendentemente l’uno dall’altro catene di acido oleico, linoleico, miristico o laurico, o come definito in una qualsiasi delle forme di realizzazione sopra o di una composizione farmaceutica che lo comprende.

Un esempio non limitativo di tali patologie comprende infezioni, sepsi, aterosclerosi, trombocitopenia, trombosi, disturbi coronarici, cardiomiopatia, danno da riperfusione post ischemia miocardica (MI/R), disturbi alle valvole cardiache, malattie neurodegenerative, cancro, diabete.

Il composto secondo la presente invenzione, in una qualsiasi delle sue forme di realizzazione potrà essere sintetizzato dal tecnico del settore, ad esempio a partire dalla D-glucosammina, secondo qualsiasi tecnica nota.

Un esempio non limitativo per la sintesi del composto dell’invenzione è fornito nella sezione degli esempi sotto.

1.1) Sintesi dei composti FP13-18

Per la sintesi dei composti FP13-17 è stata adottata una strategia divergente a partire dalla D-glucosammina che viene dapprima trattata con sodio azide ed anidride triflica per ottenere l’azido-derivato in posizione C2, che viene successivamente protetta nelle posizioni C4 e C6 come 4,6-di-O-benzilidene ed infine viene protetta in posizione C1 come terz-butildimetilsilil etere (TBDMS) per ottenere il composto **1** come intermedio comune di tutte le molecole. (Schema 1)

Schema 1. sintesi dell'intermedio 1

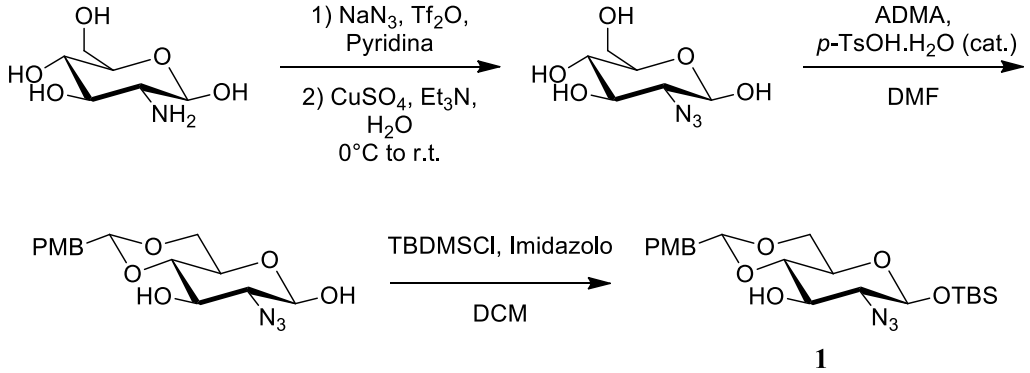

1

Per la sintesi dei composti FP13, FP14 and FP17 che recano in C2 e C3 due catene identiche l'intermedio **1** è stato trattato con trifenilfosfina (Ph3P) in tetraidrofurano (THF)/acqua per ridurre l'azide in ammina e produrre l'intermedio 2 (Schema 2 A).

I gruppi ossidrili liberi delle posizioni C2 e C3 dello zucchero sono stati quindi esterificati con acido miristico, oleico e linoleico in presenza dell'agente condensante 1-Etil-3-(3-dimetilamminopropil)carbodiimide (EDC), ed una quantità catalitica di dimetilamminopiridina (DMAP) in diclorometano, dando rispettivamente i composti **3**, **4**, **5** e **6**.

Schema 2.

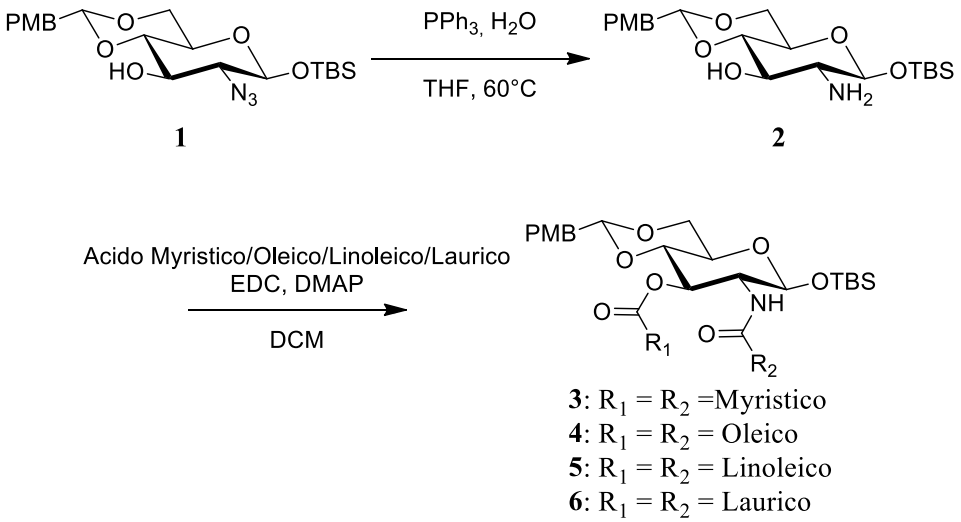

1 **2**

3: $R_1 = R_2$ =Myristico
4: $R_1 = R_2$ = Oleico
5: $R_1 = R_2$ = Linoleico
6: $R_1 = R_2$ = Laurico

Per la sintesi dei composti con due catene differenti in C2 e C3 è stata seguita un'altra via sintetica (Schema 2 B) dove l'intermedio azido-glucosio **1** è stato esterificato nella posizione C3 usando acido miristico in presenza di DMAP ed EDC in diclorometano a dare l'intermedio **7** che dopo riduzione dell'azide ad ammina con trifenilfosfina in THF/acqua (**8**) e successiva esterificazione con acido linoleico o oleico ha dato rispettivamente i composti **9** (R1 = miristico; R2 = linoleico) e **10** (R1 = miristico; R2 = oleico).

Schema 3.

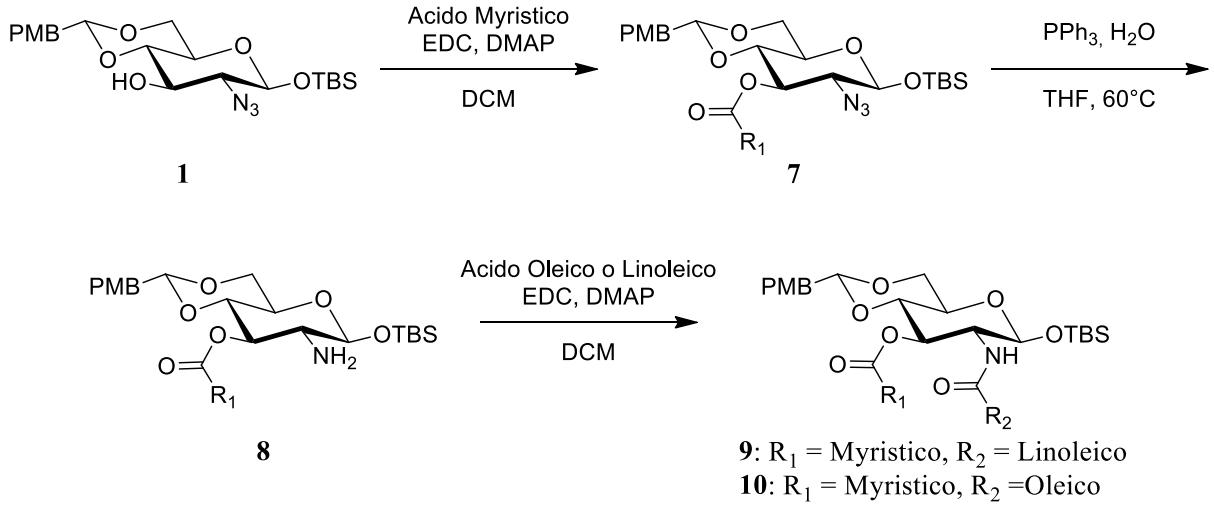

Gli intermedi **3**, **4**, **5**, **6**, **9** e **10** sono stati trasformati nei prodotti finali tramite la stessa sequenza di reazioni (Schema 3). L'apertura regioselettiva del benzilidene con sodio cianoboroidruro ed acido cloridrico seguita da trattamento con anidride succinica ed infine deprotezione del gruppo para-metossibenzile in C6 tramite trattamento acido (acido trifluoroacetico, TFA) ha dato i prodotti finali FP 13-18 (Schema 3).

I composti FP13-18 sono solubili in DMSO fino ad una concentrazione di 100 mg/ml.

Schema 4:

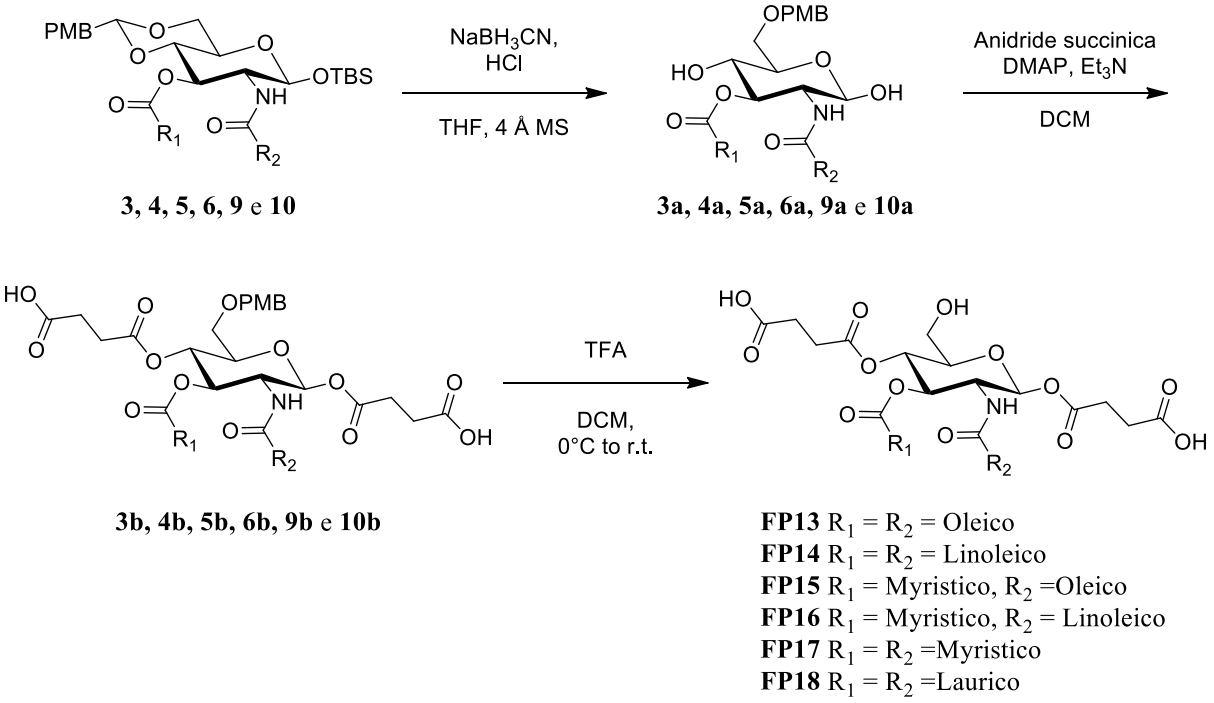

7. ESEMPI

Gli esempi sotto riportati mostrano un modo per realizzare i composti della presente invenzione e riportano dati sperimentali, chimici e biologici, ottenuti con gli stessi.

1.2) Protezione con azide

E' stato messo, in una fiasca a due colli asciutta riempita di argon, NaN_3 (1.2 eq.) in Piridina (2 ml/mmol). La reazione è stata raffreddata in un bagno ghiacciato ed è stato aggiunto Tf_2O (1.4 eq.) a gocce. La miscela è stata mescolata in ghiaccio per 3 ore.

E' stata aggiunta in una seconda fiasca glucosammina (1 eq.) in piridina/H_2O (1:3, 1 ml/mmol). La reazione è stata raffreddata a 0 °C ed è stato aggiunto $CuSO_4$ (0.065 eq.) e poi TEA (2 eq.). La miscela è stata mescolata per 30 min. La prima preparazione è stata trasferita nella seconda e la miscela è stata riscaldata a temperatura ambiente e mescolata per 24 ore. La reazione è stata monitorata mediante TLC (AcOEt/MeOH/H_2O 7:3:0.1, R_f = 0.6)

Work-up: la metà del solvente è stata fatta evaporare sotto vuoto, è stato aggiunto toluene (1:1) ed è stato fatto co-evaporare sotto vuoto più volte fino alla comparsa di un precipitatio bianco. Il prodotto è stato utilizzato senza purificazione nel passaggio successivo assumendo una resa del 100%.

1.3) Formazione del benzilidene

La glucosammina protetta con azide (1 eq.) della precedente reazione è stata sciolta in DMF_{Dry} (~1 ml/mmol). Sono stati aggiunti anisaaldeide dimetil acetale (ADMA, 1.1 eq.) ed acido *para*-toluen-solfonico (p-TsOH, 0.02 eq.) e la reazione è stata lasciata reagire sul rotavapor (60 °C, 250 mbar) per 30 min. La reazione è stata monitorata mediante TLC (AcOEt /EtP 6:4, R_f = 0.7).

Work-up: La reazione è stata bloccata con TEA (0.04 eq.) e fatta evaporare sotto vuoto. Il prodotto è stato purificato su colonna cromatografica flash (AcOEt/EtP 1:1) a dare il prodotto come polvere gialla. Resa globale delle due reazioni: 80%.

1.4) Protezione anomerica con terz-butildimetilsilano (TBDMS)

Il composto ottenuto dopo la procedura 3. (1 eq.) è stato sciolto in DCM_{Dry} (2 ml/mmol) in argon e raffreddato fino a - 10 °C. E' stato aggiunto *terz*-butildimetilsilil cloruro (1.2 eq.) insieme ad imidazolo (2.5 eq.) e la reazione è stata seguita da TLC (EtP/AcOEt 8:2, R_f = 0.9).

Work-up: È stata aggiunta H_2O (0.2 ml/mmol) e la miscela è stata diluita con CH_2Cl_2 (2 ml/mmol) e lavato con H_2O (2 ml/mmol). Lo strato acquoso è stato estratto con CH_2Cl_2 (2x 1 ml/mmol), e gli strati organici combinati sono stati essiccati con $NaSO_4$ e concentrati sotto vuoto. Il residuo è stato purificato su colonna cromatografica flash (AcOEt/EtP 1:9) a dare il prodotto come olio giallastro con resa del 75%.

1.5) Idrolisi dell'azide ad ammina

Il carboidrato protetto con ammina idoneo (1 eq.) è stato sciolto in THF (10 ml/mmol) ed è stato aggiunto PPh_3 (3 eq.). La reazione è stata mescolata 30 min a temperature ambiente e quindi scaldata a 60 °C. A questo punto, è stata aggiunta H_2O (1 ml/mmol) . La reazione è stata seguita da TLC (AcOEt/EtP 2:8, $R_f = 0.2$)

Work-up: La miscela è stata asciugata sotto vuoto e purificata su colonna cromatografica flash (AcOEt/EtP 1:9) to a dare il prodotto desiderato come olio giallastro con una resa del 85%.

1.6) Acilazione

Sono stati sciolti in una fiasca asciutta riempita con argon le catene di acidi grassi idonee (4 eq.) e EDC (6 eq.) in DCM (5 ml/mmol). La miscela è stata mescolata 30 min a temperatura ambiente. In una seconda fiasca asciutta riempita con argon è stato sciolto il carboidrato (1 eq.) in DCM (5 ml/mmol) e, quindi, è stato trasferito nella prima fiasca. La miscela è stata mescolata 5 min prima di aggiungere DMAP (1 eq.). La reazione è stata monitorata mediante TLC (AcOEt/EtP 2:8, $R_f = 0.7$).

Work-up: La miscela è stata diluita con DCM (5 ml/mmol) e lavata con $NaHCO_3$ saturo e salina. La fase organica è stata recuperata ed essiccata con $NaSO_4$, filtrata fatta evaporare sotto vuoto prima di essere purificata su colonna cromatografica flash (AcOEt/EtP 0.5:9.5) a a dare il prodotto desiderato come olio giallastro con resa del 60%.

1.7) Apertura regioselettiva one-pot del benzilidene e deprotezione TBDMS

In una fiasca asciutta e pulita sono stati scolti: il prodotto della procedura 6. (1 eq.), $NaBH_3CN$ (15 eq.) e un setaccio molecolare 4 Å (200 mg/mmol) in THF anidro (45 ml/mmol). La miscela è stata mescolata a temperatura ambiente per 2 ore e, quindi, raffreddata a 0 °C. È stata aggiunta a gocce una soluzione di HCl (1 M in diossano, 18 eq.) e la miscela è stata mescolata per 1 ora a 0 °C e altre 3 ore temperatura ambiente. (AcOEt/EtP 1:1, $R_f = 0.3$)

Work-up: è stata aggiunta trietilammina (0.5 mL/mmol) per terminare la reazione. è stato filtrato attraverso setaccio molecolare in Celite e lavato con etere. Il filtrato e l'eluato sono stati combinati e lavati con $NaHCO_3$ saturo e salina, asciugati con Na_2SO_4 e infine fatti evaporare sotto vuoto. Il residuo è stato purificato su colonna cromatografica flash (AcOEt/EtP 4:6) a dare il prodotto desiderato come olio incolore con una resa del 62%.

1.8) Acido 1,4 -ossobutanoico

Ad una soluzione del carboidrato idoneo (1 eq.) e DMAP (6 eq.) in DCM (50 ml/mmol) è stata aggiunta anidride succinica (6 eq.). La miscela è stata mescolata tutta la notte e monitorata mediante TLC (DCM/MeOH 5% + 1% acido formico, $R_f = 0.4$).

Work-up: la miscela è stata concentrata sotto vuoto e purificata su colonna cromatografica flash (DCM/MeOH 2% + 1% acido formico) a dare il prodotto desiderato come olio giallastro con resa del 80%.

1.9) Deprotezione del *para*-metossibenzilidene (PMB)

Ad una soluzione di monosaccaride (1 eq.) in DCM (100 ml/mmol) a 0 °C, è stato aggiunto TFA (10 eq.). La miscela è stata lasciata scaldare a temperatura ambiente. La reazione è stata monitorata mediante TLC (DCM/MeOH 5% + 1% acido formico, $R_f = 0.2$).

Work-up: la miscela è stata trattata con $NaHCO_3$ saturo ed estratta due volte con DCM (20 ml/mmol). La fase organica è stata lavata con fisiologica., asciugata con Na_2SO_4, filtrata, e il solvente è stato fatto evaporare sotto vuoto. Il residuo è stato portato in cromatografia su colonna (DCM/MeOH 2% to 10% + 1% acido formico) a dare il prodotto finale come olio marrone con una resa del 75 %.

8. Caratterizzazione dei composti intermedi e finali

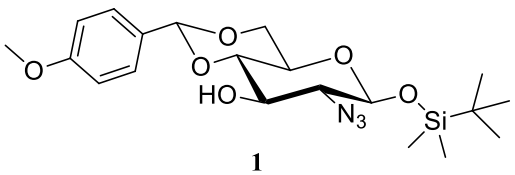

1

1 (4aR,6S,7R,8R,8aS)-7-azido-6-((terz-butildimetilsilil)ossi)-2-(4-metossifenil)esaidro-pirano[3,2-d][1,3]diossin-8-ol.

^{1}H NMR (400 MHz, $CDCl_3$) δ 7.39 (d, *J* = 8.7 Hz, 2H, 2*H_{Ar}), 6.89 (d, *J* = 8.5 Hz, 2H, 2*H_{Ar}), 5.48 (s, 1H, CH_{PMB}), 4.64 (d, *J* = 7.6 Hz, 1H, H_1), 4.27 (dd, *J* = 10.5, 4.9 Hz, 1H, H_4), 3.84 –

3.67 (m, 4H, OMe, H_{6a}), 3.58 (dt, *J* = 28.0, 9.2 Hz, 2H, H_3, H_{6b}), 3.46 – 3.37 (m, 1H, H_5), 3.32 (t, *J* = 8.5 Hz, 1H, H_2), 0.94 (s, 9H, ^{t}Bu), 0.16 (s, 6H, 2*Me-Si). **^{13}C NMR (400 MHz, $CDCl_3$) δ** 159.2, 129.9, 128.8, 113.4, 102.0, 100.7, 81.2, 70.7, 67.9, 6.7, 56.0, 49.8, 25.8–25.5, 18.6, -2.9, -3.3.

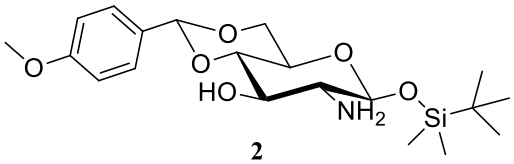

2

2 (4aR,6S,7R,8R,8aS)-7-ammino-6-((terz-butildimetilsilil)ossi)-2-(4-metossifenil)esaidropirano[3,2-d][1,3]diossin-8-olo.

^{1}H NMR (400 MHz, $CDCl_3$) δ 7.41 (d, *J* = 8.6 Hz, 2H, 2*H_{Ar}), 6.88 (d, *J* = 8.6 Hz, 2H, 2*H_{Ar}), 5.48 (s, 1H, CH_{PMB}), 4.56 (d, *J* = 7.4 Hz, 1H, H_1), 4.25 (dd, *J* = 10.4, 4.8 Hz, 1H, H_4), 3.84 – 3.71 (m, 4H, OMe, H_{6a}), 3.64 (t, *J* = 9.2 Hz, 1H, H_3), 3.54 (t, *J* = 8.9 Hz, 1H, H_{6b}), 3.44 (dt, *J* = 14.1, 7.1 Hz, 1H, H_5), 2.75 (t, *J* = 8.6 Hz, 1H, H_2), 0.92 (s, 9H, ^{t}Bu), 0.13 (s, 6H, 2*Me-Si). **^{13}C NMR (400 MHz, $CDCl_3$) δ** 159.2, 130.0, 128.8, 113.6, 102.1, 100.2, 80.6, 71.2, 67.9, 64.7, 60.7, 56.0, 25.6–25.6, 18.6, - 4.8, -5.3.

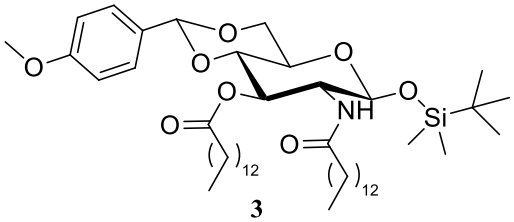

3

3 (4aR,6S,7R,8R,8aS)-6-((terz-butildimetilsilil)ossi)-2-(4-metossifenil)-7-tetradecanammido esaidropirano[3,2-d][1,3]diossin-8-il tetradecanoato.

^{1}H NMR (400 MHz, $CDCl_3$) δ 7.35 (d, *J* = 8.7 Hz, 2H, 2*H_{Ar}), 6.86 (d, *J* = 8.8 Hz, 2H, 2*H_{Ar}), 5.46 (s, 1H, CH_{PMB}), 5.17 (t, *J* = 10.0 Hz, 1H, H_3), 4.72 (d, *J* = 7.8 Hz, 1H, H_1), 4.26 (dd, *J* = 10.6, 5.1 Hz, 1H, H_5), 4.07 (dd, *J* = 17.9, 9.3 Hz, 1H, H_2), 3.83 – 3.76 (m, 4H, OMe_{PMB}, H_{6a}), 3.70 (t, *J* = 9.4 Hz, 1H, H_4), 3.53 – 3.43 (m, 1H, H_{6b}), 2.39 – 2.22 (m, 2H, $CH_{2\alpha\ Ammide}$), 2.16 – 2.02 (m, 2H, $CH_{2\alpha\ Estere}$), 1.74 – 1.49 (m, 4H, 2*$CH_{2\beta}$), 1.25 (s, 44H, 22*CH_2), 0.96 – 0.78 (m, 15H, ^{t}Bu + 2*CH_3), 0.09 (s, 3H, Si-Me_a), 0.07 (s, 3H, Si-Me_b).**^{13}C NMR (400 MHz, $CDCl_3$) δ** 175.3, 174.4, 159.2, 129.9, 128.7, 113.5, 102.0, 97.7, 78.5, 71.0, 67.9, 64.3, 56.0, 54.6, 37.7, 34.1, 31.2, 29.2–28.5, 25.3, 25.1, 22.8, 18.6, 14.0, -2.9, -3.3.

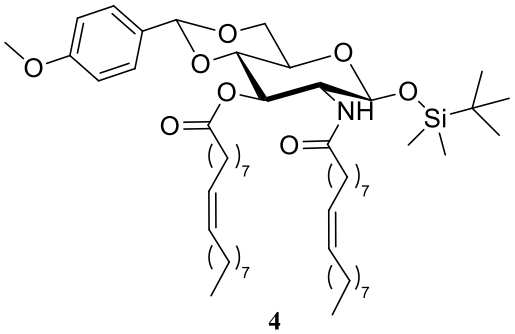

4

4 (4aR,6S,7R,8R,8aS)-6-((terz-butildimetilsilil)ossi)-2-(4-metossifenil)-7-oleammido-esaidro pirano[3,2-d][1,3]diossin-8-il oleato.

^{1}H NMR (400 MHz, $CDCl_3$) δ 7.35 (d, *J* = 8.6 Hz, 2H, 2*H_{Ar}), 6.85 (d, *J* = 8.7 Hz, 2H, 2*H_{Ar}), 5.67 (d, *J* = 9.6 Hz, 1H, NH), 5.45 (s, 1H, $H_{1\,\alpha}$), 5.40 – 5.23 (m, *J* = 10.2, 4.7 Hz, 4H, 4*CH=), 5.18 (t, *J* = 10.0 Hz, 1H, H_3), 4.69 (d, *J* = 7.9 Hz, 1H,$H_{1\,\beta}$), 4.23 (dd, *J* = 10.5, 4.8 Hz, 1H, H_5), 4.08 (dd, *J* = 18.2, 9.9 Hz, 1H, H_2), 3.82 – 3.74 (m, 4H, Me_{PMB}, H_{6a}), 3.69 (t, *J* = 9.5 Hz, 1H, H_4), 3.53 – 3.39 (m, 1H, H_{6b}), 2.40 – 2.22 (m, 2H, $CH_{2\alpha\ Ammide}$), 2.15 – 2.02 (m, 2H, , $CH_{2\alpha\ Estere}$), 2.02 – 1.93 (m, 8H, 4*CH_2-=), 1.62 – 1.46 (m, 4H, 4*$CH_{2\beta}$), 1.39 – 1.15 (m, 40H, 40*CH_2), 0.94 – 0.77 (m, 15H, ^{t}Bu, 2*Me), 0.07 (s, 3H, Si-Me_a), 0.04 (s, 3H, Si-Me_b). **^{13}C NMR (400 MHz, $CDCl_3$) δ** 174.3, 172.6, 160.0, 130.0, 129.7, 127.4, 113.5, 101.3, 97.3, 78.7, 71.7, 68.6, 66.6, 56.3, 55.2, 36.9, 34.3, 31.9, 29.8, 29.5, 29.4, 29.3, 29.1, 27.2, 25.6, 25.5, 25.0, 22.7, 17.8, 14.1, - 4.1, - 5.2.

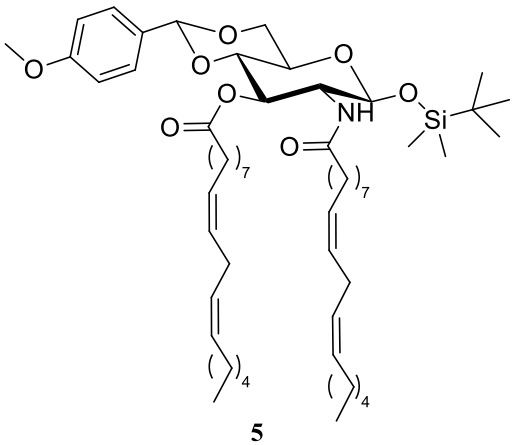

5

5 (9Z,12Z)-(4aR,6S,7R,8R,8aS)-6-((terz-butildimetilsilil)ossi)-2-(4-metossifenil)-7-((9Z,12Z)-ottadeca-9,12-dienammido)esaidropirano[3,2-d][1,3]diossin-8-il ottadeca-9,12-dienoato

^{1}H NMR (400 MHz, $CDCl_3$) δ 7.35 (d, *J* = 8.8 Hz, 2H, 2*CH_{Ar}), 6.86 (d, *J* = 8.8 Hz, 2H, 2*CH_{Ar}), 5.46 (s, 1H, $H_{1\alpha}$), 5.36 (m, *J* = 16.6, 14.2, 8.0 Hz, 9H, 8*CH=, CH_{PMB}), 5.16 (t, *J* = 10.0 Hz, 1H, H_3), 4.73 (d, *J* = 7.9 Hz, 1H, $H_{1\beta}$), 4.27 (dd, *J* = 10.6, 5.1 Hz, 1H, H_5), 4.06 (dd, *J* = 18.3, 9.7 Hz, 1H, H_2), 3.79 (m, 4H, OMe, H_{6a}), 3.70 (t, *J* = 9.4 Hz, 1H, H_4), 3.47 (m, 1H, H_{6b}), 2.76 (d, *J* = 3.8 Hz, 4H, 2*=CH_2=), 2.30 (m, 2H, $CH_{2\alpha\ Ammide}$), 2.05 (m, 10H, 4*CH2-=, $CH_{2\alpha\ Estere)}$, 1.56 (m, 2H, 2*$CH_{2\beta}$), 1.29 (m, 28H, 14*CH_2), 0.88 (m, 16H, ^{t}Bu, 2*Me), 0.10 (s, 3H, Si-Me_a), 0.08 (s, 3H, Si-Me_b). **^{13}C NMR (400 MHz, $CDCl_3$) δ** 174.2, 172.6, 160.1, 130.2, 130.0, 127.9, 127.4, 113.5, 101.3, 97.4, 78.6, 71.4, 68.6, 66.7, 56.4, 55.2, 36.91, 34.3, 31.5, 29.5, 27.2, 25.6, 25.5, 25.0, 22.6, 17.8, 14.1, -4.1, -5.3.

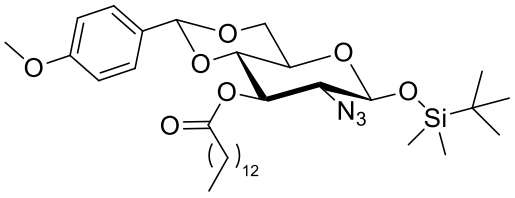

6

6 (2R,4aR,6S,7R,8R,8aS)-6-((tert-butyldimethylsilyl)oxy)-7-dodecanamido-2-(4-methoxyphenyl)hexahydropyrano[3,2-d][1,3]dioxin-8-yl dodecanoate

^{1}H NMR (400 MHz, CDCl3) δ 7.35 (d, *J* = 8.7 Hz, 2H, 2*H_{Ar}), 6.86 (d, *J* = 8.8 Hz, 2H, 2*H_{Ar}), 5.46 (s, 1H, CH_{PMB}), 5.37 (t, *J* = 10.0 Hz, 1H, H_3), 4.72 (d, *J* = 7.8 Hz, 1H, H_1), 4.26 (dd, *J* = 10.6, 5.1 Hz, 1H, H_5), 4.37 (dd, *J* = 17.9, 9.3 Hz, 1H, H_2), 3.83 – 3.76 (m, 4H, OMe_{PMB}, H_{6a}), 3.70 (t, *J* = 9.4 Hz, 1H, H_4), 3.53 – 3.43 (m, 1H, H_{6b}), 2.39 – 2.22 (m, 2H, $CH_{2\ \alpha\ Ammide}$), 2.16 – 2.02 (m, 2H, $CH_{2\ \alpha\ Estere}$), 1.74 – 1.49 (m, 4H, 2*$CH_{2\beta}$), 1.25 (s, 44H, 22*CH_2), 0.96 – 0.78 (m, 15H, ^{t}Bu + 2*CH_3), 0.09 (s, 3H, Si-Me_a), 0.07 (s, 3H, Si-Me_b). **^{13}C NMR (400 MHz, $CDCl_3$) δ** 175.3, 174.4, 159.2, 129.9, 128.7, 113.5, 102.0, 97.7, 78.5, 71.0, 67.9, 64.3, 56.0, 54.6, 37.7, 34.1, 31.2, 29.2–28.5, 25.3, 25.1, 22.8, 18.6, 14.0, -2.9, -3.3.

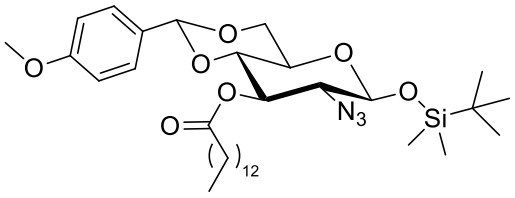

7

7 (4aR,6S,7R,8R,8aS)-7-azido-6-((terz-butildimetilsilil)ossi)-2-(4-metossifenil) esaidropirano[3,2-d][1,3]diossin-8-il tetradecanoato

^{1}H NMR (400 MHz, $CDCl_3$) δ 7.33 (d, *J* = 8.7 Hz, 2H, 2*CH_{Ar}), 6.85 (d, *J* = 8.7 Hz, 2H, 2*CH_{Ar}), 5.43 (s, 1H, CH_{PMP}), 5.12 (t, *J* = 9.9 Hz, 1H, H_3), 4.71 (d, *J* = 7.6 Hz, 1H, $H_{1\square}$), 4.27 (dd, *J* = 10.4, 4.8 Hz, 1H, H_5), 3.82 – 3.72 (m, 4H, OMe+H_{6a}), 3.61 (t, *J* = 9.5 Hz, 1H, H_4), 3.52 – 3.44 (m, 1H, H_{6b}), 3.44 – 3.34 (m, 1H, H_2), 2.36 (t, *J* = 7.4 Hz, 2H, $CH_{2\square}$), 1.70 – 1.54 (m, 4H, $CH_{2\square}$), 1.36 – 1.14 (m, 20H, 10*CH_2), 0.94 (s, 9H,$_{tBu}$), 0.88 (t, *J* = 6.8 Hz, 3H, Me), 0.23 – 0.13 (m, 6H, 2*Me-Si). **^{13}C NMR (400 MHz, $CDCl_3$) δ** 174.4, 159.2, 129.9, 128.7, 113.6, 102.0, 100.3, 78.8, 71.4, 67.9, 64.4, 56.1, 46.5, 34.1, 31.7, 29.1–28.7, 25.8–25.67, 25.3, 22.9, 18.6, 14.0, -2.9, -3.3.

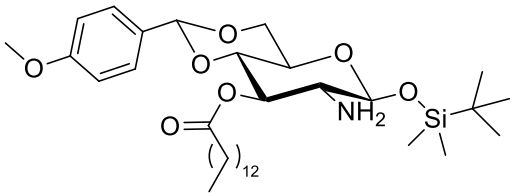

7

8 (4aR,6S,7R,8R,8aS)-7-ammino-6-((terz-butildimetilsilil)ossi)-2-(4-metossifenil) esaidropirano[3,2-d][1,3]diossin-8-il tetradecanoato

^{1}H NMR (400 MHz, $CDCl_3$) δ 7.34 (d, *J* = 8.6 Hz, 2H, 2*CH_{Ar}), 6.84 (d, *J* = 8.6 Hz, 2H, 2*CH_{Ar}), 5.43 (s, 1H,$CH_{\text{-PMP}}$), 5.10 (t, *J* = 9.8 Hz, 1H, H_3), 4.57 (d, *J* = 7.6 Hz, 1H, $H_{1\square}$), 4.25 (dd, *J* = 10.4, 4.8 Hz, 1H, H_5), 3.82 – 3.67 (m, 4H, H_{6a} +OMe), 3.63 (t, *J* = 9.4 Hz, 1H, H_4), 3.49 (td, *J* = 9.7, 5.0 Hz, 1H, H_{6b}), 2.82 (dd, *J* = 9.8, 7.6 Hz, 1H, H_2), 2.35 (t, *J* = 7.4 Hz, 2H, $CH_{2\square}$), 1.67 – 1.53 (m, 2H, $CH_{2\beta}$), 1.48 (s, 2H, NH_2), 1.17 (m, 20H, 10*CH_2), 0.91 (s, 9H, ^{t}Bu), 0.87 (t, *J* = 6.7 Hz, 3H, Me), 0.13 (s, 6H, 2*Si-Me).**^{13}C NMR (400 MHz, $CDCl_3$) δ** 174.4, 159.2, 130.0, 113.6, 102.0, 99.6, 77.6, 71.7, 67.9, 64.4, 58.1, 56.0, 34.1, 31.6, 29.4– 28.8 (m), 25.6–25.5, 25.3, 22.9, 18.6, 14.0, - 2.89, -3.3.

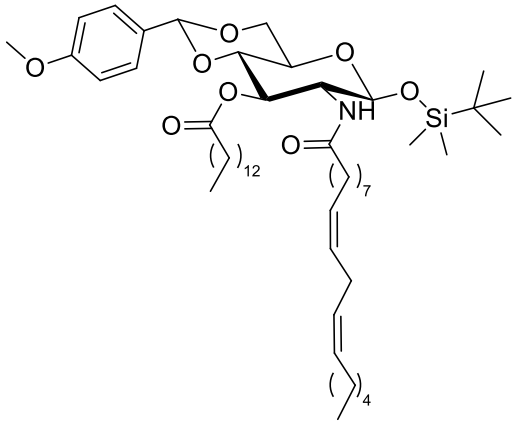

8

9 (4aR,6S,7R,8R,8aS)-6-((terz-butildimetilsilil)ossi)-2-(4-metossifenil)-7-((9Z,12Z)-ottadeca-9,12-dienammido)esaidropirano[3,2-d][1,3]diossin-8-il tetradecanoato

^{1}H NMR (400 MHz, $CDCl_3$) δ 7.35 (d, *J* = 8.7 Hz, 2H, 2*CH_{Ar}), 6.86 (d, *J* = 8.8 Hz, 2H, 2*CH_{Ar}), 5.46 (s, 1H, CH_{PMB}), 5.42 – 5.26 (m, 5H, 4*CH= +$H_{1□}$), 5.19 (t, *J* = 10.0 Hz, 1H, H_3), 4.72 (d, *J* = 7.9 Hz, 1H, $H_{1□}$), 4.26 (dd, *J* = 10.5, 5.0 Hz, 1H, H_5), 4.11 – 4.03 (m, 1H, H_2), 3.80 – 3.66 (m, 5H, OMe+H_{6a}+H_4), 3.44 (dd, *J* = 9.6, 4.9 Hz, 1H, H_{6b}), 2.76 (t, *J* = 6.5 Hz, 2H, =CH_2=), 2.39 – 2.23 (m, 2H, $CH_{2□□Ammide□}$, 2.16 – 1.99 (m, 6H, 2*CH_2= + $CH_{2□□Estere}$), 1.64 – 1.48 (m, 4H, 2*$CH_{2□}$), 1.40 – 1.14 (m, 34H, 17*CH_2), 0.91 – 0.81 (m, 15H, ^{t}Bu+2*Me), 0.08 (s, 3H, Si-Me_a), 0.06 (s, 3H, Si-Me_b).**^{13}C NMR (400 MHz, $cdcl_3$) δ** 175.0, 174.3, 172.6, 160.0, 130.2, 128.0, 113.5, 101.3, 96.4, 78.7, 69.9, 68.6, 66.5, 62.7, 55.6, 55.2, 36.9, 34.3, 31.9, 31.5, 30.4–28.2, 27.2, 25.6, 22.7, 22.6, 17.9, 14.1, - 4.0, -5.2.

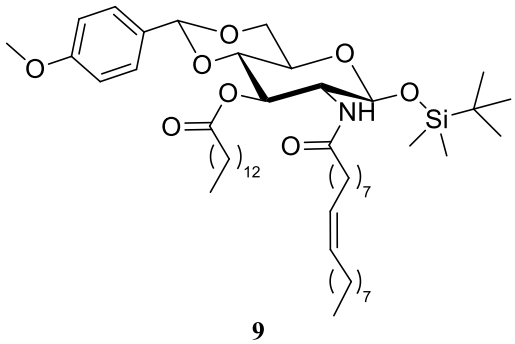

9

10 (4aR,6S,7R,8R,8aS)-6-((terz-butildimetilsilil)ossi)-2-(4-metossifenil)-7-oleammidoesa idropirano[3,2-d][1,3]diossin-8-il tetradecanoato

^{1}H NMR (400 MHz, $CDCl_3$) δ 7.35 (d, *J* = 8.7 Hz, 2H, 2CH_{Ar}), 6.86 (d, *J* = 8.8 Hz, 2H, 2CH_{Ar}), 5.50 – 5.40 (m, 2H, $H_{1□}$, CH_{PMB}), 5.34 (t, *J* = 6.1 Hz, 2H, 2*CH=), 5.17 (t, *J* = 10.1 Hz, 1H,

H_3), 4.73 (d, *J* = 7.9 Hz, 2H,$H_{1'}$), 4.27 (dd, *J* = 10.5, 4.8 Hz, 1H, H_5), 4.06 (dd, *J* = 18.3, 9.6 Hz, 1H, H_2), 3.83 – 3.74 (m, 4H, OMe+H_{6a}), 3.70 (t, *J* = 9.4 Hz, 1H, H_4), 3.55 – 3.41 (m, 1H, H_{6b}), 2.40 – 2.20 (m, 2H, $CH_{2\ Ammide}$), 2.16 – 2.04 (m, 2H, $CH_{2\ Estere}$), 2.00 (d, *J* = 5.9 Hz, 4H, 2*CH_2-=), 1.55 (s, 4H, 2*CH_{2b}), 1.39 – 1.13 (m, 40H, 20*CH_2), 0.95 – 0.83 (m, 15H, ^{t}Bu+2*Me), 0.09 (s, 3H, Me_a-Si), 0.07 (s, 3H, Me_b-Si). **^{13}C NMR (400 MHz, $CDCl_3$) δ** 174.3, 172.6, 160.0, 130.0, 129.7, 127.4, 114.3, 113.5, 101.2, 97.3, 78.7, 71.7, 68.6, 66.6, 56.3, 55.2, 36.9, 34.3, 31.9, 29.4, 27.2, 25.5, 25.0, 22.7, 17.8, 14.1, - 4.0, - 5.2.

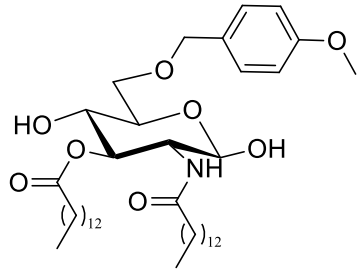

3a

3a (2R,3R,4R,5S,6R)-2,5-diidrossi-6-(((4-metossibenzil)ossi)metil)-3-tetradecanammidotetraidro-2H-piran-4-il tetradecanoato

^{1}H NMR (400 MHz, $CDCl_3$) δ 7.25 (d, *J* = 9.4 Hz, 2H, 2*CH_{Ar}), 6.87 (d, *J* = 8.6 Hz, 2H, 2*CH_{Ar}), 5.89 (d, *J* = 9.1 Hz, 1H, $H_{1'}$), 5.22 – 5.09 (m, 2H, $H_{1'}$ +H_3), 4.50 (m, 2H, $CH_{2\ PMB}$), 4.25 – 4.14 (m, 1H, H_2), 4.03 (m, 1H, H_5), 3.79 (s, 3H, OMe), 3.76 – 3.59 (m, 3H, H_4+ 2*H_6), 2.33 (m, 2H, 2*$CH_{2\ Ammide}$), 2.24 – 2.02 (m, 2H, 2*$CH_{2\ Estere}$), 1.63 – 1.46 (m, 4H, 2*$CH_{2'}$), 1.37 – 1.16 (m, 20H, 10*CH_2), 0.87 (t, *J* = 6.7 Hz, 6H, 2*Me).**^{13}C NMR (400 MHz, $CDCl_3$) δ** 175.1, 173.3, 159.5, 129.5, 113.7, 91.9, 73.2, 70.4, 69.9, 69.4, 55.3, 36.9, 34.3, 31.9, 30.4-28.4, 25.6, 23.8, 24.7, 22.8, 14.1.

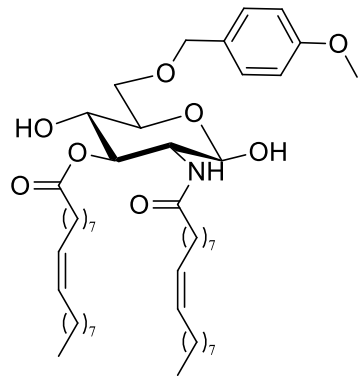

4a

4a (2R,3R,4R,5S,6R)-2,5-diidrossi-6-(((4-metossibenzil)ossi)metil)-3-oleammidotetraidro-2H-piran-4-il oleato

^{1}H NMR (400 MHz, $CDCl_3$) δ 7.26 (s, 2H, 2*CH_{Ar}), 6.88 (d, *J* = 8.6 Hz, 2H, 2*CH_{Ar}), 5.77 (d, *J* = 9.4 Hz, 1H, H_1), 5.34 (s, 4H, 4*CH=), 5.19 – 5.10 (m, 1H, H_3), 4.52 (q, *J* = 11.6 Hz, 2H, $CH_{2\ PMB}$), 4.29 – 4.15 (m, 1H, H_2), 4.10 – 3.97 (m, 1H, H_5), 3.80 (s, 3H, Me_{PMB}), 3.74 – 3.63 (m, *J* = 8.1 Hz, 3H, H_4+2*H_6), 2.33 (dd, *J* = 13.8, 7.4 Hz, 2H, $CH_{2\ Ammide}$), 2.12 (dd, *J* = 12.9, 7.5 Hz, 2H, $CH_{2\ Estere}$), 2.00 (d, *J* = 5.9 Hz, 8H, 4*CH_2-CH=), 1.57 (s, 8H, 2*$CH_{2\beta}$), 1.26 (s, 45H, 20*CH_2), 0.88 (t, *J* = 6.8 Hz, 6H, 2*Me). **^{13}C NMR (400 MHz, $CDCl_3$) δ** 175.1, 173.1, 159.3, 130.0, 129.7, 129.5, 113.8, 91.8, 73.4, 73.2, 70.5, 70.0, 69.8, 55.3, 51.7, 36.7, 34.3, 31.9, 30.3-28.1, 27.2, 25.6, 24.9, 22.7, 14.1.

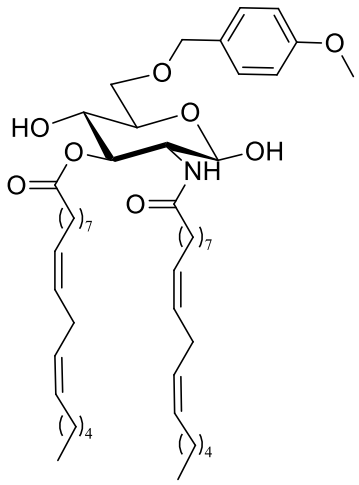

5a

5a (9Z,12Z)-(2R,3R,4R,5S,6R)-2,5-diidrossi-6-(((4-metossibenzil)ossi)metil)-3-((9Z,12Z)-ottadeca-9,12-dienammido)tetraidro-2H-piran-4-il ottadeca-9,12-dienoato

^{1}H NMR (400 MHz, $CDCl_3$) δ 7.29 – 7.19 (m, 2H, 2*CH_{Ar}), 6.88 (d, *J* = 8.6 Hz, 2H, 2*CH_{Ar}), 5.76 (d, *J* = 9.7 Hz, 1H, $H_{1\beta}$), 5.44 – 5.25 (m, 8H, 8*CH=), 5.23 (s, 1H, $H_{1\alpha}$), 5.20 – 5.09 (m, 1H, H_3), 4.59 – 4.43 (m, 2H, $CH_{2\ PMB}$), 4.22 (td, *J* = 11.0, 3.7 Hz, 1H, H_2), 4.06 – 4.01 (m, 1H, H_5), 3.80 (s, 3H, OMe), 3.69 (d, *J* = 4.8 Hz, 3H, 2*H_6+H_4), 2.76 (t, *J* = 6.2 Hz, 4H, 2*=CH_2=), 2.40 – 2.28 (m, 2H, $CH_{2\ Ammide}$), 2.16 – 2.08 (m, 2H, $CH_{2\ Estere}$), 2.07 – 1.95 (m, 8H, 4*CH_2-=), 1.73 – 1.48 (m, 4H, 2*$CH_{2\beta}$), 1.40 – 1.18 (m, 28H, 14*CH_2), 0.88 (t, *J* = 6.8 Hz, 6H, 2*Me). **^{13}C NMR (400 MHz, CD_3OD) δ** 171.1, 169.1, 155.4, 126.3, 126.0, 125.6, 125.5, 124.1, 123.9, 109.9, 87.8, 69.4, 66.5, 66.0, 65.9, 64.9, 51.3, 47.8, 32.8, 30.4, 27.6, 26.2–24.7, 23.2, 21.7, 18.6, 17.1, 10.2.

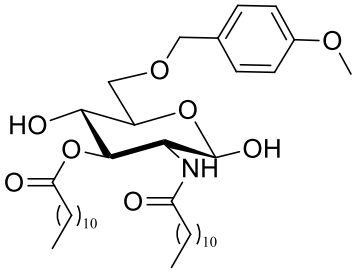

6a

6a (2R,3R,4R,5S,6R)-3-dodecanamido-2,5-dihydroxy-6-(((4-methoxybenzyl)oxy)methyl)tetrahydro-2H-pyran-4-yl dodecanoate

^{1}H NMR (400 MHz, $CDCl_3$) δ 7.35 (d, *J* = 8.7 Hz, 2H, 2*H_{Ar}), 6.86 (d, *J* = 8.8 Hz, 2H, 2*H_{Ar}), 5.46 (s, 1H, CH_{PMB}), 5.17 (t, *J* = 10.0 Hz, 1H, H_3), 4.72 (d, *J* = 7.8 Hz, 1H, H_1), 4.26 (dd, *J* = 10.6, 5.1 Hz, 1H, H_5), 4.07 (dd, *J* = 17.9, 9.3 Hz, 1H, H_2), 3.83 – 3.76 (m, 4H, OMe_{PMB}, H_{6a}), 3.70 (t, *J* = 9.4 Hz, 1H, H_4), 3.53 – 3.43 (m, 1H, H_{6b}), 2.39 – 2.22 (m, 2H, $CH_{2\ \alpha\ Ammide}$), 2.16 – 2.02 (m, 2H, $CH_{2\ \alpha\ Estere}$), 1.74 – 1.49 (m, 4H, 2*$CH_{2\beta}$), 1.25 (s, 44H, 22*CH_2). **^{13}C NMR (400 MHz, $CDCl_3$) δ** 175.1, 173.3, 159.5, 129.5, 113.7, 91.9, 73.2, 70.4, 69.9, 69.4, 55.3, 36.9, 34.3, 31.9, 30.4-28.4, 25.6, 23.8, 24.7, 22.8, 14.1.

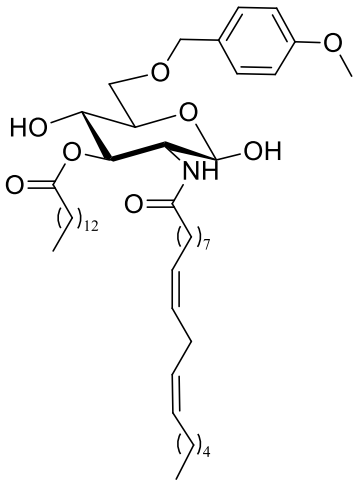

8a

8a (2R,3R,4R,5S,6R)-2,5-diidrossi-6-(((4-metossibenzil)ossi)metil)-3-((9Z,12Z)-ottadeca-9,12-dienammido)tetraidro-2H-piran-4-il tetradecanoato

^{1}H NMR (400 MHz, $CDCl_3$) δ 7.27 (d, *J* = 8.6 Hz, 2H, 2*CH_{Ar}), 6.88 (d, *J* = 8.6 Hz, 2H, 2*CH_{Ar}), 5.94 (d, *J* = 9.2 Hz, 1H, $H_{1\square}$, 5.43 – 5.26 (m, 4H, 4*CH=), 5.21 (d, *J* = 2.3 Hz, 1H, $H_{1\square}$), 5.17 – 5.10 (m, 1H, H_3), 4.58 – 4.43 (m, 2H, $CH_{2\ PMB}$), 4.23 – 4.12 (m, 1H, H_2), 4.10 – 4.01 (m, 1H, H_5), 3.80 (s, 3H, OMe), 3.75 – 3.66 (m, 3H, H_4+2*H_6), 2.76 (t, *J* = 5.9 Hz, 2H, =CH_2=), 2.43 – 2.30 (m, 2H, $CH_{2\square\ Ammide}$), 2.16 – 2.07 (m, 2H, $CH_{2\square\ Estere}$), 2.08 – 1.98 (m, 4H,

2*CH_2-=), 1.69 – 1.49 (m, 4H, 2*CH_2□), 1.44 – 1.19 (m, 34H, 17*CH_2), 0.94 – 0.82 (m, 6H, 2*Me). **^{13}C NMR (400 MHz, $CDCl_3$) δ** 175.2, 173.5, 159.8, 130.1, 129.7, 128.0, 127.9, 113.9, 91.7, 74.7, 73.4, 70.0, 68.0, 59.9, 55.3, 51.8, 40.8, 36.7, 34.3, 29.9, 27.2, 25.6, 24.9, 22.6, 14.1.

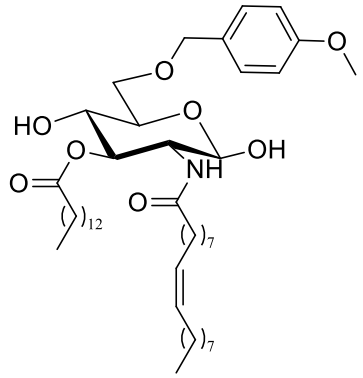

9a

9a (2R,3R,4R,5S,6R)-2,5-diidrossi-6-(((4-metossibenzil)ossi)metil)-3-oleammidotetraidro-2H-piran-4-il tetradecanoato

^{1}H NMR (400 MHz, $CDCl_3$) δ 7.29 – 7.21 (m, 2H, 2*CH_{Ar}), 6.88 (d, *J* = 8.5 Hz, 2H, 2*CH_{Ar}), 5.91 (d, *J* = 9.3 Hz, 1H, H_1□), 5.41 – 5.28 (m, 2H, 2*CH=), 5.20 (s, 1H, H_1□), 5.19 – 5.09 (m, 1H, H_3), 4.51 (q, *J* = 11.5 Hz, 2H, $CH_{2\ PMB}$), 4.23 – 4.13 (m, 1H, H_2), 4.07 – 3.98 (m, 1H, H_5), 3.80 (s, 3H, OMe), 3.74 – 3.64 (m, 3H, 2*H_6+H_4), 2.42 – 2.27 (m, 2H, CH_2□ $_{Ammide}$), 2.20 – 2.06 (m, 2H, CH_2□ $_{Estere}$), 2.06 – 1.91 (m, 4H, 2*CH_2-=), 1.64 – 1.48 (m, 4H, 2*CH_2□), 1.39 – 1.17 (m, 40H, 20*CH_2), 0.87 (t, *J* = 6.7 Hz, 6H, 2*Me). **^{13}C NMR (400 MHz, CD_3OD) δ** 175.3, 173.2, 163.3, 130.3, 130.2, 129.8, 129.8, 129.6, 114.0, 92.1, 73.5, 72.1, 70.7, 70.2, 69.2, 55.4, 51.8, 36.9, 34.5, 32.1, 30.5–28.5, 27.4, 27.3, 25.8, 25.1, 22.8, 14.3.

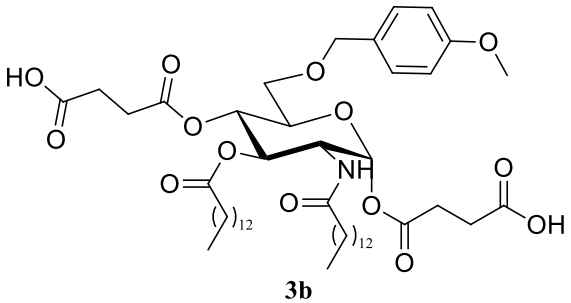

3b

3b acido 4,4'-(((2S,3R,4R,5S,6R)-6-(((4-metossibenzil)ossi)metil)-3-tetradecanammido-4-(tetradecanoilossi)tetraidro-2H-piran-2,5-diil)bis(ossi))bis(4-ossobutanoico)

^{1}H NMR (400 MHz, CD_3OD) δ 7.25 (d, *J* = 8.4 Hz, 2H, 2*$CH_{a\ Ar}$), 6.88 (d, *J* = 8.4 Hz, 2H, 2*$CH_{b\ Ar}$), 6.11 (d, *J* = 3.4 Hz, 1H, H_1), 5.35 – 5.26 (m, 1H, H_3), 5.22 (t, *J* = 9.7 Hz, 1H, H_4), 4.46 – 4.33 (m, 3H, H2, $CH_{2\ PMB}$), 4.08 – 4.00 (m, 1H, H_5), 3.78 (s, 3H, OMe), 3.67 – 3.50 (m,

2H, 2*H_6), 2.78 – 2.41 (m, 8H, 4*CH_2-COO), 2.37 – 2.21 (m, 4H, 2*$CH_{2\alpha}$), 1.62 – 1.48 (m, 4H,2*$CH_{2\beta}$), 1.39 – 1.21 (m, 40H, 20*CH_2), 0.97 – 0.82 (m, 6H, 2*Me). **^{13}C NMR (400 MHz, CD_3OD) δ** 174.9, 174.5, 173.1, 171.0, 170.9, 147.4, 129.4, 129.3, 113.0, 90.3, 74.2, 72.5, 70.6, 70.0, 60.8, 54.0, 50.5, 33.3, 31.4, 30.3–27.0, 24.3, 22.1, 12.8.

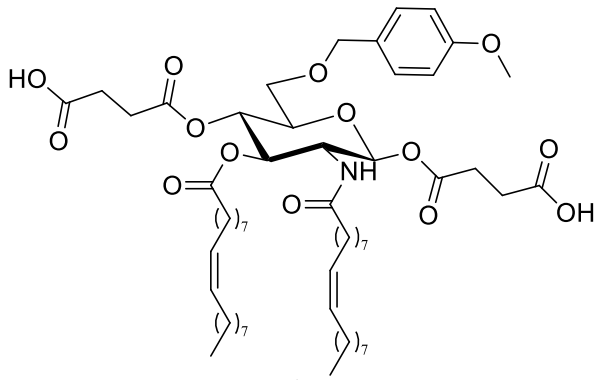

4b

4b acido 4,4'-(((2S,3R,4R,5S,6R)-6-(((4-metossibenzil)ossi)metil)-3-oleammido-4-(oleoilossi) tetraidro-2H-piran-2,5-diil)bis(ossi))bis(4-ossobutanoico)

^{1}H NMR (400 MHz, $CDCl_3$) δ 7.24 (d, *J* = 8.6 Hz, 2H, 2*CH_{Ar}), 6.86 (d, *J* = 8.6 Hz, 2H, 2*CH_{Ar}), 6.21 (d, *J* = 3.3 Hz, 1H, $H_{1\alpha}$), 5.87 (d, *J* = 8.3 Hz, 1H, $H_{1\beta}$), 5.47 – 5.29 (m, 4H, 4*CH=), 5.26 (t, *J* = 10.0 Hz, 1H, H_4), 5.20 – 5.09 (m, 1H, H_3), 4.54 – 4.33 (m, 3H, CH_{2PMB}, H_2), 3.88 (d, *J* = 9.2 Hz, 1H, H_5), 3.79 (s, 3H, OMe), 3.58 – 3.42 (m, 2H, 2*H_6), 2.90 – 2.36 (m, 8H, 4*CH_2-COO), 2.26 (t, *J* = 7.5 Hz, 2H, $CH_{2\ Ammide}$), 2.08 (dd, *J* = 13.2, 7.0 Hz, 2H, $CH_{2\ Estere}$), 2.00 (d, *J* = 5.3 Hz, 8H, 4*CH_2-=), 1.53 (s, 4H, 2*$CH_{2\beta}$), 1.26 (s, 40H, 20*CH_2), 0.87 (t, *J* = 6.6 Hz, 6H, 2*Me). **^{13}C NMR (400 MHz, $CDCl_3$) δ** 172.1, 169.7, 168.1, 164.3, 163.9, 154.0, 124.9, 124.8, 124.6, 124.5, 124.4, 124.4, 108.5, 86.1, 69.8, 68.0, 66.0, 63.3, 62.5, 50.1, 45.8, 31.2-29.0, 26.7, 24.0, 22.0, 20.3, 19.6, 17.5, 9.0.

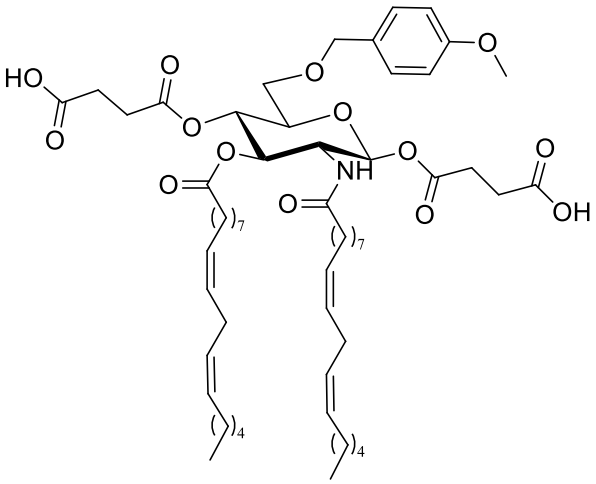

5b

5b acido 4,4'-(((2S,3R,4R,5S,6R)-6-(((4-metossibenzil)ossi)metil)-3-((9Z,12Z)-ottadeca-9,12-dienammido)-4-((9Z,12Z)-ottadeca-9,12-dienoilossi)tetraidro-2H-piran-2,5-diil)bis(ossi))bis(4-ossobutanoico)

^{1}H NMR (400 MHz, $CDCl_3$) δ 7.28 – 7.19 (m, 2H, 2*CH_{Ar}), 6.86 (d, *J* = 8.6 Hz, 2H, 2*CH_{Ar}), 6.21 (d, *J* = 3.4 Hz, 1H, H_{1a}), 5.45 – 5.28 (m, 8H, 8*CH=), 5.25 (t, *J* = 8.6 Hz, 1H, H_4), 5.14 (t, *J* = 10.6 Hz, 1H, H_3), 4.53 – 4.34 (m, 3H, H_2+ $CH_{2\ PMB}$), 3.93 – 3.82 (m, 1H, H_5), 3.80 (s, 3H,OMe), 3.58 – 3.42 (m, 2H, 2*H_6), 2.87 – 2.72 (m, 4H, 2*=CH_2=), 2.72 – 2.52 (m, 8H, 4*CH_2-COO), 2.44 – 2.38 (m, 2H, $CH_{2\ Ammide}$), 2.28 (t, *J* = 7.7 Hz, 2H, $CH_{2\ Estere}$), 2.13 – 1.97 (m, 8H, 4*CH_2=), 1.64 – 1.46 (m, 4H, 2*$CH_{2\ b}$), 1.42 – 1.17 (m, 28H, 14*CH_2), 0.88 (t, *J* = 6.8 Hz, 6H, 2*Me).**^{13}C NMR (101 MHz, $cdcl_3$) δ** 173.7, 173.0, 169.4, 168.7, 130.3, 129.7, 128.1, 127.8, 113.9, 90.9, 73.1, 70.9, 67.6, 65.8, 55.3, 53.8, 31.5, 30.7–28.1, 27.2, 25.6, 24.7, 22.6, 14.1.

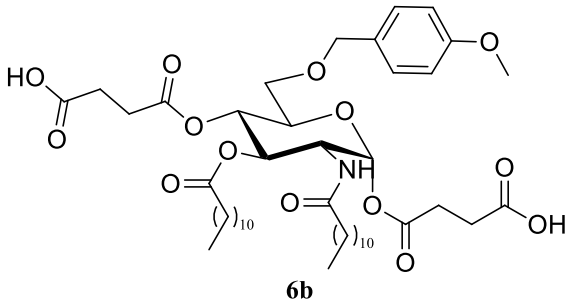

6b

6b 4,4'-(((2S,3R,4R,5S,6R)-3-dodecanamido-4-(dodecanoyloxy)-6-(((4-methoxybenzyl)oxy)methyl)tetrahydro-2H-pyran-2,5-diyl)bis(oxy))bis(4-oxobutanoic acid)

^{1}H NMR (400 MHz, $CDCl_3$) δ 7.26 (s, 2H, 2*CH_{Ar}), 6.88 (d, *J* = 8.6 Hz, 2H, 2*CH_{Ar}), 5.77 (d, *J* = 9.4 Hz, 1H, H_1), 5.19 – 5.10 (m, 1H, H_3), 4.52 (q, *J* = 11.6 Hz, 2H, $CH_{2\ PMB}$), 4.29 – 4.15 (m, 1H, H_2), 4.10 – 3.97 (m, 1H, H_5), 3.80 (s, 3H, Me_{PMB}), 3.74 – 3.63 (m, *J* = 8.1 Hz, 3H,

H_4+2*H_6), 2.33 (dd, *J* = 13.8, 7.4 Hz, 2H, $CH_{2\ \alpha\ Ammide}$), 2.12 (dd, *J* = 12.9, 7.5 Hz, 2H, $CH_{2\ \alpha\ Estere}$), 1.57 (s, 8H, 2*$CH_{2\ \beta}$), 1.26 (s, 45H, 20*CH_2), 0.88 (t, *J* = 6.8 Hz, 6H, 2*Me). **^{13}C NMR (400 MHz, CD_3OD) δ** 174.9, 174.5, 173.1, 171.0, 170.9, 147.4, 129.4, 129.3, 113.0, 90.3, 74.2, 72.5, 70.6, 70.0, 60.8, 54.0, 50.5, 33.3, 31.4, 30.3–27.0, 24.3, 22.1, 12.8.

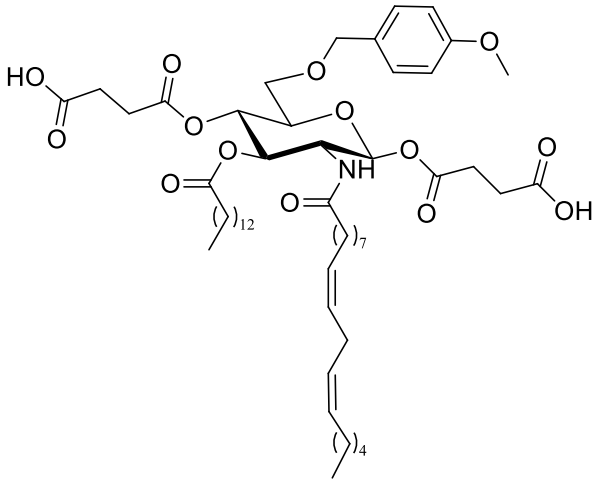

8b

8b acido 4,4'-(((2S,3R,4R,5S,6R)-6-(((4-metossibenzil)ossi)metil)-3-((9Z,12Z)-ottadeca-9,12-dienammido)-4-(tetradecanoilossi)tetraidro-2H-piran-2,5-diil)bis(ossi))bis(4-ossobutanoico) **^{1}H NMR (400 MHz, $CDCl_3$) δ** 7.23 (d, *J* = 8.9 Hz, 2H, 2*CH_{Ar}), 6.85 (d, *J* = 8.3 Hz, 2H, 2*CH_{Ar}), 6.21 (d, *J* = 2.8 Hz, 1H, H_1), 5.45 – 5.33 (m, 4H, 4*CH=), 5.19 -5.14 (m, 2H, H_4 + H_3), 4.53 – 4.35 (m, 2H, $CH_{2\ PMB}$), 4.30 – 4.21 (m, 1H, H_2), 4.00 - 3.98 (m, 1H, H_5), 3.79 (s, 3H, OMe), 3.57 – 3.41 (m, 2H, 2*H_6), 2.81 – 2.42 (m, 10H, 4*CH_2-COO + =CH_2=), 2.40 – 2.14 (m, 4H, 2*CH_2□), 2.09 - 2.00 (m, 4H, 2*CH_2=), 1.57 -1.50 (m, 4H, 2*CH_2□), 1.34 - 1.32 (m, 34H, 17*CH_2), 1.07 – 0.75 (m, 3H, 2*Me). **^{13}C NMR (400 MHz, $CDCl_3$) δ** 175.7, 175.3, 174.5, 173.0, 171.8, 159.1, 132.5, 130.2, 129.1, 128.5, 113.4, 91.4, 73.6, 71.5, 70.7, 69.2, 56.0, 54.4, 37.8, 34.1, 31.2, 30.1, 29.3-27.9, 25.3, 25.1, 23.0, 14.1.

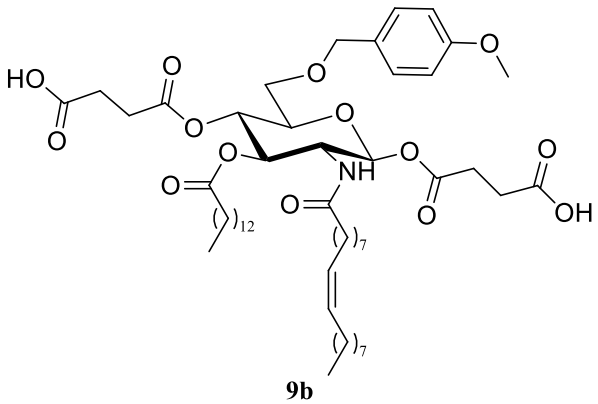

9b

9b acido 4,4'-(((2S,3R,4R,5S,6R)-6-(((4-metossibenzil)ossi)metil)-3-oleammido-4-(tetradecanoilossi) tetraidro-2H-piran-2,5-diil)bis(ossi))bis(4-ossobutanoico)

^{1}H NMR (400 MHz, $CDCl_3$) δ 7.23 (d, *J* = 8.6 Hz, 2H, 2*CH_{Ar}), 6.86 (d, *J* = 8.7 Hz, 2H, 2*CH_{Ar}), 6.22 (d, *J* = 2.9 Hz, 1H, $H_{1b)}$, 5.43 – 5.28 (m, 2H, 2*CH=), 5.23 (t, *J* = 9.1 Hz, 1H, H_4), 5.16 (t, *J* = 9.9 Hz, 1H, H_3), 4.55 – 4.34 (m, 2H, $CH_{2\ PMB}$), 4.21 – 4.11 (m, 1H, H_2), 3.94 – 3.87 (m, 1H, H_5), 3.80 (s, 3H, OMe), 3.58 – 3.43 (m, 2H, 2*H_6), 2.75 – 2.56 (m, 8H, 4*CH_2-COO), 2.26 (t, *J* = 7.7 Hz, 2H, $CH_{2a\ Ammide}$), 2.08 (t, *J* = 7.3 Hz, 2H, , $CH_{2a\ Estere}$), 2.03 – 1.90 (m, 4H, 2*CH_2-=), 1.60 – 1.46 (m, 4H, , CH_{2b}), 1.41 – 1.14 (m, 40H, 20*CH_2), 0.87 (t, *J* = 6.4 Hz, 6H, 2*Me).

^{13}C NMR (400 MHz, $CDCl_3$) δ 177.8, 176.6, 173.3, 172.6, 168.9, 159.3, 130.0, 129.6, 113.7, 91.2, 73.2, 71.2, 68.7, 67.8, 55.3, 51.9, 36.3, 34.3, 31.9, 29.9-28.4, 27.2, 25.4, 24.7, 22.8, 14.0.

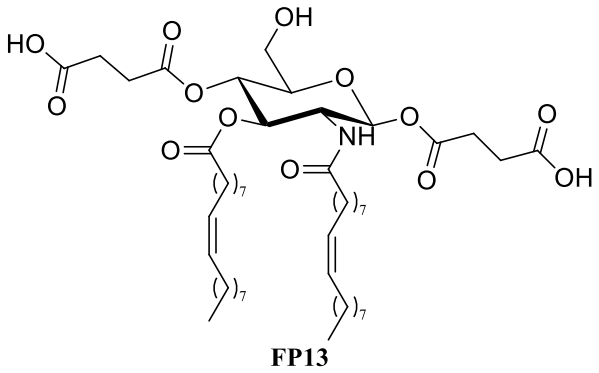

FP13

FP13 acido 4,4'-(((2S,3R,4R,5S,6R)-6-(idrossimetil)-3-oleammido-4-(oleoilossi)tetraidro-2H-piran-2,5-diil)bis(ossi))bis(4-ossobutanoico)

^{1}H NMR (400 MHz, CD_3OD) δ 6.15 (d, *J* = 3.2 Hz, 1H, H_1), 5.41 – 5.28 (m, 5H, 4*CH=, H_3), 5.16 (t, *J* = 9.9 Hz, 1H, H_4), 4.41 (dd, *J* = 10.5, 3.4 Hz, 1H, H_2), 3.96 (ddd, *J* = 7.5, 4.7, 2.3 Hz, 1H, H_5), 3.69 – 3.52 (m, 2H, 2*H_6), 2.80 – 2.48 (m, 8H, 4*CH_2-COO), 2.40 – 2.21 (m, 2H, $CH_{2\ Ammide}$), 2.17 (t, *J* = 5.1 Hz, 2H, $CH_{2\ Estere}$), 2.11 – 1.95 (m, 4H, 4*CH_2-=), 1.69 – 1.47 (m, 4H, 2*$CH_{2\ \beta}$), 1.46 – 1.16 (m, 40H,20*CH_2), 1.01 – 0.77 (m, 6H, 2*Me). **^{13}C NMR (400 MHz, CD_3OD) δ** 175.1, 174.8, 173.3, 171.4, 171.2, 129.4, 90.5, 72.2, 70.2, 68.5, 60.0, 50.6, 35.4, 33.6, 31.7-29.0, 26.8, 25.6, 24.5, 22.3, 13.1. **MS (ESI^-) m/z** calcolato (M-H) $C_{50}H_{84}NO_{13}^-$ = 906,59, trovato = 906.60.

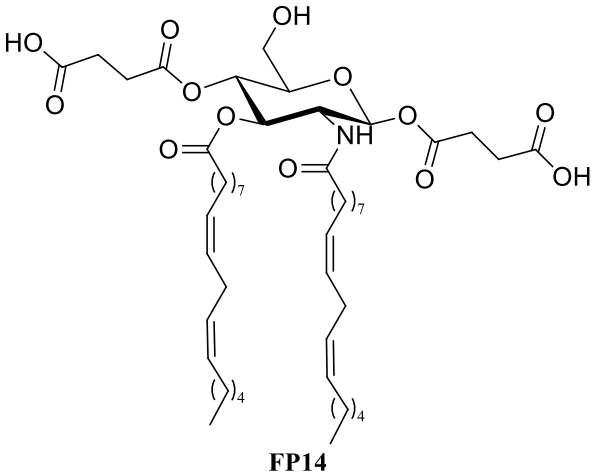

FP14

FP14 acido 4,4'-(((2S,3R,4R,5S,6R)-6-(idrossimetil)-3-((9Z,12Z)-ottadeca-9,12-dienammido)-4-((9Z,12Z)-ottadeca-9,12-dienoilossi)tetraidro-2H-piran-2,5-diil)bis(ossi))bis(4-ossobutanoico)

^{1}H NMR (400 MHz, $CDCl_3$) δ 6.19 (d, *J* = 2.8 Hz, 1H, $H_{1\alpha}$), 5.90 (d, *J* = 7.8 Hz, 1H, $H_{1\beta}$), 5.44 – 5.28 (m, 8H, 8*CH=), 5.28 – 5.21 (m, 1H, H_3), 5.21 – 5.12 (m, 1H, H_4), 4.44 (t, *J* = 9.0 Hz, 1H, H_2), 3.87 – 3.75 (m, 1H, H_5), 3.70 (s, 1H, H_{6a}), 3.60 (s, 1H, H_{6b}), 2.76 (t, *J* = 6.0 Hz, 4H, 2*=CH_2=), 2.72 – 2.53 (m, 8H, 2*CH_2-COOH), 2.40 – 2.24 (m, 4H, 2*$CH_{2\alpha}$), 2.10 – 1.99 (m, 8H,4*CH_2-COOH), 1.61 – 1.45 (m, 4H, 2*CH_2), 1.45 – 1.11 (m, 28H, 14*CH_2), 0.96 – 0.78 (m, 6H, 2*Me). **^{13}C NMR (400 MHz, $CDCl_3$) δ** 176.8, 176.4, 174.8, 173.5, 170.7, 169.7, 130.2, 127.8, 91.2, 72.2, 70.2, 68.0, 60.9, 51.1, 36.4, 34.1, 31.8, 31.5-27.2, 25.5, 24.9, 22.6, 14.1. **MS (ESI^-) m/z** calcolato (M-H) $C_{50}H_{80}NO_{13}^-$ = 902,56, trovato = 902.60

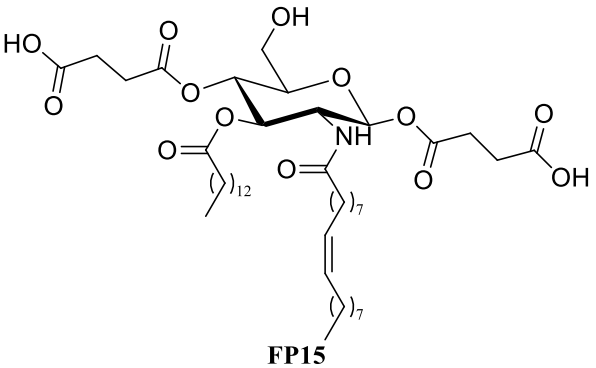

FP15

FP15 acido 4,4'-(((2S,3R,4R,5S,6R)-6-(idrossimetil)-3-oleammido-4-(tetradecanoilossi)tetraidro-2H-piran-2,5-diil)bis(ossi))bis(4-ossobutanoico)

^{1}H NMR (400 MHz, $CDCl_3$) δ 6.20 (d, *J* = 3.3 Hz, 1H, $H_{1\ \alpha}$), 5.90 (d, *J* = 8.7 Hz, 1H, $H_{1\ \beta}$), 5.40 – 5.27 (m, 2H, 2*CH=), 5.28 – 5.12 (m, 2H, H_3+H_4), 4.42 (t, *J* = 8.4 Hz, 1H, H_2), 3.82 – 3.75 (m, 1H, H_5), 3.74 – 3.53 (m, 2H, 2*H_6), 2.85 – 2.54 (m, 8H, 4*CH_2-COOH), 2.29 (t, *J* =

7.6 Hz, 2H, $CH_{2\,Ammide}$), 2.15 – 2.05 (m, 2H, $CH_{2\,Estere}$), 2.05 – 1.94 (m, 4H, 2*CH_2-=), 1.61 – 1.47 (m, 4H, 2*$CH_{2\beta}$), 1.29 (d, *J* = 28.5 Hz, 40H, 20*CH_2), 0.88 (t, *J* = 6.8 Hz, 6H, 2*Me). **^{13}C NMR (400 MHz, $CDCl_3$) δ** 176.4, 176.1, 174.8, 174.0, 171.2, 170.3, 130.0, 129.6, 91.1, 72.2, 70.2, 68.2, 60.8, 51.1, 36.3, 34.1, 29.4-27.2, 27.2, 24.9, 14.1. **MS (ESI$^-$) m/z** calcolato (M-H) $C_{46}H_{78}NO_{13}^-$ =852,55, trovato = 852,50

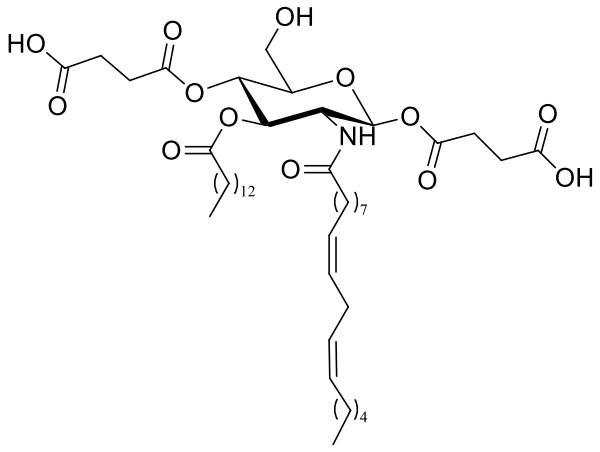

FP16

FP16 acido 4,4'-(((2S,3R,4R,5S,6R)-6-(idrossimetil)-3-((9Z,12Z)-ottadeca-9,12-dienammido)-4-(tetradecanoilossi)tetraidro-2H-piran-2,5-diil)bis(ossi))bis(4-ossobutanoico) **^{1}H NMR (400 MHz, $CDCl_3$) δ** 6.19 (s, 1H, $H_{1\alpha}$), 5.91 (d, *J* = 6.8 Hz, 1H, $H_{1\beta}$), 5.43 – 5.30 (m, 4H, 4*CH=), 5.27 (dd, *J* = 23.7, 9.8 Hz, 1H, H_3), 5.21 – 5.11 (m, 1H, H_4), 4.50 – 4.37 (m, 1H, H_2), 3.82 (dd, *J* = 9.5, 3.2 Hz, 1H, H_5), 3.77 – 3.53 (m, 2H, H_{6a}+H_{6b}), 2.83 – 2.73 (m, 2H, 4*=CH_2=), 2.73 – 2.49 (m, 8H, 2*CH_2-COOH), 2.39 – 2.23 (m, 4H, 2*$CH_{2\alpha}$), 2.10 – 1.98 (m, 4H,2*CH_2-=), 1.53 (dd, *J* = 5.4, 2.9 Hz, 4H, 2*$CH_{2\beta}$), 1.43 – 1.09 (m, 34H, 17*CH_2), 0.86 (m, 6H, 2*Me). **^{13}C NMR (400 MHz, $CDCl_3$) δ** 176.6, 176.3, 174.8, 173.4, 171.6, 170.7, 130.2, 127.8, 91.2, 72.2, 70.1, 68.1, 60.8, 51.2, 36.4, 34.0, 31.9, 31.5, 30.8–27.9, 27.1, 25.6, 24.9, 22.7, 14.1. **MS (ESI$^-$) m/z** calcolato (M-H) $C_{46}H_{76}NO_{13}^-$ = 850,53, trovato = 850.50

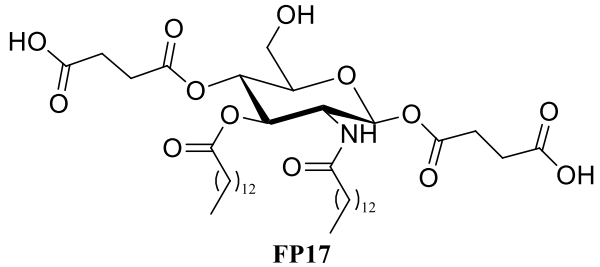

FP17

FP17 acido 4,4'-(((2S,3R,4R,5S,6R)-6-(idrossimetil)-3-tetradecanammido-4-(tetradecanoilossi)tetraidro-2H-piran-2,5-diil)bis(ossi))bis(4-ossobutanoico)

^{1}H NMR (400 MHz, $CDCl_3$) δ 6.19 (s, 1H, $H1_a$), 5.94 (d, *J* = 7.4 Hz, 1H, $H1_b$), 5.32 – 5.20 (m, 1H, H_3), 5.20 – 5.07 (m, 1H, H_4), 4.51 – 4.37 (m, 1H, H_2), 3.89 – 3.75 (m, 1H, H_5), 3.75 – 3.52 (m, 2H, 2*H_6), 2.85 – 2.48 (m, 8H, 4*CH_2-COO), 2.39 – 2.22 (m, 2H, $CH_{2\ Ammide}$), 2.16 – 1.96 (m, 2H, $CH_{2\ Estere}$), 1.64 – 1.45 (m, 4H, 2*CH_{2b}), 1.44 – 1.00 (m, 40H, 20*CH_2), 0.99 – 0.80 (m, 6H, 2*Me). **^{13}C NMR (400 MHz, CD_3OD) δ** 176.3, 175.0, 173.7, 171.0, 170.0, 91.3, 72.3, 70.3, 68.3, 61.0, 55.0, 34.3, 32.0-29.4, 25.6, 25.0, 22.8, 14.3. **MS (ESI$^-$) m/z** calcolato (M-H) $C_{42}H_{72}NO_{13}^-$= 798,50, trovato = 798.50

FP18 4,4'-(((2S,3R,4R,5S,6R)-3-dodecanamido-4-(dodecanoyloxy)-6-

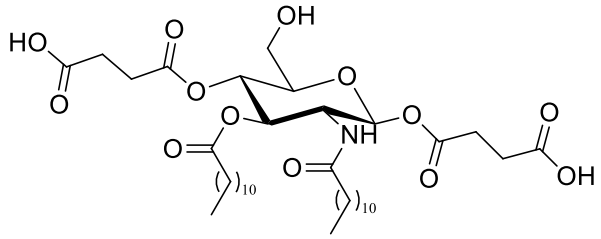

FP18

(hydroxymethyl)tetrahydro-2H-pyran-2,5-diyl)bis(oxy))bis(4-oxobutanoic acid)

^{1}H NMR (400 MHz, $CDCl_3$) δ (ppm): 175.13 (C_{Amide}), 173.15 (C_{Ester}), 159.35 ($C_{Ar\ OMe}$) 130.01 (C_{Ar}), 129.68 ($CH_{2\ Ar}$),113.83 ($CH_{2\ Ar}$), 91.84 (H_1), 73.36 ($CH_{2\ PMB}$), 73.25 (C_5), 70.49 (C_3), 70.01 (C_4), 69.85 (C_6), 55.27 (MeO_{PMB}), 51.72 (C_2), 36.71 ($C_{\alpha\ Amide}$), 34.31 ($C_{\alpha\ Ester}$), 31.91 (2*$CH_{2\ \omega-2}$), 30.33 - 28.11 (18*CH_2), 25.62 ($C_{\beta\ Ester}$), 24.93 ($C_{\beta\ Amide}$), 22.69 (2*$CH_{2\ \omega-1}$), 14.15 (2*Me). **^{13}C NMR (400 MHz, CD_3OD) δ** 176.3, 175.0, 173.7, 171.0, 170.0, 91.3, 72.3, 70.3, 68.3, 61.0, 55.0, 34.3, 32.0-29.4, 25.6, 25.0, 22.8, 14.3. **MS (ESI$^-$) m/z** calcolato (M-H) $C_{38}H_{65}NO_{13}^-$= 743.45, trovato = 743.50.

9. Biologia

1.1) Preparazione della soluzione stock dei composti

Al fine di ottenere una soluzione stock a concentrazione 10 mM dei composti, è stato risospeso un milligrammo di ciascun compost nel solvente indicato nella tabella sotto.

:

Composto	**P.M. (g/mol)**	**Solventr**
FP7	847.77	H_2O:DMSO 1:1
FP13	908.21	Etanolo:DMSO 1:1
FP14	904.18	Etanolo:DMSO 1:1

FP15	854.12	Etanolo:DMSO 1:1
FP16	852.1	Etanolo:DMSO 1:1

I composti sono stati agitati fino a quando completamente disciolti in soluzione.

1.2) Saggio con cellule HEK-Blue hTLR4

Cellule HEK-Blue ™ hTLR4 (InvivoGen) sono state messe in coltura secondo le istruzioni del produttore. In breve, le cellule sono state coltivate in terreno ad alto glucosio DMEM complementate con siero fetale bovino (FBS) al 10%, glutammina 2 mM, antibiotici e 1× HEK-Blue ™ Selection (InvivoGen). Le cellule sono state staccate utilizzando una spatola per cellule, contate e seminate in una piastra a 96 pozzetti ad una densità di 4×10^4 cellule per pozzetto. Dopo incubazione tutta la notte (37 °C, 5% CO_2, umidità 95%), il terreno di coltura è stato rimpiazzato con DMEM senza rosso fenolo complementato con il composto da saggiare. Dopo 30 minuti di pre incubazione con le molecole di sintesi FP13-17, le cellule sono state stimolate 100 ng/mL LPS di *E. coli* O55:B5 (Sigma-Aldrich) e incubate tutta la notte. I surnatanti contenenti SEAP sono stati raccolti e incubati con paranitrofenilfosfato (pNPP) per 2−4 ore al buio a temperatura ambiente. La densità ottica dei pozzetti è stata determinata utilizzando un lettore di micropiastre impostato a 405 nm. I risultati sono stati normalizzati con il controllo positivo (LPS da solo) ed espressi come media percentuale ± SEM di almeno tre esperimenti indipendenti

1.3) Esperimenti su cellule HEK-Blue hTLR4

I monosaccaridi FP13-16 sono stati saggiati per la loro capacità di attivare o inibire l'attivazione e il segnale di TLR4 stimolato da LPS nelle cellule HEK-Blue TM hTLR4 (Invivogen). Le cellule HEK-Blue™ hTLR4 sono stabilmente trasfettate in modo da esprimere i recettori umani del complesso di riconoscimento del LPS (TLR4, MD-2 e CD14) e un gene reporter inducibile SEAP (secreted embryonic alkaline phosphatase) posto sotto il controllo dei fattori di trascrizione NF-κB e AP-1- La stimolazione con un ligando TLR4 attiva NF-□B e AP-1 che inducono la produzione e la secrezione di SEAP. Questa linea cellulare è disegnata in modo specifico per studiare l'attivazione del TLR4 umano monitorando l'attivazione di NF-□B.
Quando forniti da soli, i composti FP13-16 erano inattivi nello stimolare il segnale TLR4 fino ad una concentrazione di 50 µM. I composti FP13-16 erano invece attivi nell'inibire in maniera dose dipendente il segnale TLR4 innescato da LPS (Figura 1).

10. RIVENDICAZIONI

1. Composto avente formula (I) in cui R1 ed R2 possono essere, indipendentemente l'uno dall'altro catene di acido oleico, linoleico, miristico o laurico.

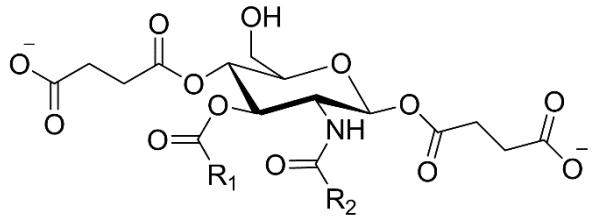

(I)

2. Composto secondo la rivendicazione 1 in cui quando R1 è una catena di acido oleico R2 è una catena di acido oleico o una catena di acido linoleico.

3. Composto secondo la rivendicazione 1 in cui quando R1 è una catena di acido linoleico R2 è una catena di acido linoleico.

4. Composto secondo la rivendicazione 1 in cui quando R1 è una catena di acido miristico R2 è una catena di acido oleico, linoleico o miristico.

5. Composto secondo la rivendicazione 1 scelto tra i composti aventi formula:

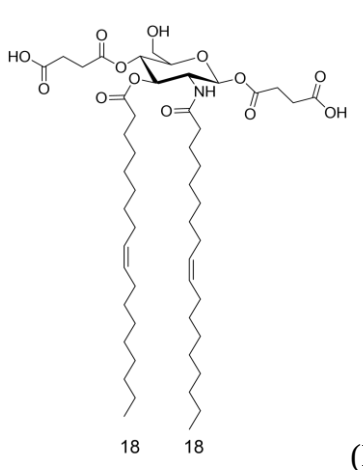

(I^a);

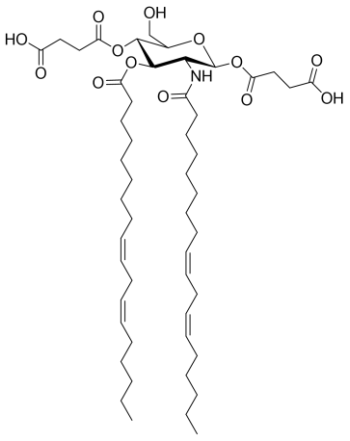

(I^b)

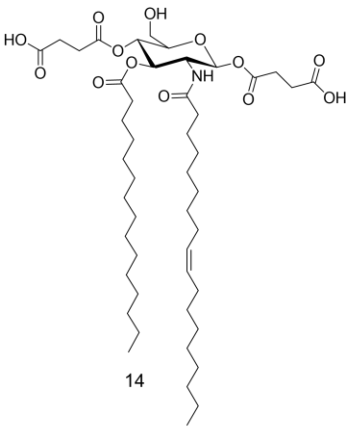

(I^c)

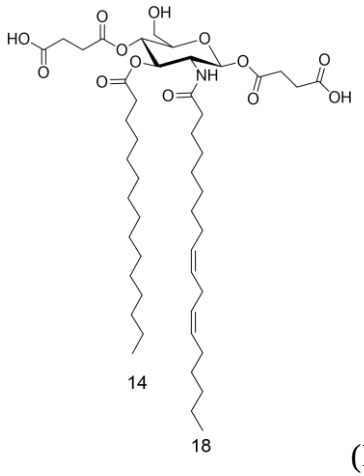

(I^d)

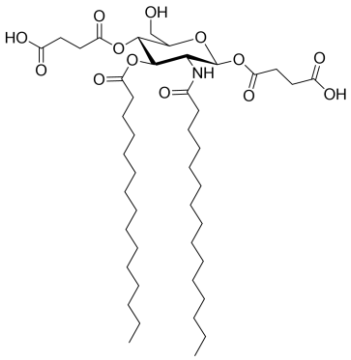

(I^e)

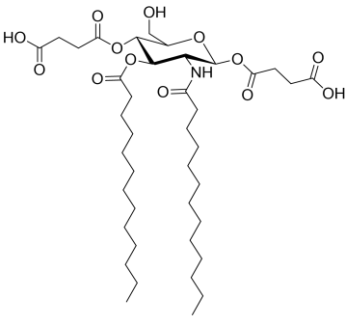

(I^f)

6. Composto secondo una qualsiasi delle rivendicazioni da 1 a 5 per uso come principio attivo farmacologico.

7. Composto per l'uso secondo la rivendicazione 6 nel trattamento di patologie in cui è necessaria una inattivazione del recettore TLR4.

8. Composto per l'uso secondo la rivendicazione 6 o 7 nel trattamento di infezioni, sepsi, aterosclerosi, trombocitopenia, trombosi, disturbi coronarici, cardiomiopatia, danno da riperfusione post ischemia miocardica (MI/R), disturbi alle valvole cardiache, malattie neurodegenerative, cancro, diabete.

9. Composizione farmaceutica comprendente un composto come definito in una qualsiasi delle rivendicazioni da 1 a 5 e almeno un veicolante o un eccipiente farmacologicamente accettabile.

10. Composizione farmaceutica secondo la rivendicazione 9 in forma liquida, iniettabile, solida, granulato, polvere, emulsione, spray, aerosol, crema.

11. Composizione farmaceutica secondo una qualsiasi delle rivendicazioni 9 o 10 per somministrazione orale, sistemica, endovenosa, topica, nebulizzata.

12. Composizione farmaceutica secondo una qualsiasi delle rivendicazioni da 9 a 11 per uso come farmaco.

13. Composizione farmaceutica per l'uso secondo la rivendicazione 12 nel trattamento di patologie in cui è necessaria una inattivazione del recettore TLR4.

14. Composizione farmaceutica per l'uso secondo la rivendicazione 12 o 13 nel trattamento di infezioni, sepsi, aterosclerosi, trombocitopenia, trombosi, disturbi coronarici, cardiomiopatia, danno da riperfusione post ischemia miocardica (MI/R), disturbi alle valvole cardiache, malattie neurodegenerative, cancro, diabete.

11. RIASSUNTO

L’invenzione riguarda nuovi antagonisti del TLR4, composizioni che li comprendono e loro uso come medicamenti.

(figura 1)

XI. Novel carboxylate-based glycolipids: TLR4 antagonism, MD-2 binding and self-assembly properties

Novel carboxylate-based glycolipids: TLR4 antagonism, MD-2 binding and self-assembly properties

Florent Cochet[1], Fabio A. Facchini[1], Lenny Zaffaroni[1], Jean-Marc Billod[2], Helena Coelho[3], Aurora Holgado[4], Harald Braun[4], Rudi Beyaert[4], Roman Jerala[5], Jesus Jimenez-Barbero[6], Sonsoles Martin-Santamaria[2], Francesco Peri[1]*

[1] Department of Biotechnology and Biosciences, University of Milano-Bicocca, Piazza della Scienza, 2; 20126 Milano (Italy).

[2] Department of Structural and Chemical Biology, Centro de Investigaciones Biologicas, CIB-CSIC, C/Ramiro de Maeztu, 9, 28040 Madrid, Spain.

[3] Molecular Recognition & Host−Pathogen Interactions Programme, CIC bioGUNE, Bizkaia Technology Park, Building 801A, 48170 Derio (Spain); UCIBIO, REQUIMTE, Departamento de Química, Faculdade de Ciências e Tecnologia, Universidade Nova de Lisboa, 2829-516 Caparica (Portugal); Department of Organic Chemistry II, Faculty of Science & Technology, University of the Basque Country, 48940 Leioa, Bizkaia (Spain).

[4] Unit for Molecular Signal Transduction in Inflammation VIB-UGent Center for Inflammation Research, VIB Technologiepark 927, 9052 Zwijnaarde, Ghent (Belgium); Department of Biomedical Molecular Biology, Ghent University Technologiepark 927, 9052 Zwijnaarde, Ghent (Belgium).

[5] Department of Biotechnology, National Institute of Chemistry, Hajdrihova 19, 1000 Ljubljana (Slovenia).

[6] Molecular Recognition & Host−Pathogen Interactions Programme, CIC bioGUNE, Bizkaia Technology Park, Building 801A, 48170 Derio (Spain); Department of Organic Chemistry II, Faculty of Science & Technology, University of the Basque Country, 48940 Leioa, Bizkaia (Spain); Ikerbasque, Basque Foundation for Science, Maria Diaz de Haro 13, 48009 Bilbao (Spain).

1. Abstract

New monosaccharide-based lipid A analogues were rationally designed through MD-2 docking studies. A panel of compounds with two carboxylate groups as phosphates bioisosteres, was synthesized with the same glucosamine-bis-succinyl core linked to different unsaturated and saturated fatty acid chains. The binding of the synthetic compounds to purified, functional recombinant human MD-2 was studied by four independent methods. All compounds bound to MD-2 with similar affinities and inhibited in a concentration-dependent manner, the LPS-stimulated TLR4 signaling in human and murine cells, while being inactive as TLR4 agonists when provided alone. A compound of the panel was tested *in vivo* and was not able to inhibit the production of proinflammatory cytokines in animals. This lack of activity is probably due to strong binding to serum albumin, as suggested by cell experiments in the presence of the serum. The interesting self-assembly property in solution of this type of compounds was investigated by computational methods and microscopy, and formation of large vesicles was observed by cryo-TEM microscopy.

2. Introduction

The Toll-like Receptor 4 (TLR4) is the mammalian receptor responsible for the Gram-negative bacterial endotoxin recognition (lipopolysaccharide, LPS and lipooligosaccharide, LOS). TLR4 is mainly expressed on the cells surface of innate immune[370] and epithelial cells,[371] allowing them to sense minute amounts of LPS released by the Gram-negative bacteria. An ordered series of interactions among the lipophilic portion of LPS and LBP,[50,372] CD14[373,374] and MD-2[89,277,375,376] co-receptors allows the formation of the activated membrane heterodimeric complex $(LPS/MD\text{-}2/TLR4)_2$[70] that triggers an intracellular signal[377] inducing the production of pro-inflammatory cytokines and chemokines.[378,379] TLR4-mediated cytokine production is an essential mechanism by which the host organism responds to infections, however, excessive stimulation of TLR4 by pathogen-associated molecular patterns (PAMPs) can cause uncontrolled cytokine production leading to serious life-threatening syndromes such

as acute sepsis and septic shock.[380] Recently, TLR4 activation by endogenous factors (DAMPs) has been associated to several inflammatory disorders and auto-immune diseases affecting a variety of organs and body functions.[223,381,382] In this context, the development of hit or lead compounds that are able to modulate TLR4 signaling is attracting increasing interest for a wide range of possible therapeutic settings.[231] TLR4 antagonists of synthetic or natural origin can block TLR4 signaling by interacting with the natural TLR4-bound co-receptor MD-2,[81] thus competing with the natural ligand LPS. Other TLR4 inhibition mechanisms are based on preventing LPS-induced receptor co-localization and dimerization (MGCs),[383] on interfering with cytosolic adaptor protein recruitment (TAK242),[158] or on the direct binding with other co-receptors such as the CD14 co-receptor.[245,340,358,384]

The type of modulation (agonism or antagonism) and the potency of TLR4 modulation by lipid A (phospholipidic part of LPS recognized by TLR4) and lipid A analogues not only depends on the interaction with CD14 and MD-2 receptors, but also on the aggregation state in solution of such amphiphilic molecules. The size and 3D shape of aggregates directly influences early stages of ligand recognition, namely the interaction with LBP and CD14 receptors.[385] Large lamellar or spherical aggregates have been associated respectively to the antagonist and agonist behavior of the lipid A variants.[87,240,241,340]

Compound E5564 (Eritoran, Fig. 75)[83] is one of the most potent TLR4 inhibitors so far. The activity of this molecule is associated to its capacity to mimic the lipid A moiety, thus competing with LPS for MD-2 binding. Eritoran consists of a glucosamine disaccharide with two phosphate groups, in C1 and C4' positions, and four lipophilic chains. Other TLR4 antagonists have glycolipid structures, as in the case of Gifu monosaccharides,[273] Lipid X and compound FP7 (Fig. 75)[358,386] or have a chemical structure unrelated to lipid A. Eritoran and FP7 are the only lipid A mimetics whose direct binding to MD-2 and the competition with natural MD-2 ligands LPS and LOS have been reported.[81,234,340,342].

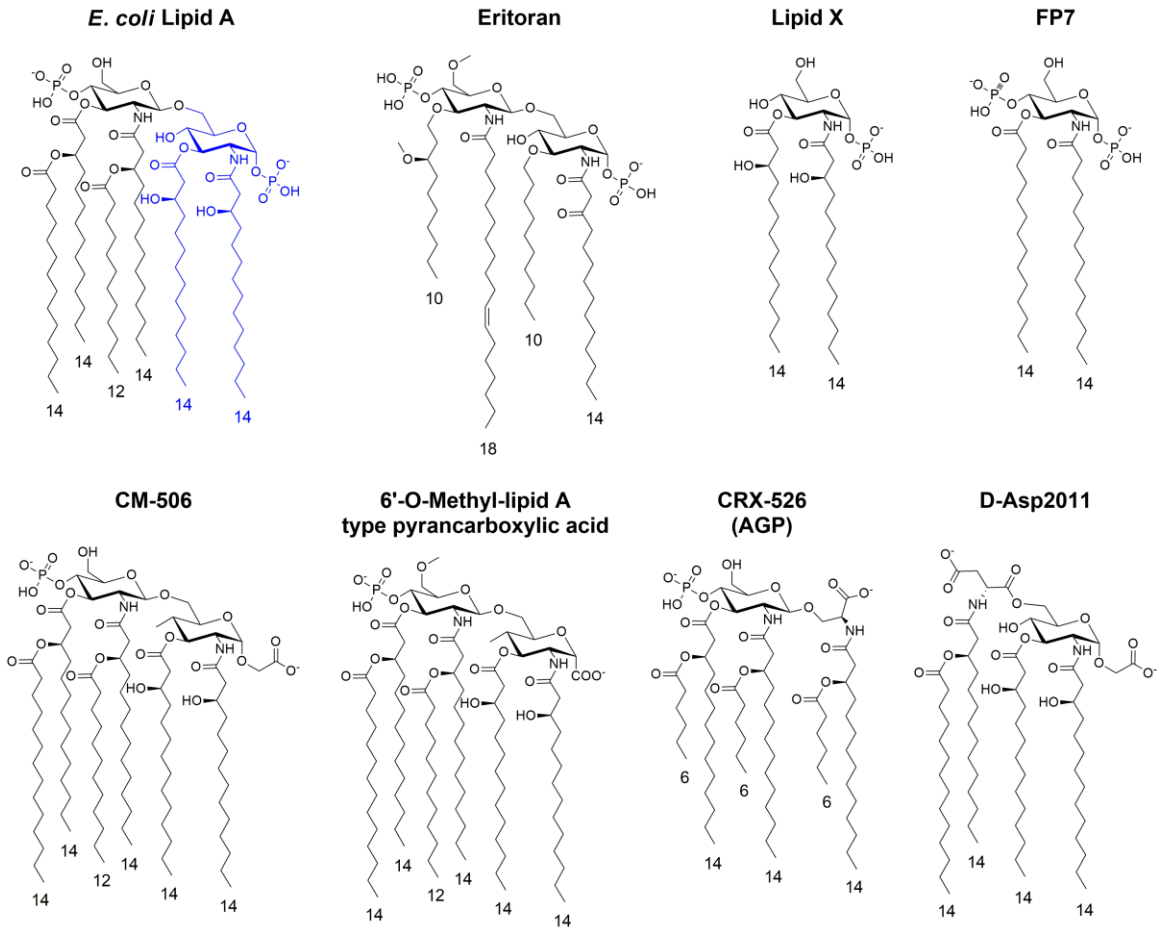

Figure 75. Chemical structures of Natural *E. coli* lipid A, **lipid X**, synthetic antagonist **E5564** (**Eritoran**) and monosaccharide **FP7**. Synthetic Lipid A mimics with carboxylic acids replacing phosphates, active as TLR4 modulators.

With the aim of obtaining lipid A mimetics with drug-like features, including increased metabolic stability, the anionic phosphate group has been replaced by the bioisosteric carboxylate group (Fig. 75)[287,387–392] and different Lipid A analogues have been reported presenting different acylation patterns together with a carboxymethyl[387–390] or a carboxyl group linked to the anomeric carbon.[391] In the case of aminoalkyl glucosaminide-4-phosphates (AGPs, or Corixa compounds, CRX),[290] the whole reducing sugar and phosphate have also been replaced by an acylated diethanolamine bound to a phosphate or a carboxylic acid.[287,392]

AGPs act as TLR4 agonists or antagonists depending on the acylation patterns and the fatty acids chains lengths, and the variants with agonist properties (CRX 526, Fig. 75) were subsequently developed as vaccine adjuvants.[291] The TLR4 agonistic/antagonist activity of

AGPs is a good indication that the bioisosteric substitution of the phosphate group in C1 by a carboxylic acid, preserves the ability to bind to MD-2 and triggers or inhibits TLR4 dimerization. While some of carboxylic acid synthetic variants of lipid A have been characterized for their immunomodulating activity in cells and in animal models, no data are available on the characterization of their direct binding to MD-2.

We report here a small series of monosaccharide-based lipid A mimetics resembling FP7, with carboxyl moieties mimicking phosphates and with unsaturated fatty acid chains. We tested the capacity of this variety of molecules to interact with the MD-2 co-receptor in multiple binding assays and we evaluated their biological activity on different cellular models. Compounds **FP13- FP17** have been rationally designed as lipid A mimetics where the phosphates have been replaced by succinate moieties, while the distance between the two carboxylate groups has been kept similar to that of the two phosphates groups in lipid A (distance of 11 to 15 Å for *E. coli* Lipid A and 8 to 15 Å for **FP13-17**).[287,387–389,391,392] Moreover, unsaturated chains (also present in Eritoran) have also been inserted to enhance the binding into the MD-2 hydrophobic pocket.[393]

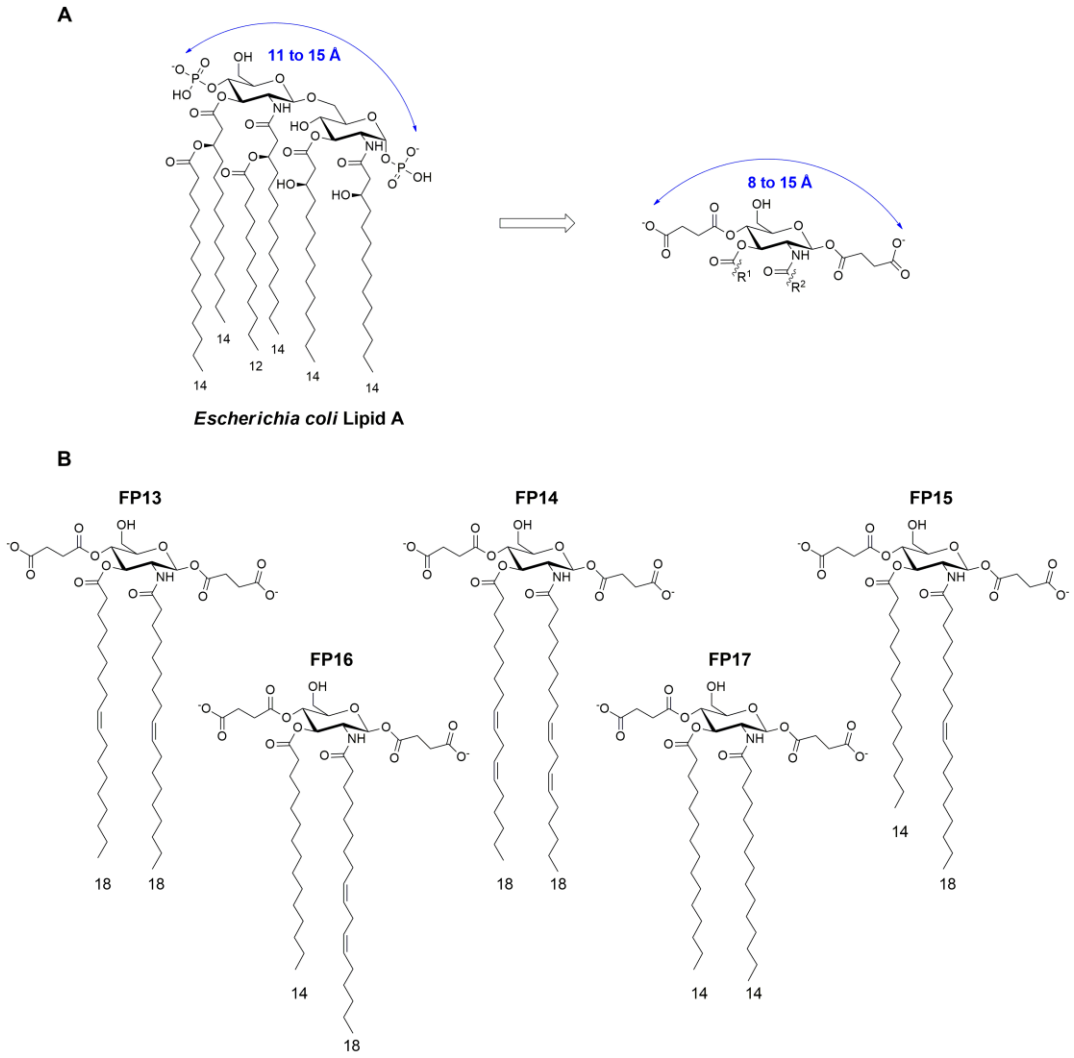

Figure 76. Monosaccharide FP13-17 are lipid A mimetics (**A**). They share a common backbone composed of a glucosamine scaffold linked to two succinyl moieties (at position C1 and C4) ensuring a similar distance to that of lipid A phosphates between the two carboxylic acids and allowing a higher flexibility. Carboxylic acid groups are evaluated as phosphate bioisoteres.[394] (**B**). Structure of the lipid A mimetics displaying their differences: **FP13** contains two oleic chains (C18, cis-9), **FP14** two linoleic chains (C18, cis, cis-9,12), **FP15** myristic at C3 (C14) and oleic at C2, **FP16** myristic at C3 and linoleic at C2 and **FP17** two myristic chains.

All compounds are based on a glucosamine scaffold, and present two units of succinic acid condensed to the hydroxyl groups at C1 and C4. As the TLR4 antagonist Eritoran presents an unsaturated chain (C18, cis-11) that has the role to increase the binding affinity for the MD-2 hydrophobic pocket,[395] we aimed to investigate the effect of unsaturated chains linked to glucosamine C2 and C3. **FP13** contains two oleic chains (C18, cis-9), **FP14** two linoleic chains (C18, cis, cis-9,12), **FP15** myristic at C3 (C14) and oleic at C2, **FP16** myristic at C3 and linoleic at C2 and **FP17** two myristic chains.

Results

3. Computational studies of the binding of FP13-17 to TLR4/MD-2

Designed monosaccharides **FP13-17** were computationally studied to predict their TLR4/MD-2 binding properties. To explore their possible binding modes, the compounds were computationally docked in a 3D model of the TLR4/MD-2 complex in antagonist conformation previously reported by us,[356] by means of the Vina docking program.[339] Compounds **FP13-17** were predicted to bind inside the MD-2 hydrophobic pocket (Fig. 77) with favorable predicted binding scores (ranging from -8.2 to -6.7 kcal/mol for the 20 best predicted poses). Two different binding orientations were identified: one similar to that for *E. coli* lipid A in PDB ID 3FXI, and a second one similar to that for antagonist lipid IVa in PDB ID 2E59 (rotated by 180 degrees along the lipid chains axis compared with agonist *E. coli* LPS in PDB ID 3FXI, Supp. Inf. Fig. S1). In all case, the fatty acid chains were inserted inside the MD-2 pocket establishing interactions with the aliphatic and aromatic residues. In particular, Phe151 was found to interact with the unsaturated moiety of oleic and linoleic acids in compounds **FP13-17**, while other hydrophobic interactions were found with side chains from Phe121, Phe147, Ile44 and Ile46 residues (Fig. 77). Regarding the polar moieties of **FP13-17** (pyranose ring of the sugar and esters groups), they were participating in a variety of polar interactions with the polar residues at the MD-2 rim, such as Tyr102 and Glu92. The carboxylate groups were predicted to establish ionic interactions with Arg96 and Arg264 (TLR4) in most of the docked poses for all the compounds (Fig. 77).

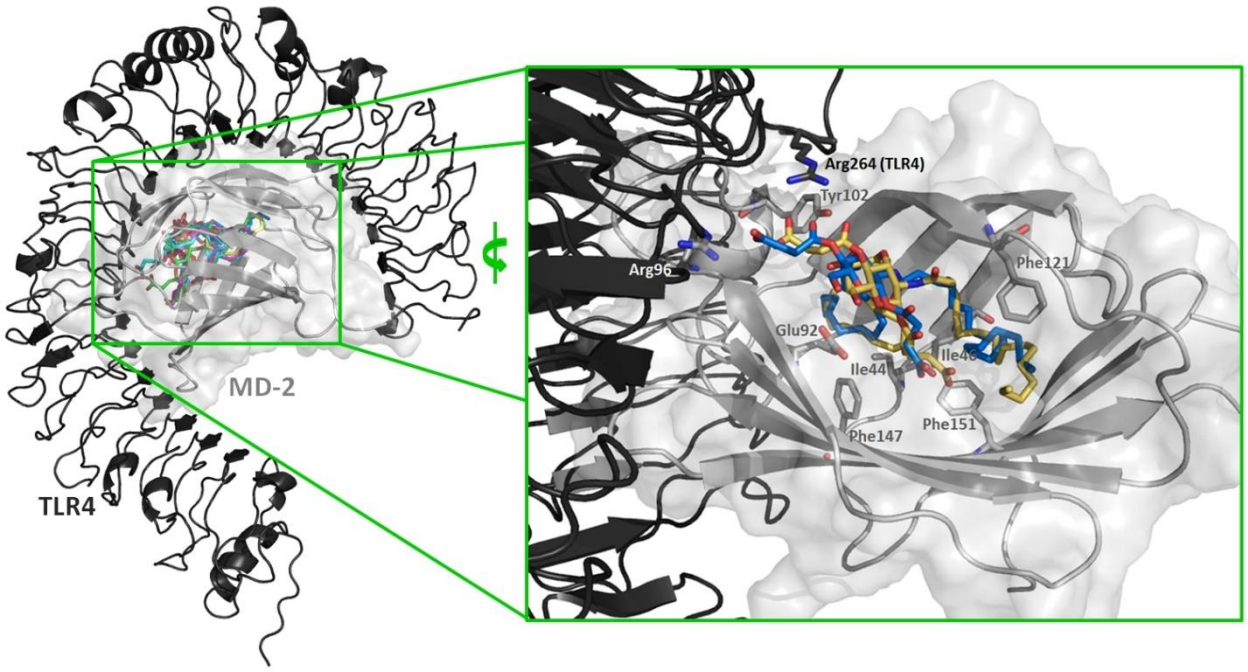

Figure 77. Best AutoDock Vina docked poses of FP13-17 within the TLR4/MD-2 complex. TLR4 and MD-2 are respectively represented in black and grey cartoon. Ligands **FP13** to **FP17** are in yellow, cyan, pink, blue and green sticks, respectively (left: general view; right: detailed view showing selected interacting residues, only **FP13** in yellow and **FP16** in blue are shown).

Selected docked binding poses obtained with Vina were submitted to re-docking with AutoDock,[338] another well-known docking program with a different scoring function. Fittingly, the best poses obtained for each ligand were in good agreement with those obtained through Vina, which supported the appropriateness of the employed approach. Predicted scores ranged from -7.38 to -4.53 kcal/mol across all the ligands with a score for the best predicted poses ranging from -7.38 to -4.69 kcal/mol. No major score or binding differences were observed among the set of ligands suggesting similar binding properties.

To study in detail the binding interactions of each ligand to the TLR4/MD-2 system, we performed molecular dynamics (MD) simulations of the complexes of TLR4/MD-2 with the best docked pose for each ligand. The dynamics of the ligands and of key residues of MD-2 were analysed. MD-2 is stable over the trajectory as shown by the RMSD and RMS fluctuation per residues analysis (Supp. Inf. Fig. S6). Polar interactions are maintained along the simulation and residue Phe126 does not undergo major conformational change (Supp. Inf. Fig. S7),

indicating that all the ligands are able to retain the antagonist conformation of MD-2, previously associated with antagonist properties.[70] Interestingly, the starting docked poses relocate, after 50 ns of MD simulation, from a slightly deep position inside the MD-2 rim towards a binding mode closer to that for lipid IVa (depicted for **FP13** in Supp. Inf. Fig. S8). These similar modes of TLR4/MD-2 binding were in agreement with a similar antagonist activity (see below).

The solubility of the ligands, which is a critical property for cellular assays, was also analyzed by calculating the logP parameter (Supp. Inf. Fig. S9). The results point toward relatively high logP values. However, they are in the range of a previously reported family of FP7 analogues.[88] Despite the high calculated logP it was however possible to dissolve all compounds in aqueous buffers and test them on cells and animals.

4. MD-2 binding properties of synthetic compounds

Compounds **FP13-17** were synthesized according to synthetic scheme S1 and procedures described in Supp. Info. and were tested for their capacity to bind to purified human MD-2 (hMD-2) Four different techniques were used: two ELISA-type plate-based assays with immobilized protein, a fluorescence displacement assay, and surface plasmon resonance (SPR).[346,396]

Direct binding of LPS and synthetic molecules **FP13-17** to hMD-2 was determined by using a monoclonal antibody that binds to free hMD-2 but not to LPS bound to the hMD-2 binding site.[397] Monoclonal mouse anti-hMD-2 (9B4) antibody specifically binds to an epitope close to the rim of the hMD-2 pocket, available for the binding only when the hMD-2 pocket is empty. This assay detected a decrease in binding to hMD-2 in the presence of LPS (Fig. 78A), similar to what has previously been reported.[398] A dose-dependent inhibition of antibody/MD-2 interaction was observed when adding molecules **FP13-17**, with a 85−95% decrease in binding obtained at concentrations of molecules **FP13-17** of 20 μM (Fig. 78A). This indicates that the synthetic molecules bind the cavity of MD-2.

The ability of synthetic molecules **FP13-17** to displace LPS from the hMD-2 pocket was assessed by ELISA. **FP13-17** molecules were added at increasing concentrations to hMD-2 that was previously incubated with biotinylated LPS. **FP13-17** molecules were able to displace biotin-LPS from the hMD-2 pocket in a similar dose-dependent manner, with the highest displacement of 40−55% obtained at a concentration of 160 μM (Fig. 78B). As a control, LPS at a concentration of 40 μM gave the highest displacement of biotin-LPS of 70% (Fig. 78B).

It has been previously shown that the fluorescent probe 1,1'-Bis(anilino)-4,4'-bis (naphthalene)−8,8' disulfonate (bis-ANS) binds to hMD-2 and it is displaced by LPS.[346] bis-ANS binds the same hMD-2 binding pocket that accommodates the fatty acid chains of lipid A and of other lipid A-like ligands, so that TLR4 modulators interacting with MD-2 in a lipid A-like manner, compete with bis-ANS and displace it from hMD-2. Synthetic compounds **FP13-17** caused a similar concentration-dependent decrease of bis-ANS fluorescence, indicating competitive binding of molecules **FP13-17** to hMD-2 (Fig. 78C).

Results of SPR data experiments based on binding of compounds to the immobilized hMD-2, showed direct interaction of the hMD-2 receptor with LPS (control, Supp. Inf. Fig. S2) and with the tested synthetic compounds **FP13-17**. K_D values derived from sensorgram analysis were 9, 35, 14, 21 and 12 μM for **FP13**, **FP14**, **FP15**, **FP16** and **FP17**, respectively (Fig. 78D-H). SPR experimental curve optimal fitting was obtained by assuming 1:1 ligand/MD-2 binding stoichiometry.

Together, the results obtained from these *in vitro* cell-free studies clearly indicate that compounds **FP13-17** directly bind to hMD-2.

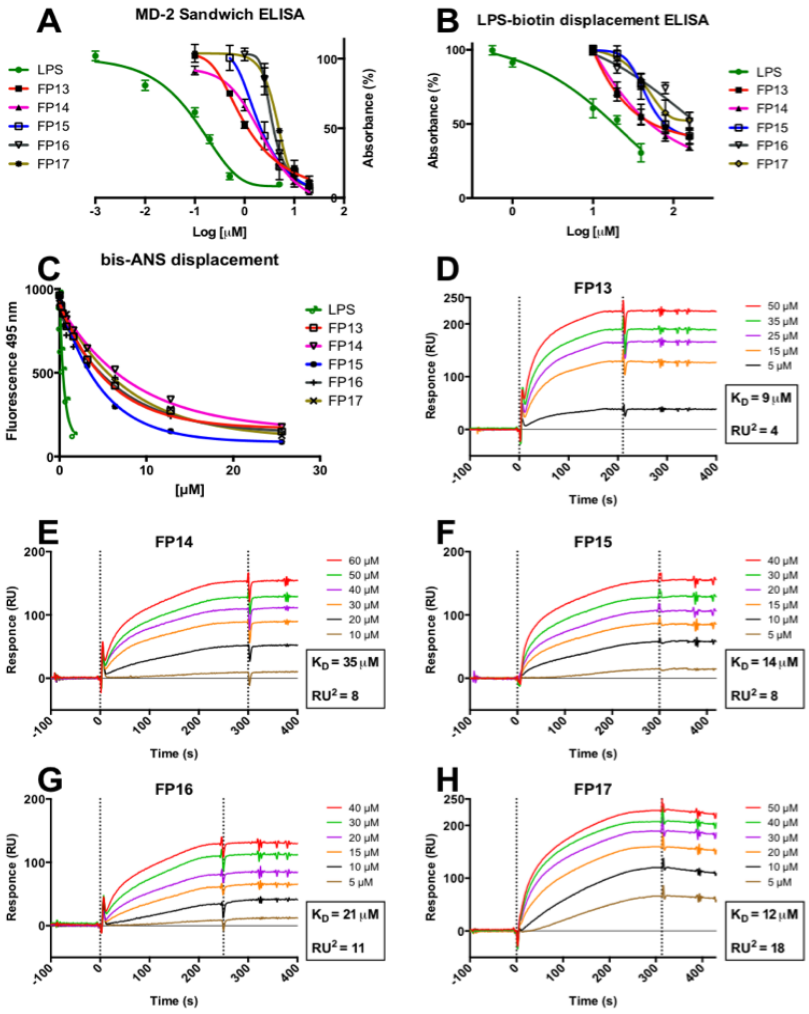

Figure 78. Binding studies on purified hMD-2 receptor. (**A**) **FP13-17** prevent anti-human hMD-2 monoclonal antibody binding in a dose-dependent manner; **(B**) **FP13-17** compete with biotin-LPS for hMD-2 binding; (**C**) **FP13-17** dose-dependently inhibit the binding of bis-ANS to hMD-2; **(D-H**) SPR analysis show direct interaction between **FP13-17** and hMD-2; K_D values are reported.

5. Inhibition of LPS-stimulated human TLR4 activation in HEK293-Blue cells

Synthetic monosaccharides were screened for their capacity to activate or inhibit LPS-stimulated TLR4 activation in HEK293-Blue hTLR4 cells. HEK293-Blue hTLR4 cells are HEK cells transfected in order to express the human receptors involved in LPS detection process (TLR4, MD-2 and membrane-bound CD14) and an inducible SEAP (secreted embryonic alkaline phosphatase) reporter gene placed under the control of NF-kB and AP-1-transcription factors. Activation of the MyD88-dependent TLR4 pathway promotes the production and secretion of SEAP in the cell culture media, which can be easily quantified. In

order to evaluate the capacity of **FP13-17** to trigger TLR4 activation, cells were treated with increasing concentrations of the compounds (0.1 to 10 µM) and incubated for 16 hours. On the other hand, to evaluate the antagonist activity, cells were pre-incubated with compounds **FP13-17** for 15 min. and stimulated with LPS for 16 hours. The results obtained revealed that none of the molecules induced TLR4 signaling up to a concentration of 10 µM, thus indicating lack of agonist activity (Data not shown). Conversely, **FP13-17** did inhibit, in a dose-dependent manner, the LPS-induced TLR4 signaling (Fig. 79). All molecules showed similar antagonist potency (IC_{50} values is in the range 2.7 to 6.6 µM, also in the same order of magnitude than that of IC_{50} of **FP7**, range, 0.46-3.42 µM).[88,274] An MTT assay revealed that the compounds did not affect cell viability at concentrations up to 10 µM (Supp. Inf. Fig. S3).

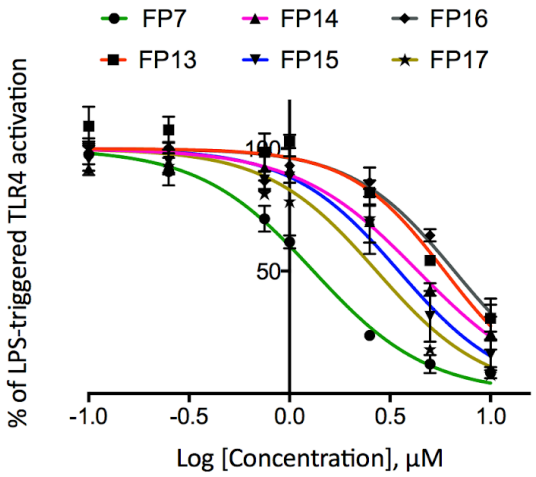

Compound	IC_{50} LPS (µM)
FP7	1.32
FP13	5.91
FP14	4.35
FP15	3.50
FP16	6.61
FP17	2.70

Figure 79. Dose-dependent inhibition of LPS-triggered TLR4 pathway activation in HEK293-Blue hTLR4 cells. Cells were pre-incubated with increasing concentrations (0.1 to 10 µM) of compounds **FP13-17** in serum-free DMEM medium and stimulated with LPS (100 ng/mL) after 15 min. SEAP levels in cell culture media were quantified after 16 hours as indicator of TLR4 activation. Data were normalized to stimulation with LPS alone and fitted to a sigmoidal 4 parameter logistic equation to obtain dose-effect curves (left panel). IC_{50} values for **FP13-17** are reported in the right panel. points represent the mean of percentage ± SEM of at least 3 independent experiments.

Inhibition of LPS signaling in murine macrophages.

To characterize the effect of synthetic compounds **FP13-17** on cells naturally expressing TLR4, we used the murine macrophage RAW 264.7-Blue cell line, which are murine RAW 264.7 macrophages with chromosomal integration of SEAP reporter construct described in the

previous section. Also in this case, the compounds did not show agonist activity when provided alone to the cells, while they inhibited LPS-stimulated SEAP secretion in a dose-dependent manner (Fig. 80) and the potency in inhibiting TLR4 signal was similar for all synthetic compounds.

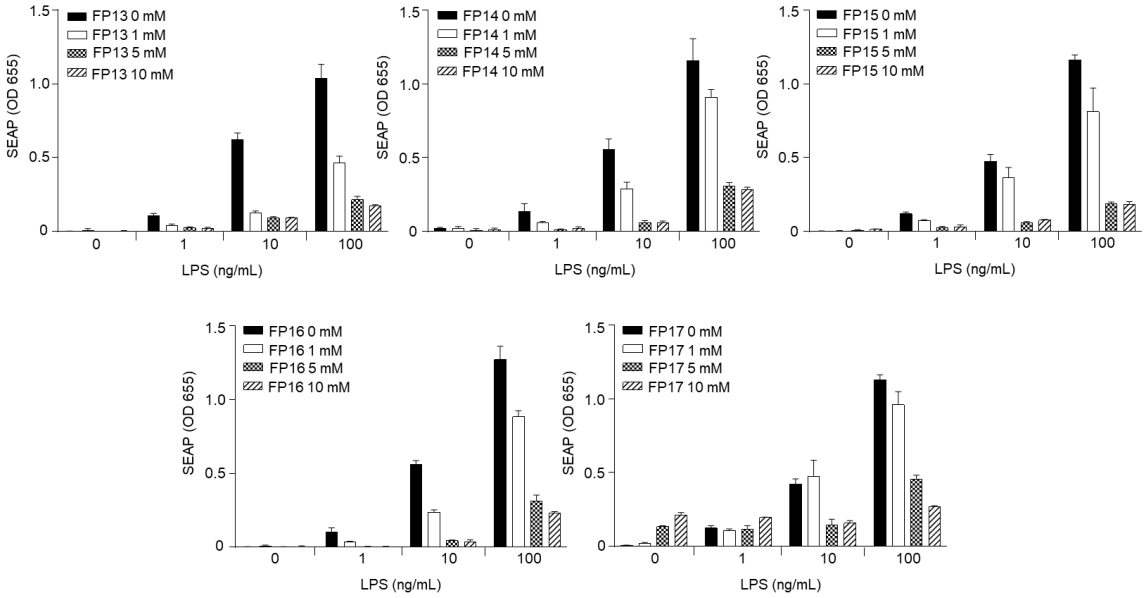

Figure 80. Inhibition of LPS-induced TLR4 signaling in RAW 264.7-Blue cells. Cells were pre-incubated with the indicated concentrations of monosaccharides **FP13-17** and stimulated with 1, 10 or 100 ng/mL *E. coli* O111:B4 LPS 30 min. later in serum-free DMEM medium. SEAP reporter levels in the cell supernatant were determined by QuantiBlue Assay 24 h later. Error bars represent the standard deviation of the mean of technical triplicates. The graph is representative of at least three independent experiments.

7. *In vivo* experiments with compound FP13.

To further investigate whether carboxylate-based lipid A mimetics are able to inhibit LPS-induced signaling *in vivo*, we injected C57BL/6 mice i.p. with 200 μg of compound **FP13** followed by the LPS injection 30 min later. After 4 h mice were sacrified and serum was analyzed for the presence of TNFα, which was strongly increased upon the LPS treatment (Supp. Inf. Fig. S4). However, in contrast to our cellular studies, **FP13** did not affect LPS-induced serum TNFα levels. The reason for this was unclear and we hypothesized poor distribution and absorption of the compound upon i.p. injection.

We therefore also explored the antagonistic capacity of **FP13** in a different *in vivo* model, where LPS and **FP13** were both administered locally in the lungs. Intratracheal (i.t.) instillation of LPS is known to cause an acute inflammatory response in mice, characterized by transient infiltration of neutrophils into the airways.[399,400] However, also in this model, treatment with **FP13** failed to suppress the LPS-induced effect (Supp. Inf. Fig. S5). These results demonstrate that **FP13** is biologically inactive in mice when administered i.p. or i.t.

We next sought to determine the possible reason for the discrepancy in the observed effect of **FP13** *in vitro* and *in vivo*. The plasma protein binding of therapeutic drugs is known to have a significant impact on their pharmacokinetics and pharmacodynamics.[401] It should be noted that the above described *in vitro* experiments were done with HEK293-Blue and RAW 264.7-Blue cells cultured in the absence of serum. Therefore, we first analyzed whether the presence of serum has an effect on the *in vitro* biological activity of **FP13**. Indeed, the antagonistic activity of **FP13** was completely neutralized when tested on RAW 264.7-Blue cells incubated in DMEM supplemented with 10% FBS (Fig. 81A). Serum albumin is the major soluble protein constituent of blood with mouse albumin serum concentrations being around 20 mg/mL.[402] In order to evaluate whether the presence of serum albumin protein is sufficient to neutralize the *in vitro* activity of **FP13**, we repeated the RAW 264.7-Blue cell assay in serum-free conditions but with the addition of 4 or 20 mg/mL BSA. Similar to addition of complete serum, also addition of BSA strongly decreased the antagonistic activity of **FP13** in a dose dependent manner (Fig. 81B and C). Together, these data indicate that binding of **FP13** to proteins interferes with its biological activity and that binding of **FP13** to albumin or other proteins present in mouse blood and the bronchoalveolar lung environment is most likely responsible for the absence of an antagonistic effect of **FP13** *in vivo*.

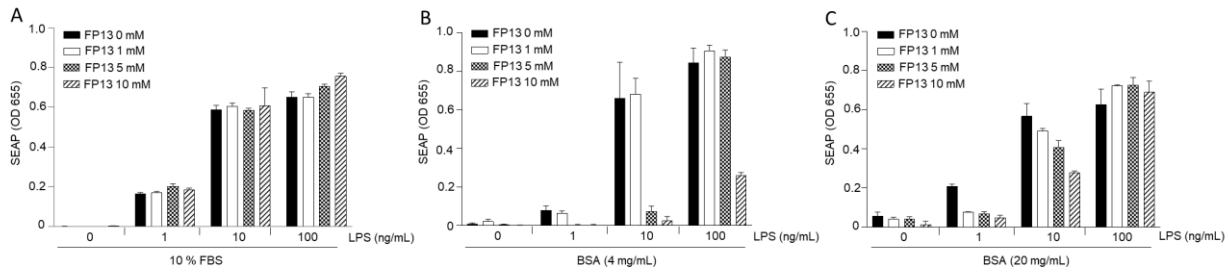

Figure 81. Presence of serum or BSA neutralizes the antagonistic activity of monosaccharide FP13 on LPS-induced TLR4 signaling in RAW 264.7-Blue cells. (**A-C**) Cells were pre-incubated with the indicated concentrations of monosaccharide **FP13** in DMEM supplemented with 10% FBS (**A**), 4 mg/mL BSA (**B**) or 20 mg/ml BSA (**C**). 30 min later cells were stimulated with 1, 10 or 100 ng/mL *E. coli* O111:B4 LPS. SEAP reporter levels in the cell supernatant were determined by QuantiBlue Assay 24 h later. Error bars represent the standard deviation of the mean of biological triplicates. The graph is representative of at least three independent experiments.

8. Cryogenic Transmission Electron Microscopy (Cryo-TEM)

We have recently described the aggregation behavior of **FP7** glycolipid, a related molecule to those described herein.[88] In particular, the analysis of the obtained NMR and TEM data (cryogenic and negative staining) permitted to show that **FP7** forms micelle structures.[234] Indeed, previous investigations had demonstrated that **FP7** has a CMC of about 9 µM.[274] Thus, the self-assembly in solution of one member of the series, namely compound **FP15**, was studied by Cryogenic Transmission Electron Microscopy (Cryo-TEM) (Fig. 82).

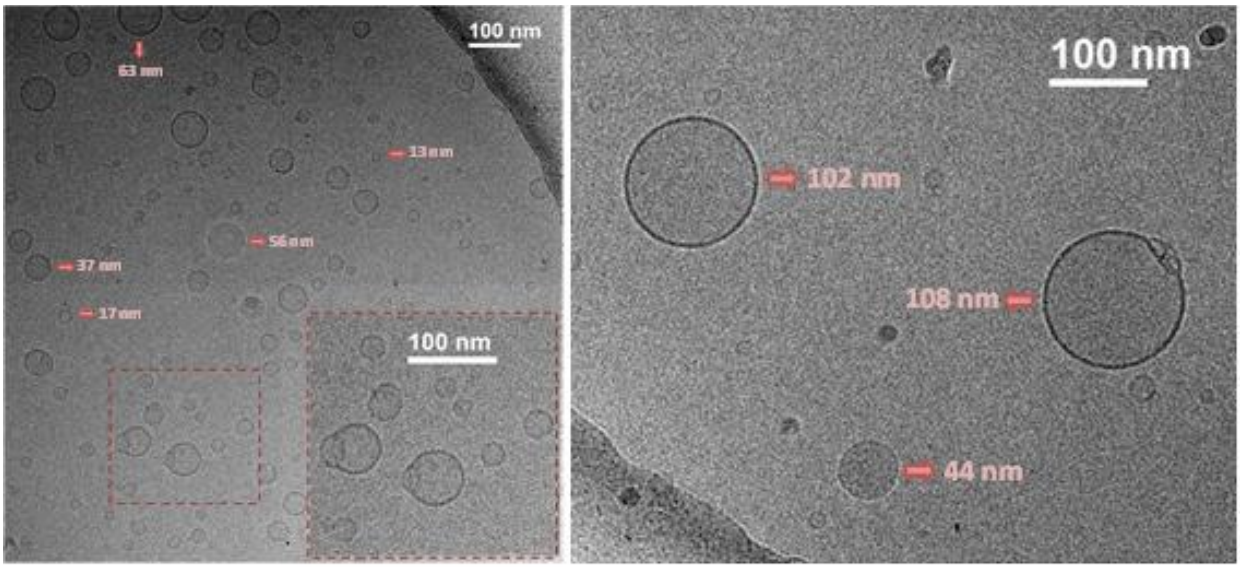

Figure 82. Cryogenic Transmission Electron Microscopy (Cryo-TEM) of FP15 (7 mg/mL) nominal magnification of 40,000 X (0.26 nm/pixel).

The detailed inspection of the cryo-TEM data shows that **FP15** mainly forms spherical and homogeneous small unilamellar vesicles (SUVs), although with rather different size distributions, from 10 to 110 nm. Moreover, it was possible to detect the presence of fusion events (as highlighted in the zoomed picture in Fig. 82, dark red squares) as well as the existence of open bilayers. The use of vitrified samples allowed the trapping of the potentially unstable structures associated with the formed intermediates in the solubilization process of the vesicles.

These experimental data show that **FP15** is able to form vesicles/liposomes displaying a bilayer.

9. Molecular dynamics (MD) simulations of FP15 self-assembly

As **FP15** was experimentally shown to spontaneously form SUVs, observed through Cryo-TEM experiments, we were eager to understand this phenomenon at an atomistic level by performing MD simulations of **FP15** in water (see Experimental Section for details). A thorough explanation and discussion about all the self-assembly simulations performed is given in Supp. Inf., the following analysis is based on one unique selected long simulation of 1 μs in total. Starting from a random mixture of **FP15** molecules and explicit water molecules, the system was observed to self-organize into a bilayer system, reaching a stable regime from 700 ns of simulation (according to the area per molecule graph, Supp. Inf. Fig. S10, left). For this reason, only the last 300 ns were considered for plotting electron density profile (Supp. Inf. Fig. S10, right) to estimate the thickness of the **FP15** layer between 40 and 70 Å. It can be grasped from Fig. 83 that the membrane is slightly curved resulting in an electron density profile with soft delimitation between the water and the **FP15** phases preventing us form precisely assessing the thickness. The graph also shows that water is present at all latitude of the membrane with a minimum at the center indicating that the vesicles might be highly permeable to water.

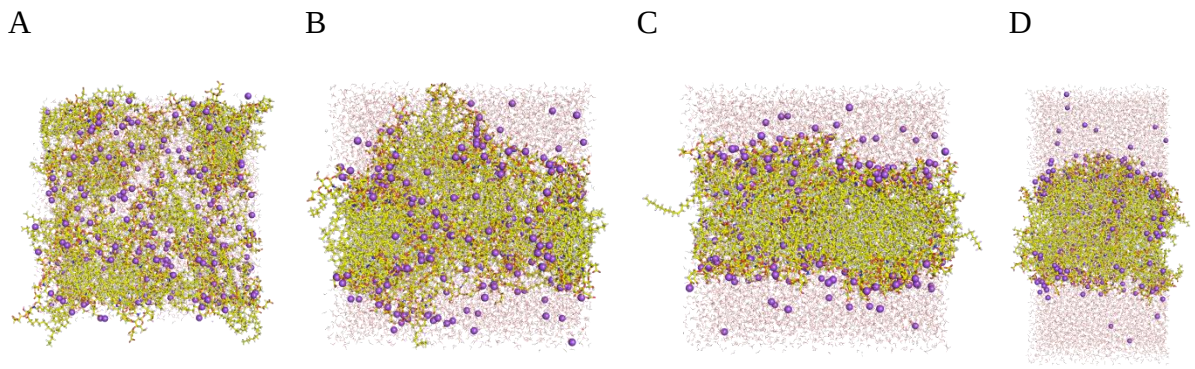

Figure 83. Representation of the evolution of the FP15-water mixture over time, t=0ns (**A**), t=50ns (**B**), t=200ns (**C**) and t=1000ns (**D**). **FP15** in represented in CPK colored sticks, ion Na^+ in violet spheres and the water molecules in thin grey and red lines.

In each layer, **FP15** is regrouped in small cluster surrounded by water accessible pores. The smallest, and what looks like the most stable cluster, is a face-to-face head group packaging assembly of two **FP15** units, stabilized through hydrogen bonds and interactions between carboxylate anion from the succinate groups through Na^+ ionic interactions. Two other assemblies of four **FP15** are observed, one in which the saccharide rings are packed in parallel, being stabilized by hydrogen bonds and ionic interactions, the other one is an in-circle assembly of **FP15**, around a spot rich in Na^+ ions, driven exclusively by ionic interactions between succinate groups and Na^+ ions (Supp. Inf. Fig. S11). Additionally, we can observe that the unsaturation in the acyl chains induces a sharp turn at the center of the membrane, preventing the different units of **FP15** to form highly organized bilayers.

10. Discussion

This study presents a new series of monosaccharide lipid A mimetics containing two carboxylates replacing lipid A phosphates. The structure of these compounds is based on a glucosamine scaffold that has been functionalized with two succinate esters in C1 and C4, and therefore expose two carboxylic acids at a mutual distance similar to that of lipid A phosphates. Saturated and/or unsaturated fatty acid chains are attached to the C2 and C3 positions of the sugar.

The structure-based design of these compounds was done by molecular docking within the TLR4/MD-2 receptor and MD simulations. All compounds showed favorable predicted binding scores and interesting binding poses into hMD-2 that suggested their putative MD-2 binding properties and their possible activity as TLR4 modulators. Compounds were synthesized starting from commercial glucosamine through a divergent strategy from a common intermediate.

For the first time in the case of carboxylic-acid-based lipid A analogues, the interaction with functional hMD-2 receptor was directly measured by using a recombinant hMD-2 expressed in yeast (*P. pastoris*).

In a first set of *in vitro* experiments, we studied the SAR of these carboxylic-acid-based lipid A analogues (**FP13-17**). Four different binding experiments between synthetic compounds **FP13-17** and hMD-2 were carried out. These were competition (displacement) experiments in which the synthetic glycolipids **FP13-17** competed with biotin-LPS, with the fluorescent MD-2 ligand bis-ANS, and with anti-MD-2 antibody for MD-2 binding. SPR measurements allowed to analyze directly the binding between synthetic glycolipids and hMD-2. All binding experiments consistently provided a similar order of affinity among hMD-2 and synthetic molecules **FP13-17**.

The biological activity was assessed on cellular models expressing human and murine TLR4/MD-2. All molecules turned out to be inactive as agonists on human and murine TLR4. However, when administered with LPS, all the carboxylate-based lipid A mimetics were able to inhibit the LPS/TLR4 signal (antagonism) in both human (HEK293) and murine (RAW 264.7) TLR4-expressing cells with a similar potency, also similar to the previously characterized monosaccharide **FP7**.

FP13-17 present very similar IC_{50} in a range from 2.7 to 6.6 μM, which is a slightly higher value compared to the IC_{50} of **FP7** (2.0 μM).

Although our results reveal **FP13** and related compounds as strong antagonists of TLR4, their biological activity is abrogated by serum albumin, which most likely explains the absence of an antagonistic effect in the two different *in vivo* models of LPS activity. We propose that direct binding of **FP13** to albumin or other proteins in serum and lungs neutralizes its biological activity *in vivo*. Definitive prove will require *in vitro* binding studies of **FP13** with albumin. Together, these data demonstrate the need for additional chemical optimization or formulation of the current compounds.

The analysis of the cryo-TEM data of one compound of the series, **FP15**, indicates that this molecule mainly generates circular and homogeneous small unilamellar vesicles (SUV), with rather different size distributions, from 10 to 110 nm of diameter, with the presence of fusion events as well as open bilayers. The fact that FP15 forms stable aggregates is an important information for the pharmacological formulation of this type of compounds in the perspective of clinical development. Interestingly, the formation of large vesicles does not abrogate the biological activity, at least at cellular level.

MD simulation shows the self-assembly with formation of clusters. Succinate groups seems to stabilize complexes to form 3 main assemblies, “face-to-face” and “packed in parallel” clusters might be the reason for the strong stability of the membrane vesicles while “in-circle assembly” cluster suggests a high permeability to water.

The main achievement of this is work is demonstrating that this type of new carboxylate-based monosaccharidic lipid A analogues strongly interact with co-receptor MD-2 displacing the natural ligand LPS and forming stable complexes.

MD-2 strong interaction and binding is very likely the main mechanism of TLR4 antagonism for this series of compounds.

Concerning the molecular design, we confirm that the carboxylic acid represents an effective bioisostere of phosphoric acid and can be used in this type of lipid A mimetics retaining MD-2

molecular recognition and binding. The replacement of phosphates with carboxylates is an important step towards druggability, as carboxylates are metabolically more stable and easier to synthesize. On the contrary, the presence of an unsaturation in the fatty acid chains seems to play a minor role since the *in vitro* affinity for the purified hMD-2 receptor and the activity on cells is almost identical for saturated (**FP17**) and unsaturated (**FP13-16**) compounds.

In conclusion, the novelty and importance of our work is the description of new carboxylate-based monosaccharidic lipid A analogues that strongly interact with the co-receptor MD-2, displacing the natural ligand LPS and forming stable complexes. The interaction and binding with MD-2 is most likely the main mechanism of TLR4 antagonism for this series of compounds. **FP13-17** showed to bind MD-2, are active on cells as TLR4 antagonists and are non-toxic at a concentration of 10 μM. The lack of *in vivo* activity is probably due to strong interaction with serum albumin and further structure optimization is in progress to improve the pharmacokinetic of these promising hit compounds.

The biological activity of this panel of compounds as TLR4 antagonists, combined with the tendency to spontaneously form vesicular aggregates, make this type of carboxylate-based lipid A analogues interesting in the perspective to exploit the self-assembled aggregates structures to modulate their pharmacokinetic and biodistribution properties in biomedical and pharmacological contexts.[244,403,404]

11. Methods

Methods for the chemical synthesis of monosaccharides and computational methods are provided at the Supp. Inf.

Preparation of recombinant MD-2 in Pichia pastoris and purification. MD-2 was produced in *Pichia pastoris*, analyzed by SDS–PAGE and its biological activity tested on 293/hTLR4a cells as described before.[88]

Antibody-sandwich ELISA for the detection of binding of compounds to MD-2. The method of antibody-sandwich ELISA for the detection of the binding of compounds to MD-2 was modified from a previous study.[88] A microtiter plate was coated overnight at 4 °C with 100 μL/well of 5 μg/mL of chicken polyclonal anti-hMD-2 antibodies, diluted in 50 mM Na_2CO_3 buffer, pH 9.6 and blocked with 1% BSA in PBS. After washing, 1 μM hMD-2 with tested compounds was added and incubated for 2 hours. 0.1 μg/mL mouse anti-hMD-2 MAb (9B4) and 0.1 μg/mL goat anti-mouse IgG conjugated with HRP in PBS were added, followed by detection at 420 nm after the addition of 100 μL of ABTS (Sigma). Chicken anti-hMD-2 polyclonal antibodies were prepared against recombinant hMD-2 by GenTel (Madison, WI, USA), monoclonal mouse anti-hMD-2 9B4 antibodies were from eBioscience (San Diego, CA, USA), and secondary goat anti-mouse IgG conjugated with horseradish peroxidase were from Santa Cruz Biotechnology (Santa Cruz, CA, USA).

Fluorescence spectroscopy assay. Fluorescence was measured on Perkin Elmer fluorimeter LS 55 (Perkin Elmer, UK) as previously described.[88] All measurements were done at 20 °C in a 5 x 5 mm quartz glass cuvette (Hellma Suprasil, Müllheim, Germany). hMD-2 protein (200 nM) and 1,1'-Bis(anilino)-4,4'-bis (naphthalene)−8,8' disulfonate (bis-ANS, 200 nM) were mixed and incubated until reaching stable relative fluorescence units (RFUs) emitted at 420–550 nm under excitation at 385 nm. Compounds, at different concentrations, were then added, followed by relative fluorescence unit (RFU) measurement at 420–550 nm.

LPS displacement assay. The ability of the compounds to displace LPS from hMD-2 hydrophobic pocket was determined by ELISA. A microtiter plate was coated overnight at 4 °C with 100 μL/well of 5 μg/mL of chicken polyclonal anti-hMD-2 antibodies, diluted in 50 mM Na_2CO_3 buffer, pH 9.6 and blocked with 1% BSA in PBS. After washing, 1 μM of hMD-2 with biotin-labeled LPS was added and incubated for 2 hours. After washing, the compounds were added at different concentration and incubated for 1.5 hours. After washing, 0.5 μg/mL HRP-

conjugated streptavidin (Sigma) in PBS was added, followed by detection at 420 nm after the addition of 100 µL ABTS (Sigma). Chicken anti-hMD-2 polyclonal antibodies were prepared against recombinant hMD-2 by GenTel (Madison, WI, USA).

Surface plasmon resonance (SPR) analysis. The binding affinity of the compounds to recombinant hMD-2 was determined using a Biacore X100 with an NTA sensor chip (Biacore, GE Healthcare, Uppsala, Sweden). Briefly, 0.5 µM hMD-2 (in 50 mM TRIS, 150 mM NaCl, 0.5% Tween 20, pH 7.5) was immobilized onto the sensor chip previously activated with 1-min. pulse of 10 mM $NiSO_4$. First flow cell was used as a reference surface to control non-specific binding. Both flow cells were injected with the analyte (in PBS, 5% DMSO, 5% EtOH, pH 7.5) at a flow rate of 10 µL/min at 25 °C in increasing concentrations. The data were analyzed with Biacore Evaluation software. K_D values were calculated by global fitting of the equilibrium binding responses from various concentrations of analytes using a 1:1 Langmuir binding model.

HEK-Blue hTLR4 cells assay. HEK-Blue hTLR4 cells (InvivoGen) were cultured according to manufacturer's instructions. Briefly, cells were cultured in DMEM high glucose medium supplemented with 10% fetal bovine serum (FBS), 2 mM glutamine, antibiotics and 1× HEK-Blue Selection (InvivoGen). Cells were detached using a cell scraper, counted and seeded in a 96-well multiwell plate at a density of 4×10^4 cells per well. After overnight incubation (37 °C, 5% CO2, 95% humidity), supernatants were replaced with new medium w/o FBS supplemented by the compound to be tested and incubated for 16 hours. For the antagonism evaluation, cells were stimulated with LPS (100 ng/mL, *E. coli* O55:B5, Sigma-Aldrich) after compounds pre-treatment and incubated for 16 hours as above. The SEAP-containing supernatants were collected and incubated with *para*-nitrophenyl phosphate (pNPP) for 2−4 h in the dark at room temperature. The wells optical density was determined using a microplate reader (labtech LT-4000) set to 405 nm.

MTT Cell Viability Assay. HEK-Blue hTLR4 cells were grown in DMEM supplemented with 10% FBS, 2 mM glutamine and antibiotics. Cells were seeded in 100 µL of DMEM w/o Phenol Red at a density of 4×10^4 cells per well and incubated overnight (37 °C, 5% CO_2, 95% humidity). Cells were treated with the higher dose of compound used in the previous experiments (10 µM) and incubated overnight. MTT solution (5 mg/mL in PBS) was added to each well and after 3 hours incubation, HCl 0.1 N in 2-propanol solution was used to dissolve formazan crystals. Formazan concentration was determined by measuring the absorbance at 570 nm.

Experiments on RAW 264.7-Blue cells

Murine RAW 264.7-Blue cells (Invivogen) derived from the murine RAW 264.7 macrophages and stably expressing an NF-κB-inducible secreted alkaline phosphatase (SEAP) reporter gene were cultured in Dulbecco's modified Eagle's medium (DMEM), supplemented with 10% Fetal bovine serum (FBS), L-Glutamine (2 mM) and sodium pyruvate (0.4 mM), in the presence of selection antibiotic Zeocin (200 µg/mL). *E. coli* O111:B4 LPS was purchased from Invivogen. Bovine serum albumin (BSA) was purchased from Sigma-Aldrich. Compounds **FP13-17** were reconstituted in DMSO/ethanol to provide a 10 mM stock solution. Further dilutions were made in cell culture medium so that the final amount of DMSO in the cell culture did not exceed 0.05 %. C57BL6/J mice were obtained from Janvier. All animal experiments were approved by the animal ethical committee of Ghent University, Faculty of Sciences. Salmonella enterica LPS used for *in vivo* studies was purchased from Sigma-Aldrich.

Biological activity assay. 5x104 RAW 264.7-Blue cells were pre-treated with compounds **FP13-17** in a total volume of 200 µl serum-free DMEM supplemented with L-Glutamine (2 mM) and sodium pyruvate (0.4 mM). In some experiments DMEM was supplemented with 10% FBS or BSA at the concentrations of 4 mg/mL and 20 mg/mL. 30 min. later, cells were

stimulated with *E. coli* O111:B4 LPS, as indicated. 24 h later cell supernatants were analyzed for SEAP production by the QUANTI-Blue Assay (Invivogen).

Cryo-TEM sample preparation. All samples were prepared in 10 mM buffer phosphate (pH 7.4) with 16% of DMSO. *Cryo-TEM* data were collected on a JEM-2200FS/CR transmission electron microscope (JEOL, Japan), equipped with an UltraScan 4000 SP (4008×4008 pixels) cooled slow-scan CCD camera (GATAN, UK). Three microliters of the compound were vitrified on Quantifoil 2/2 grids, using Vitrobot (FEI) and were analyzed at nitrogen liquid temperature with a TEM operated at 200kV in low dose conditions.

AUTHOR INFORMATION

Corresponding Author

* Prof. Francesco Peri: ✉ francesco.peri@unimib.it; ☎ (+39) 02-6448-3453

Funding Sources

This study was financially supported by the H2020-MSC-ETN-642157 project TOLLerant. RJ was partially funded by the research program P4-0176 by the Slovenian Research Agency.

ACKNOWLEDGEMENTS

TOLLerant project (H2020-MSC-ETN-642157), the Italian Ministry for Foreign Affairs and International Cooperation (MAECI) and Spanish MINECO (CTQ2014-57141-R and CTQ2017-88353-R grants) are acknowledged. Vesna Hodnik of University of Ljubljana for the help with SPR, Sandra Delgado of CIC BioGUNE for the Cryo-TEM images.

Ethical Approval

All animal experiments were approved by the Ethical Committee for Animal Experimentation of Ghent University – Faculty of Sciences.

Author Contributions

FC synthesized all the molecules. FAF performed biological tests on cells. LZ and HB produced and purified the hMD-2 protein. LZ and RJ performed binding tests with hMD-2. FC, JMB and SMS performed the computational chemistry work. FC, HC, JJB performed TEM analysis. AH and RB performed *in vivo* tests and cell experiments. FP supervised the work and wrote the manuscript. FC and SMS contributed to write the manuscript. All authors reviewed the manuscript.

Additional Information

Supplementary information is available to reviewers and Editor

Competing interests:

The authors declare no competing interests.

12. References

1. Czerkies, M. & Kwiatkowska, K. Toll-Like Receptors and their Contribution to Innate Immunity: Focus on TLR4 Activation by Lipopolysaccharide. *Adv. Cell Biol.* **4,** 1–23 (2014).
2. Cario, E. *et al.* Lipopolysaccharide Activates Distinct Signaling Pathways in Intestinal Epithelial Cell Lines Expressing Toll-Like Receptors. *J. Immunol.* **164,** 966–972 (2000).
3. Hailman, E. Lipopolysaccharide (LPS)-binding protein accelerates the binding of LPS to CD14. *J. Exp. Med.* **179,** 269–277 (1994).
4. Lamping, N. *et al.* Effects of site-directed mutagenesis of basic residues (Arg 94, Lys 95, Lys 99) of lipopolysaccharide (LPS)-binding protein on binding and transfer of LPS and subsequent immune cell activation. *J. Immunol.* **157,** 4648–56 (1996).
5. Kim, J. I. *et al.* Crystal structure of CD14 and its implications for lipopolysaccharide signaling. *J. Biol. Chem.* **280,** 11347–11351 (2005).
6. Kelley, S. L., Lukk, T., Nair, S. K. & Tapping, R. I. The Crystal Structure of Human Soluble CD14 Reveals a Bent Solenoid with a Hydrophobic Amino-Terminal Pocket. *J. Immunol.* **190,** 1304–1311 (2013).
7. Walsh, C. *et al.* Elucidation of the MD-2/TLR4 Interface Required for Signaling by Lipid IVa. *J. Immunol.* **181,** 1245–1254 (2008).
8. Park, B. S. & Lee, J.-O. Recognition of lipopolysaccharide pattern by TLR4 complexes. *Exp. Mol. Med.* **45,** e66–e66 (2013).
9. Visintin, A., Mazzoni, A., Spitzer, J. A. & Segal, D. M. Secreted MD-2 is a large

polymeric protein that efficiently confers lipopolysaccharide sensitivity to Toll-like receptor 4. *Proc. Natl. Acad. Sci.* **98,** 12156–12161 (2001).

10. Ohto, U., Fukase, K., Miyake, K. & Shimizu, T. Structural basis of species-specific endotoxin sensing by innate immune receptor TLR4/MD-2. *Proc. Natl. Acad. Sci.* **109,** 7421–7426 (2012).
11. Park, B. S. *et al.* The structural basis of lipopolysaccharide recognition by the TLR4-MD-2 complex. *Nature* **458,** 1191–5 (2009).
12. Palsson-McDermott, E. M. & O'Neill, L. A. J. Signal transduction by the lipopolysaccharide receptor, Toll-like receptor-4. *Immunology* **113,** 153–162 (2004).
13. Akira, S. & Takeda, K. Toll-like receptor signalling. *Nat. Rev. Immunol.* **4,** 499–511 (2004).
14. Ryu, J.-K. *et al.* Reconstruction of LPS Transfer Cascade Reveals Structural Determinants within LBP, CD14, and TLR4-MD2 for Efficient LPS Recognition and Transfer. *Immunity* **46,** 38–50 (2017).
15. Beutler, B. & Poltorak, A. Sepsis and evolution of the innate immune response. *Crit. Care Med.* **29,** S2–S7 (2001).
16. Liu, Y., Yin, H., Zhao, M. & Lu, Q. TLR2 and TLR4 in Autoimmune Diseases : a Comprehensive Review. *Clin. Rev. Allergy Immunol.* **47,** 136–147 (2014).
17. Kuzmich, N. *et al.* TLR4 Signaling Pathway Modulators as Potential Therapeutics in Inflammation and Sepsis. *Vaccines* **5,** 34 (2017).
18. Zaffaroni, L. & Peri, F. Recent advances on Toll-like receptor 4 modulation: new therapeutic perspectives. *Future Med. Chem.* **10,** 461–476 (2018).
19. Peri, F. & Piazza, M. Therapeutic targeting of innate immunity with Toll-like receptor 4 (TLR4) antagonists. *Biotechnol. Adv.* **30,** 251–260 (2012).
20. Shirey, K. A. *et al.* The TLR4 antagonist Eritoran protects mice from lethal influenza infection. *Nature* **497,** 498–502 (2013).
21. Flacher, V. *et al.* Mannoside Glycolipid Conjugates Display Anti-inflammatory Activity by Inhibition of Toll-like Receptor-4 Mediated Cell Activation. *ACS Chem. Biol.* **10,** 2697–2705 (2015).
22. Matsunaga, N., Tsuchimori, N., Matsumoto, T. & Ii, M. TAK-242 (Resatorvid), a Small-Molecule Inhibitor of Toll-Like Receptor (TLR) 4 Signaling, Binds Selectively to TLR4 and Interferes with Interactions between TLR4 and Its Adaptor Molecules. *Mol. Pharmacol.* **79,** 34–41 (2011).
23. Calabrese, V., Cighetti, R. & Peri, F. Molecular simplification of lipid A structure:

TLR4-modulating cationic and anionic amphiphiles. *Mol. Immunol.* **14,** 1–9 (2014).

24. Ciaramelli, C. *et al.* Glycolipid-based TLR4 modulators and fluorescent probes: rational design, synthesis and biological properties. *Chem. Biol. Drug Des.* 1–13 (2016). doi:10.1111/cbdd.12749
25. Peri, F. & Calabrese, V. Toll-like receptor 4 (TLR4) modulation by synthetic and natural compounds : an update. *J. Med. Chem.* **57,** 3612–3622 (2014).
26. Perrin-Cocon, L. *et al.* TLR4 antagonist FP7 inhibits LPS-induced cytokine production and glycolytic reprogramming in dendritic cells, and protects mice from lethal influenza infection. *Sci. Rep.* **7,** 40791 (2017).
27. Kitchens, R. L. & Munford, R. S. CD14-dependent internalization of bacterial lipopolysaccharide (LPS) is strongly influenced by LPS aggregation but not by cellular responses to LPS. *J. Immunol.* **160,** 1920–1928 (1998).
28. Gutsmann, T., Schromm, A. B. & Brandenburg, K. The physicochemistry of endotoxins in relation to bioactivity. *Int. J. Med. Microbiol.* **297,** 341–352 (2007).
29. Schromm, A. B. *et al.* Biological activities of lipopolysaccharides are determined by the shape of their lipid A portion. *Eur. J. Biochem.* **267,** 2008–2013 (2000).
30. Opal, S. M. *et al.* Effect of Eritoran, an Antagonist of MD2-TLR4, on Mortality in Patients With Severe Sepsis. *J. Am. Med. Assoc.* **309,** 1154–1162 (2013).
31. Tamai, R. *et al.* Cell activation by monosaccharide lipid A analogues utilizing Toll-like receptor 4. *Immunology* **110,** 66–72 (2003).
32. Cighetti, R. *et al.* Modulation of CD14 and TLR4·MD-2 Activities by a Synthetic Lipid A Mimetic. *ChemBioChem* **15,** 250–258 (2014).
33. Xu, Y. *et al.* Discovery of novel small molecule TLR4 inhibitors as potent anti-inflammatory agents. *Eur. J. Med. Chem.* **154,** 253–266 (2018).
34. Shirey, K. A. *et al.* Novel strategies for targeting innate immune responses to influenza. *Mucosal Immunol.* **9,** 1173–1182 (2016).
35. Facchini, F. A. *et al.* Co-administration of Antimicrobial Peptides Enhances Toll-like Receptor 4 Antagonist Activity of a Synthetic Glycolipid. *ChemMedChem* **13,** 280–287 (2018).
36. Kusama, T. *et al.* Synthesis and biological activities of lipid A analogs: modification of a glycosidically bound group with chemically stable polar acidic groups and disaccharide backbone with tetradecanoyl or N-dodecanoylglycyl Groups. *Chem. Pharm. Bull.* **39,** 3244–3253 (1991).
37. Liu, W.-C., Oikawa, M., Fukase, K., Suda, Y. & Kasumoto, S. A divergent synthesis of

lipid A and its chemically stable unnatural analogues. *Bull. Chem. Soc. Jpn.* **72,** 1377–1385 (1999).

38. Fujimoto, Y. *et al.* Synthesis of lipid A and its analogues for investigation of the structural basis for their bioactivity. *J. Endotoxin Res.* **11,** 341–347 (2005).
39. Fukase, Y. *et al.* Synthesis of Rubrivivax gelatinosus lipid A and analogues for investigation of the structural basis for immunostimulating and inhibitory activities. *Bull. Chem. Soc. Jpn.* **81,** 796–819 (2008).
40. Mochizuki, T. *et al.* Synthesis and biological activities of lipid A-type pyrancarboxylic acid derivatives. *Carbohydr. Res.* **324,** 225–230 (2000).
41. Lewicky, J. D., Ulanova, M. & Jiang, Z. Improving the immunostimulatory potency of diethanolamine-containing lipid A mimics. *Bioorg. Med. Chem.* **2,** 20–23 (2013).
42. Fort, M. M. *et al.* A Synthetic TLR4 Antagonist Has Anti-Inflammatory Effects in Two Murine Models of Inflammatory Bowel Disease. *J. Immunol.* **174,** 6416–6423 (2005).
43. Johnson, D. A. *et al.* Synthesis and biological evaluation of new class of vaccine adjuvants: aminoalkyl glucosamine 4-phosphates (AGPs). *Bioorg. Med. Chem. Lett.* **9,** 2273–2278 (1999).
44. Johnson, D. a. Synthetic TLR4-active glycolipids as vaccine adjuvants and stand-alone immunotherapeutics. *Curr. Top. Med. Chem.* **8,** 64–79 (2008).
45. Resman, N. *et al.* Essential Roles of Hydrophobic Residues in Both MD-2 and Toll-like Receptor 4 in Activation by Endotoxin. *J. Biol. Chem.* **284,** 15052–15060 (2009).
46. Rajaiah, R., Perkins, D. J., Ireland, D. D. C. & Vogel, S. N. CD14 dependence of TLR4 endocytosis and TRIF signaling displays ligand specificity and is dissociable in endotoxin tolerance. *Proc. Natl. Acad. Sci.* **112,** 8391–8396 (2015).
47. Sestito, S. E. *et al.* Amphiphilic Guanidinocalixarenes Inhibit Lipopolysaccharide (LPS)- and Lectin-Stimulated Toll-like Receptor 4 (TLR4) Signaling. *J. Med. Chem.* **60,** 4882–4892 (2017).
48. Trott, O. & Olson, A. AutoDock Vina: improving the speed and accuracy of docking with a new scoring function, efficient optimization and multithreading. *J. Comput. Chem.* **31,** 455–461 (2010).
49. Morris, G. M. *et al.* AutoDock4 and AutoDockTools4: Automated docking with selective receptor flexibility. *J. Comput. Chem.* **30,** 2785–2791 (2009).
50. Facchini, F. A. *et al.* Structure–Activity Relationship in Monosaccharide-Based Toll-Like Receptor 4 (TLR4) Antagonists. *J. Med. Chem.* **61,** 2895–2909 (2018).
51. Huang, J. X. *et al.* Molecular Characterization of Lipopolysaccharide Binding to Human

α -1-Acid Glycoprotein. *J. Lipids* **2012,** 1–15 (2012).

52. Manček-Keber, M. & Jerala, R. Structural similarity between the hydrophobic fluorescent probe and lipid A as a ligand of MD-2. *FASEB J.* **20,** 1836–1842 (2006).
53. Viriyakosol, S. *et al.* Characterization of Monoclonal Antibodies to Human Soluble MD-2 Protein. *Hybridoma* **25,** 349–357 (2006).
54. Resman, N. *et al.* Taxanes inhibit human TLR4 signaling by binding to MD-2. *FEBS Lett.* **582,** 3929–3934 (2008).
55. Cighetti, R. *et al.* Modulation of CD14 and TLR4×MD-2 activities by a synthetic lipid A mimetic. *ChemBioChem* **15,** 250–258 (2014).
56. Okamoto, T. *et al.* Multiple contributing roles for NOS2 in LPS-induced acute airway inflammation in mice. *Am. J. Physiol. Cell. Mol. Physiol.* **286,** L198–L209 (2004).
57. Poynter, M. E., Irvin, C. G. & Janssen-Heininger, Y. M. W. A Prominent Role for Airway Epithelial NF- B Activation in Lipopolysaccharide-Induced Airway Inflammation. *J. Immunol.* **170,** 6257–6265 (2003).
58. Belpaire, F. M. & Bogaert, M. G. Pharmacokinetic and pharmacodynamic consequences of altered binding of drugs to alpha 1-acid glycoprotein. *Prog. Clin. Biol. Res.* **300,** 337–50 (1989).
59. Zaias, J., Mineau, M., Cray, C., Yoon, D. & Altman, N. H. Reference values for serum proteins of common laboratory rodent strains. *J. Am. Assoc. Lab. Anim. Sci.* **48,** 387–90 (2009).
60. Hashim, R. *et al.* Dry Thermotropic Glycolipid Self-Assembly:A Review. *J. Oleo Sci.* **67,** 651–668 (2018).
61. Kameta, N., Matsuzawa, T., Yaoi, K., Fukuda, J. & Masuda, M. Glycolipid-based nanostructures with thermal-phase transition behavior functioning as solubilizers and refolding accelerators for protein aggregates. *Soft Matter* **13,** 3084–3090 (2017).
62. Baccile, N. *et al.* Self-Assembly Mechanism of pH-Responsive Glycolipids: Micelles, Fibers, Vesicles, and Bilayers. *Langmuir* **32,** 10881–10894 (2016).
63. Cochet, F. & Peri, F. NUOVI ANTAGONISTI DEL TLR4 UMANO. SIB BI5153R, 1–41 (2018).

XII. Cy7N-LOS and Alexa568-LPS for imaging studies

Synthesis of the new cyanine-labelled bacterial endotoxin LOS-Cy7N for intracellular imaging and in vivo microscopy studies

Tung-Cheng Wang[a], Florent Cochet[b], Fabio Alessandro Facchini[b], Lenny Zaffaroni[b], Christelle Serba[c], Simon Pascal[c], Chantal Andraud[c], Olivier Maury[c], Thomas Huser[a], Francesco Peri[b*]

[a] *Biomolecular Photonics, Department of Physics, University of Bielefeld, 33615 Bielefeld, Germany.*

[b] *Department of Biotechnology and Biosciences, University of Milano-Bicocca, Piazza della Scienza, 2; 20126 Milano, Italy.*

[c] *Univ. Lyon, ENS de Lyon, CNRS UMR 5182, Université Lyon 1, Laboratoire de Chimie, 46 Allée d'Italie, 69364 Lyon Cedex 07, France.*

1. Abstract

Fluorescent LPS/LOS are fundamental molecular tools for the investigation of their distribution into the body and the understanding of receptor-dependent cellular trafficking of gram-negative bacteria endotoxins. Cy7 derivatives are known for their fluorescence in the near-infrared region providing an excellent contrast on biological samples. We exploited the far-red fluorescence emission of amino-heptamethine fluorophore (Cy7N), possessing a large Stokes-shift. The fluorophore Cy7N, featuring sulfonate side-chains, provides a good solubility in aqueous medium and the central amino substitution, while allowing a convenient bio-conjugation to LOS, confers optimal optical properties: important stokes shift and strong emission in the biological transparency window, increasing the imaging contrast. It was showed that Cy7N conjugated to LOS can be excited by default filter-set of Cy5 and fluoresces into deep red spectrum for low-background imaging. The large Stoke-shift feature of Cy7N permits to obtain two-colors images by using one excitation for double-labelling of two cyanine dyes. Contrarily to commercially available fluorescent LPS, LOS-Cy7N was purified by chromatography with a high level of chemical purity. The study demonstrates that LOS internalization is CD14-dependent but, by co-treatment of two types of fluorescent endotoxins, it was showed for the first time that LOS and LPS undergo different internalization speed in cells: endocytosis of LOS is much faster than LPS upon cell surface binding.

2. Introduction

Endotoxins (lipopolysaccharide, LPS and its truncated version lipooligosaccharide, LOS), also defined as pathogen-associated molecular patterns (PAMPs), are very toxic molecules released from the cell wall of gram-negative bacteria (GNB) and they are able to activate host inflammatory and immune response at picomolar concentrations through the interaction with a specific pattern recognition receptor (PRR), the Toll-like Receptor 4 (TLR4). Severe sepsis and septic shock are life-threatening pathologies still lacking pharmacological treatment deriving from excessive TLR4 activation by circulating bacterial endotoxins.[1]

Endotoxins and other PAMPs are also fundamental molecular players in the communication of gut microbiota with other organs and body districts, including the central nervous system.[2] LPS activation of endothelial TLR4 in the brain has recently been proposed as a model of pathogenesis for brain diseases, including cerebral cavernous malformations (CCMs) that are a cause of stroke and seizures.[2] In this model, GNB in the gut are the source of LPS that enters circulating blood, activates brain endothelial TLR4 receptors, and, in turn, drives intracellular signaling to induce the pathology. The ability to track endotoxins in the body can therefore provide some important information about the molecular mechanisms by which intestinal microbial communities influence other organs and communicate with the brain, while the possibility to visualize TLR4-mediated LPS transport in cells can be used to clarify molecular mechanisms of TLR4 activation and signaling.

LPS is transported to cell membranes by the sequential action of LPS-binding protein (LBP) and CD14. LBP acts to transfer LPS monomers out of LPS aggregates to a binding site on CD14, the LPS-CD14 complex then facilitates LPS transfer to TLR4-bound MD-2 adaptor and the formation of the activated homodimer $(TLR4/MD\text{-}2/LPS)_2$.[3] Ligand-induced formation of the TLR4/MD-2 homodimer on the plasma membrane of TLR4-HEK cells has recently been investigated using fluorescently-tagged TLR4 and quantitative single-molecule localization microscopy (SMLM).[4] Interestingly, 48% of fluorescent TLR4 molecules on the cell membrane were present as dimers even in the absence of LPS. The addition of *E. coli* LPS agonist induced the formation of 74% dimer, while the treatment with the antagonist Rhodobacter sphaeroides LPS gave 100% monomeric TLR4.

Once bound to MD-2 and associated to TLR4 into the homodimer, LPS initiates two independent signal pathways:[5,6] the MyD88-dependent pathway, which starts at the cell membrane with the formation of the Myddosome,[7] a macromolecular signaling complex formed by MyD88 and IRAK members leading to NF-κB activation and production of inflammatory cytokines. Alternatively, the TRIF-dependent pathway is activated which signals from the early endosomes, and also leads to the formation of the supramolecular Triffosome complex to drive type I interferon production and delayed NF-κB activation.[8]

Data using single molecule fluorescence (SMF) show that LPS stabilizes preformed TLR4/MD2 dimers to drive signaling,[4] however other published studies suggest that, under certain circumstances, TLR4 clustering may occur.[9] While the majority of biophysical studies on LPS/TLR4 have used fluorescently-labelled TLR4 to determine its localization on the cell membrane, leading to eventual clustering and endocytosis of the TLR4 receptor complex (containing also CD14 and MD-2 receptors), fluorescent LPS/LOS are fundamental molecular tools for investigating the body distribution and receptor-dependent cellular trafficking of GNB endotoxin. Moreover, the conjugations of fluorescent agents reported so far were accomplished solely with LPS,[10-13] by which the fluorophores were chemically attached to the hydroxyl groups of O-antigen which is absent in LOS. Therefore, the labelling on LOS is still undocumented and should provide useful complementary information.

To that end we thought to use cyanine-based fluorophores widely used in protein labelling for microscopic imaging[14,15] and in particular Cy7 derivative known for their fluorescence in the near-infrared region (NIR) providing an excellent contrast on biological samples. However, Cy7 dyes suffer some inherent drawbacks such their very small Stockes-shift making the imaging experiment more difficult. Here, we explored the possibility to exploit the far-red fluorescence emission of amino-heptamethine fluorophore (Cy7N), featuring larger Stokes-shift.[16] These dyes where functionalized with a carboxyl-diethylenglycolamine (CDE) linker to label LOS endotoxin through the reaction with a nucleophilic phosphoethanolamine group on LOS to obtain the fluorescently-tagged LOS-Cy7N conjugate for *in vitro* microscopy studies. The cyanine fluorescent scaffold has already been used for numerous imaging applications including intracellular pH determination or ion sensing,[17-19] as contrast agent for surgery,[20] and for cancer detection and therapy.[21-23] Cy7N was chosen specifically, because it combines some particularly interesting photophysical properties,[14,15] with the possibility to functionalize the central cyclohexene moiety with linkers containing terminal reactive groups for bio-

conjugation (as CDE-Cy7N, structure **6**, Fig. 84). The intense fluorescence of Cy7N is localized in the far-red to NIR (λ_{em} = 764 nm), in the biological transparent window where absorption and scattering of biological material are minimum.[24] These dyes are further characterized by a large Stokes shift (Δ = 3440 cm^{-1}) and consequently enable bio-imaging experiment with an improved signal-to-noise ratio. In the present study we successfully label the LOS with Cy7N. The fractions of conjugates were well isolated by chromatography, verified on gel electrophoresis and tested on its immunostimulatory activity before it was applied on cell imaging by confocal fluorescence microscopy. The use of Cy7N-labeled LOS enables us for the first time to explore its cell binding, internalization and vesicle transportation in CD14-transfected HEK-293T cells.

3. Synthesis of conjugable CDE-Cy7N

The Cy7N fluorophores were designed introducing sulfonate functions to optimize their solubility in biological media, while the rigidity of the heptamethine skeleton was ensured by a *tert*-butyl cyclohexenyl framework, limiting fluorescence losses by nonradiative deexcitation.[25] The synthesis of the reference amino-heptamethine Cy7N (compound **4,** Figure 84) and carboxyl-diethylenglycolamine (CDE)-functionalized Cy7N (CDE-Cy7N, compound **6**) was carried out using classical conditions.[26,27] Briefly, the corresponding chloro-heptamethine precursor was substituted in presence of *n*-propylamine or 2-[2-(2-aminoethoxy)ethoxy]acetic acid in DMF to afford dyes **4** and **6** as blue solids in 45% and 25% yields, respectively (Scheme S1).

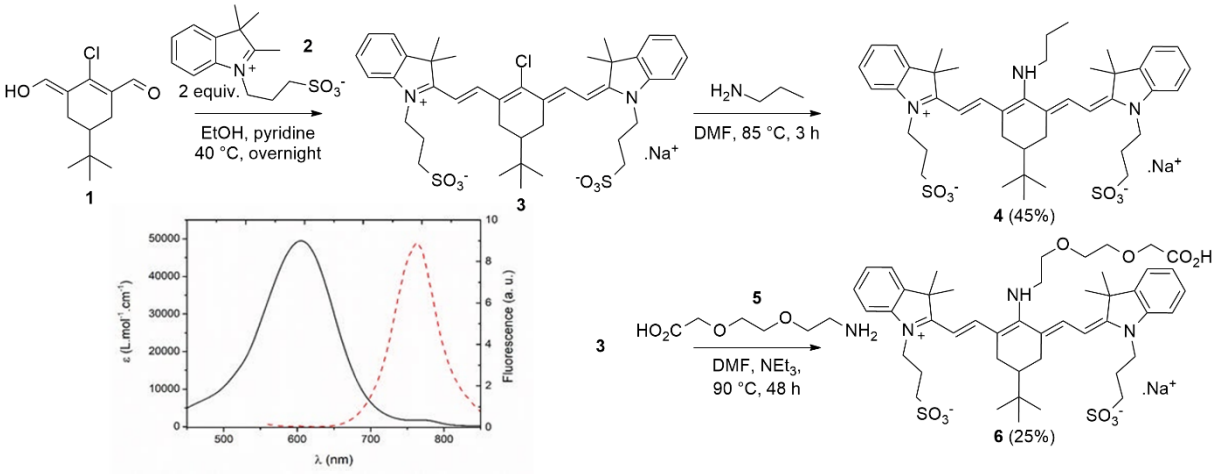

Figure 84. Synthesis of the reference amino-heptamethine dye (Cy7N, 4) and corresponding functionalized analogue (CDE-Cy7N, **6**). Absorption (black, plain line) and fluorescence (red, dashed line) spectra of **4** in water. λ_{abs} = 605 nm; λ_{em} = 764 nm; ϕ_{fl} = 0.06.

4. Site-specific bioconjugation of CED-Cy7N to LOS

LOS (10 mg, 1 equiv.) extracted and purified from *E. coli* strain MG1655, bearing two nucleophilic ethanolamine functions on sugar phosphates (Figure 85), was dissolved in imidazole/HCl buffer (pH = 6.2). CDE-Cy7N **6** (5 equiv.) was added together with the condensing agent 1-ethyl-3-(3-dimethylaminopropyl) carbodiimide (EDC, 5 equiv.), and a catalytic amount of the acyl-transfer catalyst N-hydroxy succinimide (NHS). The mixture was stirred overnight at room temperature, then extracted with dichloromethane and the aqueous phase containing the conjugation product was purified by chromatography through 2 cycles of PD-10 column giving LOS-Cy7N. The purity of the conjugate was assessed by discontinuous SDS-PAGE (18% separating gel and 5% stacking gel) and silver staining (Fig. 85). The attachment of CDE-Cy7N to LOS has been designed to be site-specific on the ethanolamine group on LOS phosphates. LOS-Cy7N was lyophilized and stored at – 20 °C.

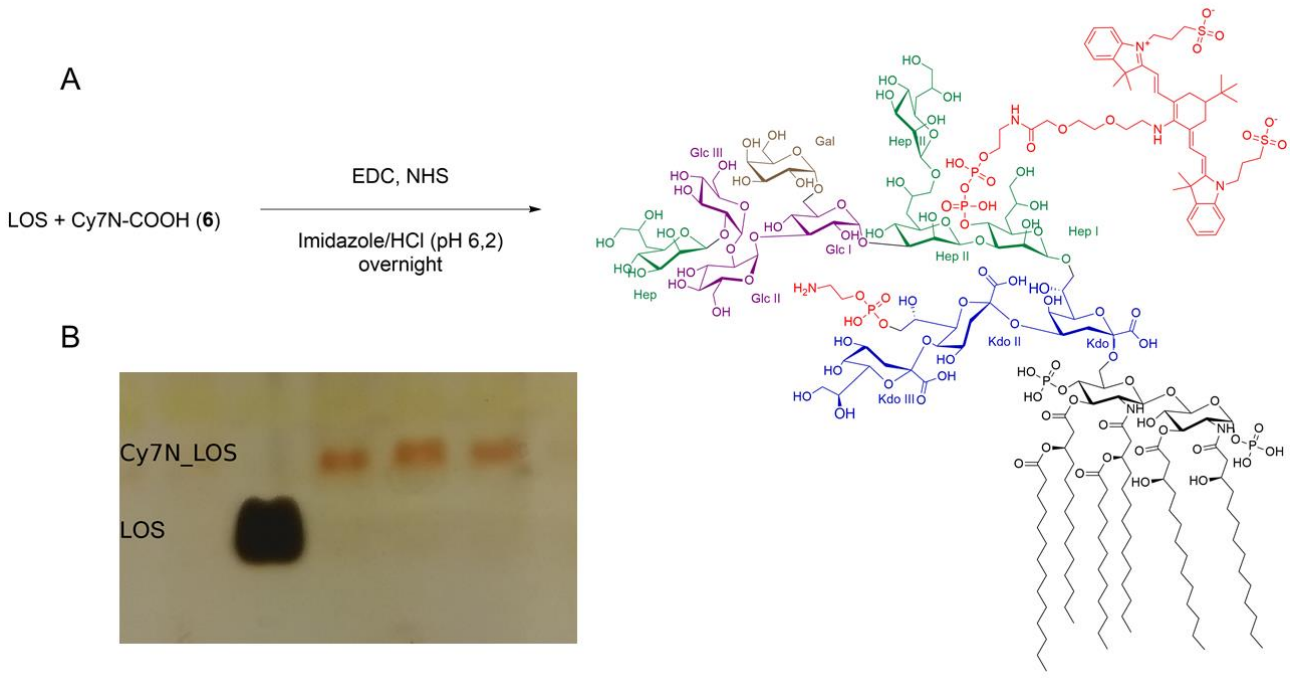

Figure 85. Fluorescence labelling of E. coli LOS (**A**) Fluorescence labelling of *E. coli* LOS with CDE-Cy7N **6** give rise to Cy7N-LOS. Please note that the conjugation of CDE-Cy7N could occur with one or both ethanolamine phosphates (only mono-labelling was observed). (**B**) SDS-PAGE of three fractions recovered after two PD-10 columns revealed by silver staining.

5. Optical properties of the Cy7N fluorophore and its conjugates

The photophysical properties of this type of cyanine dyes were investigated in the reference fluorophore Cy7N **4** and fluorescence spectra were recorded in water (Figure 84). The chromophore presents a broad absorption band centred at 605 nm and an emission in the far-red range, characterized by a particularly large Stokes shift (*ca.* 3440 cm^{-1}). The fluorescence

quantum yield is however noticeably decreased in water, as already reported for analogous polymethine derivatives.[25] Introduction of functional group on CDE-Cy7N **6** has no influence on the optical properties.[25,27,28]

To know if LOS-Cy7N retains such properties for biological applications, we directly recorded the spectra from living cells briefly treated with LOS-Cy7N on the confocal microscope. Using supercontinuum laser, which provides variable laser lines in visible range, an excitation spectrum scanning can be assessed by imaging-based intensity measurement. On the other hand, we can also choose a fixed excitation laser line and move the detection slit step by step to get emission spectrum. All images were taken on CD14-transfected cells treated with LOS-Cy7N, then briefly washed and maintained in PBS during acquisition. The results from live-cell image scanning were plotted together with those of CDE-Cy7N **6** obtained by fluorimeter (Fig. 86). The excitation spectrum of LOS-Cy7N on living cells measured was consistent with that of CDE-Cy7N **6** despite some fluctuations among individual image frames. However, the peak of emission spectrum (λ_{ems} = 705 nm) of live cell-binding LOS-Cy7N was surprisingly blue-shifted by approximately 50 nm. This can possibly be due to the protonation of the Cy7N itself because it is known to be sensitive to pH change as it is internalized into cell compartments (e.g. lysosomes) where the acidity can play a crucial role[18] or it may be due to the cell environment (interaction with biological sample).

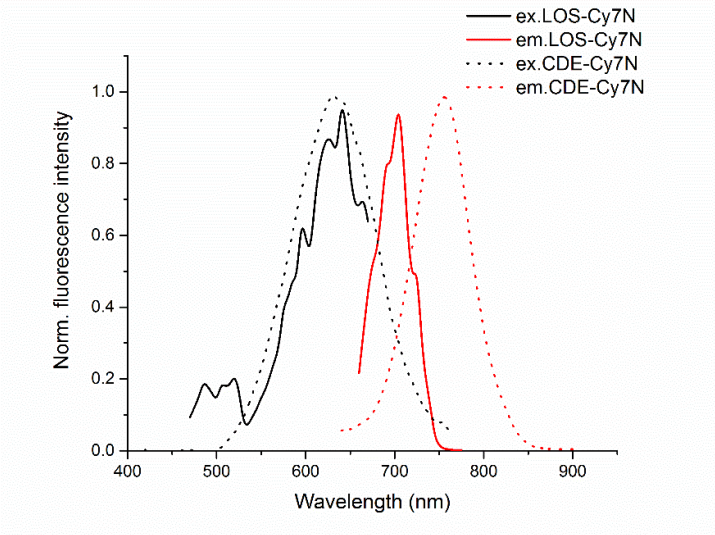

Figure 86. Normalized excitation (ex) and emission (em) spectra of CDE-Cy7N 6 in solution and LOS-Cy7N in living cells. 1mg/mL of CDE-Cy7N **6** was used to measure the excitation and emission spectra on a spectrophotometer (λ_{exc} = 630 nm; λ_{em} = 755 nm). The spectra of LOS-Cy7N were assessed directly on the confocal scanning microscope. The excitation curve was obtained by changing excitation laser lines (470-670 nm) in constant power mode while the fluorescence signal (690-800 nm) was detected in photon-counting mode of the hybrid detector (HyD) with pinhole size set to 2 Airy disk units. The emission plot was obtained with a fixed 633 nm laser line and signals were collected by 5 nm stepwise movement of detection sliders and the intensity was corrected by the quantum efficiency of the HyD.

6. Evaluation of LOS-Cy7N bioactivity

The bioactivity of LOS-Cy7N in terms of capacity to activate TLR4 was assayed on HEK-Blue hTLR4 reporter cells. This cell line has stable expression of all proteins of TLR4 receptor complex, namely TLR4, MD-2 and membrane-bound CD14, and an inducible secreted embryonic alkaline phosphatase (SEAP) reporter gene placed under the control of transcription factors NF-κB and AP-1. The activation of TLR4-mediated MyD88-dependent pathway induces the activation of NF-κB and AP-1 leading to production and secretion of SEAP in the cell culture media. The levels of SEAP can be easily determined by incubating the enzyme with *para*-nitrophenyl phosphate (pNPP). Cells were treated with increasing concentrations of both fluorescently-labelled LOS-Cy7N and LOS (10^{-7} to 10^{1} μg/mL), and SEAP levels were quantified after 16 hours of incubation. The results revealed that LOS-Cy7N was active in inducing TLR4 activation, though the addition of Cy7N fluorophore partially reduced the immunogenicity compared to LOS (Fig. 87). Although the potency of LOS-Cy7N as TLR4 agonist is three order of magnitude lower than LOS (EC_{50} of LOS-Cy7N and unconjugated LOS are, respectively, 0.1 μg/mL and 0.45 ng/mL respectively), Cy7N-labeled LOS activates TLR4 pathway in a comparable way than the unlabelled molecule at a concentration of 1 μg/mL.

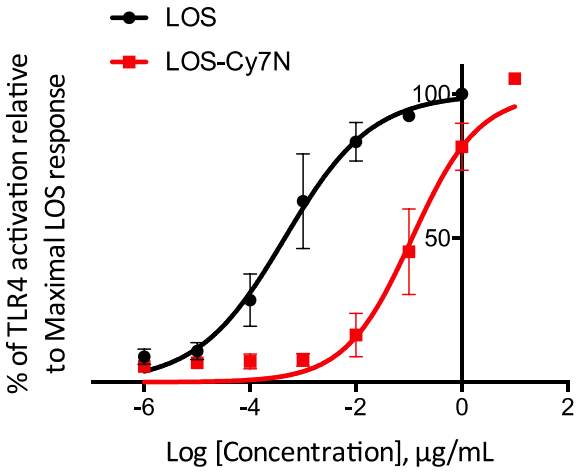

Treatment	EC_{50} (μg/mL)
LOS	$4.5 \cdot 10^{-4}$
LOS-Cy7N	$1.1 \cdot 10^{-1}$

Figure 87. Bioactivity of LOS-Cy7N and unconjugated LOS in HEK-Blue hTLR4 cells. Cells were treated with the indicated concentrations of LOS-Cy7N and unconjugated LOS and incubated for 16 hours. Supernatants were collected and SEAP levels were quantified by pNPP assay as indicator of TLR4 activation. Data were normalized compared to maximal TLR4 activation obtained by stimulating cells with 1 μg/mL LOS. Concentration-dependent data were fitted to a sigmoidal four-parameter logistic equation to determine EC_{50} values. Data points represent the mean of percentage ± SEM of at least three independent experiments. EC_{50} values for Cy7N-labeled and unconjugated LOS are shown in the table on the right.

7. Cell imaging of Cy7N-labeled LOS

In the present work the application of conjugated LOS was performed in cellular assays through imaging by confocal fluorescence microscopy. Since the LOS-Cy7N has TLR4 agonist properties it very likely directly binds to CD14 co-receptor and to MD-2. We chose to transiently express CD14 in HEK-293T cells because the introduction of CD14 in non-immune cells was shown to evaluate the binding ability of fluorescently labelled LPS[13] and it is also required to promote inflammatory endocytosis.[29,30] In one hour of incubation the fluorescent signal of Cy7N-LOS was found in CD14-positive cells which were immunolabeled with the corresponding antibody, but not in the cells which did not express CD14 after transfection (Fig. 88A). It is indicated that the LOS retains its ability to bind to the cells after bioconjugation and the binding is a CD14-dependent, which is consistent with the observations by using Cy5-LPS.[31]

In single cell level LOS-Cy7N was noticeably found on the plasma membrane but primarily in internalized vesicles (Fig. 88B), which suggested that CD14 promotes the uptake of LOS-Cy7N into the early endosomes. We expected to observe co-internalization of membrane-bound CD14 with LOS-Cy7N. However, CD14 was predominantly produced as soluble form in the cytoplasm. It is logically assumed that only a limited amount of CD14 gained the glycosylphosphatidylinositol inositol (GPI) linker to be anchored to the plasma membrane, where its presence is overwhelmed by cytoplasmic one and thus beyond the detection of single optical section of confocal microscopy. Therefore, we were unable to detect colocalization of membrane-bound CD14 with LOS-Cy7N (Fig. 88B). For comparison to previously reported fluorescent ligands,[13] we used Alexa 488-conjugated LPS to treat the cells in the same condition. Although the binding of LPS-Alexa488 was also found on the CD14-expressing cells, it mainly resided on the cell surface without obvious internalization (Fig. 88C). This is the first direct comparison of cellular uptakes between fluorescent LOS and LPS, and the striking difference between the two localizations suggests that LOS-Cy7N seems to be internalized faster than LPS-Alexa488 in the early time point. To further investigate the uptakes of the two fluorescent endotoxins, we then treated the cells with both ligands and prolonged the incubation time to more than two hours. The result of the cotreatment showed that LPS-Alexa488, although primarily located on the plasma membrane, could be internalized as well and even together with LOS-Cy7N in the extended incubation (Fig. 89). The observation of cell treatment revealed that the efficiency of the LOS-Cy7N internalization is better than the one previously reported. The delayed uptake of LPS-Alexa488 could be explained by either the

fluorophores have direct impact on endocytosis or different uptake mechanisms are used for each type of endotoxin molecules. Nonetheless, it is well characterized that once the LPS are internalized they undergo endocytic pathway to be processed, degraded in lysosomes which is important for signal termination.[32] To see if the LOS-Cy7N are directed in the same route, cells were treated with LOS-Cy7N and LysoTracker Green (Fig. 90). Here we also identified that a subset of the endocytosed LOS-Cy7N was indeed colocalized with lysosomal marker, which indicates that they were sorted to lysosomes for detoxification.

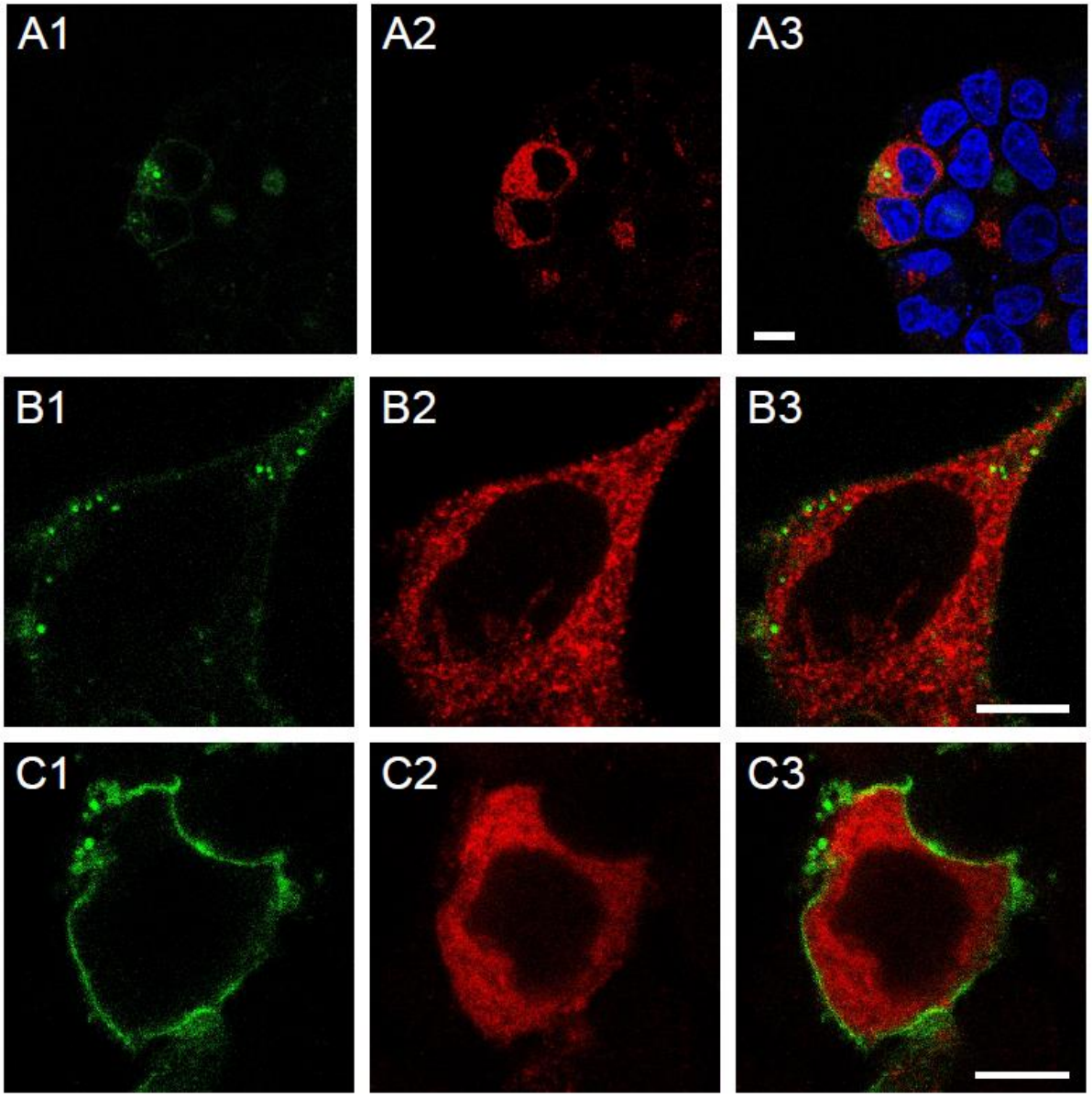

Figure 88. Specific binding of LOS-Cy7N and LPS-Alexa488 to CD14-transfected HEK-293T cells imaged by confocal fluorescence microscopy. Cells were treated with LOS-Cy7N (green, **A** and **B**) and LPS-Alexa488 (green, **C**) for 60 min, respectively, fixed and followed by immunostaining with anti-CD14 antibody (red). (**A**) LOS-Cy7N is visualized on two CD14-expressing cells whereas it is absent in other cells. Here, all nuclei were countered stained with DAPI (blue). (**B**) The cell surface bound LOS-Cy7N is rapidly internalized into the CD14-immunopositive cells as endosomal vesicles, (**C**) while

LPS-Alexa488 mostly resided on the plasma membrane and formed clusters outside of the cells via possible exocytosis. Scale bar = 10 μm.

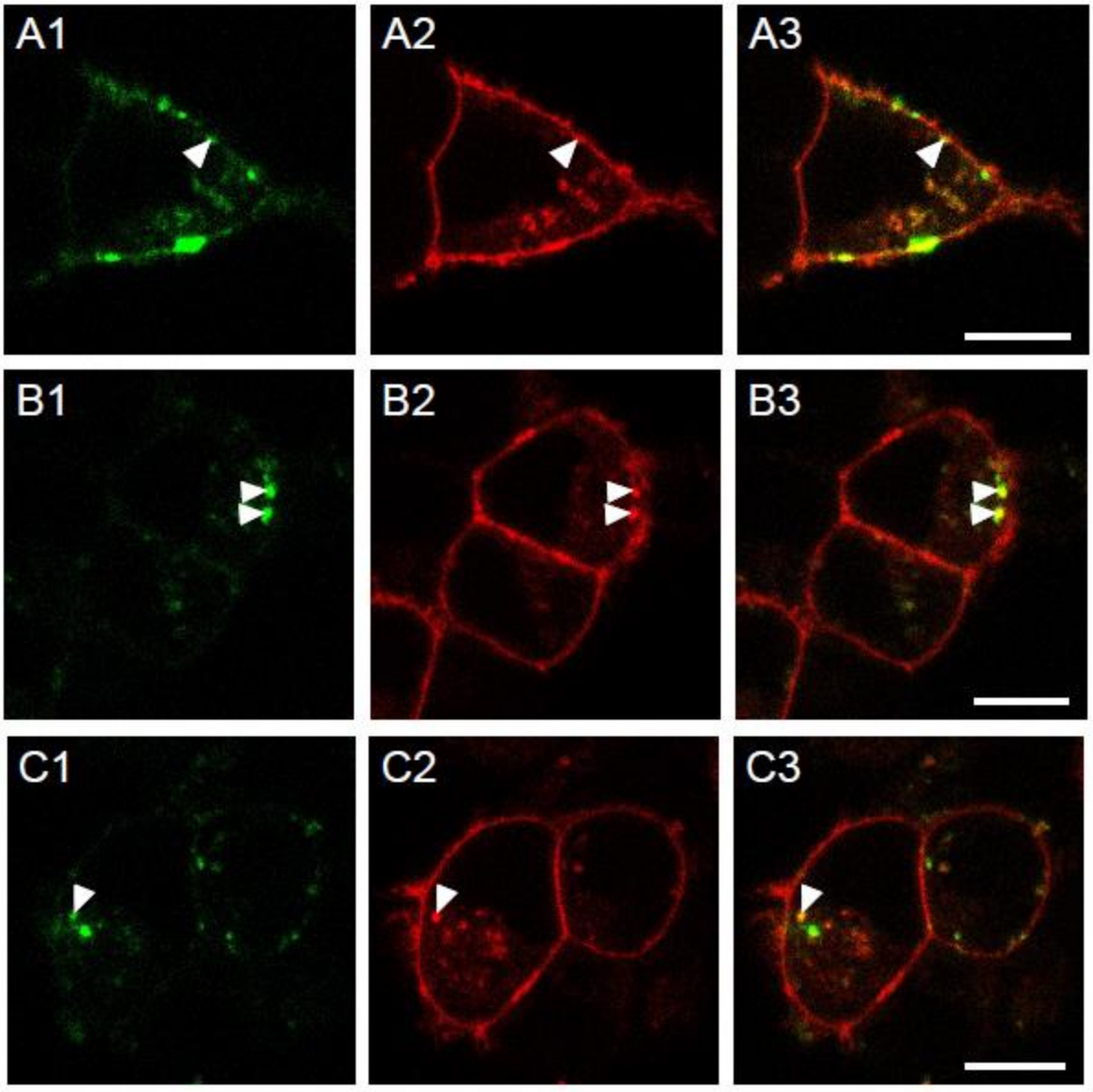

Figure 89. Confocal microscopic images of transfected HEF-293T cells co-treated with LOS-Cy7N (green) and LPS-Alexa488 (red) for two hours. Colocalization of the two ligands is found on the cell surface (**A**), in endosomal vesicles just beneath the plasma membrane (**B**) and in the cytoplasm (**C**). Arrows depict the colocalization of the two endotoxin ligands. Note that fluorescent ligands are not homogeneously distributed on cell surface, they instead appear as organized domain structures which are more pronounced for LOS-Cy7N. Scale bar = 10 μm.

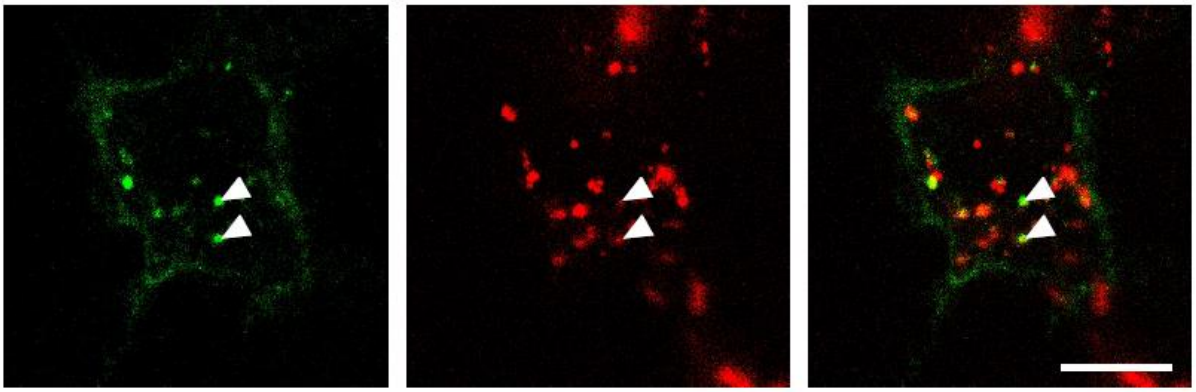

Figure 90. Subcellular localization study of internalized vesicles. Cells were first treated with LOS-Cy7N (green), briefly washed with PBS, then incubated with lysotracker (red) before imaging. The arrowheads depict the overlapped endosomes. Scale bar = 10 nm.

8. Discussion

The fluorophore Cy7N, featuring sulfonate side-chains provides a good solubility in aqueous medium which is a critical parameter for imaging. Importantly, the central amino substitution, while allowing a convenient bio-conjugation to LOS, confers optimal optical properties such as an important Stokes shift and a strong emission in the biological transparency window which are highly beneficial for imaging contrast. We showed here that Cy7N can be excited by default filter-set of Cy5 and fluoresces into deep red spectrum for low-background imaging. The large Stoke-shift feature of Cy7N, which trespasses beyond the Cy5 emission, also permits to obtain two-colours images by using one excitation for double-labelling of two cyanine dyes.

The Cy7N derivative **6**, functionalized on the central nitrogen atom with an ethylene glycol carboxyl linker was successfully conjugated to the amino group of LOS extracted from *E. coli,* that is very toxic and is the natural agonist of TLR4. Contrarily to commercially available fluorescent LPS, the fluorescently labelled endotoxin LOS-Cy7N was purified by chromatography with a high level of chemical purity.

It was deduced that only one dye was bonded to LPS since electrophoresis demonstrated a homogeneous average molecular weight and the photo-bleaching assay showed only one drop of intensity.

The conjugation reaction consists of amide formation by condensation between the carboxyl group of CDE-Cy7N and the ethanol amino group on LOS phosphates (Fig. 85). This site-specific attachment turned out to be important to partially retain the activity of the conjugate as TLR4 agonist. The LOS-Cy7N conjugate was active to stimulate human TLR4 in HEK-blue cells with a lower potency than LOS.

The use of Cy7N as a fluorescent tag for biological events was proved with cell images on the confocal microscope. The CD14 coreceptor plays a pivotal role in both endotoxin presentation to TLR4/MD-2 and in the internalization of homo-dimeric (TLR4/MD-2/ligand)$_2$ complex. In particular CD14 is required for TLR4 internalization[29,30] and LPS[31] into the endosomal network. Our study of using the newly synthesized LOS-Cy7N clearly showed that OS internalization is also CD14-dependent and by cotreatment of two types of fluorescent endotoxins, we for the first time showed the different internalization speed of endotoxins in the cells: the LOS undergoes the endocytosis much faster than LPS upon cell surface binding. The molecular mechanism of CD14-mediated endocytic pathway is however less understood: Tyrosine kinase Syk and PLCγ2 are involved as downsteam effectors for LPS-induced endocytosis of TLR4.[30] Both clathrin and dynamin were proposed for the formation of LPS-internalized vesicles.[32,33] It would be interesting to know if the above-mentioned mechanisms also apply for LOS or other approaches help facilitate the internalization of LOS.

The formation of internalized endotoxins in early endosomes provides the second signaling source other than MyD88-dependent pathway. It is triggered through the adaptors TRAM and TRIF.[34,35] These adaptors mediate the activation of the transcription factor interferon regulatory factor-3 (IRF3), which regulates type I interferon (IFN) expression.[6] Since the LOS-Cy7N was internalized at early time points, while LPS remained in plasma membrane, the timing of signal triggers may result in different cell responses upon stimuli. For instance, LOS-induced cytotoxicity may largely rely on endosomal signaling rather than MyD88-dependent signaling and thus promotes different cell reactions as compared with the cell surface-bound LPS in the first phase of cell activation. In fact, different mechanism of actions between two types of endotoxins has been shown that the LOS can activate inflammasome in dendritic cells in the absence of other accessories which are otherwise required for LPS.[36]

Ectopically expression of CD14 in HEK-293T cells proved to be essential for both surface binding and subsequent internalization of LOS-Cy7N and LPS-Alexa488, of which the non-transfected cells are not capable. However, we did not observe the presence of membrane-bound CD14 (mCD14) on confocal microscope. Perhaps it would be possible to visualize mCD14 on total internal reflection fluorescence microscope, by which the localization of mCD14 on cell surface could be detected and its colocalization with fluorescent endotoxins can be clearly determined. Interestingly, similar study was conducted by introducing mCD14-EGFP

in U373 cells, where its expression was expressed intensively on cell surface. The authors also found that internalized BODIPY-LPS did not colocalize with mCD14-EGFP, suggesting that mCD14 did not accompany LPS during endocytic movement.[37] Such phenomenon would likely depend on cell types as the LPS-induced CD14 internalization was obviously shown in macrophages by flow cytometry.[30] However, whether mCD14, at least in imaging-based study, is internalized together with the TLR4-LPS receptor complex is still an open question.

LOS-Cy7N showed interesting physicochemical properties for the microscopy of biological media, and its use as a tagged tool to study the role of endotoxin molecules in the dialogue between gut microbiota and other body organs included gut-brain axis can be envisaged.

9. Materials and methods

Synthesis. ^{1}H NMR spectra was recorded on a Bruker Advance operating at 500.10 MHZ. Data are listed in parts per million (ppm) and are reported relative to residual solvent peaks being used as internal standard. High resolution mass spectrometry measurements were performed at Centre Commun de Spectrometrie de Masse (Villeurbanne, France). Starting materials were purchased from Sigma Aldrich®, Acros Organics® or Alfa Aesar® with the best available quality grade. All reactions were routinely performed under argon atmosphere in anhydrous solvents. Column chromatography were performed using Acros Organics® (0.035-0.070 mm) silica gel or neutral aluminium oxide (50-200 µm, 60 Å). Compounds **1**,[38] **2**,[39] **3**[26] and **4**[26] were prepared following previously reported protocols. **5** is simply prepared from the commercially available Fmoc-protected compound.

Compound 6. 100 mg of **3** (0.12 mmol, 1 equiv.) and 59 mg of **5** (0.36 mmol, 3 equiv.) were dissolved in 3 mL of anhydrous DMF and 150 µL of Et_3N (9 equiv.) were added. The mixture was stirred at 80 °C for 2 days in the dark. After the solution was cooled down to room temperature, the solvent was evaporated under reduced pressure. The crude was dissolved in 1 mL of brine, and 2 mL of H_2O and was purified on automatic column (reverse phase bonded silica, C18-HP, 30 µm). The elution started with a mixture of H_2O:MeCN (90:10) and ended with 100% MeCN. After evaporation of the MeCN, water was removed by lyophilization overnight to afford the product as a blue solid in a 25% yield (26 mg).

^{1}H NMR (CD_3OD, 300 MHz, 25 °C): δ 7.82 (d, ^{3}J = 13 Hz, 2H), 7.38 (d, ^{3}J = 7 Hz, 2H), 7.30 (t, ^{3}J = 7 Hz, 2H), 7.18 (d, ^{3}J = 8 Hz, 2H), 7.08 (t, ^{3}J = 7 Hz, 2H), 5.99 (d, ^{3}J = 13 Hz, 2H), 4.17

(t, ^3J = 7 Hz, 4H), 4.12 (s, 2H), 3.93 (t, 2H), 3.79 (t, 2H), 3.78 (s, 2H), 2.93 (t, ^3J = 6 Hz, 4H), 2.82 (m, 2H), 2.20 (q, ^3J = 6 Hz, 4H), 2.03 (t, ^3J = 13 Hz, 2H), 1.70 (s, 6H), 1.69 (s, 6H), 1.31 (m, 1H), 1.09 (s, 9H). **^{13}C NMR (CD_3OD, 125.75 MHz, 25°C):** 172.8, 168.0, 143.0, 140.0, 139.7, 128.1, 122.6, 121.7, 108.8, 94.5, 70.3, 69.9, 68.0, 66.4, 49.6, 44.8, 44.3, 41.5, 39.1 32.3, 27.8, 27.7, 26.3, 26.2, 23.2, 22.1. **HRMS (ESI$^-$)**: $[M]^-$ = 880.3845 (calc. for $C_{46}H_{62}N_3O_{10}S_2$: 880.3882). **UV-Vis (CH_3OH)**: λ_{max} = 630 nm (ε_{max} = 76500 $L.mol^{-1}.cm^{-1}$).

Absorption and fluorescence

UV-visible-NIR absorption spectra were recorded on a Jasco® V-670 spectrophotometer in spectrophotometric grade solvents (ca. 10^{-5} mol L^{-1}). Molar extinction coefficients (ε) were precisely determined at least two times. The luminescence spectra were measured using a Horiba-Jobin Yvon Fluorolog-3® Spectro fluorimeter, equipped with a three slit double grating excitation and emission monochromator with dispersions of 2.1 nm/mm (1200 grooves/mm). The steady-state luminescence was excited by unpolarized light from a 450W xenon CW lamp and detected at an angle of 90° for diluted solution measurements (10 mm quartz cuvette) by a red-sensitive Hamamatsu R928 photomultiplier tube. Spectra were reference corrected for both the excitation source light intensity variation (lamp and grating) and the emission spectral response (detector and grating). Fluorescence quantum yields Q were measured in diluted solution with an optical density lower than 0.1 using the following equation $Q_x/Q_r = [A_r(\lambda)/A_x(\lambda)][n_x^2/n_r^2][D_x/D_r]$ were A is the absorbance at the excitation wavelength (λ), n the refractive index and D the integrated intensity. "r" and "x" stand for reference and sample. Excitation of reference and sample compounds was performed at the same wavelength. Cresyl violet was used as reference (ϕ_{fl} = 0.55 in MeOH).

LOS extraction and purification

For lipooligosaccharide (LOS) extraction, *E. coli* strain MG1655 was grown at 37 °C in LD for 16 hours. Culture was aseptically diluted 1:100 in fresh medium and grown until mid-logarithmic phase (OD_{600} = 0.7-0.8). Cells were harvested by centrifugation (5000 G, 20 min), washed in 50 mM NaH_2PO_4 pH 8.0 and cell pellets were stored at – 20 °C before extraction. LOS was selectively extracted from dry cell pellets using phenol chloroform-light petroleum (PCP) procedure.[40] Briefly, a solution of aqueous 90% phenol chloroform-light petroleum (2:5:8 v/v/v), to which solid phenol was added until limpidness, was prepared. Dry cell pellets were suspended in PCP solutions (2.5%, w/v), stirred for 30 minutes and extracted three times.

Then, the light solvents were removed under vacuum and LOS was precipitated from the remaining phenol solution by adding water. The solid was centrifuged, collected, suspended in water and dialyzed (cut-off 1000 Da) against distilled water for 3 days. Finally, it was lyophilized, and pure LOS was recovered. Samples obtained from this procedure was analysed by discontinuous SDS-PAGE (Sodium Dodecyl Sulphate Polyacrylamide Electrophoresis). The gel was prepared with 15% separating gel and 5% stacking gel. The gel was stained according to the silver stain procedure for lipopolysaccharide.[41]

HEK-Blue hTLR4 cells

HEK-Blue hTLR4 cells (InvivoGen) were cultured according to manufacturer's instructions. Briefly, cells were cultured (37 °C, 5% CO_2, 95% humidity) in DMEM high glucose medium supplemented with 10% foetal bovine serum (FBS), 2 mM glutamine, antibiotics and 1× HEK-Blue Selection (InvivoGen).

Confocal microscopy

HEK-293T cells and hCD14 plasmid were gifts of Dr. Roman Jerala (Chemistry Institute, Slovenia). Cells were seeded in glass-bottom imaging chambers (ibidi), transfected with plasmids in mixture of polyethyleneimine. After 48hr post transfection cells were treated with 1µg/mL of Alexa Fluor® 488-LPS (ThermoFischer, L23351) or Cy7N-LOS for indicated time before they were washed with PBS and then fixed with 4% of paraformaldehyde. For immunofluorescence, cells were briefly permeabilized with 0.1% Triton X-100, blocked with 3% (w/v) BSA, followed by immunostaining with anti-CD14 antibody (Novus Biologicals, clone:4B4F12, 1:200) and secondary antibody conjugated with Alexa 568 (ThermoFischer, 1:1000). Lysosomes were stained with 50 nM LysoTracker Green (ThermoFischer, L7526) according to manufacturer's instructions. Cell images were acquired on Leica TCS SP8 microscope using 60x/1.2NA water objective. Fluorescent labels were sequentially imaged by selecting individual excitation lines from supercontinuum laser. Controls were conducted to make sure images free of cross talks.

References

1. Whitfield, C. & Trent, M. S. Biosynthesis and Export of Bacterial Lipopolysaccharides. *Annu. Rev. Biochem.* **83,** 99–128 (2014).

2. Tang, A. T. *et al.* Endothelial TLR4 and the microbiome drive cerebral cavernous malformations. *Nature* **545,** 305–310 (2017).

3. Ryu, J.-K. *et al.* Reconstruction of LPS Transfer Cascade Reveals Structural Determinants within LBP, CD14, and TLR4-MD2 for Efficient LPS Recognition and Transfer. *Immunity* **46,** 38–50 (2017).

4. Krüger, C. L., Zeuner, M.-T., Cottrell, G. S., Widera, D. & Heilemann, M. Quantitative single-molecule imaging of TLR4 reveals ligand-specific receptor dimerization. *Sci. Signal.* **10,** eaan1308 (2017).

5. Rosadini, C. V. & Kagan, J. C. Early innate immune responses to bacterial LPS. *Curr. Opin. Immunol.* **44,** 14–19 (2017).

6. Akira, S. & Takeda, K. Toll-like receptor signalling. *Nat. Rev. Immunol.* **4,** 499–511 (2004).

7. Lin, S.-C., Lo, Y.-C. & Wu, H. Helical assembly in the MyD88-IRAK4-IRAK2 complex in TLR/IL-1R signalling. *Nature* **465,** 885–890 (2010).

8. Tan, Y. & Kagan, J. C. Microbe-inducible trafficking pathways that control Toll-like receptor signaling. *Traffic* **18,** 6–17 (2017).

9. Motshwene, P. G. *et al.* An Oligomeric Signaling Platform Formed by the Toll-like Receptor Signal Transducers MyD88 and IRAK-4. *J. Biol. Chem.* **284,** 25404–25411 (2009).

10. Troelstra, A. *et al.* Saturable CD14-dependent binding of fluorescein-labeled lipopolysaccharide to human monocytes. *Infect. Immun.* **65,** 2272–7 (1997).

11. Duheron, V. *et al.* Dual Labeling of Lipopolysaccharides for SPECT-CT Imaging and Fluorescence Microscopy. *ACS Chem. Biol.* **9,** 656–662 (2014).

12. Thieblemont, N., Thieringer, R. & Wright, S. D. Innate Immune Recognition of Bacterial Lipopolysaccharide: Dependence on Interactions with Membrane Lipids and Endocytic Movement. *Immunity* **8,** 771–777 (1998).

13. Triantafilou, K., Triantafilou, M. & Fernandez, N. Lipopolysaccharide (LPS) labeled with alexa 488 hydrazide as a novel probe for LPS binding studies. *Cytometry* **41,** 316–320 (2000).

14. Yuan, L., Lin, W., Zheng, K., He, L. & Huang, W. Far-red to near infrared analyte-responsive fluorescent probes based on organic fluorophore platforms for fluorescence imaging. *Chem. Soc. Rev.* **42,** 622–661 (2013).

15. Guo, Z., Park, S., Yoon, J. & Shin, I. Recent progress in the development of near-infrared fluorescent probes for bioimaging applications. *Chem. Soc. Rev.* **43,** 16–29 (2014).

16. Peng, X. *et al.* Heptamethine Cyanine Dyes with a Large Stokes Shift and Strong Fluorescence: A Paradigm for Excited-State Intramolecular Charge Transfer. *J. Am. Chem. Soc.* **127,** 4170–4171 (2005).

17. Guo, Z., Kim, G.-H., Yoon, J. & Shin, I. Synthesis of a highly Zn2+-selective cyanine-based probe and its use for tracing endogenous zinc ions in cells and organisms. *Nat. Protoc.* **9,** 1245–1254 (2014).

18. Sun, C. *et al.* A New Near-Infrared Neutral pH Fluorescent Probe for Monitoring Minor pH Changes and its Application in Imaging of HepG2 Cells. *Appl. Biochem. Biotechnol.* **172,** 1036–1044 (2014).

19. Zhu, M., Shi, C., Xu, X., Guo, Z. & Zhu, W. Near-infrared cyanine-based sensor for Fe 3+ with high sensitivity: its intracellular imaging application in colorectal cancer cells. *RSC Adv.* **6,** 100759–100764 (2016).

20. Njiojob, C. N. *et al.* Tailored Near-Infrared Contrast Agents for Image Guided Surgery. *J. Med. Chem.* **58,** 2845–2854 (2015).

21. Meng, X. *et al.* Dual-Responsive Molecular Probe for Tumor Targeted Imaging and Photodynamic Therapy. *Theranostics* **7,** 1781–1794 (2017).

22. Shen, Z. *et al.* A Near-Infrared, Wavelength-Shiftable, Turn-on Fluorescent Probe for the Detection and Imaging of Cancer Tumor Cells. *ACS Chem. Biol.* **12,** 1121–1132 (2017).

23. Yen, S. K. *et al.* Design and Synthesis of Polymer-Functionalized NIR Fluorescent Dyes–Magnetic Nanoparticles for Bioimaging. *ACS Nano* **7,** 6796–6805 (2013).

24. Frangioni, J. In vivo near-infrared fluorescence imaging. *Curr. Opin. Chem. Biol.* **7,** 626–634 (2003).

25. Pascal, S. *et al.* Keto-polymethines: a versatile class of dyes with outstanding spectroscopic properties for in cellulo and in vivo two-photon microscopy imaging. *Chem. Sci.* **8,** 381–394 (2017).

26. Pascal, S. *et al.* Expanding the Polymethine Paradigm: Evidence for the Contribution of a Bis-Dipolar Electronic Structure. *J. Phys. Chem. A* **118,** 4038–4047 (2014).

27. Peng, X. *et al.* Heptamethine Cyanine Dyes with a Large Stokes Shift and Strong Fluorescence: A Paradigm for Excited-State Intramolecular Charge Transfer. *J. Am. Chem. Soc.* **127,** 4170–4171 (2005).

28. Grichine, A. *et al.* Millisecond lifetime imaging with a europium complex using a commercial confocal microscope under one or two-photon excitation. *Chem. Sci.* **5,** 3475–3485 (2014).

29. Zanoni, I. *et al.* CD14 Controls the LPS-Induced Endocytosis of Toll-like Receptor 4. *Cell* **147,** 868–880 (2011).

30. Tan, Y., Zanoni, I., Cullen, T. W., Goodman, A. L. & Kagan, J. C. Mechanisms of Toll-like Receptor 4 Endocytosis Reveal a Common Immune-Evasion Strategy Used by Pathogenic and Commensal Bacteria. *Immunity* **43,** 909–922 (2015).

31. Latz, E. *et al.* Lipopolysaccharide Rapidly Traffics to and from the Golgi Apparatus with the Toll-like Receptor 4-MD-2-CD14 Complex in a Process That Is Distinct from the Initiation of Signal Transduction. *J. Biol. Chem.* **277,** 47834–47843 (2002).

32. Husebye, H. *et al.* Endocytic pathways regulate Toll-like receptor 4 signaling and link innate and adaptive immunity. *EMBO J.* **25,** 683–692 (2006).

33. Klein, D. C. G. *et al.* CD14, TLR4 and TRAM Show Different Trafficking Dynamics During LPS Stimulation. *Traffic* **16,** 677–690 (2015).

34. Kagan, J. C. *et al.* TRAM couples endocytosis of TLR4 to the induction of interferon beta. *Nat. Immunol.* **9,** 361–368 (2008).

35. Tanimura, N., Saitoh, S., Matsumoto, F., Akashi-Takamura, S. & Miyake, K. Roles for LPS-dependent interaction and relocation of TLR4 and TRAM in TRIF-signaling. *Biochem. Biophys. Res. Commun.* **368,** 94–99 (2008).

36. Zanoni, I. *et al.* Similarities and differences of innate immune responses elicited by smooth and rough LPS. *Immunol. Lett.* **142,** 41–47 (2012).

37. Vasselon, T., Hailman, E., Thieringer, R. & Detmers, P. A. Internalization of Monomeric Lipopolysaccharide Occurs after Transfer Out of Cell Surface Cd14. *J. Exp. Med.* **190,** 509–522 (1999).

38. Reynolds, G. A. & Drexhage, K. H. Stable heptamethine pyrylium dyes that absorb in the infrared. *J. Org. Chem.* **42,** 885–888 (1977).

39. Flanagan, J. H., Khan, S. H., Menchen, S., Soper, S. A. & Hammer, R. P. Functionalized Tricarbocyanine Dyes as Near-Infrared Fluorescent Probes for Biomolecules. *Bioconjug. Chem.* **8,** 751–756 (1997).

40. Galanos, C., Lüderitz, O. & Westphal, O. A New Method for the Extraction of R Lipopolysaccharides. *Eur. J. Biochem.* **9,** 245–249 (1969).

41. Kittelberger, R. & Hilbink, F. Sensitive silver-staining detection of bacterial lipopolysaccharides in polyacrylamide gels. *J. Biochem. Biophys. Methods* **26,** 81–86 (1993).

CONCLUSION

The early phases of drug development, characterization of drug interactions, mechanism of action and selection of promising candidates to perform pre-clinical studies were the central points of this manuscript. Indeed, in chapter VIII were studied the interactions leading to a strong binding, setting the early stages of the drug development process. It was highlighted that while the polysaccharide O-chain seems dispensable to TLR4 activation and signalling, sugars of the core oligosaccharide play a significant role in TLR4 activation. Kdo has an important role for the agonist activity: the fully synthetic lipid A containing Kdo units (Re-LPS) are always founded more active than their counterparts lacking Kdo even if the increase in the agonist activity is not paralleled by the number of interactions between the Kdo units and MD-2/TLR4/TLR4* complex. It should be considered that the number of interactions actually observed with X-ray may not be exhaustive, since Kdo and Hep carbohydrates protrude from MD-2 binding site, the high rotational freedom of core oligosaccharide can hamper the observation of the interactions with the TLR4/MD-2 complex. In analogy with agonists, antagonists should also benefit from additive interaction of Kdo units with TLR4/MD-2 complex. The production of lipid A variants linked to different number of Kdo units permit to define that Re-LPS is the minimal chemical motif required for the maximal activation of $(TLR4/MD\text{-}2/LPS)_2$ complex. The synthesis of lipid A mimetics, bearing one to three Kdo units linked with non-natural bonds resistant to enzymatic hydrolysis, would provide a new generation of TLR4 antagonists that should improve potency and specificity. Another important parameter that determines the efficiency of agonist and antagonist presentation to the TLR4/MD-2 receptor complex is the tendency of the ligands to form supramolecular aggregates in solution. The amphiphilic character of natural lipid As and synthetic lipid A analogues favours the formation of aggregates in solution. The stability of aggregates may determine, in turn, the affinity of the ligands for the adaptor proteins (LBP, CD14 and MD-2). The addition of hydrophilic sugar moieties to lipid A analogs could improve the water solubility, increase the CMC values of molecules, and favour interaction with adaptor proteins. In addition, the role of Kdo and Hep sugars in the binding with LBP and CD14 receptors has still to be investigated. Due to the important function of these two LPS-binding proteins in determining the efficiency of agonist or antagonist presentation to the final TLR4/MD-2 complex, an increase in affinity due to the presence of additive sugars could greatly influence the type and intensity of TLR4 response. CD14 has a leading role in the process of endocytosis of TLR4/MD-2 complex ending by intracellular signalling through the TRAM/TRIF complex formation. The differential

affinity of different LPS forms for CD14 (complete S-LPS versus R-LPS lacking the O-chain) was clearly evidenced. This review presents some examples in which the presence of Kdo in natural or synthetic lipid A variants (mono- or disaccharides) improves the TLR4 activity if compared to simple lipid A or complete S-LPS. The synthesis and the biological characterization of lipid A analogs, glycosylated with Kdo and/or Hep (or mimetics of these sugars), is still largely unexplored. We have suggested that glycosylated lipid A analogues can provide in the next future a new generation of synthetic molecules to be developed as drugs targeting TLR4.

On chapter IX and X, a new series of monosaccharide glycolipids compounds (**FP13**, **FP14**, **FP15**, **FP16**, and **FP17**) presenting two carboxylic groups in C1 and C4 with a different combination of saturated and/or unsaturated fatty acid chains attached to the C2 and C3 positions of the glucosamine moiety was presented. *In vitro* binding experiments with purified functional hMD-2 consistently provided the same order of affinity among hMD-2 and synthetic molecules: **FP13**>**FP14**=**FP15**>**FP16**>**FP17**. The biological activity assessed on human HEK-TLR4 cells provided results for the **FP13-17** series as TLR4 antagonists whit IC_{50} values in the low μM range, very similar to the IC_{50} of the TLR4 antagonist **FP7**. Taken together, these data suggest that the TLR4 antagonistic property of this **FP13-17** series is based on the competition with LPS for the binding to the TLR4/ MD-2 complex. Cryo-TEM data from a representative of this series of amphiphilic molecules, showed that when in solution there is a tendency to form vesicles/liposomes displaying a double layer. This can influence the TLR4 activity in this series of compounds. We found that the carboxylic acid represents a suitable substitute of phosphoric acid in the case of monosaccharide glycolipids as TLR4 modulators without loos of any biological activity. The contribution of unsaturated chains seems to play a minor role.
However, a complete understanding of the aggregation properties in solution of the synthetic monosaccharide glycolipids presented in this thesis is crucial. In fact, FT-IR, NMR, SAXS, and cryo-TEM analysis of these compounds is ongoing and will soon help to clarify this important point. To conclude, we can state that the study presented in this manuscript provides important chemical and biological data (structural and functional) and will hopefully contribute to the development of future TLR4-based therapeutics.

The chapter XI permit to highlight that the fluorophore Cy7N with sulfonate side-chains provides a good solubility in aqueous medium which is a critical parameter for imaging. Importantly, the central amino substitution, while allowing a convenient bio-conjugation to LOS, confers optimal optical properties such as an important Stokes shift and a strong emission in the biological transparency window which are highly beneficial for imaging contrast. We

showed that Cy7N can be excited by default filter-set of Cy5 and fluoresces into deep red spectrum for low-background imaging and that the large stoke-shift of Cy7N permits to obtain two-colors images by using one excitation for the double-labelling of two cyanine dyes. Cy7N was successfully conjugated to the amino group of LOS extracted from *E. coli* K-12, one of the most potent natural agonists of TLR4. The fluorescently labelled endotoxin, LOS-Cy7N, was extensively purified by chromatography leading to a high level of chemical purity. The conjugation reaction consists of an amide bond formation by condensation between the carboxyl group of CDE-Cy7N and the ethanol amino group of LOS. This site-specific attachment turned out to be important to retain the maximum of the conjugate activity. The LOS-Cy7N conjugate was active to stimulate human TLR4 in HEK-blue cells with a lower potency than LOS. The use of Cy7N as a fluorescent tag was proved with cell images on the confocal microscope. It was observed that the CD14 co-receptor plays a pivotal role in both endotoxin presentation to TLR4/MD-2 and in the $(TLR4/MD\text{-}2/ligand)_2$ complex internalization process. CD14 was found to be required for TLR4 internalization as endosome. The LOS-Cy7N study clearly showed that LOS internalization is CD14-dependent but, by co-treatment with two types of fluorescent endotoxins, we highlight for the first time the different internalization speed of endotoxins in the cells, indeed, LOS undergoes the endocytosis much faster than LPS upon cell surface binding. The observed formation of internalized endotoxins in early endosomes provides a second signaling source, other than the MyD88-dependent pathway. Since LOS-Cy7N was internalized at early time points while LPS remained in plasma membrane, the timing of signal triggers may result in different cell responses upon stimuli. For instance, LOS-induced cytotoxicity may largely rely on endosomal signaling rather than MyD88-dependent signaling. Then, they may promote different cell reactions regarding the LPS bounded at the cell surface. The ectopic expression of CD14 in HEK-293 cells proved to be essential for both the surface binding and subsequent internalization of LOS-Cy7N and LPS-Alexa488, however, membrane-bound CD14 (mCD14) was not observed on confocal microscope. Such phenomenon would likely depend on cell types since the LPS-induced CD14 internalization was demonstrated by flow cytometry on macrophages. However, whether mCD14 is internalized together with the TLR4-LPS receptor complex is still an open question, at least in imaging-based study.

Since LOS-Cy7N showed interesting physicochemical properties for the microscopy of biological media, its use as a tag tool to study the role of endotoxin molecules in under consideration.

SECONDMENTS

Three secondments of two months were performed:

1. CIB–CSIC, Madrid, Spain (March to May 2016):

Computational chemistry and docking studies were performed under the supervision of Prof. Sonsoles Martín Santamaría and with the guidance of Jean-Marc Billod (ESR1). It leads me to learn the Python language and how to use computational software as PyMOL, Maestro, Chimera, AutoDock4 and VINA. I learned how to refine a protein from a PDB crystal structure, to construct a ligand file, define a suitable grid for the docking, run the docking and analyse the results. A screening was realized on 30 rationally designed compounds to obtain, based on the predicted activity, an idea of the most promising structures to be synthesized. It resulted that compounds with unsaturation on the fatty acids and carboxylic acids as polar groups presented the best scores. Consecutively, compounds were synthesised and tested *in vitro* and *in vivo*.

2. Lofarma, Milan, Italy (November 2016 and February 2018):

Under the supervision of Dr. Gianni Mistrello. this secondment aims to set-up an experiment for the test of a new TLR4 agonist molecule (FP11) on mice. Several formulations were studied and it was chosen to use L-Tyrosine as depot adjuvant, which is fully metabolizable and has been successfully employed in allergy vaccines, and L-α-Phosphatidylcholine as surfactant. I visit and learn about all the different sectors of this pharmaceutical industry (production, regulation, marketing…), the GxP associated (Good "Manufacturing, Clinical, Laboratory, Storage, Distribution and Review" Practice) and the REACH compliance policy.

3. CIC bioGUNE, Bilbao, Spain (September to November 2017):

Advanced NMR and microscopy studies were conducted, under supervision of Prof. Jesus Jimenez-Barbero and with the tight collaboration of Helena Coelho (ESR7). The interactions of the synthesized compounds with purified hMD-2 protein were studied by NMR, mainly by DOSY and STD experiments. Analysis of the compounds' behaviour led us to think about highly ordered aggregates since NMR experiments did not demonstrate significative modification with or without the presence of the MD-2 protein. The three-dimensional shape in biological environment was accessed through cryo-TEM (Transmission Electro-Microscopy) and it was discovered that compounds auto-assemble as liposomes once in aqueous media.

COMMUNICATIONS

1. Congresses:

- TOLL 2015 (Marbella, Spain), from 30th September to 3rd October 2015 - poster presentation.
- BtBs Day (Milan, Italy) 15th December 2015 - poster presentation.
- International endotoxin and innate immunity society biennial congress (Curio Haus, Hamburg, Germany), from 22nd to 24th September 2016.
- BtBs Day (Milan, Italy) 2nd December 2016 - poster presentation.
- Eurocarb 2017 (Barcelona, Spain) 2nd to 6th July 2017 - poster presentation.
- BtBs Day (Milan, Italy)
- CDCO 2018 (Milan, Italy) 9th to 13th September 2018 - poster presentation.

2. Public dissemination events:

- The wonderful journey of a molecule in our body: from drugs to functional food (EXPO 2015, Milan, Italy) 24th September 2015.
- Meet me tonight (researcher's night, Milan, Italy) from 30th September to 1st October 2016 - poster presentation and scientific divulgation about carbohydrates.

3. TOLLerant school and dissemination events:

- TOLLerant European Summer School (Milan, Italy) from 22nd to 24th September 2015.
- 2nd TOLLerant Meeting (Madrid, Spain) from 24th to 27th May 2016.
- 3rd TOLLerant meeting (Ljubljana, Slovenia) from 14th 2016 to 16th December 2016.
- 4th TOLLerant meeting (Naples, Italy) from 5th 2017 to 7th June 2017.
- 5th TOLLerant meeting (Ghent, Belgium) from 12th 2017 to 15th December 2017.

PATENT AND PUBLICATIONS

1. Cochet, F. & Peri, F. The Role of Carbohydrates in the Lipopolysaccharide (LPS)/Toll-Like Receptor 4 (TLR4) Signalling. *Int. J. Mol. Sci.* **18,** 2318 (2017).

2. Cochet, F. & Peri, F. NUOVI ANTAGONISTI DEL TLR4 UMANO, SIB BI5153R, 2018.

3. Cochet, F. *et al.* Novel carboxylate-based glycolipids: TLR4 antagonism, MD-2 binding and self-assembly properties, submitted to Scientific reports.

4. Wang T-C.; Cochet F. *et al.* A novel fluorophore Cy7N for microscopic imaging studies of bacterial lipopolysaccharides, in preparation.

5. Cochet F. *et al.* Synthesis and biological characterization of iron oxide nanoparticles functionalized with TLR4 and TLR7 agonists, in preparation.

REFERENCES

1. Jones, J. D. G. & Dangl, J. L. The plant immune system. *Nature* **444,** 323–329 (2006).
2. Rowley, A. F. & Powell, A. Invertebrate Immune Systems-Specific, Quasi-Specific, or Nonspecific? *J. Immunol.* **179,** 7209–7214 (2007).
3. Parham, P. *The immune system, fourth edition*. (Garland Sciences, 2015).
4. Dranoff, G. Cytokines in cancer pathogenesis and cancer therapy. *Nat. Rev. Cancer* **4,** 11–22 (2004).
5. Tang, D., Kang, R., Coyne, C. B., Zeh, H. J. & Lotze, M. T. PAMPs and DAMPs: signal 0s that spur autophagy and immunity. *Immunol. Rev.* **249,** 158–175 (2012).
6. Mogensen, T. H. Pathogen Recognition and Inflammatory Signaling in Innate Immune Defenses. *Clin. Microbiol. Rev.* **22,** 240–273 (2009).
7. Kumar, H., Kawai, T. & Akira, S. Pathogen Recognition by the Innate Immune System. *Int. Rev. Immunol.* **30,** 16–34 (2011).
8. Oosting, M. *et al.* Human TLR10 is an anti-inflammatory pattern-recognition receptor. *Proc. Natl. Acad. Sci.* **111,** E4478–E4484 (2014).
9. Morger, J. *et al.* Naturally occurring Toll-like receptor 11 (TLR11) and Toll-like receptor 12 (TLR12) polymorphisms are not associated with Toxoplasma gondii infection in wild wood mice. *Infect. Genet. Evol.* **26,** 180–184 (2014).
10. Hidmark, A., von Saint Paul, A. & Dalpke, A. H. Cutting Edge: TLR13 Is a Receptor for Bacterial RNA. *J. Immunol.* **189,** 2717–2721 (2012).
11. O'Neill, L. A. J., Golenbock, D. & Bowie, A. G. The history of Toll-like receptors — redefining innate immunity. *Nat. Rev. Immunol.* **13,** 453–460 (2013).
12. Feldman, N., Rotter-Maskowitz, A. & Okun, E. DAMPs as mediators of sterile inflammation in aging-related pathologies. *Ageing Res. Rev.* **24,** 29–39 (2015).
13. Chen, G. Y. & Nuñez, G. Sterile inflammation: sensing and reacting to damage. *Nat. Rev. Immunol.* **10,** 826–837 (2010).
14. McCarthy, C. G. *et al.* Toll-like receptors and damage-associated molecular patterns: novel links between inflammation and hypertension. *Am. J. Physiol. Circ. Physiol.* **306,** H184–H196 (2014).
15. Kawasaki, T. & Kawai, T. Toll-Like Receptor Signaling Pathways. *Front. Immunol.* **5,** 1–8 (2014).
16. Takeda, K. & Akira, S. TLR signaling pathways. *Semin. Immunol.* **16,** 3–9 (2004).
17. Kumar, H., Kawai, T. & Akira, S. Toll-like receptors and innate immunity. *Biochem.*

Biophys. Res. Commun. **388,** 621–625 (2009).

18. Yang, L. & Seki, E. Toll-Like Receptors in Liver Fibrosis: Cellular Crosstalk and Mechanisms. *Front. Physiol.* **3,** 1–18 (2012).
19. Akira, S. & Hoshino, K. Myeloid Differentiation Factor 88–Dependent and –Independent Pathways in Toll-Like Receptor Signaling. *J. Infect. Dis.* **187,** S356–S363 (2003).
20. Zanoni, I. *et al.* CD14 Controls the LPS-Induced Endocytosis of Toll-like Receptor 4. *Cell* **147,** 868–880 (2011).
21. Triantafilou, M. & Triantafilou, K. Lipopolysaccharide recognition: CD14, TLRs and the LPS-activation cluster. *Trends Immunol.* **23,** 301–304 (2002).
22. Cochet, F. & Peri, F. The Role of Carbohydrates in the Lipopolysaccharide (LPS)/Toll-Like Receptor 4 (TLR4) Signalling. *Int. J. Mol. Sci.* **18,** 2318 (2017).
23. Zanin-Zhorov, A. *et al.* Cutting Edge: T Cells Respond to Lipopolysaccharide Innately via TLR4 Signaling. *J. Immunol.* **179,** 41–44 (2007).
24. Reynolds, J. M., Martinez, G. J., Chung, Y. & Dong, C. Toll-like receptor 4 signaling in T cells promotes autoimmune inflammation. *Proc. Natl. Acad. Sci.* **109,** 13064–13069 (2012).
25. Kajava, A. V. Structural diversity of leucine-rich repeat proteins 1 1Edited by F. Cohen. *J. Mol. Biol.* **277,** 519–527 (1998).
26. Kobe, B. The leucine-rich repeat as a protein recognition motif. *Curr. Opin. Struct. Biol.* **11,** 725–732 (2001).
27. Gay, N. J. & Gangloff, M. Structure and Function of Toll Receptors and Their Ligands. *Annu. Rev. Biochem.* **76,** 141–165 (2007).
28. Matsushima, N. *et al.* Comparative sequence analysis of leucine-rich repeats (LRRs) within vertebrate toll-like receptors. *BMC Genomics* **8,** 124 (2007).
29. Kim, H. M. *et al.* Crystal Structure of the TLR4-MD-2 Complex with Bound Endotoxin Antagonist Eritoran. *Cell* **130,** 906–917 (2007).
30. Ohto, U., Yamakawa, N., Akashi-Takamura, S., Miyake, K. & Shimizu, T. Structural Analyses of Human Toll-like Receptor 4 Polymorphisms D299G and T399I. *J. Biol. Chem.* **287,** 40611–40617 (2012).
31. Botos, I., Segal, D. M. & Davies, D. R. The Structural Biology of Toll-like Receptors. *Structure* **19,** 447–459 (2011).
32. Bella, J., Hindle, K. L., McEwan, P. A. & Lovell, S. C. The leucine-rich repeat structure. *Cell. Mol. Life Sci.* **65,** 2307–2333 (2008).

33. Billod, J.-M., Lacetera, A., Guzmán-Caldentey, J. & Martín-Santamaría, S. Computational Approaches to Toll-Like Receptor 4 Modulation. *Molecules* **21,** 994 (2016).
34. JERALA, R. Structural biology of the LPS recognition. *Int. J. Med. Microbiol.* **297,** 353–363 (2007).
35. BARTHOLOMEW, J. W. & MITTWER, T. The Gram stain. *Bacteriol. Rev.* **16,** 1–29 (1952).
36. Beveridge, T. Use of the Gram stain in microbiology. *Biotech. Histochem.* **76,** 111–118 (2001).
37. Beveridge, T. J. Structures of gram-negative cell walls and their derived membrane vesicles. *J. Bacteriol.* **181,** 4725–33 (1999).
38. Erridge, C., Bennett-guerrero, E. & Poxton, I. R. Structure and function of lipopolysaccharides. *Microbes Infect.* **4,** 837–851 (2002).
39. Qiao, S., Luo, Q., Zhao, Y., Zhang, X. C. & Huang, Y. Structural basis for lipopolysaccharide insertion in the bacterial outer membrane. *Nature* **511,** 108–111 (2014).
40. Pieretti, G. *et al.* A combined fermentative-chemical approach for the scalable production of pure E. coli monophosphoryl lipid A. *Appl. Microbiol. Biotechnol.* **98,** 7781–7791 (2014).
41. Wimmer, N., Brade, H. & Kosma, P. Synthesis of neoglycoproteins containing d-glycero-d-talo-oct-2-ulopyranosylonic acid (Ko) ligands corresponding to core units from Burkholderia and Acinetobacter lipopolysaccharide. *Carbohydr. Res.* **329,** 549–560 (2000).
42. Caroff, M. & Karibian, D. Structure of bacterial lipopolysaccharides. *Carbohydr. Res.* **338,** 2431–2447 (2003).
43. Moran, A. P. Biological and serological characterization of Campylobacter jejuni lipopolysaccharides with deviating core and lipid A structures. *FEMS Immunol. Med. Microbiol.* **11,** 121–130 (1995).
44. Rietschel, E., Kirikae, T., Schade, F. U. & Schmidt, G. The Chemical Structure of Bacterial Endotoxin in Relation to Bioactivity. *Immunobiol.* **187,** 169–190 (1993).
45. Holst, O., Brennan, patrick J. & Itzstein, M. von. *Microbial Glycobiology*. (Elsevier, 2010). doi:10.1016/B978-0-12-374546-0.X0001-6
46. Aurell, C. A. & Wistrom, A. O. Critical Aggregation Concentrations of Gram-Negative Bacterial Lipopolysaccharides (LPS). *Biochem. Biophys. Res. Commun.* **253,** 119–123

(1998).

47. Sasaki, H. & White, S. H. Aggregation Behavior of an Ultra-Pure Lipopolysaccharide that Stimulates TLR-4 Receptors. *Biophys. J.* **95,** 986–993 (2008).
48. Tobias, P. S. Isolation of a lipopolysaccharide-binding acute phase reactant from rabbit serum. *J. Exp. Med.* **164,** 777–793 (1986).
49. Han, J., Mathison, J. C., Ulevitch, R. J. & Tobias, P. S. Lipopolysaccharide (LPS) binding protein, truncated at Ile-197, binds LPS but does not transfer LPS to CD14. *J. Biol. Chem.* **269,** 8172–5 (1994).
50. Lamping, N. *et al.* Effects of site-directed mutagenesis of basic residues (Arg 94, Lys 95, Lys 99) of lipopolysaccharide (LPS)-binding protein on binding and transfer of LPS and subsequent immune cell activation. *J. Immunol.* **157,** 4648–56 (1996).
51. Beamer, L. J., Carroll, S. F. & Eisenberg, D. The BPI/LBP family of proteins: A structural analysis of conserved regions. *Protein Sci.* **7,** 906–914 (2008).
52. Ooi, C. E., Weiss, J., Elsbach, P., Frangione, B. & Mannion, B. A 25-kDa NH2-terminal fragment carries all the antibacterial activities of the human neutrophil 60-kDa bactericidal/permeability-increasing protein. *J. Biol. Chem.* **262,** 14891–4 (1987).
53. Elsbach, P. & Weiss, J. Role of the bactericidal/permeability-increasing protein in host defence. *Curr. Opin. Immunol.* **10,** 45–49 (1998).
54. Kim, Y. J. & Lee, J. Recognition of Lipopolysaccharides by TLR4 and its Accessory Proteins. *Bio Des.* **1,** 3–12 (2013).
55. Ulevitch, R. J. & Tobias, P. S. Receptor-Dependent Mechanisms of Cell Stimulation by Bacterial Endotoxin. *Annu. Rev. Immunol.* **13,** 437–457 (1995).
56. Kim, J.-I. *et al.* Crystal Structure of CD14 and Its Implications for Lipopolysaccharide Signaling. *J. Biol. Chem.* **280,** 11347–11351 (2005).
57. Cunningham, M. D. *et al.* CD14 employs hydrophilic regions to 'capture' lipopolysaccharides. *J. Immunol.* **164,** 3255–63 (2000).
58. Dziarski, R., Viriyakosol, S., Kirkland, T. N. & Gupta, D. Soluble CD14 Enhances Membrane CD14-Mediated Responses to Peptidoglycan: Structural Requirements Differ from Those for Responses to Lipopolysaccharide. *Infect. Immun.* **68,** 5254–5260 (2000).
59. Juan, T. S.-C. *et al.* Identification of a Lipopolysaccharide Binding Domain in CD14 between Amino Acids 57 and 64. *J. Biol. Chem.* **270,** 5219–5224 (1995).
60. Shapiro, R. A. *et al.* Identification of CD14 residues involved in specific lipopolysaccharide recognition. *Infect. Immun.* **65,** 293–7 (1997).
61. Stelter, F. *et al.* Mutation of Amino Acids 39-44 of Human CD14 Abrogates Binding of

Lipopolysaccharide and Escherichia coli. *Eur. J. Biochem.* **243,** 100–109 (1997).

62. Viriyakosol, S. & Kirkland, T. N. A Region of Human CD14 Required for Lipopolysaccharide Binding. *J. Biol. Chem.* **270,** 361–368 (1995).
63. Juan, T. S.-C., Hailman, E., Kelley, M. J., Wright, S. D. & Lichenstein, H. S. Identification of a Domain in Soluble CD14 Essential for Lipopolysaccharide (LPS) Signaling but Not LPS Binding. *J. Biol. Chem.* **270,** 17237–17242 (1995).
64. Muroi, M., Ohnishi, T. & Tanamoto, K. Regions of the Mouse CD14 Molecule Required for Toll-like Receptor 2- and 4-mediated Activation of NF-κB. *J. Biol. Chem.* **277,** 42372–42379 (2002).
65. Stelter, F. *et al.* Differential impact of substitution of amino acids 9-13 and 91-101 of human CD14 on soluble CD14-dependent activation of cells by lipopolysaccharide. *J. Immunol.* **163,** 6035–44 (1999).
66. Derewenda, U. *et al.* The Crystal Structure of a Major Dust Mite Allergen Der p 2, and its Biological Implications. *J. Mol. Biol.* **318,** 189–197 (2002).
67. Friedland, N., Liou, H.-L., Lobel, P. & Stock, A. M. Structure of a cholesterol-binding protein deficient in Niemann-Pick type C2 disease. *Proc. Natl. Acad. Sci.* **100,** 2512–2517 (2003).
68. Wright, C. S., Zhao, Q. & Rastinejad, F. Structural Analysis of Lipid Complexes of GM2-Activator Protein. *J. Mol. Biol.* **331,** 951–964 (2003).
69. Ohto, U., Fukase, K., Miyake, K. & Satow, Y. Crystal Structures of Human MD-2 and Its Complex with Antiendotoxic Lipid IVa. *Science (80-.).* **316,** 1632–1634 (2007).
70. Park, B. S. *et al.* The structural basis of lipopolysaccharide recognition by the TLR4-MD-2 complex. *Nature* **458,** 1191–5 (2009).
71. Means, T. K. *et al.* Differential effects of a Toll-like receptor antagonist on Mycobacterium tuberculosis-induced macrophage responses. *J. Immunol.* **166,** 4074–4082 (2001).
72. Nagai, Y. *et al.* Essential role of MD-2 in LPS responsiveness and TLR4 distribution. *Nat. Immunol.* **3,** 667–672 (2002).
73. Viriyakosol, S., Kirkland, T. N., Soldau, K. & Tobias, P. S. MD-2 binds to bacterial lipopolysaccharide. *J. Endotoxin Res.* **6,** 489–491 (2000).
74. Rietschel, E. T. *et al.* Bacterial endotoxin: molecular relationships of structure to activity and function. *FASEB J.* **8,** 217–225 (1994).
75. Teghanemt, A., Zhang, D., Levis, E. N., Weiss, J. P. & Gioannini, T. L. Molecular Basis of Reduced Potency of Underacylated Endotoxins. *J. Immunol.* **175,** 4669–4676 (2005).

76. Erridge, C., Bennett-Guerrero, E. & Poxton, I. R. Structure and function of lipopolysaccharides. *Microbes Infect.* **4,** 837–851 (2002).
77. Galanos, C. *et al.* Synthetic and natural Escherichia coli free lipid A express identical endotoxic activities. *Eur. J. Biochem.* **148,** 1–5 (1985).
78. Wang, B., Han, Y., Li, Y., Li, Y. & Wang, X. Immuno-Stimulatory Activity of Escherichia coli Mutants Producing Kdo2-Monophosphoryl-Lipid A or Kdo2-Pentaacyl-Monophosphoryl-Lipid A. *PLoS One* **10,** e0144714 (2015).
79. Gioannini, T. L. *et al.* Isolation of an endotoxin-MD-2 complex that produces Toll-like receptor 4-dependent cell activation at picomolar concentrations. *Proc. Natl. Acad. Sci.* **101,** 4186–4191 (2004).
80. Lu, Y.-C., Yeh, W.-C. & Ohashi, P. S. LPS/TLR4 signal transduction pathway. *Cytokine* **42,** 145–151 (2008).
81. Shirey, K. A. *et al.* The TLR4 antagonist Eritoran protects mice from lethal influenza infection. *Nature* **497,** 498–502 (2013).
82. Hennessy, E. J., Parker, A. E. & O'Neill, L. A. J. Targeting Toll-like receptors: emerging therapeutics? *Nat. Rev. Drug Discov.* **9,** 293–307 (2010).
83. Opal, S. M. *et al.* Effect of Eritoran, an Antagonist of MD2-TLR4, on Mortality in Patients With Severe Sepsis. *J. Am. Med. Assoc.* **309,** 1154–1162 (2013).
84. Union, E. Phase Iii Study for Severe Sepsis Treatment Eritoran (E5564) Does Not Meet Primary Endpoint. *Media* 11–12 (2011).
85. GALANOS, C. *et al.* Endotoxic properties of chemically synthesized lipid A part structures. Comparison of synthetic lipid A precursor and synthetic analogues with biosynthetic lipid A precursor and free lipid A. *Eur. J. Biochem.* **140,** 221–227 (1984).
86. Muroi, M. & Tanamoto, K. Structural Regions of MD-2 That Determine the Agonist-Antagonist Activity of Lipid IVa. *J. Biol. Chem.* **281,** 5484–5491 (2006).
87. Schromm, A. B. *et al.* Biological activities of lipopolysaccharides are determined by the shape of their lipid A portion. *Eur. J. Biochem.* **267,** 2008–2013 (2000).
88. Facchini, F. A. *et al.* Structure–Activity Relationship in Monosaccharide-Based Toll-Like Receptor 4 (TLR4) Antagonists. *J. Med. Chem.* **61,** 2895–2909 (2018).
89. Park, B. S. & Lee, J.-O. Recognition of lipopolysaccharide pattern by TLR4 complexes. *Exp. Mol. Med.* **45,** e66–e66 (2013).
90. Paramo, T., Piggot, T. J., Bryant, C. E. & Bond, P. J. The Structural Basis for Endotoxin-induced Allosteric Regulation of the Toll-like Receptor 4 (TLR4) Innate Immune Receptor. *J. Biol. Chem.* **288,** 36215–36225 (2013).

91. Hajjar, A. M., Ernst, R. K., Tsai, J. H., Wilson, C. B. & Miller, S. I. Human Toll-like receptor 4 recognizes host-specific LPS modifications. *Nat. Immunol.* **3,** 354–359 (2002).
92. Barton, G. M. Toll-Like Receptor Signaling Pathways. *Science (80-.).* **300,** 1524–1525 (2003).
93. Takaoka, A. *et al.* DAI (DLM-1/ZBP1) is a cytosolic DNA sensor and an activator of innate immune response. *Nature* **448,** 501–505 (2007).
94. Kato, H. *et al.* Differential roles of MDA5 and RIG-I helicases in the recognition of RNA viruses. *Nature* **441,** 101–105 (2006).
95. O'Neill, L. A. J. & Bowie, A. G. The family of five: TIR-domain-containing adaptors in Toll-like receptor signalling. *Nat. Rev. Immunol.* **7,** 353–364 (2007).
96. Gay, N. J., Symmons, M. F., Gangloff, M. & Bryant, C. E. Assembly and localization of Toll-like receptor signalling complexes. *Nat. Rev. Immunol.* **14,** 546–558 (2014).
97. Kieser, K. J. & Kagan, J. C. Multi-receptor detection of individual bacterial products by the innate immune system. *Nat. Rev. Immunol.* **17,** 376–390 (2017).
98. Yamamoto, M. *et al.* Essential role for TIRAP in activation of the signalling cascade shared by TLR2 and TLR4. *Nature* **420,** 324–329 (2002).
99. Yamamoto, M. Role of Adaptor TRIF in the MyD88-Independent Toll-Like Receptor Signaling Pathway. *Science (80-.).* **301,** 640–643 (2003).
100. Yamamoto, M. *et al.* TRAM is specifically involved in the Toll-like receptor 4–mediated MyD88-independent signaling pathway. *Nat. Immunol.* **4,** 1144–1150 (2003).
101. Horng, T., Barton, G. M., Flavell, R. A. & Medzhitov, R. The adaptor molecule TIRAP provides signalling specificity for Toll-like receptors. *Nature* **420,** 329–333 (2002).
102. Bonham, K. S. *et al.* A Promiscuous Lipid-Binding Protein Diversifies the Subcellular Sites of Toll-like Receptor Signal Transduction. *Cell* **156,** 705–716 (2014).
103. Lin, S.-C., Lo, Y.-C. & Wu, H. Helical assembly in the MyD88-IRAK4-IRAK2 complex in TLR/IL-1R signalling. *Nature* **465,** 885–890 (2010).
104. Kagan, J. C., Magupalli, V. G. & Wu, H. SMOCs: supramolecular organizing centres that control innate immunity. *Nat. Rev. Immunol.* **14,** 821–826 (2014).
105. Medzhitov, R. & Horng, T. Transcriptional control of the inflammatory response. *Nat. Rev. Immunol.* **9,** 692–703 (2009).
106. Jain, A., Kaczanowska, S. & Davila, E. IL-1 Receptor-Associated Kinase Signaling and Its Role in Inflammation, Cancer Progression, and Therapy Resistance. *Front. Immunol.* **5,** 1–8 (2014).

107. Tan, Y., Zanoni, I., Cullen, T. W., Goodman, A. L. & Kagan, J. C. Mechanisms of Toll-like Receptor 4 Endocytosis Reveal a Common Immune-Evasion Strategy Used by Pathogenic and Commensal Bacteria. *Immunity* **43,** 909–922 (2015).
108. Kagan, J. C. *et al.* TRAM couples endocytosis of Toll-like receptor 4 to the induction of interferon-β. *Nat. Immunol.* **9,** 361–368 (2008).
109. Fitzgerald, K. A. *et al.* LPS-TLR4 Signaling to IRF-3/7 and NF-κB Involves the Toll Adapters TRAM and TRIF. *J. Exp. Med.* **198,** 1043–1055 (2003).
110. Kim, E. *et al.* TANK-binding kinase 1 and Janus kinase 2 play important roles in the regulation of mitogen-activated protein kinase phosphatase-1 expression after toll-like receptor 4 activation. *J. Cell. Physiol.* 1–12 (2018). doi:10.1002/jcp.26787
111. Cui, Y. *et al.* Mycobacterium bovis Induces Endoplasmic Reticulum Stress Mediated-Apoptosis by Activating IRF3 in a Murine Macrophage Cell Line. *Front. Cell. Infect. Microbiol.* **6,** 1–12 (2016).
112. Funami, K., Matsumoto, M., Oshiumi, H., Inagaki, F. & Seya, T. Functional interfaces between TICAM-2/TRAM and TICAM-1/TRIF in TLR4 signaling. *Biochem. Soc. Trans.* **45,** 929–935 (2017).
113. Betzig, E. *et al.* Imaging Intracellular Fluorescent Proteins at Nanometer Resolution. *Science (80-.).* **313,** 1642–1645 (2006).
114. Rust, M. J., Bates, M. & Zhuang, X. Sub-diffraction-limit imaging by stochastic optical reconstruction microscopy (STORM). *Nat. Methods* **3,** 793–796 (2006).
115. Heintzmann, R. & Huser, T. Super-Resolution Structured Illumination Microscopy. *Chem. Rev.* **117,** 13890–13908 (2017).
116. Cario, E. Toll-like receptors in inflammatory bowel diseases: A decade later. *Inflamm. Bowel Dis.* **16,** 1583–1597 (2010).
117. Stoll, L., Denning, G. & Weintraub, N. Endotoxin, TLR4 Signaling and Vascular Inflammation: Potential Therapeutic Targets in Cardiovascular Disease. *Curr. Pharm. Des.* **12,** 4229–4245 (2006).
118. Ghoshal, S., Witta, J., Zhong, J., de Villiers, W. & Eckhardt, E. Chylomicrons promote intestinal absorption of lipopolysaccharides. *J. Lipid Res.* **50,** 90–97 (2009).
119. Jia, L. *et al.* Hepatocyte Toll-like receptor 4 regulates obesity-induced inflammation and insulin resistance. *Nat. Commun.* **5,** 3878 (2014).
120. Curtiss, L. K. & Tobias, P. S. Emerging role of Toll-like receptors in atherosclerosis. *J. Lipid Res.* **50,** S340–S345 (2009).
121. Erridge, C. The Roles of Toll-Like Receptors in Atherosclerosis. *J. Innate Immun.* **1,**

340–349 (2009).

122. Stifano, G. *et al.* Chronic Toll-like receptor 4 stimulation in skin induces inflammation, macrophage activation, transforming growth factor beta signature gene expression, and fibrosis. *Arthritis Res. Ther.* **16,** R136 (2014).
123. Panzer, R., Blobel, C., Fölster-Holst, R. & Proksch, E. TLR2 and TLR4 expression in atopic dermatitis, contact dermatitis and psoriasis. *Exp. Dermatol.* **23,** 364–366 (2014).
124. Abdollahi-Roodsaz, S. *et al.* Inhibition of toll-like receptor 4 breaks the inflammatory loop in autoimmune destructive arthritis. *Arthritis Rheum.* **56,** 2957–2967 (2007).
125. Cao, L., Tanga, F. Y. & DeLeo, J. A. The contributing role of CD14 in toll-like receptor 4 dependent neuropathic pain. *Neuroscience* **158,** 896–903 (2009).
126. Thakur, K. K. *et al.* Therapeutic implications of toll-like receptors in peripheral neuropathic pain. *Pharmacol. Res.* **115,** 224–232 (2017).
127. Bettoni, I. *et al.* Glial TLR4 receptor as new target to treat neuropathic pain: Efficacy of a new receptor antagonist in a model of peripheral nerve injury in mice. *Glia* **56,** 1312–1319 (2008).
128. Tang, A. T. *et al.* Endothelial TLR4 and the microbiome drive cerebral cavernous malformations. *Nature* **545,** 305–310 (2017).
129. Fan, J. *et al.* Hemorrhagic Shock Induces NAD(P)H Oxidase Activation in Neutrophils: Role of HMGB1-TLR4 Signaling. *J. Immunol.* **178,** 6573–6580 (2007).
130. Casula, M. *et al.* Toll-like receptor signaling in amyotrophic lateral sclerosis spinal cord tissue. *Neuroscience* **179,** 233–243 (2011).
131. De Paola, M. *et al.* Synthetic and natural small molecule TLR4 antagonists inhibit motoneuron death in cultures from ALS mouse model. *Pharmacol. Res.* **103,** 180–187 (2016).
132. Bachtell, R. *et al.* Targeting the Toll of Drug Abuse: The Translational Potential of Toll-Like Receptor 4. *CNS Neurol. Disord. Drug Targets* **14,** 692–9 (2015).
133. Liu, J., Buisman-Pijlman, F. & Hutchinson, M. R. Toll-like receptor 4: innate immune regulator of neuroimmune and neuroendocrine interactions in stress and major depressive disorder. *Front. Neurosci.* **8,** 1–15 (2014).
134. Hung, Y.-Y., Wu, M.-K., Huang, T.-L., Huang, K.-W. & Huang, G. Y.-L. Association between toll-like receptor 4 expression and symptoms of major depressive disorder. *Neuropsychiatr. Dis. Treat.* **11,** 1853 (2015).
135. Ulevitch, R. J. Therapeutics targeting the innate immune system. *Nat. Rev. Immunol.* **4,** 512–520 (2004).

136. De La Rica, A. S., Gilsanz, F. & Maseda, E. Epidemiologic trends of sepsis in western countries. *Ann. Transl. Med.* **4,** 325–325 (2016).
137. Bouza, C., López-Cuadrado, T., Saz-Parkinson, Z. & Amate-Blanco, J. M. Epidemiology and recent trends of severe sepsis in Spain: a nationwide population-based analysis (2006-2011). *BMC Infect. Dis.* **14,** 3863 (2014).
138. Vincent, J.-L. *et al.* Sepsis in European intensive care units: Results of the SOAP study*. *Crit. Care Med.* **34,** 344–353 (2006).
139. Kumar, A. *et al.* Duration of hypotension before initiation of effective antimicrobial therapy is the critical determinant of survival in human septic shock*. *Crit. Care Med.* **34,** 1589–1596 (2006).
140. Pruinelli, L. *et al.* Delay Within the 3-Hour Surviving Sepsis Campaign Guideline on Mortality for Patients With Severe Sepsis and Septic Shock*. *Crit. Care Med.* **46,** 500–505 (2018).
141. Martin, G. S., Mannino, D. M., Eaton, S. & Moss, M. The Epidemiology of Sepsis in the United States from 1979 through 2000. *N. Engl. J. Med.* **348,** 1546–1554 (2003).
142. Reinhart, K. *et al.* Recognizing Sepsis as a Global Health Priority — A WHO Resolution. *N. Engl. J. Med.* **377,** 414–417 (2017).
143. Bone, R. C. American College of Chest Physicians/Society of Critical Care Medicine Consensus Conference. *Crit. Care Med.* **20,** 864–874 (1992).
144. Levy, M. M. *et al.* 2001 SCCM/ESICM/ACCP/ATS/SIS International Sepsis Definitions Conference. *Intensive Care Med.* **29,** 530–538 (2003).
145. Singer, M. *et al.* The Third International Consensus Definitions for Sepsis and Septic Shock (Sepsis-3). *JAMA* **315,** 801 (2016).
146. Napolitano, L. M. Sepsis 2018: Definitions and Guideline Changes. *Surg. Infect. (Larchmt).* **19,** 117–125 (2018).
147. Ramachandran, G. Gram-positive and gram-negative bacterial toxins in sepsis. *Virulence* **5,** 213–218 (2014).
148. Morrison, D. C. & Ryan, J. L. Endotoxins and Disease Mechanisms. *Annu. Rev. Med.* **38,** 417–432 (1987).
149. Delvos, U., Janssen, B. & Muller-Berghaus, G. Effect of lipopolysaccharides on cultured human endothelial cells. *Blut* **55,** 101–108 (1987).
150. Hoshino, K. *et al.* Cutting edge: Toll-like receptor 4 (TLR4)-deficient mice are hyporesponsive to lipopolysaccharide: evidence for TLR4 as the Lps gene product. *J. Immunol.* **162,** 3749–52 (1999).

151. Bone, R. C. *et al.* A Controlled Clinical Trial of High-Dose Methylprednisolone in the Treatment of Severe Sepsis and Septic Shock. *N. Engl. J. Med.* **317,** 653–658 (1987).
152. Ziegler, E. J. *et al.* Treatment of Gram-Negative Bacteremia and Septic Shock with HA-1A Human Monoclonal Antibody against Endotoxin. *N. Engl. J. Med.* **324,** 429–436 (1991).
153. Fisher, C. J. *et al.* Treatment of Septic Shock with the Tumor Necrosis Factor Receptor:Fc Fusion Protein. *N. Engl. J. Med.* **334,** 1697–1702 (1996).
154. Abraham, E. *et al.* Efficacy and safety of monoclonal antibody to human tumor necrosis factor alpha in patients with sepsis syndrome. A randomized, controlled, double-blind, multicenter clinical trial. TNF-alpha MAb Sepsis Study Group. *JAMA* **273,** 934–41 (1995).
155. Fisher, C. J. *et al.* Initial evaluation of human recombinant interleukin-1 receptor antagonist in the treatment of sepsis syndrome: a randomized, open-label, placebo-controlled multicenter trial. *Crit. Care Med.* **22,** 12–21 (1994).
156. Bernard, G. R. *et al.* The Effects of Ibuprofen on the Physiology and Survival of Patients with Sepsis. *N. Engl. J. Med.* **336,** 912–918 (1997).
157. Eisen, D. P. *et al.* AspiriN To Inhibit SEPSIS (ANTISEPSIS) randomised controlled trial protocol. *BMJ Open* **7,** e013636 (2017).
158. Matsunaga, N., Tsuchimori, N., Matsumoto, T. & Ii, M. TAK-242 (Resatorvid), a Small-Molecule Inhibitor of Toll-Like Receptor (TLR) 4 Signaling, Binds Selectively to TLR4 and Interferes with Interactions between TLR4 and Its Adaptor Molecules. *Mol. Pharmacol.* **79,** 34–41 (2011).
159. Rice, T. W. *et al.* A randomized, double-blind, placebo-controlled trial of TAK-242 for the treatment of severe sepsis*. *Crit. Care Med.* **38,** 1685–1694 (2010).
160. Lee, K.-M. & Seong, S.-Y. Partial role of TLR4 as a receptor responding to damage-associated molecular pattern. *Immunol. Lett.* **125,** 31–39 (2009).
161. Tsung, A. *et al.* The nuclear factor HMGB1 mediates hepatic injury after murine liver ischemia-reperfusion. *J. Exp. Med.* **201,** 1135–1143 (2005).
162. Goligorsky, M. S. TLR4 and HMGB1: partners in crime? *Kidney Int.* **80,** 450–452 (2011).
163. Li, Z., Xiao, X. & Yang, M. Asiatic Acid Inhibits Lipopolysaccharide-Induced Acute Lung Injury in Mice. *Inflammation* **39,** 1642–1648 (2016).
164. Kuno, M. *et al.* THE NOVEL SELECTIVE TOLL-LIKE RECEPTOR 4 SIGNAL TRANSDUCTION INHIBITOR TAK-242 PREVENTS ENDOTOXAEMIA IN

CONSCIOUS GUINEA-PIGS. *Clin. Exp. Pharmacol. Physiol.* **36,** 589–593 (2009).

165. Gárate, I. *et al.* Toll-like 4 receptor inhibitor TAK-242 decreases neuroinflammation in rat brain frontal cortex after stress. *J. Neuroinflammation* **11,** 8 (2014).
166. Ortega-Cava, C. F. *et al.* Strategic Compartmentalization of Toll-Like Receptor 4 in the Mouse Gut. *J. Immunol.* **170,** 3977–3985 (2003).
167. Sartor, R. B. Microbial Influences in Inflammatory Bowel Diseases. *Gastroenterology* **134,** 577–594 (2008).
168. Cario, E. & Podolsky, D. K. Intestinal epithelial Tollerance versus inTollerance of commensals. *Mol. Immunol.* **42,** 887–893 (2005).
169. Rodríguez, L. A. G., Ruigómez, A. & Panés, J. Acute Gastroenteritis Is Followed by an Increased Risk of Inflammatory Bowel Disease. *Gastroenterology* **130,** 1588–1594 (2006).
170. Cario, E. & Podolsky, D. K. Differential alteration in intestinal epithelial cell expression of toll-like receptor 3 (TLR3) and TLR4 in inflammatory bowel disease. *Infect. Immun.* **68,** 7010–7 (2000).
171. Kamada, N. *et al.* Unique CD14+ intestinal macrophages contribute to the pathogenesis of Crohn disease via IL-23/IFN-γ axis. *J. Clin. Invest.* **118,** (2008).
172. Meijssen, M. A., Brandwein, S. L., Reinecker, H. C., Bhan, A. K. & Podolsky, D. K. Alteration of gene expression by intestinal epithelial cells precedes colitis in interleukin-2-deficient mice. *Am. J. Physiol.* **274,** G472-9 (1998).
173. De Mattos, B. R. R. *et al.* Inflammatory bowel disease: An overview of immune mechanisms and biological treatments. *Mediators Inflamm.* **2015,** (2015).
174. Mowat, C. *et al.* Guidelines for the management of inflammatory bowel disease in adults. *Gut* **60,** 571–607 (2011).
175. Rufo, P. A. & Bousvaros, A. Current therapy of inflammatory bowel disease in children. *Paediatr. Drugs* **8,** 279–302 (2006).
176. Reichel, C., Streit, J., Ott, K. & Wunsch, S. Appropriateness of Crohn's Disease Therapy in Gastroenterological Rehabilitation. *Digestion* **82,** 239–245 (2010).
177. Targan, S. R. *et al.* A Short-Term Study of Chimeric Monoclonal Antibody cA2 to Tumor Necrosis Factor α for Crohn's Disease. *N. Engl. J. Med.* **337,** 1029–1036 (1997).
178. Thomas, S. & Baumgart, D. C. Targeting leukocyte migration and adhesion in Crohn's disease and ulcerative colitis. *Inflammopharmacology* **20,** 1–18 (2012).
179. Hanauer, S. B. Risks and benefits of combining immunosuppressives and biological agents in inflammatory bowel disease: is the synergy worth the risk? *Gut* **56,** 1181–1183

(2007).

180. van Schouwenburg, P. A., Rispens, T. & Wolbink, G. J. Immunogenicity of anti-TNF biologic therapies for rheumatoid arthritis. *Nat. Rev. Rheumatol.* **9,** 164–172 (2013).

181. Sørensen, L. K., Havemose-Poulsen, A., Sønder, S. U., Bendtzen, K. & Holmstrup, P. Blood Cell Gene Expression Profiling in Subjects With Aggressive Periodontitis and Chronic Arthritis. *J. Periodontol.* **79,** 477–485 (2008).

182. Kim, K.-W. *et al.* Human rheumatoid synovial fibroblasts promote osteoclastogenic activity by activating RANKL via TLR-2 and TLR-4 activation. *Immunol. Lett.* **110,** 54–64 (2007).

183. Huang, Q., Ma, Y., Adebayo, A. & Pope, R. M. Increased macrophage activation mediated through toll-like receptors in rheumatoid arthritis. *Arthritis Rheum.* **56,** 2192–2201 (2007).

184. Huang, Q.-Q. & Pope, R. M. The role of toll-like receptors in rheumatoid arthritis. *Curr. Rheumatol. Rep.* **11,** 357–64 (2009).

185. Huang, Q.-Q. *et al.* Heat Shock Protein 96 Is Elevated in Rheumatoid Arthritis and Activates Macrophages Primarily via TLR2 Signaling. *J. Immunol.* **182,** 4965–4973 (2009).

186. Roelofs, M. F. *et al.* Identification of Small Heat Shock Protein B8 (HSP22) as a Novel TLR4 Ligand and Potential Involvement in the Pathogenesis of Rheumatoid Arthritis. *J. Immunol.* **176,** 7021–7027 (2006).

187. Taniguchi, N. *et al.* High mobility group box chromosomal protein 1 plays a role in the pathogenesis of rheumatoid arthritis as a novel cytokine. *Arthritis Rheum.* **48,** 971–981 (2003).

188. Park, J. S. *et al.* Involvement of Toll-like Receptors 2 and 4 in Cellular Activation by High Mobility Group Box 1 Protein. *J. Biol. Chem.* **279,** 7370–7377 (2004).

189. Schaefer, L. *et al.* The matrix component biglycan is proinflammatory and signals through Toll-like receptors 4 and 2 in macrophages. *J. Clin. Invest.* **115,** 2223–2233 (2005).

190. Abdollahi-Roodsaz, S. *et al.* Stimulation of TLR2 and TLR4 differentially skews the balance of T cells in a mouse model of arthritis. *J. Clin. Invest.* **118,** 205–216 (2008).

191. Sacre, S. M. *et al.* The Toll-Like Receptor Adaptor Proteins MyD88 and Mal/TIRAP Contribute to the Inflammatory and Destructive Processes in a Human Model of Rheumatoid Arthritis. *Am. J. Pathol.* **170,** 518–525 (2007).

192. Friedman, B. & Cronstein, B. Methotrexate Mechanism in Treatment of Rheumatoid

Arthritis. *Jt. Bone Spine* (2018). doi:10.1016/j.jbspin.2018.07.004

193. Lomonte, A. B. V. *et al.* Tofacitinib, an oral Janus kinase inhibitor, in patients from Brazil with rheumatoid arthritis. *Medicine (Baltimore).* **97,** e11609 (2018).
194. Vanags, D. *et al.* Therapeutic efficacy and safety of chaperonin 10 in patients with rheumatoid arthritis: a double-blind randomised trial. *Lancet* **368,** 855–863 (2006).
195. Libby, P. Inflammation in atherosclerosis. *Nature* **420,** 868–874 (2002).
196. De Kleijn, D. & Pasterkamp, G. Toll-like receptors in cardiovascular diseases. *Cardiovasc. Res.* **60,** 58–67 (2003).
197. Frantz, S., Ertl, G. & Bauersachs, J. Mechanisms of Disease: Toll-like receptors in cardiovascular disease. *Nat. Clin. Pract. Cardiovasc. Med.* **4,** 444–454 (2007).
198. Edfeldt, K., Swedenborg, J., Hansson, G. K. & Yan, Z. Expression of toll-like receptors in human atherosclerotic lesions: a possible pathway for plaque activation. *Circulation* **105,** 1158–61 (2002).
199. Xu, X. H. *et al.* Toll-like receptor-4 is expressed by macrophages in murine and human lipid-rich atherosclerotic plaques and upregulated by oxidized LDL. *Circulation* **104,** 3103–8 (2001).
200. Doherty, T. M., Fisher, E. A. & Arditi, M. TLR signaling and trapped vascular dendritic cells in the development of atherosclerosis. *Trends Immunol.* **27,** 222–227 (2006).
201. Frantz, S. *et al.* Toll4 (TLR4) expression in cardiac myocytes in normal and failing myocardium. *J. Clin. Invest.* **104,** 271–280 (1999).
202. Frantz, S., Kelly, R. A. & Bourcier, T. Role of TLR-2 in the Activation of Nuclear Factor κB by Oxidative Stress in Cardiac Myocytes. *J. Biol. Chem.* **276,** 5197–5203 (2001).
203. Zhu, X. *et al.* MyD88 and NOS2 are essential for Toll-like receptor 4-mediated survival effect in cardiomyocytes. *Am. J. Physiol. Circ. Physiol.* **291,** H1900–H1909 (2006).
204. Tavener, S. A. Immune Cell Toll-Like Receptor 4 Is Required for Cardiac Myocyte Impairment During Endotoxemia. *Circ. Res.* **95,** 700–707 (2004).
205. Frantz, S. *et al.* Tissue-Specific Effects of the Nuclear Factor κB Subunit p50 on Myocardial Ischemia-Reperfusion Injury. *Am. J. Pathol.* **171,** 507–512 (2007).
206. Birks, E. J. *et al.* Increased toll-like receptor 4 in the myocardium of patients requiring left ventricular assist devices. *J. Hear. Lung Transplant.* **23,** 228–235 (2004).
207. HA, T. *et al.* Reduced cardiac hypertrophy in toll-like receptor 4-deficient mice following pressure overload. *Cardiovasc. Res.* **68,** 224–234 (2005).
208. Anker, S. D. & Coats, A. J. S. How to RECOVER from RENAISSANCE? The significance of the results of RECOVER, RENAISSANCE, RENEWAL and ATTACH.

Int. J. Cardiol. **86,** 123–130 (2002).

209. Mahaffey, K. W. Effect of Pexelizumab, an Anti-C5 Complement Antibody, as Adjunctive Therapy to Fibrinolysis in Acute Myocardial Infarction: The COMPlement inhibition in myocardial infarction treated with thromboLYtics (COMPLY) Trial. *Circulation* **108,** 1176–1183 (2003).
210. Bomfim, G. F. *et al.* Toll-like receptor 4 contributes to blood pressure regulation and vascular contraction in spontaneously hypertensive rats. *Clin. Sci.* **122,** 535–543 (2012).
211. Cani, P. D. *et al.* Metabolic Endotoxemia Initiates Obesity and Insulin Resistance. *Diabetes* **56,** 1761–1772 (2007).
212. Cani, P. & Delzenne, N. The Role of the Gut Microbiota in Energy Metabolism and Metabolic Disease. *Curr. Pharm. Des.* **15,** 1546–1558 (2009).
213. Brun, P. *et al.* Increased intestinal permeability in obese mice: new evidence in the pathogenesis of nonalcoholic steatohepatitis. *Am. J. Physiol. Liver Physiol.* **292,** G518–G525 (2007).
214. Erridge, C., Attina, T., Spickett, C. M. & Webb, D. J. A high-fat meal induces low-grade endotoxemia: evidence of a novel mechanism of postprandial inflammation. *Am. J. Clin. Nutr.* **86,** 1286–1292 (2007).
215. Kim, J. J. & Sears, D. D. TLR4 and Insulin Resistance. *Gastroenterol. Res. Pract.* **2010,** 1–11 (2010).
216. Dasu, M. R., Devaraj, S., Park, S. & Jialal, I. Increased Toll-Like Receptor (TLR) Activation and TLR Ligands in Recently Diagnosed Type 2 Diabetic Subjects. *Diabetes Care* **33,** 861–868 (2010).
217. Liang, C.-F., Liu, J. T., Wang, Y., Xu, A. & Vanhoutte, P. M. Toll-Like Receptor 4 Mutation Protects Obese Mice Against Endothelial Dysfunction by Decreasing NADPH Oxidase Isoforms 1 and 4. *Arterioscler. Thromb. Vasc. Biol.* **33,** 777–784 (2013).
218. Walter, S. *et al.* Role of the Toll-Like Receptor 4 in Neuroinflammation in Alzheimer's Disease. *Cell. Physiol. Biochem.* **20,** 947–956 (2007).
219. Geisse, J. *et al.* Imiquimod 5% cream for the treatment of superficial basal cell carcinoma: results from two phase III, randomized, vehicle-controlled studies. *J. Am. Acad. Dermatol.* **50,** 722–733 (2004).
220. Northfelt, D. W. *et al.* A Phase I Dose-Finding Study of the Novel Toll-like Receptor 8 Agonist VTX-2337 in Adult Subjects with Advanced Solid Tumors or Lymphoma. *Clin. Cancer Res.* **20,** 3683–3691 (2014).
221. Sacre, S. M. *et al.* Inhibitors of TLR8 Reduce TNF Production from Human Rheumatoid

Synovial Membrane Cultures. *J. Immunol.* **181,** 8002–8009 (2008).

222. Piao, W. *et al.* Recruitment of TLR adapter TRIF to TLR4 signaling complex is mediated by the second helical region of TRIF TIR domain. *Proc. Natl. Acad. Sci.* **110,** 19036–19041 (2013).
223. Zaffaroni, L. & Peri, F. Recent advances on Toll-like receptor 4 modulation: new therapeutic perspectives. *Future Med. Chem.* **10,** 461–476 (2018).
224. Lucas, K. & Maes, M. Role of the Toll Like Receptor (TLR) Radical Cycle in Chronic Inflammation: Possible Treatments Targeting the TLR4 Pathway. *Mol. Neurobiol.* **48,** 190–204 (2013).
225. Ireton, G. C. & Reed, S. G. Adjuvants containing natural and synthetic Toll-like receptor 4 ligands. *Expert Rev. Vaccines* **12,** 793–807 (2013).
226. Johnson, A. G. STUDIES ON THE O ANTIGEN OF SALMONELLA TYPHOSA: V. ENHANCEMENT OF ANTIBODY RESPONSE TO PROTEIN ANTIGENS BY THE PURIFIED LIPOPOLYSACCHARIDE. *J. Exp. Med.* **103,** 225–246 (1956).
227. Evans, J. T. *et al.* Enhancement of antigen-specific immunity via the TLR4 ligands MPL adjuvant and Ribi.529. *Expert Rev. Vaccines* **2,** 219–29 (2003).
228. Coler, R. N. *et al.* A Synthetic Adjuvant to Enhance and Expand Immune Responses to Influenza Vaccines. *PLoS One* **5,** e13677 (2010).
229. Cameron, D. J. & Stromberg, B. V. The ability of macrophages from head and neck cancer patients to kill tumor cells. Effect of prostaglandin inhibitors on cytotoxicity. *Cancer* **54,** 2403–8 (1984).
230. Yang, D., Satoh, M., Ueda, H., Tsukagoshi, S. & Yamazaki, M. Activation of tumor-infiltrating macrophages by a synthetic lipid A analog (ONO-4007) and its implication in antitumor effects. *Cancer Immunol. Immunother.* **38,** 287–93 (1994).
231. Peri, F. & Piazza, M. Therapeutic targeting of innate immunity with Toll-like receptor 4 (TLR4) antagonists. *Biotechnol. Adv.* **30,** 251–260 (2012).
232. David, S. A. Towards a rational development of anti-endotoxin agents: novel approaches to sequestration of bacterial endotoxins with small molecules. *J. Mol. Recognit.* **14,** 370–387 (2001).
233. López-Abarrategui, C., Del Monte-Martínez, A., Reyes-Acosta, O., Franco, O. L. & Otero-González, A. J. LPS inmobilization on porous and non-porous supports as an approach for the isolation of anti-LPS host-defense peptides. *Front. Microbiol.* **4,** 389 (2013).
234. Facchini, F. A. *et al.* Co-administration of Antimicrobial Peptides Enhances Toll-like

Receptor 4 Antagonist Activity of a Synthetic Glycolipid. *ChemMedChem* **13,** 280–287 (2018).

235. Kwa, A., Kasiakou, S. K., Tam, V. H. & Falagas, M. E. Polymyxin B: similarities to and differences from colistin (polymyxin E). *Expert Rev. Anti. Infect. Ther.* **5,** 811–821 (2007).
236. da Silva, T. A. *et al.* CD14 is critical for TLR2-mediated M1 macrophage activation triggered by N-glycan recognition. *Sci. Rep.* **7,** 7083 (2017).
237. Manukyan, M. *et al.* Binding of lipopeptide to CD14 induces physical proximity of CD14, TLR2 and TLR1. *Eur. J. Immunol.* **35,** 911–921 (2005).
238. Asai, Y., Hashimoto, M. & Ogawa, T. Treponemal glycoconjugate inhibits Toll-like receptor ligand-induced cell activation by blocking LPS-binding protein and CD14 functions. *Eur. J. Immunol.* **33,** 3196–3204 (2003).
239. Wang, X. & Quinn, P. J. in 3–25 (2010). doi:10.1007/978-90-481-9078-2_1
240. Mueller, M. *et al.* Aggregates are the biologically active units of endotoxin. *J. Biol. Chem.* **279,** 26307–26313 (2004).
241. Gutsmann, T., Schromm, A. B. & Brandenburg, K. The physicochemistry of endotoxins in relation to bioactivity. *Int. J. Med. Microbiol.* **297,** 341–352 (2007).
242. Brandenburg, K. & Wiese, A. Endotoxins: Relationships between Structure, Function, and Activity. *Curr. Top. Med. Chem.* **4,** 1127–1146 (2004).
243. Brandenburg, K., Kusumoto, S. & Seydel, U. Conformational studies of synthetic lipid A analogues and partial structures by infrared spectroscopy. *Biochim. Biophys. Acta - Biomembr.* **1329,** 183–201 (1997).
244. Hashim, R. *et al.* Dry Thermotropic Glycolipid Self-Assembly:A Review. *J. Oleo Sci.* **67,** 651–668 (2018).
245. Calabrese, V., Cighetti, R. & Peri, F. Molecular simplification of lipid A structure: TLR4-modulating cationic and anionic amphiphiles. *Mol. Immunol.* **14,** 1–9 (2014).
246. Seydel, U., Oikawa, M., Fukase, K., Kusumoto, S. & Brandenburg, K. Intrinsic conformation of lipid A is responsible for agonistic and antagonistic activity. *Eur. J. Biochem.* **267,** 3032–3039 (2000).
247. Israelachvili, J. N., Mitchell, D. J. & Ninham, B. W. Theory of self-assembly of hydrocarbon amphiphiles into micelles and bilayers. *J. Chem. Soc. Faraday Trans. 2* **72,** 1525 (1976).
248. von Minden, H. . *et al.* Thermotropic and lyotropic properties of long chain alkyl glycopyranosides. Part II. Disaccharide headgroups. *Chem. Phys. Lipids* **106,** 157–179

(2000).

249. Vill, V. & Hashim, R. Carbohydrate liquid crystals: structure–property relationship of thermotropic and lyotropic glycolipids. *Curr. Opin. Colloid Interface Sci.* **7,** 395–409 (2002).
250. Shearman, G. C. *et al.* Calculations of and Evidence for Chain Packing Stress in Inverse Lyotropic Bicontinuous Cubic Phases. *Langmuir* **23,** 7276–7285 (2007).
251. Barón, M. Definitions of basic terms relating to low-molar-mass and polymer liquid crystals (IUPAC Recommendations 2001). *Pure Appl. Chem.* **73,** 845–895 (2001).
252. Hashim, R., Sugimura, A., Minamikawa, H. & Heidelberg, T. Nature-like synthetic alkyl branched-chain glycolipids: a review on chemical structure and self-assembly properties. *Liq. Cryst.* **39,** 1–17 (2012).
253. Tschierske, C. Amphotropic liquid crystals. *Curr. Opin. Colloid Interface Sci.* **7,** 355–370 (2002).
254. Velayutham, T. S. *et al.* Phase sensitive molecular dynamics of self-assembly glycolipid thin films: A dielectric spectroscopy investigation. *J. Chem. Phys.* **141,** 085101 (2014).
255. Velayutham, T. S. *et al.* Molecular dynamics of anhydrous glycolipid self-assembly in lamellar and hexagonal phases. *Phys. Chem. Chem. Phys.* **18,** 15182–15190 (2016).
256. Liao, G. *et al.* Thermotropic liquid crystalline properties of amphiphilic branched chain glycolipids. *Liq. Cryst.* **33,** 361–366 (2006).
257. Abeygunaratne, S., Hashim, R. & Vill, V. Evidence for uncorrelated tilted layer structure and electrically polarized bilayers in amphiphilic glycolipids. *Phys. Rev. E* **73,** 011916 (2006).
258. von Minden, H. ., Milkereit, G. & Vill, V. Effects of carbohydrate headgroups on the stability of induced cubic phases in binary mixtures of glycolipids. *Chem. Phys. Lipids* **120,** 45–56 (2002).
259. Bayach, I., Manickam Achari, V., Wan Iskandar, W. F. N., Sugimura, A. & Hashim, R. Computational insights into octyl- D -xyloside isomers towards understanding the liquid crystalline structure: physico-chemical features. *Liq. Cryst.* **43,** 1503–1513 (2016).
260. Mitchell, F. L., Miles, S. M., Neres, J., Bichenkova, E. V & Bryce, R. A. Tryptophan as a Molecular Shovel in the Glycosyl Transfer Activity of Trypanosoma cruzi Trans-sialidase. *Biophys. J.* **98,** L38–L40 (2010).
261. Gurtovenko, A. A. & Vattulainen, I. Molecular Mechanism for Lipid Flip-Flops. *J. Phys. Chem. B* **111,** 13554–13559 (2007).
262. Seydel, U., Scheel, O., Müller, M., Brandenburg, K. & Blunck, R. A K+ channel is

involved in LPS signaling. *J. Endotoxin Res.* **7,** 243–7 (2001).

263. Papavlassopoulos, M. *et al.* MaxiK Blockade Selectively Inhibits the Lipopolysaccharide-Induced I B- /NF- B Signaling Pathway in Macrophages. *J. Immunol.* **177,** 4086–4093 (2006).
264. Mueller, M., Lindner, B., Dedrick, R., Schromm, A. B. & Seydel, U. Endotoxin: physical requirements for cell activation. *J. Endotoxin Res.* **11,** 299–303 (2005).
265. Müller, M., Scheel, O., Lindner, B., Gutsmann, T. & Seydel, U. The role of membrane-bound LBP, endotoxin aggregates, and the MaxiK channel in LPS-induced cell activation. *J. Endotoxin Res.* **9,** 181–186 (2003).
266. Blunck, R. *et al.* New Insights Into Endotoxin-Induced Activation of Macrophages: Involvement of a K+ Channel in Transmembrane Signaling. *J. Immunol.* **166,** 1009–1015 (2001).
267. Scior, T. *et al.* Three-Dimensional Mapping of Differential Amino Acids of Human, Murine, Canine and Equine Tlr4/Md-2 Receptor Complexes Conferring Endotoxic Activation By Lipid a, Antagonism By Eritoran and Species-Dependent Activities of Lipid Iva in the Mammalian Lps Se. *Comput. Struct. Biotechnol. J.* **7,** 1–11 (2013).
268. Scior, T., Alexander, C. & Zaehringer, U. Reviewing and identifying amino acids of human , murine , canine and equine TLR4 / MD-2 receptor complexes conferring endotoxic innate immunity activation by LPS / lipid A , or antagonistic effects by Eritoran , in contrast to species-dependent modulation. (2013).
269. Rietschel, E. T. *et al.* Bacterial endotoxin: molecular relationships of structure to activity and function. *FASEB J.* **8,** 217–225 (1994).
270. Brandenburg, K. *et al.* Biophysical Characterization of Triacyl Monosaccharide Lipid A Partial Structures in Relation to Bioactivity. *Biophys. J.* **83,** 322–333 (2002).
271. Matsuura, M., Kiso, M. & Hasegawa, A. Activity of monosaccharide lipid A analogues in human monocytic cells as agonists or antagonists of bacterial lipopolysaccharide. *Infect. Immun.* **67,** 6286–92 (1999).
272. Funatogawa, K., Matsuura, M., Nakano, M., Kiso, M. & Hasegawa, A. Relationship of structure and biological activity of monosaccharide lipid A analogues to induction of nitric oxide production by murine macrophage RAW264.7 cells. *Infect. Immun.* **66,** 5792–8 (1998).
273. Tamai, R. *et al.* Cell activation by monosaccharide lipid A analogues utilizing Toll-like receptor 4. *Immunology* **110,** 66–72 (2003).
274. Cighetti, R. *et al.* Modulation of CD14 and TLR4×MD-2 activities by a synthetic lipid

A mimetic. *ChemBioChem* **15,** 250–258 (2014).

275. Kusumoto, S. *et al.* Chemical synthesis of lipid A for the elucidation of structure- activity relationships. *Bact. Lipopolysaccharides Struct. Synth. Biol. Act.* 237 (1983).
276. Imoto, M. *et al.* Total synthesis of Escherichia coli lipid A, the endotoxin principle of cell-surface lipopolysaccharide.pdf. *Bull. Chem. Soc. Jpn.* **60,** 2205–2214 (1987).
277. Ohto, U., Fukase, K., Miyake, K. & Shimizu, T. Structural basis of species-specific endotoxin sensing by innate immune receptor TLR4/MD-2. *Proc. Natl. Acad. Sci.* **109,** 7421–7426 (2012).
278. Tanamoto, K. -i. & Azumi, S. Salmonella-Type Heptaacylated Lipid A Is Inactive and Acts as an Antagonist of Lipopolysaccharide Action on Human Line Cells. *J. Immunol.* **164,** 3149–3156 (2000).
279. Johnson, D. A., Sowell, C. G., Keegan, D. S. & Livesay, M. T. Chemical Synthesis of the Major Constituents of Salmonella Minnesota Monophosphoryl Lipid A. *J. Carbohydr. Chem.* **17,** 1421–1426 (1998).
280. Johnson, D. A. *et al.* 3- O -Desacyl Monophosphoryl Lipid A Derivatives: Synthesis and Immunostimulant Activities †. *J. Med. Chem.* **42,** 4640–4649 (1999).
281. Coler, R. N. *et al.* Development and characterization of synthetic glucopyranosyl lipid adjuvant system as a vaccine adjuvant. *PLoS One* **6,** 1–12 (2011).
282. Pantel, A. *et al.* A new synthetic TLR4 agonist, GLA, allows dendritic cells targeted with antigen to elicit Th1 T-cell immunity in vivo. *Eur. J. Immunol.* **42,** 101–109 (2012).
283. Heeke, D. S. *et al.* Identification of GLA/SE as an effective adjuvant for the induction of robust humoral and cell-mediated immune responses to EBV-gp350 in mice and rabbits. *Vaccine* **34,** 2562–2569 (2016).
284. Santini-Oliveira, M. *et al.* Schistosomiasis vaccine candidate Sm14/GLA-SE: Phase 1 safety and immunogenicity clinical trial in healthy, male adults. *Vaccine* **34,** 586–594 (2016).
285. Falloon, J. *et al.* A phase 1a, first-in-human, randomized study of a respiratory syncytial virus F protein vaccine with and without a toll-like receptor-4 agonist and stable emulsion adjuvant. *Vaccine* **34,** 2847–2854 (2016).
286. Gregg, K. A. *et al.* Rationally Designed TLR4 Ligands for Vaccine Adjuvant Discovery. *MBio* **8,** 1–14 (2017).
287. Lewicky, J. D., Ulanova, M. & Jiang, Z. Improving the immunostimulatory potency of diethanolamine-containing lipid A mimics. *Bioorg. Med. Chem.* **2,** 20–23 (2013).
288. Lewicky, J. D., Ulanova, M. & Jiang, Z.-H. Synthesis of a dimeric monosaccharide lipid

A mimic and its synergistic effect on the immunostimulatory activity of lipopolysaccharide. *Carbohydr. Res.* **346,** 1705–1713 (2011).

289. Piazza, M. *et al.* A Synthetic Lipid A Mimetic Modulates Human TLR4 Activity. *ChemMedChem* **7,** 213–217 (2012).
290. Johnson, D. A. *et al.* Synthesis and biological evaluation of new class of vaccine adjuvants: aminoalkyl glucosamine 4-phosphates (AGPs). *Bioorg. Med. Chem. Lett.* **9,** 2273–2278 (1999).
291. Johnson, D. a. Synthetic TLR4-active glycolipids as vaccine adjuvants and stand-alone immunotherapeutics. *Curr. Top. Med. Chem.* **8,** 64–79 (2008).
292. Stöver, A. G. *et al.* Structure-Activity Relationship of Synthetic Toll-like Receptor 4 Agonists. *J. Biol. Chem.* **279,** 4440–4449 (2004).
293. Cluff, C. W. *et al.* Synthetic Toll-Like Receptor 4 Agonists Stimulate Innate Resistance to Infectious Challenge. *Infect. Immun.* **73,** 3044–3052 (2005).
294. Mason, K. W. *et al.* Reduction of nasal colonization of nontypeable Haemophilus influenzae following intranasal immunization with rLP4/rLP6/UspA2 proteins combined with aqueous formulation of RC529. *Vaccine* **22,** 3449–3456 (2004).
295. Zhu, D., Barniak, V., Zhang, Y., Green, B. & Zlotnick, G. Intranasal immunization of mice with recombinant lipidated P2086 protein reduces nasal colonization of group B Neisseria meningitidis. *Vaccine* **24,** 5420–5425 (2006).
296. Kiso, M., Ishida, H. & Hasegawa, A. Synthesis of Biologically Active, Novel Monosaccharide Analogs of Lipid A. *Agric. Biol. Chem.* **48,** 251–252 (1984).
297. Matsuura, M. *et al.* Biological activities of chemically synthesized analogues of the nonreducing sugar moiety of lipid A. *FEBS Lett.* **167,** 226–230 (1984).
298. Nishijima, M. *et al.* Macrophage activation by monosaccharide precursors of Escherichia coli lipid A. *Proc. Natl. Acad. Sci.* **82,** 282–286 (1985).
299. Kusumoto, S., Yamamoto, M. & Shiba, T. Chemical syntheses of lipid X and lipid Y, acyl glucosamine 1-phosphates isolated from escherichia coli mutants. *Tetrahedron Lett.* **25,** 3727–3730 (1984).
300. Aschauer, H., Grob, A., Hildebrandt, J., Schuetze, E. & Stuetz, P. Highly purified lipid X is devoid of immunostimulatory activity. Isolation and characterization of immunostimulating contaminants in a batch of synthetic lipid X. *J. Biol. Chem.* **265,** 9159–64 (1990).
301. Van Dervort, A. L., Doerfler, M. E., Stuetz, P. & Danner, R. L. Antagonism of lipopolysaccharide-induced priming of human neutrophils by lipid A analogs. *J.*

Immunol. **149,** 359–66 (1992).

302. Danner, R. L., Van Dervort, A. L., Doerfler, M. E., Stuetz, P. & Parrillo, J. E. Antiendotoxin activity of lipid A analogues: requirements of the chemical structure. *Pharm. Res.* **7,** 260–3 (1990).
303. Macher, I. A convenient synthesis of 2-deoxy-2-[(R)-1-hydroxytetradecanamido]-3-O-[(R)-3-hydroxytetradecanoyl]-α-d-glucopyranose 1-phosphate (lipid X). *Carbohydr. Res.* **162,** 79–84 (1987).
304. Perera, P. Y., Manthey, C. L., Stütz, P. L., Hildebrandt, J. & Vogel, S. N. Induction of early gene expression in murine macrophages by synthetic lipid A analogs with differing endotoxic potentials. *Infect. Immun.* **61,** 2015–23 (1993).
305. Lam, C. *et al.* SDZ MRL 953, a novel immunostimulatory monosaccharidic lipid A analog with an improved therapeutic window in experimental sepsis. *Antimicrob. Agents Chemother.* **35,** 500–505 (1991).
306. Knopf, H. P. *et al.* Discordant adaptation of human peritoneal macrophages to stimulation by lipopolysaccharide and the synthetic lipid A analogue SDZ MRL 953. Down-regulation of TNF-alpha and IL-6 is paralleled by an up-regulation of IL-1 beta and granulocyte colony-stimulat. *J. Immunol.* **153,** 287–99 (1994).
307. Kiani, a *et al.* Downregulation of the proinflammatory cytokine response to endotoxin by pretreatment with the nontoxic lipid A analog SDZ MRL 953 in cancer patients. *Blood* **90,** 1673–83 (1997).
308. Stern, A. *et al.* SDZ MRL 953, a lipid A analog as selective cytokine inducer. *Prog. Clin. Biol. Res.* **392,** 549–65 (1995).
309. Toda, M., Sasaki, Y. & Shimoji, K. Preparation and testing of 2-deoxy-2-acylaminoglucopyranose 4-sulfates as immunostimulants. (1988). doi:WO 9956744 A1 19991111
310. Masaaki, T., SHIMOJI, K. & YUTARO, S. Preparation of glucosamine derivatives as immunostimulants and antitumor agents. (1987).
311. Shimizu, T. *et al.* Mitogenic activity and lethal toxicity of lipid A analogs, glucosamine-phosphate carrying aromatic alkyl groups, in mice. *Biol. Pharm. Bull.* **16,** 932–4 (1993).
312. Hawkins, L. D. A Novel Class of Endotoxin Receptor Agonists with Simplified Structure, Toll-Like Receptor 4-Dependent Immunostimulatory Action, and Adjuvant Activity. *J. Pharmacol. Exp. Ther.* **300,** 655–661 (2002).
313. Imoto, M. *et al.* Chemical synthesis of phosphorylated tetraacyl disaccharide corresponding to a biosynthetic precursor of lipid A. *Tetrahedron Lett.* **25,** 2667–2670

(1984).

314. Imoto, M. *et al.* Chemical Synthesis of a Biosynthetic Precursor of Lipid A with a Phosphorylated Tetraacyl Disaccharide Structure. *Bull. Chem. Soc. Jpn.* **60,** 2197–2204 (1987).
315. Meng, J., Lien, E. & Golenbock, D. T. MD-2-mediated Ionic Interactions between Lipid A and TLR4 Are Essential for Receptor Activation. *J. Biol. Chem.* **285,** 8695–8702 (2010).
316. Mayer, H., Merkofer, T., Warth, C. & Weckesser, J. Position and configuration of double bonds of lipid A-associated monounsaturated fatty acids of Proteobacferia and Rhodobacter capsulatus 37b4. *J. Endotoxin Res.* **3,** 345–352 (1996).
317. Takayama, K., Qureshi, N., Beutler, B. & Kirkland, T. N. Diphosphoryl lipid A from Rhodopseudomonas sphaeroides ATCC 17023 blocks induction of cachectin in macrophages by lipopolysaccharide. *Infect. Immun.* **57,** 1336–8 (1989).
318. Qureshi, N., Honovich, J. P., Hara, H., Cotter, R. J. & Takayama, K. Location of fatty acids in lipid A obtained from lipopolysaccharide of Rhodopseudomonas sphaeroides ATCC 17023. *J. Biol. Chem.* **263,** 5502–4 (1988).
319. Qureshi, N. *et al.* Chemical reduction of 3-oxo and unsaturated groups in fatty acids of diphosphoryl lipid A from the lipopolysaccharide of Rhodopseudomonas sphaeroides: Comparison of biological properties before and after reduction. *J. Biol. Chem.* **266,** 6532–6538 (1991).
320. Kaltashov, I. A., Doroshenko, V., Cotter, R. J., Takayama, K. & Qureshi, N. Confirmation of the structure of lipid A derived from the lipopolysaccharide of Rhodobacter sphaeroides by a combination of MALDI, LSIMS, and tandem mass spectrometry. *Anal. Chem.* **69,** 2317–22 (1997).
321. Loppnow, H. *et al.* Cytokine induction by lipopolysaccharide (LPS) corresponds to lethal toxicity and is inhibited by nontoxic Rhodobacter capsulatus LPS. *Infect. Immun.* **58,** 3743–50 (1990).
322. Lipid, A. & Therapy, C. *Lipid A in Cancer Therapy*. **667,** (Springer New York, 2010).
323. Christ, W. J. *et al.* Total Synthesis of the Proposed Structure of Rhodobacter sphaeroides Lipid A Resulting in the Synthesis of New Potent Lipopolysaccharide Antagonists. *J. Am. Chem. Soc.* **116,** 3637–3638 (1994).
324. Rose, J. R., Christ, W. J., Bristol, J. R., Kawata, T. & Rossignol, D. P. Agonistic and antagonistic activities of bacterially derived Rhodobacter sphaeroides lipid A: comparison with activities of synthetic material of the proposed structure and analogs.

Infect. Immun. **63,** 833–9 (1995).

325. Qureshi, N., Takayama, K. & Kurtz, R. Diphosphoryl lipid A obtained from the nontoxic lipopolysaccharide of Rhodopseudomonas sphaeroides is an endotoxin antagonist in mice. *Infect. Immun.* **59,** 441–444 (1991).
326. Manthey, C. L., Qureshi, N., Stütz, P. L. & Vogel, S. N. Lipopolysaccharide antagonists block taxol-induced signaling in murine macrophages. *J. Exp. Med.* **178,** 695–702 (1993).
327. Kutuzova, G. D., Albrecht, R. M., Erickson, C. M. & Qureshi, N. Diphosphoryl Lipid A from Rhodobacter sphaeroides Blocks the Binding and Internalization of Lipopolysaccharide in RAW 264.7 Cells. *J. Immunol.* **167,** 482–489 (2001).
328. Kirkland, T. N., Qureshi, N. & Takayama, K. Diphosphoryl lipid A derived from lipopolysaccharide (LPS) of Rhodopseudomonas sphaeroides inhibits activation of 70Z/3 cells by LPS. *Infect. Immun.* **59,** 131–6 (1991).
329. Lynn, W. A., Raetz, C. R., Qureshi, N. & Golenbock, D. T. Lipopolysaccharide-induced stimulation of CD11b/CD18 expression on neutrophils. Evidence of specific receptor-based response and inhibition by lipid A-based antagonists. *J. Immunol.* **147,** 3072–9 (1991).
330. Christ, W. J., Rossignol, D. P., Kobayashi, S. & Kawata, T. SUBSTITUTED LIPOSACCHARIDES USEFUL IN THE TREATMENT AND PREVENTION OF ENDOTOXEMIA - 5,935,938-. (1995).
331. Mullarkey, M. Inhibition of Endotoxin Response by E5564, a Novel Toll-Like Receptor 4-Directed Endotoxin Antagonist. *J. Pharmacol. Exp. Ther.* **304,** 1093–1102 (2002).
332. Leon, C. G., Tory, R., Jia, J., Sivak, O. & Wasan, K. M. Discovery and Development of Toll-Like Receptor 4 (TLR4) Antagonists: A New Paradigm for Treating Sepsis and Other Diseases. *Pharm. Res.* **25,** 1751–1761 (2008).
333. Brandenburg, K. *et al.* Physicochemical characteristics of triacyl lipid A partial structure OM-174 in relation to biological activity. *Eur. J. Biochem.* **267,** 3370–3377 (2000).
334. Onier, N. *et al.* Expression of inducible nitric oxide synthase in tumors in relation with their regression induced by lipid A in rats. *Int. J. Cancer* **81,** 755–760 (1999).
335. Onier, N. *et al.* Cure of colon cancer metastasis in rats with the new lipid A OM 174. Apoptosis of tumor cells and immunization of rats. *Clin. Exp. Metastasis* **17,** 299–306 (1999).
336. Martin, O. R. *et al.* Synthesis and Immunobiological Activity of an Original Series of Acyclic Lipid A Mimics Based on a Pseudodipeptide Backbone. *J. Med. Chem.* **49,**

6000–6014 (2006).

337. Akamatsu, M. *et al.* Synthesis of lipid A monosaccharide analogues containing acidic amino acid: Exploring the structural basis for the endotoxic and antagonistic activities. *Bioorg. Med. Chem.* **14,** 6759–6777 (2006).
338. Morris, G. M. *et al.* AutoDock4 and AutoDockTools4: Automated docking with selective receptor flexibility. *J. Comput. Chem.* **30,** 2785–2791 (2009).
339. Trott, O. & Olson, A. AutoDock Vina: improving the speed and accuracy of docking with a new scoring function, efficient optimization and multithreading. *J. Comput. Chem.* **31,** 455–461 (2010).
340. Perrin-Cocon, L. *et al.* TLR4 antagonist FP7 inhibits LPS-induced cytokine production and glycolytic reprogramming in dendritic cells, and protects mice from lethal influenza infection. *Sci. Rep.* **7,** 40791 (2017).
341. Imai, Y. *et al.* Identification of Oxidative Stress and Toll-like Receptor 4 Signaling as a Key Pathway of Acute Lung Injury. *Cell* **133,** 235–249 (2008).
342. Shirey, K. A. *et al.* Novel strategies for targeting innate immune responses to influenza. *Mucosal Immunol.* **9,** 1173–1182 (2016).
343. Pérez-Regidor, L., Zarioh, M., Ortega, L. & Martín-Santamaría, S. Virtual Screening Approaches towards the Discovery of Toll-Like Receptor Modulators. *Int. J. Mol. Sci.* **17,** 1508 (2016).
344. Peri, F. & Calabrese, V. Toll-like Receptor 4 (TLR4) modulation by synthetic and natural compounds : an update Toll-like Receptor 4 (TLR4) modulation by synthetic and natural compounds : an update. **4,** (2013).
345. Yamada, M. *et al.* Discovery of Novel and Potent Small-Molecule Inhibitors of NO and Cytokine Production as Antisepsis Agents: Synthesis and Biological Activity of Alkyl 6-(N-Substituted sulfamoyl)cyclohex-1-ene-1-carboxylate. *J. Med. Chem.* **48,** 7457–7467 (2005).
346. Manček-Keber, M. & Jerala, R. Structural similarity between the hydrophobic fluorescent probe and lipid A as a ligand of MD-2. *FASEB J.* **20,** 1836–1842 (2006).
347. Morrison, D. C. & Jacobs, D. M. Binding of polymyxin B to the lipid A portion of bacterial lipopolysaccharides. *Immunochemistry* **13,** 813–818 (1976).
348. Velkov, T., Thompson, P. E., Nation, R. L. & Li, J. Structure−Activity Relationships of Polymyxin Antibiotics. *J. Med. Chem.* **53,** 1898–1916 (2010).
349. Sil, D. *et al.* Bound To Shock: Protection from Lethal Endotoxemic Shock by a Novel, Nontoxic, Alkylpolyamine Lipopolysaccharide Sequestrant. *Antimicrob. Agents*

Chemother. **51,** 2811–2819 (2007).

350. Miller, K. A. *et al.* Lipopolysaccharide Sequestrants: Structural Correlates of Activity and Toxicity in Novel Acylhomospermines. *J. Med. Chem.* **48,** 2589–2599 (2005).
351. Wu, W. *et al.* Structure–activity relationships of lipopolysaccharide sequestration in guanylhydrazone-bearing lipopolyamines. *Bioorg. Med. Chem.* **17,** 709–715 (2009).
352. Burns, M. R. *et al.* Polycationic Sulfonamides for the Sequestration of Endotoxin. *J. Med. Chem.* **50,** 877–888 (2007).
353. Chen, W., Yan, W. & Huang, L. A simple but effective cancer vaccine consisting of an antigen and a cationic lipid. *Cancer Immunol. Immunother.* **57,** 517–530 (2008).
354. Tanaka, T. *et al.* DiC14-amidine cationic liposomes stimulate myeloid dendritic cells through toll-like receptor 4. *Eur. J. Immunol.* **38,** 1351–1357 (2008).
355. Chen, X. *et al.* Topomimetics of Amphipathic β-Sheet and Helix-Forming Bactericidal Peptides Neutralize Lipopolysaccharide Endotoxins. *J. Med. Chem.* **49,** 7754–7765 (2006).
356. Sestito, S. E. *et al.* Amphiphilic Guanidinocalixarenes Inhibit Lipopolysaccharide (LPS)- and Lectin-Stimulated Toll-like Receptor 4 (TLR4) Signaling. *J. Med. Chem.* **60,** 4882–4892 (2017).
357. Piazza, M. *et al.* Glycolipids and Benzylammonium Lipids as Novel Antisepsis Agents: Synthesis and Biological Characterization. *J. Med. Chem.* **52,** 1209–1213 (2009).
358. Peri, F. & Calabrese, V. Toll-like receptor 4 (TLR4) modulation by synthetic and natural compounds : an update. *J. Med. Chem.* **57,** 3612–3622 (2014).
359. Koo, J. E., Park, Z. Y., Kim, N. D. & Lee, J. Y. Sulforaphane inhibits the engagement of LPS with TLR4/MD2 complex by preferential binding to Cys133 in MD2. *Biochem. Biophys. Res. Commun.* **434,** (2013).
360. Urpi-Sarda, M. *et al.* Virgin olive oil and nuts as key foods of the Mediterranean diet effects on inflammatory biomarkers related to atherosclerosis. *Pharmacol. Res.* **65,** 577–583 (2012).
361. Wu, Y., Chen, H.-D., Li, Y.-H., Gao, X.-H. & Preedy, V. R. in 68–90 (2012). doi:10.3920/978-90-8686-729-5_5
362. Cicerale, S., Conlan, X. A., Sinclair, A. J. & Keast, R. S. J. Chemistry and Health of Olive Oil Phenolics. *Crit. Rev. Food Sci. Nutr.* **49,** 218–236 (2008).
363. Visioli, F., Poli, A. & Gall, C. Antioxidant and other biological activities of phenols from olives and olive oil. *Med. Res. Rev.* **22,** 65–75 (2002).
364. Maiuri, M. C. *et al.* Hydroxytyrosol, a phenolic compound from virgin olive oil, prevents

macrophage activation. *Naunyn. Schmiedebergs. Arch. Pharmacol.* **371,** 457–465 (2005).

365. Iacono, A. *et al.* Effect of oleocanthal and its derivatives on inflammatory response induced by lipopolysaccharide in a murine chondrocyte cell line. *Arthritis Rheum.* **62,** 1675–1682 (2010).
366. Beauchamp, G. K. *et al.* Ibuprofen-like activity in extra-virgin olive oil. *Nature* **437,** 45–46 (2005).
367. Xagorari, A., Roussos, C. & Papapetropoulos, A. Inhibition of LPS-stimulated pathways in macrophages by the flavonoid luteolin. *Br. J. Pharmacol.* **136,** 1058–1064 (2002).
368. Xagorari, a *et al.* Luteolin inhibits an endotoxin-stimulated phosphorylation cascade and proinflammatory cytokine production in macrophages. *J. Pharmacol. Exp. Ther.* **296,** 181–7 (2001).
369. Fang, H.-L., Lai, J.-T. & Lin, W.-C. Inhibitory effect of olive oil on fibrosis induced by carbon tetrachloride in rat liver. *Clin. Nutr.* **27,** 900–907 (2008).
370. Czerkies, M. & Kwiatkowska, K. Toll-Like Receptors and their Contribution to Innate Immunity: Focus on TLR4 Activation by Lipopolysaccharide. *Adv. Cell Biol.* **4,** 1–23 (2014).
371. Cario, E. *et al.* Lipopolysaccharide Activates Distinct Signaling Pathways in Intestinal Epithelial Cell Lines Expressing Toll-Like Receptors. *J. Immunol.* **164,** 966–972 (2000).
372. Hailman, E. Lipopolysaccharide (LPS)-binding protein accelerates the binding of LPS to CD14. *J. Exp. Med.* **179,** 269–277 (1994).
373. Kim, J. I. *et al.* Crystal structure of CD14 and its implications for lipopolysaccharide signaling. *J. Biol. Chem.* **280,** 11347–11351 (2005).
374. Kelley, S. L., Lukk, T., Nair, S. K. & Tapping, R. I. The Crystal Structure of Human Soluble CD14 Reveals a Bent Solenoid with a Hydrophobic Amino-Terminal Pocket. *J. Immunol.* **190,** 1304–1311 (2013).
375. Walsh, C. *et al.* Elucidation of the MD-2/TLR4 Interface Required for Signaling by Lipid IVa. *J. Immunol.* **181,** 1245–1254 (2008).
376. Visintin, A., Mazzoni, A., Spitzer, J. A. & Segal, D. M. Secreted MD-2 is a large polymeric protein that efficiently confers lipopolysaccharide sensitivity to Toll-like receptor 4. *Proc. Natl. Acad. Sci.* **98,** 12156–12161 (2001).
377. Palsson-McDermott, E. M. & O'Neill, L. A. J. Signal transduction by the lipopolysaccharide receptor, Toll-like receptor-4. *Immunology* **113,** 153–162 (2004).
378. Akira, S. & Takeda, K. Toll-like receptor signalling. *Nat. Rev. Immunol.* **4,** 499–511

(2004).

379. Ryu, J.-K. *et al.* Reconstruction of LPS Transfer Cascade Reveals Structural Determinants within LBP, CD14, and TLR4-MD2 for Efficient LPS Recognition and Transfer. *Immunity* **46,** 38–50 (2017).
380. Beutler, B. & Poltorak, A. Sepsis and evolution of the innate immune response. *Crit. Care Med.* **29,** S2–S7 (2001).
381. Liu, Y., Yin, H., Zhao, M. & Lu, Q. TLR2 and TLR4 in Autoimmune Diseases : a Comprehensive Review. *Clin. Rev. Allergy Immunol.* **47,** 136–147 (2014).
382. Kuzmich, N. *et al.* TLR4 Signaling Pathway Modulators as Potential Therapeutics in Inflammation and Sepsis. *Vaccines* **5,** 34 (2017).
383. Flacher, V. *et al.* Mannoside Glycolipid Conjugates Display Anti-inflammatory Activity by Inhibition of Toll-like Receptor-4 Mediated Cell Activation. *ACS Chem. Biol.* **10,** 2697–2705 (2015).
384. Ciaramelli, C. *et al.* Glycolipid-based TLR4 modulators and fluorescent probes: rational design, synthesis and biological properties. *Chem. Biol. Drug Des.* 1–13 (2016). doi:10.1111/cbdd.12749
385. Kitchens, R. L. & Munford, R. S. CD14-dependent internalization of bacterial lipopolysaccharide (LPS) is strongly influenced by LPS aggregation but not by cellular responses to LPS. *J. Immunol.* **160,** 1920–1928 (1998).
386. Cighetti, R. *et al.* Modulation of CD14 and TLR4·MD-2 Activities by a Synthetic Lipid A Mimetic. *ChemBioChem* **15,** 250–258 (2014).
387. Kusama, T. *et al.* Synthesis and biological activities of lipid A analogs: modification of a glycosidically bound group with chemically stable polar acidic groups and disaccharide backbone with tetradecanoyl or N-dodecanoylglycyl Groups. *Chem. Pharm. Bull.* **39,** 3244–3253 (1991).
388. Liu, W.-C., Oikawa, M., Fukase, K., Suda, Y. & Kasumoto, S. A divergent synthesis of lipid A and its chemically stable unnatural analogues. *Bull. Chem. Soc. Jpn.* **72,** 1377–1385 (1999).
389. Fujimoto, Y. *et al.* Synthesis of lipid A and its analogues for investigation of the structural basis for their bioactivity. *J. Endotoxin Res.* **11,** 341–347 (2005).
390. Fukase, Y. *et al.* Synthesis of Rubrivivax gelatinosus lipid A and analogues for investigation of the structural basis for immunostimulating and inhibitory activities. *Bull. Chem. Soc. Jpn.* **81,** 796–819 (2008).
391. Mochizuki, T. *et al.* Synthesis and biological activities of lipid A-type pyrancarboxylic

acid derivatives. *Carbohydr. Res.* **324,** 225–230 (2000).

392. Fort, M. M. *et al.* A Synthetic TLR4 Antagonist Has Anti-Inflammatory Effects in Two Murine Models of Inflammatory Bowel Disease. *J. Immunol.* **174,** 6416–6423 (2005).
393. Resman, N. *et al.* Essential Roles of Hydrophobic Residues in Both MD-2 and Toll-like Receptor 4 in Activation by Endotoxin. *J. Biol. Chem.* **284,** 15052–15060 (2009).
394. Cochet, F. & Peri, F. NUOVI ANTAGONISTI DEL TLR4 UMANO. 1–41 (2018).
395. Rajaiah, R., Perkins, D. J., Ireland, D. D. C. & Vogel, S. N. CD14 dependence of TLR4 endocytosis and TRIF signaling displays ligand specificity and is dissociable in endotoxin tolerance. *Proc. Natl. Acad. Sci.* **112,** 8391–8396 (2015).
396. Huang, J. X. *et al.* Molecular Characterization of Lipopolysaccharide Binding to Human *α* -1-Acid Glycoprotein. *J. Lipids* **2012,** 1–15 (2012).
397. Viriyakosol, S. *et al.* Characterization of Monoclonal Antibodies to Human Soluble MD-2 Protein. *Hybridoma* **25,** 349–357 (2006).
398. Resman, N. *et al.* Taxanes inhibit human TLR4 signaling by binding to MD-2. *FEBS Lett.* **582,** 3929–3934 (2008).
399. Okamoto, T. *et al.* Multiple contributing roles for NOS2 in LPS-induced acute airway inflammation in mice. *Am. J. Physiol. Cell. Mol. Physiol.* **286,** L198–L209 (2004).
400. Poynter, M. E., Irvin, C. G. & Janssen-Heininger, Y. M. W. A Prominent Role for Airway Epithelial NF- B Activation in Lipopolysaccharide-Induced Airway Inflammation. *J. Immunol.* **170,** 6257–6265 (2003).
401. Belpaire, F. M. & Bogaert, M. G. Pharmacokinetic and pharmacodynamic consequences of altered binding of drugs to alpha 1-acid glycoprotein. *Prog. Clin. Biol. Res.* **300,** 337–50 (1989).
402. Zaias, J., Mineau, M., Cray, C., Yoon, D. & Altman, N. H. Reference values for serum proteins of common laboratory rodent strains. *J. Am. Assoc. Lab. Anim. Sci.* **48,** 387–90 (2009).
403. Kameta, N., Matsuzawa, T., Yaoi, K., Fukuda, J. & Masuda, M. Glycolipid-based nanostructures with thermal-phase transition behavior functioning as solubilizers and refolding accelerators for protein aggregates. *Soft Matter* **13,** 3084–3090 (2017).
404. Baccile, N. *et al.* Self-Assembly Mechanism of pH-Responsive Glycolipids: Micelles, Fibers, Vesicles, and Bilayers. *Langmuir* **32,** 10881–10894 (2016).
405. Case, D. A. *et al. AMBER 14*. (University of California, San Francisco, 2014).
406. Frisch, M. J. *et al. Gaussian 09*. (Gaussian, Inc., Wallingford CT, 2009).
407. Kirschner, K. N. *et al.* GLYCAM06: A generalizable biomolecular force field.

Carbohydrates. *J. Comput. Chem.* **29,** 622–655 (2008).

408. Maier, J. A. *et al.* ff14SB: Improving the Accuracy of Protein Side Chain and Backbone Parameters from ff99SB. *J. Chem. Theory Comput.* **11,** 3696–3713 (2015).

409. Martínez, L., Andrade, R., Birgin, E. G. & Martínez, J. M. PACKMOL: A package for building initial configurations for molecular dynamics simulations. *J. Comput. Chem.* **30,** 2157–2164 (2009).

ACKNOWLEDGMENTS

First of all, I would like to thank the European Community for the MCSA Action. It allowed me to perform a doctorate with freedom and optimal conditions. The action leads me to develop a broader knowledge with additional skill: computational and analytical chemistry research, international and interdisciplinar collaboration, project management, language learning. The MCSA action and the close collaboration of the TOLLerant project members allowed me to be committed to the entire drug development process.

I would like to thank all the collaborators of Bicocca. First, thank you Prof. Peri for the great opportunity you gave me to be part of your research group. I enjoyed to work with you and to learn from you. You have always been available and helpful, thank you a lot for everything.

Thank you Lenny, we had amazing three years together. I learn most of what I know in Italian thanks to you, from pelo declensions until s……osa ;-). Joke apart, you made me feel home in Italy, thank you for all the discussions we had. I wish you the best buddy.

Grazie Fabio per queste 3 anni di lavoro e risate. Non so quanto tempo abbiamo passato ad discutere e confrontarsi sull lavoro o meno. Sei un amico precioso, grazie di tutto.

Andrea, prima che tu arrivessi era un altro mondo. Grazie a te ho trovato un collega chimico con chi potevo discutere. Grazie per tutto il tempo passato insieme (da Jambon e in lab).

Grazie Michela, mia tesista, è stato un piacerre lavorare con te. Sempre sorridente e vogliosa di imparare. Ho imparato tantissimo al tuo contatto, ti voglio bene.

Vorrei anche ringraziare Sylvia, abbiamo passato momenti indimenticabili da quanto sei diventatta chimica. E sempre bello interfaciarsi con te, grazie davero.I would like to thank my co-tutors which were always open to discuss, Prof. Airoldi and Prof. Bertini, as well as all the close collaborators of the 4th floor: Valentina, Stefania, Laura, Marica, Alessio, Dylan, Andrea, Luca, Prof. Cipolla, Prof. La Ferla, Prof. Nicotra, Laura, Linda, Sofia, Gepo, Alice, Roberto, Matia, Rana, Alessandro, Carlota, Matilde, Federica, Monica, Veronica.

Gracias a Prof. Martín-Santamaría por su cálida bienvenida en su grupo de investigación, sus explicaciones y valiosos consejos. Estaba muy feliz de aprender de ella. También agradezco a todos los colaboradores de su grupo de investigación: Jean-Marc, Alessandra, Joan, Lucia, Malik, Tamara y Aurora por su apoyo.

Gracias también al Prof. Jiménez-Barbero por la investigación e interacciones dentro de su grupo de investigación, sus aclaraciones y valiosos consejos. Tuve el honor de aprender de

él. También agradezco a todos los colaboradores de su grupo de investigación: Helena, la 3 Ana, Sandra, Luca, Ilaria, José y Pablo.

Thanks to the Lofarma industry and more precisely to Dr. Mistrelo and Stefania who permitted me to learn about the drug-discovery and drug-development from an industrial point of view.

Je tiens à remercier ma famille, mes parents, grands-parents, mon frère et ma sœur qui m'ont permis d'être où et qui je suis. C'est grâce à leur support et leurs conseils que j'ai pu me construire et m'épanouir. Du fond du cœur je vous en remercie de tout ce que vous avez fait pour moi (même si je n'ai pas toujours compris tout de suite que c'était pour mon bien).

Merci à Marie, tu m'as permis de survivre dans cet environnement étranger, on a tout traversé ensemble et tu m'as appris énormément sur beaucoup d'aspects de la vie. Je ne t'en remercierais jamais assez. Je te souhaite tout le bonheur du monde.

Je voudrais également remercier mes amis Damien, Dindon et Gino, ainsi que leurs familles. C'est grâce aux amis que, peu importe les défis de la vie, on se relève et on en sort grandit. Je suis heureux de vous avoir à mes côtés les copains, vous me trouverez toujours aux vôtres.

Finally, I want to thank all the people that take part of my life during those three years, even if not explicitly noticed, you know you are part of my heart. Thank you all!

ANNEXES I: SUPPLEMENTARY INFORMATION - NOVEL CARBOXYLATE-BASED GLYCOLIPIDS: TLR4 ANTAGONISM, MD-2 BINDING AND SELF-ASSEMBLY PROPERTIES

Florent Cochet[1], Fabio A. Facchini[1], Lenny Zaffaroni[1], Jean-Marc Billod[2], Helena Coelho[3], Aurora Holgado[4], Harald Braun[4], Rudi Beyaert[4], Roman Jerala[5], Jesus Jimenez-Barbero[6], Sonsoles Martin-Santamaria[2], Francesco Peri[1]*

[1] Department of Biotechnology and Biosciences, University of Milano-Bicocca, Piazza della Scienza, 2; 20126 Milano (Italy).

[2] Department of Structural and Chemical Biology, Centro de Investigaciones Biologicas, CIB-CSIC, C/Ramiro de Maeztu, 9, 28040 Madrid, Spain.

[3] Molecular Recognition & Host−Pathogen Interactions Programme, CIC bioGUNE, Bizkaia Technology Park, Building 801A, 48170 Derio (Spain); UCIBIO, REQUIMTE, Departamento de Química, Faculdade de Ciências e Tecnologia, Universidade Nova de Lisboa, 2829-516 Caparica (Portugal); Department of Organic Chemistry II, Faculty of Science & Technology, University of the Basque Country, 48940 Leioa, Bizkaia (Spain).

[4] Unit for Molecular Signal Transduction in Inflammation VIB-UGent Center for Inflammation Research, VIB Technologiepark 927, 9052 Zwijnaarde, Ghent (Belgium); Department of Biomedical Molecular Biology, Ghent University Technologiepark 927, 9052 Zwijnaarde, Ghent (Belgium).

[5] Department of Biotechnology, National Institute of Chemistry, Hajdrihova 19, 1000 Ljubljana (Slovenia).

[6] Molecular Recognition & Host−Pathogen Interactions Programme, CIC bioGUNE, Bizkaia Technology Park, Building 801A, 48170 Derio (Spain); Department of Organic Chemistry II, Faculty of Science & Technology, University of the Basque Country, 48940 Leioa, Bizkaia (Spain); Ikerbasque, Basque Foundation for Science, Maria Diaz de Haro 13, 48009 Bilbao (Spain).

INDEX:

Molecular modeling

Structure construction and refinement. The 3D structures of ligands **FP13**, **FP14**, **FP15**, **FP16** and **FP17** were built with PyMOL using the 3D structure of **FP7**, previously reported,[88] as template. All structures were then optimized at the Hartree-Fock level. For the human TLR4/MD-2 system, we used a computational 3D model in antagonist conformation previously modeled by us. Information about the construction of the 3D coordinates of this TLR4/MD-2 model can be found here.[356]

The 3D structures of ligands **FP13**, **FP14**, **FP15**, **FP16** and **FP17** were built with PyMOL using the 3D structure of **FP7**, previously reported,[88] as template. All structures were then optimized at the Hartree-Fock level. For the human TLR4/MD-2 system, we used a computational 3D model in antagonist conformation previously modeled by us. Information about the construction of the 3D coordinates of this TLR4/MD-2 model can be found here.[356]

Parameters Derivation. The missing parameters for the MD simulations were calculated using the standard Antechamber procedure for Amber14.[405] Briefly, ligand structures, already refined at the AM1 level of theory, were optimized and their atomic partial charges were calculated with Gaussian09/e1[406] at the Hartree−Fock level (HF/6-31G* Pop = MK iop(6/33 = 2), iop(6/42 = 6)). Partial charges were derived and formatted for AmberTools15 and Amber14 with Antechamber, assigning the general AMBER force field (GAFF) atom types. The atom types of the atom constituting the saccharide ring were changed to the GLYCAM force field atom types.[407] The GAFF parameters for the phosphate group were modified as reported here.[88]

Docking calculations of ligands FP13-17. AutoDock Vina 1.1.2 [339] was used for the docking of the ligands in the human TLR4/MD-2 antagonist model and AutoDock 4.2 [338] was used to re-dock some selected poses. In AutoDock 4.2, the Lamarckian evolutionary algorithm was chosen, and all parameters were kept default except for the number of genetic algorithm runs that was set to 200 to enhance the sampling. AutoDockTools 1.5.6[338] was used to assign the Gasteiger-Marsili empirical atomic partial charges to the atoms of both the ligands and the

receptor. Nonpolar hydrogens were merged for all the ligands. The structure of the receptor was always kept rigid, whereas the structure of the ligand was set flexible. Regarding the docking boxes, spacing was set to the default value of 1 Å for Vina, and of 0.375 Å for AutoDock. The size of the box was set to 33.00 Å in the x-axis, 40.50 Å in the y-axis and 35.25 Å in the z-axis, and the center of the box was located equidistant to the center of mass of residues Arg90 (MD-2), Lys122 (MD-2) and Arg264 (TLR4).

Molecular dynamics (MD) simulations. MD simulations of selected docked TLR4/MD-2/ligand complexes were performed with amber14 and amber16. The proteins were described by the ff14SB all-atom force field,[408] the saccharide core of the ligands by the GLYCAM_06j-1 force field[407] and the other moieties of the ligands were parametrized with the GAFF force field. The simulation box was designed such as the edges are distant of at least 10 Å of any atoms. The system was solvated with the TIP3P water molecules model. Na^+ and Cl^- ion were added to counterbalance the eventual charges of the protein-ligand systems. All the simulations were performed with the same equilibration and production protocol. First, the system was submitted to 1000 steps of steepest descent algorithm followed by 7000 steps of conjugate gradient algorithm. A 100 kcal mol^{-1} A^{-2} harmonic potential constraint was applied on the proteins and the ligands. In the subsequent steps, the harmonic potential was progressively lowered (respectively to 10, 5, 2.5 and 0 kcal mol^{-1} A^{-2}) for 600 steps of conjugate gradient algorithm each time. Next, the system was heated from 0 K to 100 K by a Langevin thermostat in the canonical ensemble (NVT) under a 20 kcal.mol^{-1}.A^{-2} harmonic potential restraint on the proteins and the ligand. Finally, the system was heated up from 100 K to 300 K in the Isothermal-isobaric ensemble (NPT) under the same restraint condition than the previous step, followed by a simulation of 100 ps in which all harmonic restraints were removed. At this point the system was ready for the production run, which was performed using the Langevin thermostat in the NPT ensemble, at a 2 fs time step.

Molecular dynamics simulations of FP15 spontaneous assembly. In the experiment **FP15** was added to a phosphate buffer (PB) and 5% DMSO preparation, we thus assume the counter ions to be Na^+. To create the starting structure for the self-assembly 128 molecules of **FP15** were randomly distributed in a cubic box of 80 $Å^3$ with Packmol.[409] The same starting random spatial distribution was simulated at different temperatures (ranging from 300K to 400K) in order to minimize the simulation time while increasing the assembly speed. Within the NpT ensemble pressure was handled both isotropically (to trigger the self-assembly) and anisotropically (for the production run of the bilayer). A total of 5 sets of simulations were conducted. A first simulation in isotropic conditions at 300K for 180 ns then anisotropic conditions at 303K for 120 ns (total of 300 ns), a second one in isotropic conditions at 310K for 200 ns, a third one in isotropic conditions at 350K for 150 ns and then 850 ns of simulation in anisotropic conditions and finally two independent simulations at 400K, one in anisotropic condition for 500ns and another one in isotropic conditions for 400ns. More explanations about the different simulations are given in SI. The MD protocol used is the same than the one described for the simulations of the docked poses at the exception that temperature was changed accordingly to the desired one and pressure during the production phase was switched from isotropic to anisotropic as mentioned above.

Chemistry. Synthesis of monosaccharides

Synthesis of **FP13-17** series was achieved following the divergent synthetic strategy depicted in the Scheme 1. D-glucosamine was treated with sodium azide and triflic anhydride to obtain the azido derivative at position C2. Positions C4 and C6 were protected as 4,6-di-O-benzylidene and position C1 was protected as *tert*-butyldimethylsilyl ether (TBS) to obtain compound **1** as a common intermediate for all compounds (Scheme S1).

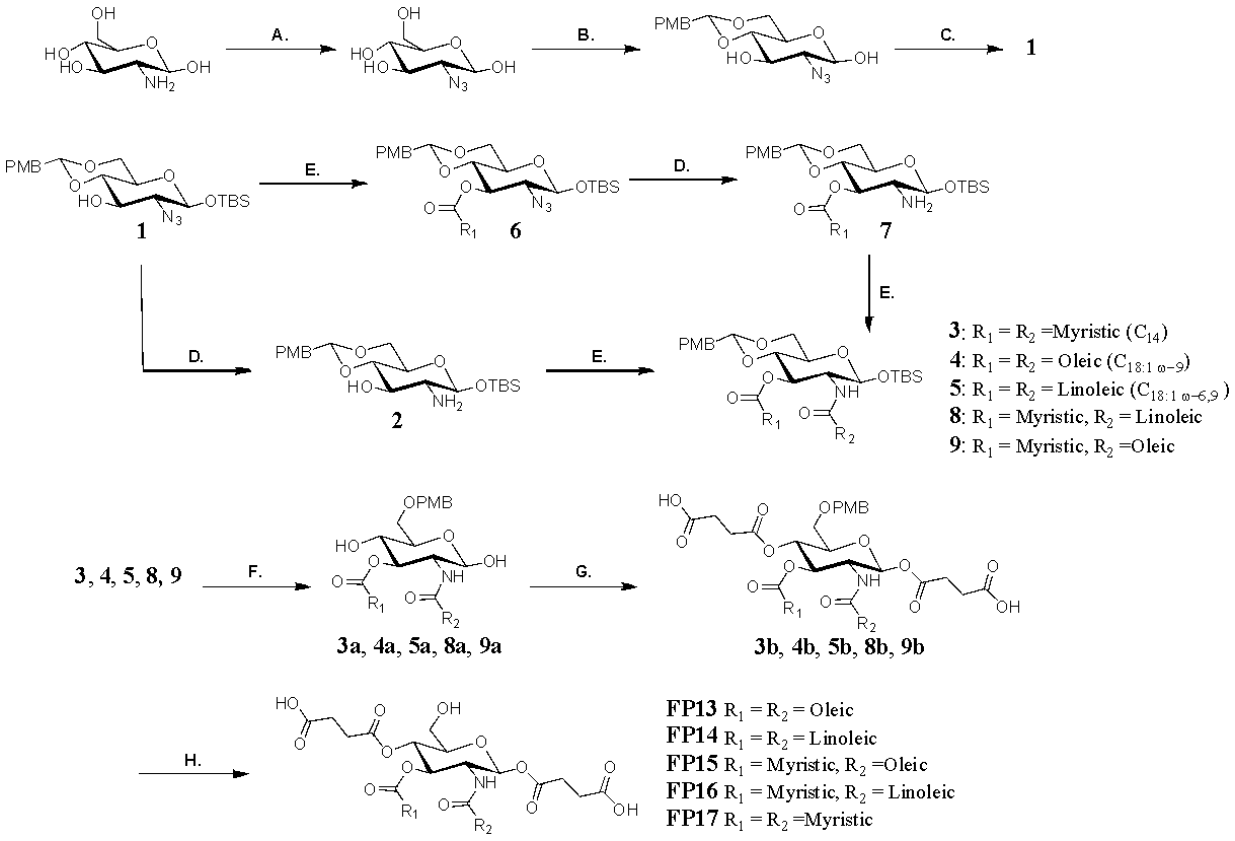

Scheme S1. Synthesis of compounds FP13-17. Reagents and conditions: **A.** i) NaN_3, Tf_2O, Pyr. ii) $CuSO_4$, Et_3N, H_2O, 0°C to r.t.; **B.** ADMA, p-TsOH.H_2O (cat.), DMF, (80%); **C.** TBDMSCl, Imidazole, DCM, (75%); **D.** PPh_3, H_2O, THF, 60°C, (85%); **E.** Myristic, Oleic or Linoleic acid, EDC, DMAP, DCM, (60%); **F.** $NaBH_3CN$, HCl, 4 Å MS, THF, (62%); **G.** Succinic anhydride, DMAP, Et_3N, DCM, (80%); **H.** TFA, DCM, 0°C to r.t., (75%).

For the synthesis of **FP13**, **FP14** and **FP17** having in glucosamine positions C2 and C3 two identical chains, **1** was treated with triphenylphosphine (PPh_3) in THF/H_2O to hydrolyze the azide into an amine thus obtaining **2**. C2 and C3 positions were then esterified with myristic, oleic or linoleic acid in the presence of the 1-ethyl-3-(3-dimethylaminopropyl)carbodiimide (EDC) as a condensing agent and a catalytic amount of dimethyl aminopyridine (DMAP) in dichloromethane giving, respectively, compounds **3**, **4** and **5**.

For the synthesis of compounds with two different chains in C2 and C3, azido-glucose **1** was esterified at position C3 using myristic acid, in the presence of DMAP and EDC in dichloromethane, to give intermediate **6**. After transformation of the azide into amine (**7**) and subsequent esterification with linoleic or oleic acid was obtained, respectively, compounds **8** (R^1=myristic; R^2=linoleic) and **9** (R^1=myristic; R^2=oleic).

Intermediates **3**, **4**, **5**, **8** and **9** were transformed into final products through the same reactions sequence. The regioselective opening of benzylidene with sodium cyanoborohydride and hydrochloric acid followed by reaction with succinic anhydride and deprotection of the para-methoxybenzyl group in position C6 by acid treatment (trifluoroacetic acid, TFA), afforded final products **FP13-17**.

Experimental procedures.

General. Commercially available reagents and solvents were used without further purification. Reactions were monitored by thin-layer chromatography (glass plates coated with silica gel 60 F254 from Merck KGaA). Products were purified with column chromatography on flash Silica gel 60A (40-63u from Fluorochem). ^1H and ^{13}C NMR spectra were recorded at room temperature in deuterated solvents on a Varian Mercury 400MHz Spectrometer. Chemical shifts (δ) are reported in parts per million (ppm) relative to TMS as internal standard or relative to the solvent [^1H: δ($CDCl_3$) = 7.26 ppm, δ(CD_3OD) = 3.31 ppm, δ(acetone-d_6) = 2.05 ppm; ^{13}C: δ($CDCl_3$) = 77.16 ppm, δ(CD_3OD) = 49.00 ppm, δ(acetone-d_6) = 29.84 ppm]. Electrospray

ionization ESI mass spectra were acquired on an AB SCIEX 2000 QTRAP LC/MS/MS with ESI source, mechanical pump and Analyst Data System.

A. ***Azide protection****:* In a two-necked flask filled with Argon was added NaN_3 (1.2 eq.) in Pyridine (2 ml/mmol). Reaction was cooled down in an ice bath and Tf_2O (1.4 eq.) was added dropwise. The reaction was stirred in ice during 3h. In a second flask was added glucosamine (1 eq.) in pyridine/H_2O (1:3, 1 ml/mmol). The reaction was cooled down to 0°C, were added $CuSO_4$ (0.065 eq.), TEA (2 eq.) and the reaction was stirred during 30 min. The first preparation was transferred in the second-one and the mixture was stirred during 24h at r.t. Reaction was monitored by TLC (AcOEt/MeOH/H_2O 7:3:0.1, R_f = 0.6). Then, half of the solvent was evaporated under vacuum, toluene was added (1:1) and co-evaporated under vacuum several times until a white precipitate appears. Product was used without further purification in the successive step, assuming 100 % yield.

B. ***Benzylidene formation***: Azide protected glucosamine (1 eq.) from the previous reaction was dissolved in DMF_{Dry} (~1 ml/mmol). Anisaldehyde dimethyl acetal (ADMA, 1.1 eq.) and para-toluene-sulfonic acid (*p*-TsOH, 0.02 eq.) were added and the reaction was performed on the rotavapor (60°C, 250 mbar) during 30 min. Reaction was monitored by TLC (AcOEt /EtP 6:4, R_f = 0.7). Then, reaction was quenched with TEA (0.04 eq.) and evaporated under vacuum. Product was purified on flash column chromatography (AcOEt/EtP 1:1) to afford the product as a yellow powder. Global yield of the two reactions: 80%.

C. ***Anomeric protection by TBDMS****:* Compound obtained after procedure *B*. (1 eq.) was dissolved in DCM_{Dry} (2 ml/mmol) under argon and cooled down until -10°C. Tert-butyldimethylsilyl chloride (1.2 eq.) was added together with imidazole (2.5 eq.). The reaction was followed by TLC (EtP/AcOEt 8:2, R_f = 0.9). Then, H_2O (0.2 ml/mmol) was added and the mixture was diluted with DCM (2 ml/mmol) and washed with H_2O (2

ml/mmol). The aqueous layer was extracted with DCM (2x 1 ml/mmol), and the combined organic layers were dried with Na_2SO_4 and concentrated under vacuum. The residue was purified on flash column chromatography (AcOEt/EtP 1:9) to afford the product as a slightly yellow oil with 75% yield.

D. ***Azide deprotection****:* The suitable azide protected carbohydrate from procedure *C* (1 eq.) was dissolved in THF (10 ml/mmol) and PPh_3 (3 eq.) was added. The reaction was stirred 30 min at r.t and, then, heated to 60°C. At this point, H_2O (1 ml/mmol) was added. The reaction was followed by TLC (AcOEt/EtP 2:8, R_f = 0.2). Then, the mixture was dried under vacuum and purified on flash column chromatography (AcOEt/EtP 1:9) to afford the desired product as a slightly yellow oil with 85% yield.

E. ***Acylation*** *(for double acylation):* Into a dry flask filled with argon were dissolved the suitable fatty acid chain (4 eq.) and EDC (6 eq.) in DCM (5 ml/mmol). The reaction was stirred 10 min at r.t. In a second dry flask filled with argon was dissolved the carbohydrate from protocol *D* (1 eq.) in DCM (5 ml/mmol) and, then, transferred into the first flask. The mixture was stirred 5 min before adding DMAP (1 eq.) and monitored by TLC (AcOEt/EtP 2:8, R_f = 0.7). Then, the mixture was diluted with DCM (5 ml/mmol) and washed with saturated $NaHCO_3$ and brine. The organic phase was dried over $NaSO_4$, filtrated and evaporated under vacuum before being purified on flash column chromatography (AcOEt/EtP 0.5:9.5) to afford the desired product as a slightly yellow oil with 60% yield.

F. ***One-pot regio-selective opening of PMP benzylidene and anomeric silyl deprotection****:* Product of procedure *E*. (1 eq.) was dissolved in dry THF (45 ml/mmol). $NaBH_3CN$ (15 eq.) and 4 Å molecular sieves (200 mg/mmol) were added. Mixture was stirred at r.t. for 2 h and, then, cooled to 0°C. A solution of HCl (1 M in dioxane, 18 eq.) was added dropwise and the mixture was stirred for 1h at 0°C and another 3h at r.t. (AcOEt/EtP 1:1,

R_f = 0.3). Et_3N (0.5 mL/mmol) was added to terminate the reaction. Molecular sieve was filtered off through Celite and washed with ether. The filtrate and wash were combined and washed with saturated $NaHCO_3$ and brine, dried over Na_2SO_4 and finally evaporated under vacuum. The residue was purified on flash column chromatography (AcOEt/EtP 4:6) to afford the desired product as a colorless oil with 62% yield.

G. ***1,4 -oxobutanoic acid formation****:* To a solution of the compound from procedure *F* (1 eq.) and DMAP (6 eq.) in DCM (50 ml/mmol) was added succinic anhydride (6 eq.). The mixture was stirred overnight and monitored by TLC (DCM/MeOH 5% + 1% formic acid, R_f = 0.4). Then, the mixture was concentrated under vacuum and purified on flash column chromatography (DCM/MeOH 2% + 1% formic acid) to afford the desired product as a slightly yellow oil with 80% yield.

H. ***PMB Deprotection****:* To a solution the compound from procedure *G* (1 eq.) in DCM (100 ml/mmol) at 0°C, was added TFA (10 eq.). The reaction was stirred at room temperature and monitored by TLC (DCM/MeOH 5% + 1% formic acid, R_f = 0.2). Then, treated by saturated $NaHCO_3$ and extracted twice by DCM (20 ml/mmol). The organic phase was washed with brine, dried over Na_2SO_4, filtrated and solvent was evaporated under vacuum. The residue was forwarded to column chromatography (DCM/MeOH 2% to 10% + 1% formic acid) to afford the final product as a brown oil with 75 % yield.

Compounds characterization:

(4aR,6S,7R,8R,8aS)-7-azido-6-((tert-butyldimethylsilyl)oxy)-2-(4-methoxyphenyl) hexahydro-pyrano[3,2-d][1,3]dioxin-8-ol (1): **^{1}H NMR (400 MHz, $CDCl_3$) δ** 7.39 (d, J = 8.7 Hz, 2H, 2*HAr), 6.89 (d, J = 8.5 Hz, 2H, 2*HAr), 5.48 (s, 1H, CHPMB), 4.64 (d, J = 7.6 Hz, 1H, H1), 4.27 (dd, J = 10.5, 4.9 Hz, 1H, H4), 3.84 – 3.67 (m, 4H, OMe, H6a), 3.58 (dt, J = 28.0, 9.2 Hz, 2H, H3, H6b), 3.46 – 3.37 (m, 1H, H5), 3.32 (t, J = 8.5 Hz, 1H, H2), 0.94 (s, 9H,

tBu), 0.16 (s, 6H, 2*Me-Si). **^{13}C NMR (400 MHz, $CDCl_3$) δ** 159.20, 129.95, 128.81, 113.36, 102.04, 100.73, 81.24, 70.68, 67.93, 64.74, 56.04, 49.77, 25.76 – 25.55, 18.59, -2.89, -3.29.

*(4aR,6S,7R,8R,8aS)-7-amino-6-((tert-butyldimethylsilyl)oxy)-2-(4-methoxyphenyl) hexahydro-pyrano[3,2-d][1,3]dioxin-8-ol (**2**):* **^{1}H NMR (400 MHz, $CDCl_3$) δ** 7.41 (d, J = 8.6 Hz, 2H, 2*HAr), 6.88 (d, J = 8.6 Hz, 2H, 2*HAr), 5.48 (s, 1H, CHPMB), 4.56 (d, J = 7.4 Hz, 1H, H1), 4.25 (dd, J = 10.4, 4.8 Hz, 1H, H4), 3.84 – 3.71 (m, 4H, OMe, H6a), 3.64 (t, J = 9.2 Hz, 1H, H3), 3.54 (t, J = 8.9 Hz, 1H, H6b), 3.44 (dt, J = 14.1, 7.1 Hz, 1H, H5), 2.75 (t, J = 8.6 Hz, 1H, H2), 0.92 (s, 9H, tBu), 0.13 (s, 6H, 2*Me-Si). **^{13}C NMR (400 MHz, $CDCl_3$) δ** 159.21, 129.98, 128.76, 113.62, 102.06, 100.22, 80.59, 71.18, 67.93, 64.74, 60.74, 56.04, 25.62 – 25.58, 18.59, - 4.79, -5.26.

*(4aR,6S,7R,8R,8aS)-6-((tert-butyldimethylsilyl)oxy)-2-(4-methoxyphenyl)-7-tetradecan amidohexahydropyrano[3,2-d][1,3]dioxin-8-yl tetradecanoate (**3**):* **^{1}H NMR (400 MHz, $CDCl_3$) δ** 7.35 (d, J = 8.7 Hz, 2H, 2*HAr), 6.86 (d, J = 8.8 Hz, 2H, 2*HAr), 5.46 (s, 1H, CHPMB), 5.17 (t, J = 10.0 Hz, 1H, H3), 4.72 (d, J = 7.8 Hz, 1H, H1), 4.26 (dd, J = 10.6, 5.1 Hz, 1H, H5), 4.07 (dd, J = 17.9, 9.3 Hz, 1H, H2), 3.83 – 3.76 (m, 4H, OMePMB, H6a), 3.70 (t, J = 9.4 Hz, 1H, H4), 3.53 – 3.43 (m, 1H, H6b), 2.39 – 2.22 (m, 2H, CH2 α Amide), 2.16 – 2.02 (m, 2H, CH2 α Ester), 1.74 – 1.49 (m, 4H, 2*CH2β), 1.25 (s, 44H, 22*CH2), 0.96 – 0.78 (m, 15H, tBu + 2*CH3), 0.09 (s, 3H, Si-Mea), 0.07 (s, 3H, Si-Meb).**^{13}C NMR (400 MHz, $CDCl_3$) δ** 175.33, 174.42, 159.17, 129.95, 128.75, 113.53, 102.03, 97.73, 78.46, 70.96, 67.91, 64.34, 56.01, 54.65, 37.75, 34.12, 31.20, 29.20 – 28.55, 25.33, 25.13, 22.84, 18.56, 14.01, -2.89, -3.29.

*(4aR,6S,7R,8R,8aS)-6-((tert-butyldimethylsilyl)oxy)-2-(4-methoxyphenyl)-7-oleamido-hexa hydropyrano[3,2-d][1,3]dioxin-8-yl oleate (**4**):* **^{1}H NMR (400 MHz, $CDCl_3$) δ** 7.35 (d, J = 8.6 Hz, 2H, 2*HAr), 6.85 (d, J = 8.7 Hz, 2H, 2*HAr), 5.67 (d, J = 9.6 Hz, 1H, NH), 5.45 (s, 1H, H1 α), 5.40 – 5.23 (m, J = 10.2, 4.7 Hz, 4H, 4*CH=), 5.18 (t, J = 10.0 Hz, 1H, H3), 4.69 (d, J = 7.9 Hz, 1H,H1 β), 4.23 (dd, J = 10.5, 4.8 Hz, 1H, H5), 4.08 (dd, J = 18.2, 9.9 Hz, 1H,

H2), 3.82 – 3.74 (m, 4H, MePMB, H6a), 3.69 (t, J = 9.5 Hz, 1H, H4), 3.53 – 3.39 (m, 1H, H6b), 2.40 – 2.22 (m, 2H, CH2 α Ester), 2.15 – 2.02 (m, 2H, , CH2 α Amide), 2.02 – 1.93 (m, 8H, 4*CH2-=), 1.62 – 1.46 (m, 4H, 4*CH2 β), 1.39 – 1.15 (m, 40H, 40*CH2), 0.94 – 0.77 (m, 15H, tBu, 2*Me), 0.07 (s, 3H, Si-Mea), 0.04 (s, 3H, Si-Meb). **^{13}C NMR (400 MHz, $CDCl_3$) δ** 174.28, 172.62, 160.02, 129.97, 129.66, 127.38, 113.49, 101.27, 97.33, 78.66, 71.72, 68.60, 66.58, 56.27, 55.22, 36.90, 34.27, 31.90, 29.77, 29.53, 29.37, 29.32, 29.10, 27.22, 25.56, 25.52, 25.02, 22.68, 17.82, 14.12, -4.12, -5.22.

*(9Z,12Z)-(4aR,6S,7R,8R,8aS)-6-((tert-butyldimethylsilyl)oxy)-2-(4-methoxyphenyl)-7-((9Z,12Z)-octadeca-9,12-dienamido)hexahydropyrano[3,2-d][1,3]dioxin-8-yl octadeca-9,12-dienoate (**5**):* **^{1}H NMR (400 MHz, $CDCl_3$) δ** 7.35 (d, J = 8.8 Hz, 2H, 2*CHAr), 6.86 (d, J = 8.8 Hz, 2H, 2*CHAr), 5.46 (s, 1H, H1 α), 5.36 (m, J = 16.6, 14.2, 8.0 Hz, 9H, 8*CH=, CHPMB), 5.16 (t, J = 10.0 Hz, 1H, H3), 4.73 (d, J = 7.9 Hz, 1H, H1 β), 4.27 (dd, J = 10.6, 5.1 Hz, 1H, H5), 4.06 (dd, J = 18.3, 9.7 Hz, 1H, H2), 3.79 (m, 4H, OMe, H6a), 3.70 (t, J = 9.4 Hz, 1H, H4), 3.47 (m, 1H, H6b), 2.76 (d, J = 3.8 Hz, 4H, 2*=CH2=), 2.30 (m, 2H, CH2 α Amide), 2.05 (m, 10H, 4*CH2-=, CH2 α Ester), 1.56 (m, 2H, 2*CH2 β), 1.29 (m, 28H, 14*CH2), 0.88 (m, 16H, tBu, 2*Me), 0.10 (s, 3H, Si-Mea), 0.08 (s, 3H, Si-Meb). **^{13}C NMR (400 MHz, $CDCl_3$) δ** 174.15, 172.61, 160.06, 130.21, 130.00, 127.87, 127.43, 113.52, 101.32, 97.41, 78.62, 71.47, 68.61, 66.70, 56.44, 55.25, 36.91, 34.26, 31.51, 29.51, 27.19, 25.61, 25.52, 25.00, 22.57, 17.85, 14.09, -4.09, -5.27.

(4aR,6S,7R,8R,8aS)-7-azido-6-((tert-butyldimethylsilyl)oxy)-2-(4-methoxyphenyl) hexahydro

*pyrano[3,2-d][1,3]dioxin-8-yl tetradecanoate (**6**):* **^{1}H NMR (400 MHz, $CDCl_3$) δ** 7.33 (d, J = 8.7 Hz, 2H, 2*CHAr), 6.85 (d, J = 8.7 Hz, 2H, 2*CHAr), 5.43 (s, 1H, CH-PMP), 5.12 (t, J = 9.9 Hz, 1H, H3), 4.71 (d, J = 7.6 Hz, 1H, H1), 4.27 (dd, J = 10.4, 4.8 Hz, 1H, H5), 3.82 – 3.72 (m, 4H, OMe+H6a), 3.61 (t, J = 9.5 Hz, 1H, H4), 3.52 – 3.44 (m, 1H, H6b), 3.44 – 3.34 (m,

1H, H2), 2.36 (t, J = 7.4 Hz, 2H, CH2α), 1.70 – 1.54 (m, 4H, CH2β), 1.36 – 1.14 (m, 20H, 10*CH2), 0.94 (s, 9H,tBu), 0.88 (t, J = 6.8 Hz, 3H, Me), 0.23 – 0.13 (m, 6H, 2*Me-Si). **^{13}C NMR (400 MHz, $CDCl_3$) δ** 174.42, 159.22, 129.95, 128.73, 113.58, 102.03, 100.29, 78.80, 71.37, 67.93, 64.37, 56.08, 46.54, 34.14, 31.67, 29.12 – 28.74, 25.76 – 25.67, 25.33, 22.94, 18.57, 14.01, -2.89, -3.29.

(4aR,6S,7R,8R,8aS)-7-amino-6-((tert-butyldimethylsilyl)oxy)-2-(4-methoxyphenyl) hexahydro

pyrano[3,2-d][1,3]dioxin-8-yl tetradecanoate (7): **^{1}H NMR (400 MHz, $CDCl_3$) δ** 7.34 (d, J = 8.6 Hz, 2H, 2*CHAr), 6.84 (d, J = 8.6 Hz, 2H, 2*CHAr), 5.43 (s, 1H,CH-PMP), 5.10 (t, J = 9.8 Hz, 1H, H3), 4.57 (d, J = 7.6 Hz, 1H, H1), 4.25 (dd, J = 10.4, 4.8 Hz, 1H, H5), 3.82 – 3.67 (m, 4H, H6a +OMe), 3.63 (t, J = 9.4 Hz, 1H, H4), 3.49 (td, J = 9.7, 5.0 Hz, 1H, H6b), 2.82 (dd, J = 9.8, 7.6 Hz, 1H, H2), 2.35 (t, J = 7.4 Hz, 2H, CH2α), 1.67 – 1.53 (m, 2H, CH2β), 1.48 (s, 2H, NH_2), 1.17 (m, 20H, 10*CH_2), 0.91 (s, 9H, tBu), 0.87 (t, J = 6.7 Hz, 3H, Me), 0.13 (s, 6H, 2*Si-Me).**^{13}C NMR (400 MHz, $CDCl_3$) δ** 174.45, 159.20, 129.98, 77, 113.58, 102.04, 99.65, 77.65, 71.69, 67.93, 64.38, 58.11, 56.04, 34.15, 31.65, 29.36 – 28.85 (m), 25.66 – 25.55, 25.33, 22.94, 18.59, 14.02, -2.89 – -3.29.

*(4aR,6S,7R,8R,8aS)-6-((tert-butyldimethylsilyl)oxy)-2-(4-methoxyphenyl)-7-((9Z,12Z)-octa deca-9,12-dienamido)hexahydropyrano[3,2-d][1,3]dioxin-8-yl tetradecanoate (**8**):* **^{1}H NMR (400 MHz, $CDCl_3$) δ** 7.35 (d, J = 8.7 Hz, 2H, 2*CHAr), 6.86 (d, J = 8.8 Hz, 2H, 2*CHAr), 5.46 (s, 1H, CHPMB), 5.42 – 5.26 (m, 5H, 4*CH= +H1β), 5.19 (t, J = 10.0 Hz, 1H, H3), 4.72 (d, J = 7.9 Hz, 1H, H1α), 4.26 (dd, J = 10.5, 5.0 Hz, 1H, H5), 4.11 – 4.03 (m, 1H, H2), 3.80 – 3.66 (m, 5H, OMe+H6a+H4), 3.44 (dd, J = 9.6, 4.9 Hz, 1H, H6b), 2.76 (t, J = 6.5 Hz, 2H, =CH2=), 2.39 – 2.23 (m, 2H, CH2α Amide), 2.16 – 1.99 (m, 6H, 2*CH2= + CH2α Ester), 1.64 – 1.48 (m, 4H, 2*CH2β), 1.40 – 1.14 (m, 34H, 17*CH2), 0.91 – 0.81 (m, 15H, tBu+2*Me), 0.08 (s, 3H, Si-Mea), 0.06 (s, 3H, Si-Meb).**^{13}C NMR (400 MHz, $CDCl_3$) δ** 175.05, 174.33,

172.65, 160.04, 130.21, 128.04, 113.53, 101.35, 96.40, 78.66, 69.95, 68.62, 66.55, 62.71, 55.58, 55.23, 36.89, 34.29, 31.92, 31.51, 30.39 – 28.18, 27.18, 25.61, 22.69, 22.57, 17.89, 14.12, -4.04, -5.21.

*(4aR,6S,7R,8R,8aS)-6-((tert-butyldimethylsilyl)oxy)-2-(4-methoxyphenyl)-7-oleamidohexa hydropyrano[3,2-d][1,3]dioxin-8-yl tetradecanoate (**9**):* **^{1}H NMR (400 MHz, $CDCl_3$) δ** 7.35 (d, J = 8.7 Hz, 2H, 2CHAr), 6.86 (d, J = 8.8 Hz, 2H, 2CHAr), 5.50 – 5.40 (m, 2H, H1a, CHPMB), 5.34 (t, J = 6.1 Hz, 2H, 2*CH=), 5.17 (t, J = 10.1 Hz, 1H, H3), 4.73 (d, J = 7.9 Hz, 2H,H1b), 4.27 (dd, J = 10.5, 4.8 Hz, 1H, H5), 4.06 (dd, J = 18.3, 9.6 Hz, 1H, H2), 3.83 – 3.74 (m, 4H, OMe+H6a), 3.70 (t, J = 9.4 Hz, 1H, H4), 3.55 – 3.41 (m, 1H, H6b), 2.40 – 2.20 (m, 2H, CH2a Amide), 2.16 – 2.04 (m, 2H, CH2a Ester), 2.00 (d, J = 5.9 Hz, 4H, 2*CH2-=), 1.55 (s, 4H, 2*CH2b), 1.39 – 1.13 (m, 40H, 20*CH2), 0.95 – 0.83 (m, 15H, tBu+2*Me), 0.09 (s, 3H, Mea-Si), 0.07 (s, 3H, Meb-Si). **^{13}C NMR (400 MHz, $CDCl_3$) δ** 174.30, 172.62, 160.02, 129.97, 129.67, 127.37, 114.29, 113.51, 101.25, 97.34, 78.66, 71.69, 68.60, 66.57, 56.26, 55.22, 36.91, 34.28, 31.92, 29.43, 27.22, 25.51, 25.03, 22.68, 17.82, 14.12, -4.01, -5.17.

*(2R,3R,4R,5S,6R)-2,5-dihydroxy-6-(((4-methoxybenzyl)oxy)methyl)-3-tetradecanamidotetra hydro-2H-pyran-4-yl tetradecanoate (**3a**):* **^{1}H NMR (400 MHz, $CDCl_3$) δ** 7.25 (d, J = 9.4 Hz, 2H, 2*CHAr), 6.87 (d, J = 8.6 Hz, 2H, 2*CHAr), 5.89 (d, J = 9.1 Hz, 1H, H1a), 5.22 – 5.09 (m, 2H, H1b +H3), 4.50 (m, 2H, CH2 PMB), 4.25 – 4.14 (m, 1H, H2), 4.03 (m, 1H, H5), 3.79 (s, 3H, OMe), 3.76 – 3.59 (m, 3H, H4+ 2*H6), 2.33 (m, 2H, 2*CH2a Amide), 2.24 – 2.02 (m, 2H, 2*CH2a Ester), 1.63 – 1.46 (m, 4H, 2*CH2b), 1.37 – 1.16 (m, 20H, 10*CH2), 0.87 (t, J = 6.7 Hz, 6H, 2*Me).**^{13}C NMR (400 MHz, $CDCl_3$) δ** 175.14, 173.33, 159.54, 129.51, 113.73, 91.91, 73.25, 70.42, 69.86, 69.39, 55.30, 36.88, 34.35, 31.91, 30.42 - 28.37, 25.62, 23.79, 24.74, 22.78, 14.10.

*(2R,3R,4R,5S,6R)-2,5-dihydroxy-6-(((4-methoxybenzyl)oxy)methyl)-3-oleamidotetrahydro-2H-pyran-4-yl oleate (**4a**):* **^{1}H NMR (400 MHz, $CDCl_3$) δ** 7.26 (s, 2H, 2*CHAr), 6.88 (d, J =

8.6 Hz, 2H, 2*CHAr), 5.77 (d, J = 9.4 Hz, 1H, H1), 5.34 (s, 4H, 4*CH=), 5.19 – 5.10 (m, 1H, H3), 4.52 (q, J = 11.6 Hz, 2H, CH2 PMB), 4.29 – 4.15 (m, 1H, H2), 4.10 – 3.97 (m, 1H, H5), 3.80 (s, 3H, MePMB), 3.74 – 3.63 (m, J = 8.1 Hz, 3H, H4+2*H6), 2.33 (dd, J = 13.8, 7.4 Hz, 2H, CH2 α amide), 2.12 (dd, J = 12.9, 7.5 Hz, 2H, CH2 α ester), 2.00 (d, J = 5.9 Hz, 8H,4*CH2-CH=), 1.57 (s, 8H, 2*CH2 β), 1.26 (s, 45H, 20*CH2), 0.88 (t, J = 6.8 Hz, 6H, 2*Me). **^{13}C NMR (400 MHz, $CDCl_3$) δ** 175.13, 173.15, 159.35 130.01, 129.68, 129.53, 113.83, 91.84, 73.36, 73.25, 70.49, 70.01, 69.85, 55.27, 51.72, 36.71, 34.31, 31.91, 30.33 - 28.11, 27.20, 25.62, 24.93, 22.69, 14.15.

*(9Z,12Z)-(2R,3R,4R,5S,6R)-2,5-dihydroxy-6-(((4-methoxybenzyl)oxy)methyl)-3-((9Z,12Z)-octadeca-9,12-dienamido)tetrahydro-2H-pyran-4-yl octadeca-9,12-dienoate (**5a**):* **^{1}H NMR (400 MHz, $CDCl_3$) δ** 7.29 – 7.19 (m, 2H, 2*CHAr), 6.88 (d, J = 8.6 Hz, 2H, 2*CHAr), 5.76 (d, J = 9.7 Hz, 1H, H1β), 5.44 – 5.25 (m, 8H, 8*CH=), 5.23 (s, 1H, H1α), 5.20 – 5.09 (m, 1H, H3), 4.59 – 4.43 (m, 2H, CH2 PMB), 4.22 (td, J = 11.0, 3.7 Hz, 1H, H2), 4.06 – 4.01 (m, 1H, H5), 3.80 (s, 3H, OMe), 3.69 (d, J = 4.8 Hz, 3H, 2*H6+H4), 2.76 (t, J = 6.2 Hz, 4H, 2*=CH2=), 2.40 – 2.28 (m, 2H, CH2 α amide), 2.16 – 2.08 (m, 2H, CH2 α ester), 2.07 – 1.95 (m, 8H, 4*CH2-=), 1.73 – 1.48 (m, 4H, 2*CH2β), 1.40 – 1.18 (m, 28H, 14*CH2), 0.88 (t, J = 6.8 Hz, 6H, 2*Me). **^{13}C NMR (400 MHz, CD_3OD) δ** 171.12, 169.14, 155.38, 126.27, 126.03, 125.65, 125.54, 124.08, 123.92, 109.86, 87.85, 69.38, 66.48, 66.06, 65.91, 64.89, 51.30, 47.84, 32.76, 30.36, 27.56, 26.24 – 24.74, 23.24, 21.66, 18.63, 17.11, 10.24.

*(2R,3R,4R,5S,6R)-2,5-dihydroxy-6-(((4-methoxybenzyl)oxy)methyl)-3-((9Z,12Z)-octadeca-9,12-dienamido)tetrahydro-2H-pyran-4-yl tetradecanoate (**8a**):* **^{1}H NMR (400 MHz, $CDCl_3$) δ** 7.27 (d, J = 8.6 Hz, 2H, 2*CHAr), 6.88 (d, J = 8.6 Hz, 2H, 2*CHAr), 5.94 (d, J = 9.2 Hz, 1H, H1β), 5.43 – 5.26 (m, 4H, 4*CH=), 5.21 (d, J = 2.3 Hz, 1H, H1α), 5.17 – 5.10 (m, 1H, H3), 4.58 – 4.43 (m, 2H, CH2 PMB), 4.23 – 4.12 (m, 1H, H2), 4.10 – 4.01 (m, 1H, H5), 3.80 (s, 3H, OMe), 3.75 – 3.66 (m, 3H, H4+2*H6), 2.76 (t, J = 5.9 Hz, 2H, =CH2=), 2.43 – 2.30 (m, 2H,

CH2α Amide), 2.16 – 2.07 (m, 2H, CH2α Ester), 2.08 – 1.98 (m, 4H, 2*CH2-=), 1.69 – 1.49 (m, 4H, 2*CH2β), 1.44 – 1.19 (m, 34H, 17*CH2), 0.94 – 0.82 (m, 6H, 2*Me). **^{13}C NMR (400 MHz, $CDCl_3$) δ** 175.25, 173.51, 159.79, 130.10, 129.66, 128.04, 127.86, 113.90, 91.71, 74.70, 73.38, 70.02, 67.97, 59.95, 55.29, 51.84, 40.79, 36.73, 34.34, 29.92, 27.18, 25.61, 24.94, 22.63, 14.13.

*(2R,3R,4R,5S,6R)-2,5-dihydroxy-6-(((4-methoxybenzyl)oxy)methyl)-3-oleamidotetrahydro-2H-pyran-4-yl tetradecanoate (**9a**):* **^{1}H NMR (400 MHz, $CDCl_3$) δ** 7.29 – 7.21 (m, 2H, 2*CHAr), 6.88 (d, J = 8.5 Hz, 2H, 2*CHAr), 5.91 (d, J = 9.3 Hz, 1H, H1α), 5.41 – 5.28 (m, 2H, 2*CH=), 5.20 (s, 1H, H1β), 5.19 – 5.09 (m, 1H, H3), 4.51 (q, J = 11.5 Hz, 2H, CH2 PMB), 4.23 – 4.13 (m, 1H, H2), 4.07 – 3.98 (m, 1H, H5), 3.80 (s, 3H, OMe), 3.74 – 3.64 (m, 3H, 2*H6+H4), 2.42 – 2.27 (m, 2H, CH2a Amide), 2.20 – 2.06 (m, 2H, CH2a Ester), 2.06 – 1.91 (m, 4H, 2*CH2-=), 1.64 – 1.48 (m, 4H, 2*CH2β), 1.39 – 1.17 (m, 40H, 20*CH2), 0.87 (t, J = 6.7 Hz, 6H, 2*Me). **^{13}C NMR (400 MHz, CD_3OD) δ** 175.26, 173.21, 163.34, 130.16, 130.16, 129.85, 129.78, 129.65, 114.00, 92.08, 73.55, 72.14, 70.72, 70.16, 69.24, 55.43, 51.76, 36.91, 34.48, 32.08, 30.54 – 28.46, 27.38, 27.33, 25.76, 25.11, 22.85, 14.29.

*4,4'-(((2S,3R,4R,5S,6R)-6-(((4-methoxybenzyl)oxy)methyl)-3-tetradecanamido-4-(tetradecaneoyloxy)tetrahydro-2H-pyran-2,5-diyl)bis(oxy))bis(4-oxobutanoic acid) (**3b**):* **^{1}H NMR (400 MHz, CD_3OD) δ** 7.25 (d, J = 8.4 Hz, 2H, 2*CHa Ar), 6.88 (d, J = 8.4 Hz, 2H, 2*CHb Ar), 6.11 (d, J = 3.4 Hz, 1H, H1), 5.35 – 5.26 (m, 1H, H3), 5.22 (t, J = 9.7 Hz, 1H, H4), 4.46 – 4.33 (m, 3H, H2, CH2 PMB), 4.08 – 4.00 (m, 1H, H5), 3.78 (s, 3H, OMe), 3.67 – 3.50 (m, 2H, 2*H6), 2.78 – 2.41 (m, 8H, 4*CH2-COO), 2.37 – 2.21 (m, 4H, 2*CH2α), 1.62 – 1.48 (m, 4H,2*CH2β), 1.39 – 1.21 (m, 40H, 20*CH2), 0.97 – 0.82 (m, 6H, 2*Me). **^{13}C NMR (400 MHz, CD_3OD) δ** 174.92, 174.54, 173.11, 171.03, 170.90, 147.45, 129.45, 129.30, 113.01, 90.26, 74.25, 72.52, 70.61, 70.00, 60.83, 53.99, 50.52, 33.34, 31.45, 30.33 – 27.03, 24.30, 22.11, 12.82.

*4,4'-(((2S,3R,4R,5S,6R)-6-(((4-methoxybenzyl)oxy)methyl)-3-oleamido-4-(oleoyloxy) tetrahydro-2H-pyran-2,5-diyl)bis(oxy))bis(4-oxobutanoic acid) (**4b**):* **^{1}H NMR (400 MHz, $CDCl_3$) δ** 7.24 (d, J = 8.6 Hz, 2H, 2*CHAr), 6.86 (d, J = 8.6 Hz, 2H, 2*CHAr), 6.21 (d, J = 3.3 Hz, 1H, H1α), 5.87 (d, J = 8.3 Hz, 1H, H1β), 5.47 – 5.29 (m, 4H, 4*CH=), 5.26 (t, J = 10.0 Hz, 1H, H4), 5.20 – 5.09 (m, 1H, H3), 4.54 – 4.33 (m, 3H, CH2PMB, H2), 3.88 (d, J = 9.2 Hz, 1H, H5), 3.79 (s, 3H, OMe), 3.58 – 3.42 (m, 2H, 2*H6), 2.90 – 2.36 (m, 8H, 4*CH2-COO), 2.26 (t, J = 7.5 Hz, 2H, CH2α ester), 2.08 (dd, J = 13.2, 7.0 Hz, 2H, CH2α amide), 2.00 (d, J = 5.3 Hz, 8H, 4*CH2-=), 1.53 (s, 4H, 2*CH2β), 1.26 (s, 40H, 20*CH2), 0.87 (t, J = 6.6 Hz, 6H, 2*Me). **^{13}C NMR (400 MHz, $CDCl_3$) δ** 172.12, 169.73, 168.12, 164.28, 163.88, 154.05, 124.86, 124.81, 124.57, 124.49, 124.43, 124.37, 108.50, 86.13, 69.83, 67.99, 65.97, 63.33, 62.48, 50.08, 45.83, 31.19 - 28.96, 26.72, 24.03, 22.02, 20.26, 19.62, 17.51, 8.96.

*4,4'-(((2S,3R,4R,5S,6R)-6-(((4-methoxybenzyl)oxy)methyl)-3-((9Z,12Z)-octadeca-9,12-dien amido)-4-((9Z,12Z)-octadeca-9,12-dienoyloxy)tetrahydro-2H-pyran-2,5-diyl)bis(oxy))bis(4-oxobutanoic acid) (**5b**):* **^{1}H NMR (400 MHz, $CDCl_3$) δ** 7.28 – 7.19 (m, 2H, 2*CHAr), 6.86 (d, J = 8.6 Hz, 2H, 2*CHAr), 6.21 (d, J = 3.4 Hz, 1H, H1a), 5.45 – 5.28 (m, 8H, 8*CH=), 5.25 (t, J = 8.6 Hz, 1H, H4), 5.14 (t, J = 10.6 Hz, 1H, H3), 4.53 – 4.34 (m, 3H, H2+ CH2 PMB), 3.93 – 3.82 (m, 1H, H5), 3.80 (s, 3H,OMe), 3.58 – 3.42 (m, 2H, 2*H6), 2.87 – 2.72 (m, 4H, 2*=CH2=), 2.72 – 2.52 (m, 8H, 4*CH2-COO), 2.44 – 2.38 (m, 2H, CH2 a Amide), 2.28 (t, J = 7.7 Hz, 2H, CH2 a Ester), 2.13 – 1.97 (m, 8H, 4*CH2=), 1.64 – 1.46 (m, 4H, 2*CH2 b), 1.42 – 1.17 (m, 28H, 14*CH2), 0.88 (t, J = 6.8 Hz, 6H, 2*Me).**^{13}C NMR (101 MHz, $CDCl_3$) δ** 173.72, 172.99, 169.41, 168.69, 130.26, 129.74, 128.10, 127.83, 113.88, 90.88, 73.10, 70.89, 67.65, 65.78, 55.27, 53.78, 31.51, 30.75 – 28.09, 27.20, 25.61, 24.75, 22.57, 14.09.

*4,4'-(((2S,3R,4R,5S,6R)-6-(((4-methoxybenzyl)oxy)methyl)-3-((9Z,12Z)-octadeca-9,12-dien amido)-4-(tetradecanoyloxy)tetrahydro-2H-pyran-2,5-diyl)bis(oxy))bis(4-oxobutanoic acid) (**8b**):* **^{1}H NMR (400 MHz, $CDCl_3$) δ** 7.23 (d, J = 8.9 Hz, 2H, 2*CHAr), 6.85 (d, J = 8.3 Hz,

2H, 2*CHAr), 6.21 (d, J = 2.8 Hz, 1H, H1), 5.45 – 5.33 (m, 4H, 4*CH=), 5.19 -5.14 (m, 2H, H4 + H3), 4.53 – 4.35 (m, 2H, CH2 PMB), 4.30 – 4.21 (m, 1H, H2), 4.00 - 3.98 (m, 1H, H5), 3.79 (s, 3H, OMe), 3.57 – 3.41 (m, 2H, 2*H6), 2.81 – 2.42 (m, 10H, 4*CH2-COO + =CH2=), 2.40 – 2.14 (m, 4H, 2*CH2a), 2.09 - 2.00 (m, 4H, 2*CH2=), 1.57 -1.50 (m, 4H, 2*CH2b), 1.34 - 1.32 (m, 34H, 17*CH2), 1.07 – 0.75 (m, 3H, 2*Me).**^{13}C NMR (400 MHz, $CDCl_3$) δ** 175.72, 175.36, 174.47, 172.98, 171.81, 159.06, 132.53, 130.17, 129.07, 128.52, 113.44, 91.45, 73.64, 71.52, 70.66, 69.21, 56.03, 54.41, 37.80, 34.14, 31.18, 30.10, 29.34 - 27.91, 25.33, 25.12, 23.01, 14.08.

*4,4'-(((2S,3R,4R,5S,6R)-6-(((4-methoxybenzyl)oxy)methyl)-3-oleamido-4-(tetradecane oyloxy)tetrahydro-2H-pyran-2,5-diyl)bis(oxy))bis(4-oxobutanoic acid) (**9b**):* **^{1}H NMR (400 MHz, $CDCl_3$) δ** 7.23 (d, J = 8.6 Hz, 2H, 2*CHAr), 6.86 (d, J = 8.7 Hz, 2H, 2*CHAr), 6.22 (d, J = 2.9 Hz, 1H, H1b), 5.43 – 5.28 (m, 2H, 2*CH=), 5.23 (t, J = 9.1 Hz, 1H, H4), 5.16 (t, J = 9.9 Hz, 1H, H3), 4.55 – 4.34 (m, 2H, CH2 PMB), 4.21 – 4.11 (m, 1H, H2), 3.94 – 3.87 (m, 1H, H5), 3.80 (s, 3H, OMe), 3.58 – 3.43 (m, 2H, 2*H6), 2.75 – 2.56 (m, 8H, 4*CH2-COO), 2.26 (t, J = 7.7 Hz, 2H, CH2a Amide), 2.08 (t, J = 7.3 Hz, 2H, , CH2a Ester), 2.03 – 1.90 (m, 4H, 2*CH2-=), 1.60 – 1.46 (m, 4H, , CH2b), 1.41 – 1.14 (m, 40H, 20*CH2), 0.87 (t, J = 6.4 Hz, 6H, 2*Me).**^{13}C NMR (400 MHz, $CDCl_3$) δ** 177.79, 176.65, 173.34, 172.62, 168.94, 159.27, 129.98, 129.63, 113.71, 91.22, 73.24, 71.20, 68.69, 67.81, 55.27, 51.91, 36.32, 34.34, 31.92, 29.94 - 28.37, 27.19, 25.40, 24.68, 22.77, 14.05.

*4,4'-(((2S,3R,4R,5S,6R)-6-(hydroxymethyl)-3-oleamido-4-(oleoyloxy)tetrahydro-2H-pyran-2,5-diyl)bis(oxy))bis(4-oxobutanoic acid) (**FP13**):* **^{1}H NMR (400 MHz, CD_3OD) δ** 6.15 (d, J = 3.2 Hz, 1H, H1), 5.41 – 5.28 (m, 5H, 4*CH=, H3), 5.16 (t, J = 9.9 Hz, 1H, H4), 4.41 (dd, J = 10.5, 3.4 Hz, 1H, H2), 3.96 (ddd, J = 7.5, 4.7, 2.3 Hz, 1H, H5), 3.69 – 3.52 (m, 2H, 2*H6), 2.80 – 2.48 (m, 8H, 4*CH2-COO), 2.40 – 2.21 (m, 2H, CH2 α amide), 2.17 (t, J = 5.1 Hz, 2H, CH2 α ester), 2.11 – 1.95 (m, 4H, 4*CH2-=), 1.69 – 1.47 (m, 4H, 2*CH2 β), 1.46 – 1.16 (m,

40H,20*CH2), 1.01 – 0.77 (m, 6H, 2*Me). **^{13}C NMR (400 MHz, CD_3OD) δ** 175.15, 174.79, 173.30, 171.45, 171.16, 129.41, 90.51, 72.22, 70.21, 68.49, 60.04, 50.59, 35.38, 33.58, 31.68 - 29.02, 26.76, 25.57, 24.55, 22.35, 13.08. **MS (ESI-)** m/z calcd (M-H) C50H84NO13-= 906,59, found = 906.60.

*4,4'-(((2S,3R,4R,5S,6R)-6-(hydroxymethyl)-3-((9Z,12Z)-octadeca-9,12-dienamido)-4-((9Z,12Z)-octadeca-9,12-dienoyloxy)tetrahydro-2H-pyran-2,5-diyl)bis(oxy))bis(4-oxobutanoic acid) (**FP14**):* **^{1}H NMR (400 MHz, $CDCl_3$) δ** 6.19 (d, J = 2.8 Hz, 1H, H1α), 5.90 (d, J = 7.8 Hz, 1H, H1β), 5.44 – 5.28 (m, 8H, 8*CH=), 5.28 – 5.21 (m, 1H, H3), 5.21 – 5.12 (m, 1H, H4), 4.44 (t, J = 9.0 Hz, 1H, H2), 3.87 – 3.75 (m, 1H, H5), 3.70 (s, 1H, H6a), 3.60 (s, 1H, H6b), 2.76 (t, J = 6.0 Hz, 4H, 2*=CH2=), 2.72 – 2.53 (m, 8H, 2*CH2-COOH), 2.40 – 2.24 (m, 4H, 2*CH2α), 2.10 – 1.99 (m, 8H,4*CH2-COOH), 1.61 – 1.45 (m, 4H, 2*CH2), 1.45 – 1.11 (m, 28H, 14*CH2), 0.96 – 0.78 (m, 6H, 2*Me). **^{13}C NMR (400 MHz, $CDCl_3$) δ** 176.78, 176.42, 174.81, 173.46, 170.72, 169.68, 130.24, 127.85, 91.24, 72.18, 70.16, 68.04, 60.88, 51.13, 36.41, 34.13, 31.84, 31.53 - 27.19, 25.53, 24.86, 22.63, 14.11. **MS (ESI-)** m/z calcd (M-H) C50H80NO13-= 902,56, found = 902.60

*4,4'-(((2S,3R,4R,5S,6R)-6-(hydroxymethyl)-3-oleamido-4-(tetradecanoyloxy)tetrahydro-2H-pyran-2,5-diyl)bis(oxy))bis(4-oxobutanoic acid) (**FP15**):* **^{1}H NMR (400 MHz, $CDCl_3$) δ** 6.20 (d, J = 3.3 Hz, 1H, H1 α), 5.90 (d, J = 8.7 Hz, 1H, H1 β), 5.40 – 5.27 (m, 2H, 2*CH=), 5.28 – 5.12 (m, 2H, H3+H4), 4.42 (t, J = 8.4 Hz, 1H, H2), 3.82 – 3.75 (m, 1H, H5), 3.74 – 3.53 (m, 2H, 2*H6), 2.85 – 2.54 (m, 8H, 4*CH2-COOH), 2.29 (t, J = 7.6 Hz, 2H, CH2 α Amide), 2.15 – 2.05 (m, 2H, CH2 α Ester), 2.05 – 1.94 (m, 4H, 2*CH2-=), 1.61 – 1.47 (m, 4H, 2*CH2 β), 1.29 (d, J = 28.5 Hz, 40H, 20*CH2), 0.88 (t, J = 6.8 Hz, 6H, 2*Me). **^{13}C NMR (400 MHz, $CDCl_3$) δ** 176.41, 176.15, 174.85, 173.99, 171.21, 170.29, 129.99, 129.64, 91.09, 72.19, 70.19, 68.20, 60.80, 51.08, 36.35, 34.14, 29.45 - 27.21, 27.18, 24.88, 14.12. **MS (ESI-)** m/z calcd (M-H) C46H78NO13- =852,55, found = 852.60

*4,4'-(((2S,3R,4R,5S,6R)-6-(hydroxymethyl)-3-((9Z,12Z)-octadeca-9,12-dienamido)-4-(tetradecaneoyloxy)tetrahydro-2H-pyran-2,5-diyl)bis(oxy))bis(4-oxobutanoic acid) (**FP16**):* **^{1}H NMR (400 MHz, $CDCl_3$) δ** 6.19 (s, 1H, H1α), 5.91 (d, J = 6.8 Hz, 1H, H1β), 5.43 – 5.30 (m, 4H, 4*CH=), 5.27 (dd, J = 23.7, 9.8 Hz, 1H, H3), 5.21 – 5.11 (m, 1H, H4), 4.50 – 4.37 (m, 1H, H2), 3.82 (dd, J = 9.5, 3.2 Hz, 1H, H5), 3.77 – 3.53 (m, 2H, H6a+H6b), 2.83 – 2.73 (m, 2H, 4*=CH2=), 2.73 – 2.49 (m, 8H, 2*CH2-COOH), 2.39 – 2.23 (m, 4H, 2*CH2α), 2.10 – 1.98 (m, 4H,2*CH2-=), 1.53 (dd, J = 5.4, 2.9 Hz, 4H, 2*CH2β), 1.43 – 1.09 (m, 34H, 17*CH2), 0.86 (m, 6H, 2*Me). **^{13}C NMR (400 MHz, $CDCl_3$) δ** 176.57, 176.33, 174.83, 173.44, 171.65, 170.71, 130.24, 127.85, 91.23, 72.16, 70.12, 68.15, 60.82, 51.19, 36.41, 34.00, 31.92, 31.51, 30.82 – 27.86, 27.07, 25.61, 24.89, 22.69, 14.13. **MS (ESI-)** m/z calcd (M-H) C46H76NO13-= 850,53, found = 850.50

*4,4'-(((2S,3R,4R,5S,6R)-6-(hydroxymethyl)-3-tetradecanamido-4-(tetradecane oyloxy)tetrahydro-2H-pyran-2,5-diyl)bis(oxy))bis(4-oxobutanoic acid) (**FP17**):* **^{1}H NMR (400 MHz, $CDCl_3$) δ** 6.19 (s, 1H, H1a), 5.94 (d, J = 7.4 Hz, 1H, H1b), 5.32 – 5.20 (m, 1H, H3), 5.20 – 5.07 (m, 1H, H4), 4.51 – 4.37 (m, 1H, H2), 3.89 – 3.75 (m, 1H, H5), 3.75 – 3.52 (m, 2H, 2*H6), 2.85 – 2.48 (m, 8H, 4*CH2-COO), 2.39 – 2.22 (m, 2H, CH2 Amide), 2.16 – 1.96 (m, 2H, CH2 Ester), 1.64 – 1.45 (m, 4H, 2*CH2b), 1.44 – 1.00 (m, 40H, 20*CH2), 0.99 – 0.80 (m, 6H, 2*Me). **^{13}C NMR (400 MHz, CD_3OD) δ** 176.30, 174.97, 173.70, 170.96, 170.01, 91.31, 72.30, 70.28, 68.31, 61.00, 55.05, 34.26, 32.03 - 29.43, 25.59, 25.00, 22.81, 14.26. **MS (ESI-)** m/z calcd (M-H) C42H72NO13-= 798,50, found = 798.50.

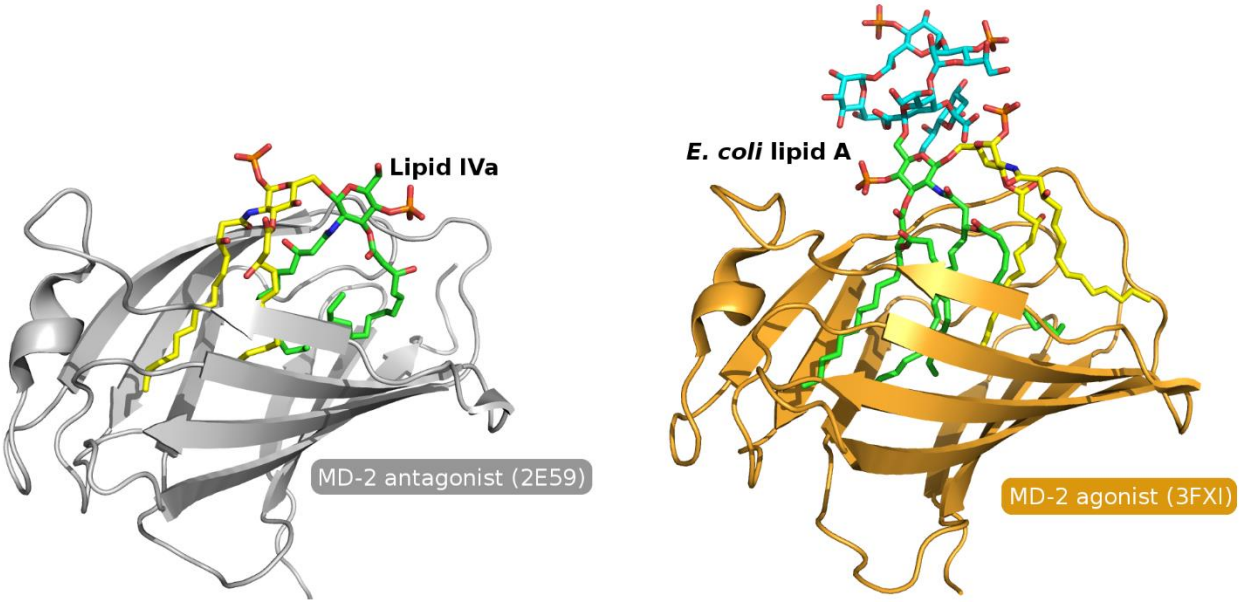

Figure S1. On the left: representation of type A (antagonist-like) binding mode as known from lipid IVa in PDB ID 2E59. On the right: representation of type B (agonist-like) binding mode as for *E. coli* lipid A in PDB ID 3FXI.

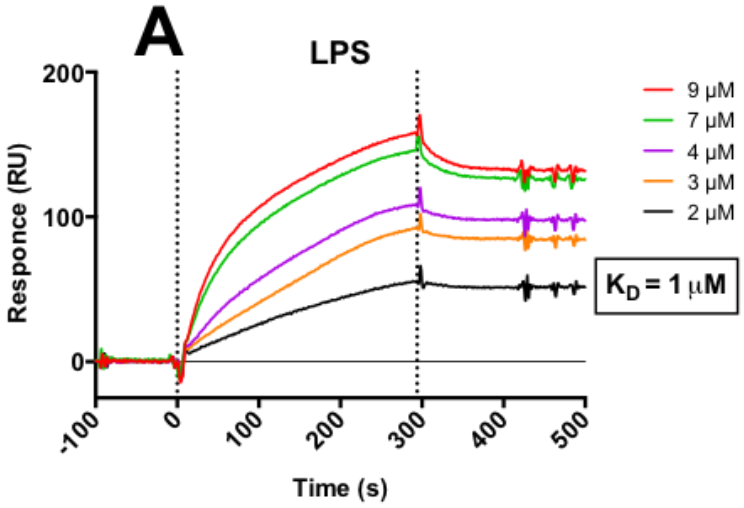

Figure S2. SPR binding studies on purified hMD-2 receptor. (A) SPR analysis show direct interaction between LPS and hMD-2 (K_D value is reported). Results are representative of at least three independent experiments.

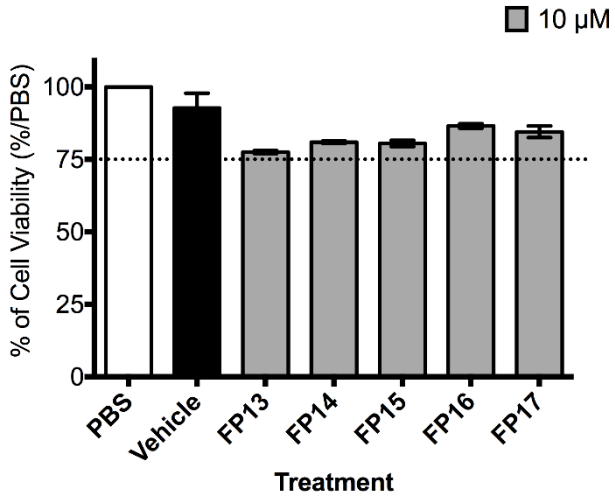

Figure S3. MTT viability assay of compounds **FP13-17** in HEK-Blue hTLR4 cells. Cells were treated with the vehicle (DMSO/EtOH 1:1) or with the indicated concentration of each compounds for 16 hours. Data were normalized with PBS administration and represent the mean of percentage ± SEM of three independent experiments.

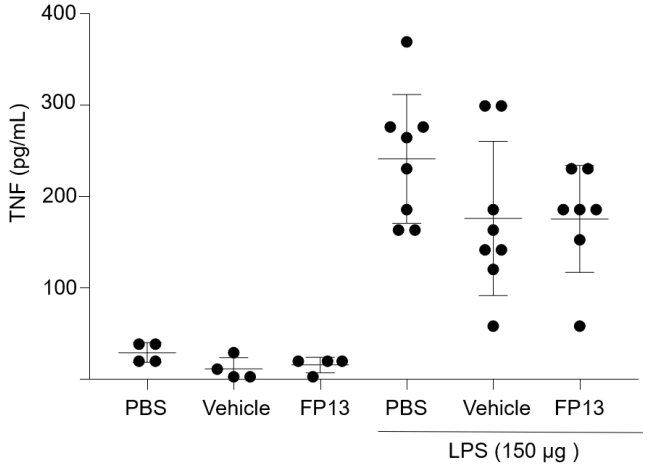

Figure S4: Monosaccharide **FP13** does not prevent increased serum TNF levels LPS-injected mice. C57BL/6 mice were injected i.p. with 200 µg **FP13**. 30 min later, the mice were i.p. injected with 150 µg of *Salmonella enterica* LPS, or vehicle and PBS as controls. Mice were sacrificed 4 h later and serum was collected. Serum TNF concentration was determined by Luminex-based Bio-Plex Multiplex system. Error bars represent the standard deviation of the mean.

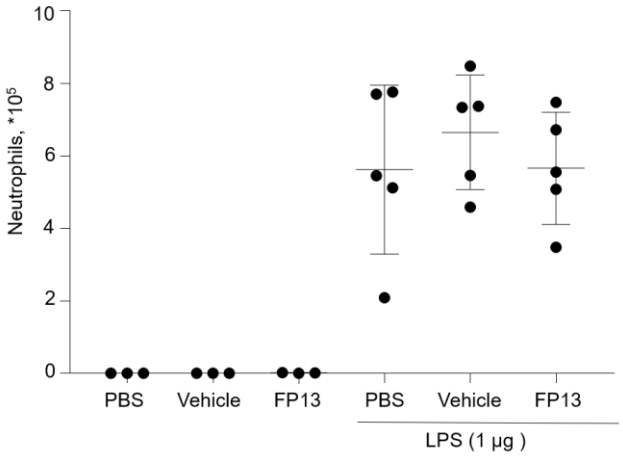

Figure S5: Monosaccharide **FP13** does not prevent lung neutrophilia upon administration of LPS in the lungs of mice.C57BL/6 mice were treated i.t. with 1 µg *Salmonella* LPS in the presence or absence of 45 µg **FP13**. PBS and vehicle were administered as controls. Mice were sacrificed 16 h later and neutrophilia in the BAL fluid was measured by flow cytometry. Error bars represent the standard deviation of the mean.

Small Unilamellar Vesicles formation: computational study.

MD simulations conducted at 300K, 303K and 310K failed to reach phase separation, in which the lipids would continuously span two dimensions interacting one with another and be separated by solvent in the third. This might be due to a too short simulation time, such system might require longer timeframes to evolve to a more stable equilibrium state. It also appears that the lipids have a tendency to freeze, which could be due to the set of parameters selected, the temperature, being controlled by a Langevin thermostat, should be distributed evenly throughout the three-dimensional space. At 350K and 400K the system reached phase separation. However, at 400K, in our attempt at starting the MD simulation under anisotropic conditions, the bilayer did not form in the two dimensions parallel to any face of the box (rather in a diagonal fashion), causing two dimensions of the box to progressively collapse over time. The other simulation (a 400-ns simulation under isotropic conditions) also reached good phase separation (data not shown). Among the two simulations to reach phase separation we selected the 350K one over the 400K one for performing an in-depth analysis, considering that the one with the lowest temperature is more likely to better represent the reality. In turn, the selected simulation was run for 1 µs, in which 150 ns were run under isotropic conditions and 850 ns under anisotropic conditions, all at 350K. In most of the MD simulations we noted that under

anisotropic conditions the system once already pre-equilibrated has a tendency to evolve very slowly.

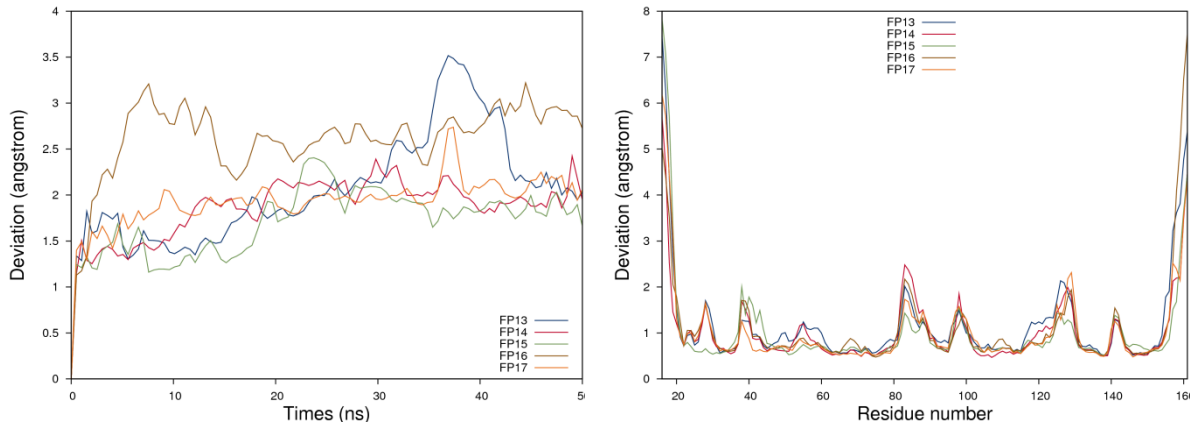

Figure S6. Molecular dynamics simulations of the TLR4/MD-2 system in complex with ligands FP13, FP14, FP15, FP16 and FP17. A) RMSD of the MD-2 backbone over time. B) RMS fluctuations per residues of MD-2.

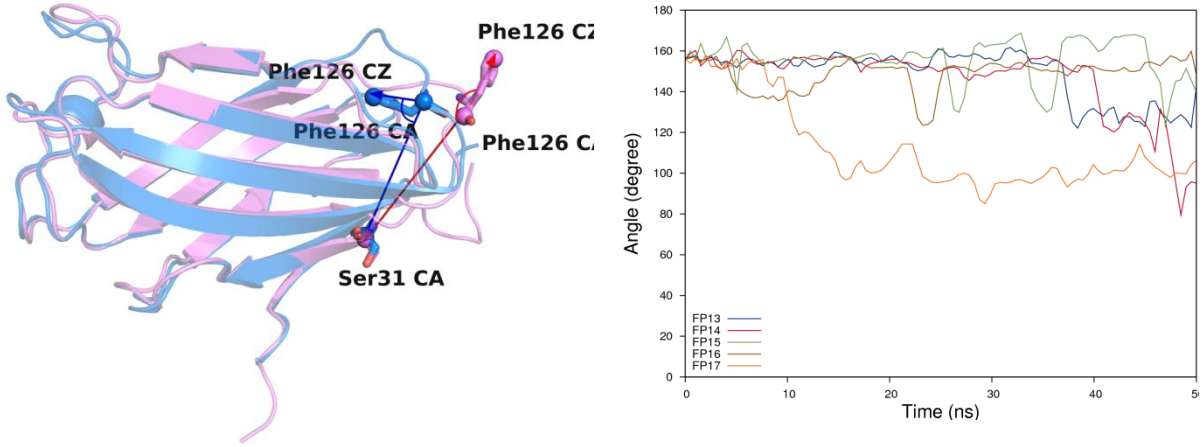

Figure S7. On the left: representation of two vectors, within MD-2, starting both from the alpha-carbon of residue Phe126 to, respectively, the zeta-carbon of the same residue and the alpha-carbon of residue Ser21. Agonist MD-2 from PDB-ID 2E59 and antagonist MD-2 from PDB-ID 3FXI are represented in semi-transparent blue and pink cartoons respectively. On the right: the angle between the two vectors defined in A is plotted within MD2 of each MD simulations.

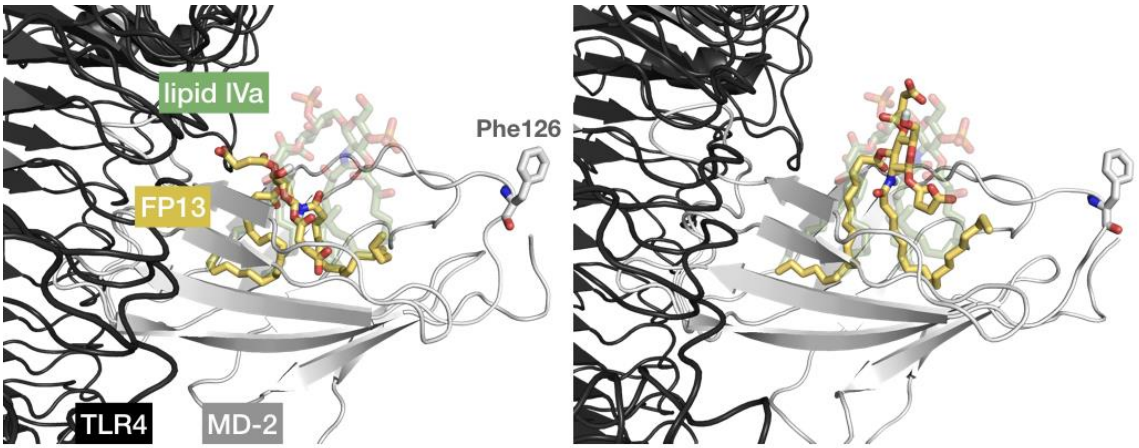

Figure S8. TLR4 and MD-2 are respectively represented in black and grey cartoon. **FP13** and lipid IVa (partially transparent) are depicted in CPK colored sticks with carbon atoms respectively colored in yellow and green. MD-2 Phe126 is in sticks. On the left: docked pose (t=0ns). On the right: end of the simulation (t=50ns).

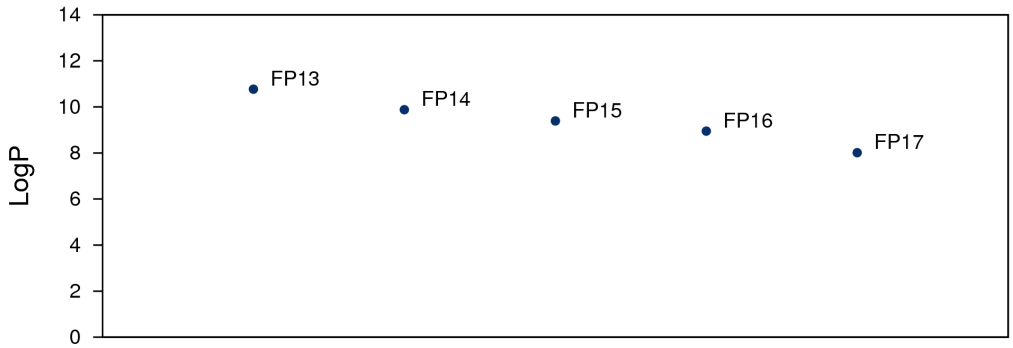

Figure S9. Computed logP values for compounds FP13, FP14, FP15, FP16 and FP17, as calculated in Maestro.†

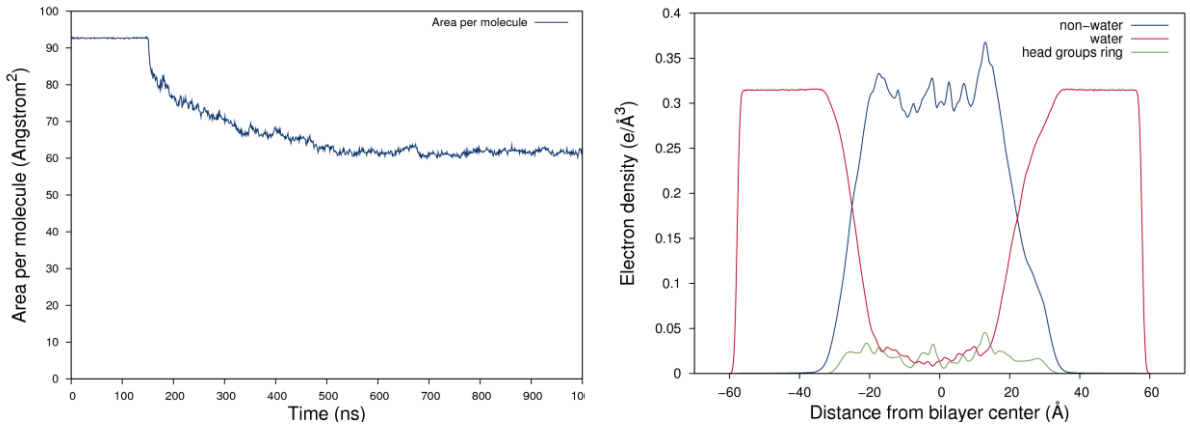

Figure S10. One the left: area per molecule over time. At t=150ns the system was switched from an isotropic to anisotropic pressure scaling. On the right: decomposed electron density of the system averaged over the 300 last ns of simulation.

† Schrödinger Release 2017-4: Maestro, Schrödinger, LLC, New York, NY, 2017.

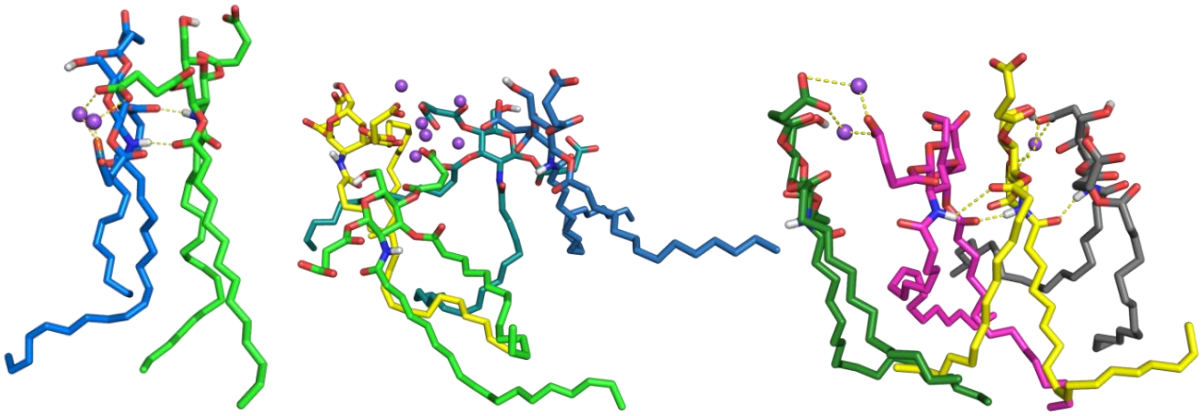

Figure S11. On the left: face to face packaging of two **FP15**. In the middle: parallel packaging of four **FP15**. On the right: clustering of four **FP15** around a Na^+ rich pocket. Each **FP15** unit has a different color to help to visually differentiate individual molecule.